THE MECHANISM OF CATALYTIC HYDROCARBON OXIDATION BY MOLECULAR OXYGEN AND HALOGENATED RUTHENIUM AND IRON PORPHYRINS

Thesis by

Eva Rachel Birnbaum

In Partial Fulfillment of the Requirements
for the Degree of
Doctor of Philosophy

California Institute of Technology

Pasadena, California

1995

(Submitted May 8th, 1995)

Acknowledgment

When I came to Caltech four years ago, I had no idea what I was getting into. Fortunately, I stumbled onto a joint project with John Bercaw and Harry Gray, who have been great advisors. They have given me tremendous freedom to explore and learn chemistry on my own, while providing full support and guidance. They promote excellent science while still managing to have fun and be wonderful, generous, people. Thank you both for a great graduate experience.

The graduate students and post docs in both of my groups have been the people who have really shaped my time here. I feel fortunate to have worked with such a great group of people. I would especially like to thank my fellow suffering souls on the porphyrin project, Julia Hodge and Mark Grinstaff, for their support. I'd like to thank Don Low, who will make a great advisor someday because he seems to know something about everything, for being a great friend and coworker. Jack Mizoguchi has been an extremely helpful and patient instructor for bio-techniques in the azurin project; hopefully something will come of that someday! Hans Nikol I would like to thank for providing inspiration in the darkest hour of thesis writing.

I would certainly like to acknowledge the people who have kept me sane while I was here: Kathy Cooke and Dave Valone, for always making me welcome in their home (and mothering me, Kathy!); Rhonda Larson and Tim Johann, for evenings of bridge, wine, and good conversation; the Pasadena Ultimate Frisbee crowd, particularly Kelly Johnson, Laura Wheeler, Kris Sullivan, and Kurt Fleischer, for many hours of great ultimate; and Tamara Hendrickson, for all the lunches where we talked about everything BUT chemistry. My parents I would like to thank for always believing in me.

Finally, I thank Mark McCleskey for bringing joy into my life; I look forward to starting our life together. Harry, you schemer, thanks for promoting the joint PhD/Mrs degree program (how embarrassing!...what is this, Harry, intra-group marriage #5?). Life has never been dull in the Gray group!

Abstract

Highly halogenated ruthenium and iron porphyrins are shown to be active catalysts for alkene oxidation with dioxygen or iodosobenzene. The synthesis and characterization of β-octachloro-tetrakis(pentafluorophenyl)porphyrinato-ruthenium(II) carbonyl [$RuTFPPCl_8(CO)$] and β-octabromo-tetrakis(pentafluorophenyl)porphyrinato-iron(III) chloride [$Fe(TFPPBr_8)Cl$] are reported. Crystal structures of $RuTFPPCl_8(CO)$ and the zinc and free ligand precursor complexes show extensive distortion of the halogenated porphyrin macrocycles due to steric interactions between the b-chlorine atoms and the pentafluorophenyl rings. ^{19}F NMR is developed as a method to characterize both paramagnetic and diamagnetic fluorinated porphyrins in solution. The anodically shifted reduction potentials and red shifted absorptions in the UV-Vis spectroscopy of the halogenated porphyrins are discussed in terms of steric and electronic effects on porphyrin frontier orbitals.

Both $Fe(TFPPBr_8)Cl$ and $RuTFPPCl_8(CO)$ catalyze the oxidation of cyclohexene with dioxygen and without added coreductant, with 73 and 296 turnovers, respectively, in 24 hours. Although both porphyrins will catalyze reactions with iodosobenzene, showing selectivity consistent with high-valent metal-oxo formation, overall activity with dioxygen is much higher. In accord with earlier work, cyclohexene oxidation by $Fe(TFPPBr_8)Cl$ is consistent with a mechanism involving porphyrin-mediated decomposition of alkyl peroxides, which generates free radicals in solution. Catalysis with $RuTFPPCl_8(CO)$ is shown to be of a photochemical nature, as irradiation with low energy light results in a dramatic increase in the reaction rate. A reaction mechanism involving olefin binding to the excited ruthenium porphyrin is suggested by laser photolysis experiments. This catalyst represents the first stable, effective metalloporphyrin catalyst for olefin oxidation with dioxygen and light.

Table of Contents

List of Figures

List of Tables

Abbreviations Used

mCPBA	*m*-chloroperoxybenzoic acid
OEP	octaethylporphyrin
SCF	supercritical fluid
SC CO_2	supercritical carbon dioxide
TBHP	*tert*-butyl hydroperoxide
TDBPP	tetrakis-(2,6-dibromophenyl)porphyrin
TDCPP	tetrakis-(2,6-dichlorophenyl)porphyrin
TDFPP	tetrakis-(2,6-difluorophenyl)porphyrin
TFPP	tetrakis(pentafluorophenyl)porphyrin
$TFPPBr_8$	b-octabromo-tetrakis(pentafluorophenyl)porphyrin
$TFPPCl_8$	b-octachloro-tetrakis(pentafluorophenyl)porphyrin
TMP	tetramesitylporphyrin
TPP	tetraphenylporphyrin

Chapter 1

Introduction to Catalysis with Metalloporphyrins

Science has "explained" nothing; the more we know the more fantastic the world becomes and the profounder the surrounding darkness.
-- Aldous Huxley, *Along the Road*, pt. 2 (1925).[1]

The whole of science is nothing more than a refinement of everyday thinking.
-- Albert Einstein, *Out of My Later Years*, ch. 12 (1950).[2]

Oxidation chemistry is one of many arenas in which chemists are attempting to devise catalysts that achieve the remarkable efficiency, selectivity, and specificity of enzymes. Cytochrome P-450, a heme-based enzyme involved in respiration, has long been a target for the generation of a biomimetic catalyst.[3,4] Found in a wide variety of tissues, this membrane-bound enzyme catalyzes the oxidation of a wide variety of organic substrates with reductively activated dioxygen.[4] In particular, the ability of P-450 to selectively activate the more inert C-H bonds is quite desirable for industrial applications. Although many catalysts have been investigated, this selectivity has yet to be duplicated by a synthetic system.

The catalytic cycle of cytochrome P-450 is shown in Figure 1.1. From the resting state as the ferric porphyrin, two reducing equivalents from NADH are required to fully activate the enzyme. The first reduces the porphyrin to the ferrous state, enabling it to bind dioxygen. A second electron reduces the bound oxygen complex, and subsequent addition of two protons induces heterolytic cleavage of the dioxygen bond and release of a water molecule to form a high-valent metal-oxo iron porphyrin. The iron oxo

intermediate, which has never been isolated from P-450 due to its high reactivity, is generally believed to be an iron(IV)oxo porphyrin radical cation. Although early steps in the cycle are well documented, assignment of the active species is largely by analogy to Compound I of the enzyme horseradish peroxidase (HRP), which has been definitively characterized as an iron(IV)oxo porphyrin π radical cation.[4,5] The active intermediate can also be directly generated with an O-atom donor such as iodosobenzene or peroxide; this "peroxide shunt" pathway is a convenient test for P-450 monooxygenase-like activity in model complexes.

A general technique in catalyst design is to model the active site of an enzyme, in the hope that one small section of the protein will exhibit the same activity as the whole. The porphyrin core of P-450 lends itself to this type of study for several reasons: reliable syntheses for porphyrins have been developed, the periphery of the porphyrin ligand is easily modified to alter the properties of the porphyrin, and the ligand has distinctive spectroscopy which facilitates investigation. Indeed, the past two decades have produced a plethora of work on metalloporphyrin derivatives.[4,6,7]

Initial investigations on a derivative of the naturally occurring protoporphyrin IX (Figure 1.2) demonstrated that a species spectroscopically similar to compound I could be generated with an O-atom donor.[8] However, rather than oxidizing substrate, this intermediate hydroxylated its own β-side chain. A synthetic analog, octaethylporphyrin, was even less stable outside of the protective protein environment. Although a high-valent iron-oxo was believed to be generated in the presence of iodosobenzene, the planar porphyrin degraded by hydroxylation at the meso position, followed by complete destruction of the porphyrin chromophore. Oxidation of a second porphyrin molecule was clearly more favorable than oxidizing substrate.[8] The protein fold, which protects the porphyrin against autooxidation, prohibits unproductive μ-oxo dimer formation, and enhances substrate-porphyrin interactions, is clearly vital for these simple planar hemes to act as catalysts. A more stable porphyrin molecule would be necessary to mimic

monooxygenase behavior in solution. And so the quest to design a better porphyrin ligand began.

A simple iron tetraphenylporphyrin, Fe(TPP)Cl, was found to oxidize hydrocarbons in the presence of PhIO.[9] Substitution at the meso position with a bulky phenyl moiety was found to reduce aggregation in solution and protect the reactive meso position from reactions leading to porphyrin degradation. Oxidation of tetramesitylporphyrinato-iron(III) chloride (Fe(TMP)Cl) with *m*-chloroperoxybenzoic acid at low temperatures produced a species that both shares spectral features with Compound I and is capable of epoxidizing alkenes.[10] Although more promising than OEP, these ligands still showed substantial degradation in solution.

The second generation of metalloporphyrin catalysts were designed to increase the lifetime of porphyrins in solution by reducing their susceptibility to oxidative degradation. Halogenation of the meso phenyl rings would raise the reduction potential as well as increase steric bulk along the porphyrin periphery, decreasing the likelihood of dimerization or hydrogen abstraction by other porphyrin molecules. Tetrakis-(pentafluorophenyl)porphyrin (TFPP) was indeed found to be more stable than TPP, and iron complexes were found to show high selectivity for epoxidation of olefins.[11] Similarly, tetrakis(2,6-dichlorophenyl)porphyrinato-iron(III) chloride [Fe(TDCPP)Cl] was found to show high activity with pentafluoroiodosobenzene.[12] Iron(III), manganese(III) and chromium(III) complexes of TDCPP all exhibited higher activity for cyclohexene oxidation with iodosobenzene than their TPP analogs, as well as higher selectivity for epoxide formation. Furthermore, the 2,6-dichlorophenylporphyrin complexes remained intact after an oxidation reaction, while the tetraphenylporphyrin complexes were completely degraded.[13]

In addition to halogenation, other elegant methods have been developed for generating steric barriers against the close approach of two porphyrin molecules. Tailed porphyrins (Figure 1.3) have an imidazole or other nitrogen containing function linked to

the porphyrin ring by a flexible hydrocarbon chain, allowing it to swing around and axially bind to the metal center in simulation of histidine coordination.[14] Picket fence,[15] strapped,[16] basket handle,[17] and capped[18] porphyrins have large organic groups that project perpendicular to the plane of the porphyrin as pickets, or, in the latter cases, actually bridge across from one side of the porphyrin ring to the other. All of the above methods provide some steric protection as well as a pocket in which the substrate may bind. Although these types of porphyrins have led to some extremely interesting work in the area of enantioselective and regioselective oxidation chemistry,[19] they have not been further pursued as general oxidation catalysts. The hydrocarbon side chains that drive the selectivity found with these metalloporphyrins, while stable enough under mild conditions, are susceptible to degradation in a highly oxidizing environment.

Instead of building a pocket around the porphyrin, the third generation catalysts have completely protected the porphyrin periphery by full substitution at both the meso and beta positions (Figure 1.4). Steric bulk from mesityl,[20,21] pentafluorophenyl,[21-28] or 2,6-dihalophenyl[22,29-32] groups at the meso carbons is paired with electron-withdrawing substituents at the β-carbons. The electronic and steric crowding created by the full periphery imparts unusual structural and spectroscopic features to the porphyrin ligand, while the steric bulk of these complexes causes severe distortion of the porphyrin macrocycle, preventing dimerization (Chapter 2 and 3). The electronic demands of the substituents have been shown to decrease oxidative degradation of the porphyrin, thereby increasing net activity.[22,28,29,33,34]

Indeed, these highly halogenated porphyrins are found to be active catalysts. Iron and manganese complexes of β-octachloro, β-octabromo,[20,22,26,28-30,34-40] and β-octanitro[32] tetraphenylporphyrin derivatives are reported to catalyze the oxidation of both alkanes and alkenes with a variety of O-atom donors, with tremendous increases in both activity and catalyst lifetime over the second generation porphyrins. For example, β-octabromo-tetramesitylporphyrinato-manganese(III) chloride catalyzes the epoxidation

of cyclooctene with hydrogen peroxide in 96% yield,[34] and the hydroxylation of adamantane with $KHSO_5$ in 62% yield.[20] Iron(III) chloride complexes of β-octachloro-tetrakis(2,6-dichlorophenyl)porphyrin catalyze the hydroxylation of heptane with iodosobenzene in 80%yield.[22] These reactions show increases in rate, total activity, selectivity, and porphyrin lifetime relative to the unhalogenated derivatives.

An even more unique finding is the activity of the third generation porphyrins with dioxygen. At 80 °C and 75 atm O_2, β-octabromo-tetrakis(pentafluorophenyl)-porphyrinato-iron(III) chloride ($Fe(TFPPBr_8)Cl$) catalyzes 17,150 turnovers of isobutane to *tert*-butyl alcohol in three hours. At slightly lower temperatures, the selectivity of the reaction for the desired alcohol can be increased to 92%.[26]

The unprecedented activity of a metalloporphyrin with dioxygen and without a coreductant gave rise to new ideas for mechanisms for O_2 activation. Most recent porphyrin literature examines catalysis with O-atom donors that attempt to directly mimic enzymatic P-450 reactions. The reports of $Fe(TFPPBr_8)Cl$ activity imply that alternate mechanisms may exist in addition to traditional high-valent metal-oxo chemistry, and prompted a more thorough investigation of this and similar third generation compounds in our lab.

This brief review of recent metalloporphyrin catalysis literature is not meant to be comprehensive, but rather to explain some of the history behind the development of the unusual perhalogenated porphyrin ligand. The more contemporary metalloporphyrin catalysts are now only distant cousins to the natural hemes they were initially designed to model. The following chapters are a more thorough investigation of the spectroscopy and catalytic properties of several fluorinated metalloporphyrins.

Chapter 2 describes the synthesis of halogenated iron and ruthenium porphyrins and their precursors. Molecular structures of β-octachloro-tetrakis(pentafluorophenyl)-porphyrinato-ruthenium(II) carbonyl, [$RuTFPPCl_8(CO)$] and the zinc and free ligand precursor complexes, are shown to be extremely distorted, in line with other halogenated

porphyrin structures. ^{19}F NMR is developed as a method for characterizing the solution structure of both paramagnetic and diamagnetic fluorinated porphyrin structures.

The unusual spectroscopy and electrochemistry of halogenated porphyrins is discussed in Chapter 3. The changes in the frontier orbital energies upon phenyl and pyrrole halogenation are described. A full molecular orbital diagram is shown for $RuTFPPCl_8(CO)$ and discussed in terms of the distortion and electron-withdrawing effects of halogenation.

Enhanced catalytic activity is observed with the highly halogenated complexes. Alkene oxidation by halogenated iron porphyrins is described in Chapter 4. $Fe(TFPPBr_8)Cl$ is an active catalyst with both iodosobenzene and dioxygen, and shows a significant increase in activity and catalyst lifetime relative to Fe(TFPP)Cl. Observations support a mechanism involving porphyrin-mediated decomposition of alkyl peroxide, as proposed earlier in our group.[37,41]

Chapter 5 is a discussion of catalysis with $RuTFPPCl_8(CO)$. Similar to the iron complex, this porphyrin is an extremely active catalyst for the oxidation of olefins under very mild conditions: 1 atm dioxygen, room temperature, and without addition of co-reductant. Alkene oxidation is also observed with iodosobenzene. Observations of oxidation reactions catalyzed by $RuTFPPCl_8(CO)$ with dioxygen are not consistent with mechanisms proposed for the activity of either the iron analog, $Fe(TFPPBr_8)Cl$, or other ruthenium porphyrins. Instead, olefin oxidation is dependent on light, possibly initiated by an interaction of the alkene with a $RuTFPPCl_8(CO)$ excited state. As oxidation mechanisms in metalloporphyrins involving electronic excited states are rare, a photochemical reaction mechanism would be an interesting result, suggesting intermediates and ideas completely distinct from traditional high-valent metal-oxo chemistry.

The final chapter investigates the use of halogenated porphyrin catalysts in supercritical carbon dioxide. An apparatus was set up to measure the solubility of three

halogenated porphyrins in supercritical carbon dioxide by optical spectroscopy. Each porphyrin was tested with both iodosobenzene and dioxygen as a catalyst for the oxidation of cyclohexene in a supercritical medium. Although the results are extremely preliminary, they suggest that selectivity was more affected than net activity by the change in solvent. More multiple oxidations of the same substrate molecule were observed relative to reactions run in methylene chloride. Supercritical carbon dioxide was shown for the first time to be a good medium for oxidation catalysis.

References

(1) Huxley, A. In *Along the Road*; George Doran: New York, 1925; pp 266.

(2) Einstein, A. *Out of my Later Years*; Greenwood Press: Westport, CT, 1950, pp 282.

(3) McMurray, T. J.; Groves, J. T. In *Cytochrome P-450*; P. K. Ortiz de Montellano, Ed.; Plenum Press: New York, 1986; pp 1-28.

(4) Gunter, M. J.; Turner, P. *Coord. Chem. Rev.* **1991**, *108*, 115-161.

(5) *Cytochrome P-450*; Ortiz de Montellano, P. K., Ed.; Plenum Press: New York, 1986.

(6) Meunier, B. *Chem. Rev.* **1992**, *92*, 1411-1456.

(7) Mansuy, D. *Coord. Chem. Rev.* **1993**, *125*, 129-142.

(8) Chang, C. K.; Kuo, M.-S. *J. Am. Chem. Soc.* **1979**, *101*, 3413-3415.

(9) Groves, J. T.; Nemo, T. E.; Myers, R. S. *J. Am. Chem. Soc.* **1979**, *101*, 1032-1033.

(10) Groves, J. T.; Haushalter, R. C.; Nakamura, M.; Nemo, T. E.; Evans, B. J. *J. Am. Chem. Soc.* **1981**, *103*, 2884-2886.

(11) Chang, C. K.; Ebina, F. *J. Chem. Soc., Chem. Commun.* **1981**, 778-779.

(12) Traylor, P. S.; Dolphin, D.; Traylor, T. G. *J. Chem. Soc., Chem. Commun.* **1984**, 279-280.

(13) Traylor, T. G.; Miksztal, A. R. *J. Am. Chem. Soc.* **1989**, *111*, 7443-7448.

(14) Collman, J. P.; Groh, S. E. *J. Am. Chem. Soc.* **1982**, *104*, 1391-1403.

(15) Gunter, M. J.; McLaughin, G. M.; Berry, K. J.; Murray, K. S.; Irving, M.; Clark, P. E. *Inorg. Chem.* **1984**, *23*, 283-300.

(16) Battersby, A. R.; Howson, W.; Hamilton, A. D. *J. Chem. Soc., Chem. Commun.* **1982**, 1266-1268.

(17) Lexa, D.; Mamenteau, M.; Saveant, J. M.; Xu, F. *Inorg. Chem.* **1986**, *25*, 4857-4865.

(18) Kim, K.; Ibers, J. A. *J. Am. Chem. Soc.* **1991**, *113*, 6077-6081.

(19) Collman, J. P.; Zhang, X.; Lee, V. J.; Uffelman, E. S.; Brauman, J. I. *Science* **1993**, *261*, 1404-1411.

(20) Hoffmann, P.; Robert, A.; Meunier, B. *Bull. Chem. Soc. Fr.* **1992**, *129*, 85-97.

(21) Mandon, D.; Ochsenbein, P.; Fischer, J.; Weiss, R.; Jayaraj, K.; Austin, R. N.; Gold, A.; White, P. S.; Brigaud, O.; Battioni, P.; Mansuy, D. *Inorg. Chem.* **1992**, *31*, 2044-2049.

(22) Bartoli, J. F.; Brigaud, O.; Battioni, P.; Mansuy, D. *J. Chem. Soc., Chem. Commun.* **1991**, 440-442.

(23) Marsh, R. E.; Schaefer, W. P.; Hodge, J. A.; Hughes, M. E.; Gray, H. B.; Lyons, J. E.; Ellis, P. E., Jr. *Acta Crystallogr.* **1993**, *C49*, 1339-1342.

(24) Schaefer, W. P.; Hodge, J. A.; Hughes, M. E.; Gray, H. B.; Lyons, J. E.; Ellis, P. E., Jr.; Wagner, R. W. *Acta Crystallogr.* **1993**, *C49*, 1342-1345.

(25) Henling, L. M.; Schaefer, W. P.; Hodge, J. A.; Hughes, M. E.; Gray, H. B.; Lyons, J. E.; Ellis, P. E., Jr. *Acta Crystallogr.* **1993**, *C49*, 1745-1747.

(26) Lyons, J. E.; Ellis, P. E., Jr.; Durante, V. A. In *Structure-Activity and Selectivity Relationships in Heterogeneous Catalysis*; R. K. Grasselli and A. W. Sleight, Eds.; Elsevier Science Publishers B.V.: Amsterdam, 1991; pp 99-116.

(27) D'Souza, F.; Villard, A.; Caemelbecke, E. V.; Franzen, M.; Boschi, T.; Tagliatesta, P.; Kadish, K. M. *Inorg. Chem.* **1993**, *32*, 4042-4048.

(28) d'A. Rocha Gonsalves, A. M.; Johnstone, R. A. W.; Pereira, M. M.; Shaw, J.; Sobral, D. N.; Abilio, J. F. *Tetrahedron Lett.* **1991**, *32*, 1355-1358.

(29) Traylor, T. G.; Tsuchiya, S. *Inorg. Chem.* **1987**, *26*, 1338-1339.

(30) Hoffmann, P.; Meunier, B. *New J. Chem.* **1992**, *16*, 559-561.

(31) Lu, W. Y.; Bartoli, J. F.; Battioni, P.; Mansuy, D. *New J. Chem.* **1992**, *16*, 621-628.

(32) Bartoli, J. F.; Battioni, P.; Foor, W. R. D.; Mansuy, D. *J. Chem. Soc., Chem. Commun.* **1994**, 23-24.

(33) Ellis, P. E., Jr.; Lyons, J. E. *Catal. Lett.* **1989**, *3*, 389-398.

(34) Banfi, S.; Mandelli, R.; Montanari, F.; Quici, S. *Gazz. Chim. Ital.* **1993**, *123*, 409-415.

(35) d'A. Rocha Gonsalves, A. M.; Pereira, M. M.; Serra, A. C.; Johnstone, R. A. W.; Nunes, M. L. P. G. *J. Chem. Soc., Perkin Trans. 1* **1994**, 2053-2057.

(36) Ellis, P. E., Jr.; Lyons, J. E. *Coord. Chem. Rev.* **1990**, *105*, 181-193.

(37) Grinstaff, M. W.; Hill, M. G.; Labinger, J. A.; Gray, H. B. *Science* **1994**, *264*, 1311-1313.

(38) Lyons, J. E.; Ellis, P. E., Jr. *Catal. Lett.* **1991**, *8*, 45-52.

(39) Traylor, T. G.; Hill, K. W.; Fann, W.; Tsuchiya, S.; Dunlap, B. E. *J. Am. Chem. Soc.* **1992**, *114*, 1308-1312.

(40) Wijesekera, T.; Matsumoto, A.; Dolphin, D.; Lexa, D. *Angew. Chem., Int. Ed. Eng.* **1990**, *29*, 1028-1030.

(41) Labinger, J. A. *Catal. Lett.* **1994**, *26*, 95-99.

Figure 1.1 -- The proposed catalytic cycle for oxidation reactions by cytochrome P-450. All steps before the generation of the high-valent metal-oxo are well documented, but the actual active intermediate has not been isolated. Addition of an O-atom donor such as iodosobenzene to the ferric porphyrin (peroxide shunt) will directly form the oxidizing species, generally believed to be $Fe^{IV}(P)(O)^{\bullet +}$ (diagram modified from reference 1).

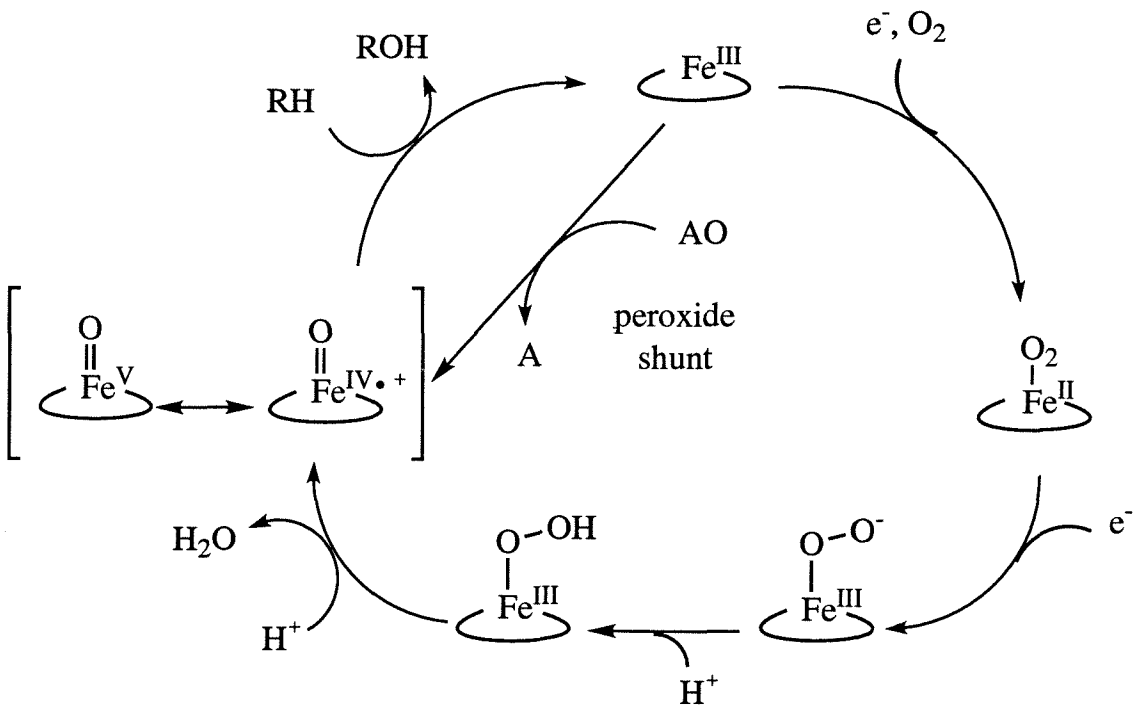
ROH
RH
Fe^III
e⁻, O2
AO
A
peroxide
shunt
O
Fe^V
O
Fe^IV•+
O2
Fe^II
e⁻
H2O
O-OH
Fe^III
O-O⁻
Fe^III
H+
H+

Figure 1.2 -- Diagram of the heme center from cytochrome P-450, protoporphyrin IX, and a synthetic equivalent, octaethylporphyrin (OEP). Naturally occurring hemes commonly bear alkyl or vinyl substituents at the pyrrole carbons.

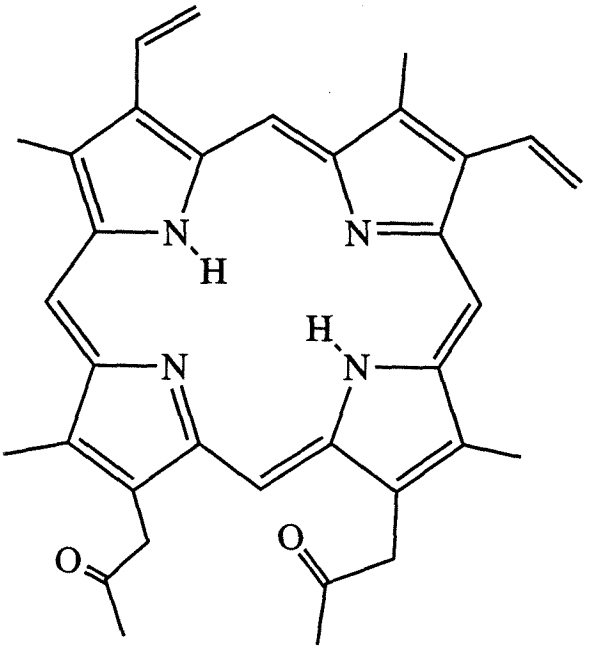

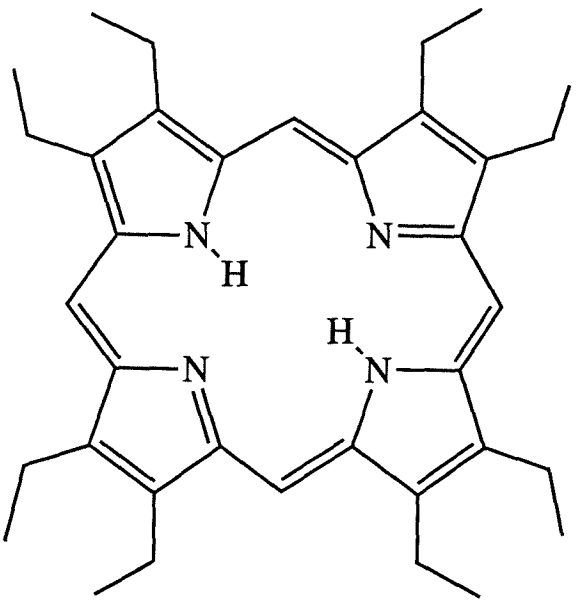

Protoporphyrin IX (above) and Octaethylporphyrin (OEP)

Figure 1.3 -- Representations of tailed, picket fence, basket handle, and capped porphyrins. The bulky ligands create a steric barrier in the plane perpendicular to the porphyrin to prevent μ-oxo dimerization.

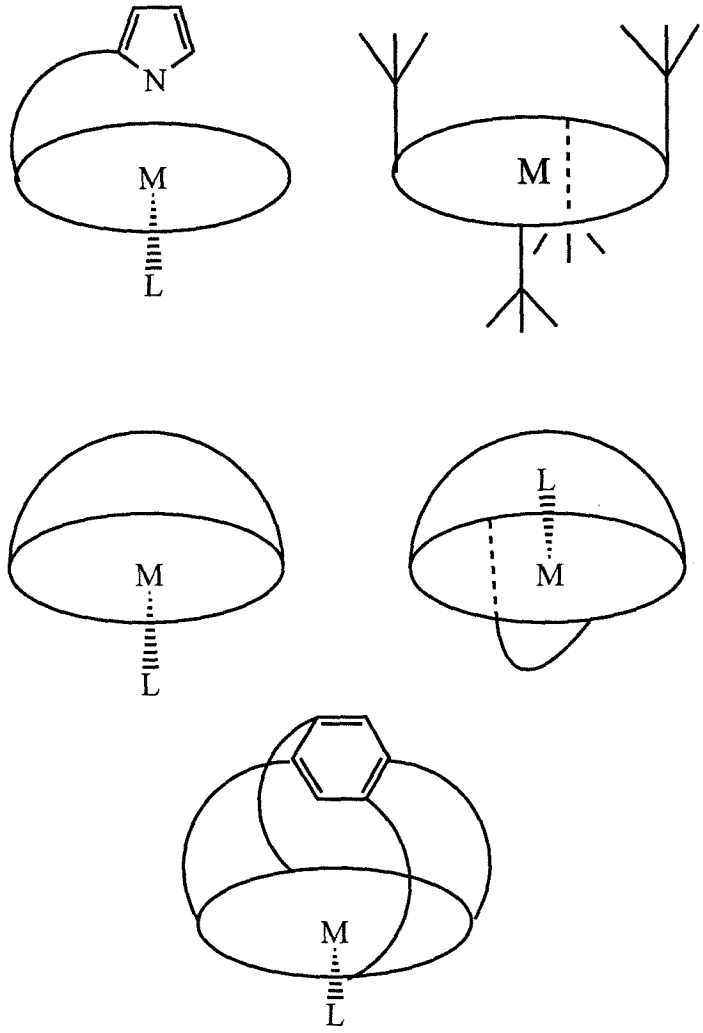

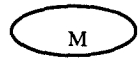

= porphyrin ring

Figure 1.4 -- Drawings of three iron complexes of second generation porphyrins showing the groups commonly substituted at the meso positions: mesityl, 2,6-dichlorophenyl, and pentafluorophenyl groups. Halogenation of the pyrrole carbons would form third generation catalysts.

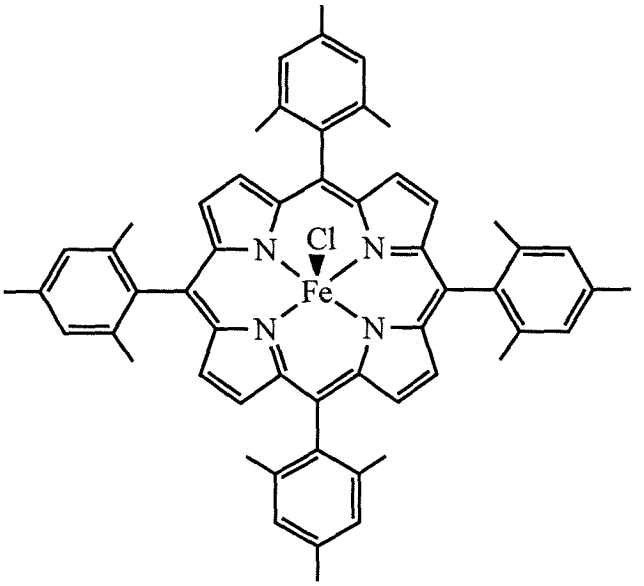

Fe(TMP)Cl

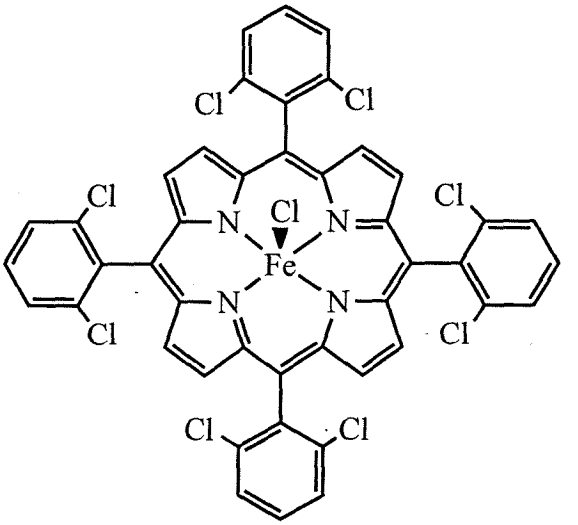

Fe(TDCPP)Cl

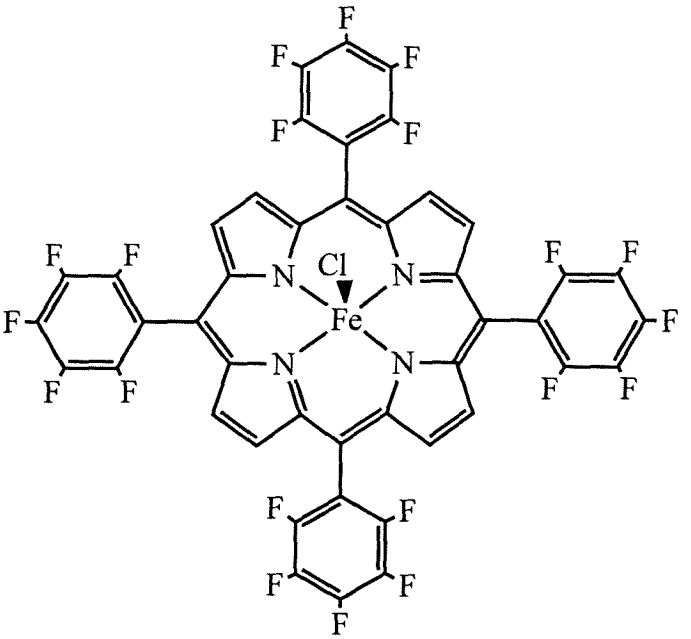

Fe(TFPP)Cl

Chapter 2

Synthesis, Molecular Structures, and Nuclear Magnetic Resonance Spectroscopy of Halogenated Porphyrins

Introduction

Biomimetic metalloporphyrin oxidation catalysts are often based on a tetraphenylporphyrin template because these complexes are not as susceptible to aggregation and are protected from degradation to oxophlorins (oxo substitution at the meso position) by meso-phenyl substitution. Mesityl (TMP) or 2,6-dichlorophenyl (TDCPP) groups at the meso positions are more successful than unsubstituted phenyl rings, since the additional steric bulk of a substituted phenyl moiety decreases the tendency to form μ-oxo dimers in solution. The next generation of metalloporphyrins further enhanced the tetraphenylporphyrin ligands with electron-withdrawing substituents at the beta positions, removing reactive C-H bonds from the porphyrin periphery and increasing the steric bulk of the molecules. Many β-substituted TDCPP and TMP metalloporphyrins have been synthesized and investigated as oxidation catalysts (see Chapter 4). In addition to these ligands, another option is to begin with a tetrakis(pentafluorophenyl)porphyrin (TFPP) template, and then halogenate the β-positions to give a perhalogenated macrocycle. These "Teflon" porphyrins are designed to be extremely resistant to normal porphyrin decomposition in oxidizing environments.

Although extremely efficient porphyrin condensation reactions have been developed,[1] allowing porphyrins to be made in high yield from the appropriate benzaldehyde and pyrrole, this methodology has not been reported to be successful for β-halo derivatives. Recent advances have developed a synthesis for the required

3,4-halogenated pyrroles,[2,3] but these compounds readily polymerize and are difficult to purify. Instead, halogenation of the β-positions is accomplished on an intact porphyrin macrocycle.[4-14] The fluorinated porphyrin, 5,10,15,20-tetrakis(pentafluorophenyl)-porphyrinato-zinc(II) (ZnTFPP), is commercially available or can be synthesized from pyrrole and pentafluorobenzaldehyde. The zinc, rather than the unmetallated porphyrin, is used because the metallated porphyrins are found to better withstand the halogenation reactions.[14]

Synthesis

Halogenation to form β-octachloro- or β-octabromo-tetrakis(pentafluorophenyl)-porphyrinato-zinc(II) ($ZnTFPPCl_8$ and $ZnTFPPBr_8$; Figure 1.1) was initially accomplished with direct addition of $Cl_{2(g)}$ or $Br_{2(l)}$. However, a less hazardous synthesis with N-halo-succinamide was developed[10] and found to proceed in good yield. Addition of excess N-halosuccinamide to a refluxing solution of ZnTFPP in methanol gave the desired product in 1-3 hours. Synthesis of the octabromo porphyrin was easier to drive to completion than that of the octachloro. The relative size of chlorine (atomic radii = 0.99) versus bromine (1.14 Å)[15] would have predicted a more difficult synthesis for $ZnTFPPBr_8$ based on the greater steric demands of eight bromines on the porphyrin periphery . However, the relative ease of synthesis of the two ligands suggests that the electronic effect, which leads to a decrease in reactivity for further substitution on the ligand, (electronegativity = 3.617 Cl, 3.365 Br)[16] is more significant. If the trend follows to fluorine, the lack of success in our lab[14] in synthesizing the β-octafluoro porphyrin is not surprising.

Although $ZnTFPPBr_8$ was readily purified by column chromatography, the large amount of partially halogenated porphyrins in the $ZnTFPPCl_8$ reaction mixture necessitated high performance liquid chromatography (HPLC). Once the β-octahalo porphyrins were isolated, they were demetallated with $HCl_{(g)}$ and purified from the zinc salts by alumina

chromatography. The yields for $H_2TFPPCl_8$ and $H_2TFPPBr_8$ were 40 and 82%, respectively, based on ZnTFPP.

Iron was inserted into the porphyrins by the standard methods: iron(II) acetate in refluxing glacial acetic acid or iron(II) chloride in DMF.[17,18] With the $TFPPBr_8$ ligand, the metal is oxidized to iron(III) during the aqueous workup, and the porphyrin isolated as the chloride salt, $Fe(TFPPBr_8)Cl$. The iron porphyrins were found to demetallate during standard column chromatography, and could only be purified by washing or recrystallization. Therefore, high quality free ligand was a prerequisite for generation of pure iron porphyrin.

Addition of pyridine to a solution of $Fe(TFPPBr_8)Cl$ reduced the metal and formed the bis-pyridine adduct. Both $Fe^{III}(TFPPBr_8)Cl$[19] and $Fe^{II}(TFPPBr_8)py_2$[20] have been crystallographically characterized. The absorption spectrum of $[Fe(TFPPCl_8)]$ in the presence of pyridine indicates formation of $Fe(TFPPCl_8)py_2$, but this species was not isolated. Attempts to synthesize $[Fe(TFPPCl_8)]$ were made using air-free, high vacuum techniques, in hopes of isolating a clean, oxygen-free sample for the anticipated investigation of O_2 activation. In retrospect, the removal of oxygen is believed to have complicated its synthesis. Allowing oxygen into the synthesis of $Fe(TFPPBr_8)Cl$ did not lead to oxygen coordination, but clean oxidation of the Fe^{II} porphyrins to $Fe^{III}(TFPPBr_8)Cl$. In the absence of oxygen, the β-octachloro porphyrin appeared to form an iron(II) complex, based on the red shifted Soret band (see Chapter 3), but with mixed axial ligands. Due to the difficulty in isolating any pure $Fe(TFPPCl_8)$ species, further work concentrated on the β-octabromo species.

Insertion of Ru from $Ru_3(CO)_{12}$ into H_2TFPPX_8 in perfluorobenzene yields a bright red (X = Cl) or green (X = Br) $RuTFPPX_8(CO)$ compound.[21] In perprotiobenzene, the extended time at reflux necessary to insert the ruthenium atom results in partial porphyrin dehalogenation and decomposition. In these reactions, ruthenium also inserts into the partially chlorinated derivatives $H_2TFPPCl_7$ and $H_2TFPPCl_6$ to form

$RuTFPPCl_7(CO)$ and $RuTFPPCl_6(CO)$, which can be isolated by sequential column chromatography and HPLC (Figure 2.2).

A single band attributable to CO stretching (1990, Cl_8; 1973 cm^{-1}, Br_8) is observed in the IR spectrum of $RuTFPPX_8(CO)$, confirming a single carbonyl ligand.[22] Identification of the other axial ligand is problematic; this ligand is labile in Ru(CO) porphyrins due to the strong trans effect of the CO.[23] Photolysis of $RuTFPPCl_8(CO)$ in pyridine results in the formation of $RuTFPPCl_8(py)_2$. After photolysis, a single symmetrically coordinated species is observed by ^{19}F NMR spectroscopy, indicating that the multiple signals in the spectrum of the carbonyl complex are due to variations in trans ligation and not dehalogenation of the porphyrin ring (*vide infra*).

Ruthenium insertion from $Ru_3(CO)_{12}$ was found to proceed in very low yield: approximately 10-20 % for $TFPPCl_8$, and less than 5 % for $TFPPBr_8$. Attempts to modify the reaction were unsuccessful. Solvent choice is limited, since any proton bearing solvent will exchange protons with the β-halogens of the porphyrin. Other ruthenium starting materials were tried, including $Ru(DMSO)_4Cl_2$, $[Ru(DMSO)_6]Cl_2$, $RuCl_3$, and $[Ru_5Cl_{12}]^{2-}$ (generated in situ). None showed significant reactivity with the $TFPPCl_8$ ligand.

Surprisingly, attempts to insert ruthenium into TFPP were also unsuccessful. Similar reaction conditions as above showed no reaction with H_2TFPP before substantial decomposition of the ligand occurred. No reports of RuTFPP have been found in the literature, although many metallated derivatives of TFPP have been synthesized.

Molecular Structures

ORTEP diagrams for $H_2TFPPCl_8$, $ZnTFPPCl_8$,[10] and $RuTFPPCl_8(CO)H_2O$[24] complexes are shown in Figure 2.3 - 2.5, with the atom numbering shown. Complete crystallographic reports are included in Appendix 2.

$H_2TFPPCl_8$ crystallized from an acetone/water solution in space group $P\bar{1}$, with two porphyrins in the unit cell. The two parallel porphyrin molecules are 4.74 Å apart, with the porphyrin centers slightly offset (center to center distance 6.1 Å). The zinc derivative, $ZnTFPPCl_8$, crystallized from a saturated *o*-dichlorobenzene solution with a solvent molecule in a parallel plane both above and below the porphyrin molecule. The solvent molecules are located 3.4 Å from the mean plane of the porphyrin (defined as the average plane of the four nitrogen atoms), a distance suggestive of a π-stacking interaction between the π systems of the porphyrin and the *o*-dichlorobenzene molecules. Aromatic solvent molecules were found to stack in a similar fashion in the crystal structure of tetraphenylporphyrinato-zinc(II) bis-toluene, $ZnTPP(C_6H_5CH_3)_2$, where two toluene molecules occupy these positions.[25] The π donor ability of the aromatic solvent may help stabilize the zinc ion in the electron deficient macrocycle. Similarly, $H_2TFPPBr_8$ was found to crystallize with an *o*-dichlorobenzene molecule stacked above each porphyrin molecule.[10]

Recrystallization of $RuTFPPCl_8(CO)$ in air from ethyl acetate and hexane gave $RuTFPPCl_8(CO)H_2O$ (Figure 2.5). An ethyl acetate molecule is hydrogen bonded to the water ligand (O ··· O 2.668 Å), and the stability provided by this hydrogen bond network may explain why no crystals were obtained with other solvents. Trans coordination of CO and H_2O to Ru is unusual, but is precedented in $RuOEP(CO)H_2O$ and the non-porphyrin compound *trans*-$RuCl_2(PEt_3)_2(CO)H_2O$.[26,27]

Chlorination of the β-pyrrole carbons induces severe tetrahedral distortions (Figures 2.6 and 2.7) reducing the molecular symmetry of the porphyrin from D_{4h} to D_2. The pairs of β-halogen atoms are located alternately above and below the average plane determined by the four central nitrogen atoms, and the phenyl rings are rotated slightly towards the mean porphyrin plane to minimize steric contact between the halogen atoms at the pyrrole positions and the ortho carbons of the pentafluorophenyl rings. The distortion of the macrocycle is quantified as the distances of the *meso* and β-carbons from the mean

plane of the porphyrin (Table 2.2). A view of the free ligand porphyrins H_2TFPP, $H_2TFPPCl_8$, and $H_2TFPPBr_8$ (Figure 2.6), generated from crystal structure coordinates, shows the increasing distortion along the series.

The three β-octachloro porphyrins described above exhibit severe distortions common to perhalogenated and other highly substituted porphyrins:[7,10,13,20,28-32] 'ruffling' or twist (distortion manifested at the *meso*- carbons) and 'saddling' (distortion manifested at the β-carbons).[33] As expected, saddling increases with halogenation (Figure 2.6), as manifested by increasing average C_β displacements from the plane from 0.051 to 0.62 to 0.90 Å in the free ligand series.[10] The free ligand, $H_2TFPPCl_8$, is the least distorted of the structurally characterized chlorinated porphyrins [$ZnTFPPCl_8$, $H_2TFPPCl_8$, $RuTFPPCl_8(CO)H_2O$, $CuTFPPCl_8$[29]], as reflected by the smaller perpendicular displacements of atoms from the mean porphyrin plane and a lack of the twisting or ruffling observed in the metallated derivatives. The saddle distortion in the free ligand (average C_β displacement = 0.62 Å) is smaller than in the metallated derivatives $ZnTFPPCl_8$ (0.75), and $CuTFPPCl_8$ (0.70),[29] but greater than in the octahedrally coordinated $RuTFPPCl_8(CO)H_2O$ (0.48 Å).[24]

Though saddled, the unmetallated $H_2TFPPCl_8$ has essentially no twist distortion (average C_m displacement = 0.023 Å). When the metal atom sits inside the core, a large twist distortion is observed: $ZnTFPPCl_8$ (0.13), $RuTFPPCl_8(CO)H_2O$ (0.20),[24] and $CuTFPPBr_8$ (0.16 Å).[28] Extended to the porphyrin periphery, this results in one halogen atom of each pyrrole being significantly farther out of the mean plane than the other. In $ZnTFPPCl_8$ the displacements differ by 0.31 Å,[10] and in $RuTFPPCl_8(CO)H_2O$ by 0.43 Å.[24] The twist distortion is apparent in the side-on view of $RuTFPPCl_8(CO)H_2O$ (Figure 2.7).

A final measure of distortion is one based on the phenyl dihedral angles; to minimize steric contact with the β-substituents, the phenyl rings rotate towards the mean porphyrin plane (Figure 2.6). The dihedral angles decrease with halogenation from 79° in

H_2TFPP to 73° in $H_2TFPPCl_8$ to 54° in $H_2TFPPBr_8$. Metallation also affects the dihedral angle. In the $TFPPCl_8$ complexes, octahedral $RuTFPPCl_8(CO)$ has a much larger dihedral angle (81°) than the free ligand (73°) or the zinc complex (59°) (Table 2.3).

Remarkably, bond lengths (Table 2.4) in the porphyrin skeleton are essentially preserved throughout the series of metalloderivatives of TPP,[25,34,35] TFPP, and $TFPPX_8$ (X= Cl, Br).[10,36] Bond lengths and angles in the porphyrin skeleton are very similar for all three $TFPPCl_8$ species, indicating that metallation does not greatly affect porphyrin bond lengths.

The Ru-C bond is slightly longer in $RuTFPPCl_8(CO)H_2O$ (Table 2.2) than in $RuOEP(CO)H_2O$ (1.785)[26] or RuTPP(CO)EtOH (1.77 Å),[37] consistent with the relatively high value of ν_{CO}.[22] The Ru-C-O bond is nearly linear in the three porphyrins, at 178.9, 178.5, and 175.8°, respectively. The Ru-O bond length (2.172 Å) is shorter for the perhalogenated porphyrin than for $RuOEP(CO)H_2O$ (2.253 Å), and closer to the distance found for *trans*-$RuCl_2(PEt_3)_2(CO)H_2O$ (2.189 Å).[26,27] Interestingly, although the Ru-N bond lengths in $RuTFPPCl_8(CO)H_2O$ and RuTPP(CO)EtOH are the same (~2.05 Å), the TPP derivative is planar, whereas the metal in the halogenated derivative is 0.11 Å out of the mean plane towards the carbonyl ligand. The distorted structure decreases the core size, and may explain why ruthenium insertion is so difficult for $TFPPCl_8$ and has almost no yield for $TFPPBr_8$.

NMR Spectra

Fluorine-19 NMR has been extremely helpful in ascertaining both the identity and purity of halogenated compounds. The 100% natural abundance of spin 1/2 ^{19}F and its high gyromagnetic ratio allow ^{19}F NMR spectra to be obtained readily.[38] As observed in ^{1}H NMR of tetraphenylporphyrins, the corresponding fluorine atoms from all four phenyl rings appear equivalent in ^{19}F NMR. The four phenyl rings on the porphyrin are related in the high degree of symmetry of the approximate D_{4h} or D_{2d} point groups of these

compounds. The chemical shifts of the fluorine atoms on the meso-phenyl rings are extremely sensitive to the metal center, its axial ligands, and the pyrrole carbon substituents, however, such that each porphyrin has a unique spectrum. Correlations in ^{19}F shifts and splitting patterns may be related to various TFPP structures.

The ^{19}F NMR for the unmetallated and zinc TFPP and $TFPPCl_8$ complexes (Figure 2.8; Table 2.5) display one set of signals each for the ortho, meta, and para fluorines. The para signal, identified by its intensity of 1/2 relative to the ortho and meta signals, is most sensitive to metallation, and shifts 1.7 ppm upfield from $H_2TFPPCl_8$ to $ZnTFPPCl_8$. The signal appears as a triplet due to coupling to the meta-Fs ($^3J_{F\text{-}F}$ = -21 Hz). The ortho signal, farthest downfield, is split into a doublet of doublets, and the meta is a triplet of doublets. The additional splitting is attributed to coupling of fluorines positioned para to one another, as only the para signal does not show any additional structure, with $^5J_{F\text{-}F}$ = 6.7 Hz. Computer simulation of the observed spectrum with only these parameters was not satisfactory. Additional coupling between meta fluorines of $^4J \approx -2$ Hz was needed to increase linewidth and generate the proper intensities in the model spectrum. The signs of the coupling constants are consistent with literature values, as are the magnitudes of the various Js (ortho > para > meta).[39]

Substitution with a paramagnetic or an axially unsymmetric metal center results in significantly different NMR spectra. As with proton NMR, fluorine resonances of the paramagnetic species exhibit a large isotropic shift from those of the diamagnetic derivatives. High spin five-coordinate $Fe^{III}TFPP(Cl)$ (Figure 2.9) or $Fe^{III}TFPP(OH)$ samples, identified by their characteristic UV-Vis and EPR spectra,[40] show *five* separate ^{19}F NMR signals that fall over a much larger window than those of the diamagnetic porphyrins. The ortho and ortho' (and meta and meta') fluorines, no longer related by an S_4 axis, now have chemical shifts separated by several ppm, and previously observed fine structure is lost due to paramagnetic line broadening. The resonances do not coalesce at temperatures up to 298 K, indicating that rotation of the phenyl rings is slow on the NMR

time scale at room temperature. A Curie plot (Figure 2.10) shows a linear relationship between the isotropic shift and inverse temperature. The isotropic shift is the sum of a contact shift (dependent on 1/T) and a dipolar shift (dependent on $1/T^2$)[41]; the linear dependence on 1/T suggests that the dipolar contribution is small. However, the lines do not intersect the origin, which may indicate some dipolar contribution is present.[42]

The axial ligand is known to affect the ^{1}H NMR shifts of paramagnetic Fe^{III} porphyrins. In general terms, the porphyrin and the axial ligand compete for bonding interactions with the metal, and the strength of these interactions affects the ring current and π electron density on the protons and therefore their chemical shift.[43] A substantial downfield shift of all five resonances (Table 5) is observed upon substitution of an $^-$OH for a Cl^- ligand on FeTFPP, consistent with axial ligand effects observed with *p*-CH_3-TPPMnX complexes. Increased π bonding between the metal and the stronger field axial ligand reduces π electron density in the porphyrin, resulting in smaller contact shifts in the ^{1}H NMR spectrum.[44] Although the direction of the shift is similar in the fluorine spectrum, the different magnitudes for the contact shift at the ortho and para positions relative to the meta are not observed. Therefore, contact shift alone is not sufficient to explain the ^{19}F NMR spectrum. This is consistent with theory that expects a large temperature independent paramagnetic contribution to fluorine chemical shifts (relative to proton). Further study involving additional compounds would be needed to fully explore this effect.

The five-coordinate $(FeTFPP)_2O$ dimer also shows 5 peaks in its NMR spectrum (Figure 2.11); however, the signals show significantly less broadening and appear in a much narrower window than the other Fe^{III} porphyrins. Strong antiferromagnetic coupling between the two metal centers[40] reduces the paramagnetic shift in the ^{19}F NMR of the μ-oxo dimer. Similarly, the resonance for the β-hydrogens in the ^{1}H NMR spectrum is shifted less in the dimer relative to the monomeric iron(III) complexes. The pyrrole protons of $(FeTFPP)_2O$ and $(FeTPP)_2O$[42] show similar isotropic shifts of 5.1 and 5.02 ppm,

respectively, from the diamagnetic Zn complexes, whereas the pyrrole protons are shifted over 70 ppm downfield in the spectrum of Fe(TFPP)Cl.

The distinctive patterns observed in ^{19}F NMR play important roles in the structural assignment of other perhalogenated compounds. The ^{19}F NMR spectrum of $Fe^{III}TFPPBr_8(Cl)$ (Figure 2.12) shows a broadened five-signal pattern similar to that of $Fe^{III}TFPP(Cl)$. The ortho fluorine resonances exhibit a smaller paramagnetic shift in the perhalogenated compound, consistent with the mixed spin character of the $Fe^{III}TFPPBr_8(Cl)$ ground state.[20] The addition of pyridine to $Fe^{III}TFPPBr_8(Cl)$ results in reduction of the iron and formation of the symmetric bis-pyridine compound, $Fe^{II}TFPPBr_8(py)_2$. The assignment of this compound was confirmed as low-spin iron(II) due to the sharp signals and splitting pattern consistent with an axially symmetric, diamagnetic species. Most unusual is the NMR of $[Fe^{II}TFPPBr_8(Cl)]^-$, produced by electrochemical reduction of $Fe^{III}TFPPBr_8(Cl)$ (Figure 2.13a). The relatively sharp signals support the reduction of the metal center, but the splitting of the ortho and meta signals suggests an axially unsymmetric porphyrin; the Fe(II) porphyrin appears to retain an association with the chloride ligand even in the reduced state.[19] Chemical reduction in methanol with ascorbic acid, however, gives a very different spectrum. Only three resonances appear instead of five, indicating a symmetric porphyrin, most likely the bis-methanol derivative $[Fe^{II}TFPPBr_8(OMe)_2]$.

NMR also revealed interesting properties of $RuTFPPCl_8(CO)H_2O$.[24] Although an X-ray structure for this compound was obtained, ^{19}F NMR on crystalline material fails to yield a simple spectrum. Instead, several 5-signal patterns are observed, suggesting that the strong trans effect of the carbonyl ligand results in lability of the sixth ligand. The unsymmetric trans coordination around the Ru again leads to dual ortho and meta signals (as in FeTFPP(Cl)), but with the diamagnetic metal center, the fine structure is retained. Upon photolysis in pyridine, a single species, $RuTFPPCl_8(py)_2$, is obtained. The simple pattern now seen in the ^{19}F NMR shows that previous overlapping signals were due to

multiple species with varying ligands trans to the CO rather than to partial decomposition or dehalogenation of the porphyrin macrocycle.

Conclusions

A series of tetrakis(pentafluorophenyl)- and β-octahalo-tetrakis(pentafluorophenyl)-porphyrins have been synthesized. TFPP derivatives have been studied to provide a comparison for understanding the spectroscopy and catalytic properties of the perhalogenated iron and ruthenium complexes (Chapters 3 - 6).

Crystal structures of unmetallated, zinc, and ruthenium octachloro-tetrakis(pentafluorophenyl) porphyrins are consistent with other structures that demonstrate that halogenation of the β-pyrrole carbons causes a severe saddling of the porphyrin macrocycle. The free base porphyrin, however, does not show the twisting distortion seen in the metallated octahalo derivatives, suggesting that the metal plays a significant role in determining the type and degree of distortion.

The distortions and metal effects observed in the structures of the halogenated metalloporphyrins are analogous to those reported for the octamethyl and octaethyl derivatives of TPP; 2,3,7,8,12,13,17,18-β-octaalkyl-5,10,15,20-tetraphenylporphyrin ($TPPX_8$, X = methyl, and ethyl).[32,45] $ZnTPPMe_8$ and $ZnTPPEt_8$ are essentially the steric analogs of $ZnTFPPCl_8$ and $ZnTFPPBr_8$, respectively. The implication is that the observed distortion is a result of the steric interactions involving the β-halo substituents, and is not electronic in origin.

Fluorine-19 NMR has been shown to be a useful tool for characterization of perhalogenated porphyrin compounds. The identification of various FeTFPPX species will allow another mechanism to study catalysis reactions, for example, by monitoring deactivation of the catalyst via formation of a μ-oxo dimer. Trends in linewidths, shift dispersions, and multiplicities all provide information on the oxidation state and coordination sphere of the metal center. As a supplement to crystallographic data, NMR

allows a more direct examination of the behavior of these highly halogenated porphyrins in solution.

Experimental

Materials Omnisolv grade methanol, acetone, dichloromethane, benzene, pyridine, dimethylformamide, and hexane were purchased from EM Science. N-chloro- and N-bromosuccinimide, glacial acetic acid, iron(II) chloride, triruthenium dodecacarbonyl, and tetraphenylporphyrinato ruthenium(II) carbonyl were purchased from Aldrich and used as received. ZnTFPP and H_2TFPP were purchased from Porphyrin Products and used as received. UV-Vis (CH_2Cl_2): ZnTFPP λ_{max} nm (ε 10^5 M^{-1} cm^{-1}); 414 (5.0), 544 (0.24); H_2TFPP λ_{max} nm 412, 506, 584. Fe^{III}TFPPCl was purchased from Aldrich and purified by chromotography on alumina before use. UV-Vis (acetone): λ_{max} nm (ε 10^5 M^{-1} cm^{-1}) 350 (0.7), 410 (1.0), 50 (0.11), 629 (0.06). RuTPP$(py)_2$ was prepared by a literature method.[46]

Methods UV-Vis spectra were recorded on a Hewlett Packard HP8452 diode array interfaced to an IBM or a Cary-14 spectrophotometer with an Olis 3820 conversion system. Infrared spectra were recorded as solutions in carbon tetrachloride or benzene on a Perkin-Elmer Model 1600 FT-IR spectrophotometer. Separation of the ruthenium porphyrins was accomplished with a Beckman Model 126 dual pump and 166 single channel detector on a Vydac C-18 reverse phase column. A 1000 W tungsten lamp was used for photolysis experiments. ^1H and ^{19}F NMR spectra were recorded on a Brüker AM-500 (tuned down to 470.56 MHz for fluorine detection) instrument in $CDCl_3$ or deuterated acetone and referenced internally to C_6H_5F at -113.6 ppm (vs. $CFCl_3$ at 0 ppm). Porphyrin purification was accomplished with alumina (Fluka or Baker 40 μ alumina) or silica (Analtech 150 Å pore, 75-100 particle size silica) column chromatography. Further purification of the zinc and ruthenium perhalogenated porphyrins was accomplished with a Beckman Model HPLC system (126 dual pump and 166 single channel detector) on a

Vydac C-18 reverse phase column with isocratic acetone:water elution. Mass spectroscopy was performed at Caltech with a cesium ion fast atom bombardment spectrometer. Elemental analysis on the perhalogenated compounds was obtained, and varied greatly by compound. Results were not satisfactory, even on crystalline samples that were pure by other criteria.

$Fe^{III}TFPP(OH)$ and $(Fe^{III}TFPP)_2O$: $Fe^{III}TFPP(OH)$ and $(Fe^{III}TFPP)_2O$ were synthesized from the chloride by published methods:[40] $Fe^{III}TFPP(Cl)$ was dissolved in benzene, and a small amount of NaOH solution was added. After stirring for several hours, the water was removed using a separatory funnel, and the benzene solution was chromatographed on neutral alumina with a benzene/acetone solution. The μ-oxo elutes first, and the hydroxide elutes with a higher percent acetone. $Fe^{III}TFPPP(OH)$: UV-Vis (acetone): λ_{max} 406, 563 nm. $(Fe^{III}TFPP)_2O$: UV-Vis; CH_2Cl_2; λ_{max} 398, 415(shoulder), 560 nm.

$H_2TFPPCl_8$: Chlorination of ZnTFPP was accomplished by a modification of earlier methods.[8,47,48] Approximately 500 mg ZnTFPP was dissolved in 50 mL dry methanol with forty equivalents of N-chlorosuccinimide, and the mixture refluxed for an hour. When chlorination of the pyrrole positions was complete, as determined by the red shift of the Soret band in the UV-Vis and thin layer chromatography on silica plates (1:1 hexane: dichloromethane) the solution was allowed to cool. The product was precipitated with water, filtered, and washed with cold hexane to remove decomposed porphyrin by-products. Further purification by HPLC was necessary to separate partially chlorinated species. Yield $ZnTFPPCl_8$ 60 to 80%. UV-Vis (CH_2Cl_2): λ_{max} nm (ε 10^5 M^{-1} cm^{-1}); 364, 440 (1.6), 572 (0.13). Mass spectrum m/z = 1314 (calc. 1313). The chlorinated zinc porphyrin was demetallated as previously by Lyons, et al.:[47] $ZnTFPPCl_8$ was redissolved in approximately 50 mL chloroform, and HCl gas was passed through a gas dispersion tube into the solution for 1-2 minutes. The volume of the reaction mixture was reduced, and the solution was chromatographed on alumina, eluting with 95% chloroform - 5%

methanol. The product, $H_2TFPPCl_8$, was collected and rotary evaporated to dryness, with a yield of approximately 95%. UV-Vis (CH_2Cl_2): λ_{max} nm (ε 10^5 M^{-1} cm^{-1}); 436 (16), 536 (1.3), 622 (0.46).

$H_2TFPPBr_8$: The bromo analog was similarly synthesized via bromination of ZnTFPP with N-bromosuccinimide. $ZnTFPPBr_8$: UV-Vis (CH_2Cl_2): λ_{max} nm (ε 10^5 M^{-1} cm^{-1}); 460 (1.9), 594 (0.17). The free ligand was obtained by demetallation with HCl gas, and the product chromatographed on alumina. UV-Vis (CH_2Cl_2): λ_{max} 454, 552, 636 nm.

$FeTFPPBr_8(Cl)$ and $[FeTFPPCl_8]$: Iron was inserted into H_2TFPPX_8 with freshly prepared iron(II) acetate in glacial acetic acid,[17] or with $Fe^{II}Cl_2$ in DMF.[18] Insertion was evident by the red color of the solution. The iron porphyrin was precipitated with brine, dried, and washed with hexane to remove impurities. UV-Vis (CH_2Cl_2) Br_8: λ_{max} nm(ε 10^5 M^{-1} cm^{-1}) 402 (8.1), 442 (8.5), 560 (1.4). With $H_2TFPPCl_8$, reactions were conducted on a high vacuum line and precipitated with deoxygenated water. UV-Vis (CH_2Cl_2): λ_{max} 404, 582 nm. Addition of pyridine to a solution of $FeTFPPX_8(Cl)$ led to formation of $Fe^{II}TFPPX_8(py)_2$. UV-Vis (CH_2Cl_2) Br_8: λ_{max} 450, 556, 588 nm; Cl: λ_{max} 438, 542, 574 nm.

$RuTFPPCl_8(CO)$: The preparation of $RuTFPPCl_8(CO)$ was based on the methods of Tsutsui[49] and Chow.[50] 300 mg $H_2TFPPCl_8$[10] reacts with 300 mg $Ru_3(CO)_{12}$ (48 h, refluxing benzene) to form $RuTFPPCl_8(CO)$. $RuTFPPCl_7(CO)$ and $RuTFPPCl_6(CO)$ also were isolated from the reaction mixture. $RuTFPPCl_n(CO)$ (n = 6,7,8) complexes were separated from unreacted free ligand by column chromatography on silica gel eluting with hexane and increasing percentages of methylene chloride. The partially chlorinated isomers were purified by HPLC, and the identity of each fraction was confirmed by mass spectroscopy. The parent peak in each mass spectrum appears at the mass for $RuTFPPCl_n$ (n = 6,7,8), with a smaller peak appearing at the mass for the monocarbonyl complex. Parent peaks appeared at m/z = 1351.2 ($RuTFPPCl_8$) , 1315.8

($RuTFPPCl_7$), and 1280.1 ($RuTFPPCl_6$). UV-Vis (CH_2Cl_2): λ_{max} nm (ε 10^5 M^{-1} cm^{-1}) 416 (1.7), 542 (0.14). $RuTFPPBr_8(CO)$ (mass spectrum; m/z =1703) was synthesized from $Ru_3(CO)_{12}$ and $H_2TFPPBr_8$ (50 h refluxing benzene). UV-Vis (CH_2Cl_2): λ_{max} 424, 560 nm.

$RuTFPPCl_8(py)_2$: Photolysis of the carbonyl was accomplished by modification of Chow's methods.[50] Pyridine solutions of $RuTFPPCl_n(CO)$ exposed to a 1000W mercury lamp for several hours lose a carbonyl ligand to form $RuTFPPCl_n(py)_2$. Loss of the carbonyl was confirmed by the disappearance of the CO stretch (IR, CCl_4 solution) and by ^{19}F-NMR spectroscopy ($CDCl_3$ solution): d ($RuTFPPCl_8(py)_2$) = -138.7 (2F, q, ortho); -152.3 (1F, t, para); -163.2 ppm (2F, m, meta). UV-Vis (CH_2Cl_2): λ_{max} 415, 510, 536 nm. ^{19}F-NMR: -138.7 (2F, q, ortho), -152.3 (1F, t, para), -163.2 ppm (2F, m, meta).

Crystal Structure Analysis: Since the halogenated porphyrin crystals lost solvent easily, a single crystal was removed directly from the crystallization solution and mounted in a capillary with silicon grease. Data were collected on an Enraf-Nonius CAD-4 diffractometer using Mo Ka radiation. Atomic scattering factors and values for *f'* were taken from Cromer and Waber[51] and Cromer,[52] and CRYM,[53] MULTAN,[54] and ORTEP[55] computer programs were used for calculations. The weights were taken as $1/\sigma^2(F_o^2)$; variances ($\sigma^2(F_o^2)$) were derived from counting statistics plus an additional term, $(0.014I)^2$; variances of the merged data were obtained by propagation of error plus another additional term, $(0.014\,\bar{I})^2$.

Purple crystals of $ZnTFPPCl_8$ were grown from a saturated solution of *o*-dichlorobenzene at 0 °C. Crystals of this compound lost solvent quickly, so one was covered with epoxy glue before being cooled to -44 °C on the diffractometer. The zinc crystal was found to be tetragonal, belonging to space group $P\bar{4}2_1c$. The structure was solved by location of the zinc atom from a Patterson map. Structure factors and Fourier calculations showed Cl1 and Cl2, and subsequent structure factor Fourier calculations gave the rest of the porphyrin. Solvent molecules were found in difference Fourier maps

calculated in their planes. The solvent molecules occupy two separate regions in the cell, each region holding one dichlorobenzene molecule. The molecules are disordered in these regions, and were initially modeled with idealized $C_6H_4Cl_2$ groups. Eventually, some of the chlorine atoms of the solvent were refined, as well as the population parameters for alternate orientations, but the carbon atoms were always positioned based on Fourier maps. For one region (C31-36 and C41-46) anisotropic displacement parameters were assigned by hand based on the maps and the refined parameters of the Cl atoms of the solvent; the other carbon atoms of the solvent were left isotropic. The disordered solvent regions are the cause, in all probability, of the somewhat larger than usual values for R and goodness of fit.

Brown crystals of $H_2TFPPCl_8$ were grown by slow evaporation from an acetone/water solution. The crystals were found to be triclinic, belonging to space group $P\bar{1}$. Porphyrin molecules were located from a Patterson map, and the two inner hydrogen atoms were located in a difference map as disordered among the four nitrogen atoms. Their positional parameters were refined, with B values fixed at 1.2 times the isotropic equivalent U_{ij} value of the bonded nitrogen atoms and the population factors assigned at one-half.

Deep red crystals of $RuTFPPCl_8(CO)(H_2O)$ were grown by slow evaporation from an ethyl acetate/hexane solution. Ruthenium atom coordinates were obtained from a Patterson map, and the remaining atoms located with structure factor-Fourier calculations. Hydrogen atoms on the solvent molecules were positioned by calculation in idealized locations with staggered geometry and a C-H bond length of 0.95 Å. Of the solvent molecules, only one ethyl acetate site is fully populated (C71,C72, O2, O3, C73, and C74). The second (C81, C82, O4, O5, C83, and C84) is half-populated, near a center of symmetry. The region occupied by hexane is not easily interpreted. There are five peaks in a difference map in an area of broadly diffuse electron density. These five were co-planar within 0.15 Å, so we fitted idealized hexane molecules to the difference density in this plane. Our model has three orientations of the hexane; there may be twice that many. We

kept the positional and thermal parameters of these idealized molecules fixed but refined their population parameters independently. The sum of the three was 0.84; we believe this represents some loss of hexane from the crystal during data collection. We kept the populations fixed in the final refinement. The final difference map has peaks of 0.88, 0.82 and 0.79 $Å^{-3}$ and valleys of -1.24 and -0.84 $Å^{-3}$ in this region.

Appendix 2 contains unit cell diagrams, final heavy atom parameters, anisotropic displacement parameters, complete distances and angles, and structure factors for $H_2TFPPCl_8$, $ZnTFPPCl_8$, and $RuTFPPCl_8(CO)H_2O$, H atom parameters for $H_2TFPPCl_8$, and intermolecular distances less than 3.5 Å for $ZnTFPPCl_8$ and $RuTFPPCl_8(CO)H_2O$.

References and Notes

(1) Lindsey, J. S.; Wagner, R. W. *J. Org. Chem.* **1989**, *54*, 828-836.

(2) Bray, B. L.; Mathies, P. H.; Naef, R.; Solas, D. R.; Tidwell, T. T.; Artis, D. R.; Muchowski, J. M. *J. Org. Chem.* **1990**, *55*, 6317-6328.

(3) Qui, Z.-M.; Burton, D. J. *Tetrahedron Lett.* **1994**, *35*, 4319-4322.

(4) Traylor, T. G.; Tsuchiya, S. *Inorg. Chem.* **1987**, *26*, 1338-1339.

(5) Wijesekera, T.; Matsumoto, A.; Dolphin, D.; Lexa, D. *Angew. Chem., Int. Ed. Eng.* **1990**, *29*, 1028-1030.

(6) Bartoli, J. F.; Brigaud, O.; Battioni, P.; Mansuy, D. *J. Chem. Soc., Chem. Commun.* **1991**, 440-442.

(7) Mandon, D.; Ochsenbein, P.; Fischer, J.; Weiss, R.; Jayaraj, K.; Austin, R. N.; Gold, A.; White, P. S.; Brigaud, O.; Battioni, P.; Mansuy, D. *Inorg. Chem.* **1992**, *31*, 2044-2049.

(8) Hoffmann, P.; Robert, A.; Meunier, B. *Bull. Chem. Soc. Fr.* **1992**, *129*, 85-97.

(9) D'Souza, F.; Villard, A.; Caemelbecke, E. V.; Franzen, M.; Boschi, T.; Tagliatesta, P.; Kadish, K. M. *Inorg. Chem.* **1993**, *32*, 4042-4048.

(10) Birnbaum, E. R.; Hodge, J. A.; Grinstaff, M. G.; Schaefer, W. P.; Marsh, R. E.; Henling, L. M.; Labinger, J. A.; Bercaw, J. E.; Gray, H. B. *Inorg. Chem.* **in press**.

(11) d'A. Rocha Gonsalves, A. M.; Johnstone, R. A. W.; Pereira, M. M.; Shaw, J.; Sobral, D. N.; Abilio, J. F. *Tetrahedron Lett.* **1991**, *32*, 1355-1358.

(12) Banfi, S.; Mandelli, R.; Montanari, F.; Quici, S. *Gazz. Chim. Ital.* **1993**, *123*, 409-415.

(13) Ochsenbein, P.; Ayougou, K.; Mondon, D.; Fischer, J.; Weiss, R.; Austin, R. N.; Jayaraj, K.; Gold, A.; Terner, J.; Fajer, J. *Angew. Chem., Int. Ed. Eng.* **1994**, *33*, 348-350.

(14) Bartoli, J. F.; Battioni, P.; Foor, W. R. D.; Mansuy, D. *J. Chem. Soc., Chem. Commun.* **1994**, 23-24.

(15) *Tables of Interatomic Distances and Configurations in Molecules and Ions*; Sutton, L. E., Ed.; The Chemical Society: London, 1965; Vol. Special Publication 18.

(16) Allred, A. L. *J. Inorg. Nucl. Chem.* **1961**, *17*, 215-221.

(17) Warburg, O.; Negelein, E. *Z. Biochem* **1932**, 14-32.

(18) Adler, A. D.; Longo, F. R.; Kampas, F.; Kim, J. *J. Inorg. Nucl. Chem.* **1970**, *32*, 2443-2445.

(19) Grinstaff, M. W.; Hill, M. G.; Labinger, J. A.; Gray, H. B. *Science* **1994**, *264*, 1311-1313.

(20) Grinstaff, M. W.; Hill, M. G.; Birnbaum, E. R.; Schaefer, W. P.; Labinger, J. A.; Gray, H. B. *Inorg. Chem.* **in press.**

(21) The axial ligand trans to the carbonyl ligand in ruthenium porphyrins is usually assumed to be solvent, and is not specifically mentioned. Unless otherwise indicated, the oxidation state of ruthenium is 2+.

(22) For reference, the CO stretch in the IR spectrum of RuTPP(CO) is at 1945 cm^{-1}: Chow, B. C.; Cohen, I. A. *Bioinorg. Chem.* **1971**, *1*, 57. Since the probable trans ligands (water, ethanol, acetone) are all O-atom donors, we would not expect any splitting of ν_{CO}.

(23) Buchler, J. W.; Kokisch, W.; Smith, P. D. *Struct. Bonding* **1978**, *34*, 79-134.

(24) Birnbaum, E. R.; Schaefer, W. P.; Labinger, J. A.; Bercaw, J. E.; Gray, H. B. *Inorg. Chem.* **1995**, *34*, 1751-1755.

(25) Scheidt, W. R.; Kastner, M. E.; Hatano, K. *Inorg. Chem.* **1978**, *17*, 706-710.

(26) Kadish, K. M.; Hu, Y.; Mu, X. H. *J. Heterocycl. Chem.* **1991**, *28*, 1821-1824.

(27) Sun, Y.; Taylor, N. J.; Carty, A. J. *Inorg. Chem.* **1993**, *32*, 4457-4459.

(28) Henling, L. M.; Schaefer, W. P.; Hodge, J. A.; Hughes, M. E.; Gray, H. B.; Lyons, J. E.; Ellis, P. E., Jr. *Acta Crystallogr.* **1993**, *C49*, 1745-1747.

(29) Schaefer, W. P.; Hodge, J. A.; Hughes, M. E.; Gray, H. B.; Lyons, J. E.; Ellis, P. E., Jr.; Wagner, R. W. *Acta Crystallogr.* **1993**, *C49*, 1342-1345.

(30) Marsh, R. E.; Schaefer, W. P.; Hodge, J. A.; Hughes, M. E.; Gray, H. B.; Lyons, J. E.; Ellis, P. E., Jr. *Acta Crystallogr.* **1993**, *C49*, 1339-1342.

(31) Bhyrappa, P.; Krishnan, V. *Inorg. Chem.* **1991**, *30*, 239-245.

(32) Barkigia, K. M.; Berber, M. D.; Fajer, J.; Medforth, C. J.; Renner, M. W.; Smith, K. M. *J. Am. Chem. Soc.* **1990**, *112*, 8851-8857.

(33) Scheidt, W. R.; Lee, Y. J. In *Metal Complexes with Tetrapyrrole Ligands I*; J. W. Buchler, Ed.; Springer-Verlag: New York, 1987; Vol. 64; pp 2-70.

(34) Hoard, J. L. *Ann. N.Y. Acad. Sci.* **1973**, *206*, 18-31.

(35) Fleischer, E. B.; Miller, C. K.; Webb, L. E. *J. Am. Chem. Soc.* **1964**, *86*, 2342-2347.

(36) Hodge, J. A. Thesis, California Institute of Technology, 1995.

(37) Bonnet, J. J.; Eaton, S. S.; Eaton, G. R.; Holm, R. H.; Ibers, J. A. *J. Am. Chem. Soc.* **1973**, *95*, 2141-2149.

(38) Harris, R. K. *Nuclear Magnetic Resonance Spectroscopy*; Pitman Publishing, Inc.: Marshfield, MA, 1983.

(39) Bovey, F. A.; Jelinski, L. *Nuclear Magnetic Resonance Spectroscopy;* 2nd ed.; Academic Press, Inc: San Diego, CA, 1988, pp 437-488.

(40) Jayaraj, K.; Gold, A.; Toney, G. E.; Helms, J. H.; Hatfield, W. E. *Inorg. Chem.* **1986**, *25*, 3516-3518.

(41) La Mar, G. N.; Eaton, G. R.; Holm, R. H.; Walker, F. A. *J. Am. Chem. Soc.* **1971**, *95*, 63-75.

(42) La Mar, G. N.; Walker, F. A. *J. Am. Chem. Soc.* **1973**, *95*, 1782-1790.

(43) Caughey, W. S.; Johson, L. F. *J. Chem. Soc., Chem. Commun.* **1969**, 1362-1363.

(44) La Mar, G. N.; Walker, F. A. *J. Am. Chem. Soc.* **1975**, *97*, 5013-5106.

(45) Sparks, L. D.; Medforth, C. J.; Park, M.-S.; Chamberlain, J. R.; Ondrias, M. R.; Senge, M. O.; Smith, K. M.; Shelnutt, J. A. *J. Am. Chem. Soc.* **1993**, *115*, 581-592.

(46) Brown, G. M.; Hopf, F. R.; Ferguson, J. A.; Meyer, T. J.; Whitten, D. G. *J. Am. Chem. Soc.* **1973**, *95*, 5939-5942.

(47) Lyons, J. E.; Ellis, P. E., Jr.; Myers, H. K., Jr.; Wagner, R. W. *J. Catal.* **1993**, *141*, 311-315.

(48) Ellis, P. E., Jr.; Lyons, J. E. *Coord. Chem. Rev.* **1990**, *105*, 181-193.

(49) Tsutsui, M.; Ostfeld, D.; Hoffman, L. M. *J. Am. Chem. Soc.* **1971**, *93*, 1820-1823.

(50) Chow, B. C.; Cohen, I. A. *Bioinorg. Chem.* **1971**, *1*, 57-63.

(51) Cromer, D. T.; Waber, J. T. *International Tables For X-ray Crystallography*; Kynoch Press: Birmingham, 1974; Vol. IV, pp 99-101.

(52) Cromer, D. T. *International Tables For X-ray Crystallography*; Kluwer Academic Publishers: Dordrecht, 1974; Vol. IV, pp 149-151.

(53) Duchamp, D. J. In Am. Crystallogr. Assoc. Meet., Paper B14: Bozeman, Montana, 1964; pp 29-30.

(54) Debaerdemaeker, T.; Germain, G.; Main, P.; Refaat, L. S.; Tate, C.; Woolfson, M. M. *MULTAN 88. Computer Programs for the Automatic Solution of Crystal Structures from X-ray Diffraction Data*, University of York, England and Louvain, Belgium, 1988.

(55) Johnson, C. K. *ORTEPII*, Report ORNL-3794: Oak Ridge National Laboratory, Oak Ridge, Tennessee, 1976.

Figure 2.1 -- The general structure of third generation pentafluorophenyl metalloporphyrins discussed in this chapter. The α, β, and meso carbons are marked.

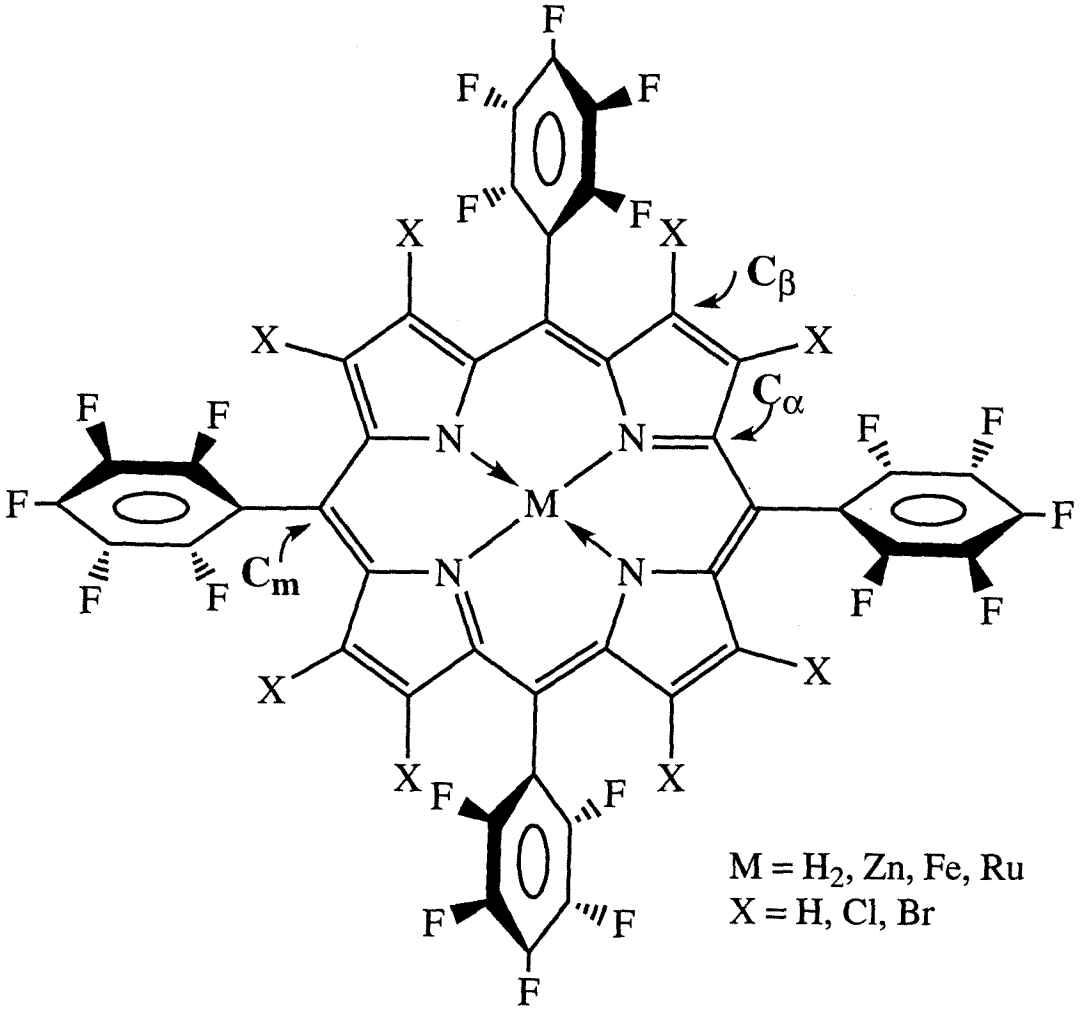
F
F
F
F
F
X
X
X
X
Cβ
Cα
N
N
M
N
N
F
F
F
F
F
F
F
F
F
F
Cm
X
X
X
X
F
F
F
F
F
M = H2, Zn, Fe, Ru
X = H, Cl, Br

Figure 2.2 -- HPLC trace showing separation of partially halogenated ruthenium porphyrins on a reverse phase C_{18} column with isocratic elution of 88% ethanol in water. Excess free ligand comes off the column earliest, followed by ruthenium porphyrins bearing increasing numbers of β-chlorines. Zinc porphyrin is likely produced from metallation of the free ligand in the stainless steel HPLC tubing.

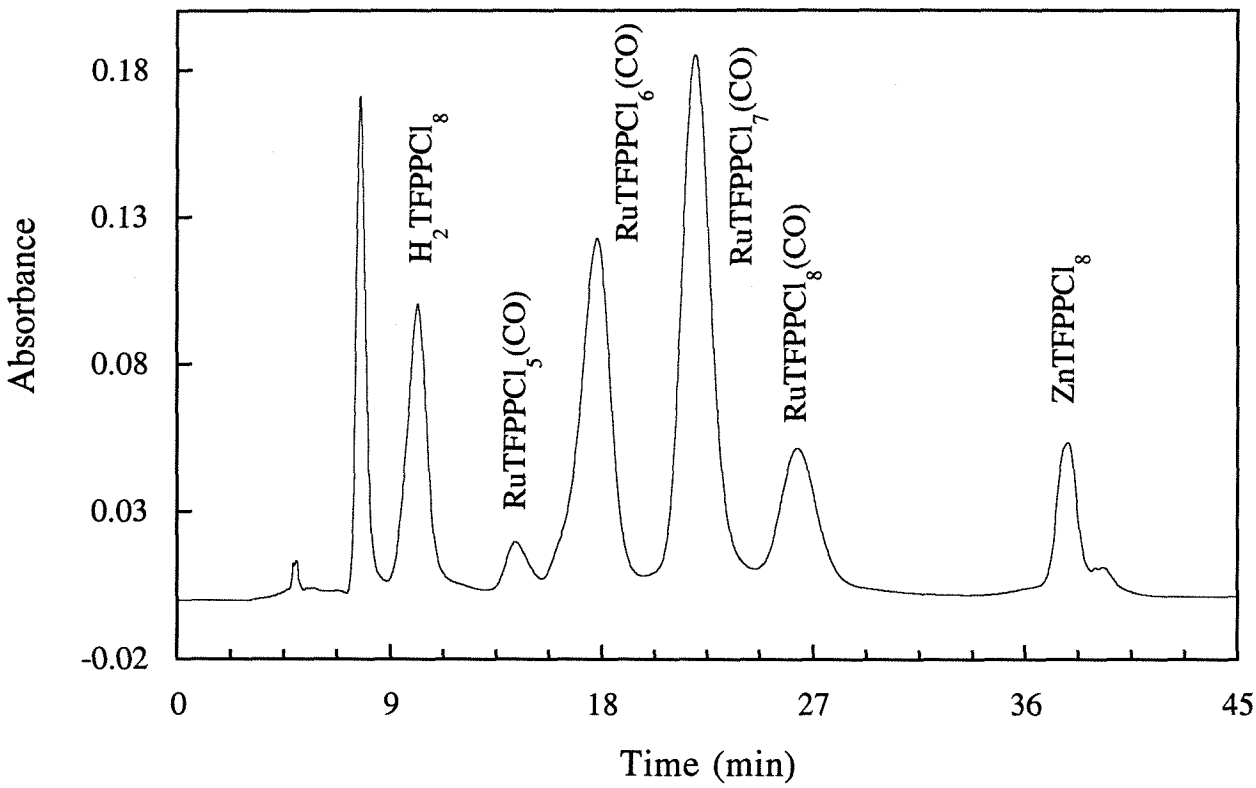
0.18
0.13
0.08
0.03
-0.02
Absorbance
0
9
18
27
36
45
Time (min)
H2TFPPCl8
RuTFPPCl5(CO)
RuTFPPCl6(CO)
RuTFPPCl7(CO)
RuTFPPCl8(CO)
ZnTFPPCl8

Figure 2.3 -- ORTEP diagram of $H_2TFPPCl_8$ with 50% probability ellipsoids of the molecule showing the numbering used. Only two hydrogen atom sites are shown.

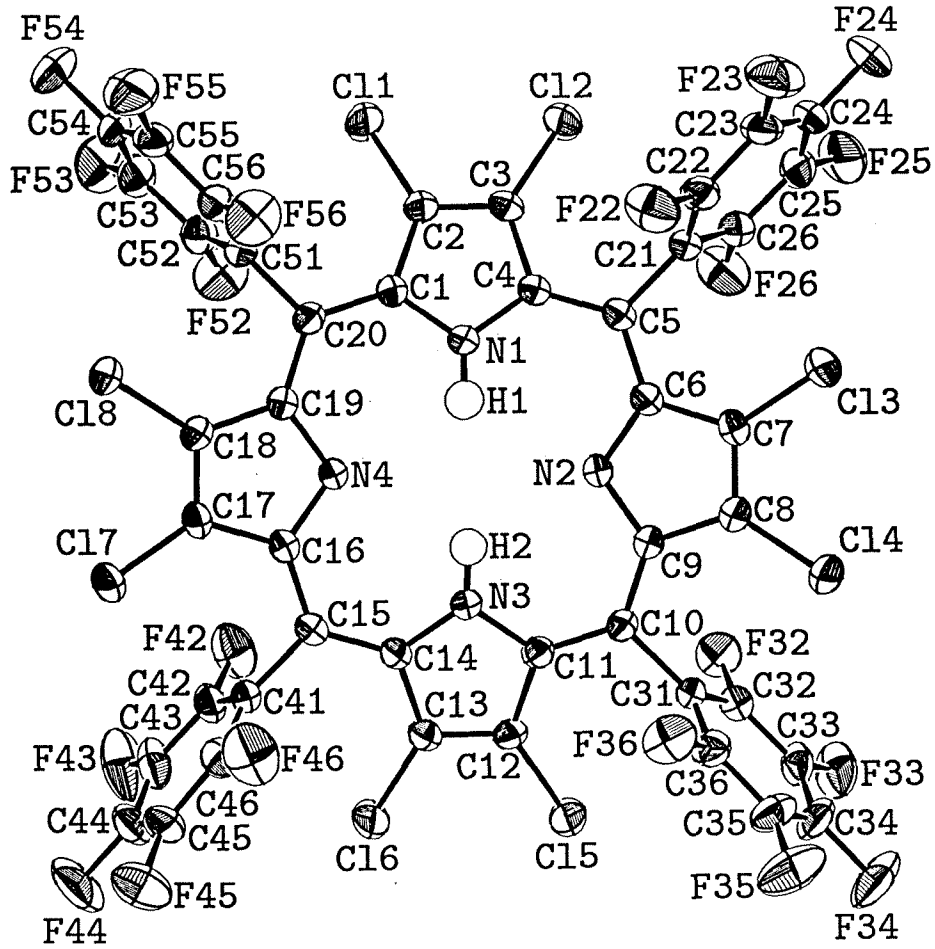
F54
F55
C54
C55
F53
C56
C53
F56
C52
C51
F52
Cl1
Cl2
C3
C2
C1
C4
C20
N1
H1
F24
F23
C23
C24
C22
F25
F22
C25
C21
C26
F26
C5
C6
Cl3
C7
N2
C8
Cl4
C9
Cl8
C19
C18
N4
C17
Cl7
C16
H2
N3
C15
C14
C11
C10
F32
C31
C32
C33
F33
C34
F34
F42
C42
C41
C43
F43
F46
C46
C44
C45
F44
F45
C13
C12
Cl6
Cl5
F36
C36
C35
F35

Figure 2.4 -- ORTEP diagram of $ZnTFPPCl_8$ with 50% probability ellipsoids of the molecule showing the numbering system used.

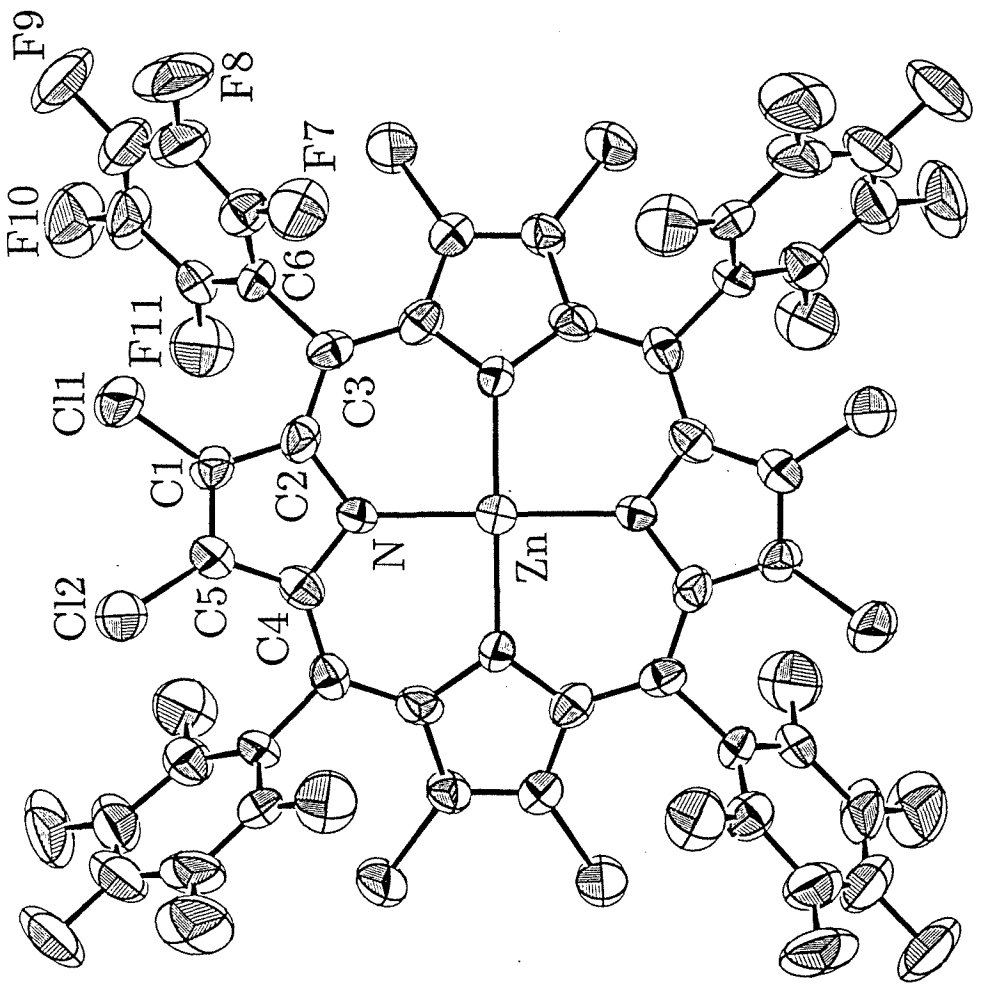
F9
F8
F10
F7
C6
F11
Cl1
C3
C1
C2
N
Zn
Cl2
C5
C4

Figure 2.5 -- ORTEP diagram of $RuTFPPCl_8(CO)H_2O$ with 50% probability ellipsoids showing the numbering system used. Atoms C21, C31, C41, and C51 (not numbered) are bonded to C3, C8, C13, and C18, respectively; carbon atoms in the pentafluorophenyl groups have the same numbers as the attached fluorine atoms.

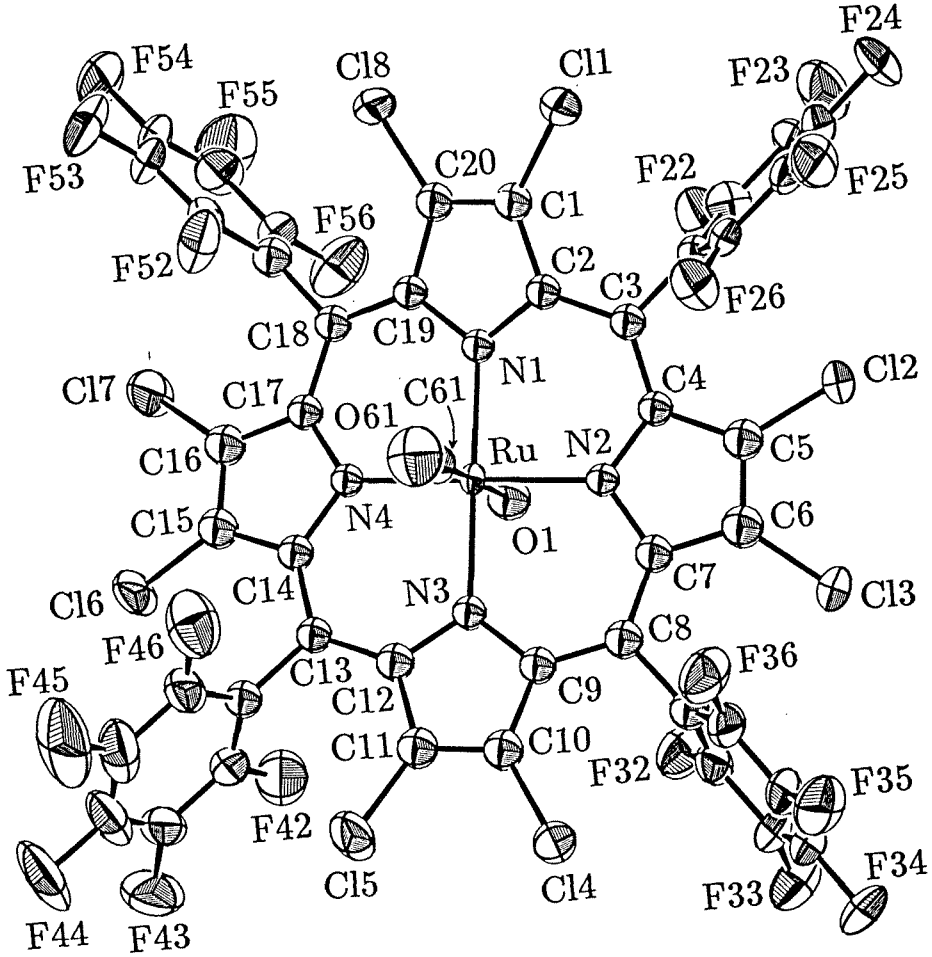
F24
F54
Cl8
Cl1
F23
F55
F53
C20
F22
F25
C1
F56
F52
C2
C3
F26
C18
C19
N1
Cl2
Cl7
C17
C61
C4
O61
Ru
N2
C5
C16
N4
C6
C15
O1
C7
Cl3
Cl6
C14
N3
C8
F46
F36
F45
C13
C12
C9
C11
C10
F32
F35
F42
Cl5
Cl4
F34
F33
F44
F43

Figure 2.6 -- Molecular representations of the series H_2TFPP, $H_2TFPPCl_8$, and $H_2TFPPBr_8$ using the actual crystal structure coordinates. From the planar H_2TFPP, the saddle distortion clearly increases upon further halogenation.

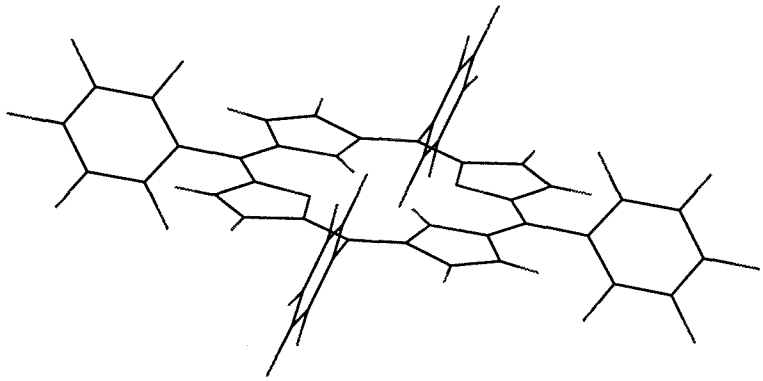

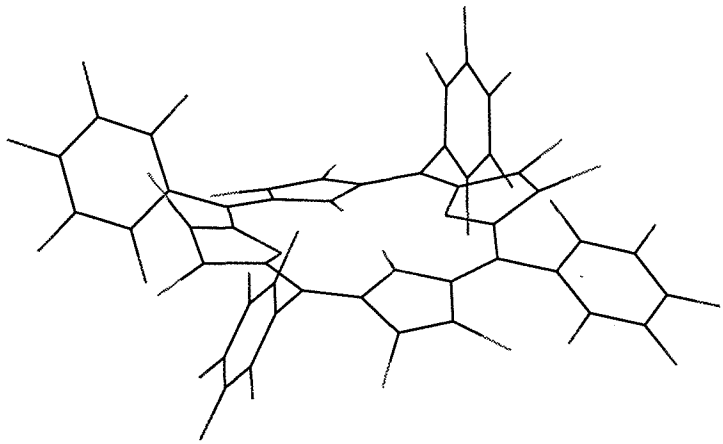

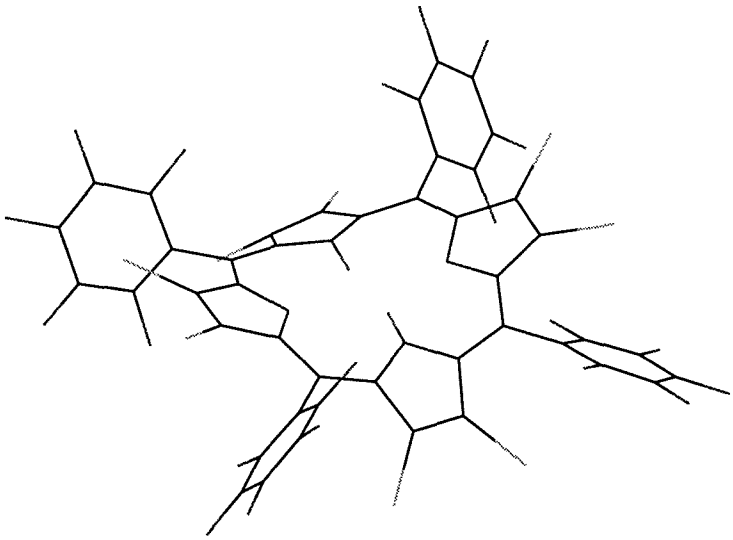

Figure 2.7 -- Edge-on view of a Chem 3D drawing of $RuTFPPCl_8(CO)H_2O$ using crystal structure coordinates. The ruffle in the porphyrin macrocycle is apparent in the different displacements of the chlorine atoms (striped) from the mean porphyrin plane.

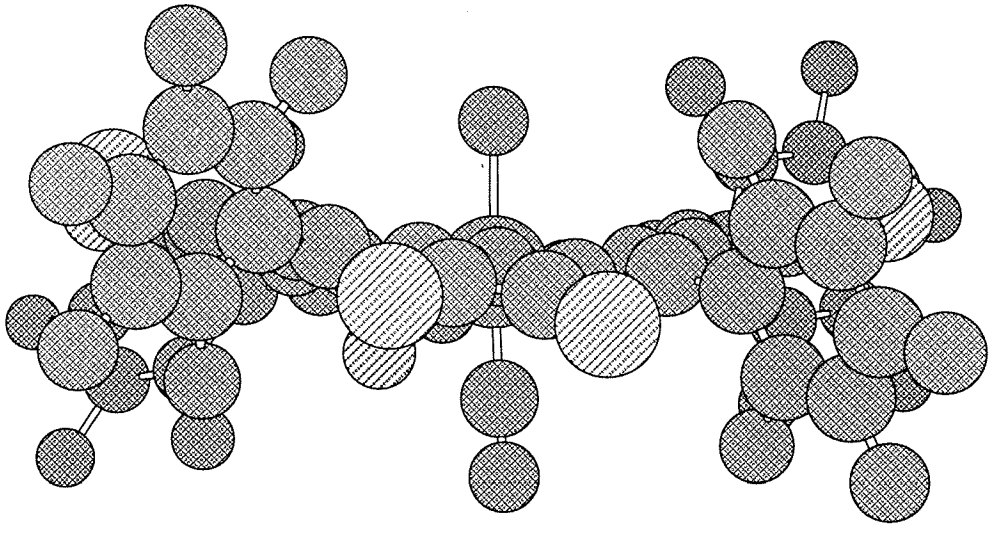

Figure 2.8 -- ^{19}F-NMR spectra of a) $H_2TFPPCl_8$ and b) $ZnTFPPCl_8$ in $CDCl_3$. The signals are assigned ortho, para, meta, from left to right. The signals for the free ligand have been enlarged to show the fine structure observed in the spectra of free ligand, zinc, and other diamagnetic metal porphyrins.

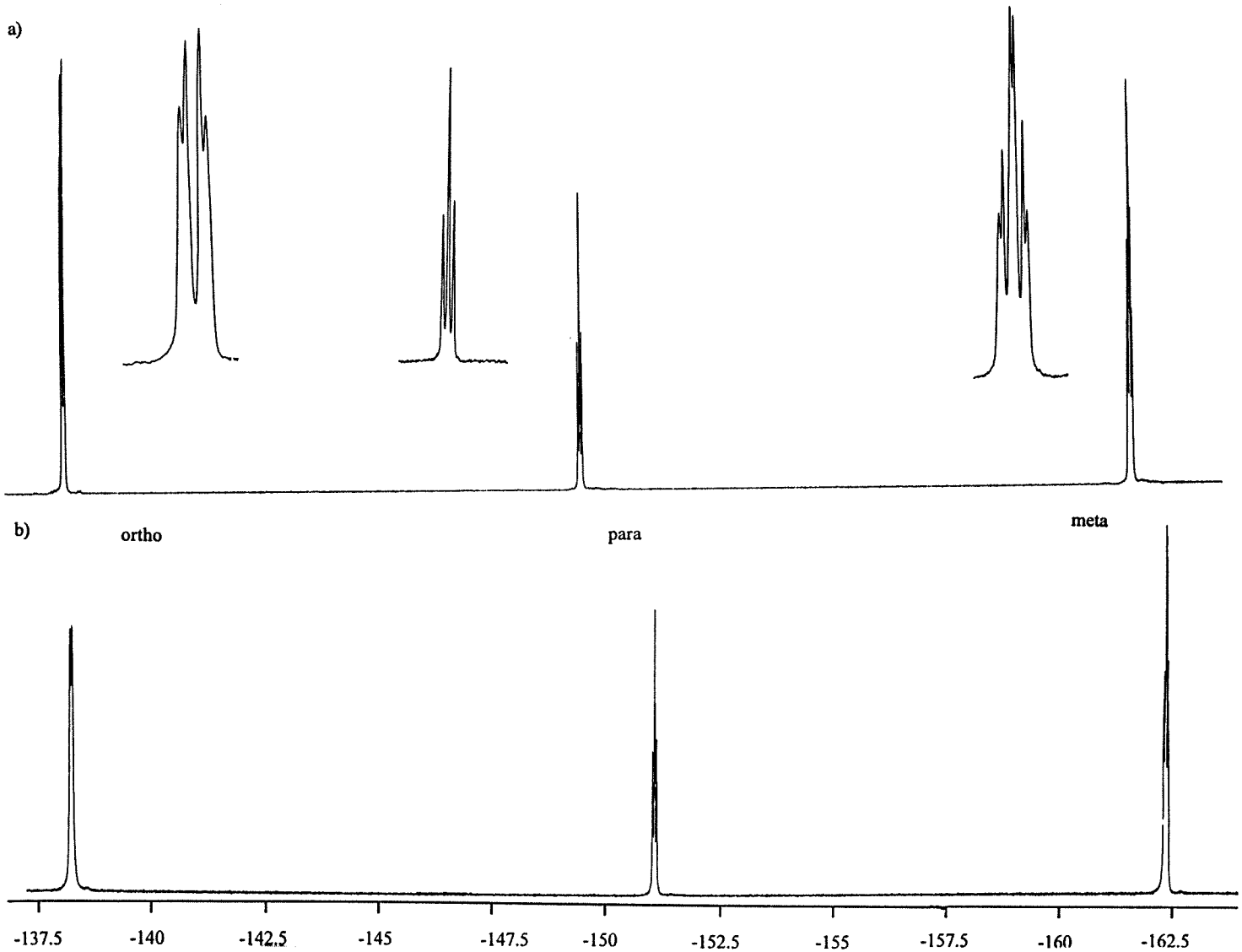
a)
b)
ortho
para
meta
-137.5
-140
-142.5
-145
-147.5
-150
-152.5
-155
-157.5
-160
-162.5

Figure 2.9 -- ^{19}F-NMR spectrum of Fe^{III}TFPP(Cl). The ortho resonances are shifted over 20 ppm downfield from those of H_2TFPP.

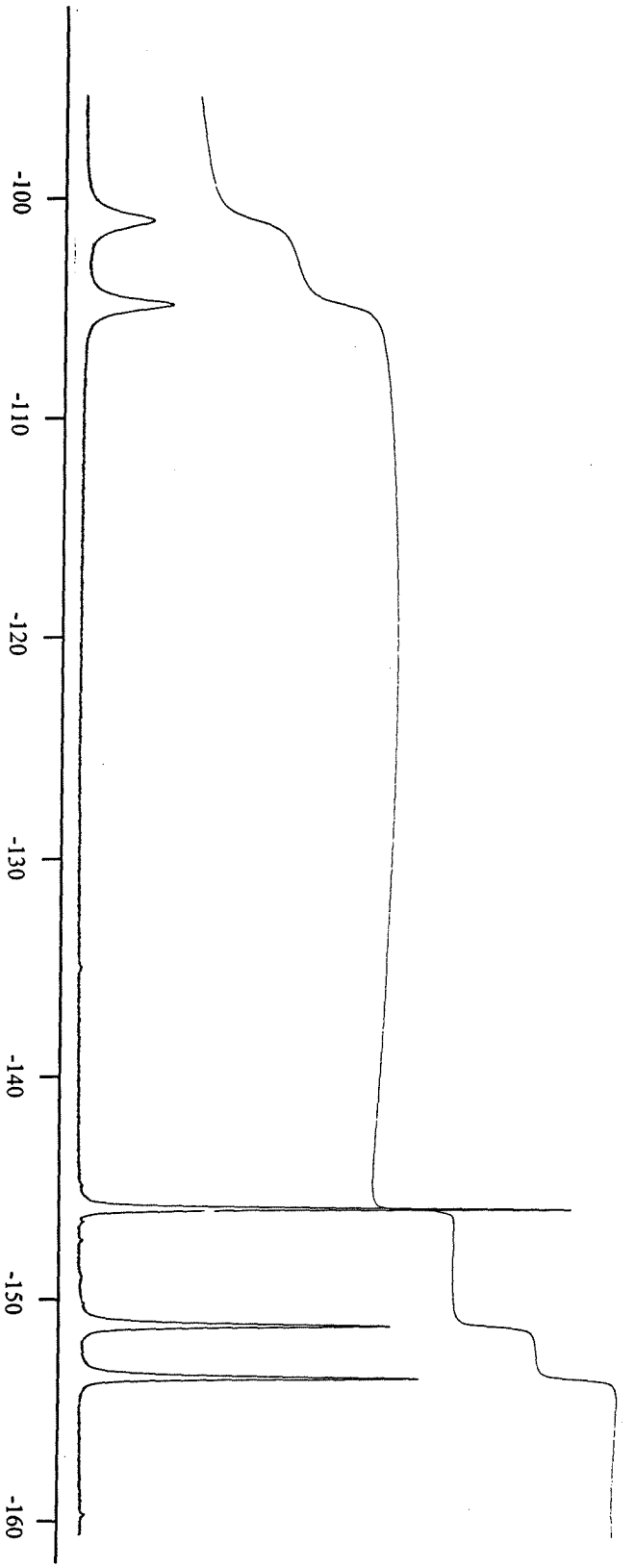
-100
-110
-120
-130
-140
-150
-160

Figure 2.10 -- Curie plot showing the temperature dependence of the chemical shift of $Fe^{III}TFPP(Cl)$ resonances. The isotropic shift is calculated relative to the diamagnetic $Zn^{II}TFPP$ complex.

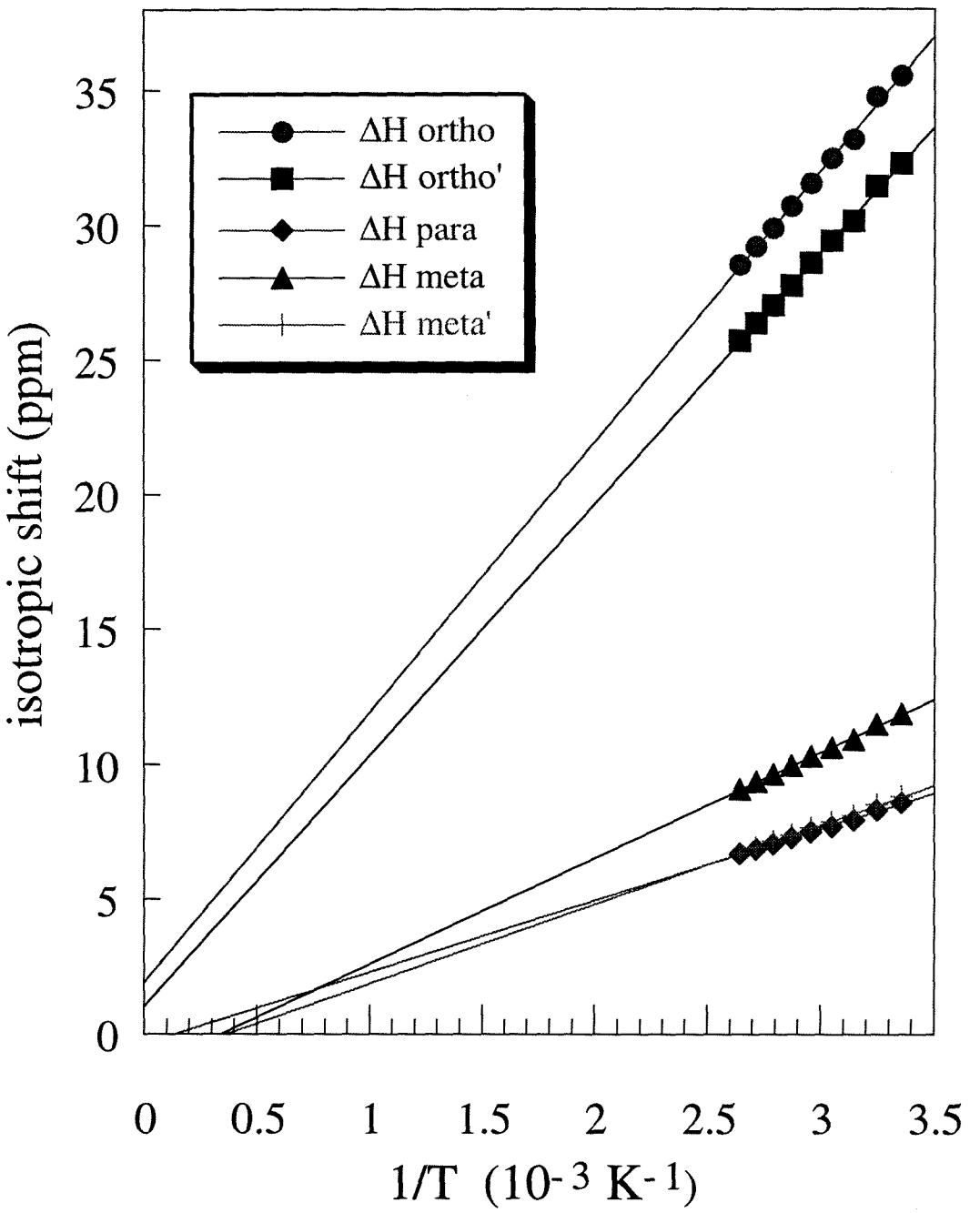
ΔH ortho
ΔH ortho'
ΔH para
ΔH meta
ΔH meta'
isotropic shift (ppm)
0
5
10
15
20
25
30
35
0
0.5
1
1.5
2
2.5
3
3.5
1/T (10-3 K-1)

Figure 2.11 -- ^{19}F-NMR spectrum of $(Fe^{III}TFPP)_2O$ in acetone-d_6. The window is much smaller than that of the paramagnetic FeTFPP(Cl) monomer due to antiferromagnetic coupling between the two iron atoms.

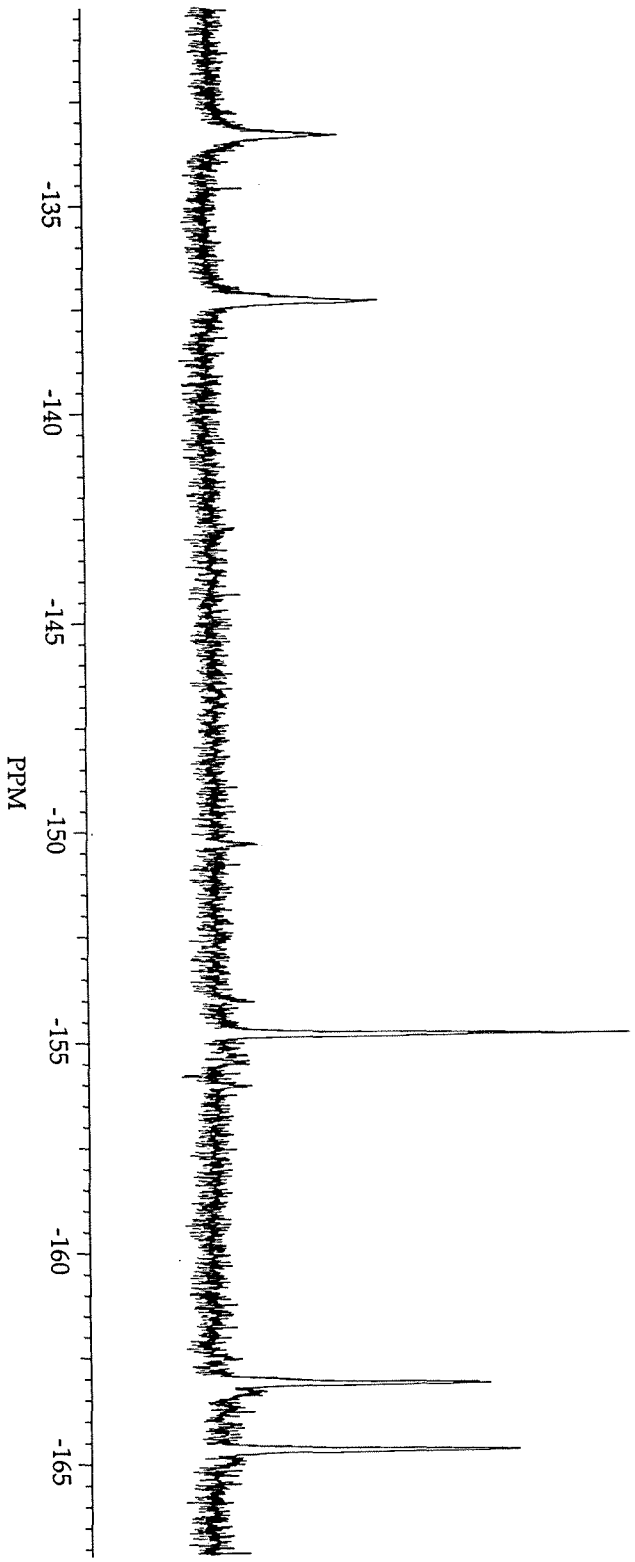
-135
-140
-145
-150
-155
-160
-165
PPM

Figure 2.12 -- ^{19}F-NMR spectrum of $Fe^{III}TFPPBr_8Cl$ in acetone-d_6. The paramagnetic shift is less than in the partially halogenated FeTFPP(Cl).

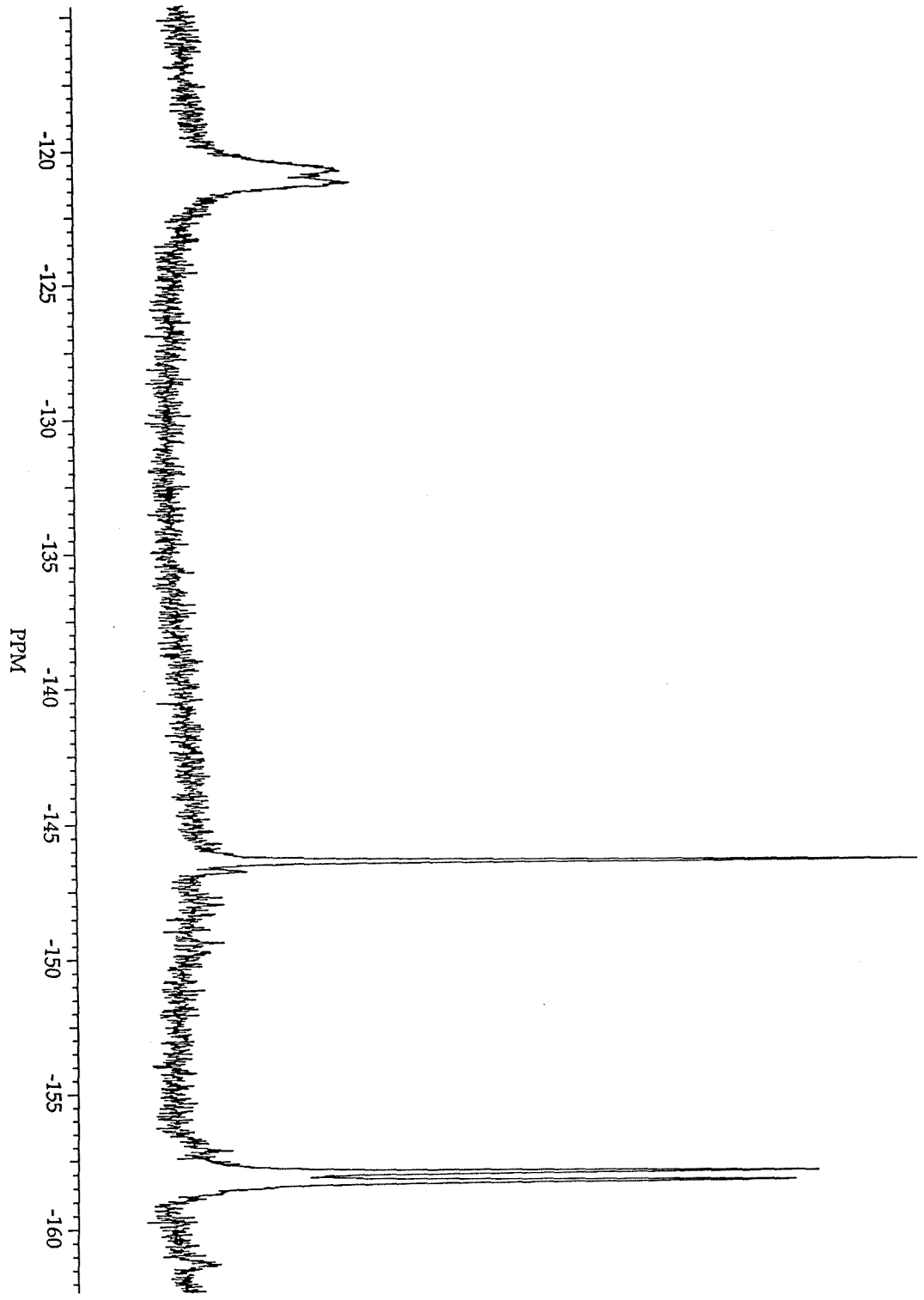
-120
-125
-130
-135
-140
-145
-150
-155
-160
PPM

Figure 2.13 -- ^{19}F-NMR spectra of electrochemically (bottom) and chemically (top) generated [Fe^{II}TFPPBr$_8$]. The five line pattern in the electrochemically generated spectrum indicates an axially unsymmetric species, [Fe^{II}(TFPPBr$_8$)Cl]$^-$, while the lack of splitting in the ortho and meta resonances in the top spectrum is suggestive of a symmetric coordination sphere, i.e. Fe^{II}(TFPPBr$_8$)(OMe)$_2$. The five spikes in the bottom spectrum are instrument noise.

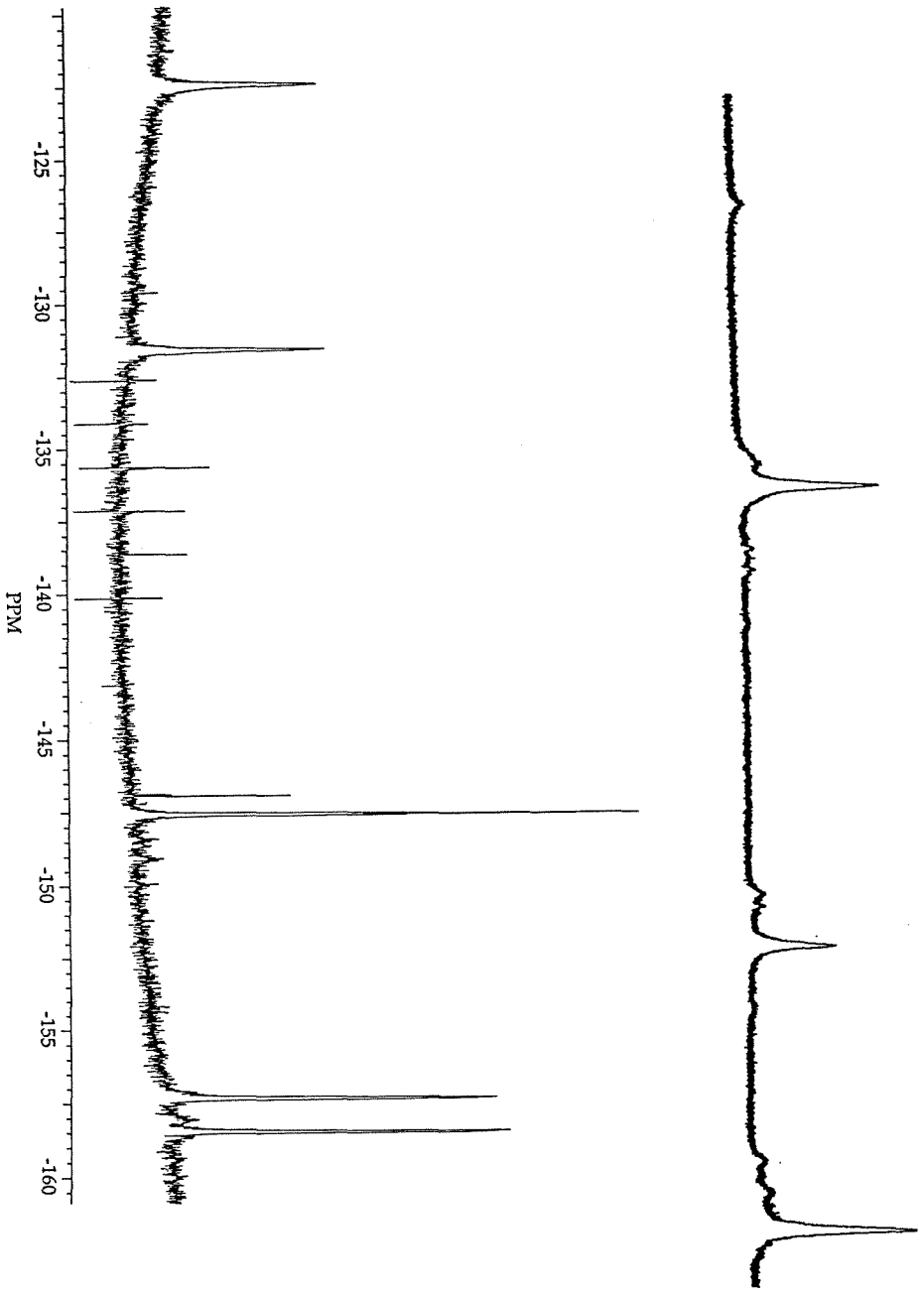
-125
-130
-135
-140
-145
-150
-155
-160
PPM

Table 2.1. X-ray Experimental Parameters.

	$H_2TFPPCl_8$	$ZnTFPPCl_8$	$RuTFPPCl_8(CO)H_2O$
formula	$C_{44}H_2Cl_8F_{20}N_4$	$C_{44}Cl_8F_{20}N_4Zn \cdot 6(C_6H_4Cl_2)$	$C_{57}H_{28}Cl_8F_{20}N_4O_5Ru$
molecular weight	1250.12	2139.48	1613.53
color	brown	dull red	dark red
shape	plate	thick needles	rectangular tablet
crystal system	triclinic	tetragonal	monoclinic
space group	$P\bar{1}$	$P\bar{4}2_1c$	$P2_1/c$
a, Å	11.066(1)	19.502(20)	14.364(3)
b, Å	14.641(3)		16.012(4)
c, Å	14.678(2)	10.916(8)	26.679(8)
a, °	88.97(1)		
β, °	76.05(1)		90.29(2)
γ, °	71.29(1)		
V, Å^3	2181.4(6)	4152(6)	6136(3)
Z	2	2	4
D_x, g cm^{-3}	1.90	1.71	1.75
radiation	MoKα		
μ, cm^{-1}	6.4	10.41	7.11
temperature, K	293	229	295
crystal size, mm	0.11 X 0.35 X 0.42	0.19 X 0.19 X 0.59	0.16 x 0.29 x 0.44
diffractometer	Enraf-Nonius Cad-4		
collection method	omega scans		
$h_{min/max}$	± 12	0/23	-15/+15
$k_{min/max}$	± 16	0/23	-17/+17
$l_{min/max}$	± 16	± 13	0/28
reflections measured	12455	8027	16,813
indep. reflections	6054	2050	8006
reflections used	6054	2050	8005
$R_{int}(F)$	0.019	0.033	0.043
R(F)	0.042	0.0949	0.089
$R_w(F^2)$	0.0061	0.0286	0.028
$(\Delta/\sigma)_{max}$	0.01	0.07	0.00 (for porphyrin)
goodness of fit	2.05	3.29	2.14

Table 2.2. Selected Average Bond Lengths (Å).

Bond	$H_2TFPPCl_8$	$ZnTFPPCl_8$	$RuTFPPCl_8(CO)H_2O$
N - C_α	1.372	1.380	1.378
C_α - C_β	1.448	1.427	1.448
C_β - C_β	1.347	1.337	1.339
C_α - C_m	1.402	1.403	1.399
N - M (or H)	0.94	2.032	2.059
N - Ct	2.075	2.029	not determined
Ru - C	—	—	1.828
Ru - O	—	—	2.172

Table 2.3. Selected Average Angles (°).

Angle	$H_2TFPPCl_8$	$ZnTFPPCl_8$	$RuTFPPCl_8(CO)H_2O$
N - M - N	—	90.2	175.5
C_α - N - C_α	109.5	106.9	177.6
N - C_α - C_m	125.4	124.2	125.1
N - C_α - C_β	107.2	107.4	107.8
C_α - C_β - C_β	107.9	108.8	108.0
C_α - C_m - C_α	125.8	126.5	126.0
C_m - C_α - C_β	127.2	128.4	127.0
Dihedral (C_6F_5 groups)	72.6	59.1	80.7
C - Ru - O	—	—	177.6

Table 2.4. Average Deviations of Atoms from the Least-Squares Plane (Å).

Atom	$H_2TFPPCl_8$	$ZnTFPPCl_8$	$RuTFPPCl_8(CO)H_2O$
N	0.088	0.10	0.06
C_m	0.023	0.13	0.20
C_β	0.625	0.79, 0.68	0.48
Cl_{odd}	1.06	1.17	1.11
Cl_{even}	1.06	1.48	0.68
M	—	0.0	0.11 (towards CO)

Table 2.5: NMR Shifts for Halogenated Porphyrins.

Compound	NMR values in acetone-d_6[a]				
	^{19}F			^{1}H	β-H
	ortho	para	meta	N-H	
					9.17
ZnTFPP	-138.5 (d)	-154.8 (t)	-163.7 (m)	—	9.40
H_2TFPP	-136.9 (d)	-151.7 (t)	-161.8 (m)	-2.91	83
FeTFPP(Cl)	-105.8, -107.7	-150.2	-153.9, -156.0	—	83
FeTFPP(OH)	-108.0, -114.5	-152.0	-156.6, -158.0	—	14.3
(FeTFPP)$_2$O	-133.3, -137.1	-154.8	-163.1, -164.7	—	
					—
ZnTFPPCl$_8$	-138.9 (d)	-151.5 (t)	-163.4 (m)	—	—
H_2TFPPCl$_8$	-140.0 (d)	-149.8 (t)	-162.4 (m)	-1.0[b]	—
RuTFPPCl$_8$(CO)[c]	-138.8, -139.3	-151.3 (t)	-163.2, -163.6	—	—
RuTFPPCl$_8$(py)$_2$	-136.9 (d)	-149.7 (t)	-161.1 (m)	—	
					—
ZnTFPPBr$_8$	-138.4 (d)	-151.7 (t)	-163.4 (m)	—	—
H_2TFPPBr$_8$	-139.7 (d)	-150.1 (t)	-162.7 (m)	-0.5[b]	—
FeTFPPBr$_8$(Cl)	-121.4, -122.3	-146.5	-158.1, -158.5	—	—
[FeTFPPBr$_8$(Cl)]$^-$ [d]	-124, -133	-148	-158, -160	—	—
[FeTFPPBr$_8$][e]	-136	-152	-163	—	—
FeTFPPBr$_8$(py)$_2$[f]	-138.6	-152.0	-163.1	—	

a. ^{19}F-NMR values are versus $CFCl_3$ at 0 ppm. ^{1}H-NMR values are versus TMS at 0 ppm. Fine structure given as follows: (d) doublet of doublets, (t) triplet, (m) multiplet.
b. Very broad; the inner nitrogen protons are much more distinct in chlorocarbon solvents such as $CDCl_3$.
c. Major set of resonances, each with fine structure as observed in diamagnetic species; other resonances are also observed, as discussed in text.
d. Produced by bulk electrolysis.
e. Produced by reduction with ascorbic acid in methanol. Presumably the bis-methanol complex (see text).
f. Values in $CDCl_3$.

Spectroscopy and Electronic Structures of Halogenated Porphyrins

Introduction

Metalloporphyrins have distinctive UV-visible spectroscopy due to the aromatic porphyrin chromophore. Two strong $\pi \rightarrow \pi^*$ absorptions in the near UV (log $\varepsilon \approx 5$ M^{-1} cm^{-1}) and visible regions (log $\varepsilon \approx 4$ M^{-1} cm^{-1}) dominate the spectrum. The higher energy transition is known as the Soret (or B) band, and the less intense, lower energy transition as the Q band. Other higher energy bands of moderate intensity often appear, designated N, L, and M with increasing energy. A typical porphyrin spectrum is pictured in Figure 3.1, with the various transitions labeled with standard porphyrin nomenclature.[1]

A satisfactory theoretical basis for these bands was developed by extension of work on polyarenes,[2,3] which developed a new method for calculating frontier molecular orbital energies for extended π systems. LCAO calculations were based on a postulate assuming free electron movement along the perimeter of the π system. Essentially, this allowed the porphyrin macrocycle to be treated as an 18-electron polyarene; after several iterations, the now-standard Gouterman four orbital model for porphyrin spectroscopy evolved from these calculations.[4,5] The frontier orbital picture is as follows (Figure 3.2); in D_{4h} symmetry, the two lowest occupied molecular orbitals consist of a nearly degenerate a_{1u} and a_{2u} pair, and the highest unoccupied molecular orbitals are a degenerate e_g set, both of π symmetry. Generally, the a_{1u} orbital is found at slightly lower energy than the a_{2u}, resulting in the two observed electronic transitions. Strong configurational interactions between the lowest energy states give rise to the different intensities in the Soret and Q bands.[5]

combination with NMR data, UV-visible spectroscopy is a valuable tool for porphyrin characterization, and in some situations, is the sole method of characterization for some intermediates in metalloporphyrin oxidation reactions.

The substituents on the porphyrin periphery are found to effect the relative energies of the porphyrin frontier molecular orbitals. Substitution at the β-positions of the porphyrin ring with electron withdrawing groups such as halogens or cyano groups has been found to substantially red-shift the Soret band.[6-8] A combination of theoretical and experimental work has separated the effects of halogenation into electronic[9-13] and steric[14-17] factors. Electrochemical data and semi-empirical calculations have both suggested that electron withdrawing substituents on the porphyrin periphery stabilize both the HOMO and the LUMO. This effect is offset by the distortion of the porphyrin macrocycle, which results in a large destabilization of the HOMO, and a smaller destabilization of the LUMO (Figure 3.2). The different magnitude of these shifts results in a red shifted electronic transition.[14,15,18,19] Characterization of non-planar β-alkyl porphyrins supports this separation of electronic and steric effects.[15] Similar to β-halo-porphyrins, these complexes have red-shifted Soret bands from the distortion-induced destabilization of frontier orbitals; however, the reduction potentials for these compounds are substantially more negative than in halogenated derivatives.

Results and Discussion

The electronic spectroscopy of the perhalogenated porphyrins described in Chapter 2 is consistent with this electronic model. The UV-Vis spectra for the zinc(II) tetraphenylporphyrin series are in Figure 3.3. Fluorination of the phenyl moiety has little effect on the Soret or Q band positions, consistent with the planar structures for both these compounds.[20,21] In fact, rather than the red shift observed with pyrrole halogenation, a slight blue shift in the Soret band is observed for both the zinc and free base porphyrins. The direction of the change may be explained by the effect of meso substitution on the

relative energy of the porphyrin HOMOs. The a_{2u} orbital, which has greater electron density at meso position,[5] is stabilized by the pentafluorophenyl groups such that it falls at lower energy than the a_{1u} orbital.[22] The a_{1u} orbital, with no density at the meso position, remains relatively unchanged in energy, resulting in a larger HOMO-LUMO gap for the TFPP compounds. Electrochemical experiments also show that the HOMO shifts more than the LUMO, as ZnTFPP is 0.57 V more difficult to oxidize, but only 0.38 V harder to reduce than ZnTPP.

The effect of pyrrole substitution is more substantial. Chlorination induces a 1405 cm^{-1} red shift in the Soret energy of $ZnTFPPCl_8$ relative to ZnTFPP; as expected, the larger bromine atom induces a greater shift (2405 cm^{-1}) in $ZnTFPPBr_8$. The magnitude of the shift is consistent with other halogenated porphyrins, i.e., H_2TMP exhibits a 2210 cm^{-1} red shift upon bromination.[23] The decrease in Soret intensity is offset by increasing strength of the Q bands (Table 3.1), consistent with a decrease in the configurational interaction upon β-halogenation.[18] However, the oscillator strength throughout the zinc porphyrin series remains fairly constant: 2.58, 3.40, 2.5, and 2.8 M^{-1} cm^{-2} (from ZnTPP to $ZnTFPPBr_8$).[24]

The anodic shift in the reduction potentials of $ZnTFPPX_8$[25] and H_2TFPPX_8 relative to the TFPP complexes (Table 3.2) also indicate that electron-withdrawing groups at the β positions stabilize both the highest occupied and lowest unoccupied molecular orbitals of tetraphenylporphyrins. Furthermore, the reduction potentials reflect the contraction of the HOMO-LUMO gap observed in the spectroscopy. Relative to H_2TFPP, $H_2TFPPCl_8$ is 0.46 V easier to reduce, but only 0.13 V harder to oxidize.

Addition of a redox active metal does not alter the observed trends. The Soret transition red shifts 1808 cm^{-1} from $Fe^{III}(TFPP)Cl$ to $Fe^{III}(TFPPBr_8)Cl$ (Figure 3.4), and the Soret bands of the bis-pyridine derivatives, $Fe^{II}(TFPPBr_8)py_2$ and $Fe^{II}(TFPPCl_8)py_2$, are also found at lower energy than those of $Fe^{II}(TFPP)py_2$ (Table 3.3). Although $Fe^{III}(TFPPBr_8)Cl$ may appear to have a split Soret at 404 and 440 nm, the higher energy

absorbance may be a chloride to iron charge transfer, as is the 351 nm band in the spectrum of Fe^{III}(TFPP)Cl. As the LMCT falls at closer energy to the Soret, it steals intensity from it, resulting in the unusually large extinction coefficient for this absorption. The reduction potential of the metal ($Fe^{III/II}$) follows the same trend as the ligand upon halogenation, increasing from -0.29, to -0.08, to 0.31 V vs. AgCl/Ag along the series Fe(TPP)Cl, Fe(TFPP)Cl, and Fe(TFPPBr$_8$)Cl.[26]

Electrochemical reduction of Fe(TFPPBr$_8$)Cl is found to red shift the Soret from 440 nm to 478 nm, similar to the 25 nm shift observed in the reduction of Fe(TPP)Cl. Chemical reduction with ascorbic acid in methanol results in a similar but less shifted spectrum (Figure 3.5). NMR (Chapter 2) of both species suggests that the first is a five-coordinate anion, [Fe^{II}(TFPPBr$_8$)Cl]$^-$, and the second a low spin six-coordinate species, likely Fe^{II}(TFPPBr$_8$)(OMe)$_2$. The spectrum obtained during the attempted synthesis of Fe(TFPPCl$_8$) was also at very low energy, 440 nm, suggesting that an Fe^{II} species was transiently formed. Addition of pyridine resulted in an optical spectrum very similar to that of Fe(TFPPBr$_8$)py$_2$, but no single species was isolated.

Following the same trends, the RuTFPPX$_8$(CO) complexes are harder to oxidize and easier to reduce than RuTPP(CO).[27] Notably, the RuTFPPX$_8$(CO)$^{+/0}$ potentials are within 0.07 V of those of the unmetallated H_2TFPPX$_8$ molecules, indicating that the first electron is removed from a ligand-based orbital. Oxidation of RuTFPPCl$_8$(py)$_2$ occurs 0.63 V lower than RuTFPPCl$_8$(CO), suggesting that the HOMO is a dπ level in the pyridine derivative. The magnitude of this shift is similar to the 0.64 V shift between the metal-centered oxidation of RuTPP(py)$_2$[28] and the ligand-centered oxidation of RuTPP(CO).[29]

This sterically induced contraction of the HOMO-LUMO gap is surprisingly small for RuTFPPCl$_8$(CO) (0.11 V relative to RuTPP(CO))[27] as extracted from the values of the +/0 and 0/- potentials). Enhanced backbonding from Ru^{II} to TFPPCl$_8$ is the likely explanation of this finding, as discussed below.

The electronic properties of perhalogenated Ru^{II} porphyrins can be interpreted in terms of a Gouterman four-orbital model[4,9] modified by the inclusion of the Ru $d\pi$ orbitals (Figure 3.6).[30] Increased backbonding in the $TFPPX_8$ complexes promotes mixing of $\pi \rightarrow e\pi^*$ and $Ru^{II} \rightarrow e\pi^*$ excited states, with the result that the Soret (mainly $\pi \rightarrow e\pi^*$) transition falls at higher energies than would be predicted by a simple one-electron (HOMO-LUMO) model.[1,31,32] The Soret band of $RuTFPPCl_8(CO)$ (418 nm) is substantially blue-shifted from that of $H_2TFPPCl_8$ (440 nm). A blue shift upon metalation with a 2nd or 3rd row metal is often observed; i.e., the Soret band of $PdTFPPCl_8$ is 705 cm^{-1} shifted from the free ligand. The magnitude of the shift in $RuTFPPCl_8(CO)$, ~ 1300 cm^{-1}, is surprisingly high, indicating that the electronic coupling of Ru^{II} to the porphyrin is unusually strong. The offsetting effect of extensive backbonding in the distorted porphyrins is the reason that the Soret bands for both $RuTFPPCl_8(CO)$ and $RuTFPPCl_8(py)_2$ (414 nm) are only slightly red-shifted from those of RuTPP(CO) (412 nm) and $RuTPP(py)_2$ (413 nm) (Figure 3.7 and 3.8).

IR data also indicate that halogenated porphyrins are π acceptors. The peak attributable to the CO stretch appears at much higher energy in the halogenated porphyrins relative to the 1945 cm^{-1} band observed for RuTPP(CO).[33] The transition energy decreases according to $RuTFPPCl_8(CO)$ (1990) > $RuTFPPCl_7(CO)$ (1987) > $RuTFPPCl_6(CO)$ (1984) > $RuTFPPBr_8(CO)$ (1973 cm^{-1}), further reflecting the increased competition between the porphyrin and the carbonyl ligand for π electron density upon halogenation.

The distortion-induced contraction of the HOMO-LUMO gap[9,10,12,14,17,18] is evidenced by a decrease of the Soret transition energy according to $RuTFPPCl_6(CO)$ (410) > $RuTFPPCl_7(CO)$ (413.5) > $RuTFPPCl_8(CO)$ (418 nm) (Figure 3.9). The Soret band of $RuTFPPBr_8(CO)$ is further red-shifted to 424 nm; as predicted,[9] the larger halogen atoms generate a greater distortion of the porphyrin, thereby producing a smaller HOMO-LUMO

gap. Porphyrin saddling also is responsible for the red shifts of the Q(0,1) bands of $RuTFPPX_8$ complexes from those of the corresponding TPP derivatives (Figure 3.7 and 3.8).

Relatively weak bands at 670 ($\varepsilon \approx 800$) and 792 nm ($\varepsilon \approx 300\ M^{-1}cm^{-1}$) are observed in the spectrum of $RuTFPPCl_8(py)_2$ (Figure 3.10). Low-lying $Ru^{II} \rightarrow e\pi^*$ ($TFPPCl_8$) transitions are expected, since the electrochemical data show that both Ru^{II} oxidation and $TFPPCl_8$ reduction are accessible. Extensive backbonding to $e\pi^*$ ($TFPPCl_8$) orbitals would stabilize d_{xz}, d_{yz} relative to d_{xy} (Figure 3.6); it is likely, then, that a d_{xy} electron is involved in both electrochemical and the 792-nm spectroscopic oxidation of Ru^{II} to Ru^{III}. No bands above 650 nm were observed in the spectrum of $RuTFPPCl_8(CO)$, consistent with the absence of any Ru^{II} oxidations in the electrochemical experiments. The $d\pi$ orbitals for $RuTFPPCl_8(CO)$ are anticipated to fall at a similar energy as the porphyrin b_2 π orbital. Any charge transfer band in this region would be obscured by the intense porphyrin $\pi \rightarrow \pi^*$ transition. However, a b_2 $d\pi \rightarrow e\pi^*$ transition may be contributing to the slight tailing on the low energy side of the Soret band of $RuTFPPCl_8(CO)$.

Spectroelectrochemistry was performed to confirm the assignment of the LUMO as metal or ligand based in the ruthenium porphyrins. Reduction of RuOEP(CO)[34] and RuTPP(CO)[35] has demonstrated distinct differences in the UV-Vis depending on the site of reduction. Formation of a radical porphyrin anion is accompanied by a broadening of the Soret, with a concomitant decrease in intensity. The Q bands disappear, and a new band around 600 - 700 nm grows into the spectrum. RuOEP(CO)(THF)[34] and RuTPP(CO)[35] in THF both show these type of spectral features upon reduction. Reduction of $RuTFPPCl_8(py)_2$ (Figure 3.11) is accompanied by a decrease in the Soret intensity, with a red shift to 420 nm, as well as a decrease in the Q band intensity. A new band appears at 580 nm, consistent with formation of a porphyrin based radical anion. Spectroelectrochemistry in a different solvent has been shown to have completely different

characteristics, indicating that the axial ligand can alter the site of reduction. Upon reduction in benzonitrile, the Soret band of RuOEP(CO) is still sharp, and shows a slight red shift. No new features are observed in the lower wavelength regions.[34] Reduction of $RuTFPPCl_8(CO)$ is shown in Figure 3.12. The Soret band decreases in intensity, and shows a similar red shift as in $RuTFPPCl_8(py)_2$, but the broadening generally associated with radical anion formation is not observed. In addition, there is no major change in the Q-band region. Isosbestic points at 270, 376, 420, and 440 nm indicate that clean reduction is occurring, but the decrease in Soret intensity suggests that this reduction may have both metal and ligand character.

Conclusion

The distortion of the porphyrin macrocycle, as observed in the crystal structures of the halogenated free ligand, zinc, and ruthenium porphyrins (Chapter 2), gives rise to the expected red shifted optical spectra and anodically shifted electrochemistry common to porphyrins substituted with electron withdrawing ligands. Only the $RuTFPPX_8$ complexes show Soret transitions at higher energy, which has been demonstrated to stem from strong coupling between the ruthenium and porphyrin orbitals. Attempts to photolyze the carbonyl ligand further support strong interactions between these orbitals; despite a relatively high ν_{CO} (indicating a correspondingly weak Ru-C bond), it is difficult to remove the carbonyl ligand with light energy. Rather than leading to dissociation, the excited state appears to decay by non-radiative pathways. No emission is observed for either the $RuTFPPCl_8(CO)$ or $Ru(TFPPCl_8)py_2$ complexes.

The highly positive reduction potentials of the perhalogenated ruthenium and iron complexes indicate that these compounds will be quite stable in a highly oxidizing environment. Further experiments will test to see if they display the high activity as oxidation catalysts for which they were designed.

Methods

Infrared spectra were recorded as solutions in carbon tetrachloride or benzene on a Perkin-Elmer Model 1600 FT-IR spectrophotometer. Electronic absorption spectra were recorded on an Olis-modified Cary-14 spectrophotometer. Electrochemistry was performed under Ar in three compartment cell consisting of a highly polished glassy carbon working electrode, a Ag/AgCl reference electrode in 1M KCl, and a platinum auxiliary electrode. The working electrode and reference electrode are connected by a modified Luggin capillary. Spectroelectrochemical experiments were performed in an optically transparent platinum working electrode.[36] Spectral changes were monitored with a Hewlett Packard 8452A diode array spectrophotometer. A 1000 W tungsten lamp was used for photolysis experiments.

Materials

Porphyrins were obtained as described in Chapter 2. Solvents were Omnisolv grade from EM Science, and used as received.

References and Notes

(1) Gouterman, M. In *The Porphyrins*; D. Dolphin, Ed.; Academic Press, Inc.: New York, NY, 1978; Vol. III; pp 1-156.

(2) Platt, J. R. *J. Chem. Phys.* **1949**, *17*, 484.

(3) Simpson, W. T. *J. Chem. Phys.* **1949**, *17*, 1218.

(4) Gouterman, M. *J. Mol. Spectrosc.* **1961**, *6*, 138-163.

(5) Gouterman, M. *J. Chem. Phys.* **1959**, *30*, 1139-1161.

(6) Callot, H. J. *Bull. Chem. Soc. Fr.* **1974**, *7*, 1492-1496.

(7) Callot, H. J.; Giraudeau, A.; Gross, M. *J. Chem. Soc., Perkin Trans. 2* **1975**, 1321-1324.

(8) Wijesekera, T.; Matsumoto, A.; Dolphin, D.; Lexa, D. *Angew. Chem., Int. Ed. Eng.* **1990**, *29*, 1028-1030.

(9) Takeuchi, T.; Gray, H. B.; Goddard, W. A., III *J. Am. Chem. Soc.* **1994**, *116*, 9730-9732.

(10) Barkigia, K. M.; Chantranupong, L.; Smith, K. M.; Fajer, J. *J. Am. Chem. Soc.* **1988**, *110*, 7566-7567.

(11) Binstead, R. A.; Crossley, M. J.; Hush, N. S. *Inorg. Chem.* **1991**, *30*, 1259-1264.

(12) Giraudeau, A.; Callot, J. H.; Gross, M. *Inorg. Chem.* **1979**, *18*, 201-206.

(13) Hodge, J. A.; Hill, M. G.; Gray, H. B. *Inorg. Chem.* **1995**, *34*, 802-812.

(14) Ochsenbein, P.; Ayougou, K.; Mondon, D.; Fischer, J.; Weiss, R.; Austin, R. N.; Jayaraj, K.; Gold, A.; Terner, J.; Fajer, J. *Angew. Chem., Int. Ed. Eng.* **1994**, *33*, 348-350.

(15) Barkigia, K. M.; Berber, M. D.; Fajer, J.; Medforth, C. J.; Renner, M. W.; Smith, K. M. *J. Am. Chem. Soc.* **1990**, *112*, 8851-8857.

(16) Mandon, D.; Ochsenbein, P.; Fischer, J.; Weiss, R.; Jayaraj, K.; Austin, R. N.; Gold, A.; White, P. S.; Brigaud, O.; Battioni, P.; Mansuy, D. *Inorg. Chem.* **1992**, *31*, 2044-2049.

(17) Senge, M. O.; Medforth, C. J.; Sparks, L. D.; Shelnutt, J. A.; Smith, K. M. *Inorg. Chem.* **1993**, *32*, 1716-1723.

(18) Bhyrappa, P.; Krishnan, V. *Inorg. Chem.* **1991**, *30*, 239-245.

(19) D'Souza, F.; Villard, A.; Caemelbecke, E. V.; Franzen, M.; Boschi, T.; Tagliatesta, P.; Kadish, K. M. *Inorg. Chem.* **1993**, *32*, 4042-4048.

(20) Scheidt, W. R.; Kastner, M. E.; Hatano, K. *Inorg. Chem.* **1978**, *17*, 706-710.

(21) Birnbaum, E. R.; Hodge, J. A.; Grinstaff, M. G.; Schaefer, W. P.; Marsh, R. E.; Henling, L. M.; Labinger, J. A.; Bercaw, J. E.; Gray, H. B. *Inorg. Chem.* **in press.**

(22) Gross, Z.; Barzilay, C. *Angew. Chem., Int. Ed. Eng.* **1992**, 1615-1617.

(23) Hoffmann, P.; Robert, A.; Meunier, B. *Bull. Chem. Soc. Fr.* **1992**, *129*, 85-97.

(24) Oscillator strength is calculated as $4.6 \times 10^{-9}\ \varepsilon\ \nu_{1/2}$.

(25) The $ZnTFPPX_8$ compounds also show anoidcally shifted electrochemistry, but are complicated by two-electron waves. See reference 13.

(26) Grinstaff, M. W.; Hill, M. G.; Birnbaum, E. R.; Schaefer, W. P.; Labinger, J. A.; Gray, H. B. *Inorg. Chem.* **in press.**

(27) The potentials of RuTPP(CO) are 0.87 (+/0) and -1.59 (0/-) V vs. SCE (CH_2Cl_2, 0.1M TBAP): Mu, X. H.; Kadish, K. M. *Langmuir* **1990**, *6*, 51-56.

(28) Brown, G. M.; Hopf, F. R.; Ferguson, J. A.; Meyer, T. J.; Whitten, D. G. *J. Am. Chem. Soc.* **1973**, *95*, 5939-5942.

(29) Kadish, K. M.; Chang, D. *Inorg. Chem.* **1982**, *21*, 3614-3619.

(30) Since pyridine is a much weaker π acceptor than CO, we would expect Ru^{II} to backbond more strongly to $TFPPCl_8$ in the bis(pyridine) than in the carbonyl derivative. For discussions of M^{II} (M = Fe, Ru, Os) backbonding to CO and py in porphyrin complexes, see: Gentemann, S.; Albaneze, J.; Garcia-Ferrer, R.; Knapp, S.; Potenza, J. A.; Schugar, H. J.; Holten, D. *J. Am. Chem. Soc.* **1994**, *116*, 281-289; Kim, D.; Su, Y. O.; Spiro, T. G. *Inorg. Chem.* **1986**, *25*, 3993-3997; Schick, G. A.; Bocian, D. F. *J. Am. Chem. Soc.* **1984**, *106*, 1682-1694.

(31) Buchler, J. W.; Kokisch, W.; Smith, P. D. *Struct. Bonding* **1978**, *34*, 79-134.

(32) Antipas, A.; Buchler, J. W.; Gouterman, M.; Smith, P. D. *J. Am. Chem. Soc.* **1978**, *100*, 3015-3024.

(33) Chow, B. C.; Cohen, I. A. *Bioinorg. Chem.* **1971**, *1*, 57-63.

(34) Kadish, K. M.; Tagliatesta, P.; Hu, Y.; Deng, Y. J.; Mu, X. H.; Bao, L. Y. *Inorg. Chem.* **1991**, *30*, 3737-3743.

(35) Mu, X. H.; Kadish, K. M. *Langmuir* **1990**, *6*, 51-56.

(36) Hill, M. G.; Mann, K. R. *Inorg. Chem.* **1991**, *30*, 1429-1431.

Figure 3.1 -- An absorption spectrum of ZnTPP, a normal porphyrin. The Soret (or B) absorption usually lies around 410 nm, and the Q bands are at lower energy. The shoulder on the Soret has been assigned as a $\pi \rightarrow \pi^*$ transition (N band).

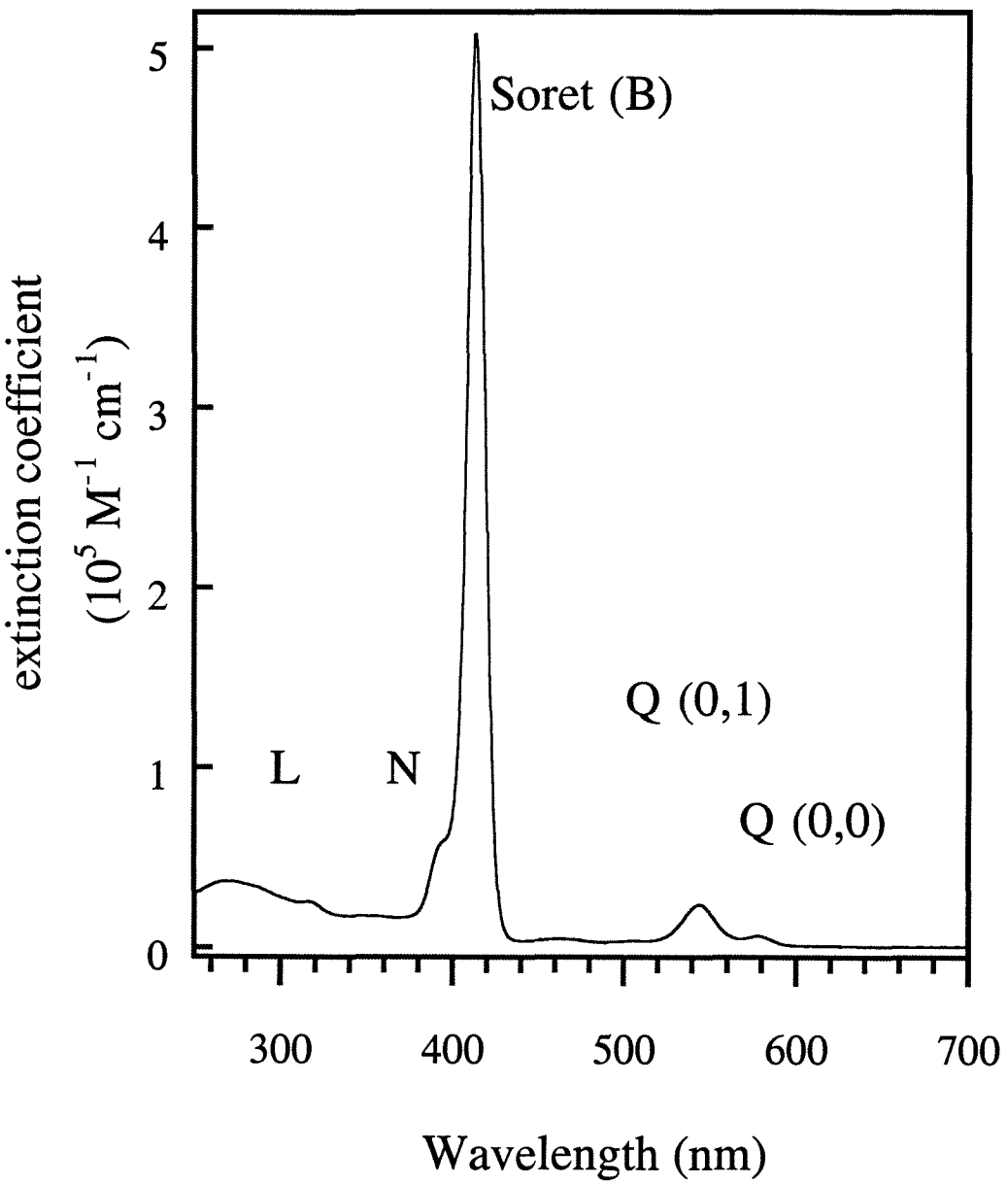
Soret (B)
Q (0,1)
Q (0,0)
L
N
extinction coefficient
(10^5 M^{-1} cm^{-1})
0
1
2
3
4
5
300
400
500
600
700
Wavelength (nm)

Figure 3.2 -- The Gouterman four orbital model for normal porphyrins is shown on the left (with D_{4h} symmetry labels). Upon fluorination of the phenyl rings, both the HOMO and the LUMO are stabilized, and the relative energy of the a_{1u} and a_{2u} HOMOs are reversed. Halogenation of the pyrrole carbons results in a further stabilization of all of the orbitals (pictured on the right). The distortion of the molecule drops the symmetry to approximately D_{2d}. The Soret transition is marked on each molecular orbital diagram with an arrow of equal length, showing the increase in the HOMO-LUMO gap in TFPP and the decrease in $TFPPCl_8$.

Gouterman Four Orbital Model

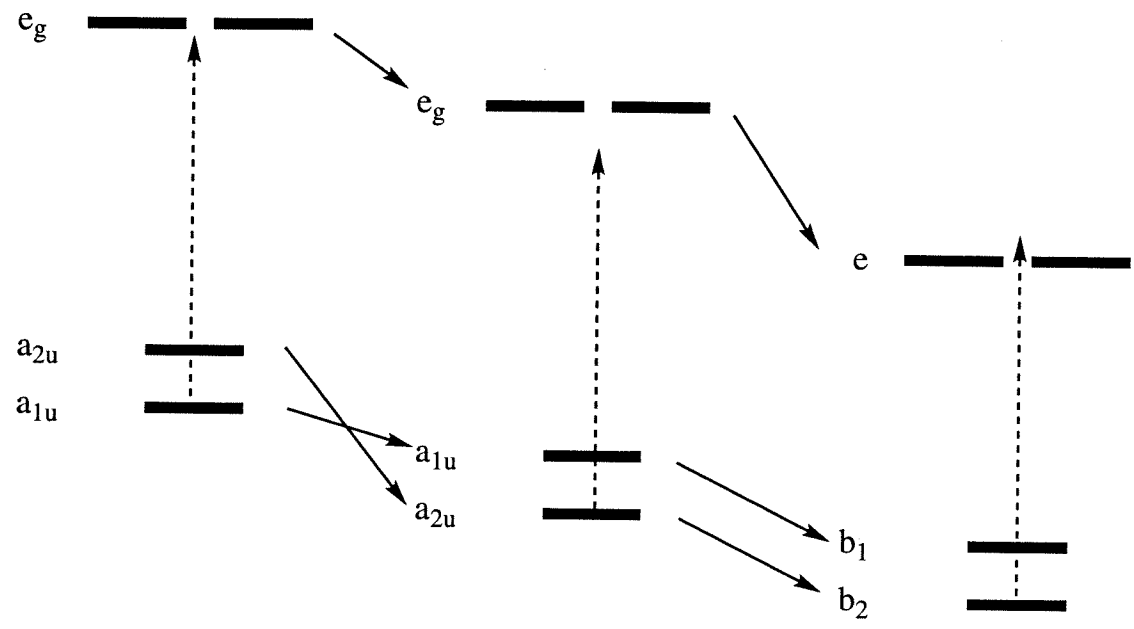

Normal orbital ordering

TPP

Addition of pentafluorophenyl groups to meso carbons

TFPP

Addition of halogens to pyrrole carbons

$TFPPCl_8$

Figure 3.3 -- The UV-Vis spectra of the ZnTPP series of porphyrins in methylene chloride. As shown in the molecular orbital diagrams in Figure 3.2, the energy of the Soret transition decreases as ZnTFPP > ZnTPP > $ZnTFPPCl_8$ > $ZnTFPPBr_8$.

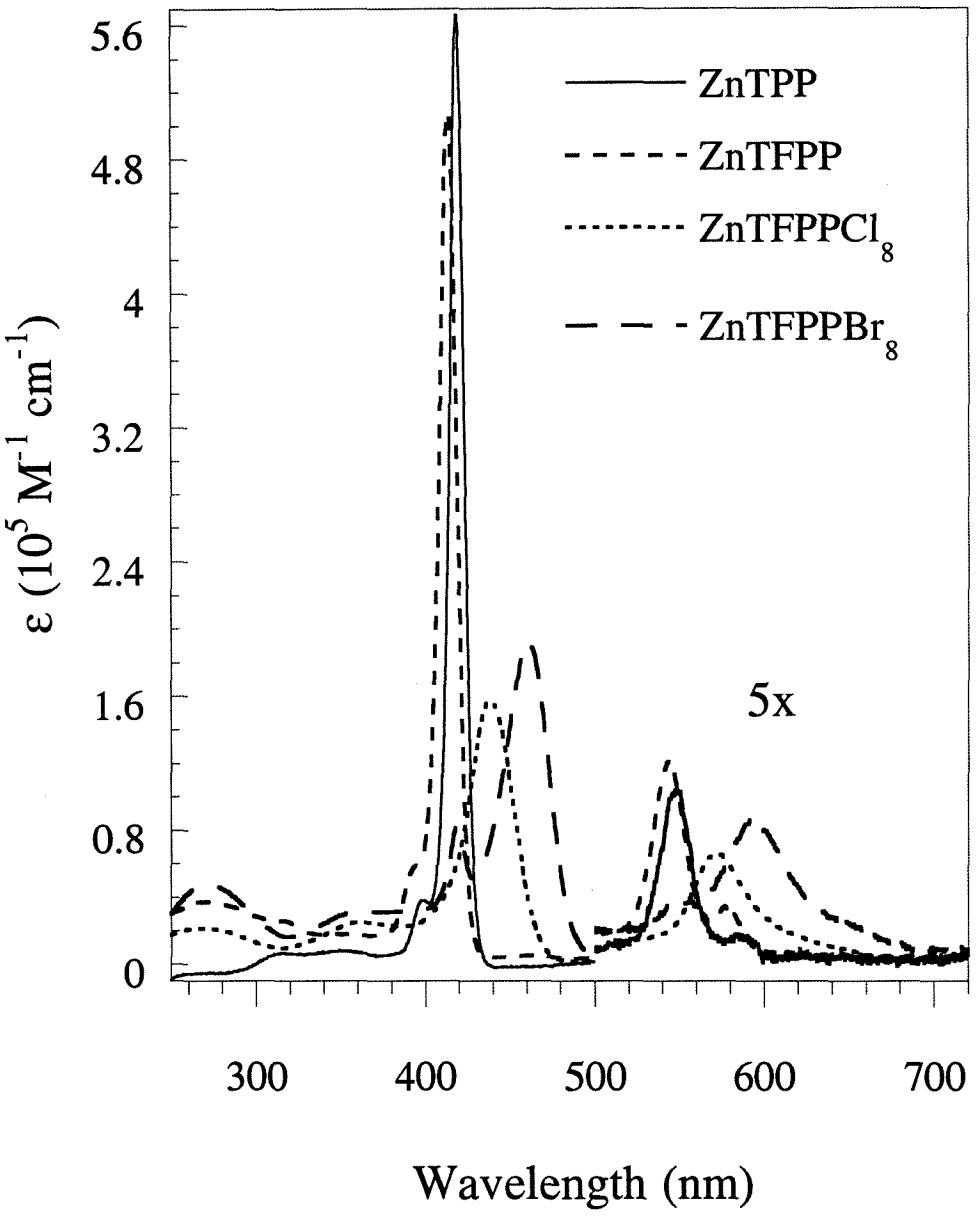
5.6
4.8
4
3.2
2.4
1.6
0.8
0
ε (10^5 M^-1 cm^-1)
ZnTPP
ZnTFPP
ZnTFPPCl8
ZnTFPPBr8
5x
300
400
500
600
700
Wavelength (nm)

Figure 3.4 -- The UV-Vis spectra of Fe(TFPP)Cl and Fe(TFPPBr$_8$)Cl in methylene chloride. The LMCT of Fe(TFPPBr$_8$)Cl mixes with the Soret band, increasing the extinction coefficient of this transition relative to the 350 nm band in Fe(TFPP)Cl.

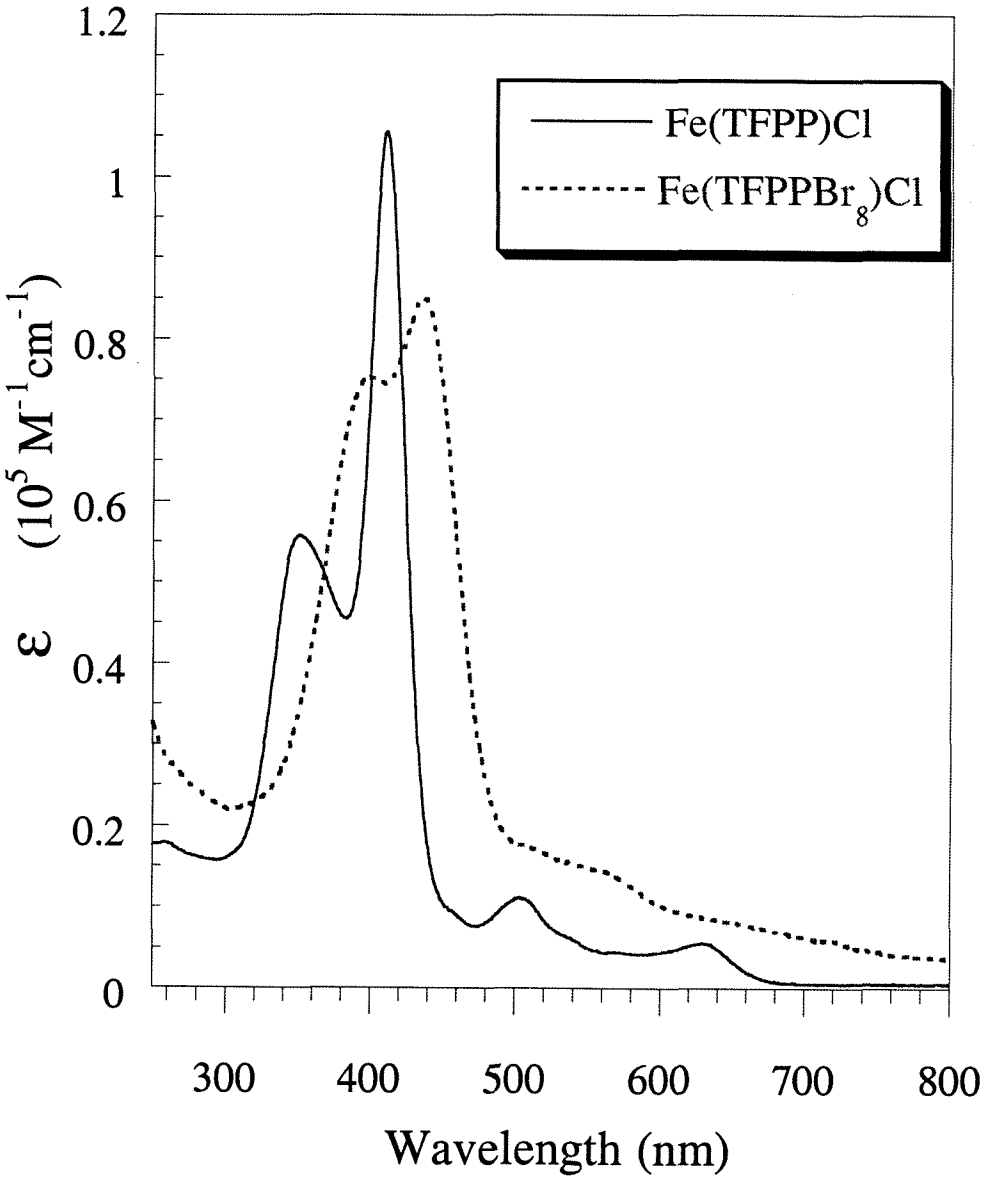
1.2
1
0.8
0.6
0.4
0.2
0
ε (10^5 M^-1cm^-1)
Fe(TFPP)Cl
Fe(TFPPBr8)Cl
300
400
500
600
700
800
Wavelength (nm)

Figure 3.5 -- The UV-Vis spectra of $[Fe^{II}(TFPPBr_8)Cl]^-$ and $[Fe^{II}(TFPPBr_8)(OCH_3)_2]$ produced by bulk electrolysis or chemical reduction in methylene chloride. The red shifted Soret band and the single Q band are consistent with formation of an iron(II) porphyrin. The axial ligands for the two complexes are determined from a combination of electrochemical data and ^{19}F NMR.

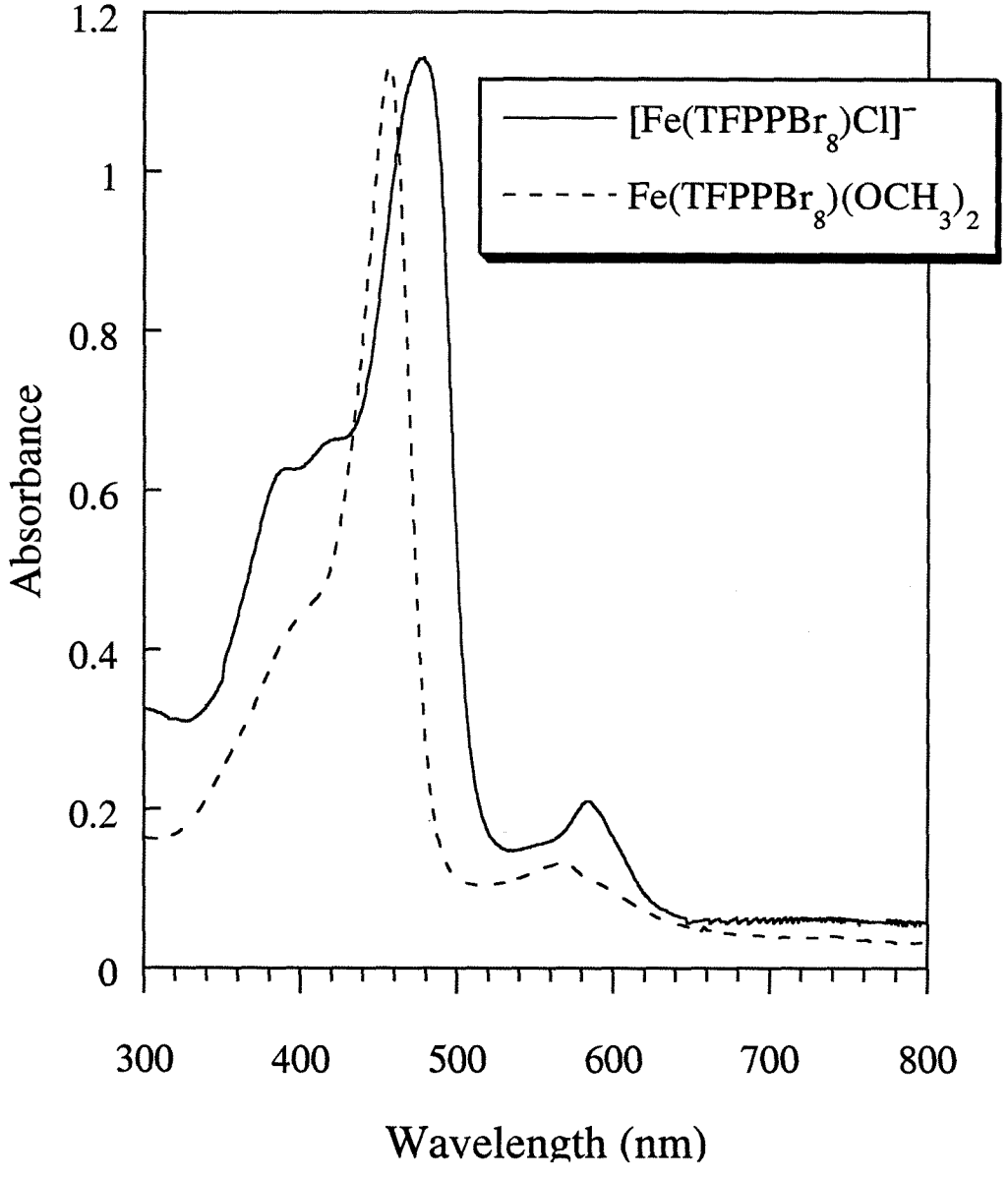
1.2
1
0.8
0.6
0.4
0.2
0
Absorbance
300
400
500
600
700
800
Wavelength (nm)
[Fe(TFPPBr8)Cl]-
Fe(TFPPBr8)(OCH3)2

Figure 3.6 -- The Gouterman four orbital model for $RuTFPPX_8$ complexes. The porphyrin $TFPPX_8$ orbitals are allowed to interact with the $d\pi$ orbitals of carbonyl or bis-pyridine ruthenium fragments (D_{2d} symmetry). Extensive π-backbonding to the carbonyl ligand strongly stabilizes the d_{xz}, d_{yz} orbitals, resulting in a ligand based HOMO for $RuTFPPX_8(CO)$. Weaker interactions in the bis-pyridine complex leaves the $d\pi$ orbitals at higher energies, consistent with a Ru-based HOMO and low energy charge transfer transitions in $RuTFPPX_8(py)_2$. The Soret transition is shown with an arrow for both complexes.

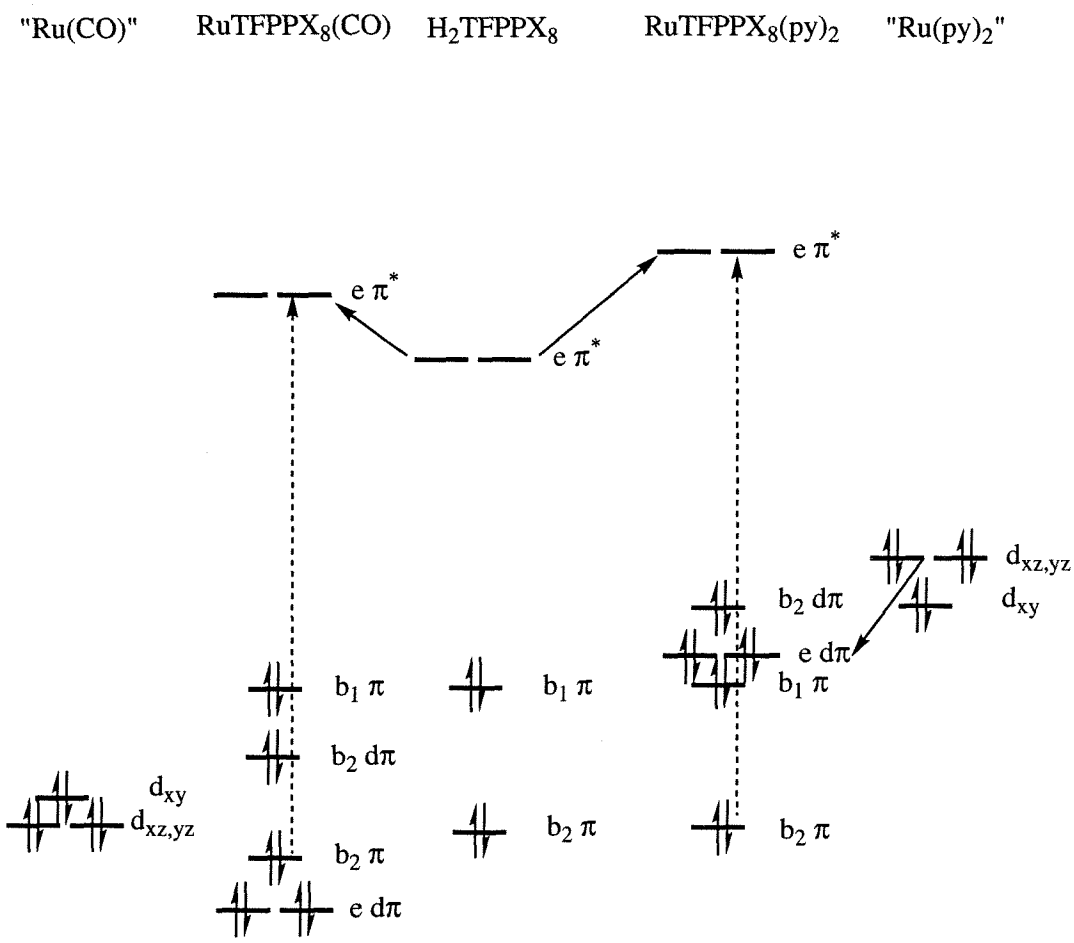
"Ru(CO)"
RuTFPPX8(CO)
H2TFPPX8
RuTFPPX8(py)2
"Ru(py)2"
e π*
e π*
e π*
dxz,yz
dxy
b2 dπ
e dπ
b1 π
b1 π
b1 π
b2 dπ
dxy
dxz,yz
b2 π
b2 π
b2 π
e dπ

Figure 3.7 -- The UV-Vis spectra of RuTPP(CO) and $RuTFPPCl_8(CO)$ in methylene chloride. Although the Soret energy is similar for the two complexes, the Q(1,0) transition is red shifted for the perhalogenated complex.

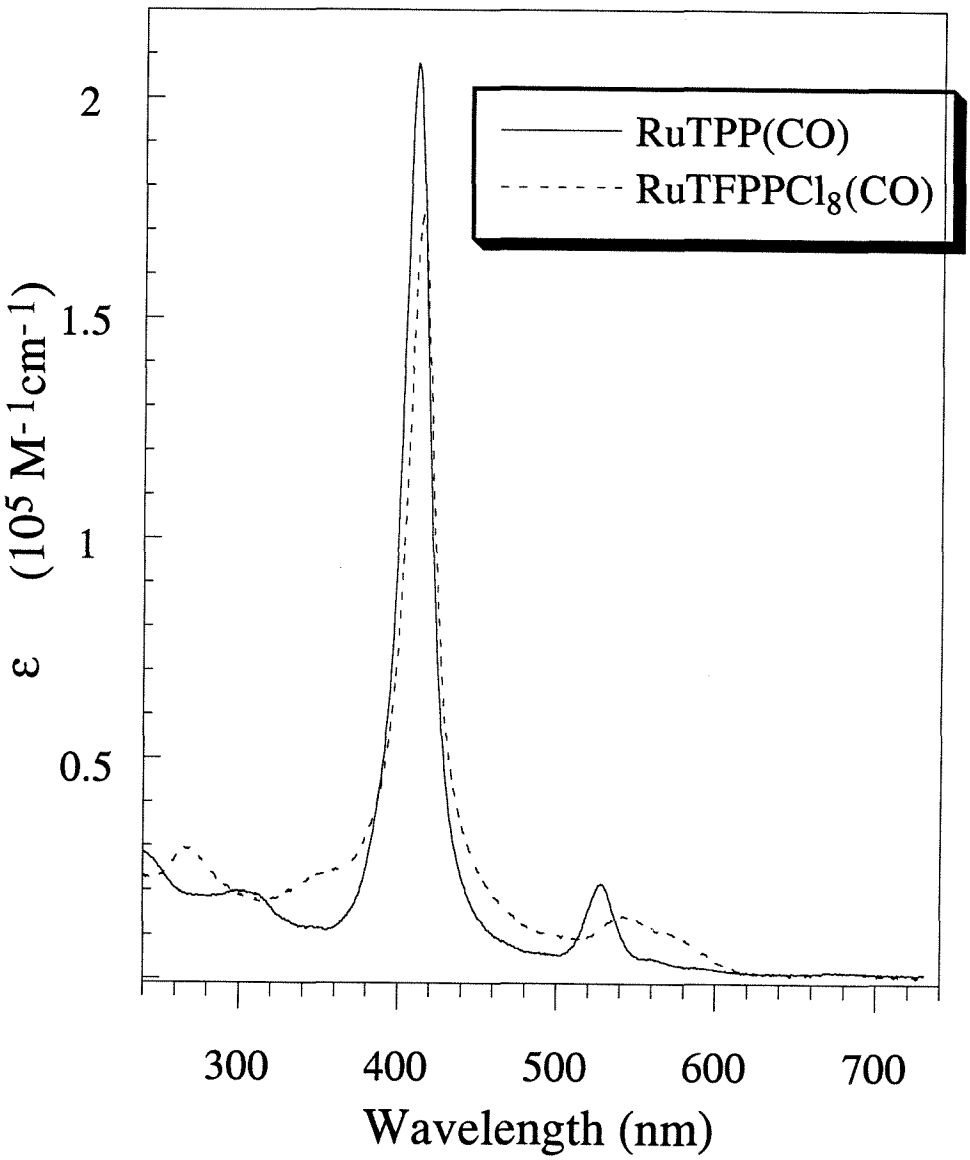
RuTPP(CO)
RuTFPPCl8(CO)
ε (10^5 M^-1cm^-1)
2
1.5
1
0.5
300
400
500
600
700
Wavelength (nm)

Figure 3.8 -- The UV-Vis spectra of $RuTPP(py)_2$ and $RuTFPPCl_8(py)_2$ in methylene chloride.

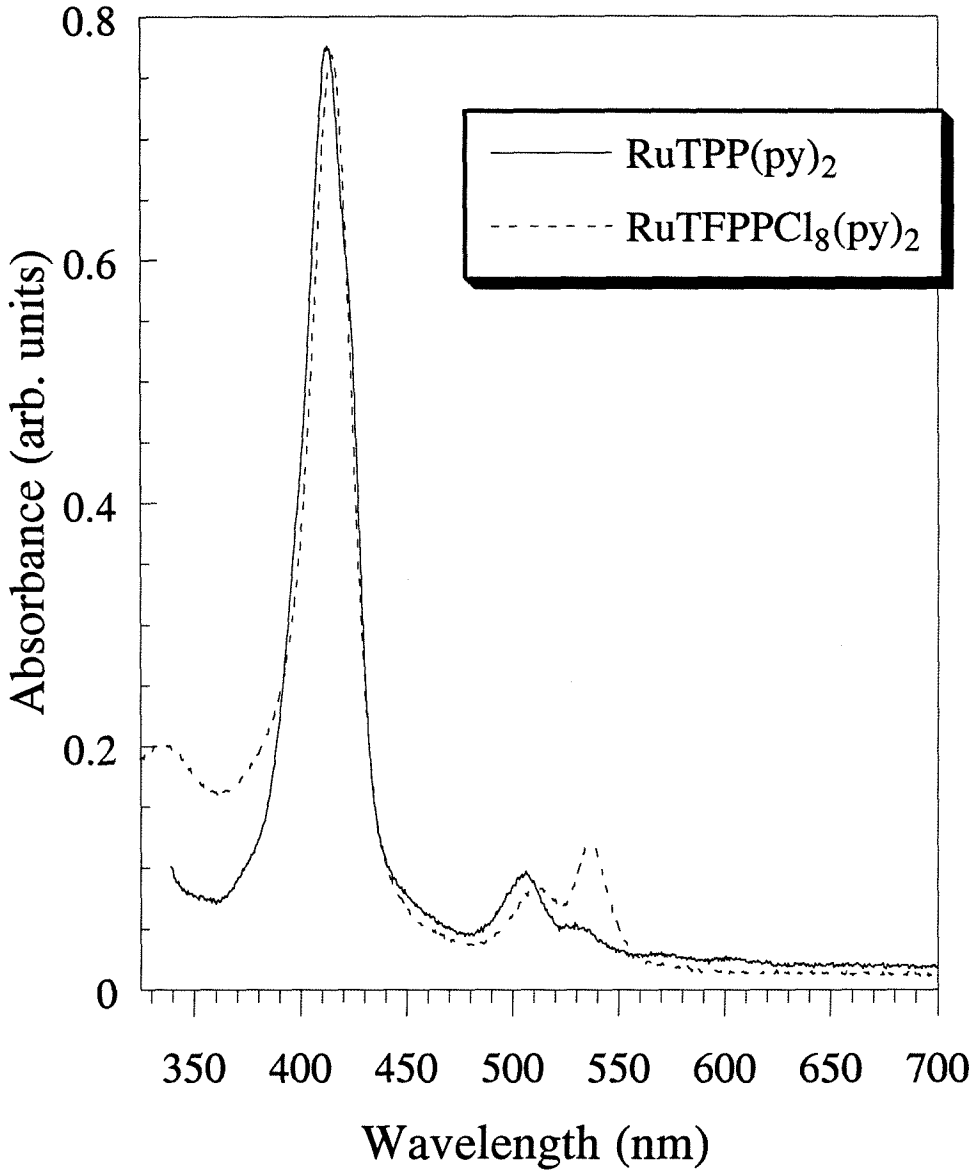
0.8
0.6
0.4
0.2
0
Absorbance (arb. units)
RuTPP(py)2
RuTFPPCl8(py)2
350
400
450
500
550
600
650
700
Wavelength (nm)

Figure 3.9 -- The UV-Vis spectra of the $RuTFPPX_n(CO)$ complexes in methylene chloride. The Soret energy decreases with halogenation: $RuTFPPCl_6(CO)$ > $RuTFPPCl_7(CO)$ > $RuTFPPCl_8(CO)$ > $RuTFPPBr_8(CO)$, with the larger bromine atoms inducing a larger red shift than chlorine. The Q bands (not shown) show a similar change in energy.

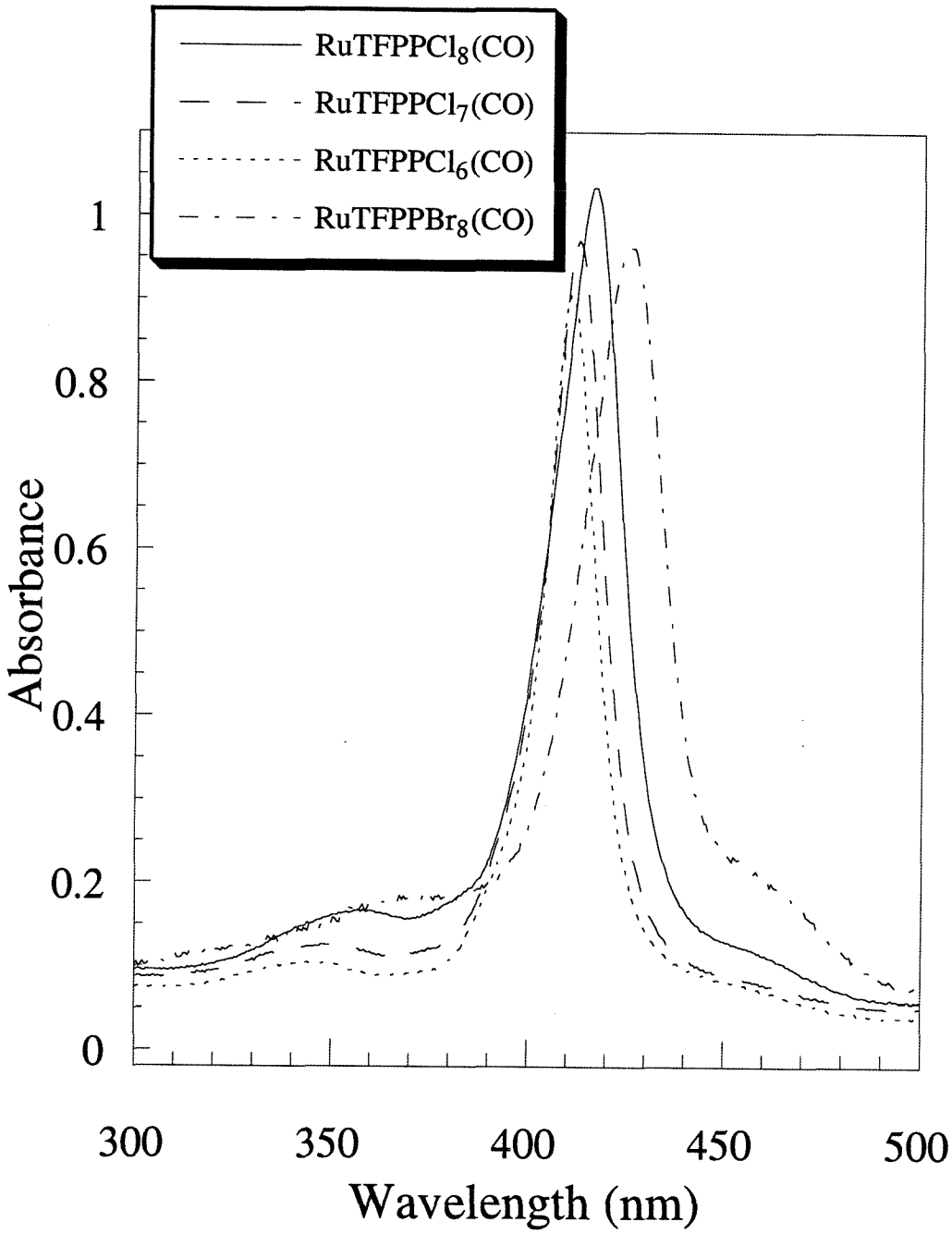
RuTFPPCl8(CO)
RuTFPPCl7(CO)
RuTFPPCl6(CO)
RuTFPPBr8(CO)
Absorbance
0
0.2
0.4
0.6
0.8
1
300
350
400
450
500
Wavelength (nm)

Figure 3.10 -- The low energy visible spectrum of $RuTFPPCl_8(CO)$ and $RuTFPPCl_8(py)_2$. The two absorptions at 670 and 792 nm in the bis-pyridine spectrum are assigned to $Ru^{II} \rightarrow e\pi^*$ ($TFPPCl_8$) transitions. MLCT transitions in the carbonyl complex are anticipated to lie at higher energy and are obscured by porphyrin $\pi \rightarrow e\pi^*$ transitions.

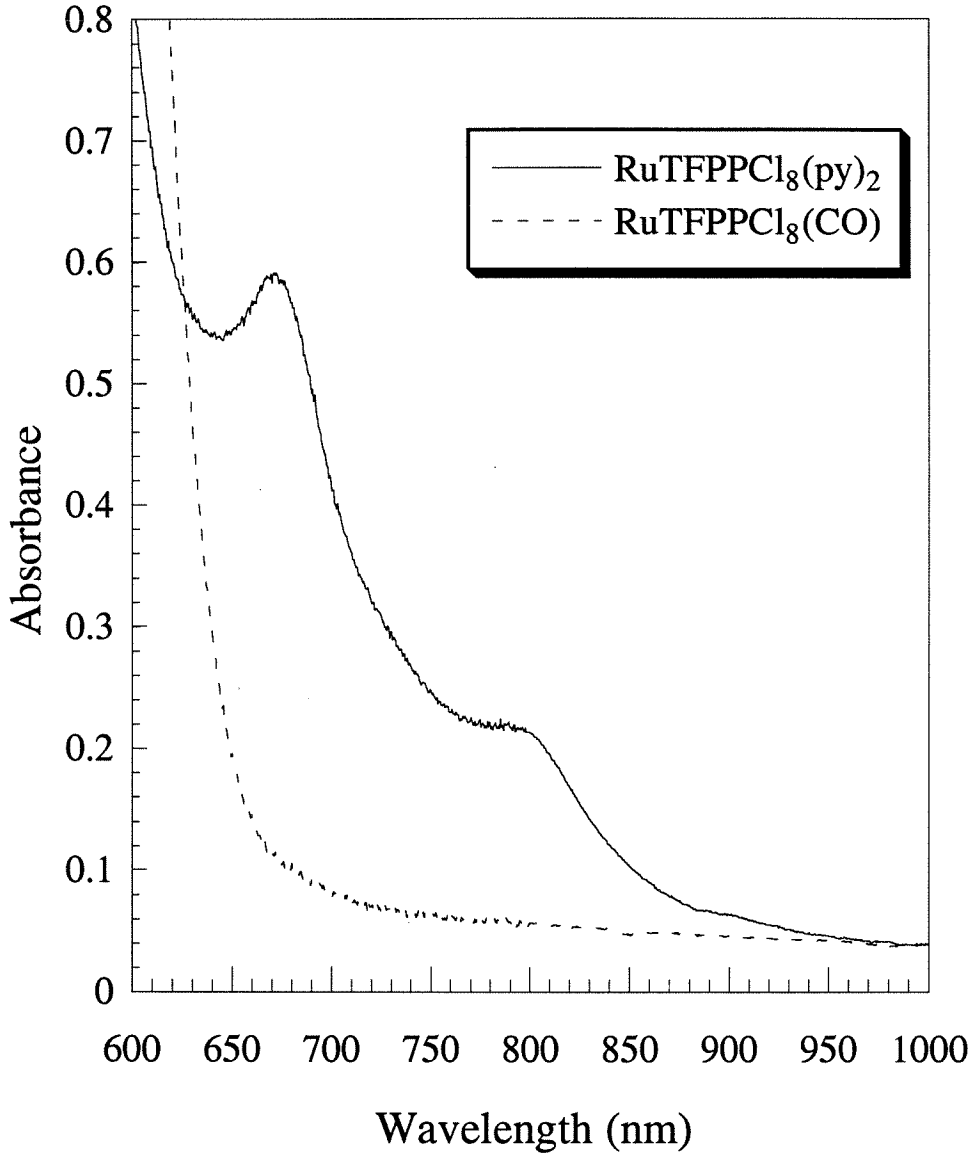
0.8
0.7
0.6
0.5
0.4
0.3
0.2
0.1
0
Absorbance
600
650
700
750
800
850
900
950
1000
Wavelength (nm)
RuTFPPCl8(py)2
RuTFPPCl8(CO)

Figure 3.11 -- Spectroelectrochemical reduction of $RuTFPPCl_8(py)_2$ in methylene chloride. The reduced species shows clear porphyrin radical character.

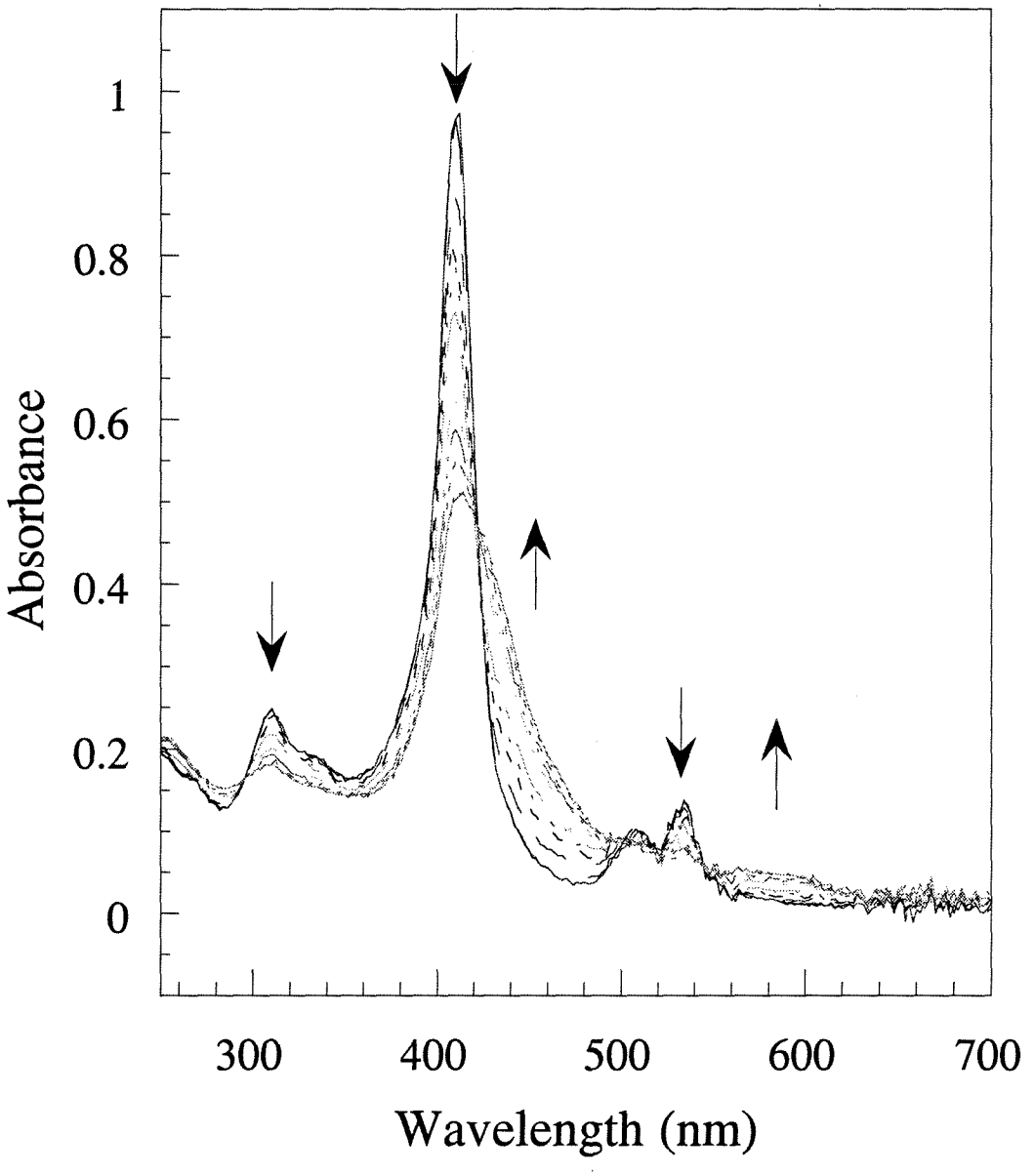
1
0.8
0.6
0.4
0.2
0
Absorbance
300
400
500
600
700
Wavelength (nm)

Figure 3.12 -- Spectroelectrochemical reduction of $RuTFPPCl_8(CO)$ in methylene chloride. While the reduced species shows a decrease in the Soret intensity, consistent with formation of a porphyrin radical anion, no change in the Q band region is observed.

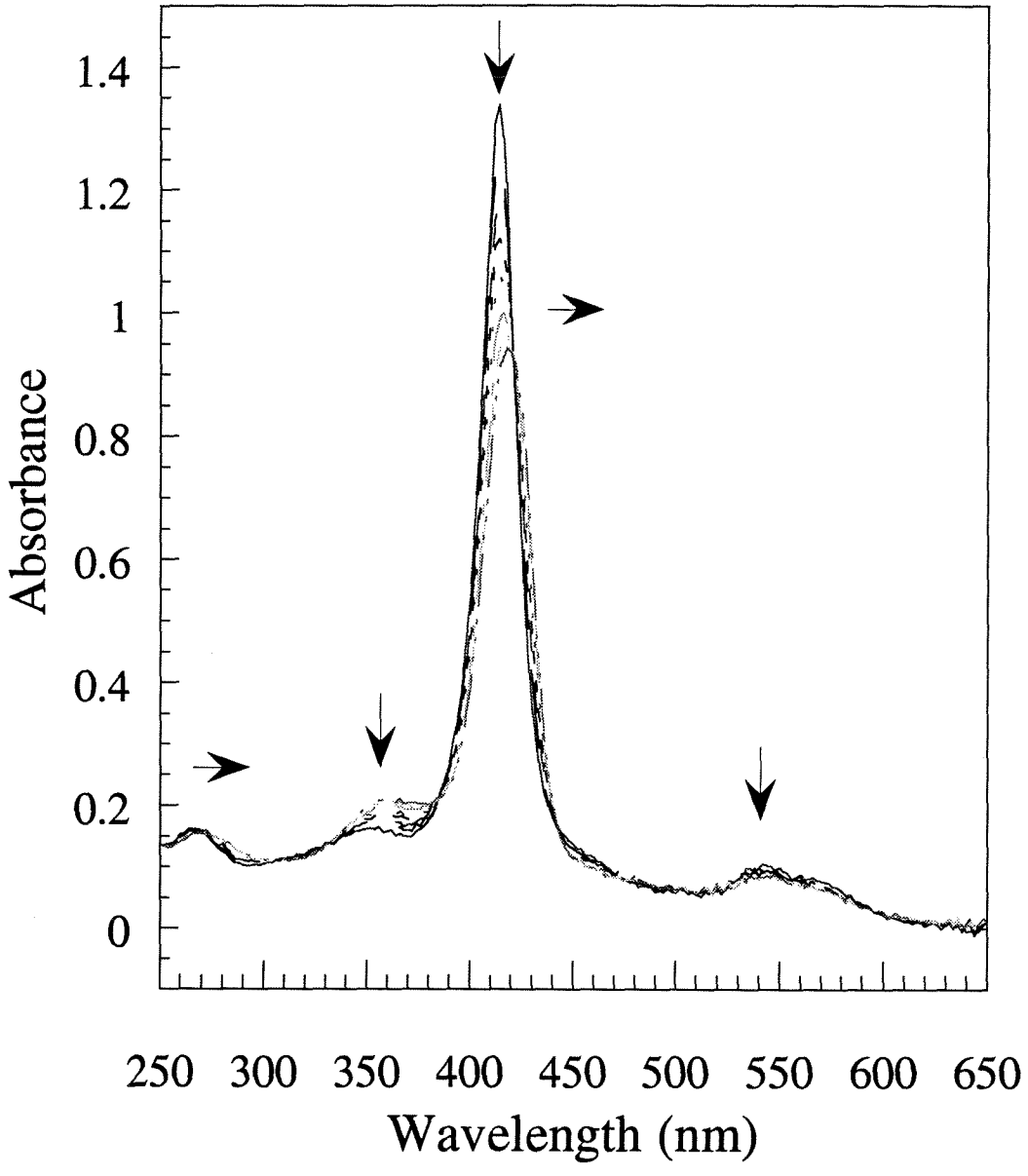
1.4
1.2
1
0.8
0.6
0.4
0.2
0
Absorbance
250 300 350 400 450 500 550 600 650
Wavelength (nm)

Table 3.1. Electronic Absorptions of Halogenated Porphyrins.

Porphyrin	L, M bands (ε, 10^3 M^{-1} cm^{-1})	Soret, nm (ε, 10^5 M^{-1} cm^{-1})	Q bands, nm (ε, 10^4 M^{-1} cm^{-1})			
ZnTPP	315 (1.0) 350 (1.5)	418 (5.6)	548 (2.1)			
ZnTFPP	318 (4)	413.5 (5.0)	544 (2.4)			
$ZnTFPPCl_8$	360 (3.0)	439 (1.6)	572 (1.3)			
$ZnTFPPBr_8$	364 (3.3)	460 (1.9)	594 (1.7)			
H_2TPP[a]		419 (4.7)	514 (1.9)	549 (0.77)	591 (0.54)	647 (0.34)
H_2TFPP[a]		412 (2.4)	506 (1.9)	584 (0.58)	659 (0.36)	
$H_2TFPPCl_8$		438 (1.6)	538 (1.3)	626 (0.46)		
$H_2TFPPBr_8$		454	532	636		
RuTPP(CO)	300 (20)	412 (2.0)	528 (2.1)			
$RuTFPPCl_8(CO)$	355 (25)	416 (1.7)	548 (1.4)	580 (1.0)		
$RuTFPPCl_7(CO)$	345	413	541	576		
$RuTFPPCl_6(CO)$	340	411	539	572		
$RuTFPPBr_8(CO)$	370	426	595			
$RuTPP(py)_2$		413	507	534		
$RuTFPPCl_8(py)_2$	355	414 (1.6)	512 (2.0)	536 (2.5)	670[b] (0.08)	790[b] (0.03)
$RuTFPPCl_7(py)_2$		414	510	536	672[b]	790[b]
$RuTFPPCl_6(py)_2$		412	508	534	674[b]	790[b]
$RuTFPPBr_8(py)_2$		424	518	572		

a. Extinction coefficients in benzene, from Longo, F. R.; Finarelli, M. G.; Kim, J. B. *J. Hetero. Chem.*, **1969**, *6*, 927-931.
b. Assigned as MCLT absorptions.

Table 3.2. Reduction Potentials of Halogenated Porphyrins.

Porphyrin[a]	$E^{\circ\prime}_{+/0}$	$E^{\circ\prime}_{M(III)/M(II)}$	$E^{\circ\prime}_{0/-}$
ZnTPP[b]	0.80	—	-1.33
ZnTFPP[b]	1.37	—	-0.95
$ZnTFPPCl_8$[b]	1.60[c]	—	-0.76
$ZnTFPPBr_8$[b]	1.55[c]	—	-0.75
H_2TPP[d]	1.08	—	-1.21
H_2TFPP	1.53	—	-0.78
$H_2TFPPCl_8$	1.66[e]	—	-0.32
$H_2TFPPBr_8$	1.56[e]	—	-0.31
RuTPP(CO)[f]	0.86		-1.46
$RuTFPPCl_6(CO)$	1.64	—	-0.76
$RuTFPPCl_7(CO)$	1.69	—	-0.69
$RuTFPPCl_8(CO)$	1.71	—	-0.64
$RuTFPPBr_8(CO)$	1.63	—	-0.84
$RuTPP(py)_2$[d]	—	0.21	—
$RuTFPPCl_6(py)_2$	—	0.89	-1.12
$RuTFPPCl_7(py)_2$	—	1.04	-0.98
$RuTFPPCl_8(py)_2$	—	1.08	-0.94
Fe(TPP)Cl[g]	1.14	-0.29	-1.07
Fe(TFPP)Cl	1.65	-0.08	-1.10
$Fe(TFPPBr_8)Cl$	—	0.31	-0.63

a. Potentials in CH_2Cl_2 solution at room temperature (V vs. AgCl/Ag, 0.1M $TBAPF_6$).
b. The zinc potentials are from reference 13.
c. $E^{\circ\prime}_{2+/0}$.
d. V. vs SCE in 0.05M THAP. From reference 12.
e. E_{pa}.
f. V. vs. SCE in 0.1 M TBAP in CH_3CN. From reference 29.
g. From reference 26.

Table 3.3. Electronic Absorptions of Halogenated Iron Porphyrins.

Porphyrin	L, M bands	Soret, nm (ε,10^5 M^{-1} cm^{-1})	Q bands, nm (ε, 10^4 M^{-1} cm^{-1})		
$Fe^{III}(TPP)Cl$[a]		419 (1.7)	510 (1.2)	573 (0.037)	656, 692 (0.028, 0.32)
$Fe^{II}(TPP)Cl$[a]		444 (1.7)	530 (0.32)	571 (0.75)	612 (0.65)
$Fe^{III}(TFPP)Cl$		411 (1.0)	351 (0.70)	504 (1.1)	621 (0.56)
"$Fe^{II}(TFPPCl_8)$"[b]	398	440	566		
$Fe^{III}(TFPPBr_8)Cl$	404 (0.81)	440 (0.85)	560 (2.0)		
$[Fe^{II}(TFPPBr_8)Cl]^-$	388, 420	478	585		
$Fe^{II}(TFPPBr_8)(OMe)_2$		454	568		
$Fe(TPP)py_2$					
$Fe(TFPP)py_2$		418	525	552	
$Fe(TFPPCl_8)py_2$		438	542	574	
$Fe(TFPPBr_8)py_2$		452	556	588	
$(FeTFPP)_2O$[c]		398 (0.62)	577 (0.7)	590 (sh)	
$Fe(TFPP)OH$[c]		406 (7.6)	563 (1.2)		

a. Spectra taken in PhCN; from reference 8.
b. Appears to be iron (II) based on the red color. See text.
c. Extinction coefficients from reference 40, Chapter 2.

Chapter 4

Mechanism of Catalytic Alkene Oxidation with Molecular Oxygen or Iodosobenzene and Halogenated Iron Porphyrins

Introduction

Since the discovery that tetraphenylporphyrinato-iron(III) chloride [Fe(TPP)Cl] catalyzes olefin epoxidation with iodosobenzene,[1] a variety of porphyrins have been tested for the ability to mediate hydrocarbon oxidation reactions utilizing assorted oxygen sources.[2] These studies have generally striven to generate high-valent metal-oxo intermediates to mimic the putative active species in cytochrome P-450. Most experiments take advantage of the peroxide shunt pathway to directly form the desired metal-oxo species, while reactions with dioxygen are usually carried out in the presence of a reductant to follow the complete P-450 oxygen activation mechanism.

The reaction of iodosobenzene (PhIO) with metalloporphyrins has been well documented.[1,3-8] The iodosobenzene polymer oxidizes $M^{III}(P)X$ complexes to $M^{V}(P)(O)$ species as shown in Eq. 1, where P = porphyrin, X = halide, ^{-}OH, etc., R = phenyl, and R' is the continuing iodosobenzene polymer.[9] Some evidence also exists for the transient

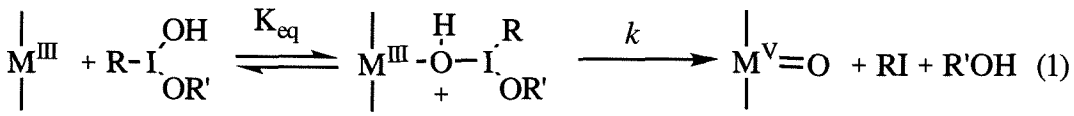

formation of a μ-oxo dimer intermediate, $(P)M^{IV}$ - O - $M^{IV}(P)^{\bullet+}$, formed from a reaction of $M^{V}(P)(O)$ with another porphyrin molecule.[10,11]

Whether the last oxidizing equivalent is more appropriately characterized as a M^{V} or as a $M^{IV}(P^{+\bullet})$ depends on the metal and porphyrin involved. Spectroscopic evidence indicates that most iron porphyrins are oxidized to form porphyrin radical cations,[12-14] as does the heme center in the enzyme horseradish peroxidase (HRP) The high-valent metal-oxo of HRP (compound I) is well characterized as $Fe^{IV}(P^{+\bullet})(O)$ and is often used as a standard for comparisons with model complexes.[15] Oxidation of $Fe^{III}(TMP)Cl$ with

m-chloroperbenzoic acid (mCPBA) at -77 °C is reported to give UV-Vis and ^{1}H NMR spectra consistent with formation of an iron(IV) porphyrin π-radical cation.[14] EXAFS and Mössbauer spectra are similar to those of HRP compound I, further supporting this assignment.[16] With other metals, such as chromium, the last electron is removed from a metal based orbital.[17] For Cr^{III}TPPCl, UV-Vis and IR spectroscopy, in combination with magnetic susceptibility measurements, indicate formation of Cr^{V}TPP(O) upon oxidation with mCPBA or PhIO.[18]

Once the high-valent metal-oxo is generated, there are a number of mechanisms for interaction with an olefin. Possible intermediates include a metallaoxetane (I), a π-radical cation (II), a carbocation (III), a carbon radical (IV), or a process of concerted oxene insertion (V) (Figure 4.1).[19] The metallocyclo intermediate has been excluded, especially for sterically encumbered porphyrins, since modeling demonstrates that the reaction coordination sphere is not large enough to accommodate formation of the four-membered ring.[20,21] Although many elegant experiments have been conducted to further probe the transition state, there is no consensus indicating a general metalloporphyrin oxidation mechanism. The academically unsatisfying conclusion seems to be that the mechanism is dependent on the metal ion and the electron density of the porphyrin and alkene substrate.[19]

Nevertheless, a few general concepts concerning the mechanism have been proposed (Figure 4.2).[17,21-23] The first step has been proposed to be association of the metal-oxo and the olefin, in some cases called a charge transfer (CT) complex. With Cr^{V}(TDBPP)(O) (TDBPP = tetrakis-(2,6-dibromophenyl)porphyrin), the formation of this complex is rate limiting,[17] and other evidence suggests this is also true for the iron derivative. The reaction of Fe(TMP)Cl with mCPBA and cyclooctene at -43 °C resulted in an observable intermediate prior to epoxide formation, again suggested to be an olefin π-complex.[13] The charge transfer complex may then react through various pathways, including concerted oxene transfer (V), electrophilic addition (III), or electron

transfer (IV).[19-21] The relative rates for each pathway are determined in each case by the electron density on the olefin and the electrochemical potential of the metal center. Unfortunately, the actual oxo transfer step is after the rate limiting formation of the CT complex, precluding its direct observation.

For the specific case of cyclohexene oxidation, different pathways are implicated for hydroxylation and epoxidation (Figure 4.3). Oxidation of deuterated cyclohexene with Fe(TPP)Cl and Cr(TPP)Cl has shown that allylic oxidation occurs via allylic hydrogen atom abstraction followed by geminate radical recombination.[24] Further experiments with partially halogenated porphyrins supported this mechanism for hydroxylation[25] and suggested that formation of cyclohexene epoxide occurs by direct electron transfer to form a carbocation intermediate (Figure 4.3). Competition between direct hydrogen abstraction and electron transfer depends on the electron density at the metal, allowing for different selectivity as observed with different metals.[25] The higher selectivity for epoxidation observed with electron-withdrawing iron porphyrins suggests that the higher reduction potential favors the electron transfer mechanism.[25] Correlations of epoxidation rates with the reduction potential or the Hammett parameter of the olefin have also been argued to support an electron transfer mechanism for Fe(TDCPP)Cl.[26]

The perhalogenated porphyrin, 2,3,7,8,12,13,17,18-octabromo-5,10,15,20-tetrakis(pentafluorophenyl)porphyrinato-iron(III) chloride, [Fe(TFPPBr$_8$)Cl], is an active catalyst for the selective oxidation of light alkanes at elevated temperatures (80 °C) and under high dioxygen pressure (80 atm).[27,28] Recently, we reported that at room temperature and one atmosphere of molecular oxygen, Fe(TFPPBr$_8$)Cl will oxidize 3-methylpentane to 3-methylpentan-3-ol.[29] We have now found that this metalloporphyrin is also an efficient catalyst for the oxidation of cyclohexene with either dioxygen or single O-atom donors such as iodosobenzene.

Results

In the presence of Fe(TFPPBr$_8$)Cl, cyclohexene oxidation to a mixture of cyclohexene oxide, 2-cyclohexen-1-ol, and 2-cyclohexen-1-one, was observed (Figures 4.4 and 4.5). The product distribution and activity varied greatly with the oxidant. With PhIO, the majority of product (77%) consisted of the epoxide. With dioxygen, mainly allylic oxidation products were generated (49 and 44% of alcohol and ketone, respectively). Reactions with styrene exhibited similar differences in product distribution with oxidant. With PhIO, the majority of the product (67%) was styrene oxide, while with dioxygen, only the cleavage product, benzaldehyde (> 95%), was observed.

Catalytic activity also varied with oxidant. Iodosobenzene reactions deactivated in 1 to 5 hours, accompanied by a shift in the Soret band from 442 to 418 nm. However, 18 ± 4 turnovers (TO) were completed during this time period, and the product distribution (Figure 4.4) was consistent between runs. Although the initial activity with PhIO was greater, overall activity was higher with dioxygen, suggesting an induction period for the latter reaction. Furthermore, in reactions with dioxygen, the perhalogenated porphyrin showed much higher activity at 24 hours (73 TO) as compared to the related porphyrins tetrakis(pentafluorophenyl)porphyrinato-iron(III) chloride (Fe(TFPP)Cl) (31 TO) and tetraphenylporphyrinato-iron(III) chloride (Fe(TPP)Cl) (< 1 TO) (Figure 4.6).

The variations in selectivity with Fe(TFPPBr$_8$)Cl can be explained by invoking different mechanisms for the two oxidants. Iodosobenzene is believed to react with metalloporphyrins to generate a high-valent metal-oxo intermediate, as described above.[30] Indeed, the large percentage of epoxide formed with PhIO and Fe(TFPPBr$_8$)Cl is consistent with a ferryl as the oxidizing species. The increase in activity from Fe(TFPPBr$_8$)Cl relative to Fe(TFPP)Cl, however, is not as great as one might predict: the positive E° $Fe^{3+/2+}$ (0.31 V vs. AgCl/Ag)[29] of the perhalogenated porphyrin would make an "Fe^{V}=O" of this porphyrin high in energy and difficulty to attain.[23] In line with

this prediction, reductive generation of a ferryl (O_2, Zn, H^+) has been shown to be inefficient for highly halogenated porphyrins.[31,32] The lower potentials of Fe(TFPP)Cl (-0.08 V)[29] and Fe(TPP)Cl (-0.29 V vs. SCE)[33] suggest that a ferryl complex can be generated more readily in these complexes. However, once formed, the ferryl can attack the C-H bonds on other porphyrins, leading to catalyst decomposition and lower net activity with these two complexes.

With dioxygen, the formation of a metal-oxo is not observed. Previously in the literature,[34] the active species was proposed to be $(P)Fe^{IV}=O$, formed by reaction of dioxygen with $(P)Fe^{II}$ to form a μ-peroxy bridged dimer (Figure 4.7). Homolytic cleavage of the dimer to $(P)Fe^{IV}=O$ would result in dioxygenase-type oxygen activation.[27,34,35] With electron-withdrawing porphyrins, it was proposed that an iron(IV)-oxo would have as much oxidizing power as a typical iron(V)-oxo porphyrin. Although the positive reduction potential of $Fe(TFPPBr_8)Cl$ is consistent with this mechanism, the increased stability of the ferrous state causes both the iron(II) and iron(III) oxidation states to be stable to oxygen. A solution of electrochemically generated $[Fe^{II}(TFPPBr_8)Cl]^-$ only shows minimal oxidation after several weeks under an O_2 atmosphere,[36] indicating that this pathway is not operative.[29] Attempts to generate an iron(IV)-oxo directly, by addition of iodosobenzene to electrochemically produced $[Fe^{II}(TFPPBr_8)Cl]^-$ in methylene chloride, resulted only in immediate conversion to $Fe^{III}(TFPPBr_8)Cl$.

The possibility of reductive ferryl generation with $Fe(TFPPBr_8)Cl$ is eliminated for several reasons. First, the lack of an added co-reductant allows no mechanism for the reduction of the ferric porphyrin to the ferrous state. Furthermore, $[Fe^{II}(TFPPBr_8)Cl]^-$ is stable to dioxygen, meaning that the oxygen binding step from the P-450 cycle does not occur. As mentioned above, reductive ferryl generation has been shown to be inefficient for halogenated iron porphyrins,[31,32] suggesting that a high-valent metal-oxo is not

implicated in reactions of Fe(TFPPBr$_8$)Cl with dioxygen. A mechanism less common to metalloporphyrins must be investigated.

Indeed, the reaction has been shown to involve formation and porphyrin-catalyzed decomposition of alkyl peroxides (Figure 4.8).[29,37] Free radicals present in solution react with oxygen to form alkyl peroxides. The alkyl peroxides, unlike dioxygen, react more readily with highly electron-deficient porphyrins such as Fe(TFPPBr$_8$)Cl (*vide infra*). The radicals generated by the Fe(TFPPBr$_8$)Cl-catalyzed peroxide decomposition react with additional molecules of substrate to form the observed products, propagating a radical chain reaction. A plot of moles product produced versus time (Figure 4.5) indicates that the reaction is autocatalytic. Competitive experiments with cyclohexene and cyclohexene-d_{10} show an isotope effect of 8.2, consistent with a mechanism involving hydrogen abstraction in the rate-determining step. Addition of a radical trap, BHT, completely inhibits the reaction. The radical chain mechanism is also consistent with the high percentage of allylic oxidation products observed in the reaction of cyclohexene with dioxygen.

Moreover, this mechanism explains the greater reactivity observed with dioxygen and Fe(TFPPBr$_8$)Cl compared to tetraphenylporphyrinato-iron(III) chloride or tetrakis(pentafluorophenyl)porphyrinato-iron(III) chloride. The electron-withdrawing TFPPBr$_8$ ligand stabilizes the ferrous state, thereby enhancing the rate of alkyl peroxide oxidation.[36] In contrast, the lower reduction potentials of Fe(TFPP)Cl and Fe(TPP)Cl make these species poor oxidants, greatly slowing the ferric $\rightarrow$ ferrous step in the catalytic cycle. Furthermore, as with ferryl complexes, any radicals generated in the presence of Fe(TFPP)Cl or Fe(TPP)Cl may decompose the porphyrin by attacking C-H bonds. Halogenation of the β positions of the porphyrin is also believed to prevent formation of a μ-oxo dimer,[29,35] which is a mode of deactivation for both Fe(TPP)Cl and Fe(TFPP)Cl in reactions with dioxygen.[38] Thus the perhalogenated porphyrin has a faster rate of catalysis but a lower rate of catalyst degradation in solution

In order to further explore the possibility of an active iron(IV) or iron(V) oxo species, the synthesis of $Fe^{III}(TFPPBr_8)OH$ was attempted. Either chemical oxidants or bulk electrolysis could be used to generate a high-valent metal-oxo from an iron(III) hydroxide porphyrin. The pentafluorophenyl derivative, Fe(TFPP)OH, has been produced by washing Fe(TFPP)Cl with NaOH in benzene.[39] Instead, we attempted to isolate the hydroxide salt directly from the iron insertion reaction. As described in Chapter 2, $Fe^{II}(OAc)_2$ in glacial acetic acid inserts into $H_2TFPPBr_8$. The red color and red shifted Soret band of this species (in situ, λ_{max} = 448 and 578 nm) are consistent with formation of $Fe^{II}(TFPPBr_8)(OAc)_2$. Instead of brine, a weak sodium hydroxide solution was used to quench the metal insertion reaction, which would provide a hydroxide ligand for the iron ion. The porphyrin that precipitated from the reaction was filtered and washed with water; the absorption spectrum of resulting solid has a maximum at 434 and a Q band at 584 nm. The blue shift from $Fe(TFPPBr_8)Cl$, as well as the shape of the spectrum, is analogous to the change from Fe(TFPP)Cl to Fe(TFPP)OH, suggesting formation of $Fe(TFPPBr_8)OH$. Purification by column chromatography resulted in a new species, with a Soret at 418, a strong shoulder at 486, and a Q band at 600 nm. This species had the same spectrum as $Fe(TFPPBr_8)Cl$ after 48 hours in a methylene chloride/PhIO solution, and may be the μ-oxo dimer. The blue shift of the Soret band and red shift in the Q bands is again the same as observed in the TFPP complexes. Although modeling has suggested that formation of $[Fe(TFPPBr_8)]_2O$ is unfavorable due to poor steric interactions, a weak complex may form. Rather than becoming a permanently unreactive species, however, this dimer may be able to break apart and undergo further reactions, as has been suggested for $(FeTFPP)_2O$.[40] An alternative explanation of catalysis with a μ-oxo dimer is that dimerization *protects* one side of the porphyrin ligand, allowing oxidation to occur on the opposite side.[41] Attempts to obtain a ^{19}F NMR of this material were unsuccessful, and due to the small amounts of compound obtained, this chemistry was not further pursued.

Conclusion

Fe(TFPPBr$_8$)Cl is a remarkably active catalyst for the oxidation of cyclohexene with dioxygen, without added coreductant or light. The mechanism does not involve traditional high-valent metal-oxo intermediates, but interacts through the lower oxidation states of the porphyrin. Catalytic oxidation and reduction of alkyl peroxides by Fe(TFPPBr$_8$)Cl generates radicals that continue free-radical chemistry in solution.

Other than halogenated porphyrins, only the highly activated porphyrin RuTMP(O)$_2$ [dioxo(tetramesitylporphyrinato)-ruthenium(VI)] is known to catalyze the aerobic epoxidation of alkenes at ambient temperatures and pressures. Although able to catalyze 26 turnovers of cyclooctene in 24 hours (versus 73 TO of cyclohexene by Fe(TFPPBr$_8$)Cl), the Ru catalyst decomposes within this time period.[42] Another electron-deficient porphyrin, β-hexanitro-tetrakis(2,6-dichlorophenyl)porphyrinato iron (III) chloride, has been shown to activate alkanes at higher temperatures and high pressures of O_2.[43] Considering the similarity of the two porphyrins, it is likely that they operate by the same peroxide decomposition mechanism. Unfortunately, the exceptional reactivity of Fe(TFPPBr$_8$)Cl with dioxygen appears to come at the expense of the selectivity found with high-valent metal-oxo species.

Methods

Oxidation reactions were run as follows. 3-4 mg of porphyrin (approximately 2-3 μmol) were added to a clean, oven-dried reaction vessel with a stir bar. For iodoso-benzene experiments, 20-30 mg of PhIO were also weighed out into the flask (~ 50 eq PhIO/Fe). The reaction vessel was then fully assembled (Figure 4.9) and flushed from the top with Ar (for PhIO reactions) or O_2, allowing gas to escape through the open stopcock. 15 mL freshly distilled methylene chloride (under Ar or saturated with dioxygen) was added by syringe into the reaction vessel, followed by 1 mL of freshly

distilled substrate. From the solubility of oxygen in methylene chloride and the volume of the flask, the dioxygen reactions were calculated to have approximately 1240 μmol of O_2, or ~ 450 equivalents based on iron. The Kontes valve and stopcock were then closed, isolating the flask from the external atmosphere. The reactions were stirred for the next 24 - 48 hours, and aliquots taken by syringe every few hours for analysis of oxidation products.

The reactions were carried out in special flasks designed to minimize evaporation from the vessel during a reaction. A stopcock was attached to the side of a 25 mL Kjeldahl flask as shown in Figure 4.9. A hose could be attached to one of the two tubes on the stopcock, such that sample aliquots were not exposed to oxygen, and additional air did not leak into the flasks when an aliquot was removed. Unfortunately, this method prohibited clean kinetic measurements, since the concentration of oxygen in the flask at any given time was unknown. However, the rather excessive caution in sealing the flask was found to be necessary, since experiments run in round bottom flasks sealed only with a rubber septum had evidence of significant evaporation and/or leakage. Even with these precautions, the reaction volume decreased due to evaporation of the volatile solvent, and measurement reliability decreased significantly after 24 hours.

Gas chromatography was performed on a Hewlett Packard with a SD 1 column. Samples were identified by retention times relative to authentic samples. An internal standard (toluene) was added to each aliquot before injection in the GC and used to determine the concentration of each product.

Materials

Porphyrins were obtained as described in Chapter 2. Iodosobenzene was purchased from TCI. Some batches were rather yellow in color, and were washed with benzene to remove impurities, with only some success. Methylene chloride, styrene, cyclohexene, *tert*-butyl hydroperoxide, and GC standards were purchased from Aldrich.

References

(1) Groves, J. T.; Nemo, T. E.; Myers, R. S. *J. Am. Chem. Soc.* **1979**, *101*, 1032-1033.

(2) Meunier, B. *Chem. Rev.* **1992**, *92*, 1411-1456.

(3) Smith, J. L.; Sleath, P. *J. Chem. Soc., Perkin Trans. 2* **1982**, 1009-1014.

(4) Traylor, T. G.; Tsuchiya, S. *Inorg. Chem.* **1987**, *26*, 1338-1339.

(5) Traylor, P. S.; Dolphin, D.; Traylor, T. G. *J. Chem. Soc., Chem. Commun.* **1984**, 279-280.

(6) Groves, J. T.; Quinn, R. *Inorg. Chem.* **1984**, *23*, 3844-3846.

(7) Chang, C. K.; Ebina, F. *J. Chem. Soc., Chem. Commun.* **1981**, 778-779.

(8) Bartoli, J. F.; Brigaud, O.; Battioni, P.; Mansuy, D. *J. Chem. Soc., Chem. Commun.* **1991**, 440-442.

(9) Traylor, T. G.; Hill, K. W.; Fann, W.; Tsuchiya, S.; Dunlap, B. E. *J. Am. Chem. Soc.* **1992**, *114*, 1308-1312.

(10) Assis, M. d. D.; Serra, O. A.; Iamamoto, Y.; Nascimento, O. R. *Inorg. Chim. Acta* **1987**, *187*, 107-114.

(11) Iamamoto, Y.; Assis, M. d. D.; Baffa, O.; Nakagaki, S.; Nascimento, O. R. *J. Inorg. Biochem.* **1993**, *52*, 191-200.

(12) Fujii, H. *J. Am. Chem. Soc.* **1993**, *115*, 4641-4648.

(13) Groves, J. T.; Watanabe, Y. *J. Am. Chem. Soc.* **1986**, *108*, 507-508.

(14) Groves, J. T.; Haushalter, R. C.; Nakamura, M.; Nemo, T. E.; Evans, B. J. *J. Am. Chem. Soc.* **1981**, *103*, 2884-2886.

(15) Hewson, W. D.; Hager, L. P. *Porphyrins* **1979**, *7*, 295-315.

(16) Penner-Hahn, J. E.; Eble, K. S.; McMurry, T. J.; Renner, M.; Balch, A. L.; Groves, J. T.; Dawson, J. H.; Hodgson, K. O. *J. Am. Chem. Soc.* **1986**, *108*, 7819-7825.

(17) He, G.-X.; Arasasingham, R. D.; Zhang, G.-H.; Bruice, T. C. *J. Am. Chem. Soc.* **1991**, *113*, 9828-9833.

(18) Groves, J. T.; W. J. Kruper, J. *J. Am. Chem. Soc.* **1979**, *101*, 7613-7615.

(19) Ostovic, D.; Bruice, T. C. *Acc. Chem. Res.* **1992**, *25*, 314-320.

(20) Ostovic, D.; Bruice, T. C. *J. Am. Chem. Soc.* **1988**, *110*, 6906-6908.

(21) Ostovic, D.; Bruice, T. C. *J. Am. Chem. Soc.* **1989**, *111*, 6511-6517.

(22) Naruta, Y.; Tani, F.; Ishihara, B.; Maruyama, K. *J. Am. Chem. Soc.* **1991**, *113*, 6865-6872.

(23) Traylor, T. G.; Nakano, T.; Dunlap, B. E.; Traylor, P. S.; Dolphin, D. *J. Am. Chem. Soc.* **1986**, *108*, 2782-2784.

(24) Groves, J. T.; Subramanian, D. V. *J. Am. Chem. Soc.* **1984**, *106*, 2177-2181.

(25) Traylor, T. G.; Miksztal, A. R. *J. Am. Chem. Soc.* **1989**, *111*, 7443-7448.

(26) Traylor, T. G.; Xu, F. *J. Am. Chem. Soc.* **1988**, *110*, 1953-1958.

(27) Ellis, P. E., Jr.; Lyons, J. E. *Coord. Chem. Rev.* **1990**, *105*, 181-193.

(28) Lyons, J. E.; Ellis, P. E., Jr. *Catal. Lett.* **1991**, *8*, 45-52.

(29) Grinstaff, M. W.; Hill, M. G.; Labinger, J. A.; Gray, H. B. *Science* **1994**, *264*, 1311-1313.

(30) Smegal, J. A.; Schardt, B. C.; Hill, C. L. *J. Am. Chem. Soc.* **1983**, *105*, 3510-3515.

(31) Ji, L.-N.; Liu, M.; Hsieh, A.-K.; Hor, T. S. A. *J. Mol. Catal.* **1991**, *70*, 247-257.

(32) Lu, W. Y.; Bartoli, J. F.; Battioni, P.; Mansuy, D. *New J. Chem.* **1992**, *16*, 621-628.

(33) Bottomley, L. A.; Kadish, K. M. *Inorg. Chem.* **1981**, *20*, 1348-1357.

(34) Lyons, J. E.; Ellis, P. E., Jr.; Durante, V. A. In *Structure-Activity and Selectivity Relationships in Heterogeneous Catalysis*; R. K. Grasselli and A. W. Sleight, Eds.; Elsevier Science Publishers B.V.: Amsterdam, 1991; pp 99-116.

(35) Ellis, P. E., Jr.; Lyons, J. E. *J. Chem. Soc., Chem. Commun.* **1989**, 1315-1316.

(36) Grinstaff, M. W.; Hill, M. G.; Birnbaum, E. R.; Schaefer, W. P.; Labinger, J. A.; Gray, H. B. submitted to *Inorg. Chem.*

(37) Labinger, J. A. *Catal. Lett.* **1994**, *26*, 95-99.

(38) Gunter, M. J.; Turner, P. *Coord. Chem. Rev.* **1991**, *108*, 115-161.

(39) Jayaraj, K.; Gold, A.; Toney, G. E.; Helms, J. H.; Hatfield, W. E. *Inorg. Chem.* **1986**, *25*, 3516-3518.

(40) Ellis, P. E., Jr.; Lyons, J. E. *Catal. Lett.* **1989**, *3*, 389-398.

(41) Chang, C. K.; Kuo, M.-S. *J. Am. Chem. Soc.* **1979**, *101*, 3413-3415.

(42) Groves, J. T.; Quinn, R. *J. Am. Chem. Soc.* **1985**, *107*, 5790-5792.

(43) Bartoli, J. F.; Battioni, P.; Foor, W. R. D.; Mansuy, D. *J. Chem. Soc., Chem. Commun.* **1994**, 23-24.

Figure 4.1 -- Intermediates that have been proposed in the literature for epoxidation by a high-valent metal-oxo. The metallaoxetane (I) and carbon radical (II) have been ruled out by recent experiments (see text), although this is not universally accepted. The carbocation (III) and carbocation radical (IV) are still considered viable intermediates, as is concerted oxygen insertion (V).

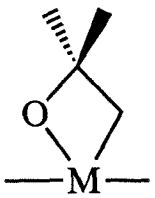

I

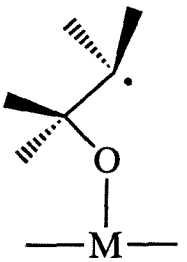

II

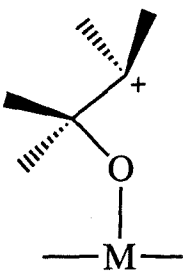

III

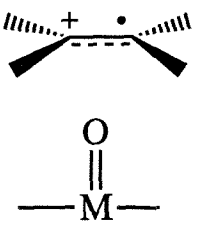

IV

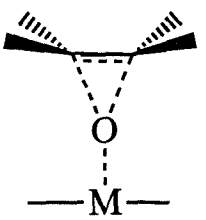

V

Figure 4.2 -- A proposed mechanism for epoxidation where the rate limiting step involves association of the olefin with the metal-oxo to form a charge transfer complex (CT). The CT can form an epoxide by concerted oxygen insertion, electrophilic addition, or electron transfer (shown from left to right). The carbocation radical (IV) can either recombine and form an epoxide, or continue on a radical pathway leading to hydroxylation or other rearrangement products. Mechanism modified from reference 19.

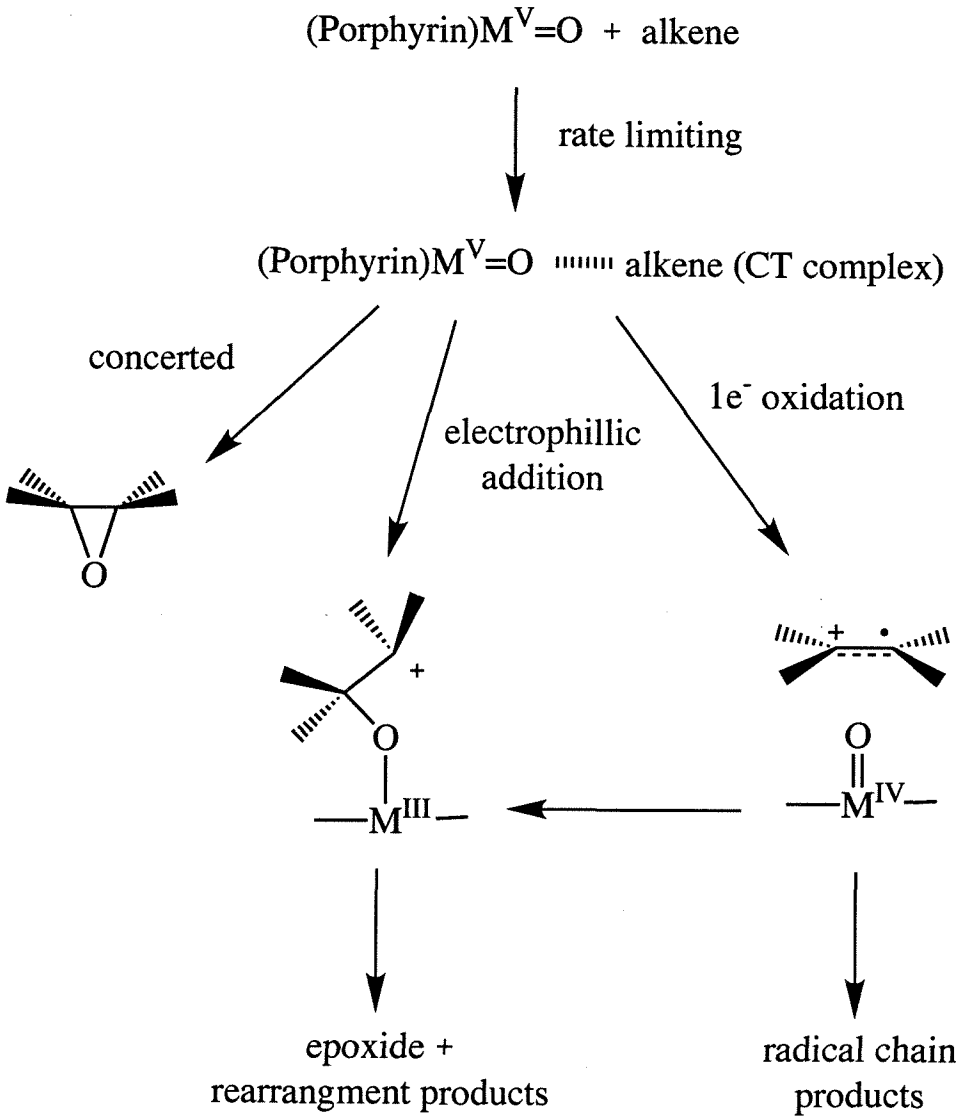
(Porphyrin)M^V=O + alkene
rate limiting
(Porphyrin)M^V=O alkene (CT complex)
concerted
electrophillic addition
1e⁻ oxidation
O
+
O
M^III
+
O
M^IV
epoxide + rearrangment products
radical chain products

Figure 4.3 -- Multiple pathways are believed to be responsible for epoxidation and hydroxylation of cyclohexene. Hydroxylation is generally believed to occur via hydrogen abstraction. In addition to the electron-transfer epoxidation mechanism shown, direct oxygen insertion may also occur. The branching ratio is dependent on the nature of the olefin, the porphyrin, and the solvent.

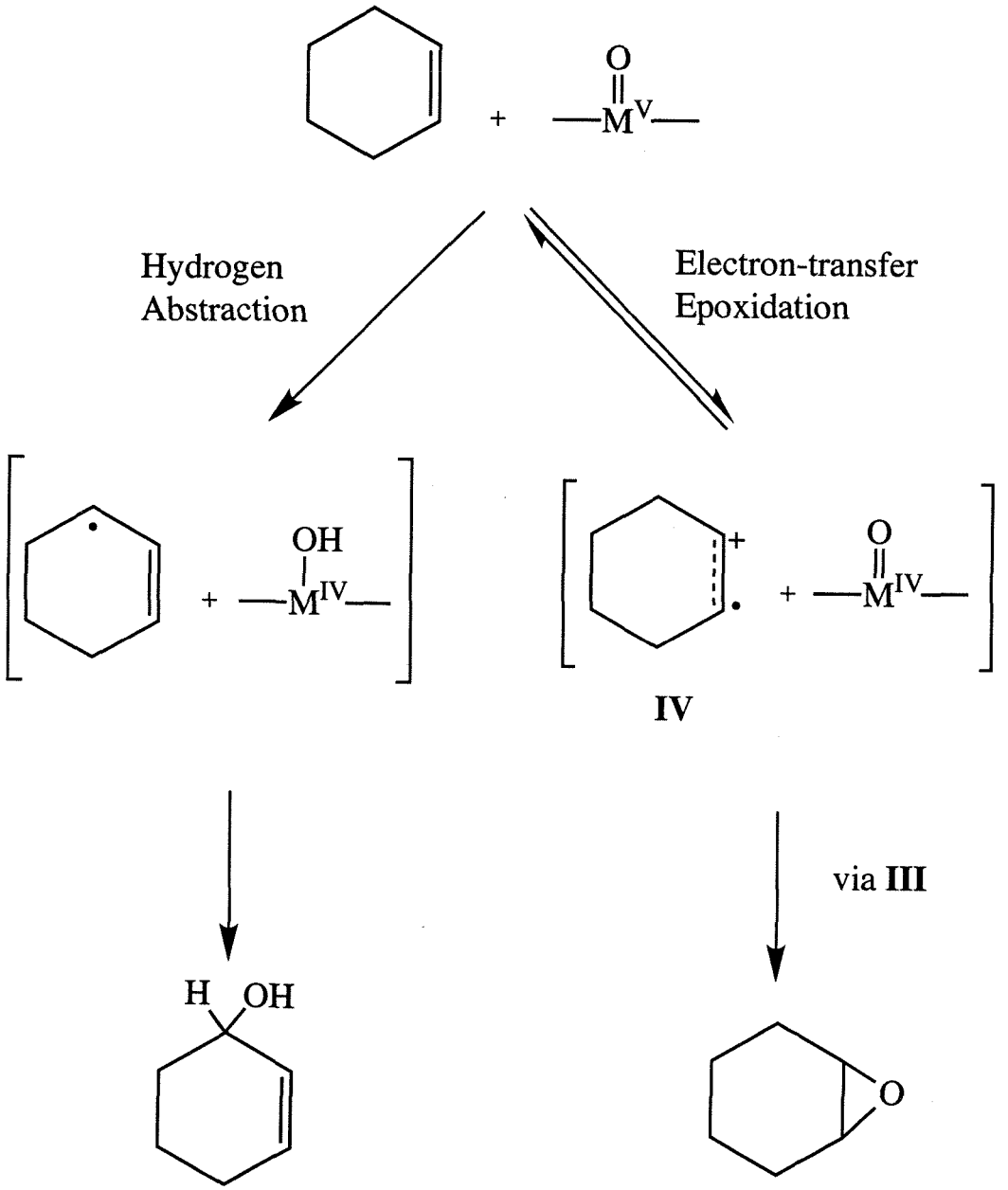
O
M^V
Hydrogen
Abstraction
Electron-transfer
Epoxidation
OH
M^IV
O
M^IV
IV
via III
H
OH
O

Figure 4.4 -- Turnovers and product distributions with cyclohexene and iron(III) porphyrins with dioxygen (at 3 hours) and PhIO (at 4 hours).

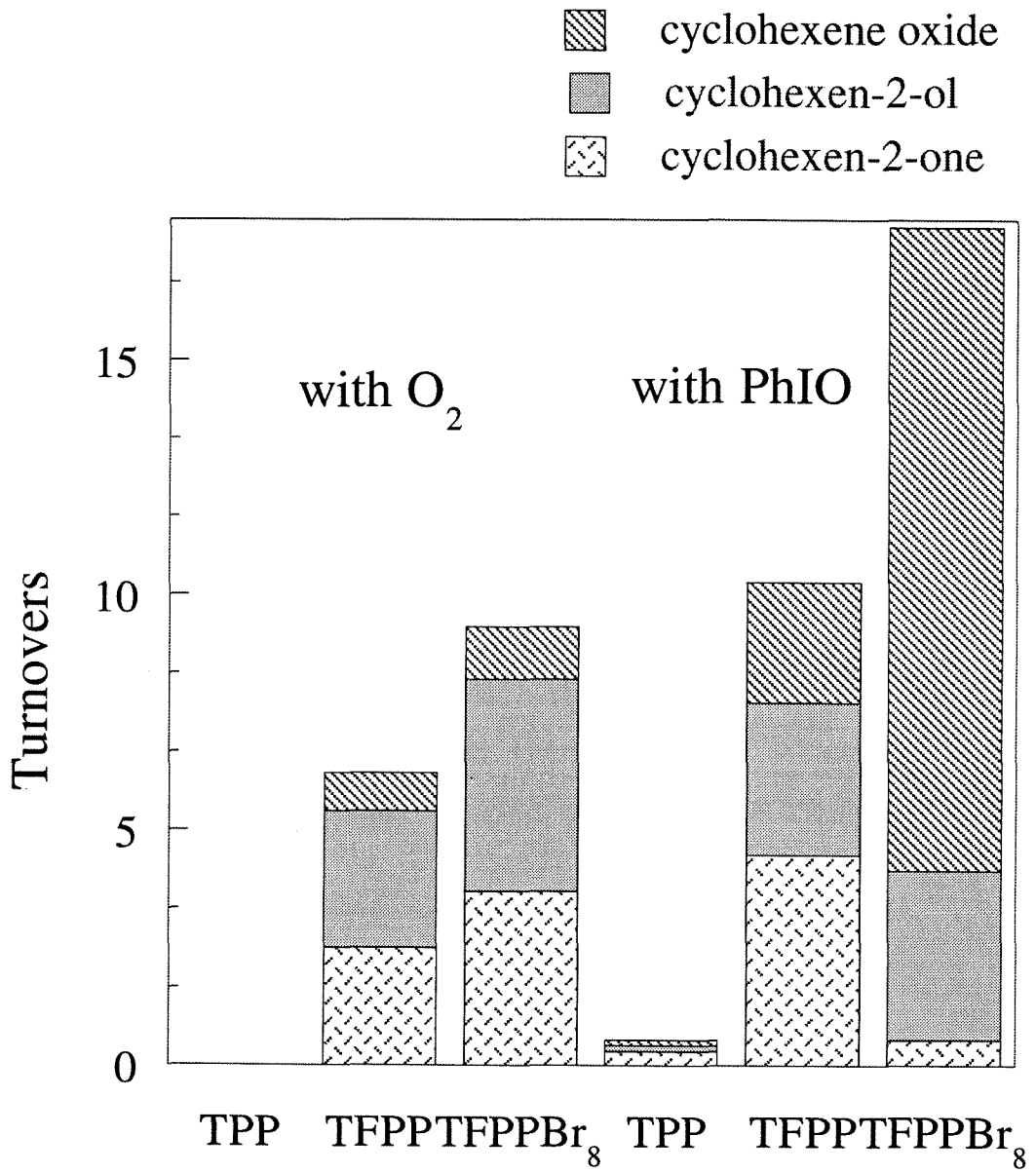
cyclohexene oxide
cyclohexen-2-ol
cyclohexen-2-one
with O_2
with PhIO
Turnovers
0
5
10
15
TPP
TFPP
TFPPBr$_8$
TPP
TFPP
TFPPBr$_8$

Figure 4.5 -- Product formation during cyclohexene oxidation with $Fe(TFPPBr_8)Cl$ and dioxygen. The curvature of the plot indicates the autocatalytic nature of the reaction.

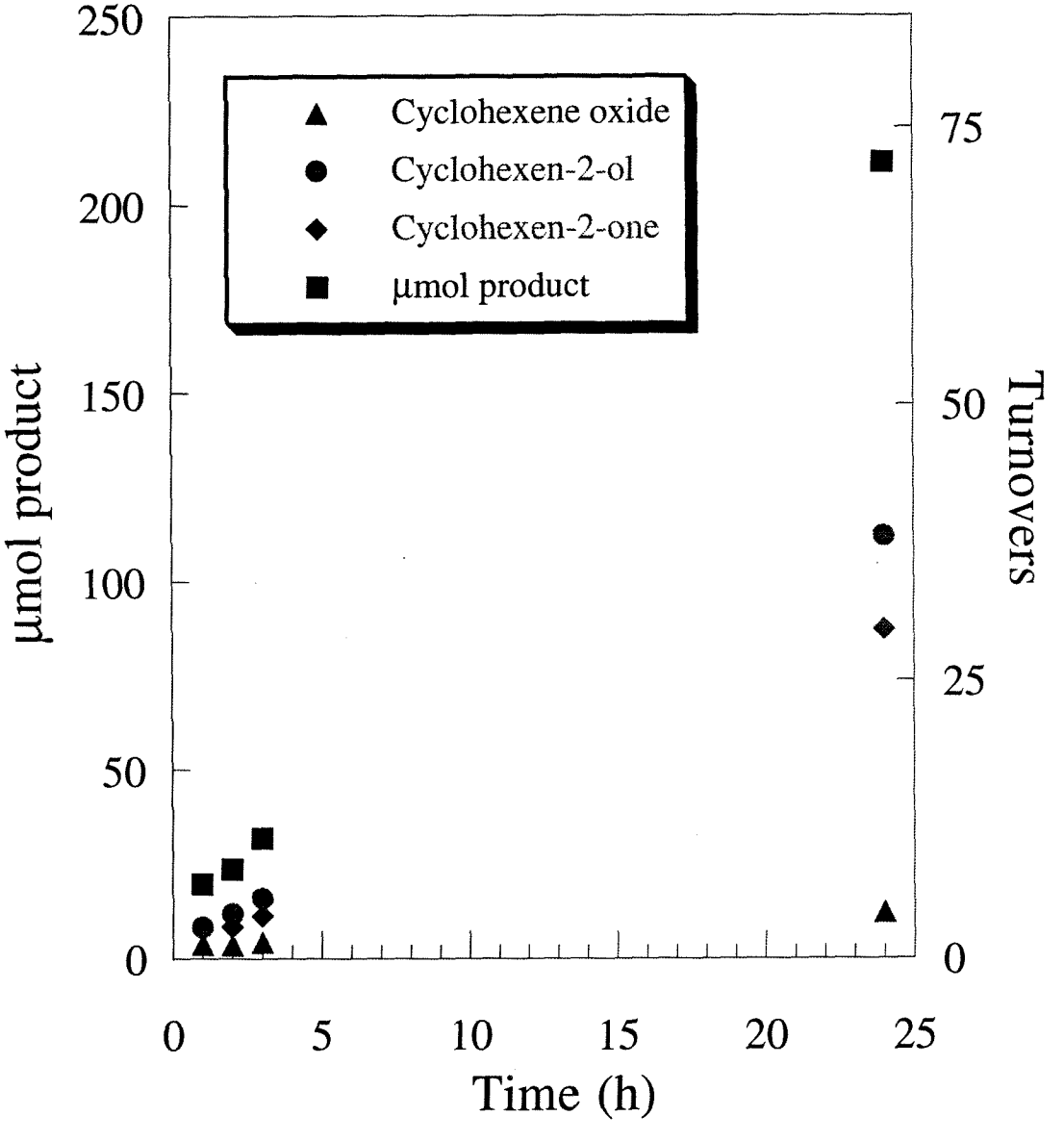
250
200
150
100
50
0
μmol product
75
50
25
0
Turnovers
0
5
10
15
20
25
Time (h)
Cyclohexene oxide
Cyclohexen-2-ol
Cyclohexen-2-one
μmol product

Figure 4.6 -- A plot of the catalytic activity (turnovers at 24 hours) observed for cyclohexene oxidation with dioxygen versus the reduction potential of the iron(III)-porphyrin catalyst (E° values: Fe(TPP)Cl < Fe(TFPP)Cl < $Fe(TFPPBr_8)Cl$).

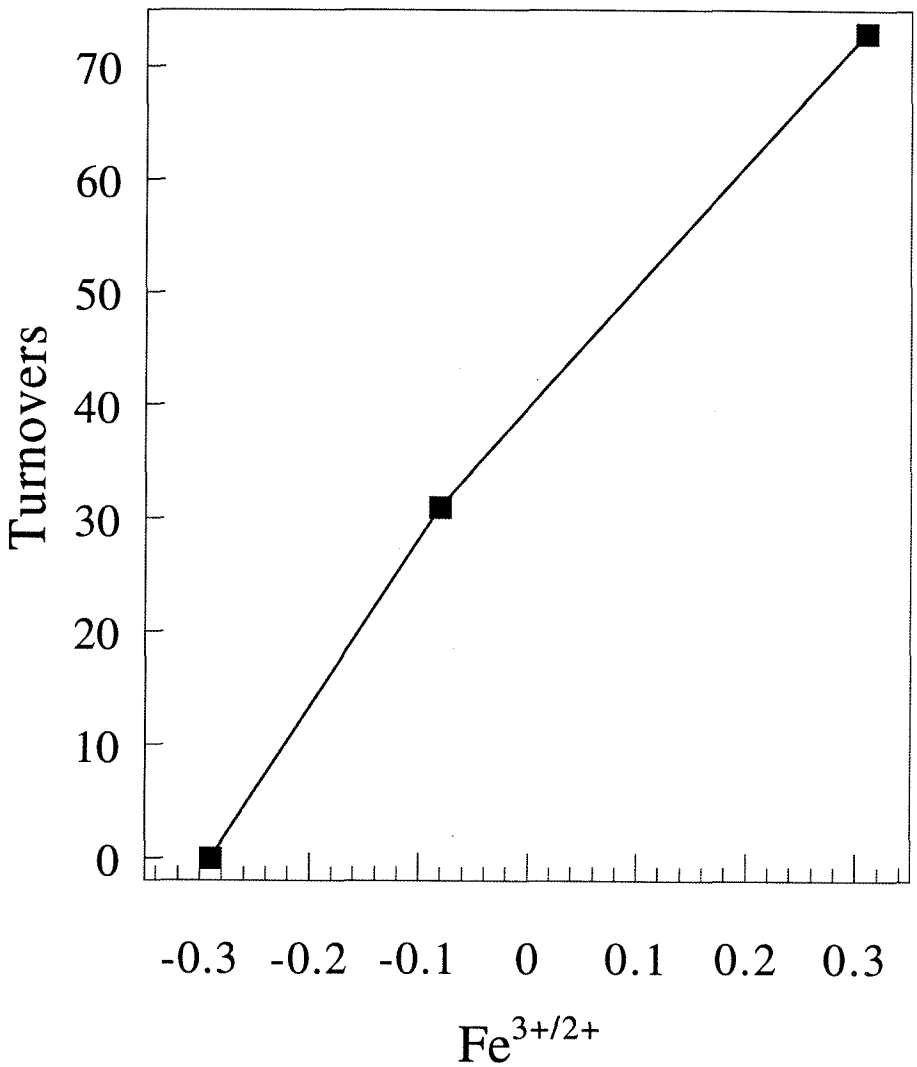
70
60
50
40
30
20
10
0
Turnovers
-0.3
-0.2
-0.1
0
0.1
0.2
0.3
Fe3+/2+

Figure 4.7 -- A proposed mechanism for direct activation of dioxygen initiated by oxygen binding to a ferrous porphyrin (modified from reference 34). The positive electrochemical potential ($Fe^{2+/3+}$) of the halogenated iron porphyrins were proposed to generate an iron(IV) oxo of comparable activity to that of a biological iron(V) oxo.

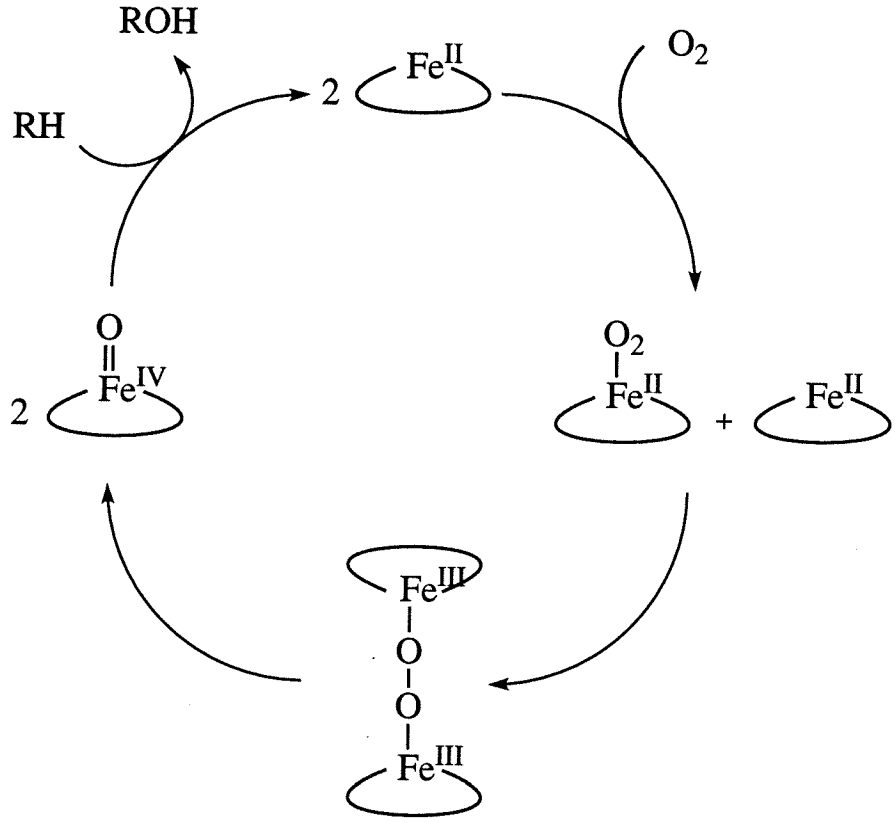

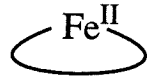

$= Fe^{II}(TFPPBr_8)$

Figure 4.8 -- The alkyl peroxide decomposition mechanism for dioxygen reactions with $Fe(TFPPBr_8)Cl$. Initiated by radicals in solution, the peroxides thereby generated are catalytically decomposed by the iron porphyrin. These radicals can further propigate the reaction.

Initiation by radicals
present in solution.

$$R\bullet + O_2 \longrightarrow ROO\bullet$$

$$ROO\bullet + RH \longrightarrow ROOH + R\bullet$$

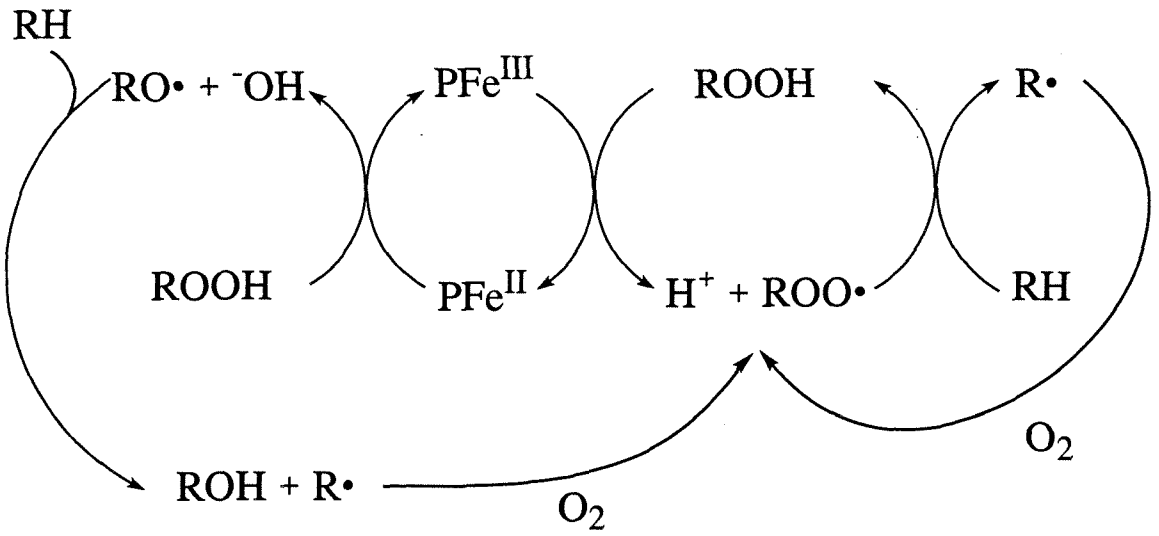

$$ROO\bullet + RO\bullet \longrightarrow \text{free radical propigation}$$

Figure 4.9 -- The modified Kjeldahl flask used for oxidation reactions. The porphyrin and iodosobenzene are added dry, then solvent and substrate are added. Aliquots can be removed without exposing the sample to air.

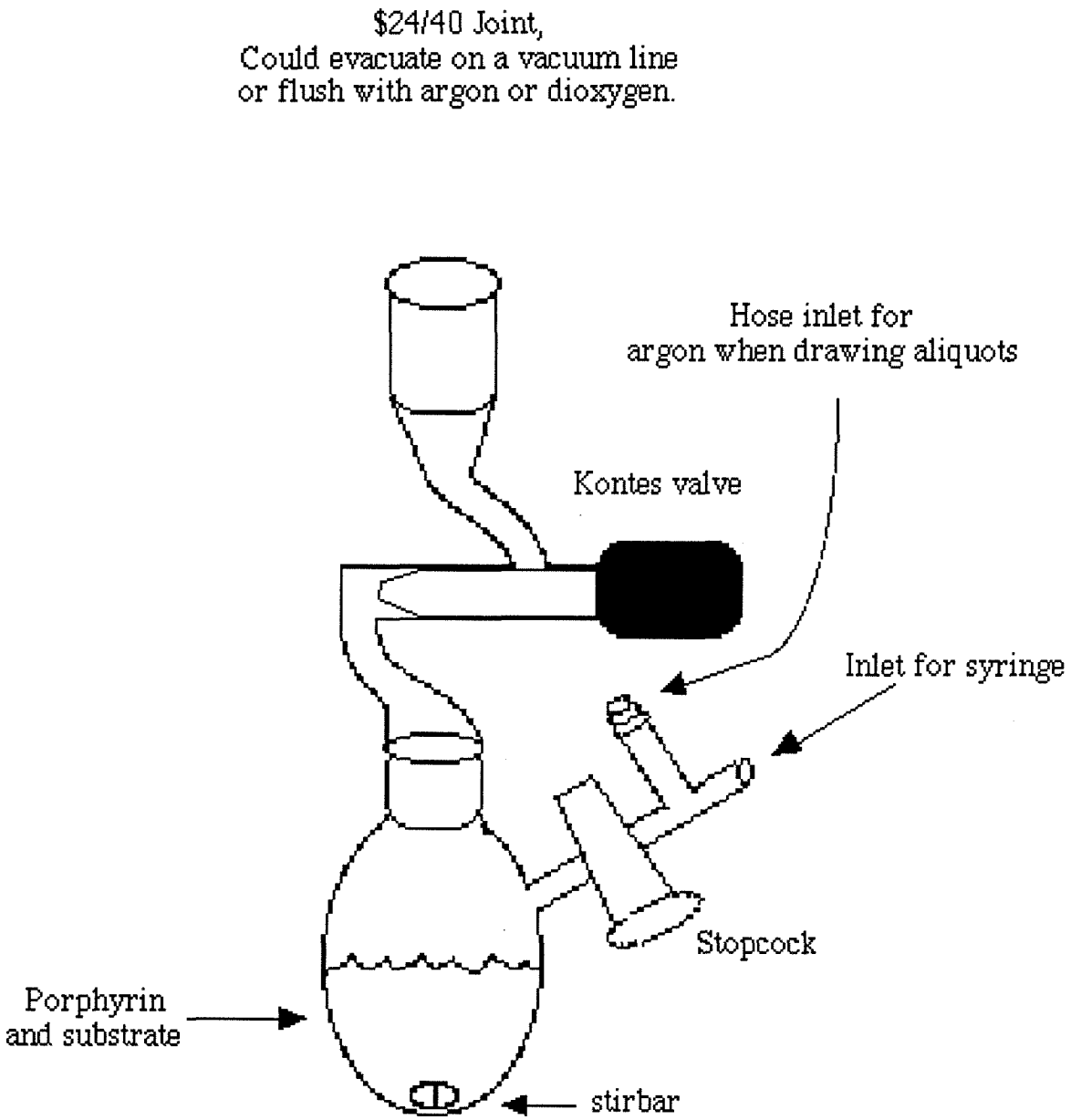
$24/40 Joint,
Could evacuate on a vacuum line
or flush with argon or dioxygen.
Hose inlet for
argon when drawing aliquots
Kontes valve
Inlet for syringe
Stopcock
Porphyrin
and substrate
stirbar

Chapter 5

On the Mechanism of Alkene Oxidation by Ruthenium Porphyrins and Molecular Oxygen

Introduction

As described in the preceding chapter, iron tetraphenylporphyrin derivatives are catalysts for the oxidation of alkenes and alkanes with oxygen donors. A smaller number of ruthenium porphyrins have also been synthesized to further explore biomimetic metalloporphyrin oxidation chemistry. Although a few have been investigated as oxidation catalysts, a greater portion of work has focused on using ruthenium porphyrins as model complexes for iron porphyrins or as systems for dihydrogen or dinitrogen activation. For example, cofacial ruthenium porphyrin dimers have been shown to bind dihydrogen in the core between the two porphyrin molecules.[1]

Ruthenium porphyrins are commonly isolated as six-coordinate Ru^{II}(porphyrin)L_2 species with $2e^-$ donor ligands such as pyridine or CO as compared to five-coordinate Fe^{III}(porphyrin)X complexes. Greater ligand field stabilization energy for the second row metal and π bonding from π acid ligands give ruthenium(II) porphyrins greater stability relative to iron hemes.[2] This increase in stability is exploited for mechanistic investigations, as intermediates in ruthenium oxidation reactions, such as (P)Ru^{IV}=O, can be isolated and better characterized than the corresponding iron porphyrin species. Furthermore, comparisons of iron, ruthenium, and osmium porphyrin spectroscopy have been useful in determining orbital energies in iron porphyrin compounds.[3-9]

Ruthenium tetramesitylporphyrins have been investigated as catalysts for the oxidation of hydrocarbons. Groves[10] found that RuTMP(CO) is oxidized to $Ru^{VI}TMP(O)_2$ with two equivalents of *m*-chloroperoxybenzoic acid (mCPBA). This species is moderately stable, and has been characterized by NMR, elemental analysis, and

UV-Vis spectroscopy. The ruthenium dioxo porphyrin complex is a competent stoichiometric oxidant of norbornene, resulting in 1.6 equivalents (eq) norbornene oxide per mole of porphyrin and a solvated $Ru^{II}TMP$ complex.[11] Transfer of the first oxygen occurs more readily than the second, indicating that the monooxo complex is not as effective an oxo transfer agent as the dioxo complex.[12] However, various N-oxides have been used as O-atom donors with $Ru^{VI}TMP(O)_2$ to catalytically oxidize alkenes[13,14] and alkanes[15] in good yields (30-90% based on N-oxide).

The carbonyl complexes RuTMP(CO), RuTPP(CO), RuOEP(CO) and RuTDFPP(CO) (TDFPP = 2,6-difluororphenylporphyrin) are also observed to catalyze hydrocarbon oxidation.[15,16] With *tert*-butyl hydroperoxide (TBHP) or sodium hypochlorite as the oxidant, over 100 turnovers of styrene in 24 hours are reported for RuTDFPP(CO), and even higher activity was reported with RuOEP(CO).[16] RuTMP(CO) and RuTPP(CO) do not show activity until addition of strong acid to the solution; once activated, both porphyrins catalyze the oxidation of adamantane with 2,6-dichloropyridine N-oxide. Activity is higher when the dioxo complex is used.[15] No mechanism was proposed to explain either the high activity with planar, unhalogenated OEP, or the "activation" of the carbonyl porphyrins by acid.

In addition to catalysis observed with N-oxides and peroxides, the dioxo ruthenium porphyrins are a unique example of porphyrin catalysis with dioxygen but without addition of a coreductant. $Ru^{VI}TMP(O)_2$ catalyzes the aerobic oxidation of olefins under mild conditions.[11] The proposed mechanism (Figure 5.1) suggests that $Ru^{IV}TMP(O)$, formed upon a single oxidation of substrate, disproportionates to reform the active Ru^{VI} species and a solvated ruthenium(II) porphyrin, $Ru^{II}TMP(S)_2$.[12] The weakly coordinated ruthenium(II) reacts with O_2 to complete the cycle. While other porphyrins such as $Ru^{VI}OEP(O)_2$ and $Ru^{VI}TPP(O)_2$ share the ability to stoichiometrically oxidize alkenes, the less sterically bulky compounds dimerize to $(Ru^{IV}P(OH))_2O$ rather than reform $Ru^{VI}P(O)_2$ in the presence of dioxygen.[17,18]

$RuTMP(O)_2$ has been utilized as a catalyst for the aerobic oxidation of thioethers, steroids, and esters.[19-22] Although these papers describe catalysis by $RuTMP(O)_2$ in good yield, few experiments have been conducted to probe the validity of the initially proposed Groves mechanism (Figure 5.1). Furthermore, there has been little comment on the unusual ability to activate dioxygen in combination with the inability of this species to oxidize alkanes. The mechanism of RuP(CO) activation by strong acid, or the possibility of a different mechanism with N-oxides (versus dioxygen) have also not been adequately addressed. In summary, although some of the extremely interesting and unique chemistry displayed by ruthenium porphyrins has been noted, little of it is well understood.

Our investigations into oxidation catalysis with perhalogenated iron porphyrins (Chapter 4) led to the synthesis and characterization of a perhalogenated ruthenium porphyrin complex, β-octachloro-tetrakis(pentafluorophenyl)porphyrinato-ruthenium(II) carbonyl ($RuTFPPCl_8(CO)$) (Chapters 2 and 3). Initially, the ruthenium porphyrin was to be used to generate stable ruthenium analogs to iron peroxy intermediates proposed in the decomposition of alkyl peroxides by $Fe(TFPPBr_8)Cl$, allowing a better understanding of the iron oxidation mechanism. Alternatively, the halogenated porphyrin could share the unusual reactivity of $Ru^{II}TMP$ with dioxygen. Catalytic activity in iron porphyrins has been shown to increase with the anodic shift in the iron reduction potential, suggesting that a halogenated ruthenium porphyrin may show higher activity than RuTMP. Indeed, $RuTFPPCl_8(CO)$ is an extremely active catalyst for olefin oxidation with dioxygen. The mechanism does not appear to be related to either the other halogenated metalloporphyrins or the unhalogenated ruthenium porphyrins, but is unique to $RuTFPPCl_8(CO)$.

Results

$RuTFPPCl_8(CO)$ is an efficient catalyst for the oxidation of alkenes with PhIO or molecular oxygen. The oxidation reactions were run under comparable conditions to those with $Fe(TFPPBr_8)Cl$ described in Chapter 4. Each reaction was initiated by addition of 1 mL substrate to 15 mL of a 0.1 mM solution of $RuTFPPCl_8(CO)$ in methylene chloride. The reaction vessel (Figure 4.9) also contained 40 equivalents iodosobenzene under argon, or if O_2 was the oxygen source, the solution and head space in the reaction vessel were saturated with dioxygen. Aliquots were taken every 2 hours and products detected by GC.

Iodosobenzene is not a very efficient oxygen source for cyclohexene oxidation with $RuTFPPCl_8(CO)$ (Figure 5.2, Table 5.1). Only 10 turnovers are observed in 24 hours, with formation of 42% epoxide. The selectivity for epoxide is less than with $Fe(TFPPBr_8)Cl$, but a notable lack of ketone is produced (< 2%). The reaction rate is highest initially, tapering off after the first 6 hours. The UV-Vis spectrum remains unchanged at the end of 24 hours, indicating that the decrease in rate is not due to porphyrin decomposition. Styrene is better oxidized by iodosobenzene and $RuTFPPCl_8(CO)$, with 26 turnovers in only 3 hours, 81% of which are styrene oxide.

The high selectivity for epoxidation observed with PhIO and $RuTFPPCl_8(CO)$ is consistent with formation of $Ru^{IV}TFPPCl_8(O)$. As described in Chapter 4, iodosobenzene reacts with metalloporphyrins to form a metal-oxo intermediate. In the presence of olefin, the oxo species forms a charge transfer complex that may lead to epoxidation via concerted oxene transfer or electrophilic addition to the carbon-carbon double bond (Figure 4.3). The decreased activity for cyclohexene oxidation by $Ru^{IV}TFPPCl_8(O)$ relative to "$Fe^{V}(TFPPBr_8)Cl(O)$" is not surprising, since the ruthenium porphyrin is one oxidation state lower than the iron analog.

Activity with dioxygen is quite substantial (Table 5.1). In 24 hours, 42 equivalents of cyclooctene are epoxidized to cyclooctene oxide. Benzaldehyde is the

sole product of styrene oxidation, producing only 2.5 turnovers in 3 hours. The greatest activity is seen in the oxidation of cyclohexene; 296 turnovers consisting of cyclohexene oxide (15%), 2-cyclohexen-1-ol (58%) and 2-cyclohexen-1-one (27%) are observed in 24 hours (Figure 5.3).

The mechanism with dioxygen is not as obvious. The different product selectivity observed in oxidation of both styrene and cyclohexene with dioxygen versus iodosobenzene suggests there is a different mechanism for the two O-atom sources. The increased amount of allylic and carbon-carbon bond cleavage oxidation products suggests that the mechanism with O_2 has a substantial radical contribution. Since reactions with PhIO are believed to go through a Ru^{IV} oxo intermediate, a different oxidizing species must be generated upon reaction with O_2. Unfortunately, the difficulty in obtaining large quantities of porphyrin has precluded the direct observation of intermediates in the dioxygen reactions. Instead, indirect methods have been used to probe the reaction mechanism. As many modes of interaction between oxygen and the porphyrin are possible, we have tried to test the viability of the most likely candidates.

A simple, direct method of dioxygen activation mimics dioxygenase rather than monooxygenase activity (Figure 4.7). Such a mechanism, initially proposed to explain oxidations with highly halogenated iron porphyrins,[23] is even more attractive for the ruthenium analogs, since no addition of coreductant would be required to initiate the cycle. Oxygen binds to $RuTFPPCl_8(CO)$, which reacts with another porphyrin molecule to form a μ-peroxo dimer, $(TFPPCl_8)Ru^{III}$-O-O-$Ru^{III}(TFPPCl_8)$. Homolytic O-O bond cleavage forms the active oxidant, Ru^{IV} monooxo, which returns to the catalyst resting state after oxidizing substrate. This mechanism is unlikely for two reasons. First, cleavage of the μ-peroxo bond to form $(P)Ru^{IV}$=O would produce the same oxidizing species as PhIO, and would therefore be expected to yield the same product distribution. This mechanism does not allow for the different selectivity observed with different oxidants. Furthermore, $Ru^{II}TFPPCl_8(CO)$ is air stable and shows no reaction with

dioxygen, even upon recrystallization from an air saturated solution. Thus the first step in the cycle does not occur.

A second possibility is that $RuTFPPCl_8(CO)$ and $Fe(TFPPBr_8)Cl$ operate by the same mechanism with oxygen (Figure 4.8). A plot of moles of cyclohexene product versus time for catalysis by $RuTFPPCl_8(CO)$ (Figure 5.3) shows a slight curvature, suggesting some initiation for this catalyst, although not as significant as observed for the iron analog. More importantly, no metal couple is accessible in the ruthenium porphyrin electrochemistry (Chapter 3), so no orbital of reasonable energy is available to transfer electrons to or from an alkyl peroxide.

The best evidence that $RuTFPPCl_8(CO)$ does not operate by an alkyl peroxide decomposition mechanism, however, is that it does not decompose peroxides at an appreciable rate. $Fe(TFPPBr_8)Cl$ has been shown to rapidly decompose *tert*-butyl hydroperoxide[24,25]; when TBHP is added to a solution of $Fe(TFPPBr_8)Cl$, oxygen is vigorously evolved. A similar concentration of $RuTFPPCl_8(CO)$ does not exhibit a visible reaction. A more sensitive analysis of hydrogen peroxide decomposition shows that the ruthenium porphyrin only decomposes 4.5 equivalents of peroxide in four hours, as measured by oxygen evolution. The iron porphyrin is much more efficient, with 68 turnovers in the same time period (Figure 5.4). The opposite relative activity is observed for cyclohexene oxidation with dioxygen, where $RuTFPPCl_8(CO)$ catalyzes 296 turnovers compared to only 73 by $Fe(TFPPBr_8)Cl$ in 24 hours. A purely radical peroxide decomposition mechanism is not consistent with these observations.

A third possibility is that this catalyst mimics the behavior of RuTMP(CO) with oxygen. A Ru^{VI} dioxo complex would be expected to exhibit different reactivity than a monooxo, thus resolving the problem of dissimilarity with the iodosobenzene results. Therefore an attempt was made to reproduce the Groves cycle with $RuTFPPCl_8(CO)$. As in the conversion of RuTMP(CO) to $Ru^{VI}TMP(O)_2$,[10] careful titration of a solution of $RuTFPPCl_8(CO)$ with mCPBA resulted in complete formation of a new species

(λ_{max} = 420, 514, 552 nm) after addition of two equivalents peroxide (Figure 5.5). Isosbestic points at 390, 417, 525, and 585 nm indicate that only a single species is formed. The slight red shift in the Soret band and the blue shift in the Q bands are consistent with spectral changes observed in the oxidation of RuOEP(CO) to $RuOEP(O)_2$,[18] suggesting that $Ru^{VI}TFPPCl_8(O)_2$ is formed. The disappearance of the carbonyl stretch in the IR indicates removal of the CO ligand, but no strong stretch is observable in the 700 to 900 cm^{-1} region, as would be expected for a ruthenium oxo.[12,18] However, this region contains strong solvent stretches, making detection of $\nu_{Ru=O}$ difficult by solution infrared spectroscopy.

The anodically shifted reduction potentials of $RuTFPPCl_8(CO)$ would destabilize the higher oxidation states relative to those of RuTPP complexes, making $Ru^{VI}TFPPCl_8(O)_2$ extremely reactive. In line with this expectation, any attempt to concentrate or isolate this species led to decomposition to a variety of porphyrin products. However, at low concentrations, such as in a range where UV-Visible spectroscopy of the porphyrin ligand is feasible (1 - 10 μM), the steps of the catalytic cycle can be observed (Figure 5.6). Addition of mCPBA to form $Ru^{VI}TFPPCl_8(O)_2$, followed by addition of a small amount of cyclohexene, results in a large decrease in the intensity of both the Soret and Q band absorptions. The bleach is not due to porphyrin decomposition, because addition of carbon monoxide gas regenerates the original spectrum with over 85% of the original intensity. The new spectrum is similar to that of $Ru^{IV}OEP(O)$[26] or $Ru^{IV}TPP(O)$,[17] with a slight blue shift in the Soret band and broad absorptions in the Q band region relative to the dioxo complex, suggesting formation of $Ru^{IV}TFPPCl_8(O)$. Increased recovery of the Soret band after 24 hours in the presence of substrate could indicate transfer of the second oxo ligand from $Ru^{IV}TFPPCl_8(O)$ to form another molecule of oxidized substrate and $Ru^{II}TFPPCl_8(S)_2$. Unfortunately, the amount of product generated was too small to be detected by the GC method used for the general catalysis experiments, and oxo-transfer to the olefin could not be confirmed.[27]

Oxidation of triphenylphosphine to triphenylphosphine oxide can be confirmed by ^{31}P NMR. Addition of two equivalents PPh_3 to a solution of $Ru^{VI}TFPPCl_8(O)_2$ led to a decrease in the 514 nm band and the 600 nm tailing associated with dioxo formation, and new Q bands at 542 and 553 nm (Figure 5.7a). Continued addition of PPh_3 resulted in a blue shift of the Q bands to 517 and 540 nm, which may correspond to the coordination of triphenylphosphine to $Ru^{II}TFPPCl_8$ (Figure 5.7b). These two steps are believed to correspond to oxidation of 2 eq PPh_3 by the dioxo porphyrin followed by coordination of PPh_3 to the solvated ruthenium(II) porphyrin.

The ^{31}P NMR of this sample after the reaction is complete does show a resonance for Ph_3PO at 29.9 ppm. A second signal, consistent with PPh_3 coordination to Ru^{II}, appears at 40 ppm in the ^{31}P NMR (no signal is observed at -6 ppm for free triphenylphosphine). For example, $Ru(COOMe)_2(CO)_2PPh_3$ has a chemical shift of 30.5 ppm.[28] Although the UV-Vis showed isosbestic conversion to "$RuTFPPCl_8(PPh_3)_2$", the ^{19}F NMR was not clean, indicating that coordination of triphenylphosphine is not quantitative. Additional peaks in the ^{19}F NMR may be due to partial degradation of the porphyrin ligand after treatment with a harsh oxidant such as mCPBA.

Addition of styrene to a solution of $Ru^{VI}TFPPCl_8(O)_2$ led to similar spectroscopic changes, indicating that the decrease in Soret intensity ("oxo transfer") is not dependent on the substrate. In the absence of a potential ligand, the Soret bleach was even more pronounced. Addition of a small amount of pyridine to this solution led to the formation of $RuTFPPCl_8(py)_2$ (confirmed by UV-Vis). The ease of formation of the bis-pyridine adduct is consistent with oxidation of substrate by $Ru^{VI}TFPPCl_8(O)_2$ to form $Ru^{II}TFPPCl_8(S)_2$ that is able to coordinate an available ligand.

These experiments suggest that $RuTFPPCl_8(CO)$ can undergo Groves type chemistry. The catalytic oxidation reactions with O_2, however, were conducted without any additional oxidant, allowing no mechanism for the initial formation of $Ru^{VI}TFPPCl_8(O)_2$ from the carbonyl species. In addition, oxo transfer is generally

accepted to be more selective than the catalysis observed in the dioxygen reactions. Although Groves chemistry is possible, it does not seem probable for the main mechanism for catalysis by $RuTFPPCl_8(CO)$ with dioxygen.

Therefore a modified mechanism is proposed, which reacts through the lower oxidation states, involving both a monooxo and a peroxo intermediate. As mentioned above, $Ru^{IV}TMP(O)$ is a weak oxo transfer agent; the more electron-withdrawing $TFPPCl_8$ ligand would be expected to result in a much more reactive monooxo complex. The reaction is initiated by a slow loss of CO (Figure 5.8). The solvated ruthenium(II) porphyrin, without the strong π acid effect of the carbonyl, would have a much lower $Ru^{III/II}$ couple, increasing the possibility of a reaction with dioxygen. Instead of forming $Ru^{IV}TFPPCl_8(O)$, as in the direct oxygen activation mechanism (Figure 4.7), the ruthenium(II) dioxygen complex could rearrange to a ruthenium peroxo species that can react with substrate. The peroxide intermediate can either abstract a hydrogen atom from substrate to form $Ru^{III}TFPPCl_8(OOH)$ or attack olefin to epoxidize one substrate molecule and form $Ru^{IV}TFPPCl_8(O)$. The branching at this point in the mechanism would accommodate the observation of allylic oxidation products from escape of R• which could initiate a free radical reaction. Decomposition of the alkyl peroxide radical to product and $RuTFPPCl_8(O)$ would result in a larger amount of epoxide formation relative to the purely radical alkyl peroxide mechanism of $Fe(TFPPBr_8)Cl$. This mechanism is similar to one proposed for stoichiometric oxidation by vanadium(V) peroxo complexes where a mixture of epoxidation and hydroxylation was observed.[29]

The modified peroxo intermediate mechanism does implicate an initiation period for the catalyst, as loss of the carbonyl ligand is required before interaction with dioxygen can occur. Chemical removal of the carbonyl ligand should abolish the initiation period and increase the amount of active catalyst, resulting in higher overall product formation. However, addition of a small amount of triethylamine-N-oxide (10 eq) or mCPBA (5-10 eq) to remove the carbonyl ligand did not increase the rate of reaction. The oxidation

reactions were initiated by addition of oxygen and cyclohexene to a solution of $RuTFPPCl_8(CO)$ and $(Et)_3NO$ or mCPBA. No change in the rate of catalysis was observed with triethylamine-N-oxide (Figure 5.9), though the product distribution was much more similar to that of $Fe(TFPPBr_8)Cl$ with dioxygen, with only 6% epoxide and 59% 2-cyclohexen-1-ol. The porphyrin spectrum was also affected by addition of $(Et)_3NO$. The Q band absorptions grew in intensity and moved to 510 and 535 nm, similar to the spectrum of $RuTFPPCl_8(py)_2$, suggesting that triethylamine may bind to ruthenium.

Reactions with mCPBA were substantially different; only 20 turnovers were observed, all within the first 2 hours. More epoxide was produced: 35% versus 15% with dioxygen alone. The lack of products suggests that the catalyst deactivated, although the spectrum was unchanged. It is possible that $Ru^{II}TFPPCl_8(L)_2$ remaining after the reaction with mCPBA dimerizes or forms another porphyrin product with a Soret at similar energy to $RuTFPPCl_8(CO)$. Although titrations with mCPBA suggest relatively stable formation of $Ru^{VI}TFPPCl_8(O)_2$, the catalysis experiments are run at significantly higher concentration of porphyrin (> 25 X). The lack of activity suggests that the carbonyl free porphyrin is not stable at higher concentrations, and perhaps dimerizes to a catalytically inactive species. In a normal cyclohexene oxidation reaction, only a small amount of ruthenium porphyrin is an active catalyst (has lost CO) at any given time. Therefore the concentration of $Ru^{IV}TFPPCl_8(O)$ is quite low, and reacts with substrate before deactivation (via dimerization) can occur. Alternatively, the mechanism proposed in Figure 5.9 may be incorrect; the carbonyl ligand may remain on the ruthenium for the duration of the reaction, and activation of the catalyst occurs by some other means.

Addition of TBHP could also serve to initiate the reaction. Unlike mCPBA, TBHP is not a strong enough oxidant to remove the carbonyl ligand. However, it is capable of generating free radicals, and could initiate a radical based reaction in solution.

Addition of 10 equivalents TBHP to a solution of $RuTFPPCl_8(CO)$ in the presence of cyclohexene and O_2 results in no increase in the number of moles of products produced (Figure 5.10a). The product distribution in these reactions is the same as with dioxygen alone.

If a larger amount of TBHP is added, the reaction is much faster, with 200 turnovers in the first hour. The product distribution is also significantly different, with 10% epoxide and 50% 2-cyclohexen-1-ol throughout the run. It is not clear if the porphyrin is involved in this chemistry, or if the TBHP has simply initiated a free radical reaction. If the data is replotted in terms of turnovers, then a significant increase in rate is observed with either 10 or 300 equivalents of TBHP (Figure 5.10b). Interpretation of this result is complicated by the fact that only 50% as much porphyrin catalyst was used in the peroxide experiment.

Phase transfer of dioxygen into the solution is not rate limiting. Although solubility of dioxygen in methylene chloride is only 10 mM, this does not limit the reaction rate. A decrease in the stir rate (Figure 5.11) or even a complete lack of stirring does not curtail the rate of product formation. In fact, as seen in Figure 5.11, the slower stirred reaction showed more turnovers in an equal time period. A completely unstirred reaction also showed slightly higher activity, suggesting that a lower concentration of oxygen in solution may enhance reactivity.

A further test of the peroxo mechanism used the presence of additional carbon monoxide to inhibit the reaction. If catalyst activation involves spontaneous loss of CO, exposure to a carbon monoxide atmosphere should shut down catalysis by pushing the equilibrium towards the inactive CO bound form. As mentioned above, both UV-Vis and IR spectroscopy indicate that the carbonyl ligand remains bound both during and after a catalytic run. However, the presence of a small amount of ruthenium porphyrin without CO would be difficult to detect by these methods. To further explore the role of the carbonyl ligand, oxidation of cyclohexene by $RuTFPPCl_8(CO)$ was conducted under a

mixture of oxygen and carbon monoxide. Rather than preventing oxidation, identical rates of product formation were observed under a 50/50 O_2/CO atmosphere. The mixed atmosphere reaction only produced less product at the 24 hour time point, since only half as much total oxygen was in the reaction vessel (Figure 5.12).

The lack of inhibition by CO, while not encouraging, does not completely rule out the loss of CO as the first step in the reaction mechanism. As described above, if the carbonyl ligand is never lost, the subsequent reaction with dioxygen would never occur. However, if the reaction with dioxygen is much faster than recombination with carbon monoxide, some ruthenium porphyrin would remain active, allowing oxidation chemistry to take place in the presence of CO. However, it is surprising that absolutely no decrease in rate is observed.

A more interesting result from the mixed atmosphere experiments is the decrease in epoxide formation. At 24 hours, epoxide comprises only 7% of the total products, compared to 15% in a pure dioxygen environment. The decrease in epoxidation is offset by an increase in the amount of 2-cyclohexen-1-one to 36%. A possible explanation for the change in product distribution is that multiple oxidation pathways with dioxygen are available, and one that favors epoxidation is inhibited by carbon monoxide, while the other is not.

To insure that a small amount of uncarbonylated porphyrin is not present, a sample was exposed to a high pressure of CO. A small amount of $RuTFPPCl_8(CO)$ in CCl_4 or CH_2Cl_2 was placed into a Parr reactor and sealed under 1100 psi of carbon monoxide for 2 or 4 days. The pressure was released from the Parr bomb, and a measured amount of the porphyrin solution (containing ~ 2 μmol porphyrin) was injected directly into a solution of methylene chloride and cyclohexene to initiate a dioxygen catalysis reaction. Some carbon monoxide remained in the porphyrin solution, but as the mixed atmosphere experiments demonstrated, the presence of a small amount of CO does not inhibit the oxidation reaction.

Catalysis with the CO treated $RuTFPPCl_8(CO)$, however, had an extremely long initiation period. In 24 hours, only ten turnovers are observed, composed entirely of allylic oxidation products. By 48 hours, the reaction has fully initiated, with 238 turnovers comprised of 7% epoxide, 53% 2-cyclohexen-1-ol, and 40% 2-cyclohexen-one, similar to the product distribution observed in the mixed atmosphere reactions.

Spectroscopy of the CO treated porphyrin showed that the porphyrin had been modified during the long exposure to CO. The infrared spectrum of the porphyrin shows a new peak at 2112 cm^{-1} in addition to the peak assigned to the CO stretch of mono-carbonyl complex at 1981 cm^{-1}. The shift of ν_{CO} to higher energy is consistent with formation of $RuTFPPCl_8(CO)_2$; calculations indicate that a single CO stretch is expected for the bis-carbonyl porphyrin (approximating the porphyrin as D_{2d} symmetry). An intense peak also appeared in the IR spectrum at 1730 cm^{-1}, as discussed below.

The UV-Vis spectrum in either methylene chloride or carbon tetrachloride showed a slight red shift of the Soret to 420 nm and a slight blue shift and broadening of the Q bands (Figure 5.13). A strong absorption was also observed at 280 nm, but is not believed to be related to the porphyrin, since it appeared at different intensity relative to the porphyrin bands in the two runs. The high energy electronic transition and the 1730 cm^{-1} IR band are consistent with signals from a ketone. It is possible that some reaction between the reactive halogenated solvent and carbon monoxide could have occurred, resulting in formation of an acyl chloride or halogenated ketone. Low molecular weight acyl chlorides have a strong absorption around 1800 cm^{-1}, while halogenated ketones are at slightly lower energy. ^1H NMR of the carbon tetrachloride solution after removal from the Parr reactor showed a weak resonance at 4.3 ppm; chloroacetyl chloride has a chemical shift of 4.6 ppm. Unfortunately, it is impossible to do more than speculate on the source of these organic-type absorptions. However, repurification of the porphyrin by column chromotography does remove the 280 nm band from the UV-Vis and the 2112 cm^{-1} band from the IR. The purified porphyrin regains

catalytic activity, suggesting that chromotography removes the second CO from the ruthenium. In the absence of another axial ligand to displace the second carbonyl, such as water or acetone available in the usual post-synthesis workup, the second carbonyl ligand remains bound. The bis-carbonyl complex has no coordination sites available for chemistry, and no catalysis is observed. The pressure experiments suggest some interesting activation of CO under high pressures, but do not elucidate the role of the carbonyl ligand in catalysis.

Oxidation reactions with cyclohexene-d_{10} show a large isotope effect in reactions with dioxygen (Figure 5.14). In competitive experiments with equal amounts of deuterated and non-deuterated cyclohexene, the ratio of products at 24 hours gives an isotope effect of 7.0. The product distribution indicates a significant difference between epoxidation and allylic oxidation. Epoxide formation has no isotope effect (ratio = 1.0), 2-cyclohexen-1-ol has an isotope effect of 14.1, and the isotope effect for 2-cyclohexen-1-one formation is twice that number (29.5), suggesting that different processes are responsible for epoxidation and hydroxylation. Both the total isotope effect (8.2) and the individual isotope effects (1.15 for epoxidation, 9.2 and 19.3 for allylic oxidation) are of similar magnitude to those of $Fe(TFPPBr_8)Cl$, suggesting that hydrogen abstraction is involved in the rate determining step.

Non-competitive experiments reveal that the two cases are not the same. With $Fe(TFPPBr_8)Cl$, no reaction was seen with cyclohexene-d_{10} alone. Presumably, spontaneous radical formation from deuterated cyclohexene is slow due to the stronger C-D bond, and the reaction is never initiated. With $RuTFPPCl_8(CO)$, however, some reaction with cyclohexene-d_{10} was observed, indicating that the ruthenium porphyrin does not initiate solely by the same mechanism as the iron porphyrin. The non-competitive isotope effect is extremely large, (mol cyclohexene products)/(mol cyclohexene-d_{10} products) = 85. A large non-competitive isotope effect (50) has been reported for the oxidation of alcohols by $[(bpy)_2(py)Ru^{IV}(O)]^{2+}$.[30] The mechanism

involves hydride transfer followed by rapid proton equilibration from the aqueous medium, which is not applicable to the organic solvent reaction of $RuTFPPCl_8(CO)$.

Further experiments probed the possibility of a photochemical reaction. Since the reaction vessel is made of glass, ambient light enters the reaction, allowing the possibility of a light activated mechanism. Porphyrins are known to sensitize singlet oxygen ,[31] and the actual oxygen transfer step could be completely unrelated to the ruthenium center. To test the possibility of singlet oxygen production, $ZnTFPPCl_8$ was used in place of $RuTFPPCl_8(CO)$. Visible light has enough energy to cause a $\pi \rightarrow \pi^*$ transition in either the zinc or ruthenium porphyrin to form a triplet excited state. The triplet can act as a sensitizer to generate singlet oxygen, which could then react with cyclohexene. Under similar conditions to catalysis with $RuTFPPCl_8(CO)$, $ZnTFPPCl_8$ produced only 3 turnovers of cyclohexene in 24 hours, all of which were allylic oxidation products. This is within the range of products observed without any catalyst (between zero and 20 μmol product, approximately equal to up to 10 turnovers), suggesting that $ZnTFPPCl_8$ does not catalyze the oxidation of cyclohexene by any mechanism. The lack of activity from the porphyrin suggests that the $TFPPCl_8$ ligand is not an efficient oxygen sensitizer. Furthermore, the products are not consistent with an organic singlet oxygen reaction. $^1O_2$ generates ketones and carbon - carbon bond cleavage products rather than epoxides and alcohols.[32]

A second control was performed by excluding light from a catalysis reaction of $RuTFPPCl_8(CO)$ with dioxygen and cyclohexene. The initiation period increased dramatically, with almost no reaction in the first 10 hours. The initiation period for one reaction was longer than the second trial, resulting in very different turnover numbers at 24 hours (Figure 5.15). Once started, however, the reaction rate does increase; at 24 hours, Run 1 has 75% of the products of an average reaction in ambient light. The second reaction, which was slower to initiate, has only 16% as much activity in 24 hours. Product distributions are similar to a reaction in the light, suggesting that the same

mechanism is operating in both cases. Although singlet oxygen is not implicated, ambient light does play a role in initiating the reaction with $RuTFPPCl_8(CO)$ and O_2. The catalyst appears to be both thermally and photochemically activated.

Photolysis with visible light dramatically increases the rate of reaction (Figure 5.16). Two identical reactions were set up, one in the presence of normal room light (one light bulb from a hood lamp), and one continuously irradiated with a tungsten lamp (150W). The visible photolysis reaction shows 3.5 times as many turnovers in 8 hours (270 vs. 77), a tremendous enhancement by relatively low energy light. No porphyrin decomposition was observed. Product distributions are similar in the two reactions, indicating that a similar reaction is occurring in both cases.

To further explore the effect of light, the photophysics of $RuTFPPCl_8(CO)$ were investigated. Samples of $RuTFPPCl_8(CO)$ in methylene chloride were irradiated with pulses from a Nd-YAG or dye laser. Laser photolysis is known to photodissociate carbonyl ligands,[8] allowing an investigation of the reactivity of the bare ruthenium porphyrin. Excitation with 355 or 480 nm light produced a transient difference spectrum consistent with promotion of an electron into the π^* e_g orbital. A positive absorbance at 620 nm (Figure 5.17) and a negative change in optical density (ΔOD) in the Soret region indicate formation of a porphyrin triplet.

The kinetics describing decay of the excited state were dependent on the atmosphere over the solution. Both the 5 μs and 50 μs transient absorption spectra from 390 to 440 nm were obtained under carbon monoxide, ethylene, oxygen, and argon atmospheres; the transient spectra at 415 nm are shown in Figures 5.18 and 5.19 (additional traces are in Appendix 5). Under CO, biexponential decay of the excited state is observed. The faster rate,[33] $k_1 = 3.9 \times 10^6\ s^{-1}$, most likely corresponds to the decay of the porphyrin triplet excited state. The lifetime, 286 ns, is much shorter than the 36 μs porphyrin-based triplet excited state of RuTPP(CO),[34] but longer than the 15 ns charge transfer excited state of $RuTPP(py)_2$.[35] Generally, ruthenium porphyrin complexes have

$^3(\pi - \pi^*)$ lifetimes of tens of microseconds, while $(d - \pi^*)$ lifetimes are only a few nanoseconds.[31] Although the transient spectrum (at t = 0; Figure 5.17) shows porphyrin triplet characteristics, the short lifetime suggests that substantial mixing of the triplet and charge transfer states is occurring. The molecular orbital diagram of $RuTFPPCl_8(CO)$ (Figure 3.6) indicates that these two transitions are expected to be very close in energy. No emission was detected either at room temperature or from 2-methyl-tetrahydrofuran glass (77 K) at any wavelength out to 1100 nm.

The second kinetic term, $k_2 = 1.3 \times 10^5\ s^{-1}$, is believed to be due to recombination of CO. The concentration of CO in chloroform is 8.5 mM; assuming pseudo first order kinetics (and a similar concentration in CH_2Cl_2), the CO recombination rate is calculated as $1.5 \times 10^7\ M^{-1}\ s^{-1}$.

As observed in the laser traces at 415 nm on a 50 μs time base (Figure 5.19), the signal does not completely return to zero. The transient at 50 μs is after the excited state has decayed, and should correspond to the spectrum of the photoproduct from loss of the carbonyl ligand. The magnitude of the ΔOD indicates that the quantum yield for loss of CO is quite small, consistent with quantum yields observed for other ruthenium porphyrins.[8] Comparisons of the transient spectra under different atmospheres at 50 μs may give some indication of the reactivity of the carbonyl free ruthenium.

Oxygen efficiently quenches the triplet at a rate of $1.25 \times 10^7\ s^{-1}$. However, comparison of the transient absorption spectra at 50 μs under CO and O_2 does not suggest that oxygen binds to ruthenium (Figure 5.20). In fact, none of the spectra from the four samples have a distinct photoproduct at 50 μs, not supporting a mechanism involving oxygen binding to $RuTFPPCl_8$ after loss of CO. Furthermore, a spectrum taken of each sample after laser photolysis (Figure 5.21) indicates that significant amounts of porphyrin decomposition occur under an oxygen atmosphere.

An ethylene atmosphere results in decay rates of $k_1 = 8.9 \times 10^6\ s^{-1}$ and $k_2 = 4.2 \times 10^5\ s^{-1}$, indicating substantial quenching of the porphyrin excited state. Since ethylene is

unable to quench an excited state by energy transfer, it must be interacting more directly with the porphyrin to protect it from decomposition. The 50 μs transient under ethylene shows the greatest bleach in the Soret region, suggesting some interaction between ruthenium and olefin on this time scale. The ethylene sample shows no decomposition after photolysis, and even shows a slight increase in the Soret intensity. One explanation for these results is that ethylene binds to the excited state of $RuTFPPCl_8(CO)$ (k_1), and also to the photodissociated ruthenium porphyrin (k_2). Approximating the concentration of ethylene in solution as 5 mM gives an ethylene recombination rate with the photodissociated $RuTFPPCl_8$ of $8.4 \times 10^7\ M^{-1}\ s^{-1}$. However, olefin complexation after loss of CO is not likely to be relevant to the catalytic mechanism since the quantum yield is very small. Photolysis of CO is only observed with high energy light (355 nm), and the oxidation reactions are only irradiated with visible wavelengths.

Under an atmosphere of argon, the excited state again shows biexponential decay kinetics with $k_1 = 7.1 \times 10^6\ s^{-1}$ and $k_2 = 7.6 \times 10^5\ s^{-1}$. These results are not consistent with the description of the ethylene and dioxygen chemistry above. It is difficult to find an explanation for the increase in the decay rates under an inert atmosphere. One possibility is that in the absence of another ligand, the excited state interacts with methylene chloride, which is not a completely inert solvent. However, the decay rate would still be expected to be slower than rates under a CO atmosphere. A second possibility is that with the high energy light needed to observe the Soret band transients, multiple reactions may occur, complicating the kinetics.

Despite these problems, it is clear that excitation under ethylene results in a different product than photolysis under an inert atmosphere. Furthermore, although oxygen quenches the triplet excited state, there is no evidence for the substantial red shift normally observed upon binding of dioxygen.[4] These experiments suggest another possible mechanism that would initiate not with oxygen binding but with olefin binding. $RuTFPPCl_8(CO)$ is not able to catalyze the hydroxylation of alkanes with dioxygen,

suggesting that the electron richness of the carbon - carbon double bond is somehow important. Toluene, which has weak methyl C-H bonds, is not oxidized, either alone or in the presence of olefin to initiate reaction. Cumene or 3-methyl pentane, which is oxidized in low yield by $Fe(TFPPBr_8)Cl$, is also inactive with the ruthenium porphyrin and dioxygen.

Some evidence for olefin binding does exist. The carbonyl stretch in the solution IR of $RuTFPPCl_8(CO)$ in CCl_4 shifts 2.2 cm^{-1} upon addition of a small amount of cyclohexene. The shift to higher energy is consistent with weak competition by the π^* orbitals of the olefin for backbonding density from the ruthenium ion.

^1H NMR of $RuTFPPCl_8(CO)$ in acetone-d_6 after 24 hours under an ethylene atmosphere showed a weak resonance at -3.6 ppm. $RuTMP(C_2H_4)$ has a singlet at -3.27 ppm, assigned to a π complex of ethylene,[36] suggesting a similar assignment for $RuTFPPCl_8(C_2H_4)$. The carbonyl ligand may remain bound to trans to the olefin, but it is not clear from the NMR data. As the signal is present under an atmosphere of ethylene gas, exchange of the bound ethylene must be slow on the NMR time scale. The ^{19}F NMR of this sample still showed several different porphyrin species, indicating that only a small fraction of the porphyrin has ethylene bound.

UV-Vis data indicates that olefin binding, if occurring, is not highly favored. A solution of $RuTFPPCl_8(CO)$ with cyclohexene showed no change after 24 hours, suggesting that any olefin complex is of low enough concentration to be swamped by the signal of the carbonyl porphyrin. Alternatively, a weak interaction with olefin might cause only small changes in the UV-Vis spectrum.

If olefin binding is not favored for the ground state, the transient spectroscopy suggests that olefin binding may be more favorable in the excited state. A mechanism for catalytic olefin oxidation via the excited state is shown in Figure 5.22. The mixing of the $^3(\pi - \pi^*)$ and $(d - \pi^*)$ orbitals indicate that visible excitation of $RuTFPPCl_8(CO)$ might populate the MLCT state which results in an oxidized metal center in the excited state.

Olefin binding to the strongly oxidizing Ru^{III} would then be more likely to occur (Figure 5.22). Once a π olefin complex is formed, it may rearrange to form a ruthenium(IV) alkyl radical complex, which would readily combine with dioxygen. The bound alkyl peroxide radical could abstract a hydrogen atom from another substrate molecule, forming a peroxide complex. From this point, several different pathways could occur. The peroxide could homolytically cleave, either thermally or photochemically, initiating a free radical reaction (not shown). Alternatively, the peroxide could decompose via an intermolecular epoxidation reaction, leaving $Ru^{III}TFPPCl_8(OH)$ (after the formal π radical anion recombines with the ruthenium), which may recombine with another radical, R•, to form ROH and return the porphyrin to the resting state of the catalytic cycle.

This mechanism has several advantages over the mechanism involving loss of CO. First, spontaneous loss of the π acid carbonyl ligand is not likely for such an electron deficient porphyrin. Second, a partial carbon monoxide mechanism would not inhibit a photochemical reaction. Third, the dramatic increase in reactivity with light is explained by a greater amount of olefin complexation, which decomposes to lead directly to product or free radicals. The branching for a radical mechanism explains the large amount of allylic radical products observed. In addition, the large non-competitive isotope effect suggests that branching for the intermolecular mechanism is favored over C-D bond cleavage by a substantial amount, as is the high percentage of epoxidation formed with cyclohexene-d_{10}.

The peroxide experiments are also consistent with this mechanism. Addition of mCPBA removes the carbonyl ligand, which leads to a less oxidizing MLCT state with less or no affinity for olefin interaction. Addition of small amounts of TBHP may enhance the branching to the radical pathway by providing radicals to propigate radical reactions.

Conclusion

> Traditional scientific method has always been at the very best, 20-20 hindsight. It's good for seeing where you've been. It's good for testing the truth of what you think you know, but it can't tell you where you ought to go.
>
> -- Robert M. Pirsig, *Zen and the Art of Motorcycle Maintenance*, (1974).[37]

$RuTFPPCl_8(CO)$ has unprecedented ability for a carbonyl porphyrin to catalyze the oxidation of olefins with dioxygen. The mechanism does not appear to be radical decomposition of alkyl peroxides, as observed with $Fe(TFPPBr_8)Cl$, or the Groves dioxo ruthenium(VI) chemistry observed with RuTMP. Instead, a novel mechanism is proposed that involves an interaction of olefin with a mixed $^3(\pi - \pi^*) - (d - \pi^*)$ excited state. The electron-withdrawing porphyrin ligand creates a highly oxidizing excited state ruthenium center, which can be stabilized by an interaction with a π donor ligand. Photochemically driven oxidation chemistry with such low energy, low intensity light is quite amazing.

The involvement of light in the mechanism is indisputable. The dramatic enhancement of catalysis by even low-energy irradiation clearly favors a photochemical reaction mechanism. This is unprecedented for this class of porphyrin catalysts. $RuTFPPCl_8(CO)$ is unique in being the first stable, effective photocatalyst for olefin oxidation with dioxygen. Moreover, the catalyst would be extremely interesting for potential commercial applications since it fulfills the desired requirements of intense, low-energy light absorption.

Once olefin binding has occurred, the following steps in the reaction mechanism are not as clear. Although a logical mechanism can be proposed, further work would be necessary to completely understand the decomposition of the bound olefin/oxygen complex to form product. The potential also exists to tune the mechanism to favor one

branch of the proposed mechanism over another to increase the selectivity for epoxidation over hydroxylation. For example, selective photolysis at 420 nm (into the Soret band) could decrease undesired radical side reactions (such as decomposition of the bound alkylperoxide). Other conditions, such as solvent, temperature, and oxygen concentration have obvious potential to change the reaction selectivity. Since phase transfer is not rate limiting, perhaps a lower concentration of oxygen would increase the activity by decreasing unfavorable quenching of the excited state by oxygen (as suggested by the higher activity in the unstirred reactions).

A continuation of this project would include a more thorough investigation of the proposed photochemical activation of olefin. The photophysics of $RuTFPPCl_8(CO)$ could be better understood, especially the fast excited state decay under an argon atmosphere. Furthermore, if ethylene is quenching the $^3(\pi - \pi^*)$ excited state, varying the concentration of olefin would allow the quenching rate to be determined by Stern-Volmer kinetics. The possibility of a reaction with solvent could also be eliminated by repeating the reaction in a more inert solvent.

Experimental

Materials -- Ruthenium porphyrins were obtained as described in Chapter 2. Iodosobenzene and cyclohexene-d_{10} was purchased from TCI. Cyclohexene, cyclooctene (Aldrich), and methylene chloride (EM Science) were distilled under argon before use. Cyclohexene oxide, 2-cyclohexen-1-ol, 2-cyclohexen-1-one, *m*-chloroperoxybenzoic acid (mCPBA), *tert*-butyl hydroperoxide (TBHP), triethylamine-N-oxide, pyridine, and styrene were purchased from Aldrich. Hydrogen peroxide and acetone were purchased from EM Science. Carbon monoxide, ethylene, and dioxygen lecture bottles were purchased from Matheson.

Methods -- General oxidation reactions were conducted as described in Chapter 4. UV-Vis, NMR, and IR spectra were obtained as described in Chapters 2 and 3.

Reaction with peroxide -- Reactivity with TBHP was only determined in a qualitative fashion. Approximately 0.2 mL TBHP was added to a mM solution of either $RuTFPPCl_8(CO)$ or $Fe(TFPPBr_8)Cl$ in methylene chloride and allowed to stir for several hours. During this time, the solution was monitored visually for the evolution of gas that would indicate peroxide decomposition. A similar reaction with hydrogen peroxide was also monitored. In this case, 10 mg of porphyrin in 10 mL acetone was degassed on a high vacuum line. Five mL of 0.6 % hydrogen peroxide in acetone (degassed) was added, and the solution allowed to stir at room temperature. Every hour, the pressure of evolved gas was measured with a Toeppler pump and the number of moles calculated. An IR of the gas indicated that it was not carbon dioxide or carbon monoxide (from the carbonyl ligand of the ruthenium porphyrin), and was assumed to be dioxygen from the recombination of radicals produced from peroxide decomposition by the porphyrin.

Titration with mCPBA -- A solution of $RuTFPPCl_8(CO)$ in methylene chloride, such that the absorbance at either the Soret or Q band was close to 1, was prepared and

the exact concentration determined by either serial dilution or from the extinction coefficient. A solution of mCPBA (mM) was prepared by serial dilution. The porphyrin solution (2.5 mL) was titrated with 10 to 20 μL aliquots of mCPBA, and monitored by UV-Vis. The changes in the spectrum were complete after addition of less than 100 μL mCPBA solution, such that the porphyrin concentration remained relatively constant.

Titration with triphenylphosphine -- Aliquots from a mM solution of PPh_3 were added to the porphyrin solution immediately after addition of mCPBA, and monitored by UV-Vis. The solution was concentrated and spiked with $CDCl_3$ for NMR analysis.

Initiation with mCPBA or $(Et)_3NO$ -- Five to ten equivalents of oxidant (approximately 1-3 mg) were added with the porphyrin to the reaction flask. Under argon, 15 mL of methylene chloride were added, and the solution allowed to stir for two minutes. The reaction vessel was flushed with dioxygen as 1 mL of cyclohexene was added to start the oxidation reaction. Product formation was measured as before.

Mixed atmosphere reactions -- $RuTFPPCl_8(CO)$, solvent, and cyclohexene were mixed together in the reaction flask under argon. A mixture of carbon monoxide and oxygen was used to flush the argon from the flask and start the oxidation reaction.

Pressurized carbon monoxide reaction -- A mM solution of $RuTFPPCl_8(CO)$ in either methylene chloride or carbon tetrachloride was placed in a glass lined Parr reactor. The reactor was connected to a carbon monoxide tank, and flushed twice before full pressurization to 1100 psi of CO. The reaction was not stirred, but allowed to rest under CO pressure for 2 or 4 days (in CCl_4 or CH_2Cl_2, respectively). The pressure was let down, the Parr reactor opened and the porphyrin solution transferred to a Teflon capped vial. One mL of solution was used to run an oxidation reaction by injecting it into the reaction just before addition of dioxygen and substrate. The concentration of $RuTFPPCl_8(CO)$ in the reaction was calculated from the absorbance of the porphyrin solution.

Initiate with TBHP -- Attempts to initiate cyclohexene oxidation reactions with peroxide were accomplished by addition of TBHP to the reaction before addition of substrate. A small amount of a dilute TBHP solution was added to a solution of $RuTFPPCl_8(CO)$ in methylene chloride. Three separate reactions were run, adding 10, 225, or 380 equivalents of TBHP, respectively.

Stir rate -- The stir rate was lowered to half of normal for these reactions. One reaction was also run without any stirring.

Isotope effect -- The isotope effect was calculated from both competitive and non-competitive experiments. Competitive experiments were run with 15 mL of methylene chloride, 2 mg $RuTFPPCl_8(CO)$, and 1 mL each of cyclohexene and cyclohexene-d_{10}. The deuterated oxidation products ran slightly slower on the GC, allowing individual determination of deuterated and non-deuterated turnover numbers. Non-competitive experiments were run with 1 mL of cyclohexene-d_{10}, and compared to reactions run with perprotio cyclohexene. The isotope effect was calculated as a ratio of turnover numbers at 24 hours, since actual rates of product formation were not determined from these experiments.

Singlet oxygen generation -- A cyclohexene oxidation reaction was run as described above, with 3 μmol $ZnTFPPCl_8$ in place of $RuTFPPCl_8(CO)$.

Light experiments -- A cyclohexene oxidation reaction was run as described above, except the entire reaction flask was wrapped in foil to prevent incidental light from affecting the reaction. The light catalyzed reaction was accomplished by photolysis of an oxidation reaction with a normal 150 watt light bulb. The light was turned on before addition of substrate, and kept on for the duration of the experiment. The reaction was placed in a water bath to maintain ambient temperature.

Laser experiments -- Solutions of $RuTFPPCl_8(CO)$ in methylene chloride were degassed by three cycles of the freeze/pump/thaw method on a high vacuum line in a quartz laser cuvette. The cuvettes were then backfilled with the desired gas (argon,

carbon monoxide, oxygen, or ethylene) to 1 atm pressure. The excitation source for the time resolved absorption experiments was the third harmonic of a Quanta-Ray Nd-YAG laser with a 20 nm pulse width; a PTi arc lamp supplied the white probe light source, and a DH 10 SA Inc. monochrometer was placed before the R955 Hamamatsu PMT detector. The analog signal was analyzed by a RTD 710A digitizer, and worked up on a 386 PC. The arc lamp power was 68 W, and in the case of weak signals the arc lamp was pulsed at 6 Hz. The signal was amplified with a fast amplifier designed at Brookhaven National Laboratories.[38] Further data manipulation was accomplished on either a 486 PC or a Macintosh IISi with computer programs written at Caltech.

References and Notes

(1) Collman, J. P.; Hutchison, J. E.; Ennics, M. S.; Lopez, M. A.; Guilard, R. *J. Am. Chem. Soc.* **1992**, *114*, 8074-8080.

(2) Chow, B. C.; Cohen, I. A. *Bioinorg. Chem.* **1971**, *1*, 57-63.

(3) Antipas, A.; Buchler, J. W.; Gouterman, M.; Smith, P. D. *J. Am. Chem. Soc.* **1978**, *100*, 3015-3024.

(4) Barringer, L. F.; Rillema, D. P.; Ham, J. H. *J. Inorg. Biochem.* **1984**, *21*, 195-207.

(5) Brown, G. M.; Hopf, F. R.; Ferguson, J. A.; Meyer, T. J.; Whitten, D. G. *J. Am. Chem. Soc.* **1973**, *95*, 5939-5942.

(6) Brown, G. M.; Hopf, F. R.; Meyer, T. J.; Whitten, D. G. *J. Am. Chem. Soc.* **1975**, *97*, 5385-5390.

(7) Eaton, G. R.; Eaton, S. S. *J. Am. Chem. Soc.* **1975**, *97*, 235-236.

(8) Hopf, F. R.; O'Brien, T. P.; Scheidt, W. R.; Whitten, D. G. *J. Am. Chem. Soc.* **1975**, *97*, 277-281.

(9) Tsutsui, M.; Ostfeld, D.; Hoffman, L. M. *J. Am. Chem. Soc.* **1971**, *93*, 1820-1823.

(10) Groves, J. T.; Quinn, R. *Inorg. Chem.* **1984**, *23*, 3844-3846.

(11) Groves, J. T.; Quinn, R. *J. Am. Chem. Soc.* **1985**, *107*, 5790-5792.

(12) Groves, J. T.; Ahn, K.-H. *Inorg. Chem.* **1987**, *26*, 3831-3833.

(13) Ohtake, H.; Higuchi, T.; Hirobe, M. *Tetrahedron Lett.* **1992**, *33*, 2521-2524.

(14) Higuchi, T.; Ohtake, H.; Hirobe, M. *Tetrahedron Lett.* **1991**, *32*, 7435-7438.

(15) Ohtake, H.; Higuchi, T.; Hirobe, M. *J. Am. Chem. Soc.* **1992**, *114*, 10660-10662.

(16) Takagi, S.; Miyamoto, T. K.; Hamaguchi, M.; Sasaki, Y.; Matsurmura, T. *Inorg. Chim. Acta* **1990**, *173*, 215-221.

(17) Ho, C.; Leung, W.-H.; Chi-Ming-Che *J. Chem. Soc., Dalton Trans.* **1991**, 2933-2939.

(18) Leung, W.-H.; Chi-Ming-Che *J. Am. Chem. Soc.* **1989**, *111*, 8812-8818.

(19) Rajapakse, N.; James, B. R.; Dolphin, D. *Catal. Lett.* **1989**, *2*, 219-226.

(20) Tavares, M.; Ramasseul, R.; Marchon, J.-C.; Maumy, M. *Catal. Lett.* **1991**, *8*, 245-252.

(21) Tavares, M.; Ramasseul, R.; Marchon, J.-C.; Bachet, B.; Brassy, C.; Marnon, J.-P. *J. Chem. Soc., Perkin Trans. 2* **1992**, 1321-1329.

(22) Tavares, M.; Ramasseul, R.; Marchon, J.-C. *Catal. Lett.* **1990**, *4*, 163-168.

(23) Ellis, P. E., Jr.; Lyons, J. E. *Coord. Chem. Rev.* **1990**, *105*, 181-193.

(24) Lyons, J. E.; Ellis, P. E., Jr.; Myers, H. K., Jr.; Wagner, R. W. *J. Catal.* **1993**, *141*, 311-315.

(25) Grinstaff, M. W.; Hill, M. G.; Birnbaum, E. R.; Schaefer, W. P.; Labinger, J. A.; Gray, H. B. submitted to *Inorg. Chem.*

(26) Sugimoto, H.; Higashi, T.; Mori, M.; Nagano, M.; Yoshida, Z.-I.; Ogoshi, H. *Bull. Chem. Soc. Jpn.* **1982**, *55*, 822-828.

(27) Attempts to repeat this experiment on a larger scale were not successful. Oxidation of $RuTFPPCl_8(CO)$ was not clean, and although product formation was observed, it was impossible to differentiate between oxo transfer from the dioxo ruthenium porphyrin and direct reaction with excess mCPBA.

(28) Evans, E. W.; Howlader, M. B. H.; Atlay, M. T. *Inorg. Chim. Acta* **1995**, *230*, 193-197.

(29) Mimoun, H.; Saussine, L.; Daire, E.; Postel, M.; Fischer, J.; Weiss, R. *J. Am. Chem. Soc.* **1983**, *105*, 3101-3110.

(30) Roecker, L.; Meyer, T. J. *J. Am. Chem. Soc.* **1987**, *109*, 746-754.

(31) Kalyanasundaram, K. *Photochemistry of Polypyridine and Porphyrin Complexes*; Academic Press, Inc.: San Diego, 1992.

(32) March, J. *Advanced Organic Chemistry;* 4th ed.; John Wiley & Sons: New York, 1992, pp 708.

(33) The faster rates are taken from the 5 μs transient spectra, and the slower rates from the 50 μs data. The two sets of rates do not show good agreement, suggesting that additional processes are contributing to the kinetics.

(34) Rillema, D. P.; Nagle, J. K.; Barringer, L. F., Jr.; Meyer, T. J. *J. Am. Chem. Soc.* **1981**, *103*, 57-82.

(35) Levine, L. M. A.; Holten, D. *J. Phys. Chem.* **1988**, *92*, 714.

(36) Rajapakse, N.; James, B. R.; Dolphin, D. *Can. J. Chem.* **1990**, *68*, 2274-2277.

(37) Pirsig, R. *Zen and the Art of Motorcycle Maintanence*; Morrow: New York, 1974, pp 412.

(38) McCleskey, T. M. Thesis, California Institute of Technology, 1994.

Figure 5.1 -- The Groves mechanism for catalytic oxidation of olefins with dioxygen by $Ru^{VI}TMP(O)_2$. The ruthenium(IV) monooxo porphyrin disproportionates to reform the active ruthenium(VI) catalyst (see reference 11).

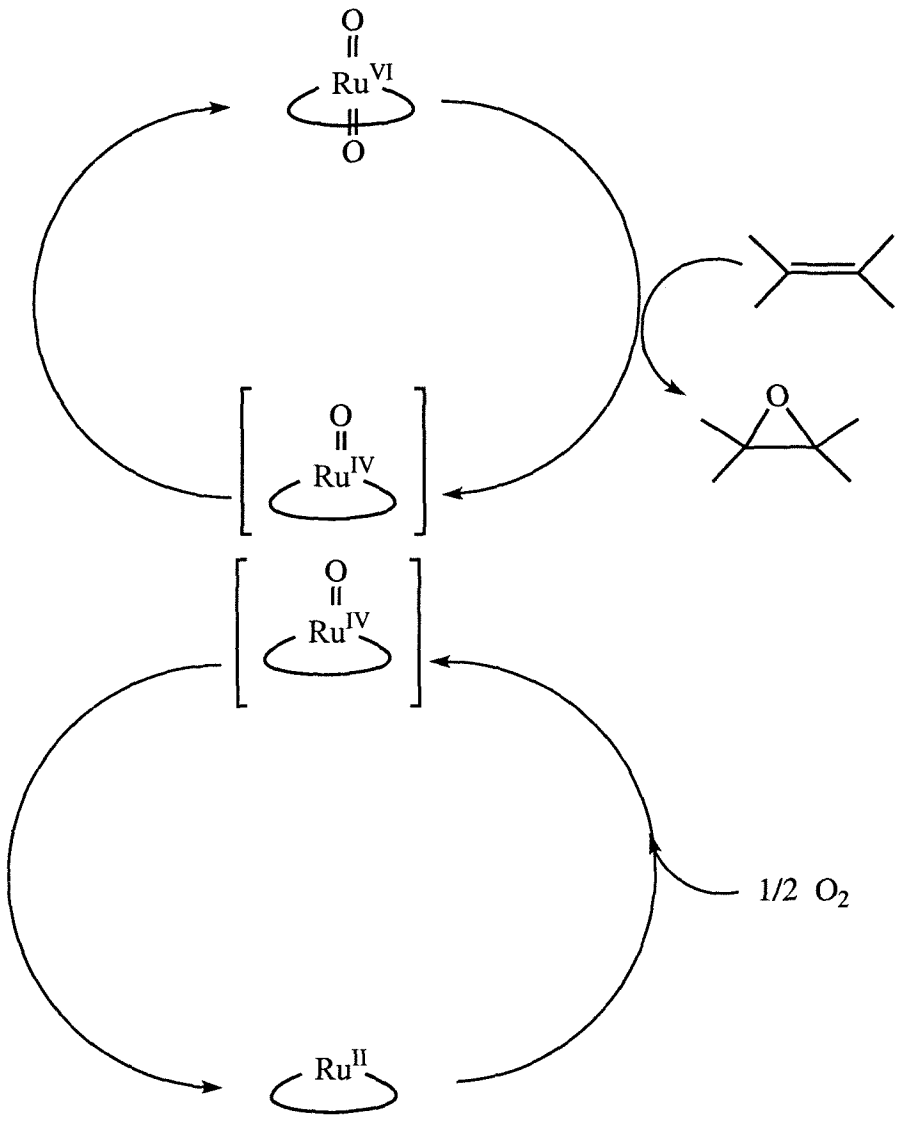

= Ruthenium tetramesitylporphyrin

Figure 5.2 -- Turnovers of cyclohexene by $RuTFPPCl_8(CO)$ with iodosobenzene in 24 hours, showing the observed product distribution. Only 25% of the available oxidant is used.

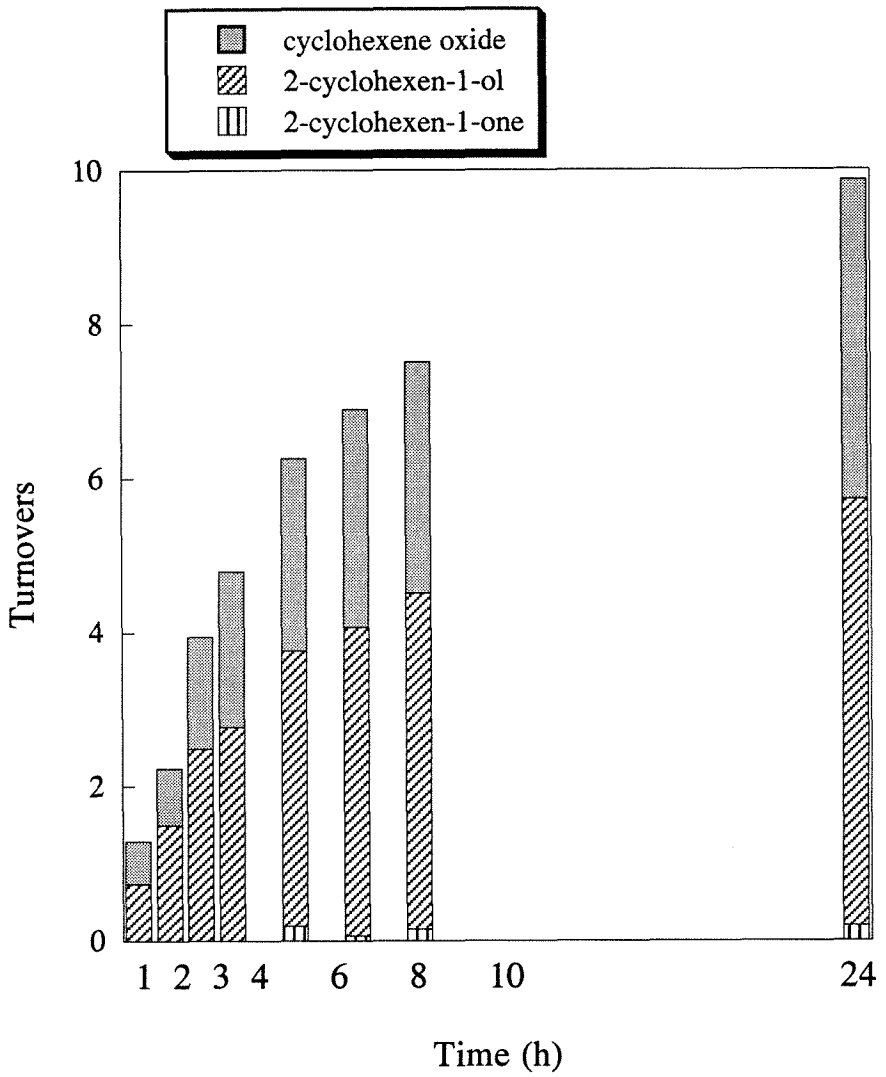
cyclohexene oxide
2-cyclohexen-1-ol
2-cyclohexen-1-one
10
8
6
4
2
0
Turnovers
1 2 3 4 6 8 10 24
Time (h)

Figure 5.3 -- Turnovers of cyclohexene by $RuTFPPCl_8(CO)$ with dioxygen in 24 hours, showing the observed product distribution. More allylic oxidation products are observed than with PhIO as the oxidant.

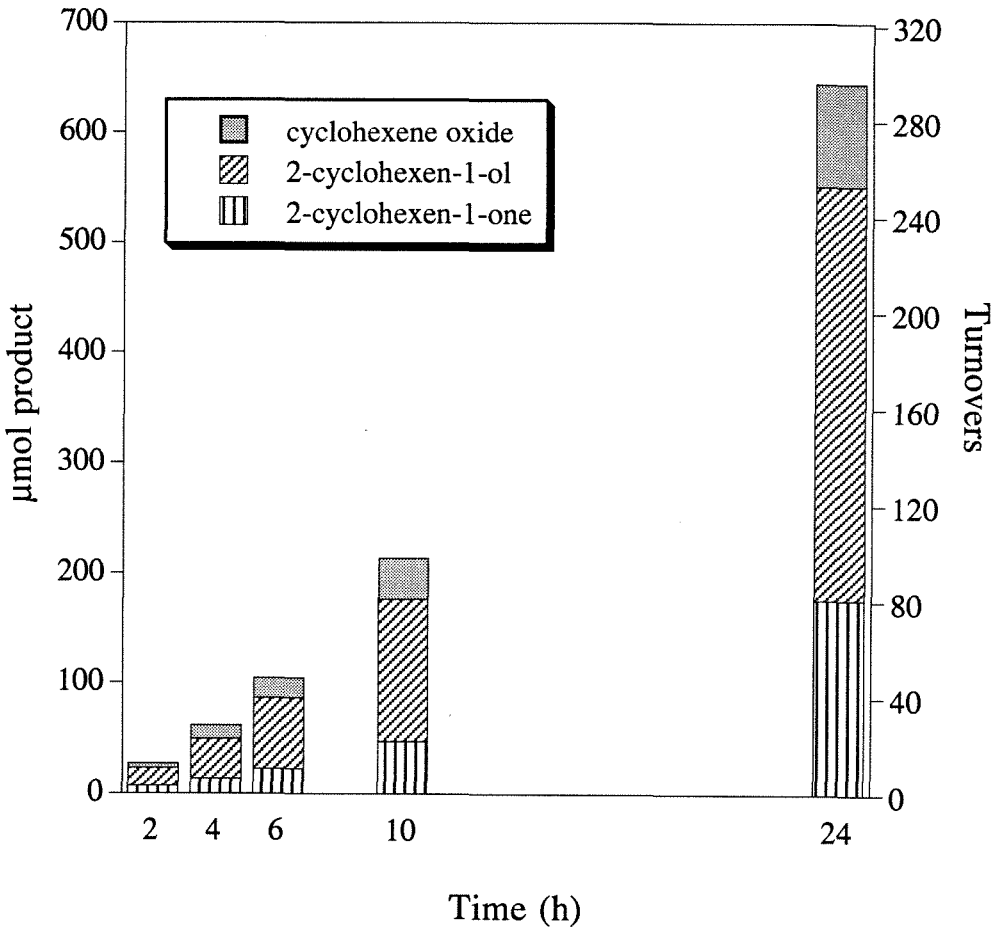
700
600
500
400
300
200
100
0
μmol product
cyclohexene oxide
2-cyclohexen-1-ol
2-cyclohexen-1-one
320
280
240
200
160
120
80
40
0
Turnovers
2
4
6
10
24
Time (h)

Figure 5.4 -- Hydrogen peroxide decomposition by $RuTFPPCl_8(CO)$ and $Fe(TFPPBr_8)Cl$ in acetone, as determined by oxygen evolution. The iron porphyrin decomposes 68 turnovers in 4 hours, while the ruthenium porphyrin shows much less activity in the same time period (4.5 TO).

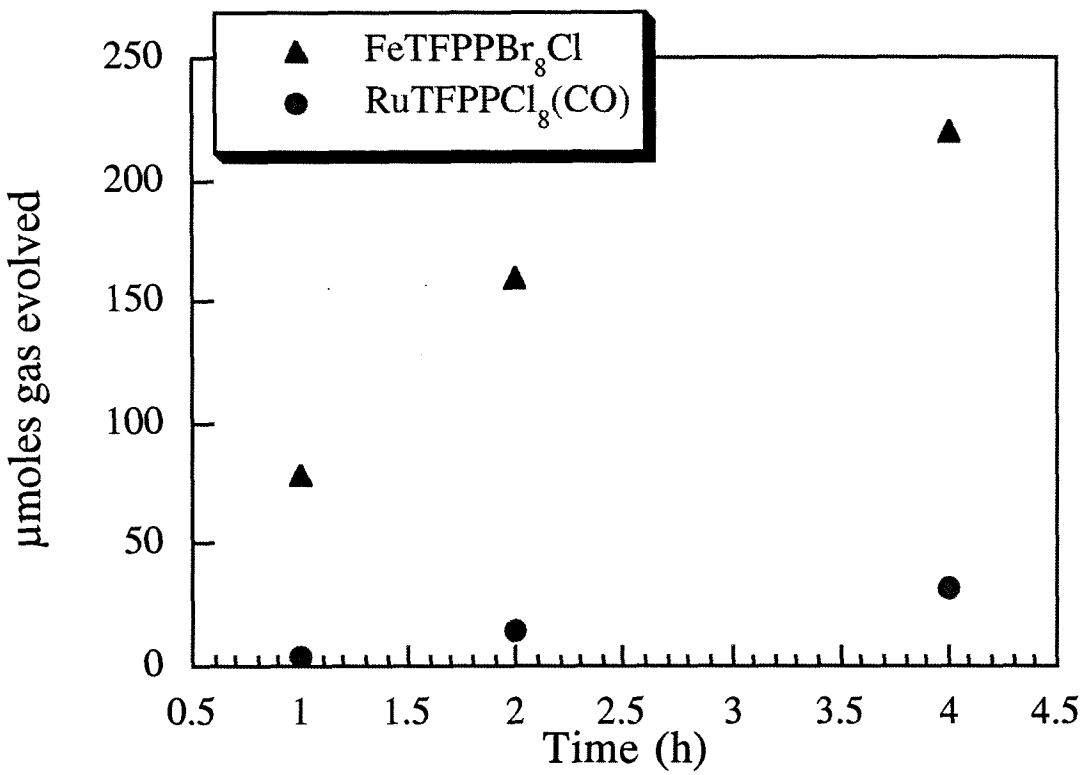
FeTFPPBr8Cl
RuTFPPCl8(CO)
250
200
150
100
50
0
µmoles gas evolved
0.5
1
1.5
2
2.5
3
3.5
4
4.5
Time (h)

Figure 5.5 -- UV-Vis spectrum of $RuTFPPCl_8(CO)$ upon titration with 2 equivalents of mCPBA to form $Ru^{VI}TFPPCl_8(O)_2$. The red shift of the Soret band to 420 nm is consistent with dioxo formation.

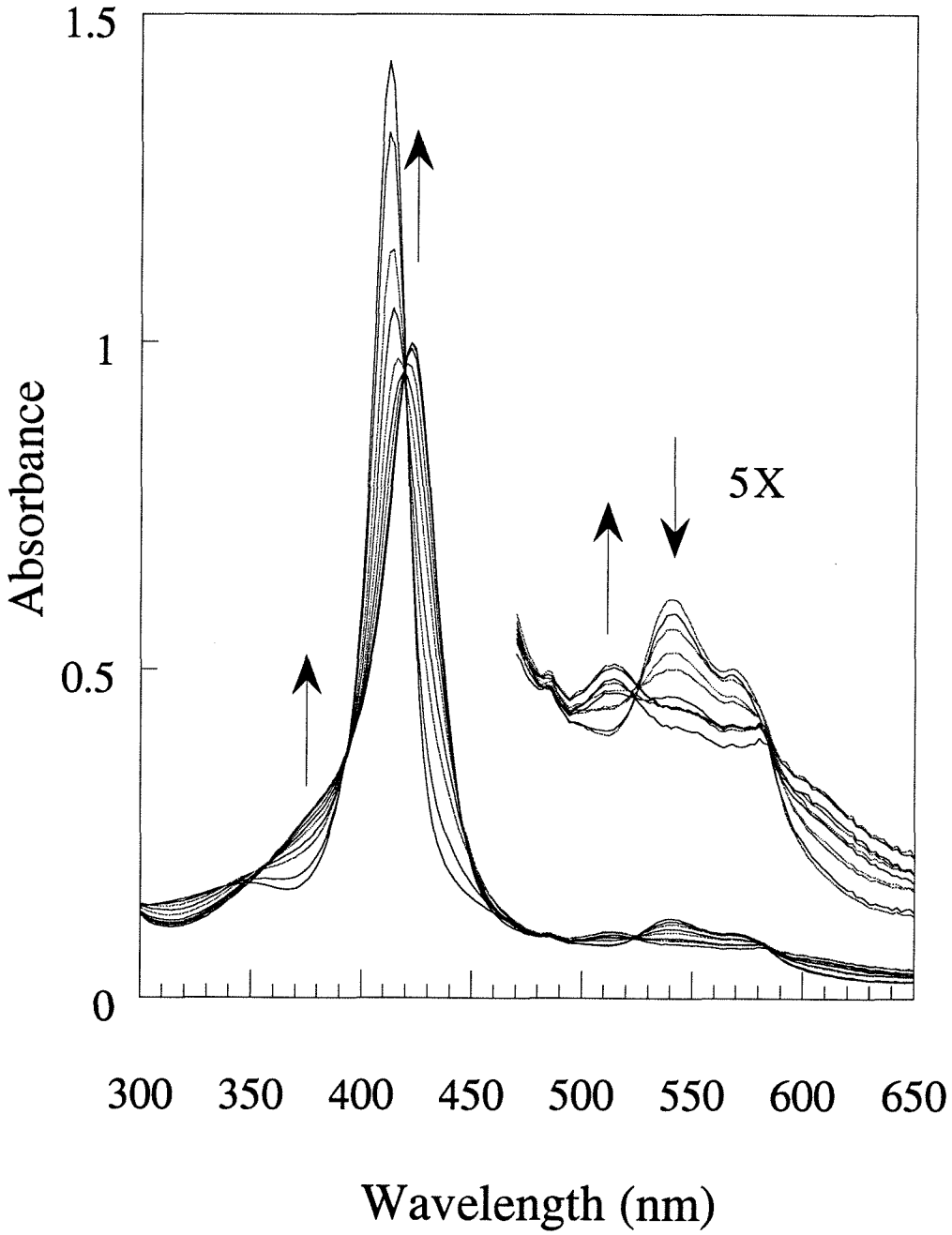
1.5
1
0.5
0
Absorbance
5X
300
350
400
450
500
550
600
650
Wavelength (nm)

Figure 5.6 -- Addition of cyclohexene to $Ru^{VI}TFPPCl_8(O)_2$. The initial decrease in Soret intensity corresponds to a single oxidation of substrate and formation of $Ru^{IV}TFPPCl_8(O)$. Eventually, the second oxo also transfers, and addition of carbon monoxide gas regenerates the original spectrum of $Ru^{II}TFPPCl_8(CO)$ with 85% of the original intensity.

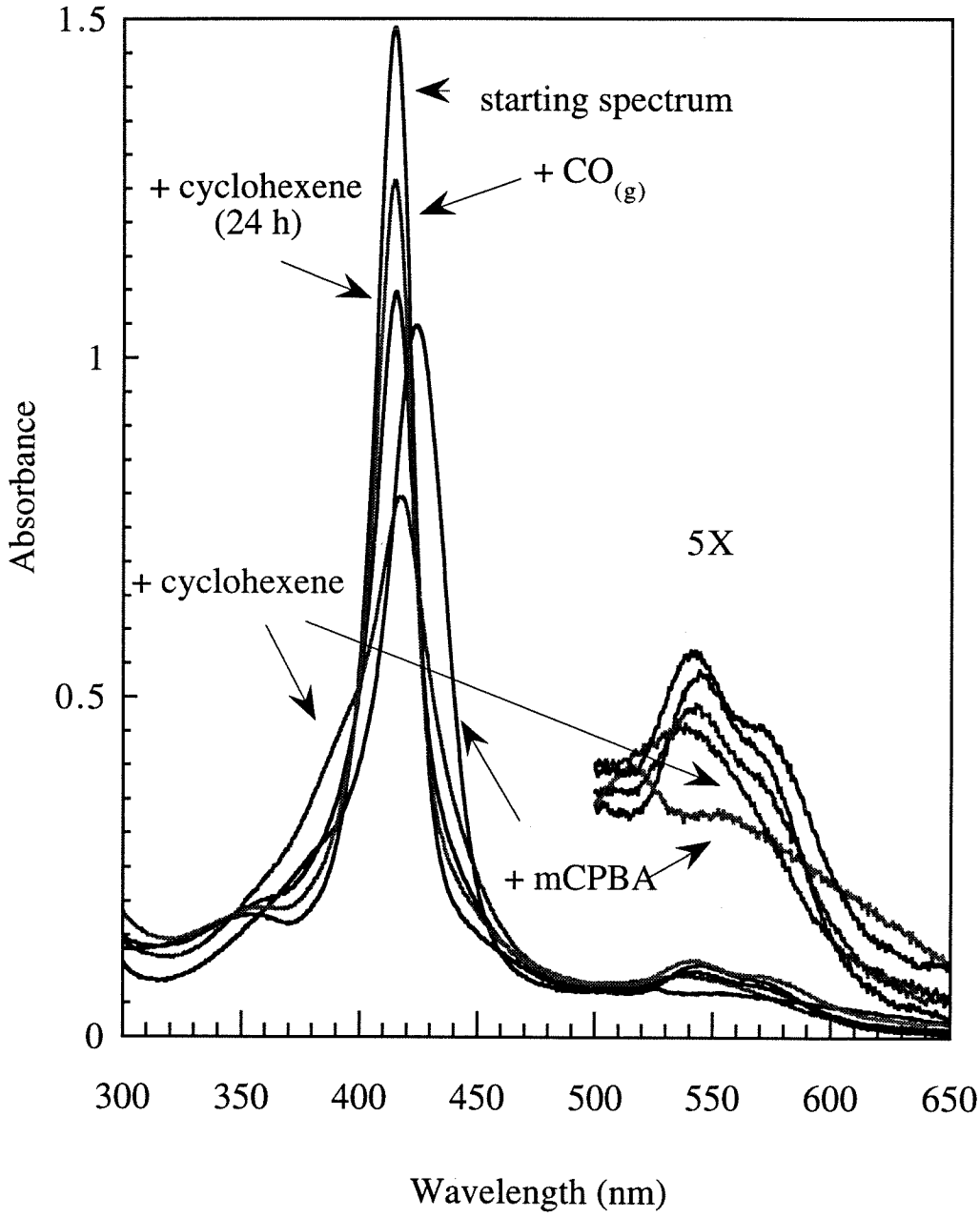
1.5
1
0.5
0
Absorbance
300
350
400
450
500
550
600
650
Wavelength (nm)
starting spectrum
+ CO(g)
+ cyclohexene
(24 h)
+ cyclohexene
5X
+ mCPBA

Figure 5.7 -- Addition of triphenylphosphine to $Ru^{VI}TFPPCl_8(O)_2$. The first 2 eq (a) are believed to correspond to transfer of both oxo ligands. Further addition of PPh_3 (2 eq, spectrum b) results in new spectral features consistent with coordination of triphenylphosphine to the ruthenium porphyrin.

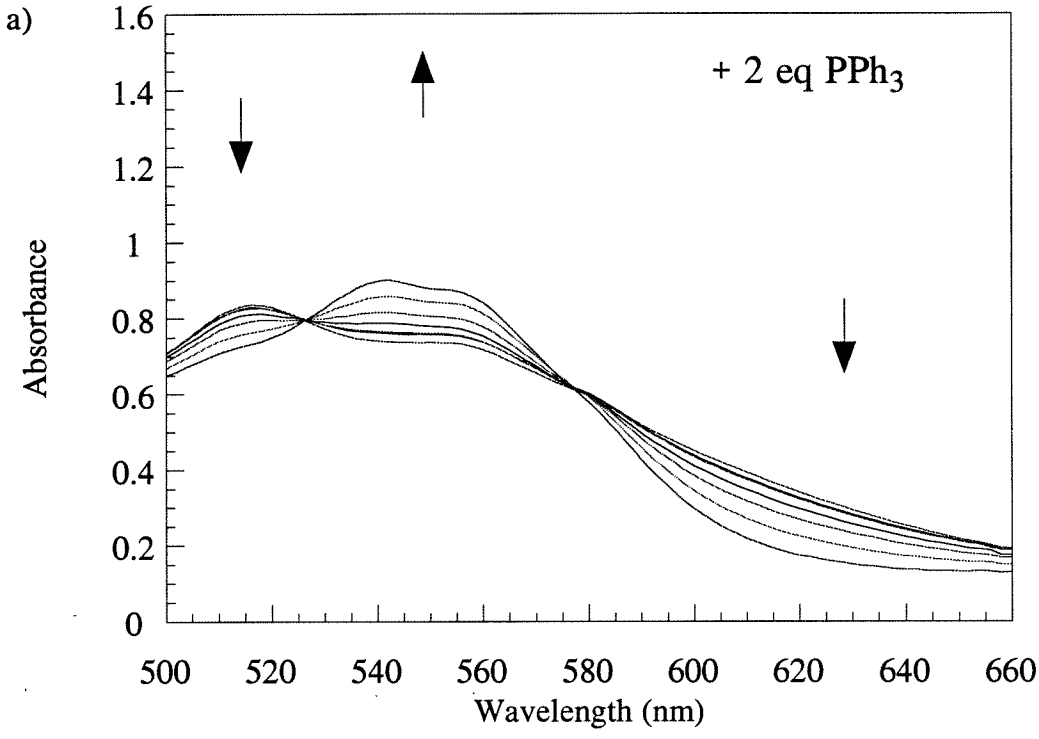
a)
+ 2 eq PPh3
Absorbance
Wavelength (nm)
0
0.2
0.4
0.6
0.8
1
1.2
1.4
1.6
500
520
540
560
580
600
620
640
660

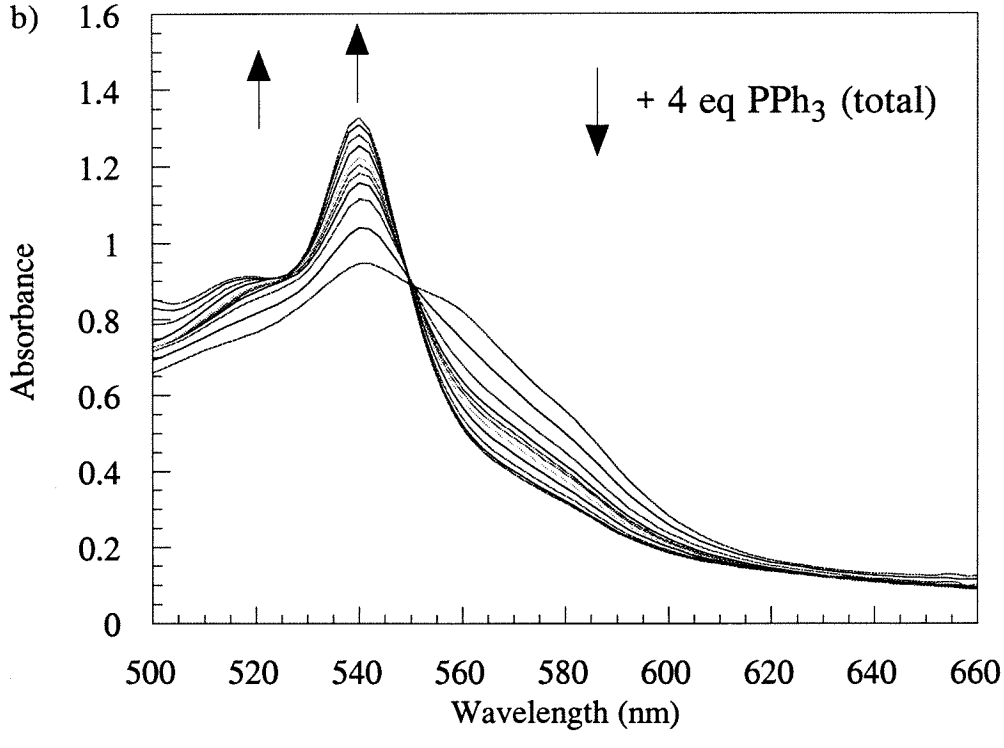
b)
+ 4 eq PPh3 (total)
Absorbance
Wavelength (nm)
0
0.2
0.4
0.6
0.8
1
1.2
1.4
1.6
500
520
540
560
580
600
620
640
660

Figure 5.8 -- A potential mechanism for oxidation of olefins by $Ru^{II}TFPPCl_8(CO)$. Initial loss of CO allows oxygen to bind to the electron poor metal center, initiating the chemistry.

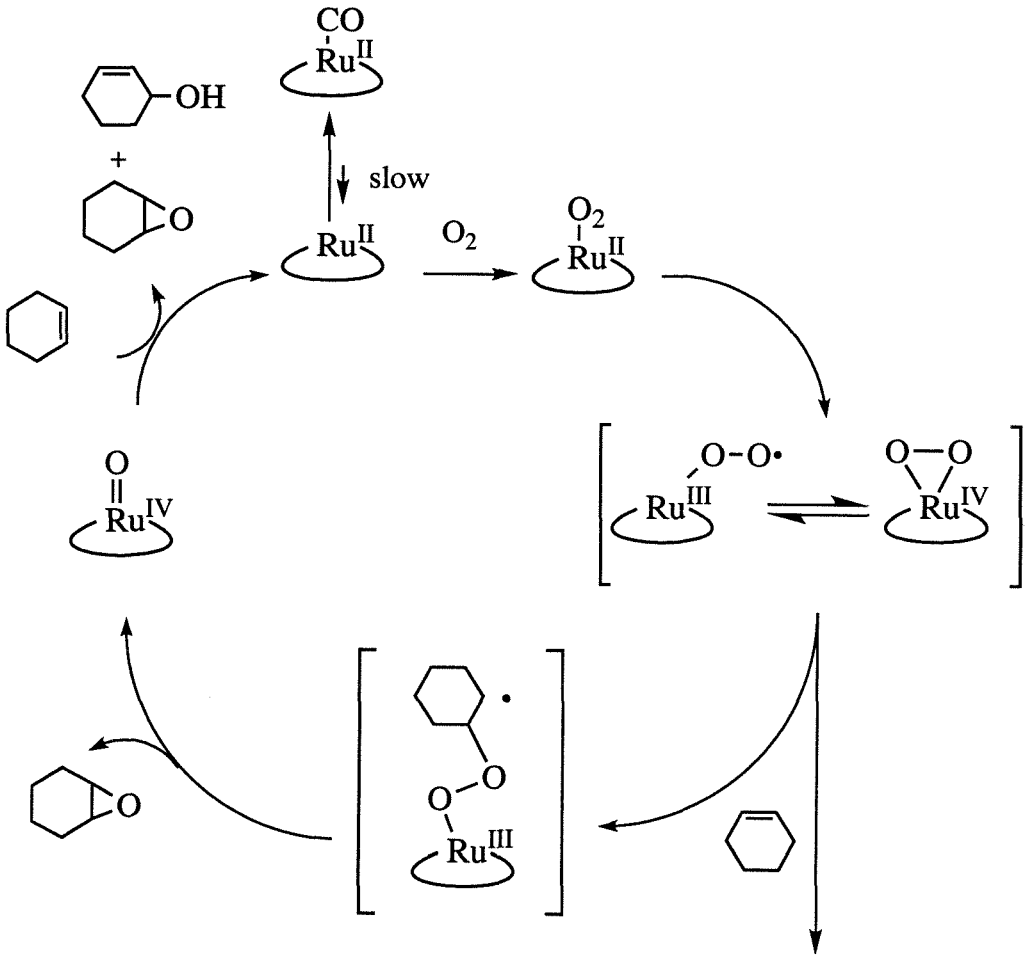

$Ru^{III}OOH + R\bullet$

↓

Free radical propigation <u>OR</u>
rebound to $Ru^{IV}(O)$ and ROH

Figure 5.9 -- Relative rates of reaction for $RuTFPPCl_8(CO)$ with dioxygen (a "normal" reaction) or in the presence of small amounts of $(Et)_3NO$ or mCPBA before addition of substrate.

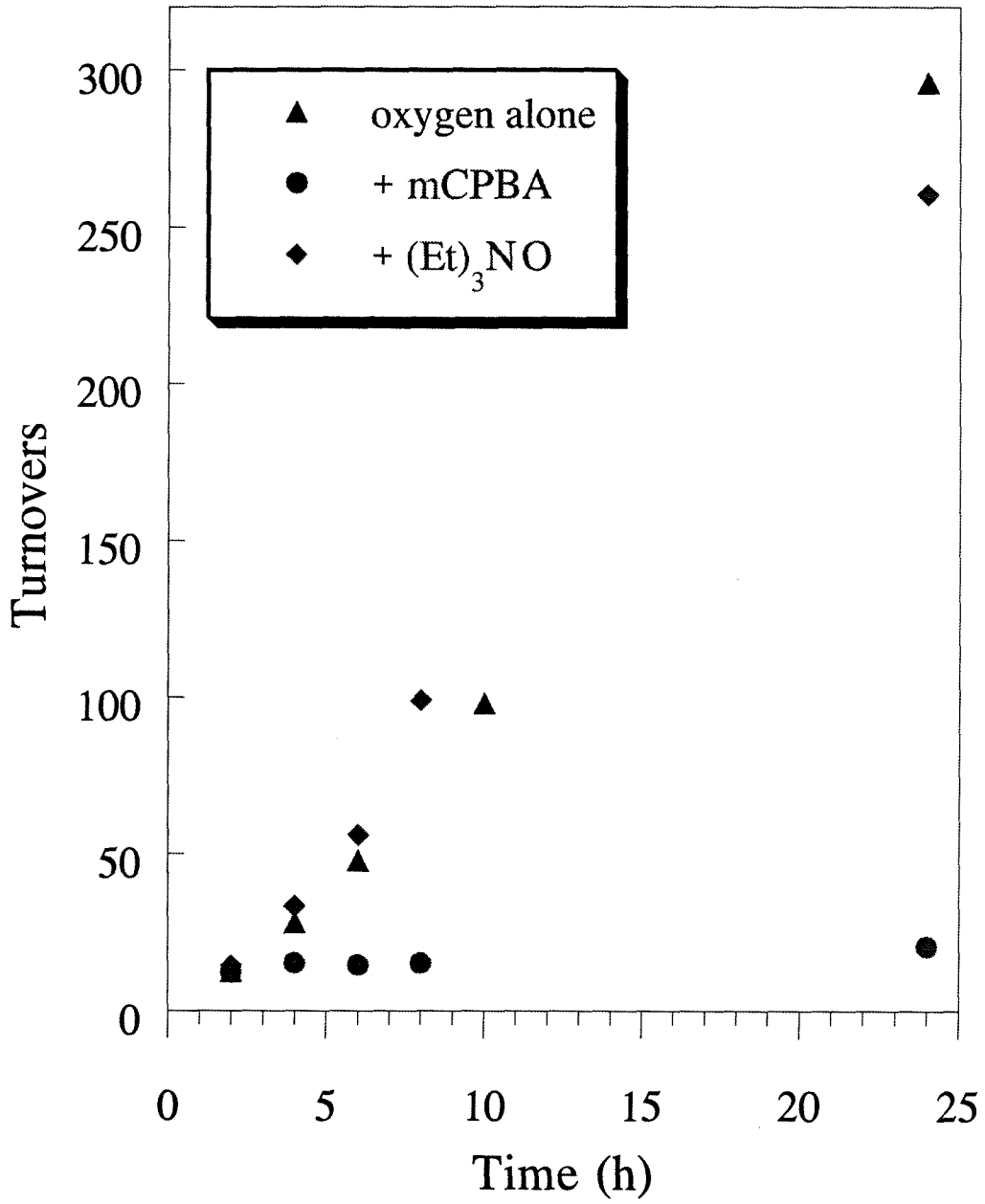
oxygen alone
+ mCPBA
+ (Et)3NO
Turnovers
300
250
200
150
100
50
0
0
5
10
15
20
25
Time (h)

Figure 5.10 -- The relative rates of cyclhexene oxidation after the addition of 10 or 300 equivalents of TBHP. Although a small addition of peroxide only induces a minor enhancement of the chemistry, the large addition appears to initiate a free radical reaction that may not be related to the ruthenium catalyst.

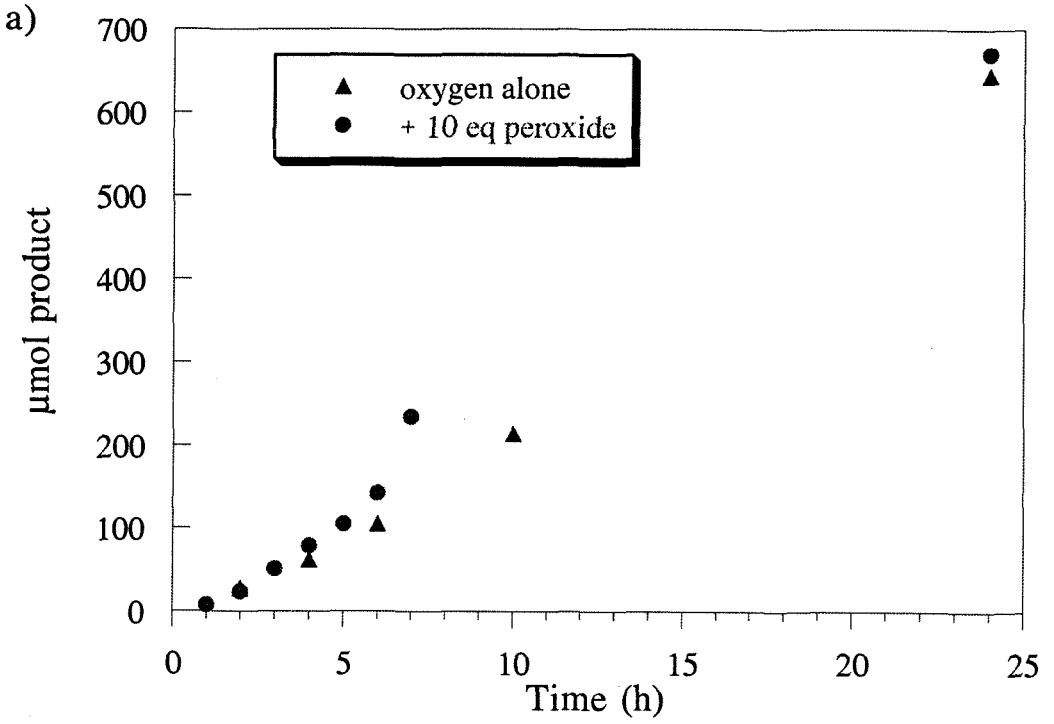
a)
oxygen alone
+ 10 eq peroxide
µmol product
0
100
200
300
400
500
600
700
0
5
10
15
20
25
Time (h)

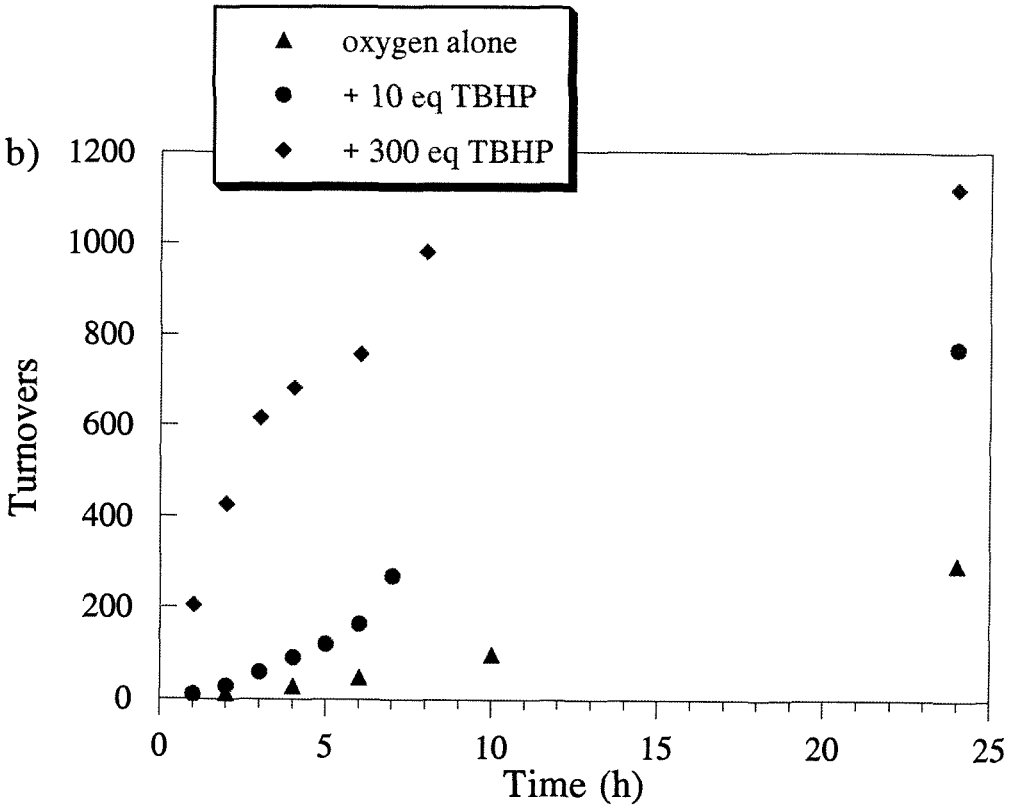
b)
oxygen alone
+ 10 eq TBHP
+ 300 eq TBHP
Turnovers
0
200
400
600
800
1000
1200
0
5
10
15
20
25
Time (h)

Figure 5.11 -- Relative turnovers in experiments stirred at two different rates indicate that phase transfer was not rate limiting. Experiments that were stirred more slowly showed slightly more activity than average.

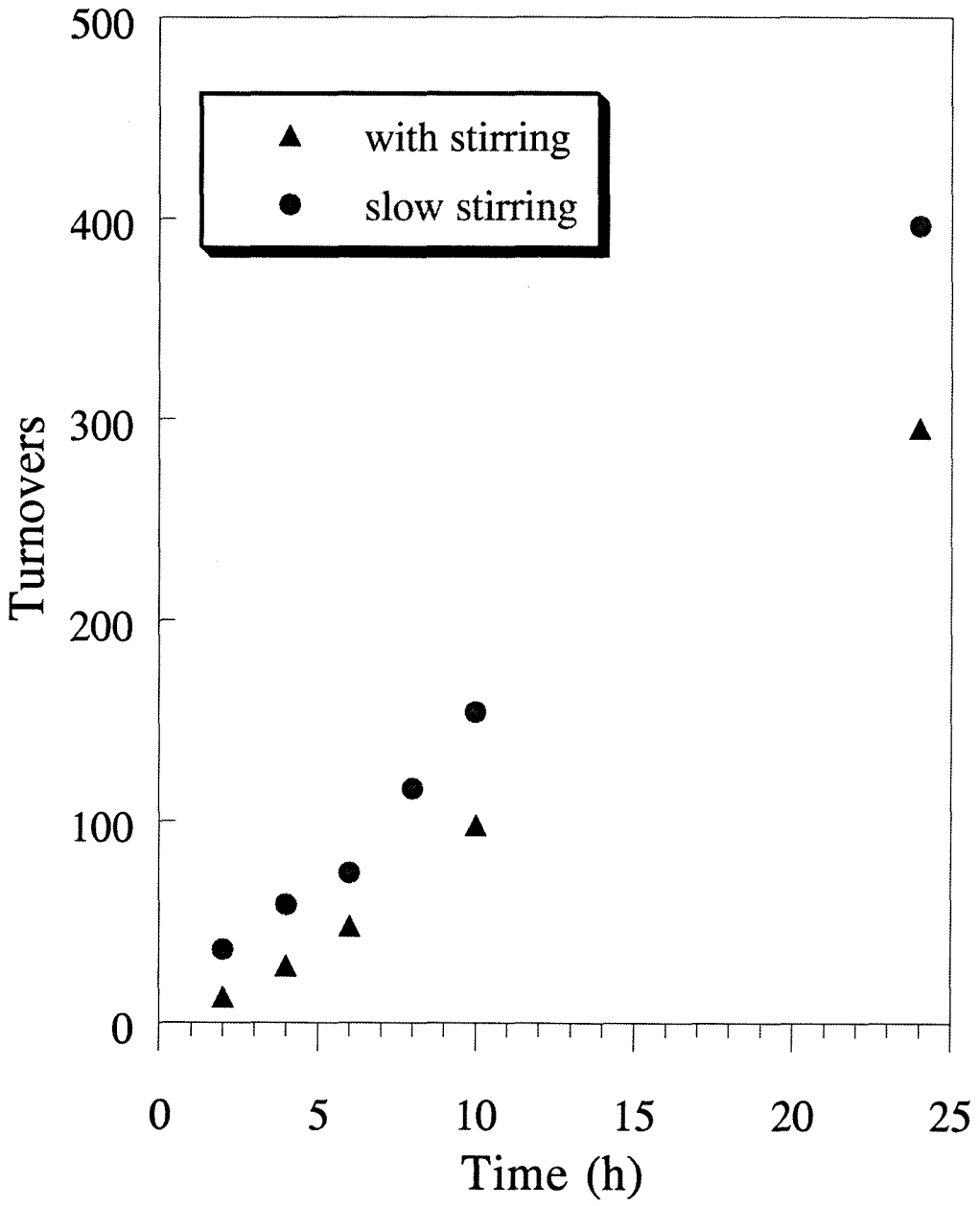
500
400
300
200
100
0
Turnovers
with stirring
slow stirring
0
5
10
15
20
25
Time (h)

Figure 5.12 -- Relative rates of cyclohexene oxidation under dioxygen or under a mixture of oxygen and carbon monoxide, indicating that CO does not inhibit catalysis by $Ru^{II}TFPPCl_8(CO)$.

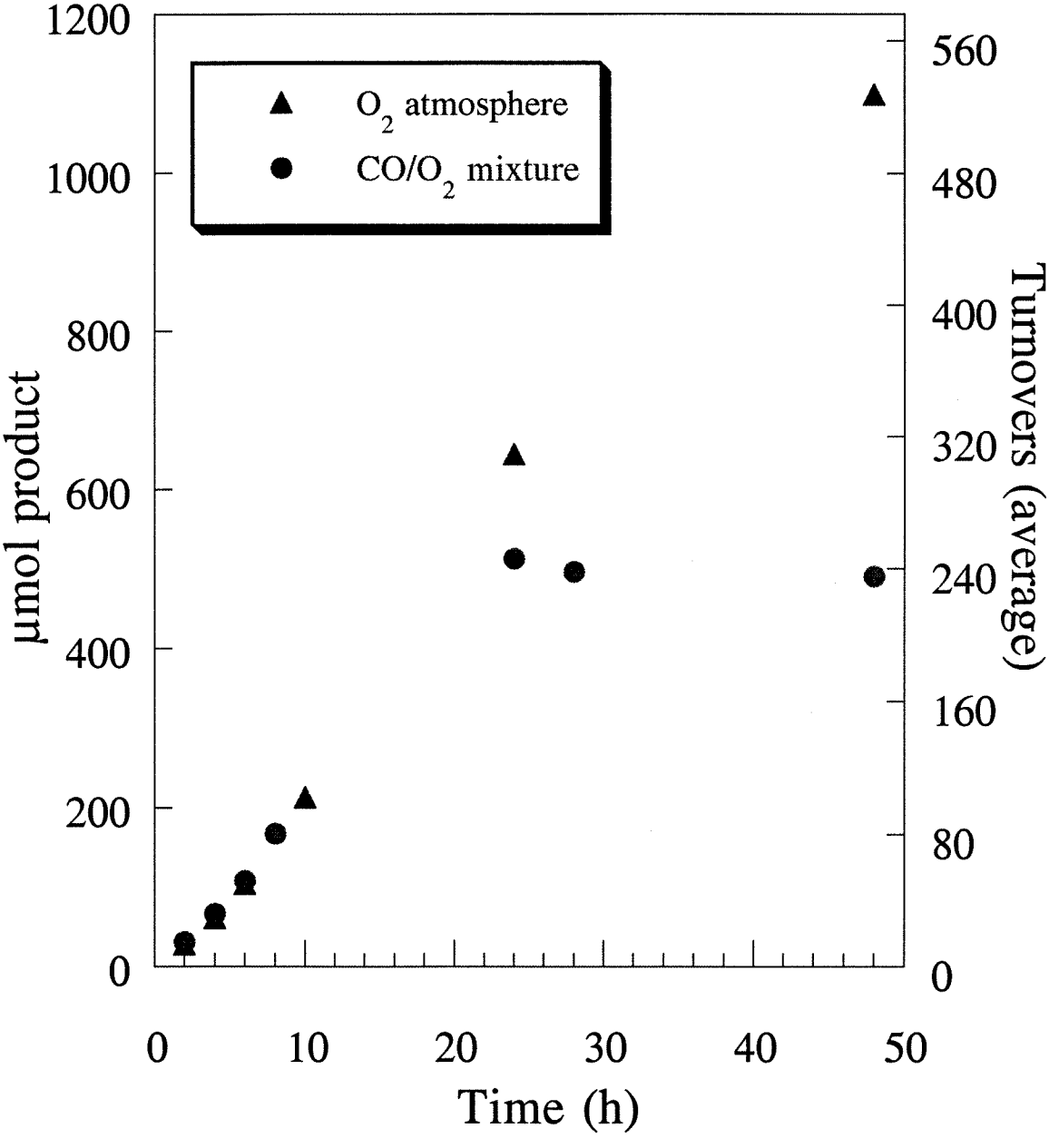
1200
1000
800
600
400
200
0
μmol product
560
480
400
320
240
160
80
0
Turnovers (average)
0
10
20
30
40
50
Time (h)
O2 atmosphere
CO/O2 mixture

Figure 5.13 -- UV-Vis spectrum of $Ru^{II}TFPPCl_8(CO)$ in carbon tetrachloride after two days in a Parr reactor under 1100 psi of carbon monoxide. The Soret band is slightly red shifted and the Q bands are slightly blue shifted from the spectrum before the Parr reactor. The absorption at 280 nm is believed to be from an organic product (see text).

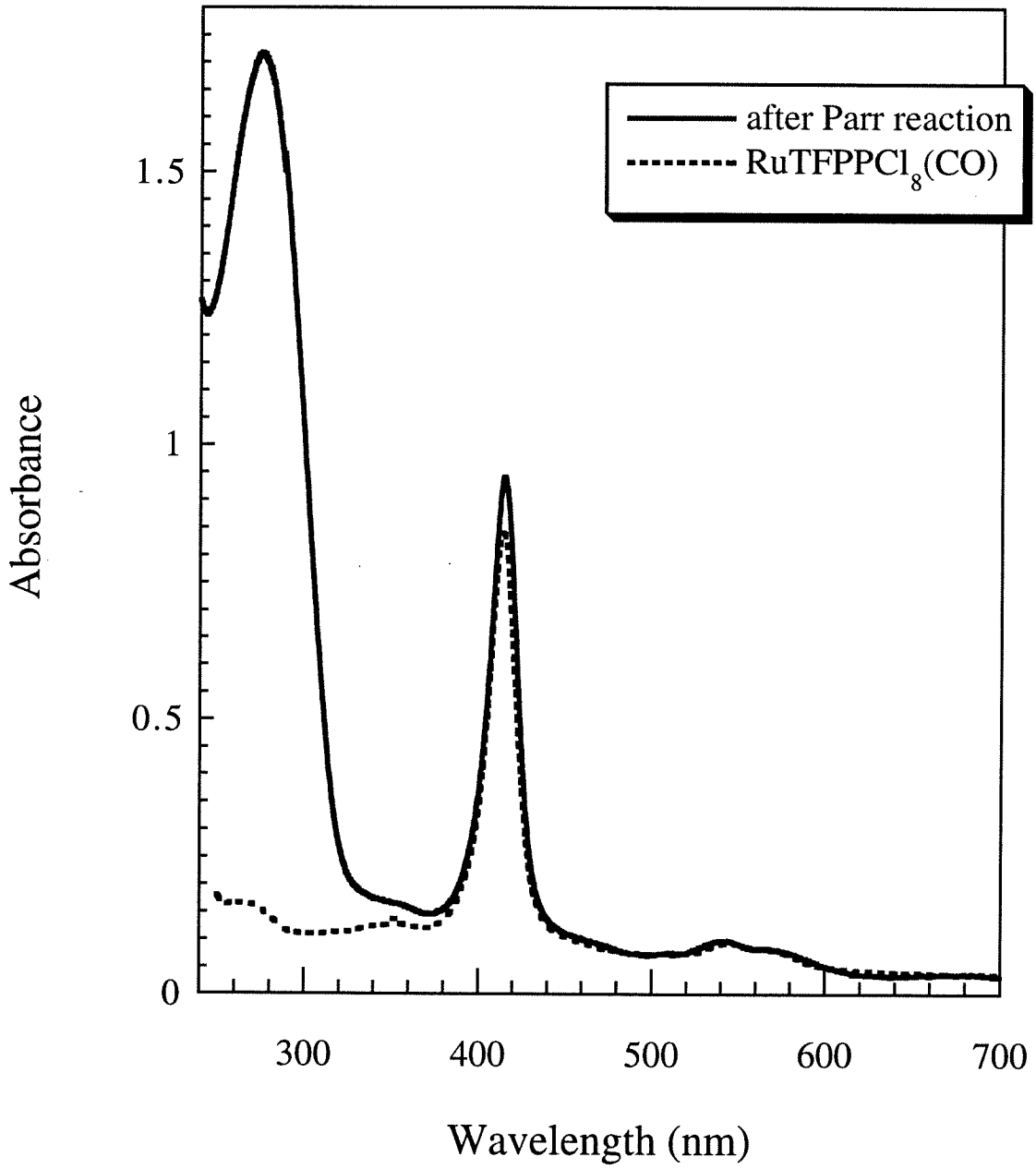
after Parr reaction
RuTFPPCl8(CO)
Absorbance
1.5
1
0.5
0
300
400
500
600
700
Wavelength (nm)

Figure 5.14 -- Relative rates of cyclohexene and cyclohexene-d_{10} oxidation by $Ru^{II}TFPPCl_8(CO)$ with dioxygen.

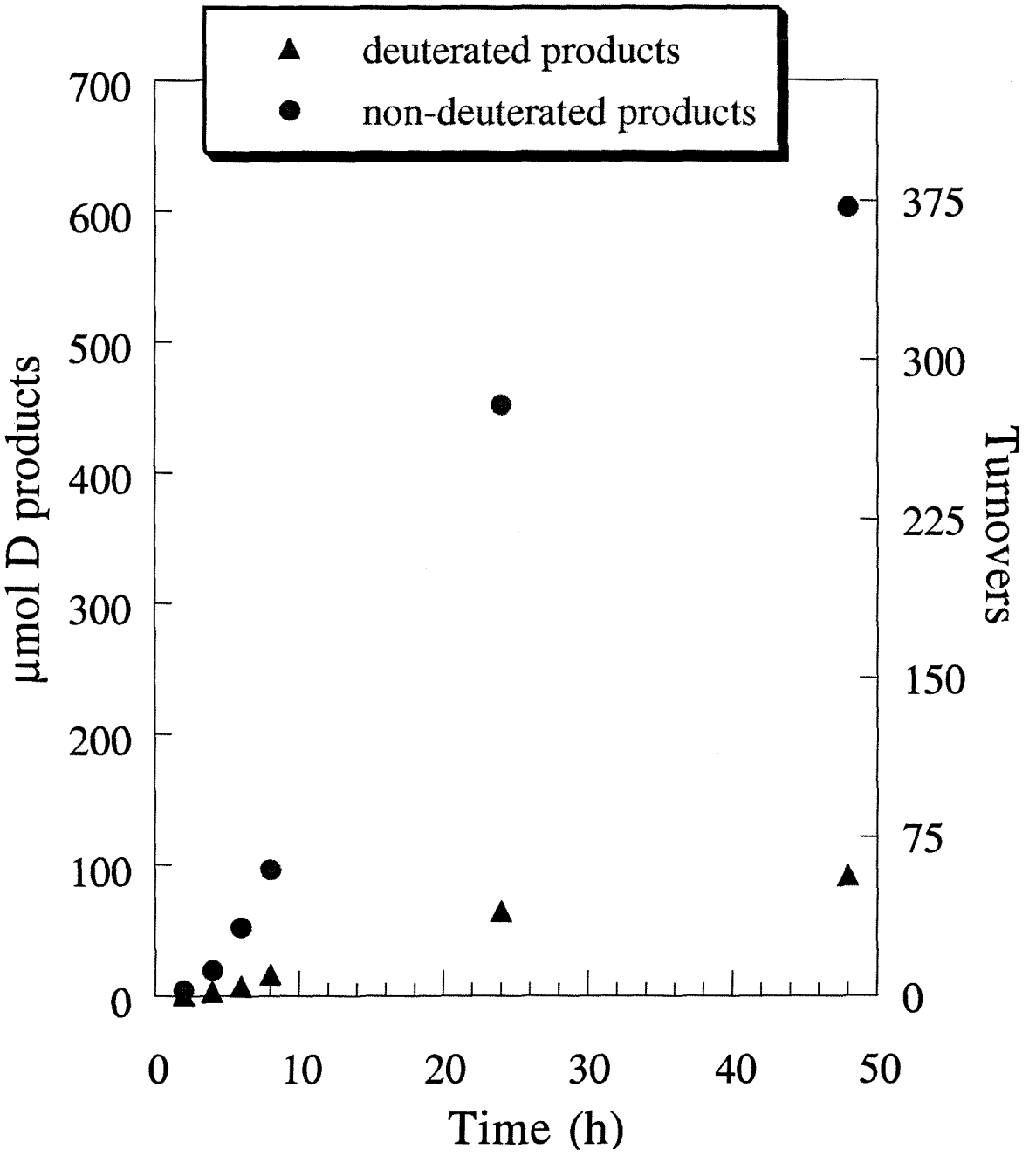
deuterated products
non-deuterated products
700
600
500
400
300
200
100
0
μmol D products
375
300
225
150
75
0
Turnovers
0
10
20
30
40
50
Time (h)

Figure 5.15 -- Cyclohexene oxidation experiments carried out in the dark showed great variability in the initiation period. Eventually both reactions showed significant reactivity.

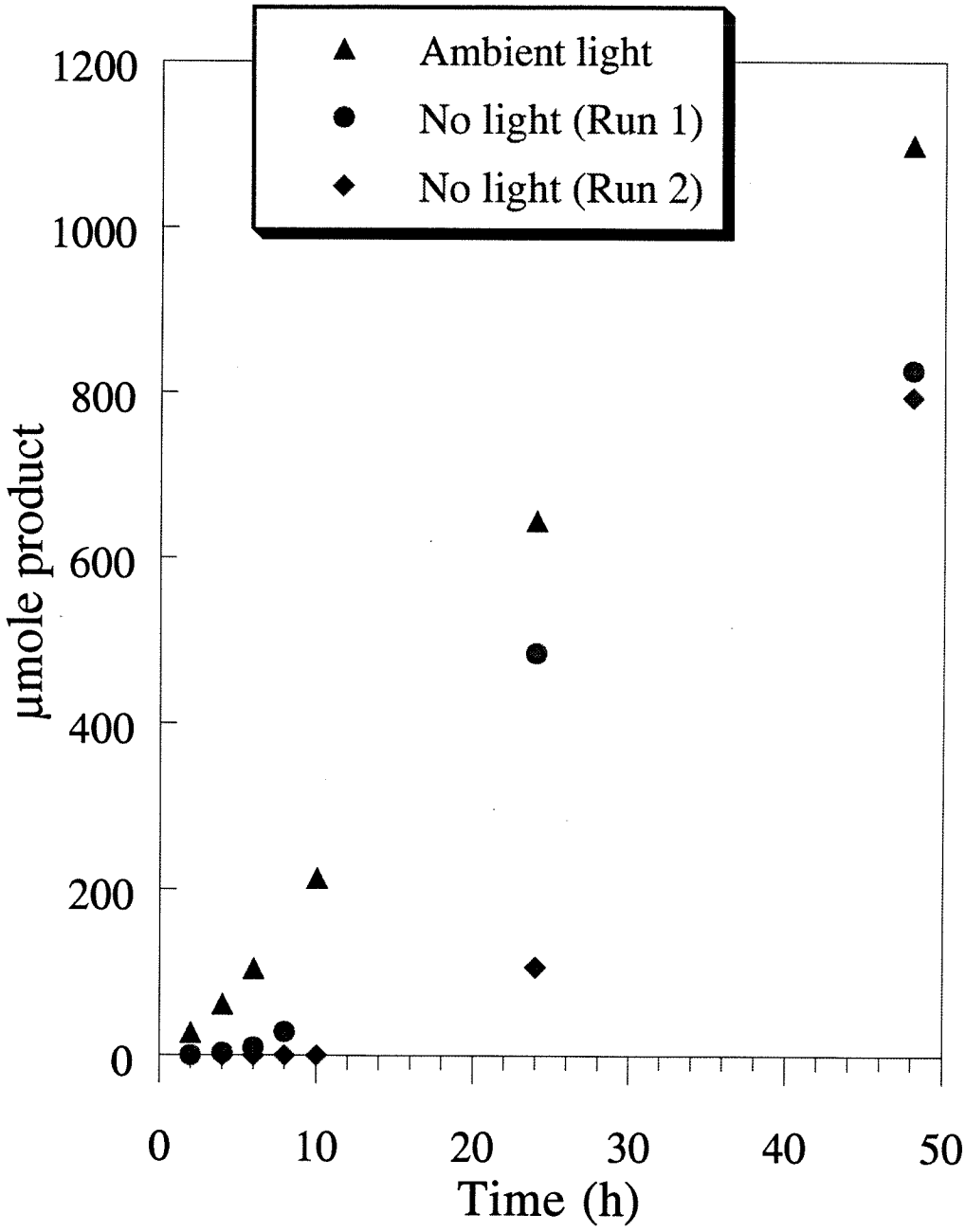
Ambient light
No light (Run 1)
No light (Run 2)
1200
1000
800
600
400
200
0
μmole product
0
10
20
30
40
50
Time (h)

Figure 5.16 -- Photolysis of a cyclohexene oxidation reaction by $Ru^{II}TFPPCl_8(CO)$ with dioxygen with a tungsten lamp dramatically increased the reaction rate.

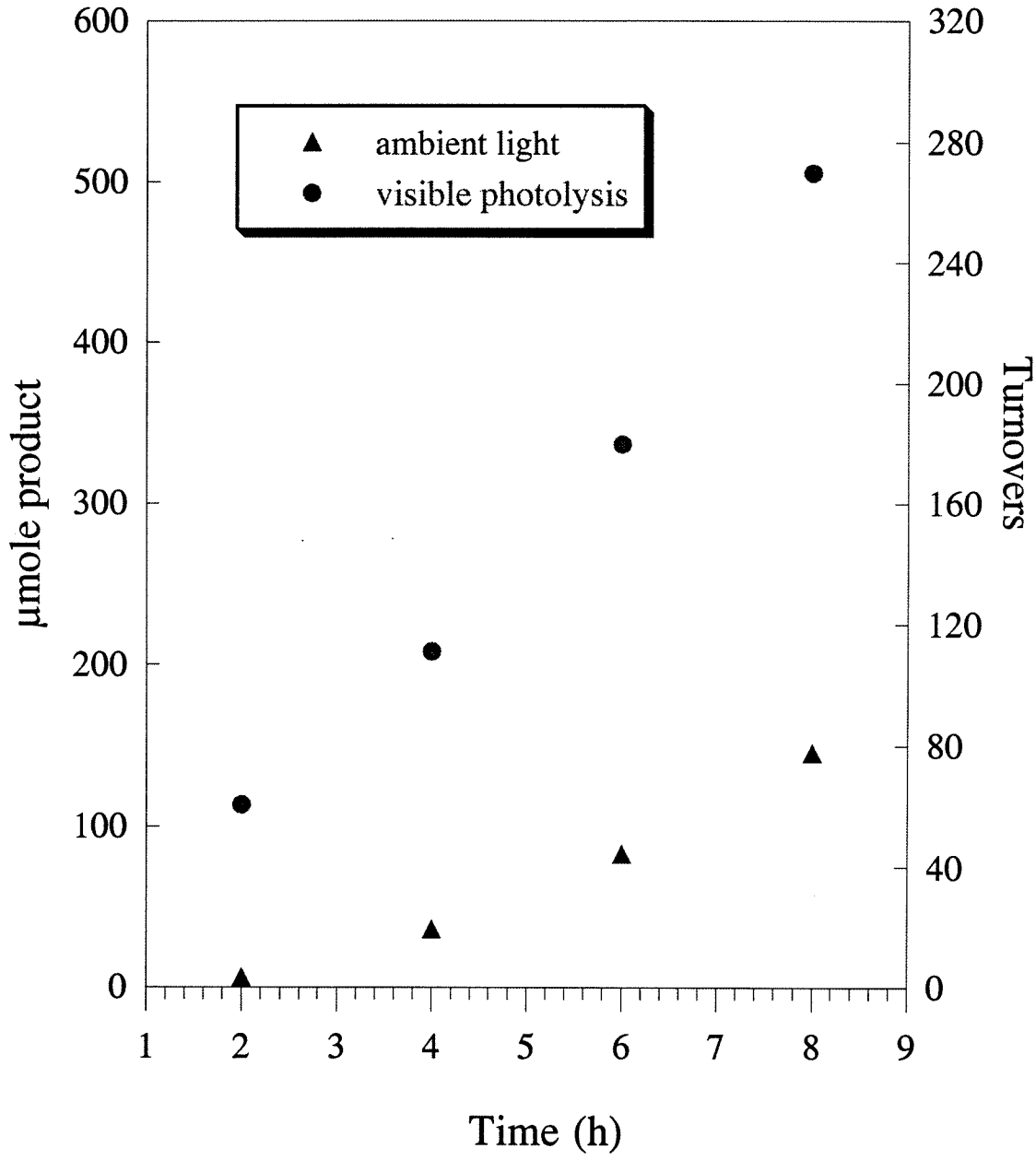
ambient light
visible photolysis
μmole product
Turnovers
Time (h)
600
500
400
300
200
100
0
320
280
240
200
160
120
80
40
0
1
2
3
4
5
6
7
8
9

Figure 5.17 -- Transient absorption spectrum in the Q band region immediately following irradiation at 480 nm. The appearance of a low energy band is consistent with formation of a porphyrin triplet excited state.

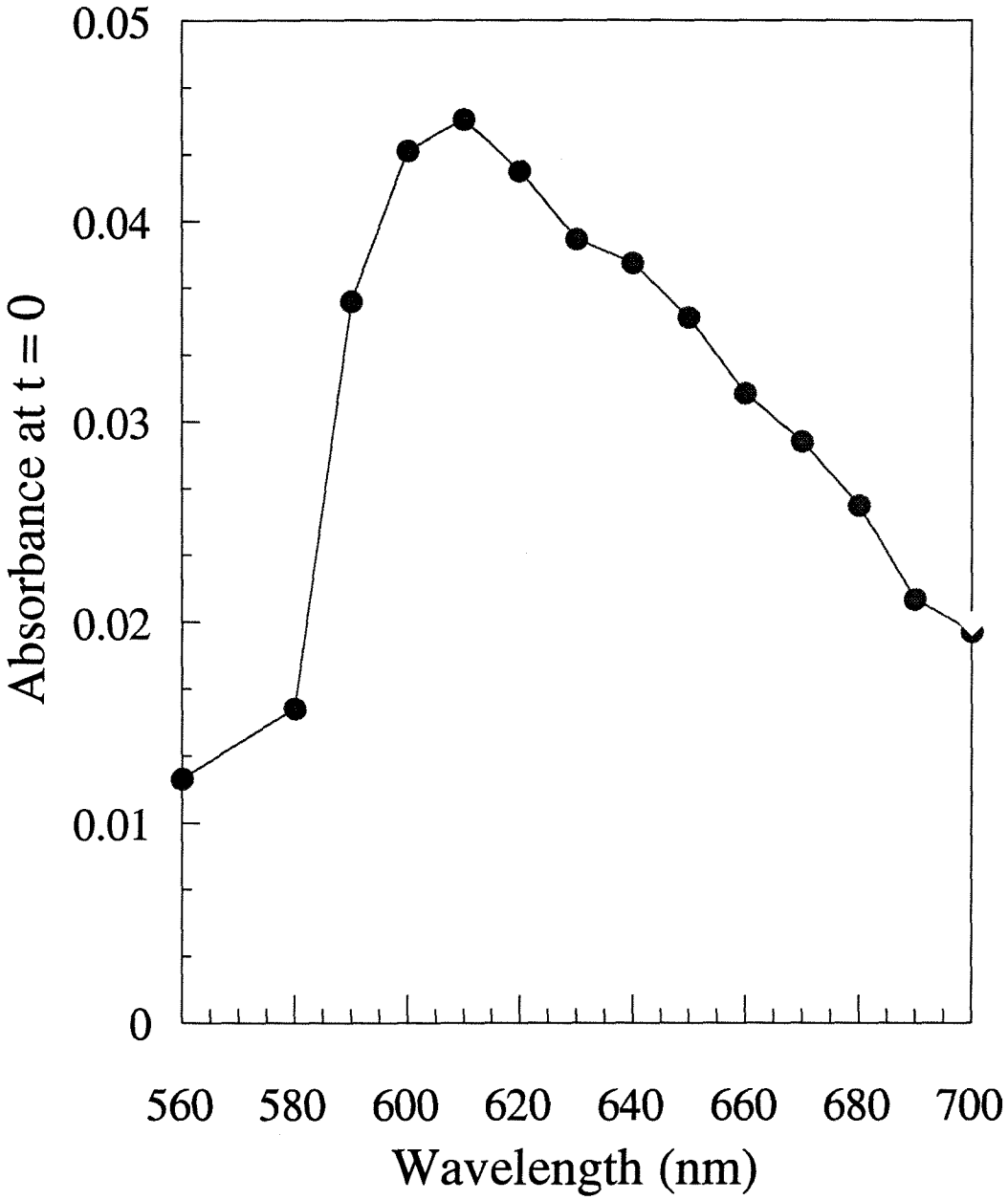
0.05
0.04
0.03
0.02
0.01
0
Absorbance at t = 0
560
580
600
620
640
660
680
700
Wavelength (nm)

Figure 5.18 -- A 5 μs transient spectrum at 415 nm for excitation of $Ru^{II}TFPPCl_8(CO)$ with 355 nm light. The sample is in methylene chloride and under an atmosphere of CO. Other transient spectra are in appendix 5.

DATA FILE: RUCO.006 1995-2-23 9:27:49
TIME RANGE: 5.0 µs INPUT V RANGE: 0.320V INPUT OFFSET: 0 %
EXPERIMENT: TRANSIENT ABSORBTION
FAST (200 MHz) QUASI-DIFFERENTIAL AMP
MODE: SINGLE-ENDED

SHOTS PRE CYCLE: 10 CYCLES: 5 PMT VOLTIGE: 702 V
EXCITATION WAVELENGTH: 355 nm OBSERVATION WAVELENGTH: 415 nm
SAMPLE: RuCl8(CO)
SOLVENT: CH2Cl2
TEMPERATURE: rt
COMMENT: under CO
COMMENT:

---> FIXED PARAMETER; ! ---> FIXED SIGN

$y(t) = C0 + C1*e^{-k1*t} + C2*e^{-k2*t}$

C0 = -1.941E-2
C1 = -1.023E-1 !k1 = 3.951E6 s^{-1}
C2 = -4.168E-2 !k2 = 8.530E5 s^{-1}

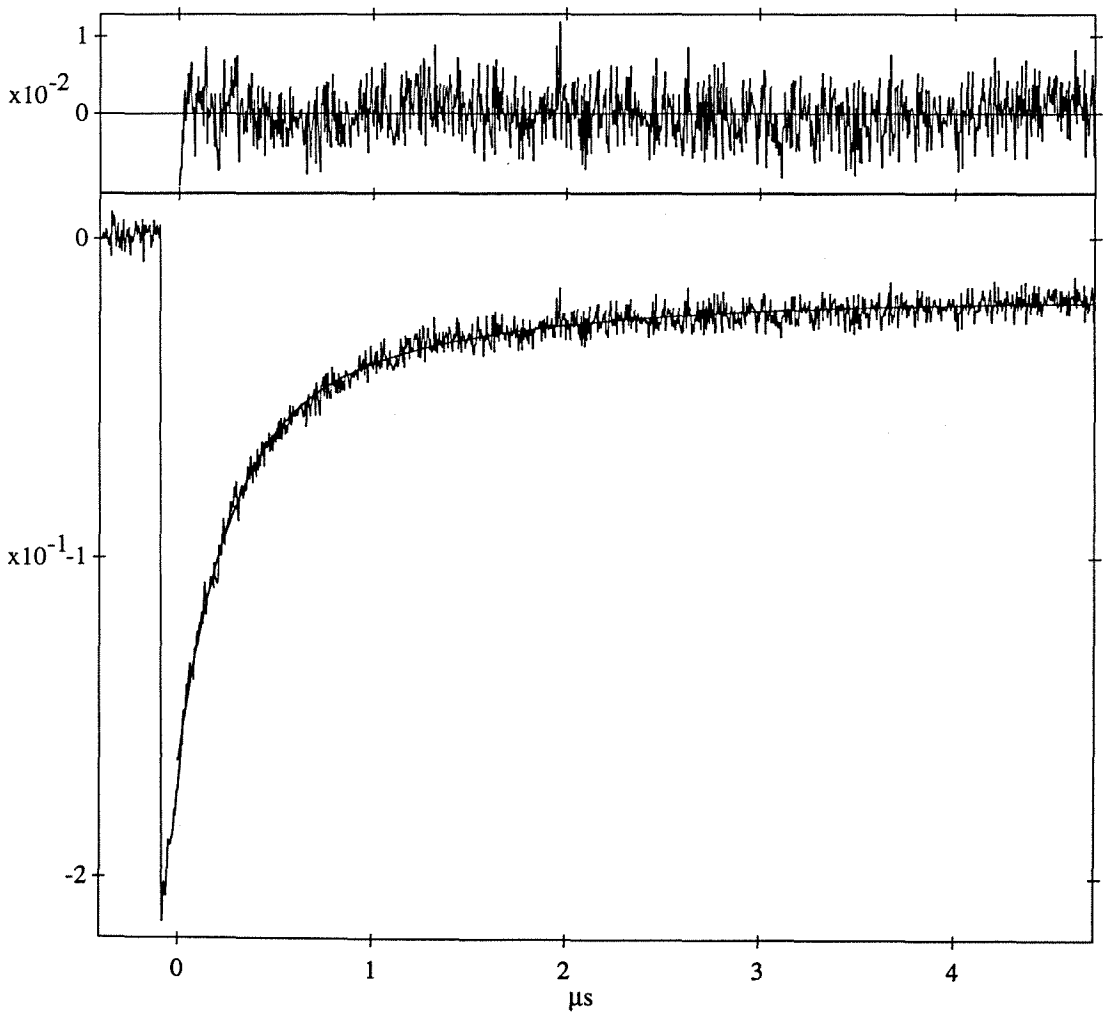

Figure 5.19 -- A 50 μs transient spectrum at 415 nm for excitation of $Ru^{II}TFPPCl_8(CO)$ with 355 nm light. The sample is in methylene chloride and under an atmosphere of CO. Other transient spectra are in appendix 5.

DATA FILE: RUCO.002 1995-2-23 8:56:56
TIME RANGE: 50 µs INPUT V RANGE: 0.320V INPUT OFFSET: 0 %
EXPERIMENT: TRANSIENT ABSORBTION
FAST (200 MHz) QUASI-DIFFERENTIAL AMP
MODE: SINGLE-ENDED

SHOTS PRE CYCLE: 10 CYCLES: 5 PMT VOLTIGE: 700 V
EXCITATION WAVELENGTH: 355 nm OBSERVATION WAVELENGTH: 415 nm
SAMPLE: RuCl8(CO)
SOLVENT: CH2Cl2
TEMPERATURE: rt
COMMENT: under CO
COMMENT:

---> FIXED PARAMETER; ! ---> FIXED SIGN

$$y(t) = C0 + C1*e^{-k1*t} + C2*e^{-k2*t}$$

C0 = -7.483E-3
C1 = -7.385E-2 !k1 = 2.196E6 s^{-1}
C2 = -2.381E-2 !k2 = 1.318E5 s^{-1}

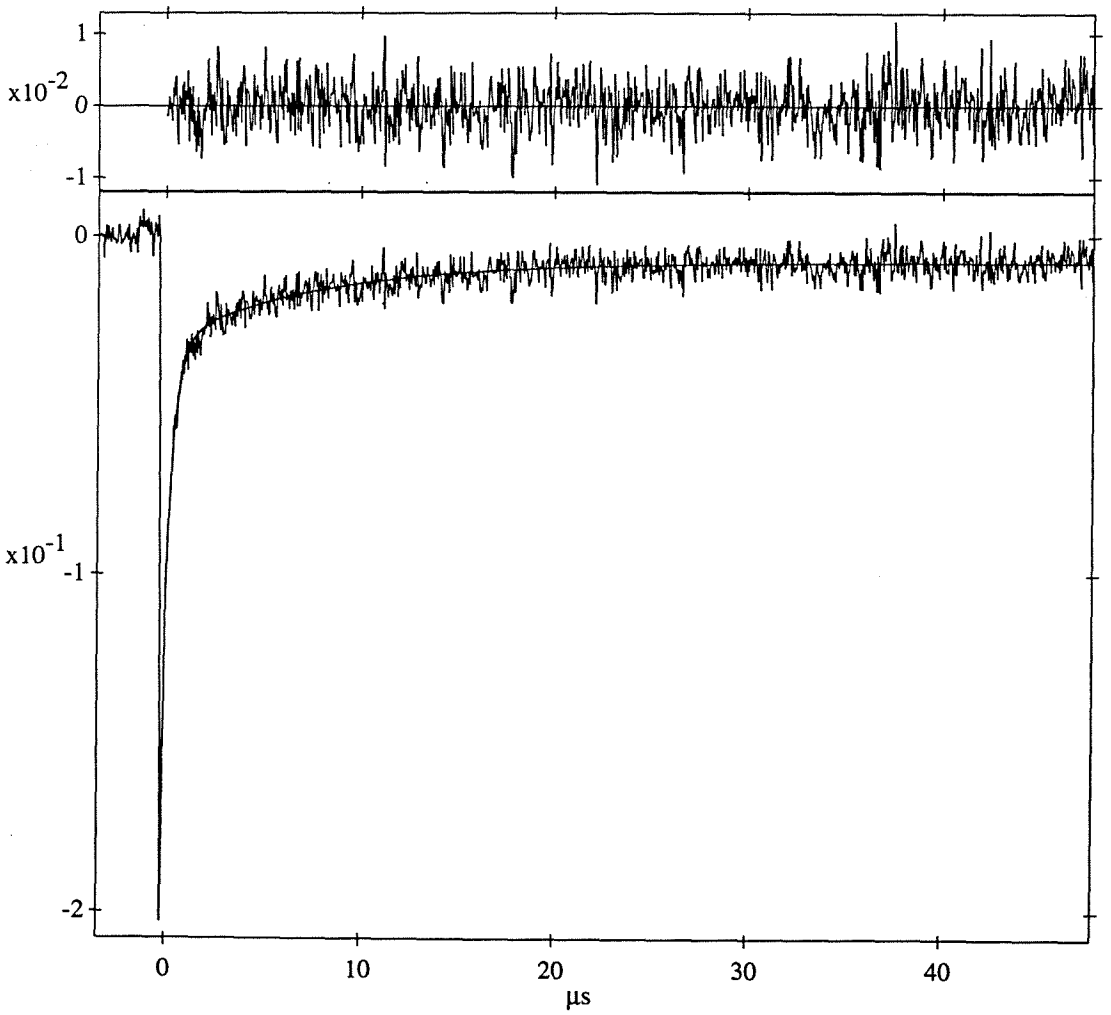

Figure 5.20 -- The 50 μs transient absorption spectrum after excitation with 355 nm light of equally concentrated solutions of $RuTFPPCl_8(CO)$ in methylene chloride under different atmospheres. The spectra are very similar; only the ethylene spectrum has a larger decrease in Soret intensity relative to the other samples.

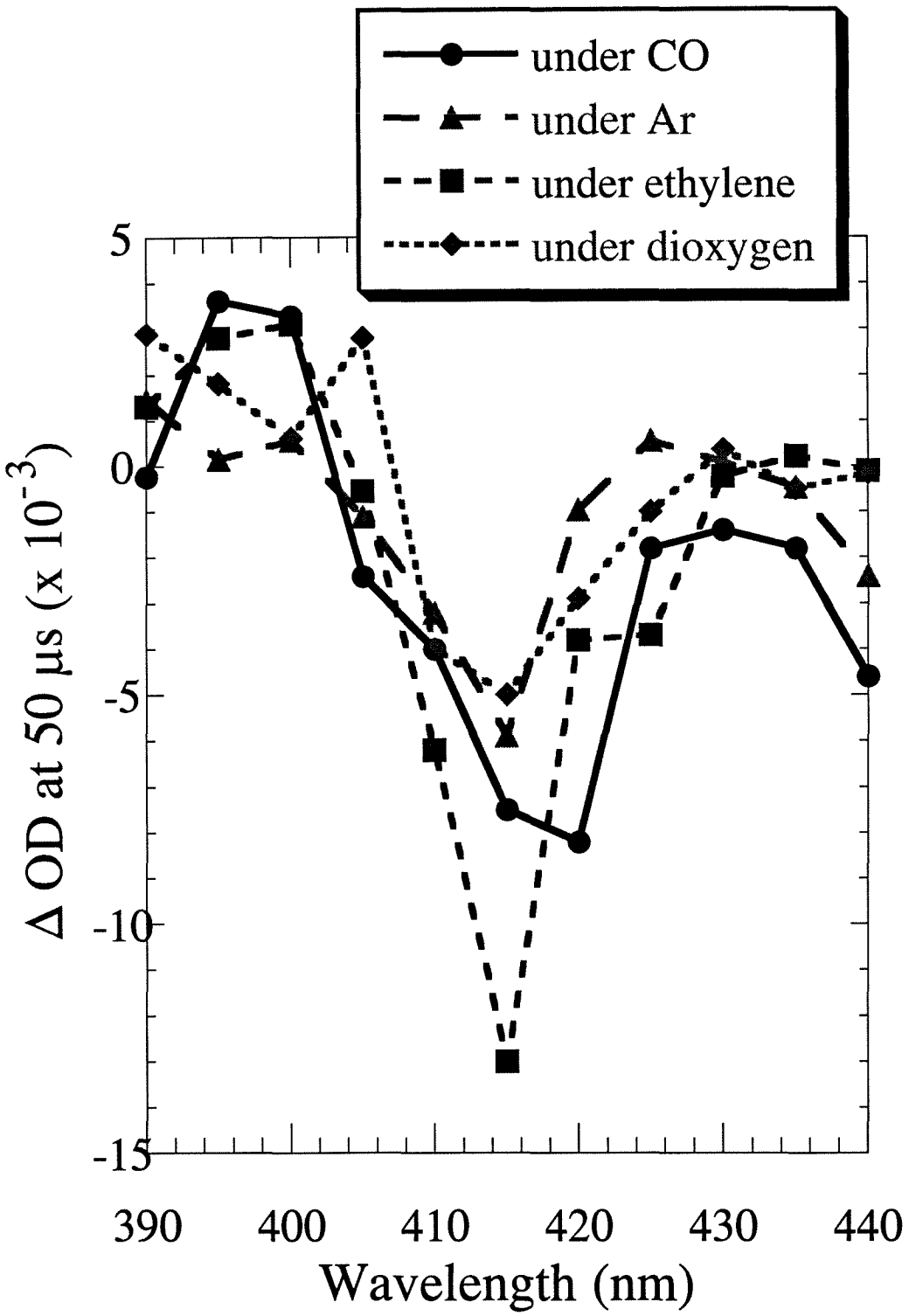
under CO
under Ar
under ethylene
under dioxygen
5
0
-5
-10
-15
Δ OD at 50 μs (x 10^-3)
390
400
410
420
430
440
Wavelength (nm)

Figure 5.21 -- UV-Vis spectra of the samples shown in Figure 5.20 after the completion of the laser photolysis experiments. The samples under argon and dioxygen show significant broadening and a decrease in the Soret intensity, but CO or ethylene atmospheres protected the porphyrin from decomposition.

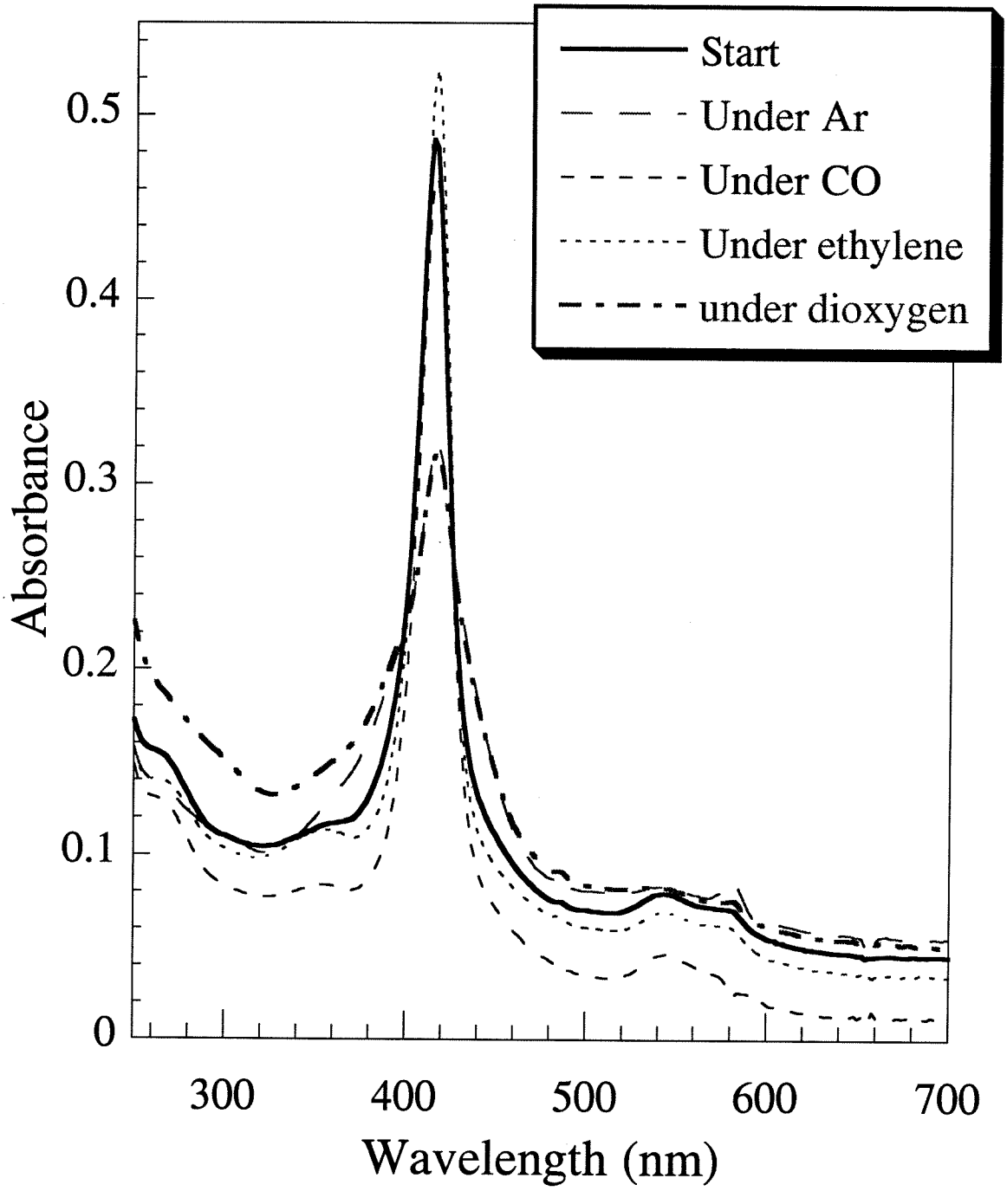
Start
Under Ar
Under CO
Under ethylene
under dioxygen
Absorbance
0.5
0.4
0.3
0.2
0.1
0
300
400
500
600
700
Wavelength (nm)

Figure 5.22 -- A mechanism for catalytic olefin oxidation by $RuTFPPCl_8(CO)$ with dioxygen involving an excited state of the porphyrin. Olefin binding is enhanced in the excited state due to the photochemical oxidation of the metal. The excited state could also be quenched by oxygen, forming singlet oxygen that could also lead to product formation.

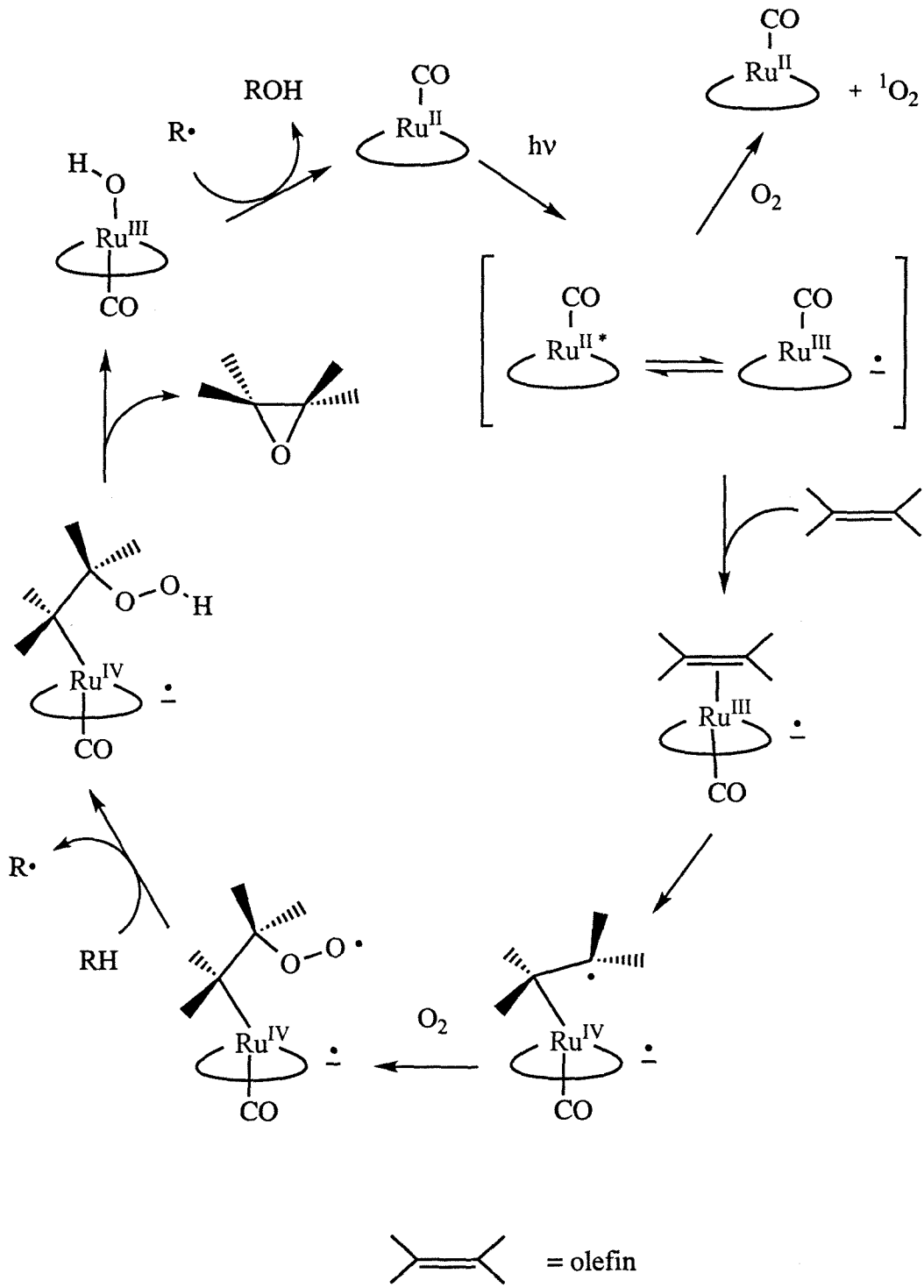
CO
Ru^II
+ ¹O₂
ROH
R•
hν
O₂
H
O
Ru^III
CO
Ru^II*
Ru^III
O
O–O
H
Ru^IV
R•
RH
O–O •
Ru^IV
O₂
= olefin

Table 5.1. Oxidation Chemistry with $RuTFPPCl_8(CO)$.

Reaction Conditions[a]	% 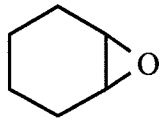	% 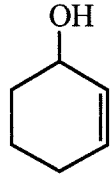	% 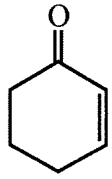	Turnovers
PhIO	42	56	2	9.9
O_2	15	58	27	296
O_2 + 10 eq $(Et)_3NO$	7	59	35	260
O_2 + 5 eq mCPBA	35	52	13	20
O_2 + 10 eq TBHP	14	54	32	770
O_2 + 300 eq TBHP	7	65	28	1119
slow str rate	14	61	25	258
CO/O_2	7	57	36	258
No light	16	59	25	200 (average)
Visible Photolysis	15	61	24	531

a. Reactions run in 15 mL of methylene chloride with approximately 1.5 - 2.0 μmol of $RuTFPPCl_8(CO)$ and 1 mL of cyclohexene. All reactions were run under 1 atm of dioxygen, except the PhIO reaction, which was under an argon atmosphere. See text and experimental section for more details.

Chapter 6

Solubility and Reactivity of Iron and Ruthenium Halogenated Porphyrins in Supercritical Carbon Dioxide

Introduction

The investigation of biomimetic metalloporphyrin catalysis has two general long range goals: first, to better understand oxidation chemistry *in vivo*, and second, the more economic objective of applying this knowledge to the design of efficient oxidation catalysts for industrial applications. The latter aim of efficiency is not specific to oxygenation, but also drives research in other areas of catalysis. Increasing pressure from the government to reduce waste as well as burgeoning costs of waste disposal have necessitated fundamental changes in catalysis methodology. Consideration of the catalyst efficiency and longevity are no longer sufficient; solvent disposal, waste stream reduction, and chemical toxicity are of increasing importance.

Supercritical carbon dioxide (SC CO_2) has recently received great attention as an environmentally friendly solvent. Non-toxic, inexpensive, and nonflammable, it is currently used for commercial extraction of hops and decaffination of coffee.[1] SC CO_2 is being further explored as a medium for uses ranging from the extraction of lanthanides from nuclear reprocessing waste[2] to dry-cleaning.[3] The primary applications and research related to SC CO_2 have focused on separation technology. The use of supercritical carbon dioxide as a solvent for chemical reactions has not been widely explored, an area where the unique attributes of supercritical fluids (SCFs) could possibly affect the desired enhancements in catalysis.

In general, SCFs have properties that range between those of gases and liquids. Gases are miscible in SCFs, eliminating phase transfer problems during hydrogenation or oxygenation catalysis in homogeneous solution. The density of a SCF is extremely

dependent on the pressure and temperature, and can vary between being "gas-like" or "liquid-like." The polarity of SC CO_2 is similar to that of halogenated hydrocarbons, indicating that it may be an excellent replacement for hazardous solvents such as carbon tetrachloride or methylene chloride.[4]

Carbon dioxide has an unusually low critical point. A phase diagram (Figure 6.1) shows the critical point at 72.8 atm and 31 °C, which is far lower than that of water (218 atm and 374 °C).[5] These conditions are easily achievable in the laboratory, albeit with care and respect, and are also feasible for industrial applications.

Supercritical carbon dioxide has recently begun to be explored as a medium for catalysis. DiSimmone conducted the free radical polymerization of methyl methacrylate in SC CO_2. High yields of quality poly(methyl methacrylate) were obtained from a single phase reaction, avoiding the aqueous and organic dispersing media used in classical polymerization techniques.[6] Noyori *et al.* have achieved formation of dimethylformamide from hydrogen gas, dimethylamine, and supercritical carbon dioxide with a ruthenium phosphine catalyst. The CO_2 serves as both solvent and reactant, driving the reaction at a rate an order of magnitude above that in an organic solvent.[7] Similarly, the miscibility of H_2 in SC CO_2 leads to very high initial rates of reaction for the formation of formic acid, catalyzed by $Ru(PMe_3)_4(H)_2$.[8] Asymmetric hydrogenation reactions with ruthenium and rhodium catalysts have demonstrated that enantioselectivity can be increased by moving from a conventional solvent to supercritical CO_2.[3] The above examples demonstrate several methods in which SCFs have improved catalytic processes.

Despite these recent successes, only one oxidative system has been investigated in SC CO_2.[9] The uncatalyzed free radical oxidation of cyclohexane with dioxygen in SC CO_2 has been reported. The conversion of cyclohexane and the ratio of cyclohexanol and cyclohexanone produced are controlled by the pressure and temperature near the critical region.[10] No other oxidations in supercritical carbon dioxide have been reported. Catalytic olefin oxidation by halogenated metalloporphyrins seems an ideal system for analysis in

SC CO_2. Since dioxygen is the only additive in these reactions (no coreductant is needed), the miscibility of O_2 with SC CO_2 has potential to increase reactivity in the SCF. Furthermore, the different solvation properties of SC CO_2 could lead to different selectivity in the oxidation reactions.

Before investigating reactivity, we determined the solubility of three halogenated porphyrins in SC CO_2. Although the dielectric constant of supercritical carbon dioxide increases with pressure, it remains quite low (only 1.8 at 2000 psi), making SC CO_2 a rather poor solvent.[4] However, since chlorinated solvents able to dissolve halogenated porphyrins (i.e., CCl_4) also have low dielectric constants, the porphyrins were anticipated to be soluble in the supercritical medium. Fe(TFPP)Cl, Fe(TFPPBr_8)Cl and RuTFPPCl_8(CO) were investigated, since their chemistry in methylene chloride had been previously studied in our laboratory.

Results

Solubility Studies

An apparatus allowing UV-Vis spectroscopy under high pressures is pictured in Figure 6.2. A tank of liquid carbon dioxide was connected to allow flow directly into the cell or into an ISCO syringe pump, which is capable of condensing CO_2 up to 5000 psi. The cell was secured with a stand on top of a stirplate in between the lamp and detector. Rubber heating tape was wrapped around the cell to maintain the temperature at 40°C during the UV-Vis experiments (Figure 6.2).

After the cell was aligned in the spectrophotometer setup, a solution of porphyrin in methylene chloride was injected into the cell through the thermocouple inlet. The thermocouple was then reattached, and the cell evacuated to remove the organic solvent. CO_2 was added, and the absorbance calculated from light intensity measurements taken at 500 psi intervals (Figure 6.3-6.6). A spectrum of each compound in methylene chloride is also displayed in each figure for comparison. The concentration of porphyrin in solution is

calculated assuming the extinction coefficients are similar in methylene chloride and in SC CO_2. Although porphyrin spectra are known to be sensitive to solvent, generally the position of the band shifts more than the extinction coefficient.

In general, solubility was found to increase with pressure. Although the spectra are quite noisy, due to refraction from mixing lines in the large cell, the main features of the porphyrin are still observable. Fe(TFPP)Cl (Figure 6.3) is the least sensitive to pressure, but has the highest solubility, with the concentration only changing from 0.27 to 0.30 μM from 2000 to 5000 psi CO_2. The Q band region is most distinct in these spectra, with a shoulder at 500 and a stronger band at 610 nm corresponding to the solution spectrum bands at 504 and 620 nm.

The resolution of the Soret band of $Fe(TFPPBr_8)Cl$ is lost in SC CO_2 (Figure 6.4). However, there is a definite increase in absorbance from 1400 to 3500 psi, and the solubility increases from 0.07 to 0.20 μM. Further increases in pressure do not cause much change in absorbance.

Unlike the iron porphyrins, the Soret band of $RuTFPPCl_8(CO)$ is quite distinct in SC CO_2. The Q band region in this spectrum, however, has a substantial amount of instrument noise (Figure 6.5). The solubility increased from almost nothing in liquid carbon dioxide (800 psi) to 0.16 μM (5000 psi). The changes of solubility with pressure for all three porphyrins are plotted in Figure 6.6. Although none of the porphyrins were soluble in liquid CO_2 (data not shown), all of them were soluble once the critical point was achieved (> 1200 psi). Surprisingly, little change in the concentration was observed at higher pressures.

Solubility Studies Discussion

The solubility of halogenated porphyrins in supercritical carbon dioxide was significantly less than in halogenated solvents. Although solubility increased with pressure as the dielectric constant increased (became more like that of a halogenated solvent), the

maximum solubility achieved was quite low (< 1 μM). Presumably SC CO_2 never became polar enough to dissolve large amounts of porphyrin.

The observed pressure broadening of electronic absorption bands is not unexpected. The $d\sigma^* \rightarrow p\sigma$ transitions in single crystals of Pt_2Cl have been shown to red shift and broaden with pressure.[11] However, the rather dramatic change in the shape of the spectrum from room temperature and one atmosphere pressure relative to SC pressure and temperature for both of the iron porphyrins is rather puzzling. The loss of resolution in the Soret bands of Fe(TFPP)Cl and Fe(TFPPBr$_8$)Cl could be ascribed to pressure broadening. Other aspects of the spectra are not as readily explained. A single intense Q band has appeared in the spectrum of Fe(TFPPBr$_8$)Cl; although absorption maxima often shift with solvent, the appearance of a new absorptions suggests that the porphyrin has been chemically altered. A blue shift in the Soret band and an increase in intensity of a band around 600 nm may be attributed to dimerization at high pressures. Relative to the 410, 510, and 620 nm bands in Fe(TFPP)Cl, (FeTFPP)$_2$O has absorption bands at 398 and 600 nm; these values match well with the observed SC CO_2 spectrum (λ_{max} = 390, 610 nm). Similarly, a μ-oxo dimer of Fe(TFPPBr$_8$)Cl would be expected to have a blue shifted Soret band and a more intense Q band relative to the monomer. The SC CO_2 spectrum of Fe(TFPPBr$_8$)Cl has maximum absorbance at 420 and 600 nm, relative to a 442 nm Soret band and weak Q bands in the solution spectrum. Although formation of a μ-oxo dimer should not have been possible in these experiments, since no oxygen was present in the cell, other dimerization modes are possible and could also account for the observed spectral changes. Contaminants from the carbon dioxide are also possible; although high purity carbon dioxide should be fairly free of impurities, no scrubbers were used. Dimerization is further suggested by the lack of pressure shifting with RuTFPPCl$_8$(CO); the ruthenium porphyrins are not as susceptible to dimerization as the iron analogs. Higher resolution spectra would have to be obtained to fully address this question.

A second complication was introduced by the use of methylene chloride. Methylene chloride was found to extract plasticizers from the O-rings used to make the seal between the sapphire windows and the cell. When the pressure was decreased, the plasticizers formed a film on the interior of the cell, possibly causing interference patterns and reducing the quality of the spectra. Furthermore, the plasticizers seem to reduce the solubility of $RuTFPPCl_8(CO)$. Addition of $RuTFPPCl_8(CO)$ as a solid to the cell resulted in much high solubility (Figure 6.7). By 3000 psi, the Soret band had already reached the maximum absorbance able to be measured by the instrument (~ 0.4).

Addition of cyclohexene resulted in a higher quality spectrum for $RuTFPPCl_8(CO)$ (Figure 6.8). No solubility is observed in liquid carbon dioxide, but the transition limit of the spectrophotometer is reached by 2000 psi, indicating that cyclohexene is an excellent co-solvent for $RuTFPPCl_8(CO)$. Cyclohexene also reduces the noise level in the ruthenium porphyrin spectrum; this effect is not understood. The structure in the Q band region changes in the presence of olefin, with a slight red shift and different intensity for the Q(1,0) and the Q(0,0) bands relative to the methylene chloride spectrum, indicating that cyclohexene may coordinate at high pressure, since no distinct Q bands were observed with SC CO_2 alone.

Despite the complications and noise levels of the spectra, lower limits for the solubility of the three halogenated porphyrins were determined. The minimal solubility of these complexes is not expected to limit the reactivity of the catalysts in supercritical carbon dioxide since the co-solvent properties of the substrate, cyclohexene, will increase the net solubility of Fe(TFPP)Cl, $Fe(TFPPBr_8)Cl$, and $RuTFPPCl_8(CO)$ in the oxidation reaction mixture.

The ability to perform UV-visible spectroscopy at high pressures is a valuable tool for studying reaction intermediates in SCF reactions. This will help determine if reaction pathways change at higher pressures. Further work to enable transient IR and emission spectroscopy in SCF systems is currently in progress at LANL.

Oxidation of Cyclohexene

We investigated the ability of Fe(TFPP)Cl, Fe(TFPPBr$_8$)Cl, and RuTFPPCl$_8$(CO) to oxidize cyclohexene in supercritical carbon dioxide. The oxidation reaction had been studied in methylene chloride (Chapter 4 and 5), providing a comparison for data in a SCF. For oxidations with dioxygen, it was thought that the miscibility of O_2 would increase the reaction rate relative to the solution chemistry.

In order to help separate solvent and pressure effects, oxygenation reactions with iodosobenzene as an oxygen source were also investigated. This chemistry should be relatively unaffected by pressure, and should help isolate the different solvation properties at high pressure.

The oxidation reactions were conducted in a small autoclave reactor (Figure 6.9). Constructed in a similar fashion to the UV-Vis apparatus, this system had an additional inlet for pressurized air. The porphyrin, cyclohexene, and iodosobenzene (if used) were added to the reactor, which was then sealed and connected to the carbon dioxide inlet. As with the UV-Vis cell, the system temperature was maintained at 40 °C and the reaction stirred to maintain equilibrium. All reactions were run at 5000 psi of CO_2 to maximize solubility of the porphyrin. At the end of the batch reaction, the pressure was let down through a metering valve, and volatile organics were collected in cold acetone. The cell was washed with additional acetone, and products were detected by GC/MS.

Two reactions were run in the UV-Vis cell in order to determine the effect of light on the ruthenium porphyrin oxidation reaction. Since irradiation with visible light dramatically enhances catalysis by RuTFPPCl$_8$(CO) with dioxygen in methylene chloride, we wanted to determine if light would also enhance cyclohexene oxidation in SC CO_2.

The results of the oxidation reactions are shown in Figures 6.10 - 6.12. With iodosobenzene, the overall activity was similar to the methylene chloride reactions for Fe(TFPP)Cl and Fe(TFPPBr$_8$)Cl. RuTFPPCl$_8$(CO) activity was considerably higher in

SC CO_2, with 21 turnovers compared to only 5 in methylene chloride (4 hour points). The product distributions for these reactions showed more variation. Notably, Fe(TFPP)Cl produced only cyclohexene oxide. For the perhalogenated iron and ruthenium complexes, higher oxidation products were observed. While reactions in methylene chloride have only been found to produce 2-cyclohexen-1-ol and 2-cyclohexen-1-one, the SC CO_2 reactions showed large peaks in the GC at later retention times. The first was identified by comparison to a library mass spectrum as 7-oxa-bicyclo[4.1.0]heptan-2-one (Figure 6.13). The second was assumed to be 4-hydroxy-2-cyclohexen-1-one due to a similar relationship in the retention times of cyclohexene oxide and 2-cyclohexen-1-ol, and since it is the logical partitioning product from the oxidation of 2-cyclohexen-1-one. Both $Fe(TFPPBr_8)Cl$ and $RuTFPPCl_8(CO)$ reactions with PhIO showed less 2-cyclohexen-1-ol than in methylene chloride, and more 2-cyclohexen-1-one, as well as 7-oxa-bicyclo[4.1.0]heptan-2-one and 4-hydroxy-2-cyclohexen-1-ol. None of the reactions used more than 30% of the available oxidant in 4 hours. A batch reaction of $Fe(TFPPBr_8)Cl$ run for 12 hours showed no more epoxide formation, but more allylic oxidation products were observed.

With air, the catalyst activities were similar in the two solvents. It is difficult to make a direct comparison, because the batch reactions in SC CO_2 were run for different times than the methylene chloride experiments. Nevertheless, it is clear that all catalysts are quite active in the supercritical solvent. Fe(TFPP)Cl (at 4 hours), $Fe(TFPPBr_8)Cl$, and $RuTFPPCl_8(CO)$ (at 12 hours) showed 11, 59, and 51 turnovers, respectively. If the higher oxidation products are considered as more than one turnover, the numbers for the latter reactions increase to 127 and 90 turnovers. As with iodosobenzene, substantial amounts of multiple oxidation products were observed in all reactions, with a decrease in the amount of 2-cyclohexen-1-ol produced. Surprisingly, a greater percentage of epoxide was also produced.

Both $Fe(TFPPBr_8)Cl$ and $RuTFPPCl_8(CO)$ had substantial initiation periods in SC CO_2. Batch reactions run for only 4 hours showed no trace of products. After 12

hours, however, significant activity was observed, as described above. Only Fe(TFPP)Cl showed activity with air in the 4 hour time period. Attempts to shorten the initiation period for $RuTFPPCl_8(CO)$ by the addition of light were not successful. Two experiments with $RuTFPPCl_8(CO)$ were conducted in the larger UV-Vis cell. Upon addition of CO_2, the solution turned a bright red, indicating that cyclohexene serves as an excellent co-solvent for the catalyst. A flashlight was used to irradiate the reaction through the cell window for the duration of the batch reaction. However, after only a few hours, the pressure dropped and the solution bleached. A reaction in the UV-Vis cell was attempted twice. The first reaction, with one atmosphere of air, bleached after 20 hours. The second, with 5 atm air, bleached within 6 hours. After bleaching was observed, the cell was let down as previously described. No product formation was detected in either light reaction.

Discussion Oxidation Experiments

The iodosobenzene reactions in supercritical carbon dioxide all showed an increase in the percent epoxide formed relative to reaction in CH_2Cl_2. As discussed in Chapter 4, epoxidation with a high-valent metal-oxo is believed to occur by a different mechanism than hydroxylation. The different solvation properties of SC CO_2 may increase the probability for electron transfer (leading to epoxidation) over hydrogen abstraction (leading to hydroxylation). The success of free radical polymerization reactions conducted in SC CO_2 suggests that radicals are quite stable in a supercritical medium. However, the solvent may change the stability of the caged radical species such that electron transfer becomes more favorable. SC CO_2 may provide a new medium for probing the oxo-transfer step in olefin oxidation reactions.

In addition to the increase in epoxide formation, there is also an increase in multiple oxidations of the same substrate molecule, both with PhIO and dioxygen. The supercritical fluid did not greatly increase the observed turnover numbers, suggesting that phase transfer is not the limiting step in the dioxygen reactions for any of the porphyrins. However, the

different solvent properties of SC CO_2 may be changing the selectivity; perhaps the catalysts are more soluble in the oxidized cyclohexene derivatives than in cyclohexene itself. Therefore, the catalyst could re-oxidize a single substrate multiple times before encountering other substrate molecules.

For $RuTFPPCl_8(CO)$, fewer turnovers are observed in the dark cell, consistent with the photochemical reaction mechanism described in Chapter 5. However, the UV-Vis suggests a greater interaction between the porphyrin and substrate in SC CO_2, indicating that olefin binding may occur in the ground state in this medium, whereas it only is effective in the excited state in a methylene chloride solution. Alternatively, a different reaction mechanism may take precedence in this solvent. Unfortunately, attempts to photolyze the reaction were complicated by the cell design. The Buna-N O-rings used to seal the sapphire windows, while having excellent resistance to supercritical carbon dioxide, are reported to have unsatisfactory resistance to alkanes,[12] suggesting that the "bleach" observed upon photolysis was not due to porphyrin decomposition but a leaking cell.

Conclusion

The preliminary results described above demonstrate that supercritical carbon dioxide is an adequate solvent replacement for methylene chloride for porphyrin-catalyzed oxidation of cyclohexene. Large rate enhancement was not observed, but changes in the reaction selectivity did occur. Most notable was the 100% selectivity observed for epoxidation of cyclohexene with Fe(TFPP)Cl and PhIO, and increased epoxidation selectivity for both $RuTFPPCl_8(CO)$ and $Fe(TFPPBr_8)Cl$ in reactions with either PhIO or O_2. For allylic oxidation products, multiple oxidations of the same substrate molecule was observed, suggesting that destruction of organics in a supercritical medium may be favorable under different conditions. A repeat of the oxidation experiments at different temperatures and pressures would reveal if the selectivity could be tuned to favor one

pathway more completely. Further experiments would be needed to determine the source of these effects.

Methods

$RuTFPPCl_8(CO)$ and $Fe(TFPPBr_8)Cl$ were synthesized as in Chapter 2. Fe(TFPP)Cl was used as received (Aldrich). Cyclohexene was from Aldrich, and distilled under argon before use. Acetone and methylene chloride were used as received from EM Science. Iodosobenzene was from TCI and used as received. Air and carbon dioxide were from Albuquerque Welding. Oxidation products were determined by injection onto an Hewlett Packard GC/MS with an auto injector and a JW Scientific DB-5 30m column. Sample identification was determined by injection of an authentic sample for cyclohexene oxide, 2-cyclohexen-1-ol, and 2-cyclohexen-1-one (Aldrich). The identity of one higher boiling peak was determined by the library on the GC MS.

Standard NPT, Swagelock, and HiP pressure rated valves and connections were used to build the high pressure systems. Stainless steel tubing (1/16" - 1/4") was used for longer connections. An ISCO brand syringe pump was used to pressurize the carbon dioxide. All systems were barricaded behind Lexan shielding, and tubing and valves were secured to the work tables to minimize damage in case of a pressure failure. All systems were equipped with relief valves or rupture discs, so the system would blow at the designed weak point in case of over-pressurization.

UV-Vis spectra were measured on a Hewlett Packard 8452 spectrophotometer. The lamp and detector were removed from the instrument cavity and placed on a laser table to allow room for the large cell. Additional focusing mirrors were placed after the lamp and before the detector to increase light intensity. Intensity data was collected in ASCII format, and loaded onto a Macintosh computer, where absorbance readings were calculated ($A = \log (I_o/I)$. I_o readings were taken at each pressure since the absorbance of CO_2 was found to change considerably around the supercritical transition. This is due to the variable

density of SC CO_2; the change in the index of refraction between the cell windows and solvent decreased at higher pressures. The stirplate was turned off when spectra were taken, in order to minimize refraction by mixing lines in solution. The large cell volume (≈ 75 mL) made it difficult to maintain a constant temperature in the cell, causing visible sheer lines due to the temperature gradient in solution. Averaging intensity data helped decrease the noise in the spectra.

The cell used for UV-Vis experiments was constructed of 316 stainless steel, with a 13.2 cm path length and 1 inch aperture on each side. The seal between the 1 cm thick sapphire windows and the metal cell was made by a Buna-N rubber O-ring, which was replaced after each use. The cell had three inlets for a thermocouple, an inlet valve, and a t-joint which contained a relief valve, an analog pressure gauge, and an outlet line. The outlet could be directed to a vacuum pump or vented to a hood.

For each sample, the cell was first mounted on the stand and aligned for maximum lamp intensity. A solution of porphyrin in methylene chloride was added through the thermocouple inlet, and then the thermocouple was fastened down. By this method, a known amount of porphyrin could be added, such that the possible absorbance in a 13.2 cm path length cell would not be above 1. The cell was evacuated, removing the solvent, and then carbon dioxide was added. The cell was sealed off at each pressure, and allowed to equilibrate to 40 ± 0.5 °C for each intensity reading. Alternatively, excess solid porphyrin was added to the cell before the windows were sealed down (the large nuts for the windows had to be tightened down on a vise).

Oxidation reactions were conducted in a cell designed by Dave Morgenstern and Sam Borkowsky at Los Alamos National Laboratory. This cell was a single 2.5" cylinder of 316 stainless steel, with a 5/8" hole bored into the center. The only openings were for a rupture disc (rated to 10000 psi), an analog pressure gauge, a thermocouple, and the main reactor valve. The total cell volume was ≈ 12 mL. The inlet lines allowed the sequential addition of compressed air and carbon dioxide to the cell. Air was always added first, so

that the CO_2 would flush any oxygen from the lines before the system was brought up to pressure. Although air or pure oxygen gas could be used with this reactor, air was used for safety reasons.

Solid porphyrin, cyclohexene, and iodosobenzene (if used) were added to the reactor, the valve was sealed on the vise, and the reactor was then attached to the inlet and letdown tubing. Air was added first, up to the pressure of the tank (110 psig) and then CO_2 up to 5000 psi. As with the UV-Vis experiments, the cell rested on a stirplate and the cell temperature was maintained at 40 °C with heating tape. As soon as the pressure reached 5000 psi, the main reactor valve was closed, and the system allowed to stir for the desired reaction time.

Oxidation reactions were let down by a HiP metering valve through 1/16" tubing, and the end of the tubing was crimped with a hammer to reduce the flow rate. The pressure was let down slowly over a period of 1-2 hours into a vial containing approximately 20 mL of cold acetone to catch volatile organics. The vial rested in a cold block of steel to maintain its temperature and reduce loss of organics. The reaction vessel was then opened and rinsed with acetone to remove residual cyclohexene and products. The rinse was collected, and the volume measured. An aliquot was taken, diluted with a known amount of toluene in acetone to standardize the GC/MS analysis, and injected onto the GC. Although there is undoubtedly some loss to evaporation, it is believed that most of the organic products are collected by this method. No mass balance calculation was attempted.

References and Notes

(1) Kaupp, G. *Angew. Chem., Int. Ed. Eng.* **1994**, *33*, 1452-1455.

(2) Laintz, K. E.; Tachikawa, E. *Anal. Chem.* **1994**, *66*, 2190-2193.

(3) Personal communication from William Tumas, Los Alamos National Laboratory, January1995.

(4) Wenclawiak, B. In *Analysis with Supercritical Fluids: Extraction and Chromatography*; B. Wenclawiak, Ed.; Springer-Verlag: Berlin, 1992.

(5) Dickerson, R. E.; Gray, H. B.; Darensbourg, M. Y.; Darensbourg, D. J. *Chemical Principles;* 4th ed.; The Benjamin/Cummings Publishing Co., Inc.: Menlo Park, CA, 1984.

(6) DeSimone, J. M.; Maury, E. E.; Meneceloglu, Y. Z.; McClain, J. B.; Romack, T. J.; Combes, J. R. *Science* **1994**, *265*, 356-359.

(7) Jessop, P. G.; Hsiao, Y.; Ikariya, T.; Noyori, R. *J. Am. Chem. Soc.* **1994**, *116*, 8851-8852.

(8) Jessop, P. G.; Ikariya, T.; Noyori, R. *Nature* **1994**, *368*, 231-233.

(9) A substantial amount of oxidation chemistry has been investigated in supercritical water. Complete oxidation of organics has been observed under these harsh conditions. For example, see Webley, P. A.; Tester, J. W. *Energy Fuels.* **1991**, *30*, 411.

(10) Srinivas, P.; Mukhopadhyay, M. *Ind. Eng. Chem. Res.* **1994**, *33*, 3118-3124.

(11) Stroud, M. A.; Drickamer, H. G.; Zietlow, M. H.; Gray, H. B.; Swanson, B. I. *J. Am. Chem. Soc.* **1989**, *111*, 66-72.

(12) Seymour, R. S. *Engineering Polymer Source Book*; McGraw-Hill: New York, 1990, pp 102.

Figure 6.1 -- Phase diagram of carbon dioxide (modified from reference 5). The critical point of CO_2 is at relatively low temperature and pressure, facilitating its use as a supercritical solvent.

Phase Diagram of Carbon Dioxide

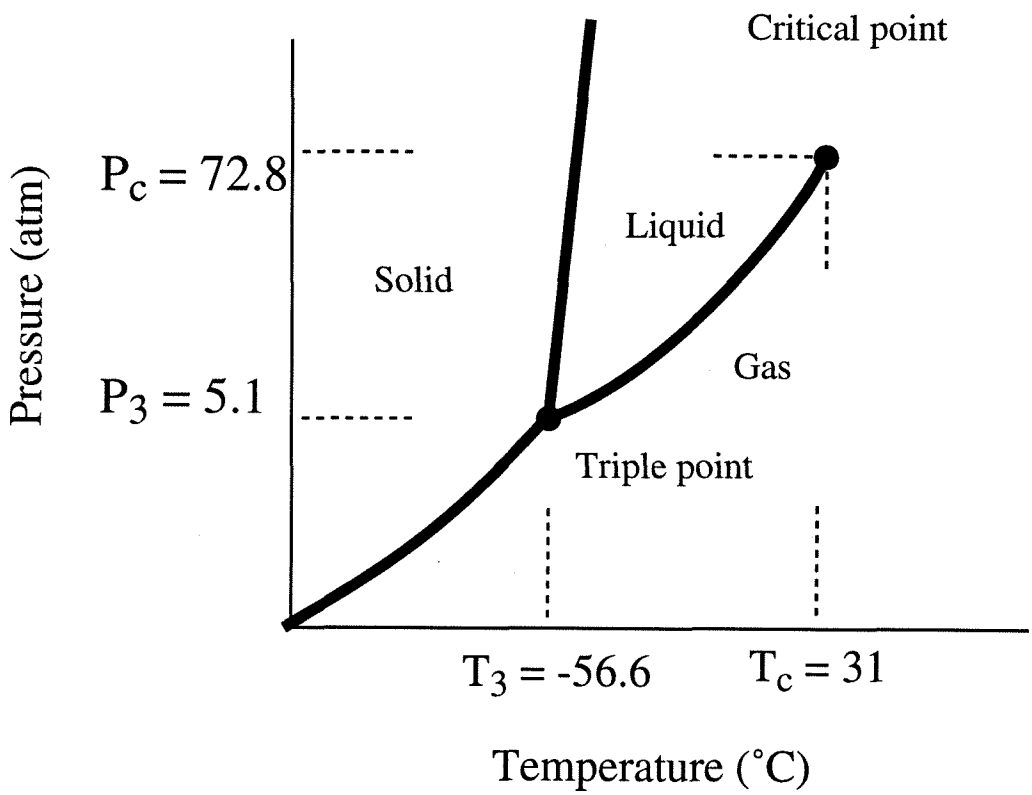

Figure 6.2 -- Apparatus used for UV-Visible spectroscopy in supercritical carbon dioxide.

UV Vis in Supercritical CO_2

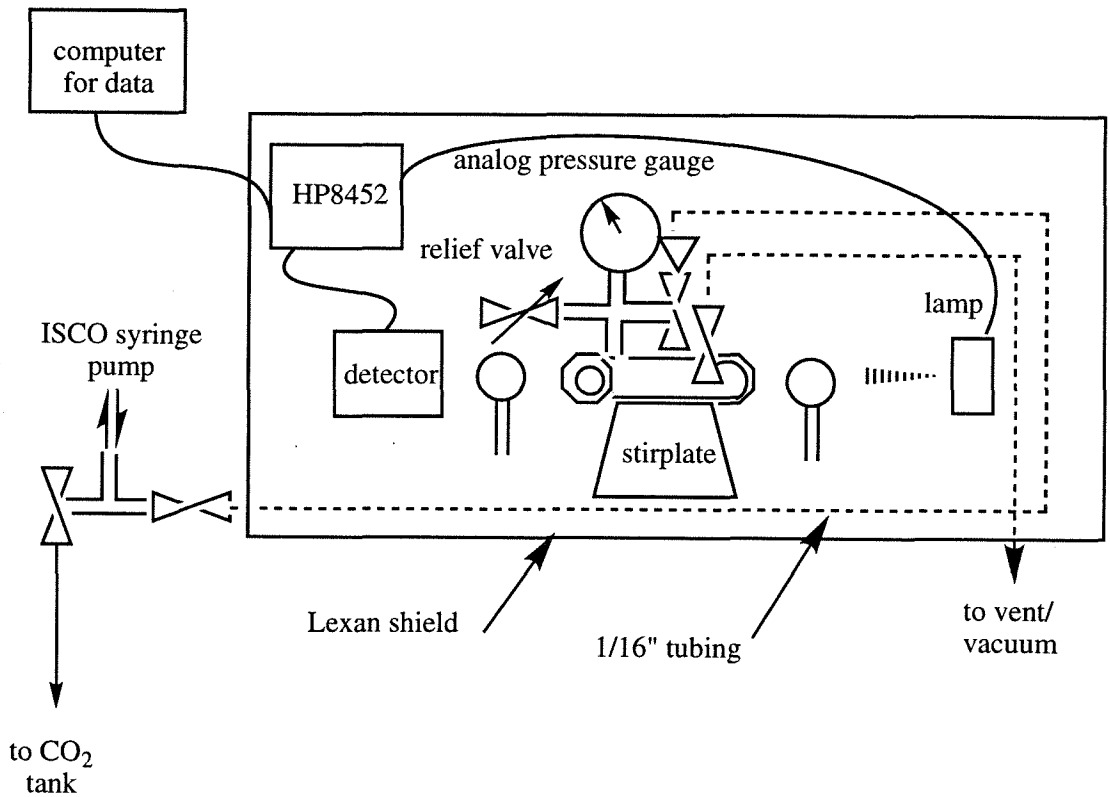

Cell characteristics: 6 inches long, 13.2 cm path length
1 inch diameter aperture with sapphire windows
75 mL cell volume, including dead space
316 stainless steel
rated to 5000 psi

Figure 6.3 -- Spectra of Fe(TFPP)Cl in methylene chloride and carbon dioxide. The spectrum in SC CO_2 is smoothed to remove noise from refracted light. The solubility did not change much with pressure, increasing only from 0.27 to 0.30 μM from 2000 to 5000 psi of CO_2.

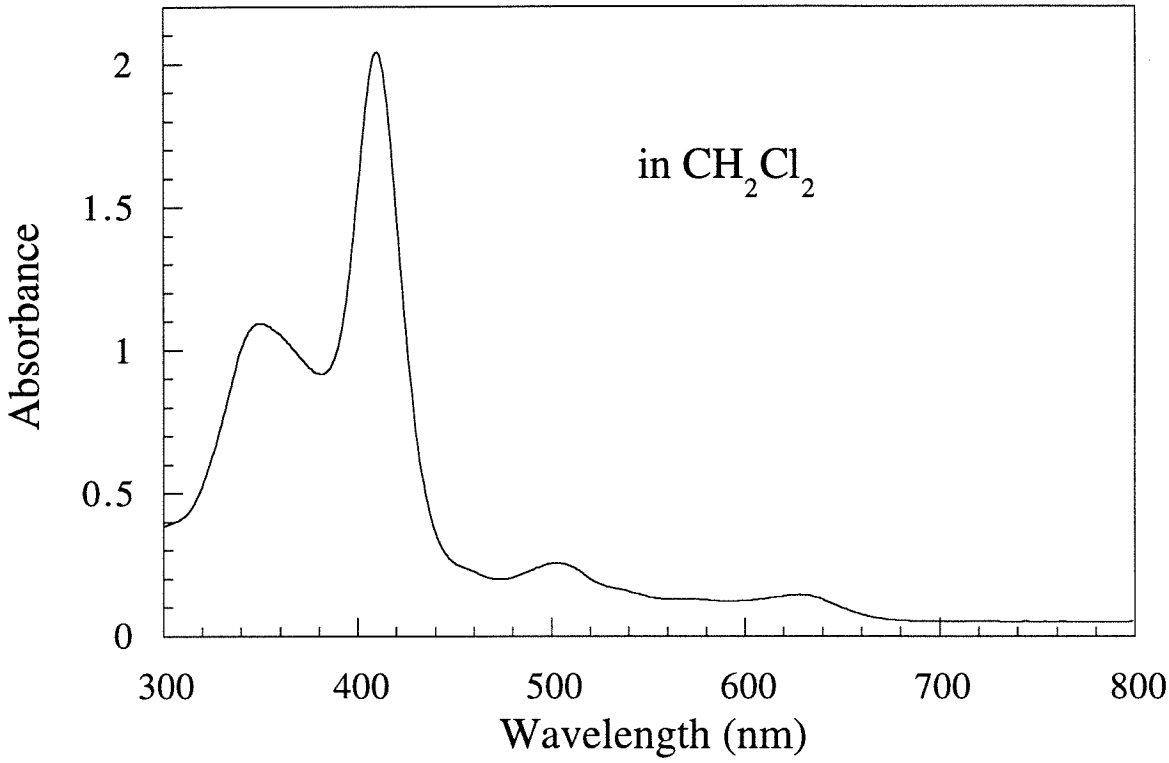
in CH_2Cl_2
Absorbance
0
0.5
1
1.5
2
300
400
500
600
700
800
Wavelength (nm)

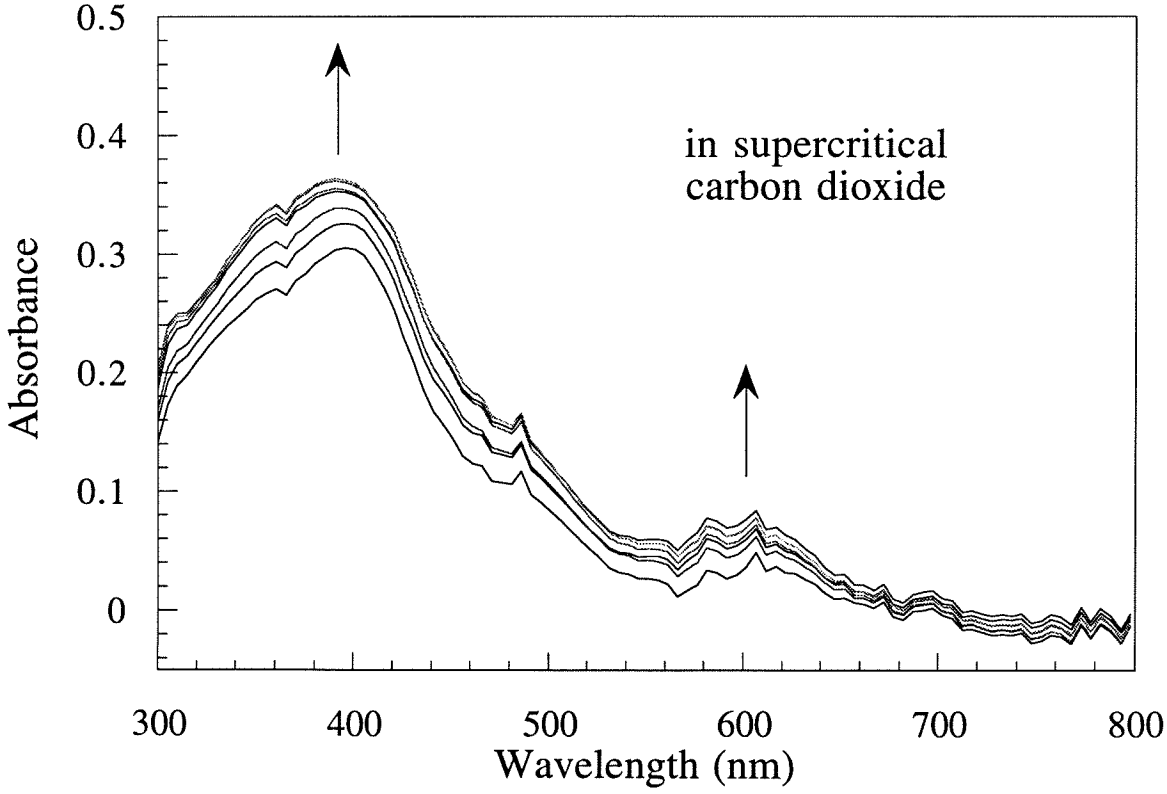
in supercritical
carbon dioxide
Absorbance
0
0.1
0.2
0.3
0.4
0.5
300
400
500
600
700
800
Wavelength (nm)

Figure 6.4 -- Spectra of $Fe(TFPPBr_8)Cl$ in methylene chloride and carbon dioxide. The spectrum in SC CO_2 is smoothed to removed noise from refracted light. The solubility increased from 0.07 to 0.20 μM from 2000 to 3500 psi of CO_2, remaining fairly constant after this pressure.

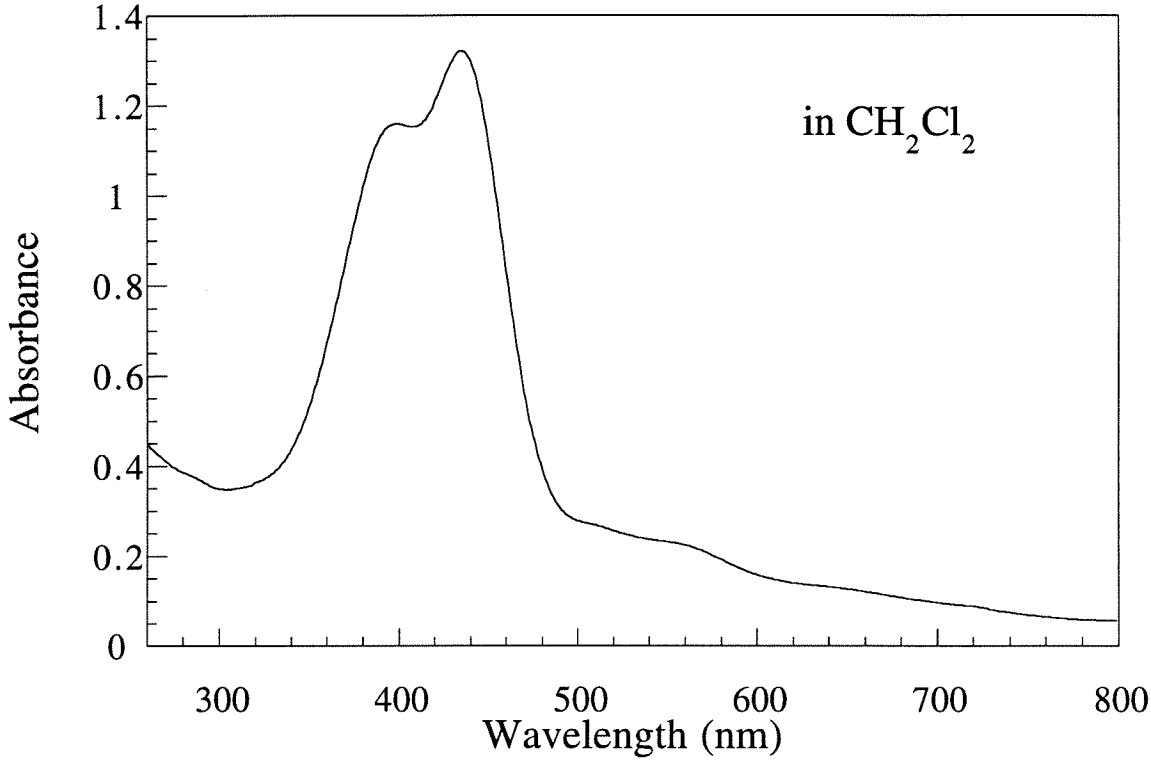
in CH_2Cl_2
Absorbance
Wavelength (nm)
0
0.2
0.4
0.6
0.8
1
1.2
1.4
300
400
500
600
700
800

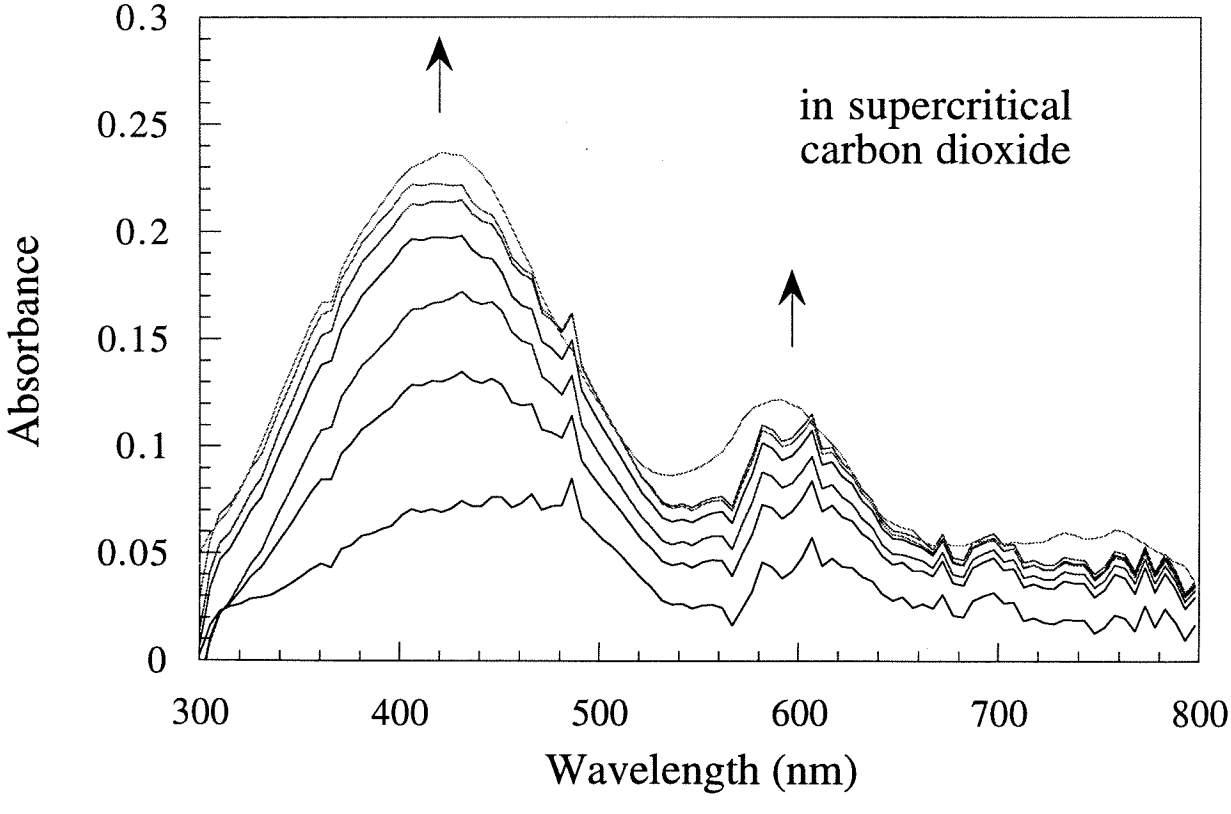
in supercritical
carbon dioxide
Absorbance
Wavelength (nm)
0
0.05
0.1
0.15
0.2
0.25
0.3
300
400
500
600
700
800

Figure 6.5 -- Spectra of $RuTFPPCl_8(CO)$in methylene chloride and carbon dioxide. The porphyrin is almost insoluble in liquid CO_2, but solubility increased to 0.16 μM at 5000 psi of CO_2. The spectra in the two different solvents match best for $RuTFPPCl_8(CO)$, suggesting no unusual interactions in the supercritical solvent.

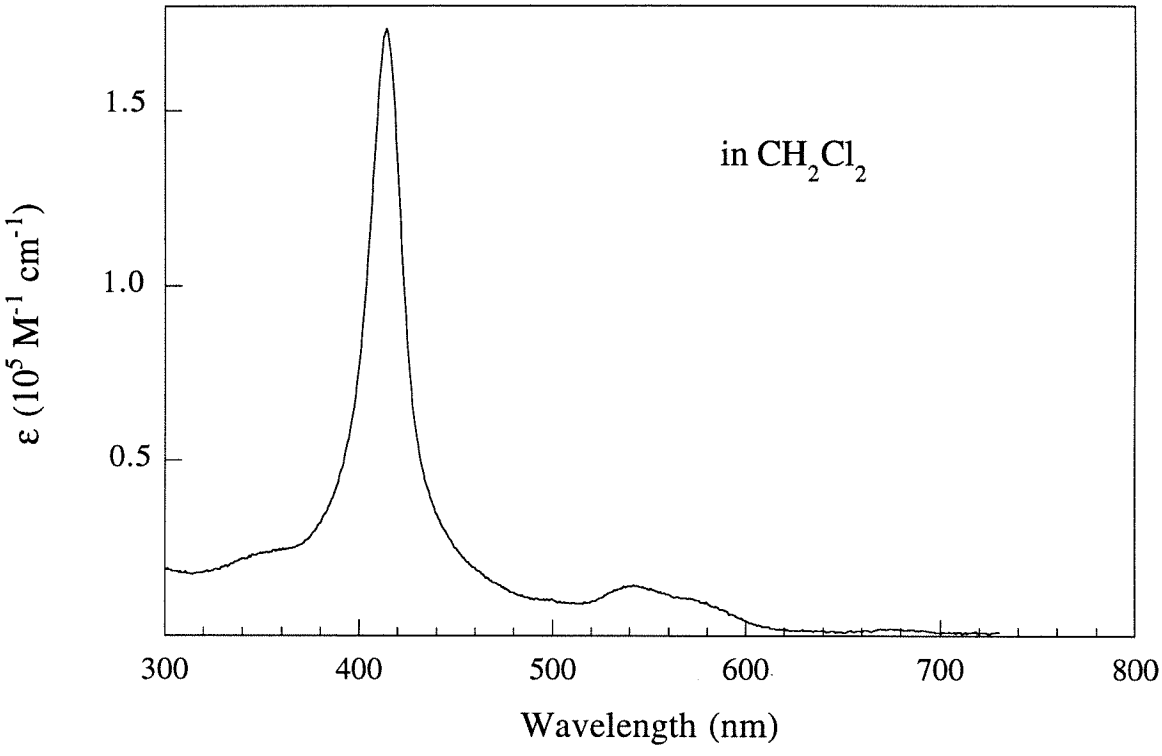
in CH_2Cl_2
ε (10^5 M^{-1} cm^{-1})
1.5
1.0
0.5
300
400
500
600
700
800
Wavelength (nm)

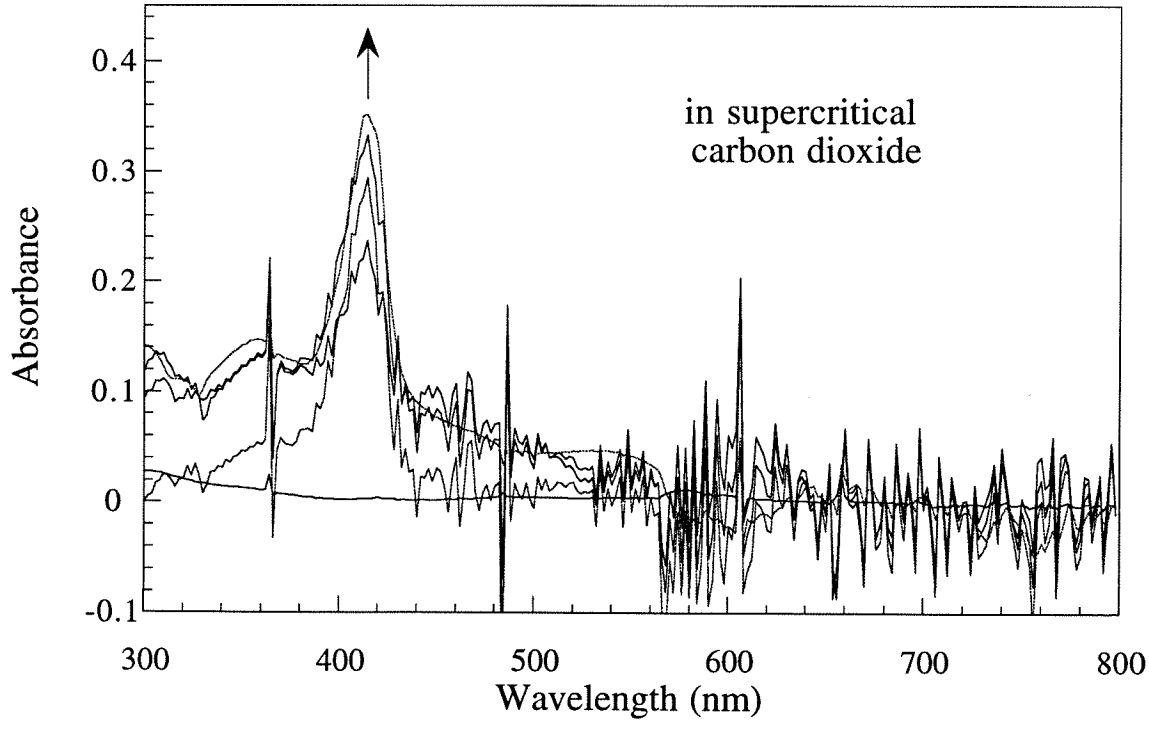
in supercritical
carbon dioxide
Absorbance
0.4
0.3
0.2
0.1
0
-0.1
300
400
500
600
700
800
Wavelength (nm)

Figure 6.6 -- A plot of solubility versus pressure for the halogenated porphyrins.

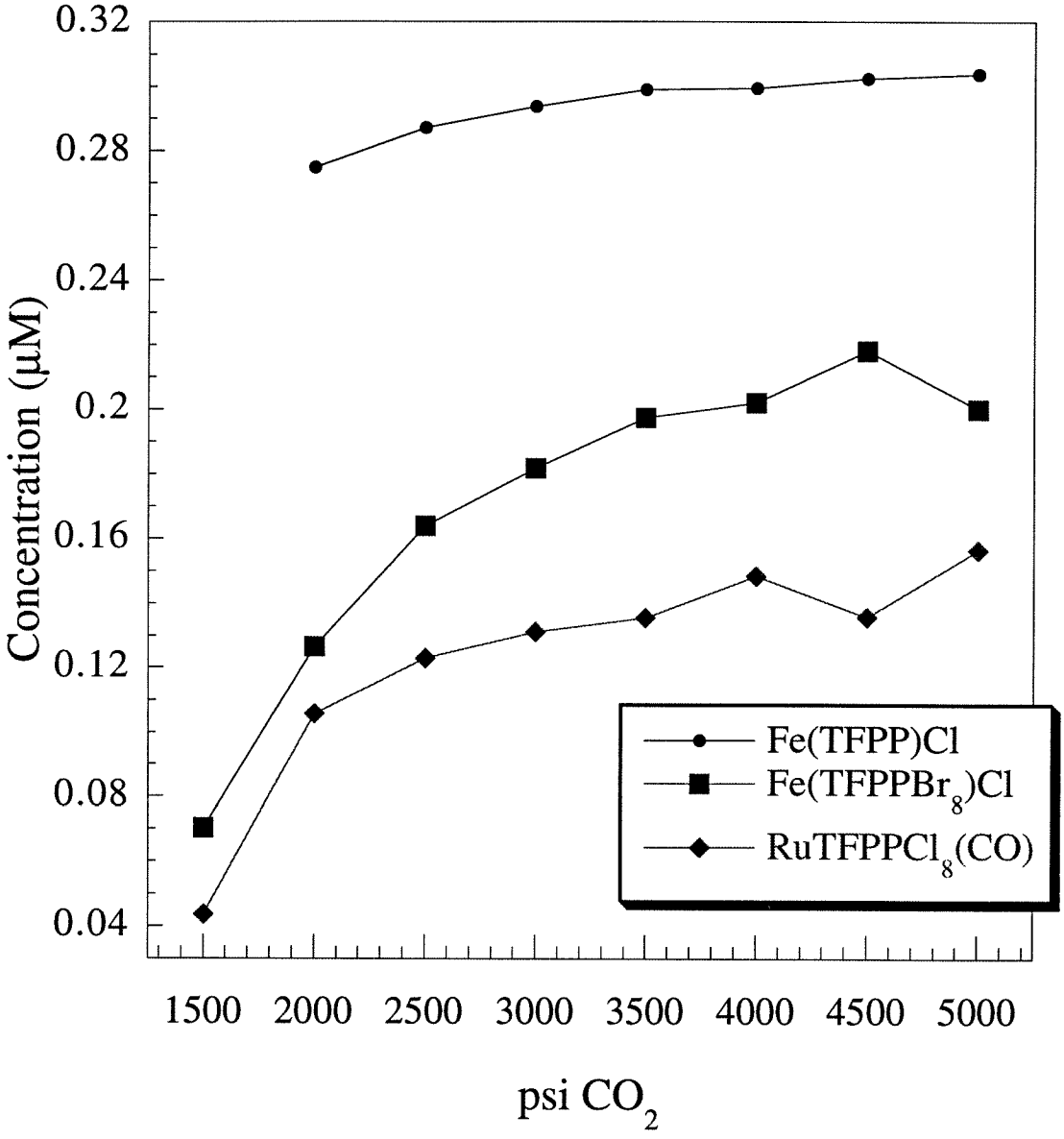
0.32
0.28
0.24
0.2
0.16
0.12
0.08
0.04
Concentration (μM)
1500
2000
2500
3000
3500
4000
4500
5000
psi CO2
Fe(TFPP)Cl
Fe(TFPPBr8)Cl
RuTFPPCl8(CO)

Figure 6.7 -- Spectrum of $RuTFPPCl_8(CO)$ in carbon dioxide. This differs from the spectrum in Figure 6.3 in that the porphyrin was added as a solid, and not as a methylene chloride solution. The solubility is much higher in this case, reaching the maximum transmission of the instrument by 3000 psi, suggesting that a deleterious interaction occurs when the porphyrin is added as a CH_2Cl_2 solution (data at 2000, 3000, and 4000 psi).

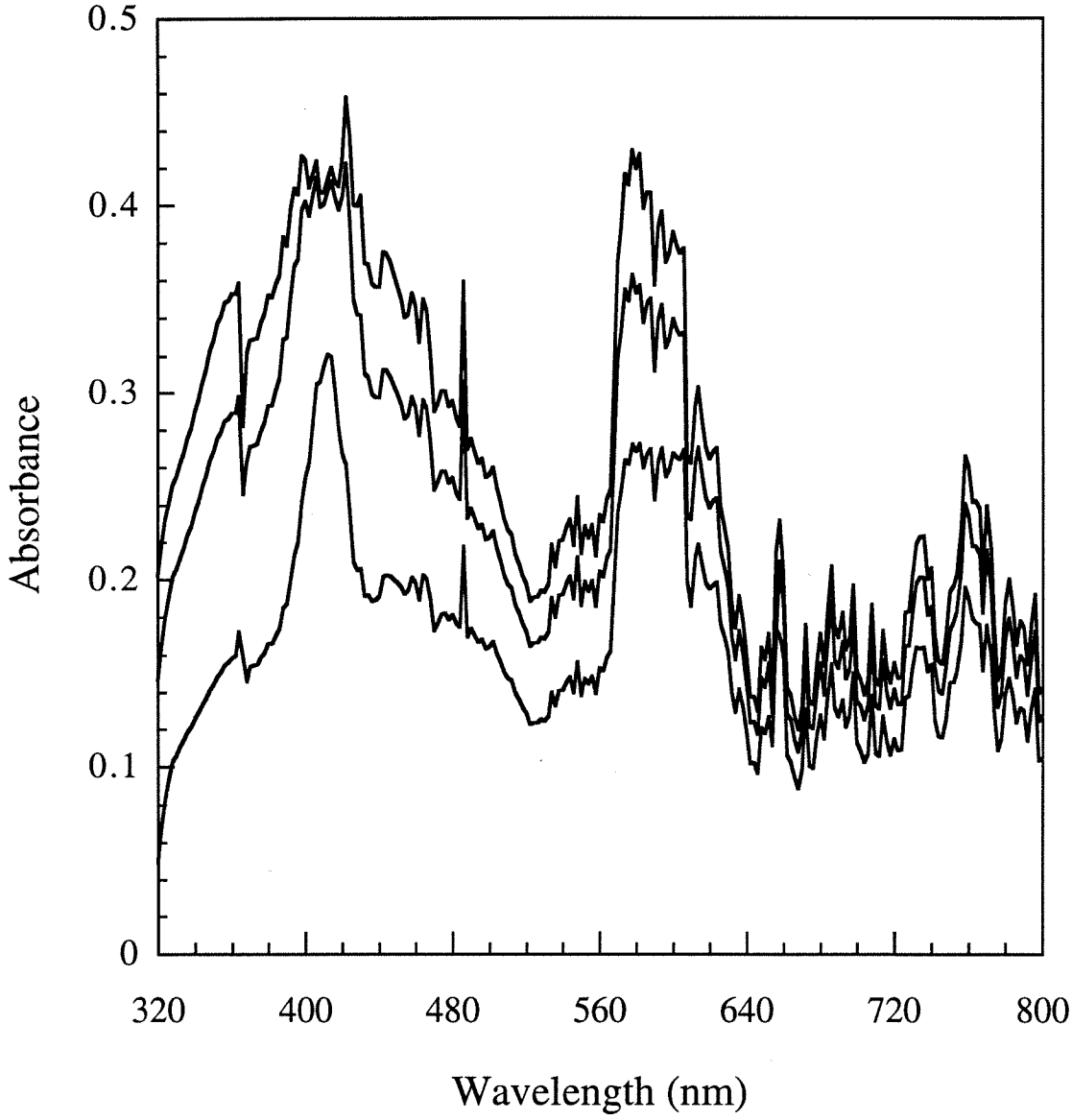
0.5
0.4
0.3
0.2
0.1
0
Absorbance
320
400
480
560
640
720
800
Wavelength (nm)

Figure 6.8 -- Spectrum of $RuTFPPCl_8(CO)$ with cyclohexene in carbon dioxide. The Q band structure is significantly different than without cyclohexene, suggesting a possible interaction or binding of alkene in the supercritical solvent (data at 800, 1200, 2000, 3000, 4000, and 5000 psi).

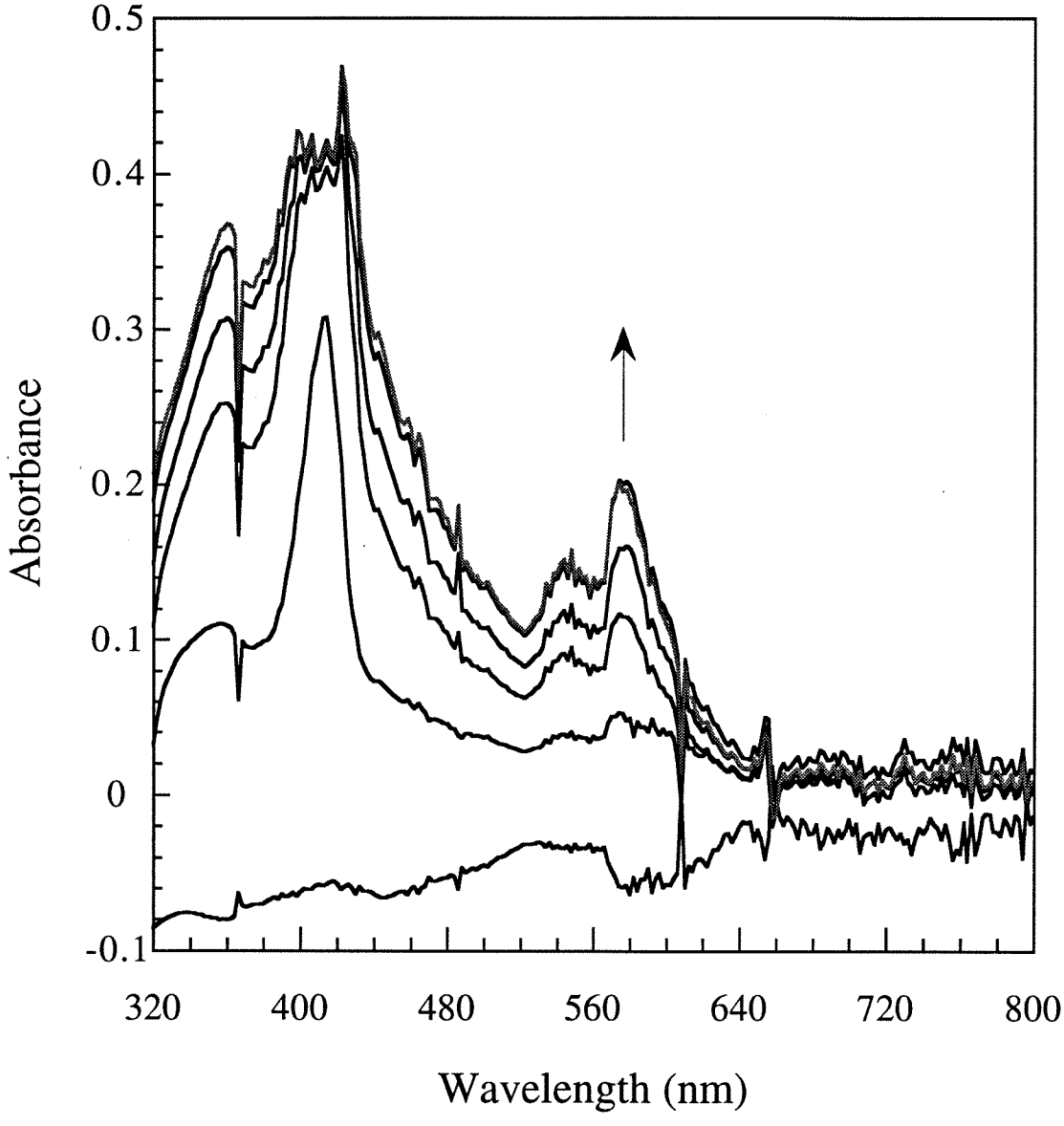
0.5
0.4
0.3
0.2
0.1
0
-0.1
Absorbance
320
400
480
560
640
720
800
Wavelength (nm)

Figure 6.9 -- Cell used for oxidation reactions with iodosobenzene or air by halogenated porphyrins in supercritical carbon dioxide.

Plumbing for High Pressure Oxygen Reactions in Small Cell

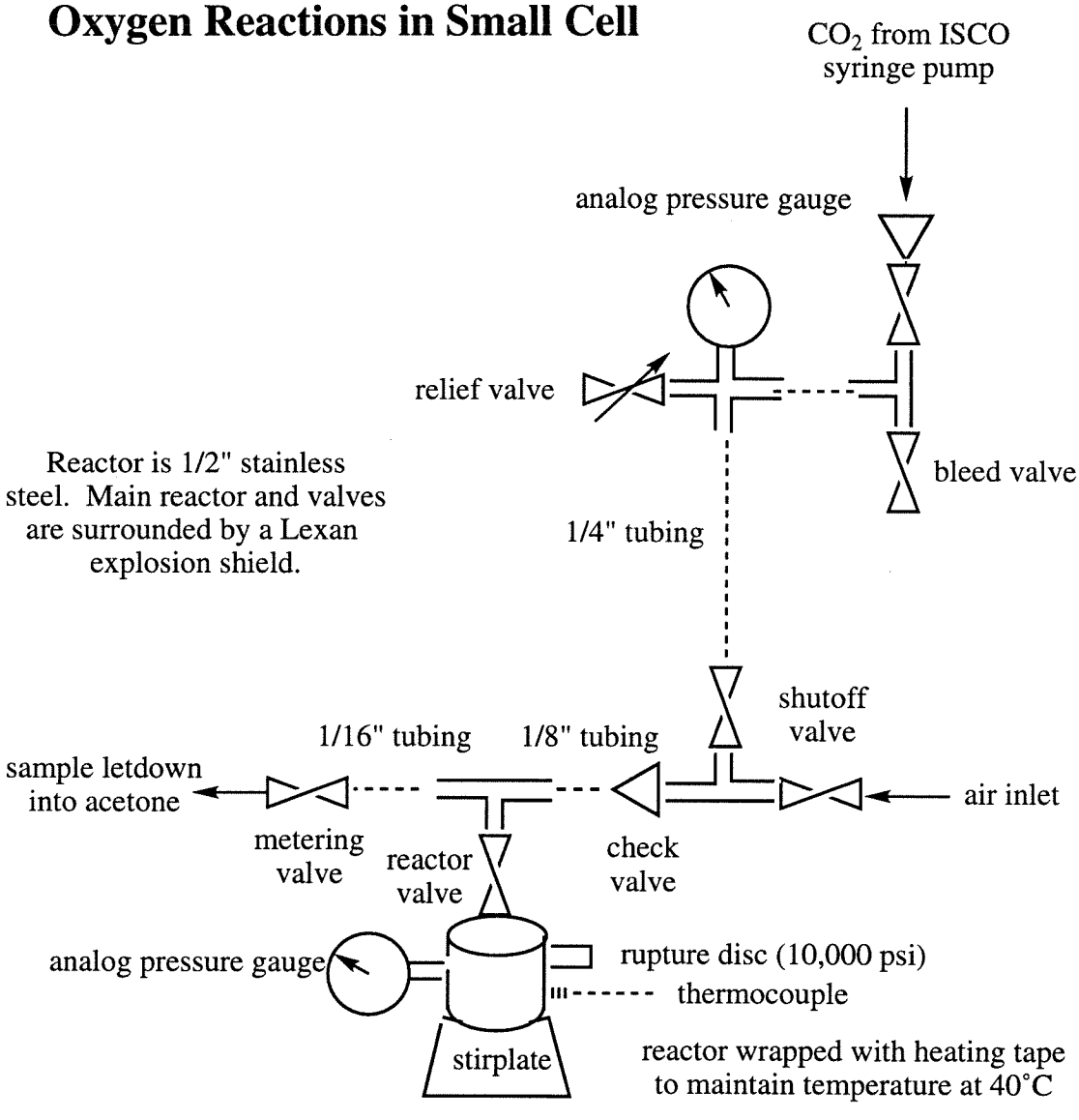

Figure 6.10 -- Turnovers of cyclohexene observed in oxidation reactions with Fe(TFPP)Cl and either iodosobenzene (left) or dioxygen (right). PhIO data is after 4 hours, and the dioxygen results are at 24 hours (CH_2Cl_2) or 12 hours (SC CO_2) in the different solvents. 100% selectivity for epoxide formation is observed with PhIO in SC CO_2.

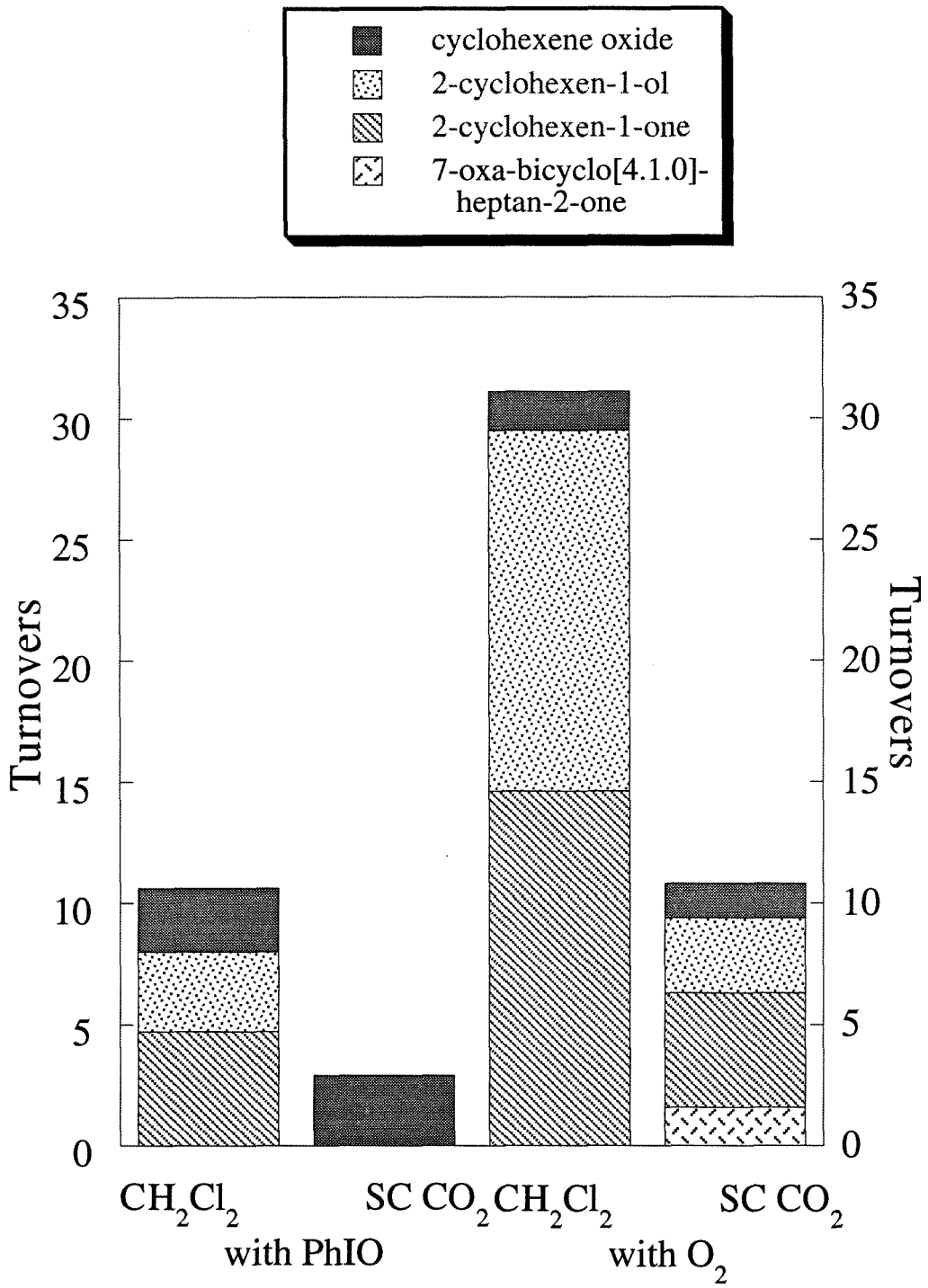
cyclohexene oxide
2-cyclohexen-1-ol
2-cyclohexen-1-one
7-oxa-bicyclo[4.1.0]-heptan-2-one
Turnovers
35
30
25
20
15
10
5
0
CH2Cl2
SC CO2
CH2Cl2
SC CO2
with PhIO
with O2

Figure 6.11 -- Turnovers of cyclohexene observed in oxidation reactions with $Fe(TFPPBr_8)Cl$ and either iodosobenzene (left) or dioxygen (right). PhIO data is after 4 hours, and the dioxygen results are at 24 hours (CH_2Cl_2) or 12 hours (SC CO_2) in the different solvents. Higher selectivity for epoxide formation is observed with dioxygen in SC CO_2 relative to CH_2Cl_2. Significant amounts of higher oxidation products are also observed.

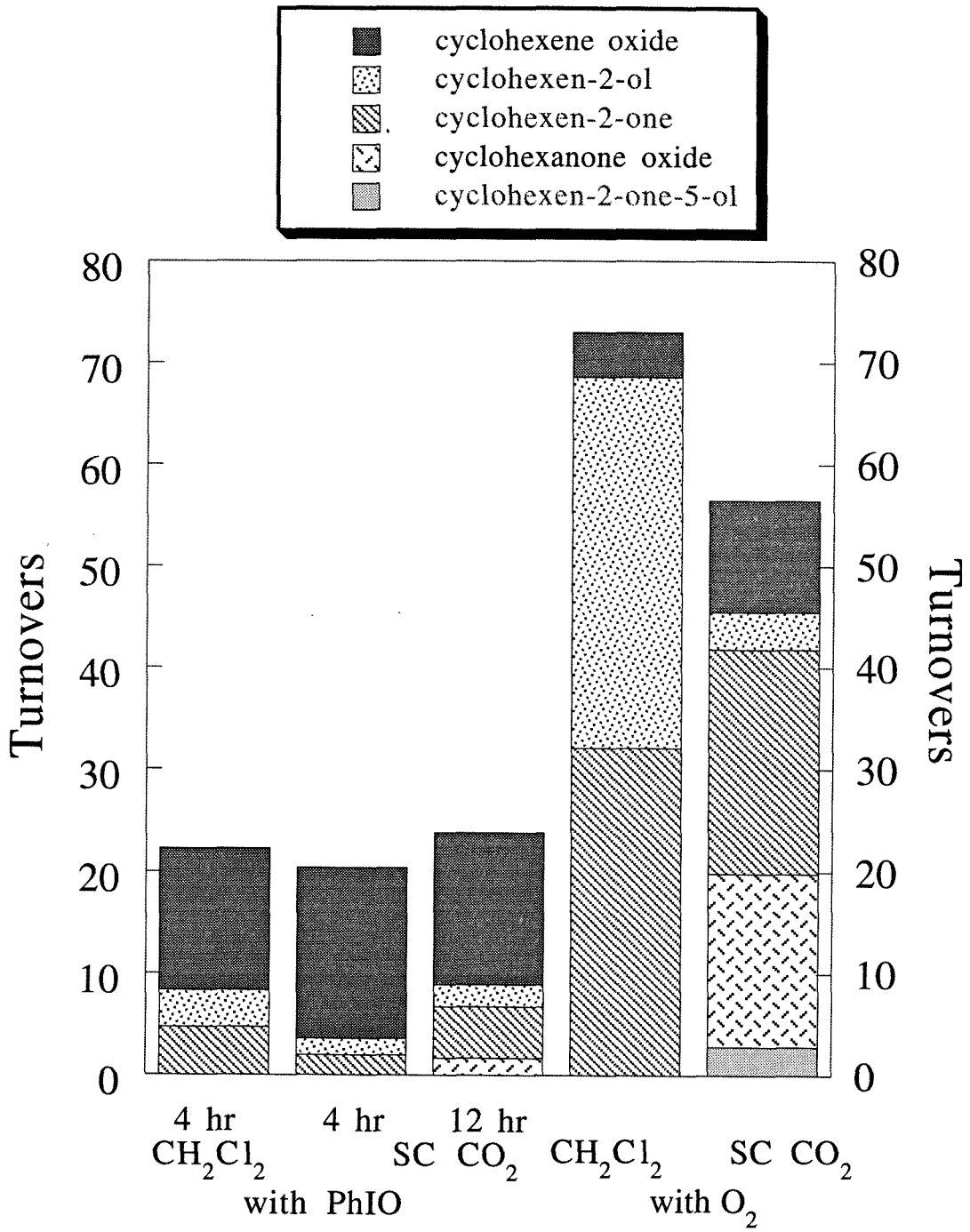
cyclohexene oxide
cyclohexen-2-ol
cyclohexen-2-one
cyclohexanone oxide
cyclohexen-2-one-5-ol
Turnovers
0
10
20
30
40
50
60
70
80
4 hr
CH_2Cl_2
4 hr
SC CO_2
12 hr
with PhIO
CH_2Cl_2
SC CO_2
with O_2

Figure 6.12 -- Turnovers of cyclohexene observed in oxidation reactions with $RuTFPPCl_8(CO)$ and either iodosobenzene (left) or dioxygen (right). PhIO data is after 4 hours, and the dioxygen results are at 24 hours (CH_2Cl_2) or 12 hours (SC CO_2) in the different solvents. Higher selectivity for epoxide formation is observed with PhIO in SC CO_2 relative to CH_2Cl_2. The dioxygen reactions are not as effective in the supercritical solvent.

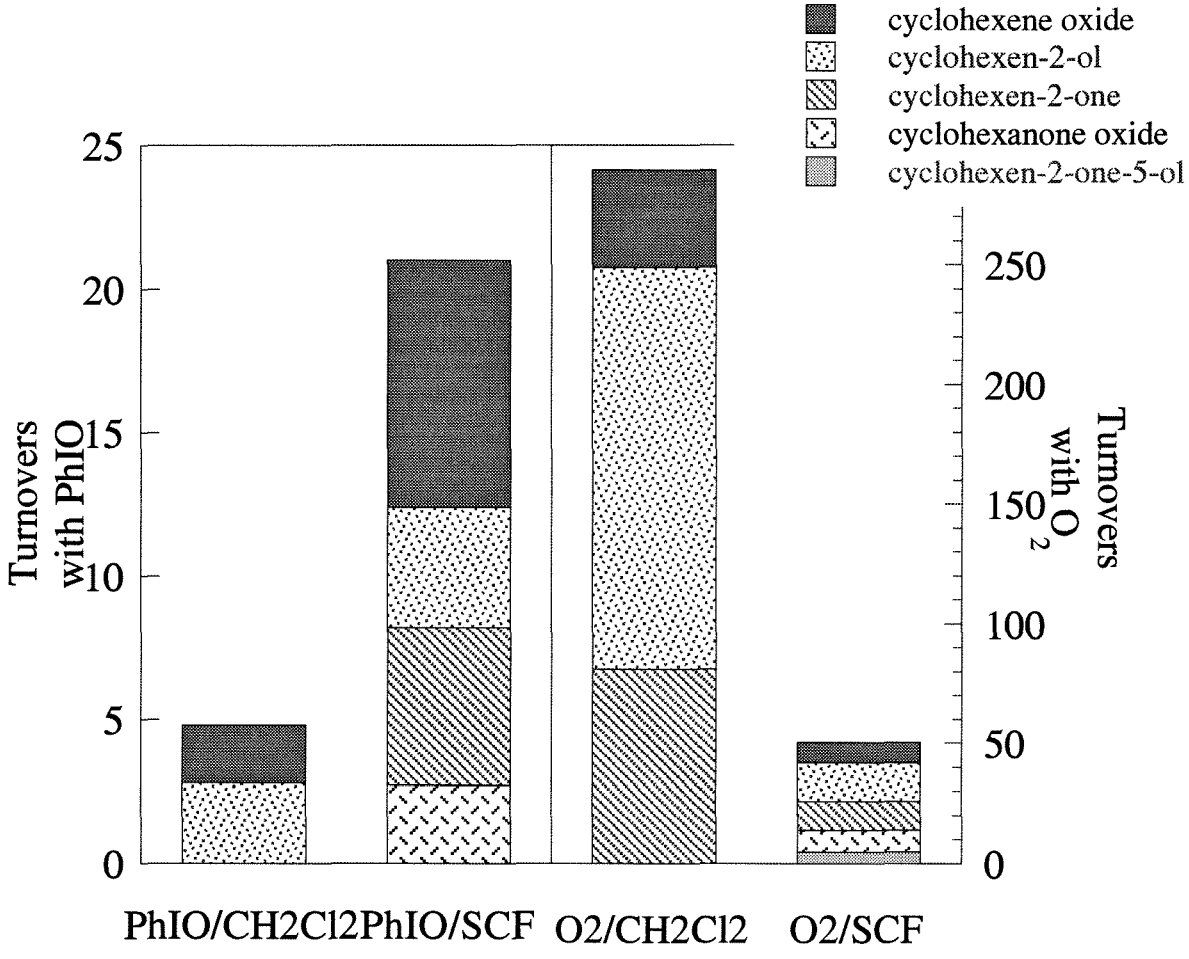
cyclohexene oxide
cyclohexen-2-ol
cyclohexen-2-one
cyclohexanone oxide
cyclohexen-2-one-5-ol
Turnovers with PhIO
Turnovers with O2
0
5
10
15
20
25
0
50
100
150
200
250
PhIO/CH2Cl2
PhIO/SCF
O2/CH2Cl2
O2/SCF

Figure 6.13 -- Partitioning mechanism to higher oxidation products.

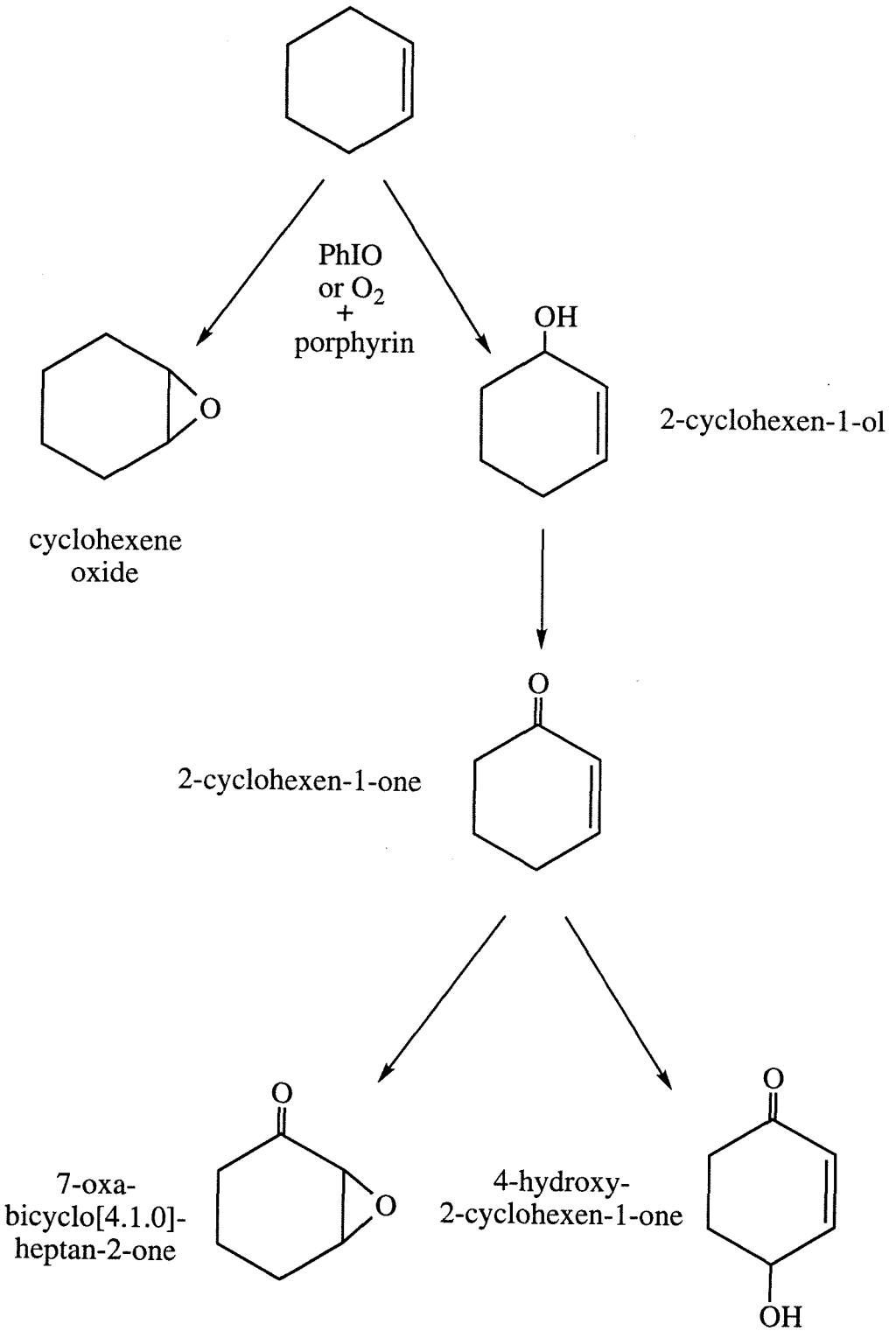
PhIO
or O_2
+
porphyrin
OH
O
2-cyclohexen-1-ol
cyclohexene
oxide
O
2-cyclohexen-1-one
O
O
7-oxa-
bicyclo[4.1.0]-
heptan-2-one
4-hydroxy-
2-cyclohexen-1-one
O
OH

Appendix 2

Crystal Structure Data

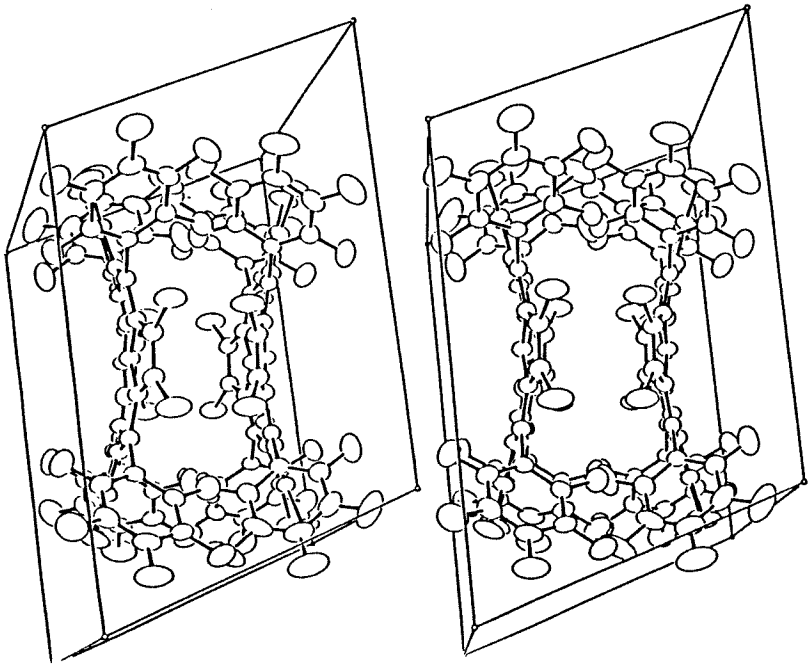

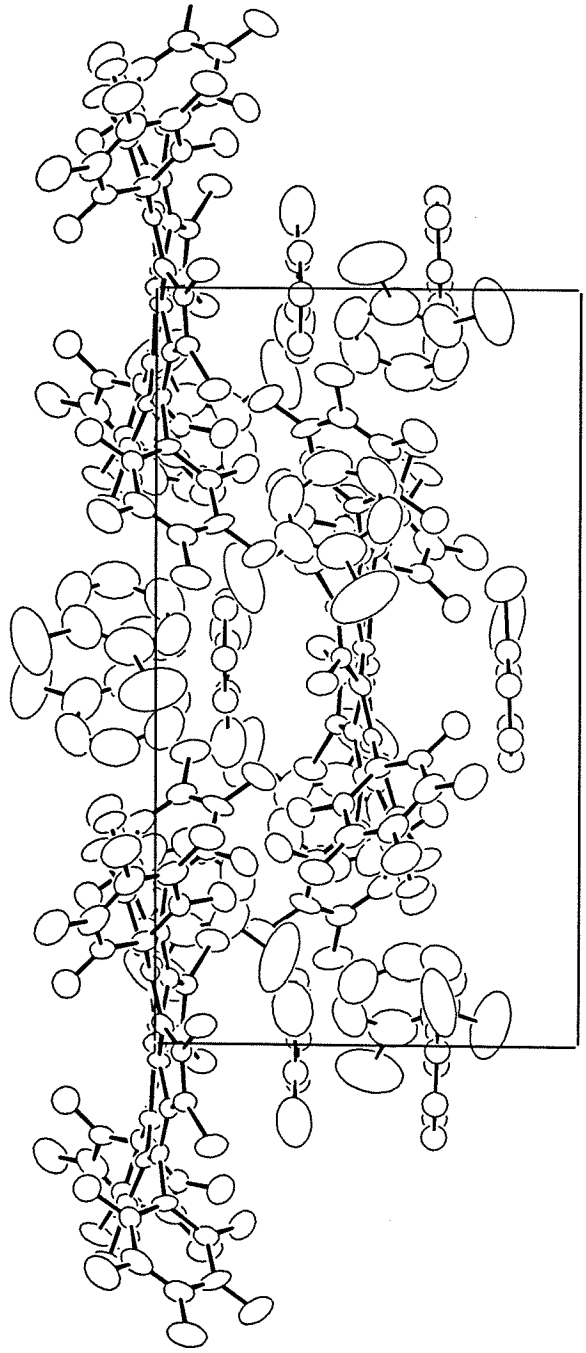

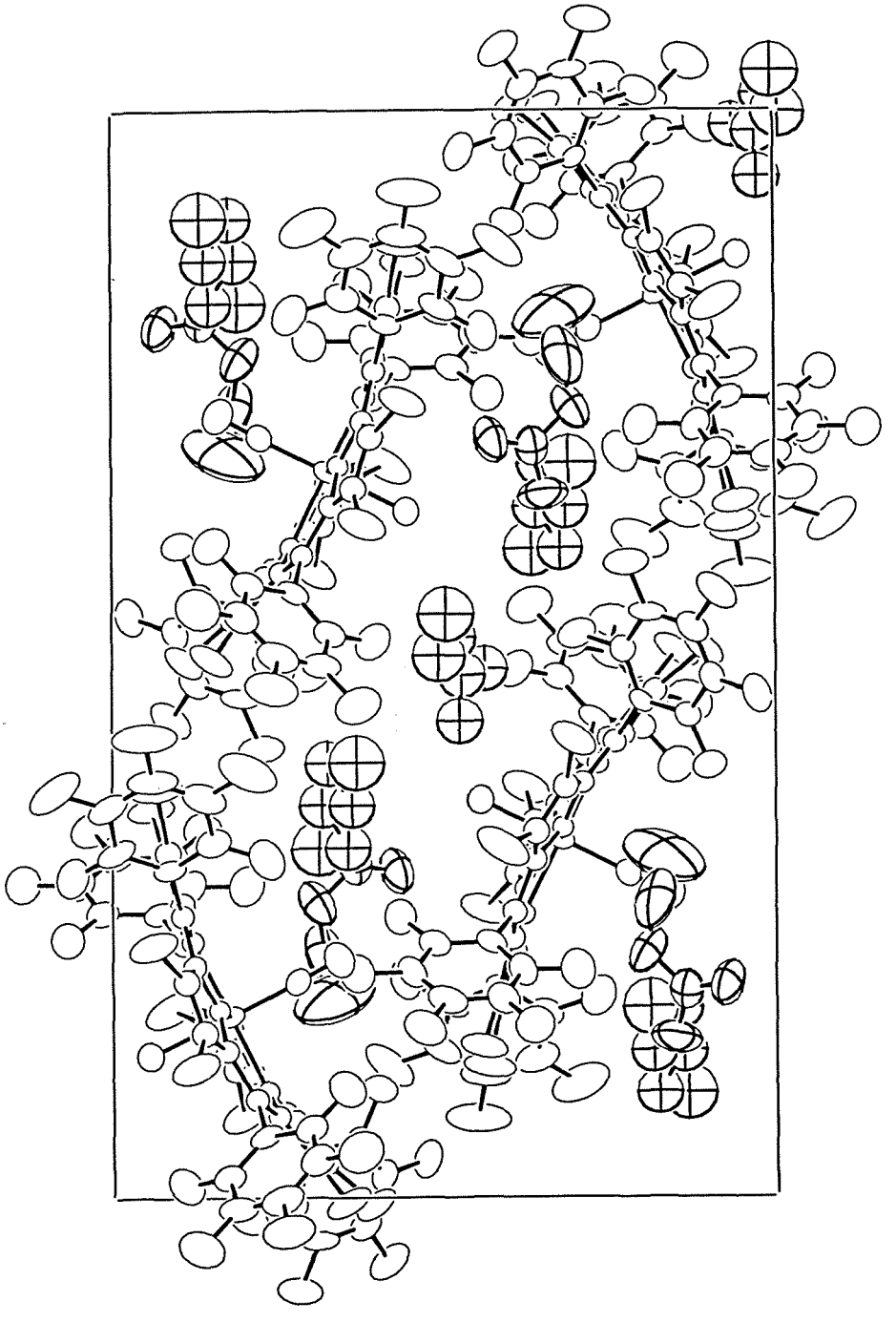

Table 1. Final Heavy Atom Parameters for Tetrakis(pentafluorophenyl)-β-octachloroporphyrin

x, y, z and $U_{eq}{}^{a} \times 10^4$

Atom	x	y	z	U_{eq}
Cl1	8772(1)	7676(1)	3695(1)	599(2)
Cl2	9105(1)	7909(1)	5768(1)	564(2)
Cl3	7030(1)	6297(1)	9358(1)	649(3)
Cl4	6863(1)	4203(1)	9784(1)	565(3)
Cl5	8296(1)	666(1)	7251(1)	551(2)
Cl6	8017(1)	388(1)	5189(1)	594(3)
Cl7	5875(1)	3260(1)	2544(1)	610(2)
Cl8	6089(1)	5349(1)	2107(1)	588(2)
N1	7751(2)	5801(2)	5404(2)	322(6)
N2	7639(2)	4666(2)	7079(2)	303(6)
N3	7448(2)	3089(2)	5970(2)	292(6)
N4	7218(2)	4335(2)	4383(2)	311(6)
C1	7855(3)	6171(2)	4534(2)	305(6)
C2	8351(3)	6968(2)	4569(2)	347(7)
C3	8477(3)	7076(2)	5450(2)	349(7)
C4	8058(3)	6354(2)	6001(2)	318(7)
C5	7890(3)	6276(2)	6972(2)	315(7)
C6	7600(3)	5516(2)	7474(2)	305(7)
C7	7306(3)	5446(2)	8484(2)	346(7)
C8	7231(3)	4562(2)	8666(2)	335(7)

Table 1. (Cont.)

Atom	x	y	z	U_{eq}
C9	7464(3)	4046(2)	7771(2)	295(7)
C10	7580(3)	3079(2)	7622(2)	285(6)
C11	7659(3)	2624(2)	6766(2)	287(6)
C12	7889(3)	1611(2)	6566(2)	308(7)
C13	7771(3)	1499(2)	5684(2)	318(7)
C14	7451(3)	2439(2)	5303(2)	278(6)
C15	7112(3)	2674(2)	4449(2)	298(7)
C16	6922(3)	3579(2)	4059(2)	310(6)
C17	6483(3)	3861(2)	3212(2)	349(7)
C18	6571(3)	4745(2)	3031(2)	350(7)
C19	7080(3)	5043(2)	3756(2)	304(7)
C20	7459(3)	5865(2)	3788(2)	299(7)
C21	7988(3)	7087(2)	7529(2)	313(7)
C22	6947(3)	7927(2)	7798(2)	356(7)
C23	6998(3)	8682(2)	8311(2)	417(9)
C24	8127(4)	8587(2)	8595(2)	454(9)
C25	9175(3)	7759(2)	8359(2)	444(8)
C26	9107(3)	7027(2)	7820(2)	390(8)
C31	7581(3)	2476(2)	8462(2)	287(6)
C32	8712(3)	2034(2)	8757(2)	346(7)

Table 1. (Cont.)

Atom	x	y	z	U_{eq}
C33	8719(3)	1485(2)	9522(2)	412(8)
C34	7567(4)	1361(2)	10009(2)	491(10)
C35	6431(3)	1784(2)	9738(2)	465(9)
C36	6446(3)	2343(2)	8980(2)	368(7)
C41	7026(3)	1869(2)	3882(2)	313(7)
C42	8108(3)	1325(2)	3209(2)	388(7)
C43	8109(4)	554(2)	2699(2)	516(9)
C44	7008(4)	292(2)	2873(3)	572(10)
C45	5909(4)	799(3)	3536(3)	573(9)
C46	5909(3)	1603(2)	4018(2)	426(8)
C51	7431(3)	6472(2)	2950(2)	306(6)
C52	8481(3)	6277(2)	2166(2)	387(8)
C53	8433(4)	6815(3)	1389(2)	478(9)
C54	7343(4)	7583(3)	1397(2)	488(9)
C55	6295(3)	7816(2)	2163(3)	454(9)
C56	6344(3)	7253(2)	2920(2)	357(7)
F22	5813(2)	8012(1)	7569(1)	587(5)
F23	5974(2)	9491(1)	8548(2)	679(6)
F24	8193(2)	9314(1)	9096(1)	721(6)
F25	10283(2)	7663(2)	8629(2)	740(6)

Table 1. (Cont.)

Atom	x	y	z	U_{eq}
F26	10183(2)	6251(1)	7549(2)	661(6)
F32	9855(2)	2125(1)	8267(1)	526(5)
F33	9839(2)	1063(1)	9778(1)	670(6)
F34	7552(2)	820(2)	10752(1)	833(7)
F35	5305(2)	1658(2)	10213(2)	825(7)
F36	5305(2)	2795(1)	8753(1)	560(5)
F42	9238(2)	1523(2)	3072(1)	628(6)
F43	9185(2)	56(2)	2043(2)	916(7)
F44	7005(3)	−470(2)	2384(2)	1022(8)
F45	4818(3)	549(2)	3707(2)	985(7)
F46	4808(2)	2121(2)	4628(2)	765(7)
F52	9591(2)	5562(1)	2157(1)	677(6)
F53	9461(2)	6597(2)	639(1)	827(7)
F54	7293(3)	8122(2)	650(2)	864(7)
F55	5208(2)	8568(1)	2179(2)	750(6)
F56	5271(2)	7458(1)	3637(1)	627(6)

[a] $U_{eq} = \frac{1}{3}\sum_i \sum_j [U_{ij}(a_i^* a_j^*)(\vec{a}_i \cdot \vec{a}_j)]$

Table 2. Selected Distances and Angles for

Tetrakis(pentafluorophenyl)-β-octachloroporphyrin

	Distance(Å)		Distance(Å)
Cl1 –C2	1.706(3)	C4 –C5	1.400(4)
Cl2 –C3	1.705(3)	C5 –C6	1.404(4)
Cl3 –C7	1.708(3)	C6 –C7	1.449(4)
Cl4 –C8	1.708(3)	C7 –C8	1.341(4)
Cl5 –C12	1.702(3)	C8 –C9	1.453(4)
Cl6 –C13	1.706(3)	C9 –C10	1.396(4)
Cl7 –C17	1.708(3)	C10 –C11	1.402(4)
Cl8 –C18	1.706(3)	C11 –C12	1.445(4)
N1 –C1	1.372(4)	C12 –C13	1.350(4)
N1 –C4	1.372(4)	C13 –C14	1.446(4)
N2 –C6	1.366(4)	C14 –C15	1.399(4)
N2 –C9	1.370(4)	C15 –C16	1.407(4)
N3 –C11	1.373(4)	C16 –C17	1.448(4)
N3 –C14	1.377(4)	C17 –C18	1.346(4)
N4 –C16	1.373(4)	C18 –C19	1.450(4)
N4 –C19	1.369(4)	C19 –C20	1.400(4)
C1 –C2	1.446(4)		
C1 –C20	1.404(4)		
C2 –C3	1.350(4)		
C3 –C4	1.445(4)		

Table 2. (Cont.)

	Angle(°)		Angle(°)
C4 –N1 –C1	109.9(2)	C6 –C7 –Cl3	129.5(2)
C9 –N2 –C6	109.4(2)	C8 –C7 –Cl3	122.2(2)
C14 –N3 –C11	109.5(2)	C8 –C7 –C6	108.3(3)
C19 –N4 –C16	109.1(2)	C7 –C8 –Cl4	122.6(2)
C2 –C1 –N1	106.8(2)	C9 –C8 –Cl4	129.8(2)
C20 –C1 –N1	125.4(3)	C9 –C8 –C7	107.6(3)
C20 –C1 –C2	127.6(3)	C8 –C9 –N2	107.4(2)
C1 –C2 –Cl1	129.4(2)	C10 –C9 –N2	125.4(3)
C3 –C2 –Cl1	122.5(2)	C10 –C9 –C8	127.1(3)
C3 –C2 –C1	108.1(3)	C11 –C10 –C9	126.0(3)
C2 –C3 –Cl2	122.7(2)	C10 –C11 –N3	125.1(3)
C4 –C3 –Cl2	129.2(2)	C12 –C11 –N3	107.2(2)
C4 –C3 –C2	108.0(3)	C12 –C11 –C10	127.6(3)
C3 –C4 –N1	106.9(2)	C11 –C12 –Cl5	129.2(2)
C5 –C4 –N1	125.9(3)	C13 –C12 –Cl5	122.7(2)
C5 –C4 –C3	127.0(3)	C13 –C12 –C11	108.1(2)
C6 –C5 –C4	125.6(3)	C12 –C13 –Cl6	121.5(2)
C5 –C6 –N2	125.1(3)	C14 –C13 –Cl6	130.4(2)
C7 –C6 –N2	107.3(2)	C14 –C13 –C12	108.0(3)
C7 –C6 –C5	127.4(3)	C13 –C14 –N3	107.1(2)

Table 2. (Cont.)

	Angle(°)
C15 –C14 –N3	125.5(2)
C15 –C14 –C13	127.3(3)
C16 –C15 –C14	125.8(3)
C15 –C16 –N4	125.5(3)
C17 –C16 –N4	107.5(2)
C17 –C16 –C15	126.9(3)
C16 –C17 –Cl7	129.1(2)
C18 –C17 –Cl7	122.9(2)
C18 –C17 –C16	107.9(3)
C17 –C18 –Cl8	122.2(2)
C19 –C18 –Cl8	130.0(2)
C19 –C18 –C17	107.8(3)
C18 –C19 –N4	107.6(2)
C20 –C19 –N4	125.3(3)
C20 –C19 –C18	127.0(3)
C19 –C20 –C1	125.6(3)

Table S1. Anisotropic Displacement Parameters for Tetrakis(pentafluorophenyl)-β-octachloroporphyrin

Atom	U_{11}	U_{22}	U_{33}	U_{12}	U_{13}	U_{23}
Cl1	990(8)	710(6)	410(5)	−647(6)	−262(5)	235(4)
Cl2	906(7)	624(6)	459(5)	−589(5)	−259(5)	119(4)
Cl3	1245(9)	425(5)	309(5)	−384(5)	−93(5)	−55(4)
Cl4	1022(8)	439(5)	247(4)	−315(5)	−78(4)	41(4)
Cl5	979(7)	284(4)	484(5)	−179(4)	−401(5)	126(4)
Cl6	1110(8)	252(4)	520(5)	−199(5)	−417(5)	35(4)
Cl7	1028(8)	488(5)	657(6)	−422(5)	−616(6)	178(4)
Cl8	1017(8)	492(5)	554(6)	−402(5)	−552(5)	253(4)
N1	476(16)	288(13)	286(14)	−200(12)	−150(12)	53(11)
N2	421(15)	286(13)	235(13)	−146(11)	−102(12)	13(11)
N3	399(15)	245(13)	269(13)	−126(11)	−127(11)	41(11)
N4	459(16)	271(13)	275(14)	−164(12)	−166(12)	43(11)
C1	385(18)	312(16)	283(16)	−166(14)	−133(14)	53(13)
C2	443(19)	359(17)	320(17)	−226(15)	−118(15)	81(13)
C3	436(19)	323(16)	384(18)	−220(15)	−147(15)	52(14)
C4	408(18)	283(16)	327(17)	−171(14)	−134(14)	49(13)
C5	385(18)	282(16)	328(17)	−146(14)	−132(14)	21(13)
C6	364(18)	274(16)	307(16)	−118(13)	−118(14)	12(13)
C7	468(19)	310(17)	261(16)	−126(14)	−89(14)	−21(13)
C8	427(19)	333(17)	255(16)	−138(14)	−85(14)	40(13)
C9	369(18)	302(16)	236(15)	−129(13)	−93(13)	40(13)
C10	329(17)	293(16)	262(16)	−121(13)	−106(13)	65(12)
C11	301(16)	286(16)	296(16)	−111(13)	−98(13)	60(13)
C12	367(17)	250(15)	338(17)	−113(13)	−131(14)	82(13)
C13	382(18)	258(15)	344(17)	−117(13)	−129(14)	11(13)
C14	318(17)	250(15)	286(16)	−100(13)	−102(13)	12(12)
C15	327(17)	279(16)	311(16)	−122(13)	−91(13)	−2(13)
C16	393(18)	311(16)	287(16)	−159(14)	−135(14)	25(13)
C17	453(19)	343(17)	334(17)	−158(15)	−213(15)	23(13)
C18	451(19)	325(17)	346(17)	−152(15)	−200(15)	100(13)
C19	376(18)	302(16)	280(16)	−142(14)	−126(14)	49(13)
C20	326(17)	299(16)	286(16)	−108(13)	−99(13)	64(12)
C21	425(19)	281(16)	295(16)	−172(14)	−128(14)	44(13)
C22	386(19)	362(18)	404(18)	−200(15)	−150(15)	80(14)
C23	540(22)	253(17)	422(19)	−137(16)	−41(17)	10(14)
C24	740(26)	390(20)	363(19)	−338(19)	−166(18)	10(15)
C25	546(22)	522(22)	432(20)	−299(19)	−264(17)	94(16)
C26	484(21)	316(17)	391(18)	−123(16)	−158(16)	36(14)
C31	399(18)	260(15)	243(15)	−139(13)	−116(14)	42(12)

Table S1. (Cont.)

Atom	U_{11}	U_{22}	U_{33}	U_{12}	U_{13}	U_{23}
C32	411(20)	330(17)	319(17)	−135(15)	−112(15)	13(14)
C33	522(22)	367(18)	347(18)	−51(16)	−239(17)	36(14)
C34	745(27)	373(19)	293(18)	−116(18)	−116(18)	140(15)
C35	490(22)	441(20)	406(20)	−181(17)	29(17)	128(16)
C36	385(19)	330(17)	401(19)	−107(15)	−135(16)	76(14)
C41	413(19)	298(16)	300(16)	−157(14)	−169(15)	45(13)
C42	460(21)	385(18)	381(18)	−145(16)	−207(16)	2(15)
C43	599(24)	436(20)	461(21)	17(19)	−279(19)	−124(17)
C44	871(31)	346(20)	657(26)	−228(21)	−437(24)	−20(18)
C45	745(28)	633(25)	678(26)	−512(23)	−420(23)	217(21)
C46	450(21)	481(20)	416(19)	−219(17)	−145(17)	55(16)
C51	389(18)	301(16)	285(16)	−169(14)	−112(14)	45(13)
C52	387(19)	396(18)	395(19)	−131(16)	−123(16)	28(15)
C53	566(23)	618(23)	307(19)	−332(20)	−22(17)	37(17)
C54	789(28)	526(22)	377(20)	−421(21)	−299(20)	215(17)
C55	559(23)	300(18)	625(24)	−154(17)	−359(20)	105(16)
C56	381(19)	335(17)	376(18)	−122(15)	−124(16)	25(14)
F22	486(12)	505(12)	829(15)	−148(10)	−287(11)	16(10)
F23	746(15)	350(11)	807(15)	−90(11)	−59(12)	−71(10)
F24	1212(19)	508(12)	648(13)	−470(13)	−342(13)	−83(10)
F25	833(16)	822(15)	872(16)	−431(13)	−559(13)	86(12)
F26	543(13)	518(12)	906(16)	−45(10)	−317(12)	−74(11)
F32	403(11)	650(13)	584(12)	−227(10)	−160(10)	108(10)
F33	760(15)	639(13)	603(13)	−28(11)	−433(12)	82(10)
F34	1148(19)	766(15)	455(12)	−179(14)	−165(12)	367(11)
F35	685(15)	841(16)	814(16)	−298(13)	111(13)	347(13)
F36	402(11)	624(12)	681(13)	−178(10)	−181(10)	186(10)
F42	434(12)	861(15)	598(13)	−242(11)	−87(10)	−140(11)
F43	807(17)	874(17)	819(16)	178(14)	−324(14)	−470(14)
F44	1617(25)	521(14)	1228(21)	−413(15)	−803(19)	−154(13)
F45	1173(21)	1190(20)	1143(20)	−981(18)	−508(17)	282(16)
F46	526(14)	1098(18)	679(15)	−393(13)	21(12)	−121(13)
F52	472(12)	650(13)	701(14)	4(11)	−17(10)	13(11)
F53	941(17)	1098(18)	423(13)	−532(15)	142(12)	7(12)
F54	1436(22)	877(16)	590(14)	−641(16)	−494(14)	462(12)
F55	817(16)	459(12)	1065(18)	−88(11)	−575(14)	203(11)
F56	442(12)	663(13)	621(13)	−62(10)	−7(11)	5(10)

$U_{i,j}$ values have been multiplied by 10^4

The form of the displacement factor is:

$$\exp -2\pi^2(U_{11}h^2a^{*^2} + U_{22}k^2b^{*^2} + U_{33}\ell^2c^{*^2} + 2U_{12}hka^*b^* + 2U_{13}h\ell a^*c^* + 2U_{23}k\ell b^*c^*)$$

Table S2. Hydrogen Atom Parameters for Tetrakis(pentafluorophenyl)-β-octachloroporphyrin

x, y and $z \times 10^4$

Atom	x	y	z	B
H1	7559(53)	5227(40)	5567(38)	3.0
H2	7773(55)	4537(41)	6517(41)	2.9
H3	7317(51)	3747(40)	5918(37)	2.8
H4	7414(55)	4351(40)	4900(40)	2.9

All atoms have a population factor of one-half.

Table S3. Complete Distances and Angles for Tetrakis(pentafluorophenyl)-β-octachloroporphyrin

	Distance(Å)		Distance(Å)
Cl1 –C2	1.706(3)	C15 –C41	1.496(4)
Cl2 –C3	1.705(3)	C16 –C17	1.448(4)
Cl3 –C7	1.708(3)	C17 –C18	1.346(4)
Cl4 –C8	1.708(3)	C18 –C19	1.450(4)
Cl5 –C12	1.702(3)	C19 –C20	1.400(4)
Cl6 –C13	1.706(3)	C20 –C51	1.506(4)
Cl7 –C17	1.708(3)	C21 –C22	1.373(4)
Cl8 –C18	1.706(3)	C21 –C26	1.381(4)
N1 –C1	1.372(4)	C22 –C23	1.372(4)
N1 –C4	1.372(4)	C22 –F22	1.343(4)
N1 –H1	0.94(6)	C23 –C24	1.375(5)
N2 –C6	1.366(4)	C23 –F23	1.331(4)
N2 –C9	1.370(4)	C24 –C25	1.361(5)
N2 –H2	0.82(6)	C24 –F24	1.335(4)
N3 –C11	1.373(4)	C25 –C26	1.375(5)
N3 –C14	1.377(4)	C25 –F25	1.342(4)
N3 –H3	0.93(6)	C26 –F26	1.337(4)
N4 –C16	1.373(4)	C31 –C32	1.380(4)
N4 –C19	1.369(4)	C31 –C36	1.373(4)
N4 –H4	0.84(6)	C32 –C33	1.370(4)
C1 –C2	1.446(4)	C32 –F32	1.342(3)
C1 –C20	1.404(4)	C33 –C34	1.369(5)
C2 –C3	1.350(4)	C33 –F33	1.335(4)
C3 –C4	1.445(4)	C34 –C35	1.363(5)
C4 –C5	1.400(4)	C34 –F34	1.336(4)
C5 –C6	1.404(4)	C35 –C36	1.368(5)
C5 –C21	1.500(4)	C35 –F35	1.340(4)
C6 –C7	1.449(4)	C36 –F36	1.343(4)
C7 –C8	1.341(4)	C41 –C42	1.374(4)
C8 –C9	1.453(4)	C41 –C46	1.380(4)
C9 –C10	1.396(4)	C42 –C43	1.365(5)
C10 –C11	1.402(4)	C42 –F42	1.341(4)
C10 –C31	1.503(4)	C43 –C44	1.359(5)
C11 –C12	1.445(4)	C43 –F43	1.339(4)
C12 –C13	1.350(4)	C44 –C45	1.362(6)
C13 –C14	1.446(4)	C44 –F44	1.338(5)
C14 –C15	1.399(4)	C45 –C46	1.385(5)
C15 –C16	1.407(4)	C45 –F45	1.337(5)

Table S3. (Cont.)

	Distance(Å)		Angle(°)
C46 –F46	1.329(4)	C4 –N1 –C1	109.9(2)
C51 –C52	1.382(4)	H1 –N1 –C1	125.9(35)
C51 –C56	1.377(4)	H1 –N1 –C4	124.1(35)
C52 –C53	1.377(5)	C9 –N2 –C6	109.4(2)
C52 –F52	1.331(4)	H2 –N2 –C6	125.7(42)
C53 –C54	1.357(5)	H2 –N2 –C9	124.9(42)
C53 –F53	1.336(4)	C14 –N3 –C11	109.5(2)
C54 –C55	1.362(5)	H3 –N3 –C11	123.1(35)
C54 –F54	1.341(4)	H3 –N3 –C14	127.4(35)
C55 –C56	1.373(5)	C19 –N4 –C16	109.1(2)
C55 –F55	1.341(4)	H4 –N4 –C16	123.6(40)
C56 –F56	1.337(4)	H4 –N4 –C19	127.3(41)
		C2 –C1 –N1	106.8(2)
		C20 –C1 –N1	125.4(3)
		C20 –C1 –C2	127.6(3)
		C1 –C2 –Cl1	129.4(2)
		C3 –C2 –Cl1	122.5(2)
		C3 –C2 –C1	108.1(3)
		C2 –C3 –Cl2	122.7(2)
		C4 –C3 –Cl2	129.2(2)
		C4 –C3 –C2	108.0(3)
		C3 –C4 –N1	106.9(2)
		C5 –C4 –N1	125.9(3)
		C5 –C4 –C3	127.0(3)
		C6 –C5 –C4	125.6(3)
		C21 –C5 –C4	117.3(2)
		C21 –C5 –C6	117.1(2)
		C5 –C6 –N2	125.1(3)
		C7 –C6 –N2	107.3(2)
		C7 –C6 –C5	127.4(3)
		C6 –C7 –Cl3	129.5(2)
		C8 –C7 –Cl3	122.2(2)
		C8 –C7 –C6	108.3(3)
		C7 –C8 –Cl4	122.6(2)
		C9 –C8 –Cl4	129.8(2)
		C9 –C8 –C7	107.6(3)
		C8 –C9 –N2	107.4(2)
		C10 –C9 –N2	125.4(3)

Table S3. (Cont.)

	Angle(°)		Angle(°)
C10 –C9 –C8	127.1(3)	F22 –C22 –C21	118.9(3)
C11 –C10 –C9	126.0(3)	F22 –C22 –C23	118.0(3)
C31 –C10 –C9	117.0(2)	C24 –C23 –C22	118.8(3)
C31 –C10 –C11	116.9(2)	F23 –C23 –C22	121.3(3)
C10 –C11 –N3	125.1(3)	F23 –C23 –C24	119.9(3)
C12 –C11 –N3	107.2(2)	C25 –C24 –C23	120.1(3)
C12 –C11 –C10	127.6(3)	F24 –C24 –C23	119.6(3)
C11 –C12 –Cl5	129.2(2)	F24 –C24 –C25	120.3(3)
C13 –C12 –Cl5	122.7(2)	C26 –C25 –C24	119.7(3)
C13 –C12 –C11	108.1(2)	F25 –C25 –C24	120.5(3)
C12 –C13 –Cl6	121.5(2)	F25 –C25 –C26	119.8(3)
C14 –C13 –Cl6	130.4(2)	C25 –C26 –C21	122.2(3)
C14 –C13 –C12	108.0(3)	F26 –C26 –C21	119.7(3)
C13 –C14 –N3	107.1(2)	F26 –C26 –C25	118.1(3)
C15 –C14 –N3	125.5(2)	C32 –C31 –C10	122.1(3)
C15 –C14 –C13	127.3(3)	C36 –C31 –C10	121.4(3)
C16 –C15 –C14	125.8(3)	C36 –C31 –C32	116.5(3)
C41 –C15 –C14	116.5(2)	C33 –C32 –C31	122.4(3)
C41 –C15 –C16	117.7(2)	F32 –C32 –C31	119.1(3)
C15 –C16 –N4	125.5(3)	F32 –C32 –C33	118.5(3)
C17 –C16 –N4	107.5(2)	C34 –C33 –C32	119.0(3)
C17 –C16 –C15	126.9(3)	F33 –C33 –C32	120.4(3)
C16 –C17 –Cl7	129.1(2)	F33 –C33 –C34	120.6(3)
C18 –C17 –Cl7	122.9(2)	C35 –C34 –C33	120.3(3)
C18 –C17 –C16	107.9(3)	F34 –C34 –C33	120.1(3)
C17 –C18 –Cl8	122.2(2)	F34 –C34 –C35	119.6(3)
C19 –C18 –Cl8	130.0(2)	C36 –C35 –C34	119.6(3)
C19 –C18 –C17	107.8(3)	F35 –C35 –C34	120.2(3)
C18 –C19 –N4	107.6(2)	F35 –C35 –C36	120.2(3)
C20 –C19 –N4	125.3(3)	C35 –C36 –C31	122.2(3)
C20 –C19 –C18	127.0(3)	F36 –C36 –C31	119.0(3)
C19 –C20 –C1	125.6(3)	F36 –C36 –C35	118.7(3)
C51 –C20 –C1	117.4(2)	C42 –C41 –C15	120.2(3)
C51 –C20 –C19	117.0(2)	C46 –C41 –C15	123.3(3)
C22 –C21 –C5	121.4(3)	C46 –C41 –C42	116.5(3)
C26 –C21 –C5	122.5(3)	C43 –C42 –C41	122.9(3)
C26 –C21 –C22	116.1(3)	F42 –C42 –C41	119.2(3)
C23 –C22 –C21	123.1(3)	F42 –C42 –C43	117.8(3)

Table S3. (Cont.)

	Angle(°)
C44 –C43 –C42	119.1(3)
F43 –C43 –C42	120.6(3)
F43 –C43 –C44	120.3(3)
C45 –C44 –C43	120.6(4)
F44 –C44 –C43	119.6(3)
F44 –C44 –C45	119.9(4)
C46 –C45 –C44	119.4(4)
F45 –C45 –C44	121.0(4)
F45 –C45 –C46	119.6(3)
C45 –C46 –C41	121.4(3)
F46 –C46 –C41	119.8(3)
F46 –C46 –C45	118.8(3)
C52 –C51 –C20	122.2(3)
C56 –C51 –C20	121.6(3)
C56 –C51 –C52	116.2(3)
C53 –C52 –C51	122.0(3)
F52 –C52 –C51	119.9(3)
F52 –C52 –C53	118.1(3)
C54 –C53 –C52	119.5(3)
F53 –C53 –C52	120.3(3)
F53 –C53 –C54	120.1(3)
C55 –C54 –C53	120.5(3)
F54 –C54 –C53	120.1(3)
F54 –C54 –C55	119.4(3)
C56 –C55 –C54	119.2(3)
F55 –C55 –C54	121.2(3)
F55 –C55 –C56	119.6(3)
C55 –C56 –C51	122.6(3)
F56 –C56 –C51	119.4(3)
F56 –C56 –C55	118.1(3)

Table S4. Observed and Calculated Structure Factors for Tetrakis(pentafluorophenyl)-β-octachloroporphyrin

The columns contain, in order, ℓ, $10F_{obs}$, $10F_{calc}$ and $10\sigma F_{obs}$. A minus sign preceding F_{obs} indicates that F^2_{obs} is negative.

-10	1	1	
1	182	227	5
2	-14	2	16
3	42	47	8
-10	2	1	
1	39	41	10
2	16	28	18
-10	3	1	
1	80	63	6
-9	1	1	
1	117	104	5
2	56	31	7
3	142	132	5
4	-21	8	14
5	11	17	21
6	73	42	7
-9	2	1	
1	50	31	7
2	23	46	13
3	60	65	7
4	61	67	8
5	156	151	5
-9	3	1	
1	84	81	6
2	54	47	8
3	71	71	7
4	60	77	8
-9	4	1	
1	65	88	7
2	36	29	11
3	38	17	11
-9	5	1	
1	110	97	5
-8	1	1	
1	931	921	8
2	278	278	4
3	55	47	7
4	119	122	5
5	40	24	8
6	152	155	5
7	98	97	6
8	5	15	26
-8	2	1	
1	116	86	4
2	206	201	4
3	139	122	4
4	65	59	7
5	12	16	19
6	196	192	5
7	130	129	5
-8	3	1	
1	288	284	4
2	261	276	4
3	174	172	4
4	100	85	5
5	68	57	7
6	117	115	5
-8	4	1	
1	132	125	5
2	48	39	8
3	220	237	4
4	203	203	5
5	79	61	6
-8	5	1	
1	60	48	7
2	53	29	8
3	188	189	5
4	65	62	7
-8	6	1	
1	129	128	5
2	149	149	5
3	76	57	7
-8	7	1	
1	115	117	5
-7	1	1	
1	26	17	10
2	46	59	7
3	84	76	5
4	33	7	9
5	145	141	4
6	137	137	5
7	54	75	8
8	73	81	7
9	-38	10	10
-7	2	1	
1	111	108	4
2	42	27	8
3	284	296	4
4	50	51	6
5	141	139	4
6	94	104	5
7	161	140	5
8	67	42	7
9	29	11	13
-7	3	1	
1	192	194	4
2	97	92	5
3	105	112	5
4	192	190	4
5	38	29	9
6	170	162	5
7	31	5	11
8	116	110	5
-7	4	1	
1	116	126	4
2	162	180	4
3	50	36	8
4	198	208	4
5	161	162	4
6	158	161	5
7	53	56	8
-7	5	1	
1	39	11	9
2	189	187	4
3	143	158	4
4	70	53	6
5	47	8	9
6	99	105	6
7	102	111	6
-7	6	1	
1	120	118	5
2	42	17	9
3	96	87	5
4	208	200	5
5	162	160	5
6	116	109	5
-7	7	1	
1	79	87	6
2	232	240	4
3	98	98	6
4	61	58	7
-7	8	1	
1	-21	7	14
2	61	88	7
3	58	77	7
-6	1	1	
1	343	362	4
2	347	349	4
3	199	185	4
4	184	183	4
5	66	44	6
6	73	68	6
7	209	213	4
8	121	112	5
9	37	23	11
10	119	112	5
-6	2	1	
1	264	272	4
2	106	120	4
3	206	212	4
4	99	107	4
5	39	24	8
6	264	268	4
7	76	61	6
8	78	69	6
9	257	257	5
10	47	58	9
-6	3	1	
1	200	199	4
2	193	192	4
3	125	125	4
4	233	236	4
5	111	132	5
6	166	177	4
7	179	176	4
8	25	34	13
9	174	160	5
10	14	28	20
-6	4	1	
1	50	26	6
2	59	17	5
3	151	148	4
4	50	41	5
5	221	222	4
6	40	27	9
7	84	74	6
8	136	154	5
9	46	29	8
-6	5	1	
1	251	257	4
2	142	145	4
3	94	78	5
4	131	122	4
5	10	10	19
6	51	34	8
7	20	35	15
8	37	48	11
-6	6	1	
1	36	17	9
2	133	139	4
3	93	93	5
4	285	271	4
5	46	27	9
6	125	139	5
7	73	72	7
-6	7	1	
1	249	261	4
2	33	50	10
3	-29	1	9
4	237	245	4
5	121	117	5
6	46	43	7
-6	8	1	
1	113	113	5
2	75	92	6
3	31	37	11
4	43	39	9
5	53	21	8
-6	9	1	
1	105	124	5
2	57	61	8
3	-43	6	8
-6	10	1	
1	80	58	6
-5	1	1	
1	159	157	3
2	278	272	3
3	521	517	5
4	539	534	5
5	73	55	5
6	134	126	4
7	287	277	4
8	-12	3	17
9	328	328	5
10	68	71	6
11	84	75	6
12	107	100	6
-5	2	1	
1	396	399	4
2	135	130	3
3	447	450	5
4	230	228	4
5	41	32	7
6	289	282	4
7	32	33	10
8	248	248	4
9	136	129	5
10	8	27	22
11	71	71	7
-5	3	1	

1	432	441	4
2	43	35	6
3	84	87	4
4	230	227	4
5	229	225	4
6	245	240	4
7	110	107	5
8	75	69	6
9	60	71	7
10	74	76	7
11	56	65	8

-5	4	1

1	208	207	3
2	113	124	4
3	68	52	5
4	380	367	4
5	46	0	7
6	16	21	14
7	52	48	6
8	-39	16	8
9	30	51	12
10	-24	12	14

-5	5	1

1	79	73	4
2	313	311	4
3	419	415	5
4	179	179	4
5	245	248	4
6	36	52	10
7	29	47	12
8	3	24	24
9	92	92	6
10	71	72	7

-5	6	1

1	249	242	4
2	134	136	4
3	331	332	4
4	80	84	5
5	38	22	8
6	44	16	9
7	123	134	5
8	16	10	17
9	86	86	6

-5	7	1

1	24	31	11
2	-22	1	11
3	3	0	22
4	66	61	6
5	53	49	8
6	150	155	5
7	142	141	5
8	62	54	8

-5	8	1

1	-23	14	12
2	-30	2	10
3	57	72	7
4	108	107	5
5	80	93	6
6	10	8	21
7	107	115	6

-5	9	1

1	99	103	5
2	-40	23	8
3	116	116	5
4	-28	31	12
5	145	131	5
6	94	100	6

-5	10	1

1	110	124	5
2	75	72	6
3	-14	43	18
4	80	81	6

-5	11	1

1	53	51	7
2	66	64	7

-4	1	1

1	522	509	5
2	359	347	4
3	63	59	4
4	98	105	4
5	211	207	3
6	89	88	4
7	332	328	4
8	139	134	4
9	272	279	4
10	155	157	4
11	183	171	5
12	70	79	7
13	-16	11	18

-4	2	1

1	977	994	8
2	430	446	4
3	352	356	4
4	165	156	3
5	151	155	3
6	175	168	4
7	336	334	4
8	208	194	4
9	150	150	4
10	179	177	4
11	88	92	6
12	-30	27	12

-4	3	1

1	591	597	5
2	353	360	4
3	58	33	5
4	306	304	4
5	335	330	4
6	301	307	4
7	369	365	4
8	136	138	4
9	125	126	5
10	-42	33	8
11	112	120	5
12	29	25	13

-4	4	1

1	167	166	3
2	191	209	3
3	94	82	4
4	80	78	4
5	427	432	5
6	139	145	4
7	33	30	9
8	146	139	4
9	54	51	8
10	17	1	16
11	-39	1	9

-4	5	1

1	615	619	6
2	58	67	5
3	27	0	9
4	415	436	4
5	205	209	4
6	77	83	5
7	160	158	4
8	167	170	4
9	-21	5	13
10	108	94	5
11	37	11	11

-4	6	1

1	187	183	3
2	354	350	4
3	64	48	5
4	95	87	4
5	99	107	5
6	314	311	4
7	58	66	7
8	-20	8	14
9	125	113	5
10	81	63	6

-4	7	1

1	84	80	5
2	78	92	5
3	67	70	5
4	269	272	4
5	151	154	4
6	71	70	6
7	130	132	5
8	326	319	5
9	133	130	5

-4	8	1

1	162	172	4
2	129	131	4
3	31	24	10
4	87	96	5
5	83	85	6
6	168	157	4
7	59	62	7
8	165	167	5

-4	9	1

1	272	265	4
2	178	168	4
3	-2	40	25
4	189	185	4
5	188	188	4
6	166	178	5
7	168	183	5

-4	10	1

1	41	38	9
2	50	16	8
3	96	83	5
4	106	94	5
5	232	245	5
6	38	35	10

-4	11	1

1	18	4	16
2	183	167	5
3	88	81	6
4	92	96	6

-4	12	1

1	57	62	7
2	95	88	6

-3	1	1

1	423	423	4
2	883	872	7
3	660	632	6
4	54	7	5
5	1223	1209	10
6	95	94	4
7	161	164	4
8	120	130	4
9	180	177	4
10	113	111	5
11	26	49	13
12	-55	14	6
13	207	207	5

-3	2	1

1	533	533	5
2	254	255	3
3	493	504	4
4	401	399	4
5	170	142	3
6	78	64	4
7	44	40	7
8	141	160	4
9	200	194	4
10	379	378	5
11	124	123	5
12	161	153	5
13	83	83	6

-3	3	1

1	791	792	7
2	55	53	4
3	188	183	3
4	159	161	3
5	835	827	7
6	-28	4	8
7	20	13	12
8	-37	6	7
9	266	259	4
10	327	314	5
11	145	138	5
12	214	207	5
13	192	196	5

-3	4	1

1	137	135	3
2	171	166	3
3	70	73	4
4	61	51	5
5	247	237	3
6	125	129	4
7	130	143	4
8	90	84	5
9	309	313	4
10	133	118	5
11	336	331	5
12	142	127	5

-3	5	1

1	527	527	5
2	197	190	3
3	57	65	5
4	45	37	5
5	154	161	4
6	68	73	5
7	121	128	4
8	39	38	7
9	164	154	4
10	70	52	7
11	200	196	5
12	51	42	8

-3	6	1

1	713	718	6
2	159	167	3
3	84	68	4
4	234	232	4
5	410	400	4
6	151	153	4
7	72	73	6
8	170	187	4
9	249	243	4
10	135	120	5
11	157	147	5

-3	7	1

1	388	375	4
2	108	106	4
3	-12	5	15
4	230	230	4
5	59	52	6
6	231	230	4
7	87	78	5
8	139	133	5
9	54	47	8
10	32	51	12
11	66	68	7

-3	8	1

1	177	179	4
2	108	102	4
3	208	219	4
4	299	307	4
5	281	274	4
6	73	60	6
7	50	50	6
8	193	181	4
9	41	67	9
10	-50	11	7

-3	9	1

1	283	265	4
2	173	169	4
3	167	168	4
4	183	197	4
5	203	192	4
6	-11	30	19
7	66	65	7
8	115	107	5
9	104	108	6

-3	10	1

1	251	250	4
2	107	107	5
3	310	307	4
4	159	132	4
5	130	116	5
6	84	77	6
7	14	12	18
8	65	35	7

-3	11	1

1	189	184	4
2	203	199	4
3	34	27	9
4	58	33	7
5	32	35	11
6	129	126	5

-3	12	1

1	99	88	5
2	205	206	5
3	101	94	5
4	170	157	5

-3	13	1

1	207	206	5

-2	1	1

1	1250	1234	10
2	1459	1455	10
3	1047	1051	9
4	142	139	3
5	977	977	8
6	309	320	4
7	399	399	4
8	109	104	4
9	69	81	5
10	316	307	4
11	81	108	6
12	49	81	8
13	28	49	13
14	157	162	5

-2	2	1

1	238	219	3
2	574	581	5
3	498	504	4
4	362	372	4
5	245	255	3
6	52	36	5
7	564	576	5
8	380	383	4
9	226	233	4
10	-11	11	18
11	242	228	4
12	146	143	5
13	75	71	7
14	222	216	5

-2	3	1

1	679	679	6
2	61	51	4
3	106	115	3
4	85	93	3
5	303	298	3
6	185	180	3
7	76	70	4
8	40	37	7
9	130	141	4
10	77	84	6
11	177	181	4
12	151	152	5
13	194	191	5

-2	4	1

1	98	99	3
2	81	94	3
3	193	196	3
4	162	166	3
5	428	429	4
6	209	204	3
7	38	44	7
8	153	159	4
9	40	48	8
10	-32	41	10
11	-33	24	10
12	-40	17	9
13	35	24	12

-2	5	1

1	503	513	5
2	287	286	3
3	285	291	3
4	497	511	5
5	223	223	3
6	297	291	4
7	51	74	6
8	210	214	4
9	96	88	5
10	57	64	7
11	66	79	7
12	232	233	5
13	21	7	16

-2	6	1

1	307	306	3
2	83	78	4
3	552	546	5
4	448	450	4
5	57	53	5
6	300	298	4
7	143	142	4
8	40	21	8
9	47	43	8
10	135	133	5
11	106	114	5
12	11	4	21

-2	7	1

1	46	38	6
2	92	87	4
3	146	142	3
4	181	181	3
5	230	227	4
6	232	230	4
7	205	211	4
8	248	251	4
9	136	116	5
10	101	107	5
11	207	191	5

-2	8	1

1	-21	27	10
2	66	72	5
3	119	112	4
4	260	261	4
5	67	54	5
6	449	433	5
7	30	12	11
8	400	404	5
9	219	221	4
10	56	49	8
11	90	80	6

-2	9	1

1	149	147	4
2	71	74	5
3	35	44	8
4	43	14	8
5	44	21	8
6	87	87	5
7	166	153	4
8	157	155	5
9	70	67	7
10	139	133	5

-2	10	1

1	28	37	9
2	101	103	5
3	151	152	4
4	173	167	4
5	367	370	5
6	138	125	5
7	243	246	4
8	-27	7	12
9	157	161	5

-2	11	1

1	108	120	5
2	67	64	6
3	63	50	7
4	330	338	5
5	226	220	4
6	44	15	9
7	158	138	5
8	279	260	5

-2	12	1

1	145	150	4
2	146	145	5
3	89	104	6
4	91	86	6
5	42	34	10
6	50	65	9

-2	13	1

1	82	80	6
2	44	27	9
3	101	83	6
4	241	222	5

-1	1	1

1	380	367	3
2	729	715	6
3	186	190	2
4	422	432	4
5	41	0	4
6	163	163	3
7	53	86	5
8	454	465	5
9	53	52	6
10	430	433	5
11	59	58	6
12	144	139	4
13	-46	6	7
14	90	96	6
15	107	107	6

-1	2	1

1	122	125	2
2	425	408	4
3	152	138	2
4	783	795	7
5	12	4	12
6	399	387	4
7	95	105	4
8	803	798	7
9	927	926	8
10	139	134	4
11	280	289	4
12	307	295	4
13	70	87	7
14	91	92	6

-1	3	1

1	446	436	4
2	207	212	2
3	214	212	3
4	378	385	4
5	120	113	3
6	31	21	7
7	626	617	6
8	193	194	3
9	55	54	6
10	139	142	4
11	-36	16	9
12	318	323	5
13	200	202	5
14	201	198	5

-1	4	1	
1	595	605	5
2	307	302	3
3	-9	5	13
4	405	405	4
5	315	326	3
6	172	164	3
7	290	283	4
8	37	25	8
9	216	210	4
10	156	165	4
11	95	87	5
12	30	47	11
13	215	207	5
14	84	82	7
-1	5	1	
1	369	368	4
2	990	1033	8
3	362	379	4
4	597	620	5
5	765	764	7
6	295	295	4
7	144	144	4
8	140	130	4
9	292	284	4
10	-15	37	16
11	17	26	14
12	77	92	6
13	66	85	7
-1	6	1	
1	214	227	3
2	189	192	3
3	654	648	6
4	584	592	5
5	331	328	4
6	26	10	9
7	87	79	4
8	674	675	6
9	204	192	4
10	116	117	5
11	227	232	4
12	156	148	5
13	117	118	6
-1	7	1	
1	640	618	6
2	163	161	3
3	249	241	3
4	107	102	4
5	51	56	6
6	138	138	4
7	359	354	4
8	91	56	5
9	798	785	7
10	33	33	11
11	74	80	6
12	-28	17	12
-1	8	1	
1	297	290	4
2	71	78	4
3	309	304	4
4	123	133	4
5	98	100	4
6	16	3	14
7	196	196	4
8	178	171	4
9	260	259	4
10	182	175	4
11	162	158	5
12	193	175	5

-1	9	1	
1	143	153	4
2	111	101	4
3	466	467	5
4	382	386	4
5	416	410	5
6	11	8	16
7	22	45	13
8	169	165	4
9	172	171	4
10	25	43	14
11	74	72	7
-1	10	1	
1	-19	24	12
2	248	251	4
3	401	399	5
4	422	415	5
5	374	368	5
6	193	179	4
7	56	43	7
8	64	49	7
9	-33	7	10
10	89	85	6
-1	11	1	
1	-42	4	7
2	100	96	5
3	36	28	8
4	631	627	6
5	47	7	7
6	177	175	4
7	-35	1	9
8	41	20	10
9	160	148	5
-1	12	1	
1	-6	5	22
2	216	211	4
3	58	34	6
4	75	83	6
5	125	128	5
6	-35	19	10
7	74	82	7
-1	13	1	
1	107	116	5
2	133	123	5
3	55	60	8
4	36	32	8
5	65	67	7
6	56	60	8
-1	14	1	
1	60	58	7
2	131	121	5
3	110	101	5
0	0	1	
2	1011	1037	8
3	91	86	3
4	651	661	5
5	491	484	4
6	580	571	5
7	104	80	3
8	177	198	3
9	-20	12	11
10	273	268	4
11	139	133	4
12	278	270	4

13	324	337	5
14	221	215	5
15	72	64	7
0	1	1	
-15	106	102	6
-14	55	42	6
-13	-20	8	14
-12	81	89	6
-11	239	232	4
-10	137	136	4
-9	596	602	6
-8	347	351	4
-7	220	203	3
-6	151	154	3
-5	216	219	3
-4	606	602	5
-3	214	204	2
-2	201	208	2
-1	52	14	3
1	193	204	2
2	869	869	7
3	289	265	3
4	200	199	2
5	1108	1103	9
6	798	798	7
7	242	247	3
8	28	46	8
9	91	83	4
10	-37	3	7
11	638	640	6
12	364	365	5
13	388	392	5
14	69	66	7
15	115	132	5
0	2	1	
-15	230	221	5
-14	336	336	5
-13	93	101	5
-12	101	120	5
-11	436	426	5
-10	697	707	6
-9	229	240	4
-8	49	42	6
-7	213	199	3
-6	309	303	3
-5	1001	1012	8
-4	754	770	6
-3	655	633	5
-2	225	236	2
-1	469	482	4
0	1133	1209	9
1	66	47	3
2	623	615	5
3	238	245	2
4	1115	1130	9
5	453	464	4
6	124	133	3
7	299	299	3
8	79	82	4
9	31	34	9
10	112	104	4
11	202	216	4
12	96	93	5
13	82	65	6
14	120	128	5
15	91	105	6
0	3	1	
-15	50	43	9
-14	55	78	8
-13	-41	30	8
-12	120	137	5
-11	299	306	4

-10	639	635	6
-9	408	423	4
-8	-6	29	17
-7	341	346	4
-6	885	853	8
-5	1988	2009	17
-4	1298	1311	11
-3	899	891	7
-2	281	283	3
-1	58	67	3
0	352	343	3
1	971	955	8
2	319	305	3
3	1286	1292	11
4	323	339	3
5	429	431	4
6	356	355	4
7	117	112	3
8	209	217	3
9	117	117	4
10	265	259	4
11	356	357	4
12	287	281	4
13	117	120	5
14	-27	39	12
15	351	352	5
0	4	1	
-15	126	132	5
-14	201	216	5
-13	166	165	5
-12	93	100	5
-11	199	203	4
-10	-28	8	9
-9	86	90	4
-8	57	63	5
-7	116	114	3
-6	1333	1332	11
-5	338	331	3
-4	274	269	3
-3	1184	1214	10
-2	195	205	2
-1	422	424	4
0	230	230	2
1	1080	1093	9
2	1332	1331	11
3	1088	1077	9
4	901	919	8
5	220	234	3
6	521	521	5
7	66	68	4
8	584	586	5
9	44	54	7
10	76	82	5
11	90	72	5
12	437	421	5
13	-19	9	15
14	48	58	9
0	5	1	
-15	197	193	5
-14	73	85	6
-13	81	88	6
-12	90	88	5
-11	577	563	6
-10	115	116	4
-9	224	239	4
-8	259	256	4
-7	-26	6	8
-6	128	129	3
-5	603	570	5
-4	206	199	3
-3	327	326	3
-2	762	774	6
-1	1048	1058	9
0	715	727	6

1	770	766	6
2	202	200	3
3	660	687	6
4	278	279	3
5	389	409	4
6	284	289	3
7	230	231	3
8	102	111	4
9	227	219	4
10	79	92	5
11	231	229	4
12	209	216	4
13	110	103	5
14	25	50	14

0 6 1

-14	166	161	5
-13	134	133	5
-12	-14	23	14
-11	339	339	4
-10	529	530	5
-9	455	446	5
-8	37	76	7
-7	287	289	4
-6	60	50	5
-5	300	293	3
-4	360	361	4
-3	435	419	4
-2	236	215	3
-1	514	513	5
0	348	345	3
1	473	484	4
2	302	316	3
3	219	230	3
4	220	233	3
5	50	18	5
6	529	530	5
7	50	56	6
8	365	378	4
9	165	153	4
10	73	84	5
11	239	238	4
12	155	163	5
13	90	93	6

0 7 1

-14	41	51	9
-13	137	142	5
-12	179	179	4
-11	116	116	5
-10	23	30	12
-9	908	911	8
-8	332	340	4
-7	31	47	8
-6	581	585	5
-5	97	95	4
-4	406	412	4
-3	84	86	4
-2	98	119	3
-1	171	171	3
0	467	484	4
1	70	79	4
2	492	509	5
3	59	58	4
4	326	320	4
5	561	558	5
6	408	416	4
7	363	364	4
8	205	215	4
9	225	221	4
10	30	22	11
11	94	91	5
12	225	225	5
13	68	51	7

0 8 1

-13	95	98	6
-12	-26	38	11
-11	122	129	5
-10	-38	17	8
-9	67	84	6
-8	258	257	4
-7	88	84	4
-6	526	531	5
-5	358	359	4
-4	494	496	5
-3	85	90	4
-2	215	218	3
-1	29	38	7
0	417	426	4
1	15	27	12
2	55	44	5
3	425	416	4
4	466	472	5
5	293	290	4
6	379	369	4
7	263	254	4
8	331	332	4
9	101	104	5
10	139	125	5
11	149	154	5
12	94	80	6

0 9 1

-13	128	140	5
-12	58	75	8
-11	-24	30	13
-10	-44	11	7
-9	31	64	10
-8	659	667	6
-7	92	90	5
-6	40	22	7
-5	268	268	4
-4	319	324	4
-3	254	253	4
-2	83	90	4
-1	27	6	9
0	163	155	3
1	307	298	4
2	260	264	4
3	347	344	4
4	434	434	5
5	487	489	5
6	31	2	9
7	13	3	16
8	427	425	5
9	155	154	4
10	54	71	8
11	-59	6	5
12	7	44	24

0 10 1

-12	225	208	5
-11	127	127	5
-10	55	59	8
-9	64	66	7
-8	-49	5	6
-7	62	85	6
-6	611	602	6
-5	288	280	4
-4	135	140	4
-3	459	457	5
-2	147	147	4
-1	95	92	4
0	499	498	5
1	57	59	6
2	203	210	4
3	457	457	5
4	213	214	4
5	369	361	4
6	192	182	4

7	75	86	6
8	65	69	7
9	250	252	4
10	-38	12	9
11	54	68	8

0 11 1

-11	196	191	5
-10	107	115	5
-9	-30	13	11
-8	174	188	4
-7	-27	39	11
-6	195	195	4
-5	31	52	10
-4	148	149	4
-3	38	48	8
-2	229	235	4
-1	395	401	4
0	245	249	4
1	15	35	13
2	71	71	5
3	280	287	4
4	249	245	4
5	133	122	4
6	258	256	4
7	128	136	5
8	370	348	5
9	49	14	7
10	56	37	8

0 12 1

-10	235	229	5
-9	58	78	7
-8	116	121	5
-7	133	138	5
-6	189	188	4
-5	215	218	4
-4	404	406	5
-3	416	420	5
-2	-24	38	11
-1	258	253	4
0	390	379	5
1	63	79	6
2	368	359	5
3	327	330	4
4	82	54	6
5	106	129	5
6	-30	9	10
7	175	166	5
8	117	109	5

0 13 1

-8	38	42	10
-7	190	174	5
-6	271	270	4
-5	67	78	7
-4	45	16	8
-3	345	350	5
-2	340	335	5
-1	34	22	10
0	194	191	4
1	224	221	4
2	305	309	4
3	250	239	4
4	124	135	5
5	-4	0	25
6	61	60	7
7	24	18	14

0 14 1

-7	223	202	5
-6	123	134	5
-5	178	184	5
-4	170	163	5

-3	73	73	6
-2	80	88	6
-1	86	96	6
0	126	121	5
1	42	30	9
2	50	47	8
3	171	160	5
4	250	236	5
5	24	31	14

0 15 1

-3	124	122	5
-2	391	376	5
-1	50	67	9
0	-49	19	7
1	141	133	5

1 -14 1

0	249	238	5
1	25	27	13
2	108	112	5
3	-34	25	9
4	91	91	6
5	147	130	5
6	195	188	5

1 -13 1

0	183	184	4
1	214	220	4
2	143	150	5
3	178	166	4
4	214	215	4
5	158	137	5
6	157	147	5
7	464	456	5
8	87	95	6

1 -12 1

0	47	25	8
1	247	246	4
2	377	380	5
3	349	336	5
4	212	199	4
5	290	299	4
6	305	294	4
7	215	219	4
8	11	55	20
9	-44	26	8
10	221	210	5

1 -11 1

0	287	283	4
1	122	134	4
2	129	147	4
3	49	83	7
4	27	30	11
5	499	493	5
6	237	225	4
7	89	92	5
8	117	125	5
9	-49	6	6
10	102	101	5
11	172	161	5

1 -10 1

0	19	13	10
1	254	255	4
2	202	197	4
3	308	309	4
4	136	130	4
5	-29	23	9
6	199	211	4

7	444	445	5
8	118	119	5
9	-35	9	9
10	252	261	4
11	19	10	16
12	99	109	6

1 -9 1

0	298	295	4
1	1022	1015	9
2	78	81	4
3	194	192	3
4	441	450	5
5	549	555	5
6	118	102	4
7	126	118	4
8	121	122	4
9	-32	48	9
10	38	27	9
11	-28	34	11
12	47	71	9
13	117	122	5

1 -8 1

0	297	304	4
1	698	683	6
2	414	420	4
3	341	354	4
4	38	43	7
5	70	73	5
6	228	233	4
7	39	38	7
8	340	348	4
9	333	327	4
10	163	164	4
11	357	373	5
12	245	237	5
13	167	159	5

1 -7 1

0	402	417	4
1	101	82	3
2	254	257	3
3	210	209	3
4	167	153	3
5	152	149	3
6	51	30	6
7	289	284	4
8	366	361	4
9	87	79	5
10	136	147	4
11	72	75	6
12	110	127	5
13	-35	30	10
14	125	132	5

1 -6 1

0	206	193	3
1	20	1	9
2	509	511	5
3	334	335	4
4	391	403	4
5	394	404	4
6	321	312	4
7	-21	40	10
8	79	60	4
9	157	153	4
10	98	101	5
11	189	197	4
12	135	135	5
13	454	455	5
14	197	193	5

1 -5 1

0	35	21	6
1	238	250	3
2	679	686	6
3	117	123	3
4	771	758	7
5	960	942	8
6	20	4	10
7	567	551	5
8	487	483	5
9	186	185	4
10	-36	1	7
11	172	175	4
12	93	108	5
13	115	125	5
14	108	106	6
15	239	231	5

1 -4 1

0	397	403	4
1	301	309	3
2	770	782	6
3	187	191	3
4	459	459	4
5	201	202	3
6	1110	1106	9
7	369	358	4
8	158	151	3
9	183	177	4
10	57	70	6
11	57	72	6
12	72	73	6
13	287	296	5
14	14	42	18
15	291	285	5

1 -3 1

0	249	254	3
1	168	171	2
2	244	250	3
3	1852	1859	15
4	227	236	3
5	565	569	5
6	475	466	4
7	646	667	6
8	118	137	3
9	472	462	5
10	273	268	4
11	252	247	4
12	110	124	5
13	351	353	5
14	-46	19	7
15	87	98	6

1 -2 1

0	1175	1149	10
1	698	683	6
2	243	238	2
3	812	796	7
4	298	277	3
5	419	434	4
6	166	165	3
7	156	159	3
8	-39	24	5
9	497	501	5
10	430	426	5
11	502	501	5
12	-45	12	7
13	148	161	5
14	284	271	5
15	250	245	5

1 -1 1

0	412	436	3
1	313	334	3
2	251	281	2
3	689	695	6
4	481	477	4
5	209	214	3
6	174	168	3
7	401	395	4
8	209	212	3
9	538	539	5
10	474	470	5
11	37	39	7
12	317	320	4
13	75	79	6
14	379	378	5
15	109	105	6

1 0 1

-15	186	174	5
-14	-26	31	13
-13	271	274	4
-12	-39	2	8
-11	77	72	5
-10	139	139	4
-9	205	207	4
-8	47	53	5
-7	399	402	4
-6	472	459	4
-5	257	261	3
-4	232	224	3
-3	43	48	5
-2	1104	1068	9
-1	134	112	2
1	219	207	2
2	860	865	7
3	969	954	8
4	28	14	7
5	590	587	5
6	633	631	6
7	63	72	4
8	719	727	6
9	570	559	5
10	123	126	4
11	65	67	6
12	60	82	6
13	416	410	5
14	222	220	4
15	295	290	5

1 1 1

-15	99	108	6
-14	254	241	5
-13	313	304	5
-12	299	291	4
-11	125	115	4
-10	554	555	5
-9	129	130	4
-8	138	137	3
-7	440	431	4
-6	228	240	3
-5	770	765	7
-4	346	336	3
-3	734	725	6
-2	212	202	2
-1	26	23	6
0	252	256	2
1	42	0	3
2	494	506	4
3	809	759	7
4	1322	1325	11
5	207	193	3
6	1113	1118	9
7	759	768	7
8	284	281	4
9	413	413	4
10	142	139	4
11	204	190	4

12	97	95	5
13	216	213	4
14	120	118	5
15	99	86	6

1 2 1

-15	272	266	5
-14	50	50	9
-13	45	56	9
-12	267	256	4
-11	131	119	4
-10	217	213	4
-9	180	175	4
-8	-24	4	9
-7	255	271	3
-6	772	765	7
-5	802	790	7
-4	1506	1519	13
-3	665	641	6
-2	529	526	4
-1	570	580	5
0	748	756	6
1	-11	12	10
2	11	23	9
3	324	329	3
4	505	507	4
5	888	876	7
6	297	285	3
7	400	399	4
8	168	164	3
9	163	167	3
10	368	363	4
11	338	332	4
12	24	47	13
13	153	152	4
14	-14	21	18
15	269	258	5

1 3 1

-15	147	152	5
-14	250	255	5
-13	22	36	13
-12	396	389	5
-11	299	290	4
-10	131	123	4
-9	52	28	6
-8	288	294	4
-7	257	244	3
-6	642	623	6
-5	566	572	5
-4	1414	1408	12
-3	315	322	3
-2	158	164	2
-1	755	704	6
0	885	869	7
1	542	536	4
2	369	365	3
3	495	492	4
4	1131	1148	9
5	124	121	3
6	633	609	6
7	173	193	3
8	557	573	5
9	268	264	4
10	572	566	6
11	131	129	4
12	76	68	6
13	218	216	4
14	74	86	7
15	106	99	6

1 4 1

-15	-32	34	11
-14	54	58	8
-13	164	186	5

-12	78	98	6
-11	200	191	4
-10	78	88	5
-9	510	509	5
-8	220	234	3
-7	341	341	4
-6	887	873	8
-5	170	156	3
-4	129	131	3
-3	808	814	7
-2	444	449	4
-1	1087	1097	9
0	200	213	2
1	304	292	3
2	348	343	3
3	447	435	4
4	426	437	4
5	544	536	5
6	236	246	3
7	262	258	3
8	436	438	4
9	386	388	4
10	105	106	4
11	-19	48	13
12	362	358	5
13	374	359	5
14	8	38	23
15	226	216	5

1 5 1

-14	94	95	6
-13	-33	12	10
-12	-56	8	5
-11	21	5	12
-10	357	359	4
-9	299	300	4
-8	284	262	4
-7	486	469	5
-6	207	205	3
-5	130	101	3
-4	20	30	9
-3	-19	9	8
-2	569	575	5
-1	225	218	3
0	572	568	5
1	189	178	2
2	867	879	7
3	1141	1140	10
4	342	329	3
5	1175	1157	10
6	54	66	5
7	42	49	5
8	256	257	4
9	412	416	4
10	168	168	4
11	113	119	5
12	121	135	5
13	174	149	5
14	229	231	5

1 6 1

-14	113	107	6
-13	151	147	5
-12	-63	10	5
-11	327	337	4
-10	159	153	4
-9	176	162	4
-8	212	208	4
-7	251	244	3
-6	609	596	6
-5	412	414	4
-4	189	195	3
-3	208	205	3
-2	320	320	3
-1	1126	1128	9
0	739	721	6
1	504	497	4
2	377	358	4
3	895	875	8
4	108	113	3
5	267	270	3
6	433	432	4
7	104	112	4
8	-26	27	9
9	172	170	4
10	89	86	5
11	425	409	5
12	179	196	4
13	63	50	7
14	43	53	10

1 7 1

-14	92	92	6
-13	11	36	20
-12	95	120	6
-11	117	113	5
-10	162	162	4
-9	115	101	4
-8	56	60	6
-7	-30	17	8
-6	661	648	6
-5	395	419	4
-4	33	52	7
-3	281	269	3
-2	91	87	3
-1	964	983	8
0	-22	24	8
1	422	403	4
2	93	95	3
3	294	279	3
4	304	314	3
5	176	179	3
6	492	491	5
7	461	468	5
8	65	69	5
9	338	348	4
10	193	187	4
11	129	127	5
12	256	259	5
13	31	15	12

1 8 1

-13	109	100	6
-12	153	141	5
-11	372	387	5
-10	271	276	4
-9	88	94	5
-8	126	132	4
-7	82	97	5
-6	380	386	4
-5	577	582	5
-4	669	673	6
-3	269	259	3
-2	419	433	4
-1	42	59	4
0	753	768	7
1	17	27	9
2	152	150	3
3	225	230	3
4	64	35	5
5	352	341	4
6	101	87	4
7	211	203	4
8	134	132	4
9	130	115	4
10	220	224	4
11	-43	3	8
12	188	180	5
13	85	84	6

1 9 1

-13	60	73	8
-12	-29	5	12
-11	-57	3	5
-10	111	103	5
-9	40	69	9
-8	134	142	4
-7	35	35	8
-6	314	313	4
-5	210	212	4
-4	666	665	6
-3	476	487	5
-2	549	547	5
-1	106	111	4
0	228	218	3
1	482	475	5
2	406	403	4
3	202	201	3
4	148	141	4
5	92	94	4
6	390	385	4
7	266	268	4
8	136	147	4
9	40	35	9
10	8	19	19
11	29	63	12
12	39	51	11

1 10 1

-12	197	187	5
-11	48	75	8
-10	498	497	5
-9	-34	10	9
-8	-48	12	6
-7	108	115	5
-6	70	71	5
-5	403	407	4
-4	153	152	4
-3	366	353	4
-2	127	132	4
-1	138	135	4
0	353	355	4
1	390	382	4
2	449	457	5
3	50	56	6
4	246	254	4
5	90	89	5
6	248	271	4
7	58	39	7
8	190	176	4
9	330	330	5
10	245	246	5
11	57	67	8

1 11 1

-11	245	245	5
-10	107	109	5
-9	-5	34	24
-8	319	328	4
-7	377	376	5
-6	180	174	4
-5	191	204	4
-4	112	125	4
-3	203	205	4
-2	357	341	4
-1	275	269	4
0	516	509	5
1	137	134	4
2	27	48	10
3	132	125	4
4	205	207	4
5	74	68	6
6	55	66	7
7	200	194	4
8	84	80	6
9	86	73	6
10	193	208	5

1 12 1

-10	55	56	8
-9	226	208	5
-8	-17	48	16
-7	55	41	7
-6	220	203	4
-5	44	57	8
-4	165	165	4
-3	438	441	5
-2	98	91	5
-1	44	44	8
0	213	219	4
1	242	234	4
2	288	287	4
3	93	86	5
4	435	424	5
5	109	115	5
6	200	193	4
7	253	255	4
8	87	91	6
9	-18	31	16

1 13 1

-9	217	221	5
-8	187	178	5
-7	109	107	5
-6	119	138	5
-5	85	77	6
-4	175	168	4
-3	15	38	16
-2	123	101	5
-1	145	149	4
0	491	496	5
1	41	8	9
2	204	199	4
3	32	41	10
4	51	53	8
5	81	83	6
6	49	74	7
7	133	130	5
8	174	181	5

1 14 1

-7	82	95	6
-6	213	205	5
-5	232	228	5
-4	110	100	5
-3	251	246	4
-2	23	6	13
-1	154	151	4
0	68	38	6
1	258	257	4
2	370	352	5
3	96	68	5
4	167	158	5
5	45	54	9
6	75	60	7

1 15 1

-4	164	157	5
-3	103	90	5
-2	178	185	5
-1	388	383	5
0	138	154	5
1	114	103	5
2	117	113	5
3	236	224	5

2 -14 1

0	141	138	5
1	162	153	5
2	119	112	5

3	268	260	5

2	-13	1

0	176	160	5
1	90	82	6
2	39	42	10
3	265	253	5
4	136	118	5
5	108	93	5
6	41	23	10
7	84	66	6

2	-12	1

0	128	120	5
1	205	190	4
2	-4	29	24
3	46	57	8
4	227	229	4
5	96	104	5
6	24	42	13
7	302	295	5
8	163	155	5
9	291	266	5

2	-11	1

0	41	53	9
1	330	324	4
2	35	52	9
3	-37	5	7
4	85	94	5
5	299	286	4
6	129	123	5
7	76	77	6
8	148	144	5
9	44	57	9
10	32	46	12

2	-10	1

0	392	389	4
1	73	69	5
2	-11	25	16
3	133	143	4
4	139	148	4
5	17	20	15
6	44	46	7
7	301	296	4
8	-30	20	10
9	94	98	5
10	153	151	5
11	297	290	5
12	77	74	7

2	-9	1

0	-28	2	8
1	158	158	4
2	287	292	4
3	193	197	4
4	93	102	4
5	336	328	4
6	537	543	5
7	160	161	4
8	192	183	4
9	109	114	5
10	265	255	4
11	326	311	5
12	-13	12	18

2	-8	1

0	44	36	6
1	498	513	5
2	88	99	4
3	56	38	5

4	467	458	5
5	545	551	5
6	210	209	4
7	92	88	4
8	30	48	8
9	163	165	4
10	156	161	4
11	-21	17	14
12	169	177	5
13	53	58	8

2	-7	1

0	275	274	3
1	572	583	5
2	390	385	4
3	485	475	5
4	267	257	3
5	139	135	3
6	549	555	5
7	6	27	19
8	155	157	4
9	417	405	5
10	128	121	4
11	-36	0	9
12	112	114	5
13	244	248	5
14	150	146	5

2	-6	1

0	78	86	4
1	354	355	4
2	279	262	3
3	25	18	8
4	244	243	3
5	530	534	5
6	511	516	5
7	221	219	3
8	653	641	6
9	353	358	4
10	211	198	4
11	-34	21	9
12	-4	50	24
13	61	61	7
14	38	46	10

2	-5	1

0	271	278	3
1	468	455	4
2	361	354	4
3	210	208	3
4	227	243	3
5	58	71	4
6	322	321	4
7	154	148	3
8	270	277	4
9	445	442	5
10	265	272	4
11	533	524	5
12	99	117	5
13	-15	26	17
14	-22	45	14
15	122	115	6

2	-4	1

0	266	262	3
1	465	481	4
2	653	659	6
3	906	926	8
4	1199	1217	10
5	302	321	3
6	273	264	3
7	952	972	8
8	430	436	4
9	645	652	6

10	326	327	4
11	33	56	9
12	-11	38	19
13	217	225	4
14	-38	17	9
15	-35	4	11

2	-3	1

0	936	944	8
1	497	500	4
2	72	63	3
3	628	622	5
4	952	916	8
5	553	567	5
6	911	873	8
7	25	23	8
8	109	119	4
9	276	279	4
10	26	13	10
11	245	244	4
12	262	262	4
13	258	263	4
14	110	108	5
15	55	64	7

2	-2	1

0	2153	2167	18
1	91	84	3
2	365	353	3
3	900	892	7
4	1253	1245	10
5	863	851	7
6	246	237	3
7	314	318	3
8	-18	34	11
9	93	99	4
10	304	309	4
11	650	644	6
12	39	56	9
13	54	91	8
14	166	167	5
15	-30	38	12

2	-1	1

0	1525	1490	13
1	61	45	3
2	341	330	3
3	300	273	3
4	1261	1271	10
5	986	983	8
6	371	360	4
7	605	582	5
8	133	146	3
9	244	255	4
10	178	184	4
11	99	109	4
12	276	282	4
13	168	185	4
14	72	74	6
15	260	238	5
16	66	62	8

2	0	1

-14	208	182	5
-13	209	202	5
-12	-30	13	11
-11	-24	18	12
-10	27	40	11
-9	74	67	5
-8	256	249	4
-7	462	441	5
-6	51	53	5
-5	1037	1059	9
-4	455	469	4

-3	543	541	5
-2	1345	1337	11
-1	1372	1340	11
0	1956	1966	16
1	293	284	3
2	387	340	3
3	84	84	3
4	184	174	2
5	207	204	3
6	717	707	6
7	100	66	3
8	179	185	3
9	594	599	6
10	-41	15	6
11	20	32	12
12	-47	4	6
13	387	389	5
14	163	171	5
15	205	206	5
16	91	95	6

2	1	1

-14	-20	26	13
-13	225	231	4
-12	122	102	5
-11	71	73	6
-10	119	120	4
-9	368	369	4
-8	-34	25	7
-7	257	242	3
-6	81	77	4
-5	555	582	5
-4	195	197	3
-3	710	700	6
-2	466	453	4
-1	438	432	4
0	22	11	7
1	144	154	2
2	288	270	3
3	183	160	2
4	163	160	2
5	604	619	5
6	1114	1128	9
7	175	187	3
8	597	607	5
9	637	625	6
10	18	34	12
11	197	202	4
12	325	338	4
13	-34	24	9
14	125	126	5
15	267	269	5
16	44	49	10

2	2	1

-14	291	285	5
-13	138	125	5
-12	125	120	5
-11	205	216	4
-10	458	455	5
-9	205	214	4
-8	500	486	5
-7	82	81	4
-6	135	132	3
-5	258	262	3
-4	976	968	8
-3	640	631	5
-2	1174	1144	10
-1	62	51	3
0	454	399	4
1	135	144	2
2	27	5	7
3	585	584	5
4	57	50	4
5	91	87	3
6	340	331	3

7	168	169	3
8	349	359	4
9	328	311	4
10	413	413	4
11	274	264	4
12	153	168	4
13	381	369	5
14	22	10	13
15	135	151	5

2	3	1

-14	307	296	5
-13	117	124	5
-12	291	290	4
-11	545	539	6
-10	369	378	4
-9	261	263	4
-8	237	239	4
-7	368	377	4
-6	150	176	3
-5	267	283	3
-4	298	278	3
-3	1246	1238	10
-2	1351	1362	9
-1	210	198	2
0	157	144	2
1	271	281	3
2	1010	968	8
3	1283	1277	11
4	1052	1060	9
5	144	150	3
6	-6	12	16
7	355	358	4
8	253	245	3
9	865	864	8
10	115	117	4
11	70	76	6
12	325	332	4
13	434	432	5
14	-17	6	16
15	38	29	11

2	4	1

-14	58	61	8
-13	116	102	5
-12	121	120	5
-11	91	104	5
-10	102	90	5
-9	369	377	4
-8	300	289	4
-7	572	575	5
-6	73	87	4
-5	532	516	5
-4	1405	1399	12
-3	638	658	5
-2	625	622	5
-1	326	332	3
0	482	484	4
1	688	694	6
2	1085	1093	9
3	1598	1604	13
4	164	162	3
5	63	79	4
6	343	341	4
7	207	219	3
8	30	28	8
9	213	210	4
10	276	268	4
11	122	140	4
12	264	260	4
13	90	96	6
14	210	198	5
15	58	49	8

2	5	1

-14	248	239	5
-13	34	54	11
-12	188	182	4
-11	79	85	6
-10	58	50	6
-9	312	314	4
-8	458	459	5
-7	605	615	6
-6	569	584	5
-5	620	594	6
-4	118	117	3
-3	143	131	3
-2	848	852	7
-1	743	756	6
0	358	357	3
1	124	122	3
2	1150	1157	10
3	1840	1829	15
4	532	534	5
5	810	789	7
6	258	259	3
7	68	73	4
8	86	94	4
9	90	92	4
10	66	74	6
11	52	78	7
12	552	562	6
13	173	187	5
14	274	258	5
15	72	88	7

2	6	1

-14	6	28	24
-13	160	174	5
-12	99	106	5
-11	227	220	4
-10	176	188	4
-9	612	606	6
-8	35	37	8
-7	48	19	6
-6	69	80	4
-5	300	301	3
-4	387	389	4
-3	565	546	5
-2	64	32	4
-1	1090	1110	9
0	556	557	5
1	84	93	3
2	67	62	4
3	708	687	6
4	1794	1778	15
5	770	756	7
6	347	345	4
7	189	211	3
8	393	392	4
9	667	674	6
10	551	551	6
11	-26	6	11
12	105	95	5
13	62	82	7
14	146	152	5

2	7	1

-13	151	146	5
-12	410	394	5
-11	102	103	5
-10	118	110	5
-9	63	48	6
-8	287	281	4
-7	605	601	6
-6	160	170	3
-5	-34	21	5
-4	231	248	3
-3	355	343	4
-2	509	510	5
-1	163	175	3

0	25	70	8
1	206	193	3
2	252	255	3
3	365	384	4
4	285	291	3
5	561	557	5
6	233	252	3
7	638	640	6
8	195	197	4
9	323	317	4
10	658	649	6
11	87	95	5
12	73	71	6
13	165	163	5
14	231	235	5

2	8	1

-13	100	105	6
-12	-42	7	8
-11	263	265	4
-10	131	131	5
-9	211	218	4
-8	319	324	4
-7	378	374	4
-6	247	238	4
-5	337	344	4
-4	46	33	6
-3	413	414	4
-2	114	117	3
-1	631	645	6
0	315	319	3
1	-35	14	5
2	85	101	4
3	41	52	6
4	114	109	3
5	7	22	16
6	713	705	6
7	354	364	4
8	170	175	4
9	260	259	4
10	224	237	4
11	77	74	6
12	261	264	5
13	355	371	5

2	9	1

-12	34	47	11
-11	103	111	5
-10	-38	12	8
-9	-33	7	8
-8	415	417	5
-7	140	131	4
-6	527	532	5
-5	73	71	5
-4	63	73	5
-3	244	250	3
-2	542	525	5
-1	379	356	4
0	970	975	8
1	270	270	3
2	-43	3	5
3	45	52	6
4	797	818	7
5	143	165	4
6	358	360	4
7	387	387	4
8	201	193	4
9	-34	24	9
10	160	152	4
11	118	125	5
12	41	56	10
13	28	29	14

2	10	1

-12	-37	25	10

-11	235	231	5
-10	84	81	6
-9	69	70	6
-8	121	129	5
-7	150	149	4
-6	380	378	4
-5	448	462	5
-4	-38	1	6
-3	173	171	4
-2	356	353	4
-1	154	154	3
0	64	80	5
1	185	179	3
2	91	93	4
3	903	917	8
4	60	62	5
5	166	165	4
6	250	254	4
7	303	280	4
8	181	169	4
9	83	82	6
10	59	63	7
11	24	51	14
12	257	249	5

2	11	1

-11	124	105	5
-10	86	83	6
-9	77	81	6
-8	200	203	4
-7	366	369	5
-6	326	327	4
-5	233	233	4
-4	61	49	6
-3	75	90	5
-2	51	45	6
-1	105	95	4
0	84	99	5
1	255	258	4
2	444	442	5
3	451	443	5
4	447	444	5
5	382	383	5
6	152	156	4
7	231	236	4
8	508	504	5
9	261	264	4
10	82	74	6
11	68	73	7

2	12	1

-10	229	217	5
-9	98	105	6
-8	-39	17	8
-7	120	103	5
-6	-44	12	7
-5	429	448	5
-4	263	274	4
-3	120	130	4
-2	216	224	4
-1	324	332	4
0	59	57	6
1	215	223	4
2	154	167	4
3	167	168	4
4	302	300	4
5	71	80	6
6	-17	35	15
7	174	183	4
8	89	91	6
9	90	95	6
10	123	125	5

2	13	1

-9	153	155	5

-8	-41	2	8
-7	-19	25	15
-6	335	313	5
-5	368	363	5
-4	13	23	17
-3	329	324	4
-2	597	585	6
-1	51	42	7
0	122	124	4
1	595	597	6
2	44	50	8
3	-37	5	8
4	77	82	6
5	186	184	4
6	-44	34	7
7	161	165	5
8	83	108	6

2 14 1

-7	50	63	9
-6	141	129	5
-5	227	222	4
-4	223	225	4
-3	44	33	9
-2	99	76	5
-1	25	38	13
0	221	211	4
1	48	48	8
2	217	209	4
3	372	373	5
4	211	220	4
5	64	74	7
6	306	286	5
7	48	27	9

2 15 1

-5	20	25	14
-4	252	255	5
-3	71	67	7
-2	59	59	7
-1	33	10	11
0	63	47	7
1	249	241	5
2	83	88	6
3	62	30	7
4	174	178	5

3 -13 1

0	124	113	5
1	241	241	5
2	170	165	5
3	204	201	5
4	166	156	5
5	334	314	5

3 -12 1

0	49	48	8
1	215	208	4
2	208	211	4
3	129	129	5
4	82	83	6
5	211	201	4
6	29	15	12
7	54	46	8
8	21	1	15

3 -11 1

0	185	173	4
1	129	133	5
2	129	139	5
3	-29	18	10
4	308	314	4
5	147	148	4
6	104	120	5
7	-15	1	17
8	-31	2	10
9	149	151	5
10	209	198	5

3 -10 1

0	243	242	4
1	372	368	5
2	265	263	4
3	171	186	4
4	-38	6	8
5	30	15	11
6	215	195	4
7	103	96	5
8	-34	32	9
9	179	182	4
10	69	81	6
11	40	8	10

3 -9 1

0	336	347	4
1	245	239	4
2	175	178	4
3	168	171	4
4	111	105	4
5	144	138	4
6	521	504	5
7	34	13	9
8	54	55	7
9	407	413	5
10	69	66	6
11	183	194	5
12	167	164	5

3 -8 1

0	101	103	4
1	178	177	4
2	94	114	4
3	218	216	4
4	57	63	6
5	583	590	6
6	56	40	6
7	468	470	5
8	81	89	5
9	409	389	5
10	218	216	4
11	141	143	5
12	-29	27	11
13	231	211	5

3 -7 1

0	50	51	6
1	40	0	7
2	9	9	16
3	-12	2	13
4	50	45	6
5	42	44	7
6	359	359	4
7	319	315	4
8	287	291	4
9	110	110	5
10	409	402	5
11	172	175	4
12	259	276	4
13	108	122	5
14	190	185	5

3 -6 1

0	138	134	3
1	124	129	3
2	29	38	6
3	103	100	3
4	310	305	4
5	131	139	3
6	203	222	3
7	132	126	4
8	347	333	4
9	527	536	5
10	177	159	4
11	252	242	4
12	61	85	7
13	55	66	8
14	281	275	5

3 -5 1

0	1296	1282	11
1	256	234	3
2	470	478	4
3	180	189	3
4	654	652	6
5	600	596	5
6	442	446	4
7	372	366	4
8	151	145	4
9	43	33	7
10	304	309	4
11	298	292	4
12	100	103	5
13	8	46	21
14	103	95	6
15	147	138	5

3 -4 1

0	95	103	3
1	291	302	3
2	155	160	3
3	520	521	5
4	506	522	5
5	283	292	3
6	115	124	3
7	556	569	5
8	362	369	4
9	91	91	4
10	-21	0	11
11	321	324	4
12	60	89	7
13	206	211	4
14	98	99	6
15	357	345	5

3 -3 1

0	605	591	5
1	853	864	7
2	20	6	8
3	161	159	3
4	228	223	3
5	750	768	6
6	448	455	4
7	107	106	3
8	27	34	9
9	30	11	7
10	461	459	5
11	755	762	7
12	100	96	5
13	86	96	6
14	167	154	5
15	-40	27	8

3 -2 1

0	576	560	5
1	409	411	4
2	300	297	3
3	188	192	3
4	747	758	6
5	357	372	4
6	125	144	3
7	325	324	4
8	240	243	3
9	8	17	17
10	195	194	4
11	560	557	6
12	108	115	5
13	-34	30	9
14	225	215	5
15	260	251	5

3 -1 1

0	608	608	5
1	1164	1156	10
2	798	797	7
3	37	3	5
4	717	720	6
5	13	26	11
6	131	137	3
7	157	161	3
8	467	469	5
9	479	479	5
10	215	208	4
11	-28	6	9
12	88	99	5
13	84	95	6
14	33	46	11
15	330	324	5
16	252	234	5

3 0 1

-14	47	22	10
-13	-38	15	9
-12	281	285	5
-11	251	252	4
-10	166	159	4
-9	192	197	4
-8	88	91	4
-7	116	125	4
-6	348	345	4
-5	360	356	4
-4	46	38	5
-3	830	821	7
-2	54	45	4
-1	46	6	4
0	152	145	2
1	2457	2436	20
2	384	374	3
3	796	810	7
4	301	303	3
5	818	810	7
6	445	445	4
7	169	163	3
8	762	774	7
9	230	238	4
10	138	124	4
11	106	103	4
12	65	93	6
13	164	158	4
14	62	59	7
15	-40	16	9
16	85	79	6

3 1 1

-14	263	260	5
-13	224	211	5
-12	275	260	5
-11	212	208	4
-10	8	27	20
-9	-12	8	16
-8	27	29	10
-7	115	106	4
-6	212	211	3
-5	358	365	4
-4	67	53	4
-3	323	321	3

-2	227	230	3
-1	1947	1987	16
0	1856	1836	15
1	503	484	3
2	666	653	6
3	134	125	3
4	255	259	3
5	718	696	6
6	39	16	6
7	941	954	8
8	72	57	4
9	355	337	4
10	247	240	4
11	234	228	4
12	279	279	4
13	402	399	5
14	201	194	4
15	57	71	8
16	62	59	8
3	2	1	
-14	101	81	6
-13	60	66	6
-12	191	183	4
-11	124	119	5
-10	231	234	4
-9	534	533	5
-8	201	211	4
-7	312	303	4
-6	547	539	5
-5	249	246	3
-4	184	187	3
-3	15	39	12
-2	712	713	6
-1	224	224	3
0	95	86	3
1	681	653	6
2	1035	1004	9
3	611	611	5
4	642	638	5
5	1252	1249	10
6	250	273	3
7	125	124	3
8	342	339	4
9	222	217	4
10	456	454	5
11	443	422	5
12	486	490	5
13	25	41	13
14	1	31	27
15	61	79	8
16	35	30	10
3	3	1	
-14	85	78	6
-13	36	59	10
-12	77	78	6
-11	100	87	5
-10	383	384	5
-9	404	420	5
-8	211	211	4
-7	252	260	4
-6	792	793	7
-5	64	52	3
-4	448	445	4
-3	32	2	6
-2	102	96	3
-1	846	835	7
0	98	89	3
1	723	705	6
2	209	210	2
3	1858	1832	16
4	150	149	3
5	254	264	3
6	524	501	5
7	577	564	5

8	286	274	4
9	311	316	4
10	244	237	4
11	26	50	11
12	256	258	4
13	341	330	5
14	27	6	13
15	186	182	5
3	4	1	
-14	-22	41	15
-13	-20	18	15
-12	23	36	12
-11	62	45	6
-10	392	390	5
-9	555	548	6
-8	241	248	4
-7	533	543	5
-6	363	380	4
-5	907	918	8
-4	116	119	3
-3	200	209	3
-2	577	587	5
-1	22	23	8
0	97	98	3
1	360	367	3
2	1819	1805	15
3	611	613	5
4	554	549	5
5	70	65	4
6	64	74	4
7	2	44	19
8	462	460	5
9	460	463	5
10	31	28	9
11	-12	55	17
12	132	137	5
13	304	303	5
14	276	286	5
15	252	252	5
3	5	1	
-13	35	54	10
-12	247	256	5
-11	132	137	5
-10	166	181	4
-9	212	208	4
-8	561	555	5
-7	117	88	4
-6	739	735	7
-5	154	158	3
-4	95	108	3
-3	23	21	8
-2	675	679	6
-1	905	884	8
0	716	711	6
1	693	693	6
2	624	609	5
3	298	303	3
4	288	283	3
5	305	291	3
6	518	531	5
7	225	248	3
8	418	425	4
9	59	56	5
10	37	45	8
11	127	139	4
12	197	203	4
13	103	102	5
14	-23	8	14
15	98	111	6
3	6	1	
-13	-19	34	16
-12	266	272	5

-11	349	338	5
-10	80	90	6
-9	189	184	4
-8	416	417	5
-7	370	367	4
-6	95	90	4
-5	263	261	3
-4	127	114	3
-3	150	146	3
-2	639	651	6
-1	63	53	4
0	127	114	3
1	11	13	12
2	257	265	3
3	541	519	5
4	446	430	4
5	179	179	3
6	590	578	5
7	679	682	6
8	153	162	4
9	476	465	5
10	331	322	4
11	78	97	6
12	88	89	6
13	208	209	5
14	186	175	5
3	7	1	
-13	70	97	7
-12	43	0	10
-11	475	468	5
-10	166	142	4
-9	79	83	5
-8	160	166	4
-7	235	249	4
-6	219	204	3
-5	113	116	4
-4	526	520	5
-3	556	572	5
-2	27	29	8
-1	836	843	7
0	366	343	4
1	641	607	6
2	60	50	4
3	570	599	5
4	188	183	3
5	4	23	18
6	289	294	4
7	93	92	4
8	296	294	4
9	240	235	4
10	262	275	4
11	167	173	4
12	129	124	5
13	109	122	5
14	41	51	10
3	8	1	
-12	15	38	18
-11	105	108	5
-10	11	39	19
-9	187	188	4
-8	378	392	4
-7	-11	21	16
-6	577	578	5
-5	88	93	4
-4	442	445	4
-3	331	330	4
-2	242	240	3
-1	191	183	3
0	473	490	4
1	78	92	4
2	26	5	8
3	43	64	5
4	172	170	3
5	423	426	4

6	214	216	3
7	56	52	6
8	9	28	17
9	243	252	4
10	35	51	10
11	23	37	12
12	65	81	7
13	236	227	5
3	9	1	
-12	178	181	5
-11	156	175	5
-10	147	153	5
-9	134	137	4
-8	11	1	18
-7	684	689	6
-6	216	211	4
-5	306	312	4
-4	320	319	4
-3	285	295	4
-2	238	227	3
-1	238	234	3
0	461	463	5
1	410	416	4
2	237	238	3
3	678	669	6
4	68	81	5
5	187	202	3
6	244	243	4
7	258	255	4
8	108	120	4
9	178	173	4
10	44	61	8
11	45	70	9
12	125	122	5
13	269	267	5
3	10	1	
-11	72	68	7
-10	39	51	10
-9	-15	43	17
-8	19	35	14
-7	155	164	4
-6	220	231	4
-5	108	100	4
-4	108	107	4
-3	446	438	5
-2	569	563	5
-1	208	198	3
0	-31	9	7
1	239	231	4
2	301	309	4
3	132	126	4
4	401	404	4
5	160	155	4
6	209	204	4
7	48	31	7
8	366	356	5
9	103	124	5
10	233	246	4
11	58	52	8
12	55	54	8
3	11	1	
-11	221	213	5
-10	193	186	5
-9	28	47	12
-8	195	197	4
-7	212	211	4
-6	96	101	5
-5	70	72	6
-4	16	47	14
-3	252	263	4
-2	383	371	4
-1	192	198	4

0	143	130	4
1	102	103	4
2	269	267	4
3	191	183	4
4	204	197	4
5	409	408	5
6	235	245	4
7	211	200	4
8	-26	27	11
9	305	288	5
10	208	208	5
11	79	87	6

3 12 1

-10	45	5	10
-9	149	136	5
-8	64	46	7
-7	69	80	6
-6	146	152	4
-5	14	19	16
-4	31	41	9
-3	-38	30	8
-2	535	541	5
-1	310	321	4
0	145	158	4
1	59	61	6
2	-25	19	10
3	143	148	4
4	41	73	8
5	181	179	4
6	-10	46	19
7	93	122	5
8	350	340	5
9	201	212	5
10	238	235	5

3 13 1

-9	115	105	5
-8	72	81	7
-7	193	184	5
-6	266	255	4
-5	143	140	5
-4	-36	2	9
-3	305	300	4
-2	-22	14	13
-1	564	556	6
0	143	152	4
1	201	208	4
2	68	72	6
3	249	259	4
4	19	28	14
5	106	116	5
6	190	200	4
7	170	169	5
8	151	148	5
9	39	39	10

3 14 1

-7	44	57	9
-6	242	238	5
-5	103	111	5
-4	-34	4	9
-3	79	82	6
-2	167	155	4
-1	313	310	4
0	36	49	10
1	249	244	4
2	362	362	5
3	62	54	7
4	94	102	5
5	131	131	5
6	111	105	5
7	89	86	6

3 15 1

-5	31	36	12
-4	-18	20	16
-3	-55	9	6
-2	107	110	5
-1	381	391	5
0	70	70	7
1	172	160	5
2	187	170	5
3	353	349	5
4	117	121	5
5	-29	27	12

3 16 1

-1	53	54	8
0	-30	0	11
1	93	87	6

4 -12 1

0	49	70	8
1	83	86	6
2	57	46	8
3	101	107	5
4	290	293	5
5	46	38	9
6	132	128	5

4 -11 1

0	44	26	9
1	241	254	4
2	174	169	4
3	162	160	4
4	251	257	4
5	169	171	5
6	98	91	5
7	107	112	5
8	-22	23	14
9	70	78	7

4 -10 1

0	100	96	5
1	237	238	4
2	47	55	7
3	-27	22	10
4	116	119	5
5	131	128	5
6	126	131	5
7	261	262	4
8	81	91	6
9	36	38	11
10	93	102	6

4 -9 1

0	32	33	10
1	60	62	5
2	440	430	5
3	54	58	7
4	18	10	12
5	57	38	7
6	766	777	7
7	93	71	5
8	176	182	4
9	268	275	4
10	41	36	9
11	14	21	18

4 -8 1

0	117	122	4
1	240	237	4
2	70	75	5
3	141	137	4
4	143	153	4
5	130	127	4
6	-15	14	13
7	223	219	4
8	643	636	6
9	93	100	5
10	238	231	4
11	142	135	5
12	93	90	6

4 -7 1

0	455	450	5
1	310	312	4
2	71	68	5
3	56	73	5
4	-31	3	8
5	41	44	7
6	73	70	5
7	337	330	4
8	163	148	4
9	224	233	4
10	179	167	4
11	30	42	12
12	153	155	5
13	305	300	5

4 -6 1

0	175	175	3
1	-26	1	8
2	52	34	5
3	321	313	4
4	560	547	5
5	278	273	4
6	222	219	4
7	176	177	4
8	54	51	6
9	79	82	5
10	177	181	4
11	379	404	5
12	-32	29	8
13	125	119	5
14	386	374	5

4 -5 1

0	42	19	6
1	227	224	3
2	718	707	6
3	729	738	6
4	226	214	3
5	-14	32	13
6	144	148	3
7	210	221	4
8	330	331	4
9	271	272	4
10	43	45	8
11	-18	34	15
12	160	174	4
13	-37	28	9
14	-33	5	11

4 -4 1

0	118	123	3
1	26	16	8
2	79	81	4
3	161	152	3
4	485	509	5
5	527	516	5
6	165	166	3
7	425	414	4
8	462	461	5
9	407	395	4
10	523	521	5
11	103	104	5
12	-57	0	5
13	182	190	5
14	193	192	5
15	165	176	5

4 -3 1

0	101	99	3
1	149	149	3
2	63	54	4
3	166	170	3
4	377	371	4
5	74	59	4
6	305	288	4
7	213	210	3
8	185	189	3
9	581	588	6
10	7	47	20
11	89	72	5
12	158	170	4
13	105	111	5
14	172	182	5
15	279	266	5

4 -2 1

0	416	408	4
1	410	419	4
2	12	9	11
3	283	284	3
4	379	383	4
5	298	308	3
6	243	239	3
7	125	126	3
8	183	185	3
9	42	44	7
10	386	385	4
11	375	373	5
12	-34	6	9
13	38	55	9
14	65	70	7
15	202	201	5

4 -1 1

0	369	344	4
1	426	430	4
2	652	644	6
3	190	185	3
4	593	598	5
5	412	418	4
6	-11	54	13
7	538	522	5
8	419	424	4
9	380	372	4
10	211	216	4
11	290	284	4
12	386	397	5
13	425	423	5
14	135	142	5
15	279	270	5

4 0 1

-13	234	234	5
-12	198	206	5
-11	-15	14	16
-10	-6	23	23
-9	42	31	8
-8	135	140	4
-7	213	209	4
-6	511	524	5
-5	53	20	5
-4	26	3	8
-3	38	29	6
-2	733	725	6
-1	572	573	5
0	1019	1018	9
1	648	665	6
2	82	93	3

3	225	221	3
4	127	134	3
5	52	60	5
6	605	606	5
7	73	83	4
8	105	113	4
9	134	126	4
10	564	551	5
11	175	170	4
12	113	120	5
13	213	230	4
14	128	122	5
15	-41	6	7
16	-25	31	13
4	1	1	
-13	-39	29	9
-12	-19	17	15
-11	166	170	5
-10	58	64	7
-9	171	164	4
-8	-25	25	10
-7	127	107	4
-6	446	457	5
-5	130	119	3
-4	278	263	3
-3	101	107	3
-2	29	11	7
-1	717	712	6
0	304	278	3
1	607	616	5
2	696	691	6
3	261	264	3
4	44	34	4
5	576	582	5
6	285	310	3
7	76	86	4
8	136	134	3
9	580	570	5
10	317	320	4
11	48	61	7
12	295	303	4
13	415	419	5
14	320	326	5
15	242	247	5
16	-38	11	10
4	2	1	
-13	76	71	7
-12	110	121	5
-11	138	134	5
-10	34	15	10
-9	-11	25	18
-8	125	117	4
-7	418	411	4
-6	407	389	4
-5	405	401	4
-4	351	343	4
-3	364	363	4
-2	63	60	4
-1	63	67	4
0	435	425	4
1	834	835	5
2	254	249	3
3	83	71	3
4	904	894	8
5	142	142	3
6	528	520	5
7	262	275	3
8	93	87	4
9	487	479	5
10	262	257	4
11	-29	23	9
12	-38	15	8
13	171	175	4
14	57	46	8

15	37	24	11
16	115	121	6
4	3	1	
-13	65	80	7
-12	80	103	6
-11	549	555	6
-10	121	119	5
-9	140	147	4
-8	100	112	4
-7	71	73	5
-6	260	254	4
-5	437	445	4
-4	233	225	3
-3	153	157	3
-2	214	221	3
-1	139	125	3
0	77	87	3
1	11	27	13
2	126	132	3
3	511	499	5
4	538	561	5
5	136	144	3
6	100	101	3
7	162	168	3
8	221	220	3
9	306	310	4
10	644	628	6
11	157	165	4
12	-53	41	6
13	80	76	6
14	78	78	6
15	15	59	18
4	4	1	
-13	73	72	7
-12	65	87	7
-11	304	305	5
-10	171	168	4
-9	435	428	5
-8	15	27	15
-7	-30	3	8
-6	111	109	4
-5	348	344	4
-4	666	677	6
-3	384	376	4
-2	218	208	3
-1	442	449	4
0	879	898	7
1	162	160	3
2	924	911	8
3	451	428	4
4	1423	1427	12
5	331	320	4
6	482	483	5
7	446	450	4
8	641	638	6
9	676	672	6
10	-30	48	9
11	-30	11	9
12	114	118	5
13	74	87	6
14	-20	44	15
15	87	96	6
4	5	1	
-13	-34	30	8
-12	171	170	5
-11	151	148	5
-10	276	266	4
-9	108	89	5
-8	228	233	4
-7	334	337	4
-6	189	178	3
-5	273	268	4

-4	271	264	3
-3	161	174	3
-2	147	137	3
-1	514	529	5
0	236	231	3
1	238	258	3
2	681	682	6
3	388	402	4
4	43	13	5
5	568	532	5
6	221	222	3
7	-10	17	15
8	475	484	5
9	250	255	4
10	408	409	5
11	301	308	4
12	442	441	5
13	280	288	5
14	165	173	5
15	-33	13	11
4	6	1	
-13	116	121	6
-12	-19	8	16
-11	166	184	5
-10	222	229	4
-9	107	93	5
-8	22	28	11
-7	371	375	4
-6	36	42	7
-5	192	200	3
-4	280	279	3
-3	326	300	4
-2	425	428	4
-1	316	334	3
0	576	574	5
1	326	325	3
2	413	387	4
3	766	727	7
4	714	699	6
5	59	55	4
6	419	408	4
7	587	591	5
8	211	208	4
9	290	289	4
10	454	457	5
11	136	151	4
12	-35	41	9
13	144	128	5
14	47	38	9
15	-37	25	10
4	7	1	
-12	39	34	11
-11	274	273	5
-10	80	69	6
-9	459	446	5
-8	362	377	4
-7	312	311	4
-6	192	191	4
-5	63	64	5
-4	325	328	4
-3	102	110	3
-2	222	216	3
-1	86	89	4
0	-18	12	10
1	112	119	3
2	423	412	4
3	22	23	9
4	747	746	7
5	579	562	5
6	266	259	4
7	-37	0	6
8	136	149	4
9	-17	34	13
10	-41	11	7

11	423	426	5
12	103	71	5
13	248	234	5
14	-7	30	23
4	8	1	
-12	29	37	13
-11	136	133	5
-10	460	455	5
-9	85	71	6
-8	49	24	8
-7	572	577	6
-6	258	256	4
-5	294	302	4
-4	555	555	5
-3	16	17	12
-2	24	39	9
-1	37	30	6
0	398	412	4
1	411	426	4
2	175	173	3
3	93	112	4
4	191	193	3
5	453	438	5
6	150	126	3
7	366	372	4
8	298	292	4
9	137	147	4
10	99	100	5
11	329	339	5
12	-44	49	8
13	-45	31	8
14	115	124	6
4	9	1	
-11	156	171	5
-10	164	162	5
-9	13	35	17
-8	100	111	5
-7	43	37	7
-6	170	172	4
-5	101	97	4
-4	133	135	4
-3	233	245	4
-2	574	573	5
-1	644	638	6
0	289	288	4
1	677	680	6
2	425	428	4
3	43	37	6
4	31	36	8
5	246	257	4
6	194	191	4
7	887	885	8
8	204	204	4
9	126	126	4
10	83	91	6
11	-50	21	5
12	115	132	5
13	241	234	5
4	10	1	
-11	152	146	5
-10	29	54	12
-9	113	120	5
-8	-37	12	7
-7	-8	38	20
-6	302	305	4
-5	190	189	4
-4	-23	26	10
-3	700	697	6
-2	87	97	4
-1	535	540	5
0	318	304	4
1	437	440	5

2	473	474	5
3	110	107	4
4	63	57	5
5	255	248	4
6	460	458	5
7	225	251	4
8	-37	36	8
9	293	284	4
10	70	86	6
11	44	60	9
12	248	237	5

4 11 1

-10	290	279	5
-9	80	83	6
-8	187	198	4
-7	113	115	5
-6	104	97	5
-5	469	486	5
-4	10	7	18
-3	183	197	4
-2	115	118	4
-1	70	69	5
0	197	190	4
1	107	111	4
2	690	698	6
3	296	296	4
4	43	44	7
5	106	114	4
6	177	185	4
7	100	105	5
8	415	411	5
9	327	346	5
10	99	95	5
11	117	114	5

4 12 1

-9	249	254	5
-8	118	121	5
-7	86	91	6
-6	243	252	4
-5	456	459	5
-4	40	30	8
-3	179	186	4
-2	154	160	4
-1	256	267	4
0	162	166	4
1	263	289	4
2	54	57	6
3	303	299	4
4	131	123	4
5	74	89	6
6	97	106	5
7	226	242	4
8	117	126	5
9	205	187	5
10	71	74	7

4 13 1

-8	285	274	5
-7	286	276	5
-6	70	37	6
-5	64	63	6
-4	259	251	4
-3	206	205	4
-2	100	105	5
-1	111	101	5
0	115	119	5
1	301	303	4
2	-41	9	6
3	259	268	4
4	445	434	5
5	31	69	11
6	45	37	8
7	160	160	5

8	35	45	11
9	52	66	8

4 14 1

-7	100	116	6
-6	122	131	5
-5	45	57	9
-4	227	235	4
-3	53	43	6
-2	203	198	4
-1	54	74	7
0	-42	10	7
1	112	124	5
2	282	268	4
3	163	143	4
4	-40	33	8
5	9	43	20
6	248	239	5
7	111	102	5
8	56	56	8

4 15 1

-5	24	29	14
-4	135	131	5
-3	33	26	11
-2	-40	13	8
-1	130	139	5
0	63	74	7
1	45	44	8
2	188	176	5
3	121	113	5
4	300	288	5
5	8	15	22
6	216	211	5

4 16 1

-1	92	93	6
0	-54	6	6
1	80	62	6

5 -11 1

0	104	107	5
1	92	79	6
2	107	115	5
3	104	99	5
4	67	81	7
5	87	84	6
6	35	29	10
7	94	99	6

5 -10 1

0	81	92	6
1	72	65	6
2	34	26	11
3	42	45	9
4	50	51	8
5	33	12	9
6	-15	3	17
7	-26	30	12
8	48	62	9
9	187	177	5

5 -9 1

0	139	156	4
1	123	124	5
2	36	41	10
3	-3	14	24
4	-3	15	25
5	126	119	5
6	138	125	5
7	340	339	5
8	63	65	7

9	28	60	12
10	162	159	5

5 -8 1

0	226	221	4
1	114	101	4
2	354	362	4
3	89	86	5
4	334	327	4
5	156	172	4
6	339	340	4
7	144	146	4
8	6	3	21
9	-35	17	9
10	357	345	5
11	87	95	6
12	128	132	5

5 -7 1

0	97	98	4
1	219	216	4
2	222	233	4
3	-17	27	12
4	200	204	4
5	91	86	5
6	172	174	4
7	86	75	5
8	69	65	6
9	-30	3	8
10	30	25	11
11	314	315	5
12	106	111	6

5 -6 1

0	226	223	4
1	133	120	4
2	325	324	4
3	168	171	4
4	29	26	8
5	166	170	4
6	115	117	4
7	487	471	5
8	60	59	6
9	132	139	4
10	75	81	6
11	138	129	5
12	11	27	20
13	179	180	5

5 -5 1

0	198	193	3
1	272	257	4
2	35	24	7
3	324	320	4
4	285	282	4
5	329	331	4
6	118	116	4
7	-12	27	14
8	506	494	5
9	183	185	4
10	199	188	4
11	142	142	5
12	159	173	5
13	-30	2	11
14	-53	11	7

5 -4 1

0	528	516	5
1	233	239	3
2	67	66	4
3	40	51	5
4	110	105	4
5	278	281	4

6	317	319	4
7	282	284	4
8	382	395	4
9	467	455	5
10	534	535	5
11	339	326	5
12	-33	38	9
13	100	111	6
14	185	191	5

5 -3 1

0	557	554	5
1	344	350	4
2	193	174	3
3	231	231	3
4	21	16	9
5	140	142	3
6	121	117	4
7	456	454	5
8	390	403	4
9	491	493	5
10	229	235	4
11	51	47	7
12	98	91	5
13	248	252	5
14	99	112	6
15	19	19	17

5 -2 1

0	316	308	4
1	308	321	3
2	168	163	3
3	352	343	4
4	242	237	3
5	83	87	4
6	101	85	4
7	263	258	4
8	335	333	4
9	294	302	4
10	49	49	7
11	188	188	4
12	440	440	5
13	477	462	5
14	207	207	5
15	110	124	6

5 -1 1

0	167	166	3
1	692	724	6
2	1019	1035	9
3	68	81	4
4	373	369	4
5	538	540	5
6	27	14	8
7	473	464	5
8	-23	27	10
9	35	50	8
10	72	88	5
11	110	123	5
12	34	24	10
13	239	243	4
14	46	58	9
15	67	78	7

5 0 1

-12	17	48	18
-11	44	39	9
-10	52	50	8
-9	48	50	8
-8	21	45	14
-7	96	83	5
-6	205	201	4
-5	533	530	5
-4	42	16	6

-3	423	419	4
-2	790	795	7
-1	83	78	4
0	35	6	6
1	237	222	3
2	284	281	3
3	102	123	3
4	1166	1150	10
5	184	169	3
6	219	212	3
7	32	29	8
8	363	354	4
9	66	66	5
10	218	219	4
11	64	55	6
12	438	435	5
13	124	132	5
14	276	273	5
15	194	181	5

5 1 1

-12	121	132	5
-11	-35	24	10
-10	66	81	7
-9	274	273	4
-8	137	144	4
-7	128	128	4
-6	443	448	5
-5	265	262	4
-4	26	53	9
-3	105	104	4
-2	346	351	4
-1	193	183	3
0	472	469	4
1	382	391	4
2	691	697	6
3	84	78	3
4	614	597	5
5	25	0	9
6	135	121	3
7	1108	1109	9
8	367	376	4
9	771	794	7
10	101	108	4
11	119	143	4
12	38	34	8
13	131	127	5
14	61	41	7
15	313	297	5

5 2 1

-12	176	158	5
-11	-22	25	14
-10	88	70	6
-9	143	143	4
-8	258	256	4
-7	202	206	4
-6	139	131	4
-5	142	143	4
-4	134	127	3
-3	365	337	4
-2	1050	1050	9
-1	468	447	4
0	498	495	5
1	173	172	3
2	195	187	3
3	48	39	5
4	648	652	6
5	120	135	3
6	341	323	4
7	163	159	3
8	38	14	7
9	284	278	4
10	200	212	4
11	259	263	4
12	150	147	4

13	522	511	6
14	312	301	5
15	88	83	6

5 3 1

-12	65	53	7
-11	123	125	5
-10	378	380	5
-9	43	61	9
-8	206	221	4
-7	192	185	4
-6	114	118	4
-5	87	93	4
-4	62	45	5
-3	91	88	4
-2	589	583	5
-1	38	44	6
0	129	125	3
1	24	31	8
2	124	129	3
3	341	333	4
4	263	262	3
5	142	148	3
6	430	410	4
7	-23	24	9
8	90	86	4
9	162	160	4
10	594	590	6
11	-46	14	6
12	393	387	5
13	291	290	4
14	215	204	5
15	153	145	5

5 4 1

-12	51	68	9
-11	238	232	5
-10	48	68	8
-9	153	145	4
-8	0	17	26
-7	55	48	6
-6	148	148	4
-5	14	13	14
-4	165	164	3
-3	417	421	4
-2	193	195	3
-1	1401	1386	12
0	97	98	3
1	149	147	3
2	318	313	3
3	242	241	3
4	586	596	5
5	374	374	4
6	66	57	4
7	104	102	4
8	298	299	4
9	265	266	4
10	-19	6	13
11	38	63	8
12	146	147	4
13	127	140	5
14	286	289	5
15	172	165	5

5 5 1

-12	35	28	12
-11	172	162	5
-10	156	166	5
-9	10	23	20
-8	347	340	4
-7	188	191	4
-6	339	338	4
-5	468	475	5
-4	133	121	3
-3	44	33	4

-2	40	32	5
-1	288	262	3
0	697	711	6
1	245	240	3
2	31	17	6
3	851	873	7
4	703	717	6
5	130	136	3
6	220	221	3
7	220	214	3
8	123	115	4
9	164	155	4
10	213	217	4
11	248	250	4
12	334	346	5
13	238	234	4
14	200	194	5
15	-59	14	6

5 6 1

-12	130	149	5
-11	93	81	6
-10	-31	15	11
-9	12	22	18
-8	167	169	4
-7	520	511	5
-6	67	57	5
-5	205	199	4
-4	18	9	10
-3	376	373	4
-2	77	64	4
-1	73	59	4
0	494	486	5
1	56	65	4
2	394	396	4
3	279	292	3
4	17	13	10
5	833	838	7
6	90	89	4
7	14	27	13
8	421	426	5
9	177	181	4
10	491	490	5
11	103	112	5
12	86	90	6
13	165	148	5
14	301	292	5
15	227	209	5

5 7 1

-12	94	74	6
-11	347	327	5
-10	97	109	6
-9	75	67	6
-8	52	45	7
-7	260	252	4
-6	572	590	6
-5	286	274	4
-4	-24	9	8
-3	61	39	5
-2	867	878	8
-1	778	774	7
0	211	216	3
1	502	484	5
2	299	289	3
3	262	261	3
4	937	947	8
5	234	228	3
6	287	300	4
7	469	462	5
8	395	391	4
9	-38	25	7
10	-33	25	9
11	402	400	5
12	-27	20	10
13	85	86	6

14	90	90	6

5 8 1

-11	150	140	5
-10	286	277	5
-9	107	95	5
-8	45	33	8
-7	637	640	6
-6	243	218	4
-5	256	253	4
-4	-28	0	8
-3	45	43	6
-2	551	564	5
-1	96	100	4
0	111	127	3
1	296	302	4
2	-19	24	9
3	37	60	7
4	50	37	5
5	331	331	4
6	270	269	4
7	349	354	4
8	435	431	5
9	636	639	6
10	17	50	15
11	339	348	5
12	-35	41	10
13	32	31	10
14	63	75	8

5 9 1

-11	57	60	8
-10	38	35	10
-9	120	121	5
-8	274	279	4
-7	245	229	4
-6	115	107	4
-5	35	32	9
-4	48	50	7
-3	258	267	4
-2	456	462	5
-1	331	332	4
0	60	55	5
1	318	322	4
2	150	150	3
3	98	85	4
4	567	565	5
5	365	373	4
6	33	30	9
7	108	103	4
8	98	103	5
9	66	77	6
10	-45	14	7
11	18	54	16
12	145	152	5
13	118	129	5

5 10 1

-10	112	105	5
-9	23	68	14
-8	117	125	5
-7	31	14	11
-6	256	252	4
-5	296	283	4
-4	200	200	4
-3	61	70	6
-2	175	190	4
-1	305	316	4
0	185	185	4
1	294	300	4
2	234	240	4
3	465	462	5
4	182	184	4
5	305	301	4
6	175	178	4

7	46	51	7
8	38	55	7
9	237	225	4
10	400	408	5
11	89	99	6
12	-47	16	8

5 11 1

-9	-30	25	11
-8	204	203	4
-7	215	218	4
-6	257	259	4
-5	156	140	4
-4	426	427	5
-3	85	84	5
-2	220	214	4
-1	189	199	4
0	80	87	5
1	220	214	4
2	419	420	5
3	625	641	6
4	134	151	4
5	714	715	7
6	237	242	4
7	-12	47	18
8	-23	44	12
9	-15	21	17
10	75	102	6
11	190	198	5

5 12 1

-9	49	65	9
-8	319	331	5
-7	270	258	5
-6	345	330	5
-5	228	235	4
-4	332	349	4
-3	159	158	4
-2	-21	5	13
-1	357	354	4
0	175	192	4
1	357	349	4
2	78	81	5
3	221	216	4
4	35	39	9
5	98	102	5
6	171	168	4
7	-50	0	6
8	77	94	6
9	-4	35	23
10	174	163	5

5 13 1

-7	126	134	5
-6	18	23	16
-5	262	248	4
-4	50	61	7
-3	265	268	4
-2	447	440	5
-1	203	206	4
0	365	363	5
1	193	199	4
2	68	81	6
3	123	131	5
4	281	287	4
5	-37	13	8
6	462	465	5
7	120	127	5
8	52	58	8
9	70	79	7

5 14 1

-6	42	72	9
-5	193	179	5
-4	372	369	5
-3	252	239	4
-2	254	242	4
-1	225	227	4
0	49	51	6
1	83	92	6
2	193	174	4
3	68	82	6
4	-3	32	25
5	80	74	6
6	85	95	6
7	206	199	5
8	103	96	6

5 15 1

-4	76	80	7
-3	265	262	5
-2	142	134	5
-1	91	93	6
0	121	110	5
1	336	321	5
2	311	302	5
3	26	38	13
4	32	36	12
5	-2	19	25
6	147	138	5

5 16 1

1	242	235	5

6 -10 1

0	15	27	18
1	87	83	6
2	32	20	11
3	133	127	5
4	-44	7	8
5	110	116	5
6	-15	43	17
7	57	63	8

6 -9 1

0	291	270	5
1	264	258	4
2	97	98	5
3	56	56	7
4	160	154	5
5	182	172	4
6	-22	14	13
7	44	59	9
8	124	115	5
9	94	107	6

6 -8 1

0	99	100	5
1	59	58	7
2	-31	6	10
3	85	91	5
4	41	46	8
5	168	162	4
6	236	237	4
7	73	59	6
8	115	111	5
9	92	68	6
10	283	266	5

6 -7 1

0	76	74	6
1	139	134	4
2	40	37	9
3	143	151	4
4	-34	21	9
5	93	83	5
6	251	248	4
7	42	41	9
8	143	146	5
9	92	110	6
10	108	97	5
11	236	229	5

6 -6 1

0	287	291	4
1	214	205	4
2	119	130	4
3	74	68	5
4	226	238	4
5	82	89	5
6	258	257	4
7	69	64	6
8	287	284	4
9	167	154	4
10	67	69	7
11	140	136	5
12	-31	4	11

6 -5 1

0	37	35	8
1	199	196	4
2	142	141	4
3	248	245	4
4	197	194	4
5	230	230	4
6	27	34	10
7	179	182	4
8	272	268	4
9	372	385	5
10	300	290	4
11	77	89	6
12	-44	0	8
13	-31	50	11

6 -4 1

0	257	250	4
1	223	218	4
2	92	74	4
3	202	205	4
4	668	695	6
5	327	323	4
6	-31	11	8
7	79	87	4
8	69	69	6
9	443	434	5
10	440	447	5
11	272	278	4
12	79	94	6
13	142	144	5
14	-27	23	13

6 -3 1

0	245	243	4
1	198	201	3
2	34	37	7
3	118	124	4
4	112	118	4
5	-11	22	15
6	204	199	4
7	125	135	4
8	114	116	4
9	62	72	6
10	48	56	8
11	124	122	5
12	39	35	9
13	62	53	7
14	331	329	5

6 -2 1

0	394	394	4
1	143	134	3
2	15	4	12
3	388	392	4
4	77	72	4
5	533	527	5
6	97	93	4
7	153	169	4
8	-15	20	14
9	185	184	4
10	83	89	5
11	251	254	4
12	485	484	5
13	68	67	7
14	70	65	7

6 -1 1

0	23	28	9
1	376	385	4
2	492	484	5
3	87	81	4
4	445	454	4
5	491	485	5
6	484	475	5
7	226	230	4
8	176	175	4
9	261	257	4
10	-35	7	8
11	-19	5	12
12	425	435	5
13	196	186	5
14	22	16	15
15	129	120	5

6 0 1

-11	120	109	5
-10	44	57	9
-9	80	95	6
-8	114	113	5
-7	79	84	6
-6	196	189	4
-5	232	230	4
-4	40	30	7
-3	232	242	4
-2	245	249	3
-1	187	179	3
0	214	206	3
1	229	226	3
2	876	866	8
3	103	85	3
4	102	85	3
5	112	104	3
6	309	315	4
7	141	134	4
8	67	80	5
9	223	232	4
10	443	437	5
11	177	173	4
12	288	287	4
13	268	268	5
14	254	262	5
15	-14	22	19

6 1 1

-11	117	113	6
-10	106	92	6
-9	-27	9	12
-8	-28	50	11
-7	67	50	6
-6	127	120	4
-5	27	22	10
-4	83	82	5
-3	109	116	4
-2	85	65	4
-1	209	206	3

0	521	535	5
1	231	240	3
2	691	710	6
3	117	107	3
4	45	28	4
5	135	141	3
6	103	103	4
7	512	498	5
8	589	595	6
9	263	252	4
10	274	260	4
11	-32	5	10
12	382	383	5
13	108	99	5
14	166	173	5
15	195	187	5

6 2 1

-11	-16	15	18
-10	64	64	7
-9	127	117	5
-8	139	151	5
-7	203	212	4
-6	453	452	5
-5	239	237	4
-4	100	103	4
-3	269	274	4
-2	311	299	4
-1	918	902	8
0	680	665	6
1	79	49	4
2	350	327	4
3	237	225	3
4	471	451	5
5	61	72	5
6	504	497	5
7	213	216	4
8	148	158	4
9	304	310	4
10	114	95	4
11	67	76	6
12	317	303	5
13	223	220	4
14	52	39	8
15	36	22	11

6 3 1

-11	-17	11	17
-10	127	132	5
-9	295	291	5
-8	130	130	5
-7	48	32	8
-6	234	229	4
-5	431	440	5
-4	259	270	4
-3	254	251	4
-2	68	48	5
-1	52	21	4
0	107	110	3
1	453	441	3
2	49	31	5
3	492	483	5
4	582	575	5
5	183	191	3
6	186	176	3
7	349	339	4
8	94	90	4
9	318	316	4
10	178	170	4
11	242	247	4
12	361	353	5
13	35	51	11
14	171	164	5
15	30	48	11

6 4 1

-11	66	67	7
-10	47	39	8
-9	92	86	6
-8	163	166	4
-7	32	24	10
-6	286	278	4
-5	38	14	8
-4	386	384	4
-3	424	413	4
-2	165	168	3
-1	169	164	3
0	88	90	4
1	172	170	3
2	593	592	5
3	478	470	5
4	168	163	3
5	160	152	3
6	340	330	4
7	266	261	4
8	173	165	4
9	119	127	4
10	229	222	4
11	461	466	5
12	220	230	4
13	290	283	5
14	327	320	5
15	214	220	5

6 5 1

-11	153	145	5
-10	-16	14	17
-9	236	239	4
-8	142	149	5
-7	175	168	4
-6	190	188	4
-5	205	212	4
-4	113	111	4
-3	191	184	3
-2	30	10	8
-1	60	29	5
0	47	41	5
1	155	168	3
2	257	248	3
3	433	438	4
4	256	238	3
5	277	270	4
6	253	244	4
7	195	197	4
8	748	756	7
9	298	306	4
10	97	102	5
11	253	257	4
12	208	213	4
13	161	153	5
14	214	205	5
15	-30	44	12

6 6 1

-11	112	114	6
-10	85	89	6
-9	207	193	4
-8	76	65	6
-7	223	213	4
-6	129	135	4
-5	124	128	4
-4	108	100	4
-3	421	418	4
-2	241	244	3
-1	158	161	3
0	291	292	4
1	57	60	5
2	197	180	3
3	576	567	5
4	411	421	4
5	94	85	4
6	71	94	5
7	439	437	5
8	43	16	7
9	154	163	4
10	378	364	5
11	328	321	5
12	104	82	5
13	44	52	9
14	118	134	5

6 7 1

-11	117	101	6
-10	38	37	11
-9	64	81	7
-8	297	304	4
-7	336	326	4
-6	144	140	4
-5	153	153	4
-4	271	271	4
-3	-25	17	9
-2	357	369	4
-1	403	396	4
0	342	334	4
1	82	74	4
2	472	463	5
3	282	278	4
4	245	228	3
5	447	433	5
6	43	40	7
7	129	129	4
8	148	162	4
9	350	353	4
10	315	322	4
11	5	0	23
12	61	60	7
13	250	248	5
14	39	42	11

6 8 1

-10	119	115	5
-9	102	89	5
-8	107	93	5
-7	559	554	6
-6	117	116	5
-5	119	120	4
-4	228	227	4
-3	122	128	4
-2	568	572	5
-1	44	9	6
0	-24	12	9
1	365	360	4
2	26	4	9
3	200	202	3
4	351	363	4
5	527	529	5
6	623	620	6
7	84	77	5
8	187	189	4
9	73	77	6
10	29	51	11
11	236	237	4
12	-27	4	12
13	97	90	6

6 9 1

-10	43	45	9
-9	-30	29	11
-8	201	210	4
-7	87	69	5
-6	67	81	6
-5	51	58	7
-4	111	121	4
-3	163	166	4
-2	68	72	5
-1	314	322	4
0	161	161	4
1	121	125	4
2	514	520	5
3	49	44	6
4	492	480	5
5	97	91	4
6	663	672	6
7	285	283	4
8	326	321	4
9	-31	28	8
10	68	74	6
11	-40	24	8
12	244	237	5
13	304	303	5

6 10 1

-9	-42	0	8
-8	98	105	6
-7	61	60	7
-6	444	442	5
-5	213	203	4
-4	34	17	10
-3	381	382	4
-2	105	87	4
-1	333	325	4
0	168	167	4
1	221	225	4
2	191	194	4
3	184	179	4
4	344	350	4
5	203	211	4
6	240	233	4
7	212	212	4
8	-31	20	10
9	130	121	5
10	209	209	4
11	-45	12	6
12	52	61	9

6 11 1

-9	60	72	8
-8	90	70	6
-7	95	99	6
-6	124	116	5
-5	374	381	5
-4	440	434	5
-3	296	306	4
-2	108	106	5
-1	-22	16	11
0	26	31	11
1	23	21	11
2	552	545	5
3	308	320	4
4	121	106	4
5	36	40	8
6	211	212	4
7	-19	38	14
8	354	360	5
9	-43	14	8
10	176	182	5
11	91	92	6

6 12 1

-8	144	141	5
-7	109	103	5
-6	11	26	19
-5	51	33	8
-4	207	195	4
-3	81	68	6
-2	193	180	4
-1	559	578	6
0	438	446	5
1	164	169	4
2	177	170	4
3	118	118	4

4	100	109	5
5	134	144	4
6	-40	0	8
7	27	37	12
8	180	162	4
9	173	182	5
10	232	216	5

6 13 1

-7	33	32	12
-6	27	41	13
-5	332	336	5
-4	113	112	5
-3	17	20	16
-2	100	101	5
-1	44	40	8
0	98	85	5
1	98	101	5
2	62	64	7
3	30	50	11
4	202	209	4
5	20	39	14
6	47	57	8
7	198	199	4
8	114	112	5
9	186	182	5

6 14 1

-5	39	46	10
-4	215	228	5
-3	73	69	6
-2	148	147	5
-1	229	228	4
0	345	337	5
1	201	213	4
2	75	72	6
3	-36	5	9
4	137	146	5
5	117	120	5
6	7	23	23
7	100	98	6

6 15 1

-3	169	150	5
-2	47	40	9
-1	352	355	5
0	250	243	5
1	106	119	5
2	287	277	5
3	109	115	5
4	379	375	5
5	142	143	5

7 -9 1

0	97	93	6
1	59	42	8
2	53	62	8
3	216	213	5
4	21	39	15
5	24	4	13
6	12	32	19

7 -8 1

0	62	55	6
1	66	56	6
2	133	150	5
3	64	66	7
4	59	85	7
5	181	180	5
6	165	168	5
7	-20	20	15
8	59	49	8
9	50	42	9

7 -7 1

0	174	166	4
1	87	86	6
2	110	124	5
3	80	110	6
4	57	47	7
5	143	145	5
6	52	58	8
7	254	252	4
8	112	118	5
9	25	25	12
10	150	142	5

7 -6 1

0	193	193	4
1	50	37	8
2	59	68	7
3	67	86	6
4	90	83	5
5	133	115	4
6	71	76	6
7	245	248	4
8	-17	30	14
9	188	196	4
10	3	40	26
11	108	101	5

7 -5 1

0	205	206	4
1	33	47	10
2	-2	27	24
3	105	96	5
4	38	16	9
5	61	58	6
6	260	253	4
7	128	119	4
8	102	106	5
9	64	28	7
10	149	155	5
11	-20	20	15
12	76	73	7

7 -4 1

0	50	33	7
1	89	98	5
2	77	61	4
3	339	350	4
4	42	34	8
5	61	56	6
6	296	302	4
7	101	96	5
8	242	243	4
9	263	269	4
10	340	359	5
11	47	64	9
12	-17	29	14
13	341	328	5

7 -3 1

0	95	88	4
1	19	27	12
2	32	15	9
3	121	95	4
4	508	514	5
5	115	112	4
6	33	1	9
7	73	72	5
8	272	274	4
9	117	120	5
10	93	93	5
11	160	153	5
12	29	39	12
13	140	131	5

7 -2 1

0	47	61	7
1	97	108	4
2	66	76	5
3	108	105	4
4	237	240	4
5	214	202	4
6	-27	12	9
7	69	72	5
8	128	125	4
9	218	220	4
10	171	167	4
11	24	8	12
12	116	106	5
13	22	5	15
14	246	242	5

7 -1 1

0	106	108	4
1	180	181	3
2	35	43	7
3	31	20	7
4	65	63	5
5	51	62	6
6	-4	41	20
7	239	246	4
8	245	246	4
9	32	46	10
10	144	154	4
11	73	63	6
12	102	111	5
13	127	128	5
14	185	167	5

7 0 1

-9	101	100	6
-8	127	148	5
-7	27	19	13
-6	42	46	9
-5	159	161	4
-4	32	4	9
-3	48	51	6
-2	62	78	5
-1	118	110	4
0	19	0	10
1	327	327	4
2	66	52	5
3	192	191	3
4	295	287	4
5	234	223	4
6	384	378	4
7	42	25	7
8	414	408	5
9	290	296	4
10	-15	52	15
11	149	139	4
12	253	264	4
13	19	47	15
14	23	29	15

7 1 1

-10	42	24	10
-9	61	87	8
-8	108	127	5
-7	30	45	12
-6	64	60	7
-5	130	130	4
-4	17	16	14
-3	61	74	6
-2	135	141	4
-1	341	342	4
0	132	131	4

1	36	33	7
2	121	120	3
3	284	291	4
4	106	93	4
5	337	331	4
6	243	250	4
7	562	578	5
8	204	202	4
9	254	254	4
10	381	373	5
11	208	198	4
12	137	148	5
13	173	179	5
14	118	100	5

7 2 1

-10	71	74	7
-9	-16	47	18
-8	61	58	6
-7	32	52	11
-6	57	70	7
-5	81	69	5
-4	117	117	4
-3	174	184	4
-2	180	187	4
-1	21	27	9
0	69	54	5
1	62	62	4
2	120	119	3
3	43	34	6
4	320	316	4
5	103	84	4
6	330	331	4
7	161	167	4
8	140	132	4
9	39	32	8
10	292	304	4
11	389	391	5
12	278	286	4
13	246	228	5
14	125	145	5
15	356	343	5

7 3 1

-10	123	126	5
-9	85	88	6
-8	88	70	6
-7	228	216	4
-6	-18	13	15
-5	81	83	5
-4	327	319	4
-3	305	307	4
-2	30	4	9
-1	276	261	4
0	127	133	4
1	221	218	4
2	38	32	7
3	27	33	10
4	803	805	7
5	252	235	4
6	202	197	4
7	380	377	4
8	191	183	4
9	33	29	10
10	156	167	4
11	336	343	5
12	67	57	7
13	125	126	5
14	35	9	11
15	170	168	5

7 4 1

-10	-34	15	11
-9	87	91	6
-8	138	138	5

-7	201	191	4
-6	114	130	5
-5	168	161	4
-4	126	123	4
-3	98	94	4
-2	45	38	7
-1	251	236	4
0	397	395	4
1	223	228	3
2	168	164	3
3	136	146	3
4	23	24	10
5	570	556	5
6	341	343	4
7	169	157	4
8	278	271	4
9	-25	13	11
10	137	137	4
11	37	13	9
12	245	250	4
13	-33	18	10
14	209	223	5

7 5 1

-10	29	34	12
-9	207	201	5
-8	124	116	5
-7	122	116	5
-6	211	200	4
-5	84	56	5
-4	91	79	5
-3	90	87	5
-2	451	434	5
-1	263	257	4
0	348	347	4
1	631	641	6
2	285	280	4
3	209	210	3
4	85	91	4
5	386	381	4
6	37	44	7
7	550	564	5
8	376	372	4
9	47	56	8
10	20	5	14
11	539	537	6
12	81	99	6
13	38	38	10
14	62	83	8

7 6 1

-10	33	5	12
-9	108	108	6
-8	81	102	6
-7	120	106	5
-6	207	192	4
-5	52	55	7
-4	64	74	6
-3	394	407	4
-2	114	117	4
-1	410	408	4
0	299	287	4
1	63	55	5
2	454	452	5
3	242	240	4
4	-22	1	10
5	208	208	4
6	152	153	4
7	292	296	4
8	452	451	5
9	565	567	6
10	206	196	4
11	105	114	5
12	629	605	6
13	120	119	5
14	-17	20	17

7 7 1

-10	102	117	6
-9	110	107	6
-8	25	30	12
-7	102	84	5
-6	44	72	8
-5	38	34	9
-4	12	5	16
-3	132	135	4
-2	327	350	4
-1	217	210	4
0	213	219	4
1	42	2	7
2	475	469	5
3	295	294	4
4	220	225	4
5	53	60	6
6	234	227	4
7	113	88	4
8	750	760	7
9	185	187	4
10	-41	5	6
11	52	72	8
12	30	5	12
13	326	315	5
14	127	123	5

7 8 1

-9	59	60	8
-8	171	175	5
-7	185	201	4
-6	90	80	5
-5	217	207	4
-4	199	193	4
-3	416	403	5
-2	259	267	4
-1	152	161	4
0	238	235	4
1	180	180	4
2	600	605	6
3	277	283	4
4	491	495	5
5	72	51	5
6	245	244	4
7	298	316	4
8	71	65	6
9	92	85	5
10	48	65	8
11	98	111	5
12	24	17	14
13	133	129	5

7 9 1

-9	137	139	5
-8	79	84	5
-7	90	91	6
-6	224	221	4
-5	32	21	10
-4	126	134	4
-3	43	19	7
-2	229	230	4
-1	125	109	4
0	200	195	4
1	179	181	4
2	423	423	5
3	76	67	5
4	143	146	4
5	446	447	5
6	54	40	7
7	292	284	4
8	359	357	5
9	72	86	6
10	-42	11	8
11	30	39	12
12	87	94	6
13	28	46	12

7 10 1

-8	-26	1	13
-7	129	133	5
-6	108	99	5
-5	18	20	14
-4	50	41	8
-3	39	60	9
-2	461	467	5
-1	156	158	4
0	127	143	4
1	-34	20	8
2	25	11	11
3	679	687	6
4	473	473	5
5	121	116	4
6	427	417	5
7	168	168	4
8	-39	32	8
9	163	163	4
10	88	106	6
11	113	121	5
12	33	8	12

7 11 1

-8	317	295	5
-7	92	85	6
-6	186	180	5
-5	122	115	5
-4	76	76	6
-3	335	345	4
-2	370	363	5
-1	175	170	4
0	155	151	4
1	33	26	10
2	-31	15	9
3	191	183	4
4	157	160	4
5	96	92	5
6	72	47	6
7	294	296	4
8	182	173	4
9	261	270	4
10	99	115	6
11	284	268	5

7 12 1

-7	97	86	6
-6	123	131	5
-5	-26	1	12
-4	215	226	4
-3	150	146	4
-2	182	187	4
-1	-30	13	10
0	186	191	4
1	496	499	5
2	419	412	5
3	-25	6	11
4	-50	9	6
5	-27	6	11
6	76	86	6
7	291	296	4
8	139	136	5
9	-34	20	10
10	33	45	12

7 13 1

-5	73	65	6
-4	91	78	6
-3	49	40	8
-2	57	43	6
-1	280	284	4
0	94	114	5
1	178	162	4
2	482	471	5
3	59	67	6
4	107	126	5
5	-32	37	10
6	77	99	6
7	-25	29	13
8	88	80	6
9	-22	3	14

7 14 1

-4	139	130	5
-3	190	190	5
-2	50	22	8
-1	99	109	5
0	113	120	5
1	-12	2	19
2	93	103	6
3	118	110	5
4	242	246	5
5	84	70	6
6	335	324	5
7	243	225	5

7 15 1

-1	29	41	12
0	91	98	6
1	14	27	18
2	214	217	5
3	197	181	5
4	144	143	5

8 -8 1

2	92	93	6
3	55	32	7
4	60	52	7

8 -7 1

0	153	140	5
1	48	52	9
2	26	31	11
3	84	107	6
4	60	66	7
5	66	73	7
6	167	160	5
7	76	84	6
8	51	66	9

8 -6 1

0	189	184	4
1	162	163	5
2	66	69	7
3	17	18	16
4	266	270	4
5	76	81	6
6	68	71	7
7	50	54	8
8	82	84	6
9	89	99	6

8 -5 1

0	44	33	7
1	35	9	10
2	239	228	4
3	51	27	8
4	52	23	8
5	109	89	5
6	109	90	5
7	65	51	7
8	328	345	5
9	-24	26	13

10	40	8	10
11	13	6	19

8 -4 1

0	88	91	5
1	38	28	9
2	325	325	4
3	100	111	5
4	399	395	5
5	119	117	5
6	93	100	5
7	242	246	4
8	233	220	4
9	37	14	9
10	35	29	11
11	82	85	6
12	144	132	5

8 -3 1

0	64	49	6
1	134	138	4
2	37	6	9
3	199	194	4
4	165	155	4
5	192	191	4
6	-33	6	9
7	145	142	4
8	110	105	5
9	361	337	5
10	54	38	8
11	180	195	5
12	-8	32	23

8 -2 1

0	155	160	4
1	137	161	4
2	298	308	4
3	139	114	4
4	82	85	5
5	59	70	6
6	34	41	9
7	54	51	7
8	212	219	4
9	8	10	21
10	431	424	5
11	148	157	5
12	105	117	6
13	67	61	7

8 -1 1

0	204	206	4
1	256	269	4
2	264	270	4
3	351	361	4
4	44	1	7
5	189	188	4
6	32	45	9
7	65	65	6
8	162	157	4
9	141	142	4
10	74	86	6
11	232	226	4
12	56	66	8
13	165	163	5

8 0 1

-8	116	113	6
-7	57	73	8
-6	81	78	6
-5	128	113	5
-4	99	108	5
-3	139	153	4
-2	93	83	5
-1	169	165	4
0	106	109	4
1	268	267	4
2	157	165	4
3	95	82	4
4	385	376	4
5	288	296	4
6	39	29	7
7	294	299	4
8	87	86	5
9	218	223	4
10	133	126	5
11	116	115	5
12	256	243	5
13	107	107	6
14	47	54	10

8 1 1

-8	41	62	10
-7	37	30	11
-6	83	78	6
-5	356	354	5
-4	67	59	6
-3	144	155	4
-2	373	377	4
-1	314	317	4
0	83	80	5
1	117	121	4
2	126	128	4
3	377	382	4
4	63	58	4
5	128	119	4
6	88	103	5
7	115	111	4
8	194	190	4
9	130	135	5
10	156	155	4
11	76	64	6
12	124	129	5
13	49	47	9
14	92	82	6

8 2 1

-9	102	101	6
-8	39	31	11
-7	191	201	5
-6	285	285	5
-5	68	42	6
-4	134	133	5
-3	104	88	5
-2	80	70	5
-1	108	113	4
0	233	230	4
1	35	4	8
2	136	135	4
3	175	173	4
4	63	47	5
5	224	221	4
6	312	306	4
7	192	193	4
8	409	416	5
9	118	120	5
10	111	131	5
11	-15	16	17
12	11	15	18
13	-22	22	15
14	354	326	5

8 3 1

-9	159	147	5
-8	31	55	12
-7	103	94	6
-6	67	58	6
-5	83	73	6
-4	169	154	4
-3	341	342	4
-2	257	266	4
-1	28	10	11
0	301	284	4
1	200	202	4
2	78	81	5
3	132	127	4
4	120	124	4
5	151	147	4
6	70	88	6
7	113	106	4
8	124	121	4
9	80	88	6
10	-39	12	8
11	90	89	6
12	96	114	6
13	125	119	5
14	144	148	5

8 4 1

-9	108	96	6
-8	1	21	29
-7	110	111	5
-6	184	190	4
-5	138	133	5
-4	45	9	9
-3	285	271	4
-2	354	353	4
-1	197	197	4
0	307	308	4
1	44	0	7
2	308	308	4
3	586	590	6
4	68	51	5
5	85	74	5
6	158	165	4
7	68	72	6
8	212	208	4
9	148	158	4
10	220	226	4
11	-24	25	13
12	34	38	10
13	140	142	5
14	87	95	6

8 5 1

-9	51	69	8
-8	13	30	20
-7	59	38	7
-6	110	114	5
-5	13	30	16
-4	29	34	11
-3	110	112	5
-2	203	207	4
-1	49	33	7
0	135	143	4
1	244	235	4
2	49	7	5
3	334	331	4
4	391	386	4
5	265	270	4
6	-29	1	9
7	149	147	4
8	46	30	7
9	252	241	4
10	390	371	5
11	367	366	5
12	66	77	7
13	245	242	5
14	187	197	5

8 6 1

-9	47	49	10
-8	120	132	5
-7	413	421	5
-6	152	133	5
-5	85	82	6
-4	109	112	5
-3	150	142	4
-2	113	111	4
-1	133	127	4
0	38	15	7
1	47	38	7
2	33	1	8
3	51	13	6
4	141	138	4
5	124	135	4
6	228	232	4
7	115	95	4
8	71	59	5
9	85	65	6
10	77	61	6
11	27	14	13
12	54	57	8
13	139	144	5

8 7 1

-8	27	8	14
-7	25	17	14
-6	275	263	5
-5	151	151	4
-4	76	76	5
-3	252	255	4
-2	195	193	4
-1	-12	3	16
0	245	240	4
1	111	101	4
2	152	153	4
3	164	173	4
4	38	44	8
5	274	258	4
6	632	622	6
7	41	35	8
8	116	107	5
9	412	406	5
10	106	118	5
11	33	39	11
12	477	469	6
13	193	177	5

8 8 1

-8	-11	16	21
-7	51	67	9
-6	110	111	5
-5	37	40	9
-4	43	55	8
-3	225	228	4
-2	378	377	5
-1	250	252	4
0	103	97	4
1	129	125	4
2	24	10	10
3	86	99	5
4	526	523	5
5	255	244	4
6	412	405	5
7	313	313	4
8	359	360	5
9	103	100	5
10	144	150	5
11	80	84	6
12	261	270	5
13	-26	24	13

8 9 1

-8	82	65	7
-7	219	233	5
-6	171	189	5
-5	198	196	4
-4	164	154	4

-3	91	89	5
-2	75	60	6
-1	209	214	4
0	52	44	6
1	233	229	4
2	33	27	9
3	52	32	7
4	34	12	9
5	74	67	6
6	278	291	4
7	208	208	4
8	500	511	5
9	208	219	4
10	37	55	10
11	91	98	6
12	12	27	21

8 10 1

-7	134	113	5
-6	68	76	6
-5	152	165	5
-4	146	136	5
-3	82	98	6
-2	118	128	5
-1	-7	0	20
0	225	226	4
1	156	157	4
2	52	44	6
3	72	61	6
4	45	13	8
5	311	299	4
6	157	147	4
7	139	145	4
8	-25	1	12
9	127	132	5
10	126	111	5
11	294	290	5

8 11 1

-6	55	61	8
-5	152	168	5
-4	103	102	5
-3	173	164	4
-2	33	37	10
-1	46	57	8
0	77	79	6
1	292	289	4
2	101	86	5
3	352	349	5
4	172	177	4
5	77	96	6
6	441	448	5
7	301	306	5
8	113	110	5
9	143	166	5
10	265	263	5

8 12 1

-5	34	9	11
-4	248	224	5
-3	117	123	5
-2	69	69	6
-1	89	108	6
0	25	37	13
1	308	311	4
2	193	179	4
3	23	21	13
4	98	90	5
5	164	169	4
6	137	150	5
7	64	77	7
8	33	14	11
9	125	138	5

8 13 1

-4	82	91	6
-3	176	160	5
-2	15	3	17
-1	8	30	21
0	122	122	5
1	65	47	7
2	67	51	6
3	305	300	5
4	64	66	7
5	50	59	8
6	58	52	8
7	375	368	5
8	228	218	5

8 14 1

-2	177	161	5
-1	7	2	23
0	247	245	5
1	69	83	7
2	267	263	5
3	339	346	5
4	-27	23	12
5	189	177	5
6	204	202	5

9 -6 1

1	79	68	6
2	40	40	10
3	28	18	13
4	86	81	6
5	41	26	10
6	143	136	5

9 -5 1

0	84	101	6
1	39	43	10
2	19	5	15
3	14	2	16
4	91	86	6
5	140	148	5
6	82	95	6
7	70	60	7
8	51	53	8

9 -4 1

0	40	21	10
1	44	23	9
2	212	201	4
3	56	36	7
4	96	100	5
5	145	151	5
6	31	2	11
7	48	69	9
8	172	163	5
9	97	85	6
10	61	54	6

9 -3 1

0	80	78	5
1	132	113	5
2	171	160	4
3	187	190	4
4	104	121	5
5	24	8	11
6	-20	33	13
7	27	4	12
8	91	98	6
9	-11	7	17
10	52	53	8
11	52	56	8

9 -2 1

0	119	106	5
1	409	430	5
2	96	86	5
3	206	216	4
4	59	52	7
5	104	112	5
6	211	225	4
7	26	43	10
8	100	99	5
9	50	55	8
10	55	52	8
11	125	110	5

9 -1 1

0	145	118	4
1	241	246	4
2	165	156	4
3	54	36	7
4	182	179	4
5	260	252	4
6	63	50	6
7	373	376	5
8	95	100	5
9	-8	33	22
10	42	26	9
11	32	44	12
12	266	267	5

9 0 1

-6	55	74	8
-5	-5	0	24
-4	-24	6	13
-3	194	189	4
-2	56	7	7
-1	98	49	5
0	114	78	5
1	76	36	6
2	125	116	4
3	105	88	5
4	36	10	9
5	41	57	8
6	246	261	4
7	83	69	5
8	57	66	6
9	-16	18	15
10	25	13	14
11	-12	9	20
12	39	48	11

9 1 1

-7	30	14	13
-6	28	17	12
-5	182	175	5
-4	69	66	7
-3	337	339	5
-2	110	71	5
-1	291	299	4
0	164	159	4
1	292	300	4
2	134	121	4
3	149	163	4
4	256	250	4
5	168	171	4
6	120	122	5
7	28	22	11
8	109	92	5
9	344	360	5
10	105	124	5
11	462	450	5
12	110	122	6
13	95	83	6

9 2 1

-7	36	32	11
-6	125	117	5
-5	57	45	8
-4	148	166	5
-3	181	182	4
-2	169	161	4
-1	93	70	5
0	115	99	4
1	222	218	4
2	374	364	4
3	144	145	4
4	197	197	4
5	49	57	7
6	165	161	4
7	442	443	5
8	81	75	6
9	-34	9	10
10	123	131	5
11	262	257	5
12	-14	35	19
13	281	275	5

9 3 1

-7	141	134	5
-6	74	77	7
-5	6	9	24
-4	147	140	5
-3	85	70	6
-2	28	4	12
-1	79	81	6
0	256	256	4
1	216	215	4
2	51	14	7
3	272	283	4
4	266	251	4
5	25	35	12
6	118	109	5
7	23	11	14
8	38	25	10
9	-27	4	12
10	44	38	9
11	89	90	6
12	261	248	5
13	234	228	5

9 4 1

-7	44	45	9
-6	111	125	6
-5	-19	9	16
-4	81	77	6
-3	206	198	4
-2	21	7	15
-1	148	133	4
0	141	100	4
1	58	12	7
2	133	139	4
3	82	62	5
4	281	287	4
5	53	43	7
6	153	153	4
7	280	284	4
8	104	99	5
9	11	26	20
10	288	298	5
11	83	88	6
12	55	38	8
13	173	165	5

9 5 1

-7	88	104	6
-6	79	68	7
-5	95	87	6
-4	179	183	5
-3	280	281	4
-2	42	28	9

-1	207	209	4
0	157	164	4
1	128	114	4
2	338	339	4
3	42	6	8
4	78	75	5
5	131	141	4
6	-19	28	14
7	106	123	5
8	32	0	11
9	330	326	5
10	-26	35	13
11	189	176	5
12	67	63	7
13	139	133	5

9 6 1

-7	46	45	8
-6	-37	4	10
-5	39	21	10
-4	156	154	5
-3	83	73	6
-2	266	268	4
-1	104	86	5
0	39	45	9
1	57	58	6
2	77	76	5
3	91	91	5
4	134	127	4
5	150	149	4
6	200	182	4
7	364	361	5
8	553	555	6
9	191	186	4
10	213	211	5
11	48	44	9
12	158	166	5

9 7 1

-7	84	80	7
-6	29	37	13
-5	194	187	5
-4	63	72	7
-3	264	274	4
-2	59	34	6
-1	310	301	4
0	113	109	5
1	114	98	4
2	17	4	15
3	114	123	4
4	66	72	6
5	29	30	11
6	105	85	5
7	159	160	4
8	67	72	7
9	290	285	5
10	105	115	5
11	63	57	8
12	56	9	8

9 8 1

-6	13	9	20
-5	58	32	8
-4	51	51	8
-3	46	25	8
-2	72	38	6
-1	178	181	4
0	66	58	6
1	262	274	4
2	214	220	4
3	43	19	8
4	19	1	14
5	16	7	15
6	48	43	8
7	196	198	4
8	275	279	4
9	52	32	8
10	141	151	5
11	-24	31	14
12	90	85	6

9 9 1

-6	55	65	7
-5	57	51	8
-4	40	36	8
-3	116	130	5
-2	302	309	4
-1	37	30	9
0	16	10	16
1	107	106	5
2	97	97	5
3	487	487	5
4	230	232	4
5	179	173	4
6	54	44	7
7	100	72	5
8	291	283	5
9	260	265	5
10	121	127	5
11	206	194	5

9 10 1

-5	-30	3	11
-4	86	102	6
-3	78	74	6
-2	21	5	13
-1	122	117	5
0	30	28	9
1	206	211	4
2	195	183	4
3	490	501	5
4	149	123	4
5	287	303	4
6	95	100	5
7	82	97	6
8	22	9	14
9	-1	33	28
10	178	170	5

9 11 1

-5	134	131	5
-4	123	127	5
-3	292	295	5
-2	313	300	5
-1	-31	15	10
0	271	270	4
1	164	163	4
2	227	214	4
3	48	68	8
4	242	254	4
5	316	318	5
6	289	289	5
7	66	62	6
8	132	138	5
9	19	0	16

9 12 1

-3	48	46	9
-2	62	41	7
-1	170	171	5
0	58	50	7
1	151	148	5
2	84	90	6
3	21	28	12
4	49	61	8
5	-28	25	9
6	24	2	14
7	103	110	5
8	117	120	5

9 13 1

-2	61	64	8
-1	174	173	5
0	172	165	5
1	75	71	6
2	27	18	13
3	85	86	6
4	-21	33	13
5	152	165	5
6	199	202	5

9 14 1

2	28	9	13
3	64	59	7

10 -4 1

2	-36	8	9
3	66	51	7
4	52	70	8
5	61	50	7
6	55	37	7

10 -3 1

0	-9	36	21
1	45	43	8
2	56	66	8
3	128	112	5
4	134	131	5
5	116	121	5
6	86	111	6
7	33	41	11
8	54	13	7

10 -2 1

0	-21	27	14
1	12	31	19
2	27	9	12
3	54	27	8
4	146	131	5
5	219	219	4
6	44	30	9
7	116	112	5
8	120	128	5
9	94	87	6

10 -1 1

0	46	3	9
1	117	138	5
2	177	174	4
3	94	69	5
4	31	15	11
5	43	21	9
6	29	12	12
7	131	141	5
8	78	76	6
9	26	19	14
10	-40	5	9

10 0 1

-4	60	31	8
-3	38	64	11
-2	33	39	11
-1	51	19	8
0	89	54	5
1	168	181	4
2	63	62	7
3	76	57	6
4	55	54	7
5	104	93	5
6	128	138	5
7	292	286	5
8	106	106	5
9	82	72	6
10	163	164	5
11	82	81	6

10 1 1

-4	94	107	6
-3	76	52	6
-2	72	74	6
-1	218	235	4
0	286	292	4
1	335	348	5
2	183	186	4
3	72	86	6
4	71	71	5
5	90	73	5
6	53	51	8
7	208	204	4
8	67	72	7
9	38	53	10
10	219	216	5
11	70	56	6

10 2 1

-5	51	46	9
-4	168	146	5
-3	61	38	7
-2	160	162	5
-1	121	116	5
0	62	48	7
1	163	151	4
2	286	286	4
3	310	305	4
4	84	81	5
5	40	28	9
6	204	205	4
7	105	91	5
8	84	78	6
9	147	137	5
10	39	25	11
11	85	80	6

10 3 1

-5	100	85	6
-4	58	53	8
-3	118	101	5
-2	80	81	6
-1	29	7	12
0	187	175	4
1	313	312	4
2	133	107	4
3	118	129	5
4	90	85	5
5	207	220	4
6	57	57	7
7	153	160	5
8	110	108	5
9	-6	18	24
10	181	188	5
11	55	56	9
12	-15	38	19

10 4 1

-5	58	62	8
-4	118	135	5
-3	90	88	6
-2	42	15	10
-1	72	72	7
0	49	48	8
1	191	186	4
2	138	114	4
3	305	300	5
4	148	140	5

5	87	76	6
6	122	125	5
7	137	111	5
8	84	83	6
9	96	100	6
10	-20	14	15
11	188	196	5
12	75	87	7

10	5	1

-5	73	99	7
-4	-31	6	12
-3	21	9	16
-2	193	157	5
-1	35	33	11
0	94	101	5
1	47	37	8
2	51	41	7
3	101	78	5
4	175	161	4
5	72	65	6
6	312	309	5
7	186	182	5
8	186	191	5
9	84	88	6
10	196	197	5
11	29	42	13

10	6	1

-5	26	52	13
-4	106	115	6
-3	91	75	6
-2	55	44	7
-1	90	89	6
0	128	129	5
1	239	256	4
2	32	31	10
3	259	250	4
4	258	254	4
5	48	5	8
6	233	226	4
7	120	120	5
8	90	96	6
9	145	152	5
10	9	13	22
11	258	256	5

10	7	1

-5	25	32	14
-4	38	43	11
-3	121	114	5
-2	277	279	5
-1	115	110	5
0	119	114	5
1	114	111	5
2	288	279	4
3	175	165	4
4	58	10	7
5	346	351	5
6	85	84	6
7	61	10	7
8	286	291	5
9	-16	29	17
10	39	39	11
11	230	224	5

10	8	1

-5	69	66	6
-4	56	13	8
-3	36	2	11
-2	59	51	7
-1	68	36	6
0	142	154	5
1	110	92	5

2	70	60	5
3	350	356	5
4	165	154	4
5	221	228	4
6	144	135	5
7	110	108	5
8	47	48	7
9	-18	16	16
10	-18	12	17

10	9	1

-4	111	126	5
-3	40	22	10
-2	90	84	6
-1	90	77	6
0	46	5	8
1	112	122	5
2	329	330	5
3	60	47	6
4	42	13	9
5	127	127	5
6	68	73	7
7	47	47	9
8	202	200	5
9	143	153	5
10	78	70	7

10	10	1

-3	80	85	6
-2	106	101	5
-1	226	226	4
0	42	38	9
1	80	105	6
2	117	115	5
3	82	83	6
4	248	253	4
5	76	85	6
6	55	41	8
7	483	454	6
8	97	90	6
9	189	186	5

10	11	1

-2	88	66	6
-1	-20	11	13
0	70	47	7
1	172	169	5
2	193	198	5
3	10	8	20
4	-6	18	23
5	50	51	8
6	236	238	5
7	163	161	5
8	203	196	5

10	12	1

-1	44	47	9
0	244	256	5
1	36	17	11
2	135	123	5
3	109	91	5
4	-20	15	13
5	64	66	7
6	103	102	6

11	-1	1

1	65	51	7
2	117	120	5
3	78	72	6
4	240	255	5
5	72	79	7
6	73	75	7
7	76	36	7

11	0	1	

0	43	11	8
1	32	47	10
2	72	62	7
3	54	63	7
4	165	158	5
5	26	40	13
6	135	123	5
7	56	45	8
8	122	112	5

11	1	1

-1	84	83	6
0	89	17	6
1	54	44	8
2	62	43	7
3	87	89	6
4	194	189	5
5	40	16	10
6	96	93	6
7	37	12	10
8	104	96	6
9	45	28	10

11	2	1

-2	119	111	5
-1	46	43	9
0	36	35	11
1	-21	0	14
2	142	116	5
3	96	78	5
4	47	36	9
5	37	30	10
6	64	79	7
7	-12	44	20
8	30	24	12
9	100	84	6

11	3	1

-2	60	49	7
-1	27	30	13
0	32	1	12
1	186	169	5
2	90	86	6
3	112	119	5
4	72	55	6
5	-18	1	16
6	107	101	5
7	116	116	5
8	208	205	5
9	42	23	9
10	25	26	15

11	4	1

-3	204	216	5
-2	230	231	5
-1	193	191	5
0	81	76	7
1	155	150	5
2	55	43	8
3	61	43	7
4	154	154	5
5	78	89	7
6	35	41	10
7	56	85	8
8	-16	4	18
9	131	137	5
10	69	53	8

11	5	1	

-3	88	62	7

-2	52	60	9
-1	34	38	12
0	88	79	6
1	43	20	8
2	149	158	5
3	71	59	7
4	76	49	6
5	64	38	7
6	154	135	5
7	103	98	6
8	106	106	6
9	124	122	6
10	-23	25	15

11	6	1

-3	117	122	6
-2	160	149	5
-1	74	87	7
0	37	37	9
1	33	35	11
2	64	55	7
3	103	77	5
4	64	41	7
5	101	98	5
6	347	357	5
7	72	71	7
8	32	31	12
9	77	89	7

11	7	1

-2	42	29	9
-1	36	37	11
0	21	57	13
1	30	27	12
2	34	24	11
3	61	31	7
4	119	124	5
5	58	42	8
6	157	143	5
7	56	31	7
8	46	54	10
9	-10	27	21

11	8	1

-2	110	85	6
-1	47	42	8
0	82	88	6
1	72	86	7
2	78	70	6
3	240	243	4
4	68	66	6
5	175	171	5
6	41	51	10
7	160	145	5
8	66	64	7

11	9	1

-1	-14	14	18
0	157	137	5
1	51	66	8
2	106	102	5
3	-24	7	13
4	-3	8	26
5	77	70	6
6	61	23	7
7	68	30	7
8	92	99	6

11	10	1

0	86	98	6
1	59	56	8
2	-6	27	24
3	20	0	13

4	20	5	15
5	130	132	5
6	49	21	9
11	11	1	
2	138	132	5
3	25	10	14
4	30	42	12
12	3	1	

3	44	41	9
4	94	91	6
5	39	1	10
12	4	1	
2	68	82	7
3	59	14	7
4	50	51	8
5	29	29	13
6	13	5	17

12	5	1	
2	25	17	15
3	83	90	7
4	39	19	12
5	182	185	5
6	110	118	6
12	6	1	
2	62	53	7
3	180	163	5

4	222	228	5
5	139	125	5
6	-6	3	25
12	7	1	
3	152	154	5
4	108	93	6
5	86	74	6

Table 1. Final Heavy Atom Parameters for Tetrakis(pentafluorophenyl)octachloroporphinato Zinc(II) · 6($C_6H_4Cl_2$).

x, y, z and $U_{eq}{}^a \times 10^4$

Atom	x	y	z	U_{eq} or B	Pop†
Zn	0	0	0	291(4)	
N	1015(4)	231(4)	95(9)	268(20)	
C1	2135(5)	108(6)	626(10)	286(26)	
C2	1542(5)	−246(5)	180(10)	297(26)	
C3	1475(5)	−943(5)	−120(11)	264(25)	
C4	1296(6)	861(6)	338(10)	287(28)	
C5	1989(6)	776(6)	720(10)	326(28)	
Cl1	2909(2)	−235(2)	1075(3)	484(8)	
Cl2	2544(2)	1359(2)	1352(3)	506(9)	
C6	2123(5)	−1340(6)	−259(11)	325(30)	
C7	2322(6)	−1829(6)	564(11)	346(29)	
F7	1935(4)	−1938(4)	1575(7)	547(20)	
C8	2900(7)	−2243(7)	393(14)	524(39)	
F8	3050(4)	−2723(4)	1207(8)	714(24)	
C9	3288(7)	−2138(8)	−611(14)	513(39)	
F9	3850(4)	−2525(5)	−810(8)	767(27)	
C10	3140(6)	−1612(7)	−1458(14)	533(41)	
F10	3529(4)	−1512(5)	−2431(8)	743(25)	
C11	2554(6)	−1232(5)	−1240(12)	329(28)	
F11	2406(4)	−770(4)	−2088(7)	549(20)	

Table 1. (Cont.)

Atom	x	y	z	U_{eq} or	B	Pop†
Cl3	4428(9)	6030(8)	1705(11)	1957(66)		0.50
Cl4	3904(6)	4528(8)	1753(12)	1411(45)		0.50
Cl5	5339(3)	910(4)	74(9)	2172(35)		
Cl6	4712(11)	1149(11)	2927(13)	2586(92)		0.47
Cl7	4300(10)	2220(11)	−277(23)	3762(115)		0.53
C31	4769	1516	620	1226		0.47
C32	4520	1628	1741	1229		0.47
C33	4060	2202	1935	1230		0.47
C34	3895	2612	964	1226		0.47
C35	4159	2490	−201	1229		0.47
C36	4608	1930	−396	1230		0.47
C41	4845	1295	1233	1225		0.53
C42	4449	1874	964	1229		0.53
C43	4104	2128	2010	1230		0.53
C44	4173	1816	3130	1225		0.53
C45	4602	1219	3265	1229		0.53
C46	4933	976	2264	1230		0.53
C14	5068	5371	1677	3.5	*	0.75
C15	4797	4709	1695	3.5	*	0.75
C16	5239	4163	1670	3.5	*	0.75

Table 1. (Cont.)

Atom	x	y	z	U_{eq} or$B$		Pop†
C17	5961	4262	1626	3.5	*	0.75
C18	6215	4923	1609	3.5	*	0.75
C19	5773	5469	1634	3.5	*	0.75
C21	4657	5072	1727	3.5	*	0.25
C22	4555	5782	1716	3.5	*	0.25
C23	5106	6237	1726	3.5	*	0.25
C24	5775	5977	1746	3.5	*	0.25
C25	5863	5255	1756	3.5	*	0.25
C26	5311	4818	1746	3.5	*	0.25

[a] $U_{eq} = \frac{1}{3}\sum_i \sum_j [U_{ij}(a_i^* a_j^*)(\vec{a}_i \cdot \vec{a}_j)]$

* Isotropic displacement parameter, B

† Population Parameter, if different from 1.0

Table 2. Anisotropic Displacement Parameters for Tetrakis(pentafluorophenyl)octachloroporphinato Zinc(II) · 6($C_6H_4Cl_2$).

Atom	U_{11}	U_{22}	U_{33}	U_{12}	U_{13}	U_{23}
Zn	246(8)	246(8)	381(15)	0	0	0
N	262(45)	193(44)	348(55)	−13(38)	−37(47)	31(47)
C1	265(59)	302(70)	290(62)	30(52)	−71(51)	−5(53)
C2	214(54)	337(62)	341(72)	12(47)	82(54)	104(56)
C3	299(61)	255(59)	239(64)	55(49)	52(58)	46(55)
C4	337(68)	274(64)	251(71)	−58(52)	−36(51)	−9(51)
C5	317(68)	269(63)	393(72)	−40(56)	−23(58)	−8(56)
Cl1	325(17)	409(18)	719(23)	64(14)	−208(17)	−66(17)
Cl2	378(18)	370(18)	769(25)	10(15)	−259(19)	−79(18)
C6	181(55)	290(61)	503(85)	31(48)	30(57)	−65(59)
C7	336(69)	372(70)	329(71)	42(58)	−33(58)	−11(59)
F7	509(48)	603(51)	529(45)	31(38)	27(41)	112(41)
C8	469(86)	385(80)	718(113)	121(71)	−235(82)	−134(74)
F8	797(59)	461(48)	885(65)	288(45)	−309(53)	66(47)
C9	315(74)	569(97)	654(99)	161(72)	−90(74)	−204(84)
F9	407(46)	766(60)	1128(75)	328(45)	−143(46)	−271(57)
C10	272(71)	624(94)	702(109)	−27(69)	196(75)	−262(88)
F10	529(52)	879(64)	822(59)	−3(45)	305(50)	−253(54)
C11	272(63)	260(63)	455(74)	−66(53)	−46(63)	−31(60)
F11	586(50)	543(48)	519(48)	−5(43)	156(41)	18(42)
Cl3	3244(222)	1771(143)	855(85)	799(149)	664(122)	−94(89)
Cl4	901(81)	2158(150)	1174(90)	−365(93)	261(71)	−130(98)
Cl5	1313(57)	1979(76)	3224(114)	−271(55)	510(69)	−1399(84)
Cl6	3216(276)	3402(265)	1139(111)	−2200(230)	−667(138)	947(142)
Cl7	2496(199)	3595(275)	5194(352)	−1801(195)	−2386(228)	3455(273)
C31	1002	925	1751	260	5	−205
C32	1368	1214	1105	−116	−302	437
C33	1272	1561	857	−193	286	−264
C34	1002	925	1751	260	5	−205
C35	1368	1214	1105	−116	−302	437
C36	1272	1561	857	−193	286	−264

Table 2. (Cont.)

Atom	U_{11}	U_{22}	U_{33}	U_{12}	U_{13}	U_{23}
C41	1156	1426	1093	−67	334	−410
C42	1426	1368	893	−222	−200	377
C43	1060	867	1763	250	−162	16
C44	1156	1426	1093	−67	334	−410
C45	1426	1368	893	−222	−200	377
C46	1060	867	1763	250	−162	16

$U_{i,j}$ values have been multiplied by 10^4

The form of the displacement factor is:

$$\exp -2\pi^2(U_{11}h^2a^{*^2} + U_{22}k^2b^{*^2} + U_{33}\ell^2c^{*^2} + 2U_{12}hka^*b^* + 2U_{13}h\ell a^*c^* + 2U_{23}k\ell b^*c^*)$$

Table 3. Complete Distances and Angles for Tetrakis(pentafluorophenyl)octachloroporphinato Zinc(II) · 6($C_6H_4Cl_2$).

	Distance(Å)		Distance(Å)
Zn –N	2.032	C23 –C24	1.401
N –C2	1.390(13)	C24 –C25	1.419
N –C4	1.371(14)	C25 –C26	1.373
C1 –C2	1.431(15)	Cl5 –C31	1.728
C1 –C5	1.337(15)	Cl5 –C41	1.758
C1 –Cl1	1.722(11)	Cl6 –C32	1.640
C2 –C3	1.405(15)	Cl7 –C42	1.541
C3 –C6	1.490(15)	C31 –C32	1.334
C3 –C4	1.401(16)	C31 –C36	1.407
C4 –C5	1.423(16)	C32 –C33	1.449
C5 –Cl2	1.716(12)	C33 –C34	1.367
C6 –C7	1.365(16)	C34 –C35	1.393
C6 –C11	1.378(16)	C35 –C36	1.416
C7 –F7	1.354(14)	C41 –C42	1.399
C7 –C8	1.399(18)	C41 –C46	1.297
C8 –F8	1.324(16)	C42 –C43	1.415
C8 –C9	1.35(2)	C43 –C44	1.372
C9 –F9	1.349(17)	C44 –C45	1.441
C9 –C10	1.41(2)	C45 –C46	1.355
C10 –F10	1.320(16)		
C10 –C11	1.381(18)		
C11 –F11	1.324(14)		
Cl3 –C14	1.792		
Cl3 –C26	1.732		
Cl4 –C15	1.779		
Cl4 –C21	1.813		
C14 –C15	1.395		
C14 –C19	1.389		
C15 –C16	1.370		
C16 –C17	1.422		
C17 –C18	1.381		
C18 –C19	1.370		
C21 –C22	1.398		
C21 –C26	1.368		
C22 –C23	1.394		

Table 3. (Cont.)

	Angle(°)		Angle(°)
N –Zn –N	90.2	C10 –C11 –C6	123.8(11)
N –Zn –N	174.1	F11 –C11 –C6	121.0(10)
Zn –N –C2	125.2	F11 –C11 –C10	115.2(11)
Zn –N –C4	42.4	C15 –C14 –Cl3	113.5
C4 –N –C2	106.9(8)	C19 –C14 –Cl3	126.2
C5 –C1 –C2	108.8(10)	C19 –C14 –C15	120.2
Cl1 –C1 –C2	128.2(8)	C14 –C15 –Cl4	123.8
Cl1 –C1 –C5	122.9(9)	C16 –C15 –Cl4	117.5
C1 –C2 –N	107.4(9)	C16 –C15 –C14	118.7
C3 –C2 –N	124.2(9)	C17 –C16 –C15	121.2
C3 –C2 –C1	128.4(10)	C18 –C17 –C16	118.8
C6 –C3 –C2	116.5(9)	C19 –C18 –C17	120.0
C4 –C3 –C2	126.5(10)	C18 –C19 –C14	121.1
C4 –C3 –C6	116.9(10)	C22 –C21 –Cl4	117.6
C3 –C4 –N	122.4(10)	C26 –C21 –Cl4	122.9
C5 –C4 –N	109.4(9)	C26 –C21 –C22	119.5
C5 –C4 –C3	128.0(10)	C23 –C22 –C21	121.3
C4 –C5 –C1	107.1(10)	C24 –C23 –C22	119.1
Cl2 –C5 –C1	122.9(9)	C25 –C24 –C23	118.3
Cl2 –C5 –C4	129.7(9)	C26 –C25 –C24	121.3
C7 –C6 –C3	122.5(10)	C21 –C26 –Cl3	128.3
C11 –C6 –C3	121.2(10)	C25 –C26 –Cl3	111.2
C11 –C6 –C7	116.4(11)	C25 –C26 –C21	120.4
F7 –C7 –C6	119.2(10)	C32 –C31 –Cl5	131.5
C8 –C7 –C6	123.0(11)	C36 –C31 –Cl5	105.3
C8 –C7 –F7	117.8(11)	C36 –C31 –C32	123.2
F8 –C8 –C7	119.8(12)	C31 –C32 –Cl6	123.2
C9 –C8 –C7	118.2(13)	C33 –C32 –Cl6	117.8
C9 –C8 –F8	121.9(13)	C33 –C32 –C31	119.1
F9 –C9 –C8	120.1(13)	C34 –C33 –C32	119.0
C10 –C9 –C8	121.9(13)	C35 –C34 –C33	121.4
C10 –C9 –F9	118.0(12)	C36 –C35 –C34	119.8
F10 –C10 –C9	121.1(12)	C35 –C36 –C31	117.5
C11 –C10 –C9	116.5(12)	C42 –C41 –Cl5	119.7
C11 –C10 –F10	122.3(12)	C46 –C41 –Cl5	110.3

Table 3. (Cont.)

	Angle(°)
C46 –C41 –C42	129.9
C41 –C42 –Cl7	129.9
C43 –C42 –Cl7	117.8
C43 –C42 –C41	112.1
C44 –C43 –C42	121.2
C45 –C44 –C43	120.4
C46 –C45 –C44	118.5
C45 –C46 –C41	118.0

Table 4. Intermolecular Distances Less Than 3.5 Å for Tetrakis(pentafluorophenyl)octachloroporphinato Zinc(II) · 6($C_6H_4Cl_2$).

	Distance(Å)		Distance(Å)
C2 –Cl4	3.487(17)	C24 –C34	2.952
C4 –C17	3.387		
Cl1 –F10	3.122(9)		
Cl2 –C33	3.441		
Cl2 –C43	3.467		
Cl2 –F8	3.413(9)		
C7 –F10	3.234(15)		
F7 –C24	3.463		
F7 –C33	3.038		
F7 –C34	3.257		
F7 –C43	3.133		
F7 –C44	3.268		
F7 –F9	3.408(11)		
F7 –F10	3.344(11)		
C8 –F10	3.038(16)		
F8 –C34	3.401		
F8 –C35	3.199		
F8 –C10	3.125(16)		
F8 –F10	2.985(12)		
F8 –C11	3.165(14)		
F8 –F11	2.970(11)		
F9 –C24	3.485		
F9 –Cl4	3.168(15)		
F9 –C36	3.254		
F10 –C46	3.244		
F11 –Cl6	3.49(2)		
F11 –C32	3.336		
F11 –C44	3.473		
F11 –Cl3	3.014(17)		
F11 –C22	3.484		
F11 –C23	3.128		
C17 –C35	3.404		
C18 –C35	3.311		
C23 –C33	3.460		
C23 –C34	3.087		

Table 5. Observed and Calculated Structure Factors for Tetrakis(pentafluorophenyl)octachloroporphinato Zinc(II) · 6($C_6H_4Cl_2$).

The columns contain, in order, h, $10F_{obs}$, $10F_{calc}$ and $10\sigma F_{obs}$. A minus sign preceding F_{obs} indicates that F^2_{obs} is negative.

h	0	0	
2	221	238	5
4	1480	1421	13
6	504	483	8
8	1446	1447	14
10	845	796	11
12	46	65	31
14	197	298	14
16	-115	48	17
18	487	566	13
20	237	146	14
22	94	102	27

h	1	0	
1	935	921	10
2	749	904	7
3	1185	1178	11
4	1176	986	11
5	506	423	7
6	366	422	7
7	380	446	8
8	714	754	9
9	822	768	10
10	71	55	22
11	481	618	10
12	712	783	11
13	231	315	12
14	245	203	13
15	192	155	15
16	-88	2	23
17	360	249	13
18	88	110	29
19	121	64	20
20	221	191	15
21	237	222	15
22	141	137	21
23	25	91	56

h	2	0	
2	830	891	10
3	464	452	6
4	659	625	7
5	437	456	7
6	244	290	8
7	-54	31	21
8	591	611	9
9	276	254	9
10	573	637	9
11	48	67	29
12	344	317	10
13	-65	97	25
14	110	189	21
15	593	652	12
16	141	176	19
17	232	123	15
18	546	505	13
19	117	171	21
20	629	582	12
21	67	11	33
22	102	70	26
23	-85	2	28

h	3	0	
3	1291	1299	14
4	1344	1356	12
5	359	373	7
6	431	208	8
7	1796	1826	16
8	-100	197	16
9	140	196	13
10	-33	36	34
11	-53	39	26
12	481	459	10
13	445	457	11
14	372	365	12
15	176	189	16
16	157	141	18
17	341	323	13
18	274	273	15
19	240	163	14
20	181	153	17
21	174	160	18
22	-30	40	50

h	4	0	
4	2581	2483	26
5	670	620	8
6	665	753	9
7	600	625	9
8	75	80	20
9	104	172	16
10	1814	1844	17
11	133	227	15
12	591	598	11
13	56	30	31
14	805	822	12
15	258	226	14
16	102	148	24
17	-37	111	45
18	450	433	13
19	314	241	12
20	-56	133	35
21	135	113	21
22	213	203	16

h	5	0	
5	1191	1145	15
6	1467	1486	14
7	460	453	9
8	1066	1029	12
9	494	501	9
10	156	116	13
11	509	469	10
12	363	374	11
13	199	236	14
14	128	165	19
15	345	337	12
16	-28	183	48
17	603	567	13
18	64	25	36
19	124	83	21
20	156	160	19
21	479	413	12
22	214	180	16

h	6	0	
6	570	647	12
7	-69	11	19
8	112	109	16
9	367	280	10
10	640	638	10
11	350	301	11
12	493	473	11
13	421	414	11
14	402	342	12
15	238	244	14
16	207	206	16
17	44	76	44
18	384	368	12
19	231	211	14
20	369	366	13
21	131	122	22
22	-109	13	22

h	7	0	
7	431	553	13
8	90	29	18
9	292	356	10
10	315	308	11
11	336	330	11
12	26	63	45
13	142	193	18
14	143	121	19
15	211	188	15
16	564	480	13
17	-106	16	22
18	285	315	13
19	217	252	15
20	97	43	26
21	183	160	18
22	-43	26	44

h	8	0	
8	1230	1226	17
9	972	949	12
10	38	41	36
11	20	86	48
12	261	279	13
13	943	904	13
14	252	221	14
15	21	31	55
16	454	398	13
17	-35	4	42
18	-30	40	47
19	57	100	36
20	293	284	14
21	92	24	28

h	9	0	
9	107	22	26
10	291	238	12
11	419	309	11
12	-98	41	20
13	352	301	12
14	53	47	36
15	484	503	13
16	-82	132	28
17	193	199	15
18	166	141	18
19	225	204	15
20	206	178	16
21	198	152	17

h	10	0	
10	425	438	16
11	478	509	11
12	145	139	18
13	150	121	19
14	214	205	16
15	447	477	13
16	-41	54	39
17	101	90	24
18	211	189	15
19	-90	98	25
20	-116	12	20

h	11	0	
11	145	251	26
12	-38	84	42
13	477	319	12
14	127	105	22
15	144	115	21
16	-54	87	34
17	103	177	24
18	126	110	22
19	-57	65	36
20	-31	11	51

h	12	0	
12	233	195	21
13	-69	98	31
14	377	325	14
15	50	115	36
16	276	291	13
17	249	255	14
18	210	175	16
19	120	114	24

h	13	0	
13	186	40	25
14	144	187	18
15	107	133	23
16	180	177	17
17	131	103	21
18	10	104	65
19	144	183	21

h	14	0	
14	-97	10	30
15	-77	61	28
16	124	56	22
17	140	105	21
18	-93	18	25

h	15	0	
15	461	424	17
16	292	288	14
17	-64	34	34

h	16	0	
16	412	433	18

h	0	1	
1	1588	1641	12
2	48	41	13
3	1174	1085	9
4	581	561	6
5	531	534	6
6	496	500	6
7	1182	1156	10
8	485	495	6
9	692	687	7
10	404	399	7
11	499	494	7
12	72	92	17
13	686	644	8
14	-60	48	22
15	496	440	8
16	-84	35	17
17	291	248	10
18	121	107	17
19	131	90	14
20	213	227	11
21	121	153	16
22	193	221	12
23	148	126	15

h	1	1	
2	379	384	4
3	880	808	7
4	1079	1050	9
5	1051	968	9
6	1281	1289	10
7	538	591	6
8	475	491	6
9	233	212	7
10	593	513	7
11	320	257	7
12	692	715	8
13	445	425	8
14	433	428	8
15	-39	44	30

16	193	217	11
17	-78	30	20
18	-79	58	21
19	30	70	36
20	350	358	9
21	-91	22	18
22	157	170	14
23	40	44	36

h 2 1

3	384	361	5
4	828	771	7
5	1293	1233	10
6	1003	904	9
7	545	502	6
8	470	425	6
9	604	601	7
10	135	144	10
11	731	759	8
12	578	545	8
13	595	561	8
14	476	396	8
15	-33	60	33
16	107	139	17
17	501	506	9
18	141	60	15
19	493	499	8
20	119	90	16
21	242	240	10
22	-61	19	26
23	-66	54	34

h 3 1

4	1038	1041	9
5	1346	1350	11
6	776	811	7
7	1048	1112	9
8	640	596	7
9	411	411	7
10	411	379	7
11	107	122	12
12	525	441	8
13	220	233	9
14	607	630	8
15	371	375	9
16	138	152	14
17	239	271	11
18	502	513	9
19	-87	49	17
20	211	228	11
21	87	68	21
22	-51	23	30

h 4 1

5	603	551	6
6	1198	1138	10
7	1166	1138	10
8	824	881	8
9	206	301	8
10	782	756	8
11	-22	169	34
12	192	220	9
13	554	545	8
14	279	298	9
15	247	272	10
16	183	221	12
17	470	464	9
18	154	167	15
19	156	155	13
20	162	148	13
21	424	385	9
22	103	82	19

h 5 1

6	268	230	6
7	597	526	7
8	347	370	7
9	806	746	8
10	676	705	8
11	-19	16	36
12	529	564	8
13	59	112	23
14	479	509	8
15	148	125	13
16	470	461	9
17	-49	55	30
18	399	403	8
19	212	204	10
20	432	410	9
21	155	155	14
22	183	178	13

h 6 1

7	218	179	7
8	588	658	7
9	387	400	7
10	380	381	7
11	759	792	9
12	189	247	10
13	260	250	9
14	253	256	10
15	279	280	10
16	-64	18	24
17	187	213	13
18	148	210	13
19	462	464	8
20	-46	70	31
21	131	162	16
22	-64	83	26

h 7 1

8	802	763	8
9	462	468	7
10	642	577	8
11	438	440	8
12	302	305	8
13	183	215	11
14	306	237	9
15	152	178	13
16	263	300	10
17	167	192	14
18	193	219	11
19	-87	39	18
20	240	249	10
21	140	105	15
22	-76	53	31

h 8 1

9	-36	98	27
10	234	283	9
11	415	462	8
12	436	459	8
13	321	323	9
14	279	273	10
15	471	451	9
16	213	236	12
17	78	82	20
18	-80	45	19
19	222	276	11
20	139	131	15
21	129	146	16

h 9 1

10	598	572	8
11	392	403	8
12	401	387	8
13	681	698	9
14	495	527	9
15	247	241	11
16	434	396	10
17	54	56	26
18	318	288	9
19	71	71	24
20	260	226	10
21	78	69	24

h 10 1

11	308	372	9
12	254	271	10
13	334	348	9
14	206	186	12
15	165	151	14
16	70	81	22
17	245	231	10
18	150	160	14
19	-5	78	57
20	88	110	21

h 11 1

12	141	137	14
13	65	101	25
14	205	301	12
15	113	171	18
16	194	221	11
17	-63	44	24
18	217	206	11
19	62	73	27
20	193	168	13

h 12 1

13	370	362	10
14	120	160	17
15	359	316	8
16	126	158	15
17	239	254	10
18	95	96	20
19	211	186	12

h 13 1

14	-53	106	25
15	146	123	13
16	173	182	12
17	126	176	16
18	142	143	15
19	140	120	16

h 14 1

15	201	217	11
16	226	251	11
17	79	35	23
18	107	122	19

h 15 1

16	401	398	9
17	171	120	13

h 0 2

0	2468	2461	17
1	848	810	7
2	74	32	11
3	641	555	6
4	1238	1198	10
5	733	762	7
6	337	297	6
7	158	149	8
8	562	501	7
9	316	350	7
10	846	868	8
11	99	98	13
12	47	23	24
13	-79	39	16
14	332	303	8
15	252	232	10
16	107	142	17
17	449	457	9
18	181	201	13
19	159	141	12
20	-9	47	52
21	-90	57	18
22	97	94	20

h 1 2

1	1160	1091	11
2	493	518	5
3	951	913	8
4	772	739	7
5	720	758	7
6	162	152	7
7	1957	1983	16
8	323	304	6
9	1034	966	9
10	462	470	7
11	885	814	9
12	641	603	8
13	550	551	8
14	341	356	8
15	442	440	9
16	214	240	11
17	226	246	11
18	-66	67	25
19	285	286	9
20	85	85	20
21	180	174	12
22	122	140	17

h 2 2

2	115	222	11
3	499	541	5
4	975	972	8
5	1246	1329	10
6	575	578	6
7	791	832	8
8	125	164	10
9	188	151	8
10	334	323	7
11	221	250	8
12	390	350	8
13	177	123	10
14	494	470	8
15	212	184	11
16	263	256	10
17	210	231	12
18	161	198	14
19	331	333	9
20	413	428	9
21	138	138	15
22	174	183	13

h 3 2

3	2365	2372	21
4	1316	1274	11
5	1676	1624	13
6	564	468	6
7	422	366	6
8	1195	1216	10
9	360	355	7
10	535	476	7
11	343	378	7
12	272	277	8
13	589	602	8
14	409	380	8
15	328	320	9
16	185	169	12
17	394	393	9

18	86	110	22
19	386	369	8
20	105	94	18
21	157	170	14
22	-69	36	24

h 4 2

4	1785	1774	16
5	1106	1040	9
6	1360	1250	11
7	883	843	8
8	633	670	7
9	498	480	7
10	230	257	8
11	28	120	31
12	345	360	8
13	166	163	11
14	540	509	8
15	340	371	9
16	330	344	9
17	317	303	10
18	370	389	8
19	219	191	10
20	324	330	9
21	19	40	46
22	92	108	21

h 5 2

5	1236	1130	12
6	481	498	6
7	523	601	7
8	414	463	7
9	422	386	7
10	399	352	7
11	310	303	8
12	346	300	8
13	530	549	8
14	194	149	11
15	41	75	31
16	368	384	9
17	365	380	10
18	101	93	17
19	255	253	10
20	156	112	13
21	356	318	9
22	24	79	44

h 6 2

6	435	459	9
7	314	223	7
8	252	252	7
9	234	248	8
10	878	857	9
11	145	188	11
12	497	494	8
13	116	132	15
14	473	440	9
15	316	242	9
16	242	214	11
17	-55	96	28
18	275	286	9
19	171	187	12
20	183	192	12
21	187	193	12
22	113	137	18

h 7 2

7	942	715	11
8	656	589	8
9	633	607	8
10	145	117	11
11	344	331	8
12	389	410	8
13	473	532	8

14	206	211	11
15	96	96	19
16	233	243	11
17	260	272	10
18	164	126	12
19	268	284	10
20	284	260	10
21	145	128	15

h 8 2

8	757	726	11
9	366	297	8
10	661	702	8
11	346	389	8
12	331	315	9
13	332	374	9
14	325	325	9
15	311	364	10
16	114	137	18
17	92	96	18
18	329	341	9
19	23	77	43
20	267	260	10
21	180	196	13

h 9 2

9	1043	959	13
10	43	85	28
11	452	398	8
12	449	458	9
13	323	336	9
14	184	176	12
15	284	340	10
16	160	210	14
17	386	386	8
18	75	69	22
19	134	180	15
20	100	110	19
21	125	153	19

h 10 2

10	395	328	12
11	346	357	9
12	215	275	11
13	234	243	11
14	414	435	9
15	99	89	20
16	282	255	9
17	116	116	16
18	174	183	12
19	81	74	22
20	262	216	11

h 11 2

11	753	725	12
12	173	188	12
13	523	520	9
14	-51	67	30
15	253	296	9
16	-49	18	28
17	225	222	11
18	178	150	12
19	94	124	20
20	47	33	33

h 12 2

12	64	66	34
13	79	95	23
14	51	147	27
15	171	149	12
16	250	246	10
17	107	97	18
18	155	180	14

19	88	79	22

h 13 2

13	105	201	24
14	122	116	15
15	289	297	9
16	-91	46	18
17	-51	79	29
18	115	107	18

h 14 2

14	338	329	12
15	343	307	9
16	208	205	11
17	114	129	18
18	148	170	15

h 15 2

15	292	324	14
16	73	108	24
17	38	81	37

h 16 2

16	262	262	15

h 0 3

1	2683	2563	21
2	2509	2369	18
3	290	311	6
4	449	476	6
5	25	80	26
6	590	612	7
7	124	98	10
8	-6	14	42
9	1406	1395	12
10	131	155	11
11	409	418	7
12	496	471	8
13	518	554	8
14	52	43	26
15	104	117	17
16	13	65	49
17	151	88	14
18	159	80	12
19	389	313	8
20	423	380	9
21	147	160	14
22	139	120	15

h 1 3

2	2875	2782	20
3	450	415	6
4	208	228	6
5	563	533	6
6	893	970	8
7	475	480	6
8	425	447	7
9	333	323	7
10	422	476	7
11	211	194	9
12	356	381	8
13	431	458	8
14	443	477	8
15	68	156	23
16	432	415	9
17	174	157	13
18	360	335	8
19	186	186	11
20	-45	48	31
21	180	181	12
22	158	173	14

h 2 3

3	440	423	6
4	379	415	6
5	235	246	6
6	168	207	8
7	505	482	7
8	492	563	7
9	611	613	7
10	379	374	8
11	460	437	7
12	179	238	10
13	195	243	10
14	213	179	10
15	396	418	9
16	281	257	10
17	132	162	16
18	122	90	14
19	242	182	10
20	119	138	16
21	-73	28	22
22	96	121	20

h 3 3

4	441	436	6
5	682	714	7
6	376	403	6
7	129	70	10
8	400	492	7
9	367	371	7
10	289	348	8
11	143	108	11
12	691	658	8
13	374	372	8
14	-70	95	20
15	39	68	32
16	633	622	9
17	166	231	14
18	186	177	11
19	183	135	12
20	466	398	9
21	-39	57	34
22	105	133	19

h 4 3

5	772	817	8
6	416	452	6
7	315	275	7
8	511	514	7
9	727	695	8
10	602	613	8
11	496	435	8
12	463	473	8
13	352	363	8
14	178	252	12
15	92	155	19
16	340	323	10
17	280	279	11
18	230	191	10
19	537	518	8
20	184	158	12
21	92	86	20
22	79	82	23

h 5 3

6	269	263	7
7	493	517	7
8	1156	1173	10
9	265	284	8
10	350	378	8
11	269	256	8
12	738	677	9
13	191	164	11
14	210	193	11
15	262	293	10

16	344	331	10
17	78	95	23
18	206	199	11
19	253	218	10
20	161	168	13
21	-91	4	18
22	74	89	45

h 6 3

7	375	408	7
8	352	377	7
9	754	792	8
10	-28	152	32
11	204	146	10
12	285	266	9
13	438	456	8
14	224	247	10
15	192	213	12
16	218	173	12
17	86	141	19
18	-40	26	31
19	189	184	12
20	-22	64	43
21	137	143	15

h 7 3

8	630	593	8
9	438	404	8
10	629	585	8
11	208	240	10
12	384	312	8
13	268	224	10
14	307	281	9
15	227	171	11
16	-46	118	32
17	185	180	11
18	353	351	9
19	148	132	14
20	193	195	12
21	-82	52	21

h 8 3

9	166	206	10
10	180	129	10
11	820	836	9
12	100	122	17
13	125	128	15
14	225	193	11
15	386	380	9
16	87	115	22
17	72	91	22
18	-107	13	14
19	270	269	10
20	-28	17	41
21	133	144	16

h 9 3

10	395	382	8
11	367	379	9
12	37	94	33
13	110	92	17
14	317	325	10
15	281	234	11
16	306	281	9
17	135	149	14
18	207	219	11
19	-105	39	15
20	55	96	29

h 10 3

11	211	281	11
12	287	231	10
13	712	607	10

14	46	138	32
15	447	367	8
16	187	176	11
17	186	188	12
18	-38	65	34
19	-20	74	46
20	92	127	21

h 11 3

12	455	395	9
13	145	173	15
14	73	104	25
15	154	181	13
16	196	209	11
17	239	238	10
18	133	153	15
19	-39	59	35

h 12 3

13	-72	112	23
14	172	190	12
15	91	47	19
16	228	197	11
17	159	95	13
18	-59	3	27
19	187	158	13

h 13 3

14	197	165	11
15	110	91	17
16	205	175	11
17	90	103	21
18	-80	36	21

h 14 3

15	405	384	9
16	218	198	11
17	168	168	14

h 15 3

16	74	102	24

h 0 4

0	525	515	8
1	748	788	7
2	1660	1612	13
3	680	754	7
4	639	616	7
5	257	270	7
6	380	335	6
7	158	177	9
8	253	279	7
9	416	457	7
10	214	238	9
11	392	341	8
12	687	698	9
13	57	153	24
14	464	476	9
15	44	92	31
16	361	359	9
17	221	253	12
18	392	381	8
19	117	128	16
20	198	182	12
21	-37	27	36
22	287	271	12

h 1 4

1	284	259	8
2	545	483	6
3	225	224	7

4	190	190	8
5	952	916	9
6	783	696	8
7	392	330	7
8	83	37	14
9	694	630	8
10	199	150	9
11	316	276	8
12	704	688	9
13	371	347	8
14	-69	90	21
15	205	171	11
16	34	47	37
17	42	48	34
18	-76	20	19
19	185	201	12
20	214	229	11
21	95	89	20
22	46	70	38

h 2 4

2	741	739	9
3	142	155	9
4	263	303	7
5	500	479	7
6	758	718	8
7	259	283	7
8	908	881	9
9	470	433	7
10	256	248	8
11	493	441	8
12	265	286	9
13	262	227	9
14	138	155	14
15	87	69	20
16	428	441	9
17	-29	43	41
18	134	84	14
19	227	187	10
20	105	103	18
21	120	119	17

h 3 4

3	668	703	9
4	565	546	7
5	937	914	9
6	234	272	7
7	166	132	9
8	266	237	7
9	291	314	8
10	310	272	8
11	73	98	19
12	582	592	8
13	326	326	9
14	38	112	32
15	563	540	9
16	259	207	11
17	114	97	18
18	78	97	21
19	521	535	9
20	115	132	17
21	173	183	13

h 4 4

4	986	897	11
5	380	371	7
6	778	800	8
7	545	561	7
8	364	314	7
9	290	286	8
10	60	117	21
11	143	200	12
12	1167	1160	11
13	454	421	8
14	226	237	10

15	172	141	13
16	519	528	9
17	72	86	21
18	314	302	9
19	71	40	23
20	372	361	9
21	118	89	17

h 5 4

5	656	716	10
6	446	431	7
7	765	808	8
8	361	313	7
9	319	330	8
10	233	240	9
11	225	238	9
12	246	194	9
13	103	151	17
14	272	283	10
15	332	298	10
16	171	193	14
17	-73	22	20
18	86	101	20
19	258	274	10
20	92	119	20
21	-46	40	32

h 6 4

6	788	762	11
7	138	203	10
8	689	612	8
9	473	442	8
10	342	320	8
11	232	191	10
12	276	220	9
13	140	187	14
14	299	296	10
15	276	291	10
16	329	269	10
17	32	58	35
18	102	158	18
19	116	91	17
20	179	166	13
21	51	45	31

h 7 4

7	786	741	11
8	442	520	8
9	847	819	9
10	206	219	10
11	531	523	8
12	256	241	10
13	179	213	12
14	264	232	10
15	137	158	16
16	187	200	11
17	211	217	11
18	165	160	13
19	300	289	10
20	23	16	44

h 8 4

8	493	474	11
9	487	492	8
10	862	894	10
11	423	457	9
12	324	350	9
13	235	184	11
14	291	289	10
15	-60	83	27
16	190	224	11
17	165	147	12
18	316	309	9
19	-73	42	22

20	63	81	27

h 9 4

9	526	509	11
10	76	119	20
11	141	56	14
12	441	411	9
13	362	335	9
14	381	380	10
15	178	168	11
16	183	155	11
17	324	334	9
18	150	123	14
19	112	114	18
20	202	216	12

h 10 4

10	228	245	14
11	299	307	9
12	192	209	12
13	-48	59	31
14	201	209	12
15	92	133	18
16	463	465	8
17	115	119	17
18	77	114	23
19	-70	54	24

h 11 4

11	393	401	13
12	170	201	13
13	202	210	12
14	196	171	11
15	247	278	10
16	390	376	9
17	207	181	11
18	114	133	17
19	251	253	11

h 12 4

12	409	448	13
13	107	148	16
14	59	86	25
15	-51	53	28
16	104	117	18
17	-53	43	29
18	-63	31	26

h 13 4

13	134	158	20
14	-72	35	21
15	198	216	12
16	70	99	25
17	182	206	13

h 14 4

14	523	478	12
15	92	79	20
16	201	187	12
17	109	86	26

h 15 4

15	-97	50	24
16	205	194	12

h 0 5

1	316	294	6
2	381	327	6
3	512	502	7
4	184	233	8
5	608	658	7
6	189	204	8
7	371	383	7
8	191	162	9
9	748	644	8
10	-48	30	24
11	298	192	9
12	522	494	8
13	659	553	9
14	202	190	11
15	-60	20	25
16	40	51	35
17	167	170	12
18	-57	69	25
19	296	299	10
20	-49	3	30
21	177	199	13

h 1 5

2	298	355	7
3	553	618	7
4	274	214	7
5	681	715	8
6	854	845	9
7	321	383	7
8	773	747	8
9	598	640	8
10	292	271	8
11	252	234	9
12	480	481	8
13	161	190	12
14	19	123	44
15	-86	38	19
16	235	234	11
17	-46	10	28
18	90	126	19
19	-19	85	45
20	62	91	27
21	97	63	20

h 2 5

3	596	605	7
4	537	485	7
5	928	929	9
6	207	213	8
7	705	671	8
8	345	299	7
9	606	633	8
10	210	201	9
11	354	356	8
12	231	224	10
13	469	462	9
14	232	228	11
15	418	375	9
16	37	75	37
17	181	143	11
18	187	183	12
19	180	213	12
20	157	116	14
21	117	119	18

h 3 5

4	396	387	7
5	456	480	7
6	467	481	7
7	271	274	8
8	432	412	7
9	315	286	8
10	337	373	8
11	435	426	8
12	703	667	9
13	97	73	18
14	205	175	11
15	186	118	12
16	449	442	10
17	292	282	9
18	363	354	9
19	143	125	14
20	271	267	10
21	112	129	18

h 4 5

5	509	486	7
6	459	478	7
7	243	223	8
8	383	416	8
9	270	251	8
10	383	395	8
11	479	511	8
12	154	149	13
13	127	141	15
14	141	136	14
15	395	415	10
16	380	322	9
17	139	170	14
18	285	278	9
19	501	460	9
20	94	97	20
21	73	82	34

h 5 5

6	524	474	7
7	432	426	7
8	461	386	8
9	341	334	8
10	298	249	9
11	282	261	9
12	202	243	11
13	376	371	9
14	142	163	15
15	235	264	11
16	200	217	10
17	-71	69	21
18	84	102	21
19	62	88	26
20	149	144	15

h 6 5

7	132	151	12
8	484	413	8
9	289	304	9
10	291	281	9
11	380	364	9
12	282	296	10
13	177	188	12
14	166	216	13
15	289	257	10
16	96	147	18
17	197	231	11
18	210	224	11
19	208	214	12
20	69	35	25

h 7 5

8	85	87	17
9	128	100	13
10	472	448	8
11	393	348	9
12	450	455	9
13	112	100	17
14	432	426	9
15	-42	77	29
16	103	130	17
17	108	114	17
18	355	342	9
19	106	63	18
20	243	219	11

h 8 5

9	479	461	8
10	158	149	12
11	492	485	9
12	-47	49	29
13	256	240	11
14	253	260	11
15	137	129	13
16	205	226	11
17	213	219	11
18	39	37	35
19	164	146	14

h 9 5

10	304	295	9
11	390	367	9
12	199	230	12
13	-69	123	24
14	401	410	8
15	193	209	11
16	294	298	9
17	108	61	17
18	87	95	21
19	19	62	47

h 10 5

11	153	137	14
12	117	180	17
13	205	222	12
14	232	193	10
15	468	447	8
16	155	156	13
17	226	231	11
18	244	211	11

h 11 5

12	361	399	10
13	229	235	10
14	103	143	17
15	114	132	17
16	264	250	10
17	125	86	16
18	224	211	12

h 12 5

13	52	145	28
14	144	180	14
15	-79	95	20
16	160	127	14
17	99	129	20

h 13 5

14	241	271	10
15	102	103	19
16	191	201	12
17	37	39	48

h 14 5

15	150	162	14
16	183	186	13

h 0 6

0	1466	1440	10
1	691	627	8
2	1081	1032	10
3	365	390	7
4	77	46	16
5	151	58	10
6	46	42	24
7	92	159	15
8	282	355	8

9	121	141	14
10	238	284	10
11	284	329	9
12	229	300	10
13	104	86	17
14	114	58	17
15	195	213	13
16	119	156	15
17	185	201	12
18	-89	51	18
19	-28	30	40
20	233	189	11

h 1 6

1	1454	1444	10
2	446	446	7
3	349	351	7
4	605	554	8
5	341	321	7
6	271	261	8
7	526	479	8
8	335	289	8
9	561	563	8
10	94	110	17
11	391	386	9
12	-24	59	40
13	148	168	14
14	86	23	21
15	378	345	10
16	121	142	15
17	-90	105	17
18	72	68	23
19	232	188	11
20	35	83	38

h 2 6

2	1337	1262	14
3	321	329	7
4	107	107	12
5	422	418	7
6	264	242	8
7	342	317	8
8	805	827	9
9	477	506	8
10	122	140	14
11	213	221	10
12	539	537	9
13	112	118	17
14	-73	66	22
15	42	40	35
16	81	67	20
17	-57	36	26
18	315	280	9
19	293	303	10
20	184	183	13

h 3 6

3	419	458	10
4	450	441	7
5	452	460	7
6	70	36	18
7	293	336	8
8	199	179	10
9	379	375	8
10	267	232	9
11	319	325	9
12	281	292	10
13	454	430	9
14	83	102	22
15	191	212	13
16	148	228	13
17	294	270	9
18	211	175	11
19	259	201	10
20	129	107	16

h 4 6

4	361	351	10
5	108	44	13
6	333	349	8
7	132	72	12
8	600	587	8
9	168	170	11
10	195	147	11
11	174	127	12
12	351	297	9
13	219	220	11
14	332	294	10
15	272	317	9
16	202	193	11
17	265	310	10
18	237	198	11
19	94	40	20
20	109	142	19

h 5 6

5	862	894	12
6	150	181	11
7	237	256	9
8	86	182	18
9	294	320	9
10	148	145	13
11	238	267	10
12	191	192	12
13	360	349	9
14	71	34	25
15	230	235	10
16	-55	8	26
17	106	97	17
18	103	103	18
19	142	152	15

h 6 6

6	268	341	12
7	325	350	8
8	188	217	11
9	299	292	9
10	525	505	9
11	342	350	9
12	314	307	10
13	63	59	26
14	305	303	10
15	297	283	9
16	269	289	10
17	-40	32	33
18	159	158	14
19	257	232	11

h 7 6

7	332	296	12
8	132	84	14
9	390	368	9
10	90	49	19
11	316	280	9
12	170	145	13
13	378	390	10
14	195	158	11
15	126	168	15
16	49	95	30
17	-49	59	29
18	134	114	15
19	226	200	11

h 8 6

8	323	393	13
9	-52	47	26
10	257	291	10
11	95	138	19
12	376	349	10
13	192	164	13
14	268	234	9
15	-18	18	45
16	235	250	10
17	-16	33	48
18	63	70	27

h 9 6

9	685	711	12
10	50	46	30
11	171	123	13
12	305	285	10
13	233	216	10
14	237	188	10
15	256	232	10
16	125	142	16
17	404	381	9
18	80	77	23

h 10 6

10	97	88	27
11	154	125	14
12	189	179	11
13	253	230	10
14	183	157	12
15	97	122	19
16	146	130	14
17	19	61	47

h 11 6

11	486	443	11
12	172	181	12
13	134	137	14
14	138	152	14
15	294	264	10
16	95	113	20
17	163	158	14

h 12 6

12	253	231	14
13	189	194	12
14	177	125	12
15	224	231	11
16	132	119	16

h 13 6

13	383	327	13
14	127	135	16
15	69	100	25

h 14 6

14	114	138	24
15	80	101	32

h 0 7

1	424	385	7
2	300	310	8
3	118	139	13
4	146	192	11
5	152	162	11
6	67	28	20
7	923	911	10
8	416	338	8
9	175	146	12
10	188	188	11
11	172	121	12
12	-55	18	27
13	48	86	32
14	-35	51	33
15	202	195	11
16	-59	71	25
17	-66	60	23
18	31	17	39
19	140	167	15

h 1 7

2	160	193	10
3	424	378	8
4	550	584	8
5	216	237	9
6	384	396	8
7	340	328	8
8	360	374	8
9	275	290	9
10	157	194	13
11	67	125	23
12	246	318	11
13	282	264	10
14	196	202	10
15	59	69	25
16	112	116	17
17	74	69	23
18	81	71	22
19	132	118	16

h 2 7

3	648	643	8
4	238	230	9
5	147	205	12
6	52	56	25
7	224	200	10
8	156	206	12
9	218	240	10
10	-80	17	18
11	567	522	9
12	171	170	13
13	379	403	10
14	189	191	11
15	117	94	15
16	214	181	11
17	181	149	12
18	163	153	13
19	153	160	15

h 3 7

4	280	257	8
5	246	245	9
6	419	390	8
7	255	213	9
8	233	240	10
9	110	87	16
10	163	145	13
11	155	153	13
12	255	274	11
13	33	79	38
14	397	365	8
15	157	162	13
16	-38	96	33
17	369	339	9
18	366	359	9
19	192	186	13

h 4 7

5	352	303	8
6	212	218	10
7	469	521	8
8	235	204	10
9	237	250	10
10	82	100	20
11	239	239	11
12	88	130	21
13	111	56	18
14	64	35	23
15	226	206	10

16	230	208	11
17	274	264	10
18	103	83	19
19	91	85	24

h 5 7

6	317	286	9
7	320	306	9
8	262	209	10
9	162	191	13
10	432	425	9
11	234	198	11
12	185	118	13
13	162	133	14
14	166	145	12
15	108	74	17
16	215	188	11
17	167	136	13
18	180	172	13

h 6 7

7	350	365	9
8	104	113	17
9	99	110	18
10	240	281	11
11	508	557	9
12	216	217	12
13	248	249	9
14	126	129	15
15	61	114	26
16	-74	32	21
17	55	85	29
18	118	149	17

h 7 7

8	448	433	9
9	99	100	18
10	57	132	28
11	125	108	17
12	532	490	10
13	31	73	36
14	-87	62	18
15	70	117	24
16	184	198	12
17	128	148	16
18	28	76	42

h 8 7

9	661	664	9
10	135	138	16
11	277	251	11
12	270	245	9
13	137	153	14
14	-45	53	30
15	167	187	13
16	57	49	28
17	159	144	14

h 9 7

10	189	196	13
11	183	203	11
12	231	253	10
13	253	244	10
14	148	116	14
15	181	162	12
16	283	291	10
17	50	84	31

h 10 7

11	381	372	8
12	-67	62	22
13	235	230	10
14	86	51	21
15	176	148	13
16	54	26	30

h 11 7

12	98	109	18
13	124	91	16
14	231	237	11
15	33	85	38
16	47	97	33

h 12 7

13	218	250	11
14	165	153	13
15	207	187	12

h 13 7

14	168	176	14

h 0 8

0	276	380	12
1	-38	13	29
2	104	17	16
3	-60	55	22
4	122	106	14
5	183	206	11
6	394	400	9
7	-39	2	31
8	615	623	9
9	69	7	23
10	69	96	24
11	-77	18	21
12	156	126	15
13	-35	32	33
14	110	146	16
15	11	79	51
16	-41	13	33
17	84	38	22
18	133	78	16

h 1 8

1	149	169	17
2	78	69	19
3	238	278	10
4	214	208	10
5	170	169	12
6	201	205	11
7	438	427	9
8	240	253	10
9	377	328	9
10	282	274	10
11	315	277	10
12	255	267	11
13	148	103	13
14	177	169	12
15	139	118	14
16	121	107	16
17	113	94	18
18	-37	35	37

h 2 8

2	256	220	13
3	362	368	8
4	324	313	9
5	155	213	12
6	250	272	10
7	514	465	9
8	86	64	20
9	171	153	13
10	306	310	10
11	155	142	14
12	433	400	9
13	134	153	14
14	206	195	11
15	173	132	12
16	66	67	25
17	78	90	23
18	282	294	10

h 3 8

3	118	188	20
4	124	136	14
5	139	155	13
6	241	256	10
7	534	531	9
8	214	205	11
9	263	261	10
10	102	96	19
11	195	203	13
12	139	138	13
13	252	284	10
14	-56	34	26
15	28	78	40
16	198	182	12
17	263	277	10
18	38	35	48

h 4 8

4	113	99	22
5	194	237	11
6	320	287	9
7	83	72	20
8	230	239	11
9	-89	66	18
10	292	273	10
11	117	86	18
12	231	225	10
13	138	141	14
14	275	291	10
15	176	146	12
16	101	106	19
17	201	216	12

h 5 8

5	213	229	15
6	137	132	14
7	177	160	12
8	259	279	10
9	200	219	12
10	119	140	17
11	234	227	11
12	164	143	12
13	209	226	11
14	96	73	19
15	102	76	18
16	162	127	13
17	245	240	11

h 6 8

6	196	208	16
7	63	65	25
8	50	80	30
9	56	5	29
10	246	214	11
11	64	71	23
12	381	373	8
13	27	27	39
14	83	85	21
15	30	48	39
16	161	160	14
17	115	112	18

h 7 8

7	334	276	13
8	-24	60	43
9	277	233	11
10	134	137	13
11	375	382	8
12	162	187	12
13	21	36	44
14	133	155	15
15	147	164	14
16	67	88	26

h 8 8

8	428	418	13
9	93	78	21
10	74	137	21
11	138	162	14
12	194	204	11
13	244	254	10
14	215	209	11
15	158	108	14
16	197	209	12

h 9 8

9	312	316	12
10	-76	43	19
11	243	225	10
12	126	122	15
13	167	170	13
14	46	35	32
15	137	113	16

h 10 8

10	233	258	14
11	73	98	23
12	63	96	26
13	-31	101	38
14	20	92	46
15	109	132	19

h 11 8

11	184	204	17
12	47	31	31
13	250	226	11
14	89	81	21

h 12 8

12	143	180	21
13	78	59	23

h 0 9

1	762	726	9
2	187	126	12
3	677	646	9
4	138	76	14
5	229	229	11
6	92	76	19
7	564	604	9
8	236	239	11
9	-48	20	31
10	152	91	12
11	230	208	10
12	167	164	12
13	48	99	30
14	165	169	13
15	83	77	22
16	112	100	18

h 1 9

2	451	463	9
3	193	224	11
4	257	190	10
5	258	289	10
6	275	299	10

7	108	36	18
8	290	289	10
9	45	60	33
10	249	242	9
11	44	67	30
12	105	144	17
13	138	132	14
14	157	155	13
15	96	94	20
16	93	47	21

h 2 9

3	193	171	11
4	208	173	11
5	147	151	14
6	97	73	19
7	360	371	10
8	96	137	20
9	209	175	12
10	184	145	11
11	316	297	9
12	6	45	55
13	91	176	20
14	81	62	22
15	100	60	19
16	67	52	26

h 3 9

4	344	318	9
5	150	149	14
6	334	310	10
7	62	78	26
8	125	121	17
9	201	147	13
10	368	371	8
11	122	94	15
12	80	98	21
13	-57	41	26
14	144	135	14
15	126	166	16
16	102	105	20

h 4 9

5	119	125	16
6	167	192	13
7	289	348	10
8	147	135	15
9	168	189	12
10	199	143	11
11	87	91	20
12	127	186	15
13	176	155	12
14	68	98	25
15	-43	69	33
16	175	135	13

h 5 9

6	202	196	12
7	42	63	34
8	219	187	12
9	49	103	28
10	309	263	9
11	76	48	22
12	79	77	22
13	65	22	25
14	199	212	12
15	83	82	22

h 6 9

7	312	356	10
8	159	168	12
9	37	48	33
10	132	169	14
11	374	362	9
12	276	234	10
13	137	171	15
14	48	34	31
15	59	96	28

h 7 9

8	152	193	13
9	155	149	13
10	279	304	9
11	122	96	16
12	27	38	41
13	232	220	11
14	164	145	14
15	54	91	30

h 8 9

9	232	249	10
10	173	119	12
11	129	113	15
12	168	154	13
13	163	142	14
14	156	153	14

h 9 9

10	-75	49	21
11	94	87	20
12	120	129	17
13	88	75	21
14	136	133	22

h 10 9

11	49	51	31
12	91	42	21
13	174	142	13

h 11 9

12	150	112	15

h 0 10

0	-21	39	57
1	-32	13	38
2	467	423	9
3	102	45	19
4	221	215	12
5	307	298	10
6	125	81	14
7	187	172	11
8	144	160	13
9	95	125	18
10	233	191	10
11	197	181	12
12	79	102	22
13	79	10	23
14	-19	60	47

h 1 10

1	215	208	17
2	40	18	35
3	186	190	13
4	260	251	11
5	192	155	13
6	72	50	21
7	374	372	8
8	134	91	14
9	-78	77	19
10	-66	68	23
11	178	186	12
12	96	88	19
13	220	189	11
14	55	38	29

h 2 10

2	171	206	19
3	83	124	22
4	120	154	17
5	169	99	14
6	228	258	10
7	165	145	12
8	145	156	13
9	157	166	13
10	191	174	12
11	43	16	32
12	-79	79	21
13	-41	47	33
14	135	134	16

h 3 10

3	310	302	14
4	118	98	18
5	206	198	10
6	92	99	18
7	181	182	11
8	199	177	11
9	153	149	13
10	103	149	18
11	174	191	13
12	78	53	23
13	197	164	12
14	62	53	28

h 4 10

4	121	123	22
5	-48	27	27
6	-63	84	22
7	28	44	38
8	109	110	17
9	16	7	47
10	173	164	12
11	82	113	22
12	202	198	12
13	84	87	22
14	125	129	17

h 5 10

5	144	191	18
6	42	30	31
7	144	130	13
8	-54	39	27
9	102	84	18
10	-28	45	40
11	133	134	15
12	94	56	20
13	202	186	12

h 6 10

6	132	144	20
7	156	168	13
8	152	133	13
9	93	112	19
10	260	259	10
11	138	150	15
12	92	29	21
13	80	60	23

h 7 10

7	283	268	13
8	-27	28	40
9	170	213	13
10	112	73	17
11	226	203	11
12	176	115	13
13	117	75	25

h 8 10

8	195	248	16
9	125	126	16
10	261	249	10
11	75	54	24
12	72	77	25

h 9 10

9	86	95	29
10	71	45	25
11	77	106	24

h 10 10

10	124	107	23

h 0 11

1	29	13	37
2	-52	67	27
3	239	234	10
4	250	262	10
5	172	149	12
6	-76	26	21
7	95	133	19
8	76	95	23
9	100	60	19
10	50	82	31
11	186	158	13
12	90	34	21

h 1 11

2	197	202	11
3	135	70	14
4	194	193	11
5	209	199	11
6	270	258	10
7	146	154	14
8	103	124	18
9	115	107	17
10	201	189	12
11	75	93	24
12	73	53	25

h 2 11

3	103	66	17
4	68	82	23
5	57	56	27
6	95	39	19
7	233	235	11
8	129	163	15
9	134	122	15
10	108	88	18
11	76	69	24
12	-50	57	35

h 3 11

4	204	220	11
5	111	69	17
6	26	94	41
7	123	94	16
8	170	164	13
9	172	198	13
10	163	147	14
11	56	19	29

h 4 11

5	131	95	15
6	70	30	24
7	105	74	18
8	43	62	33

9	159	149	14
10	-73	50	23
11	205	199	12
h	5	11	
6	-45	39	31
7	120	125	16
8	90	125	20
9	123	96	16
10	126	97	16
11	86	53	22
h	6	11	
7	205	203	12
8	69	27	25
9	167	130	13
10	81	31	23
h	7	11	

8	148	132	15
9	102	103	19
10	192	205	18
h	8	11	
9	159	194	14
h	0	12	
0	77	145	31
1	30	37	39
2	330	332	9
3	68	5	25
4	84	25	22
5	244	264	11
6	269	233	10
7	156	125	14
8	75	33	24
h	1	12	

1	287	299	14
2	69	9	24
3	179	150	13
4	100	103	19
5	122	138	16
6	88	30	21
7	95	109	20
8	93	29	21
h	2	12	
2	245	234	15
3	88	57	21
4	82	82	22
5	126	126	16
6	109	105	18
7	115	71	18
8	126	128	17
h	3	12	
3	197	174	17

4	-23	46	44
5	-37	46	36
6	127	139	16
7	136	131	16
8	103	104	19
h	4	12	
4	207	179	16
5	57	29	28
6	85	95	22
7	113	120	18
h	5	12	
5	-42	51	44
6	56	106	29
7	91	74	21
h	6	12	
6	131	137	23

Table 1. Final Refined Parameters for

Aquo, Carbonyl Tetrakis(Pentafluorophenyl)octachloroporphyrin Ruthenium(II).

x, y, z and $U_{eq}{}^{a} \times 10^4$

Atom	x	y	z	U_{eq} or B
Ru	2126(.5)	1763(.5)	1683(.3)	291(2)
Cl1	2662(2)	3927(2)	−61(1)	647(9)
C1	2188(6)	3188(6)	328(3)	2.8(2) *
C2	2635(6)	2714(6)	722(3)	2.3(2) *
N1	1953(5)	2315(4)	990(3)	2.1(1) *
C3	3597(6)	2573(6)	795(3)	2.5(2) *
C4	3997(6)	2090(5)	1169(3)	2.3(2) *
N2	3546(5)	1785(5)	1581(3)	2.1(1) *
C5	4960(6)	1836(6)	1202(4)	3.1(2) *
Cl2	5843(2)	1956(2)	773(1)	748(11)
C6	5069(7)	1380(6)	1619(4)	3.4(2) *
Cl3	6082(2)	876(3)	1761(1)	992(14)
C7	4191(6)	1364(6)	1874(4)	2.8(2) *
C8	4026(6)	1052(6)	2355(4)	2.8(2) *
C9	3163(6)	1023(6)	2593(4)	2.7(2) *
N3	2306(5)	1189(5)	2367(3)	2.4(2) *
C10	2978(7)	796(6)	3109(4)	3.2(2) *
Cl4	3744(2)	581(2)	3587(1)	695(10)
C11	2051(7)	828(6)	3186(4)	3.1(2) *
Cl5	1570(2)	663(3)	3763(1)	813(12)

Table 1. (Cont.)

Atom	x	y	z	U_{eq} or B	
C12	1613(6)	1046(6)	2710(4)	2.8(2)	*
C13	659(6)	1038(6)	2602(3)	2.5(2)	*
C14	261(6)	1224(6)	2135(3)	2.5(2)	*
N4	715(5)	1586(4)	1736(3)	2.1(1)	*
C15	−708(7)	1098(6)	1993(4)	3.3(2)	*
Cl6	−1575(2)	602(2)	2313(1)	767(11)	
C16	−798(7)	1367(6)	1519(4)	3.4(2)	*
Cl7	−1825(2)	1228(3)	1192(1)	805(11)	
C17	82(6)	1708(6)	1360(3)	2.5(2)	*
C18	263(6)	2147(6)	908(3)	2.5(2)	*
C19	1108(6)	2475(6)	757(3)	2.3(2)	*
C20	1280(6)	3034(6)	342(4)	2.8(2)	*
Cl8	500(2)	3514(2)	−50(1)	718(10)	
C21	4245(6)	2982(6)	425(4)	309(24)	
C22	4358(7)	2698(7)	−51(4)	460(30)	
C23	4973(8)	3078(8)	−388(4)	532(39)	
C24	5459(7)	3762(8)	−242(5)	494(34)	
C25	5369(7)	4056(7)	223(4)	418(31)	
C26	4771(6)	3684(6)	558(4)	347(26)	
C31	4834(6)	696(7)	2634(4)	390(29)	

Table 1. (Cont.)

Atom	x	y	z	U_{eq} or B
C32	4985(7)	−153(7)	2647(4)	460(30)
C33	5726(7)	−491(8)	2911(4)	521(32)
C34	6323(7)	34(9)	3166(4)	564(41)
C35	6179(7)	870(8)	3155(4)	497(34)
C36	5457(7)	1178(7)	2890(4)	485(33)
C41	14(6)	853(7)	3025(4)	375(30)
C42	−182(7)	60(9)	3185(4)	548(36)
C43	−756(8)	−63(10)	3598(5)	655(40)
C44	−1151(9)	600(13)	3840(5)	801(57)
C45	−984(9)	1377(11)	3683(5)	758(46)
C46	−419(7)	1509(8)	3273(4)	544(34)
C51	−564(6)	2279(7)	567(4)	403(29)
C52	−1167(7)	2958(7)	633(4)	472(32)
C53	−1943(7)	3056(8)	342(5)	581(38)
C54	−2128(7)	2515(10)	−26(5)	613(48)
C55	−1549(8)	1857(9)	−110(4)	626(38)
C56	−765(7)	1723(8)	184(4)	487(30)
F22	3874(5)	2015(4)	−195(2)	706(20)
F23	5056(5)	2762(5)	−849(3)	832(25)
F24	6020(5)	4122(5)	−576(3)	818(22)

Table 1. (Cont.)

Atom	x	y	z	U_{eq} or B
F25	5857(4)	4728(4)	369(3)	648(19)
F26	4692(4)	4006(4)	1018(2)	581(18)
F32	4412(4)	−675(4)	2400(3)	665(19)
F33	5841(5)	−1327(4)	2922(3)	768(21)
F34	7021(4)	−306(5)	3428(3)	789(23)
F35	6777(4)	1349(4)	3402(3)	763(22)
F36	5338(4)	2009(4)	2890(3)	741(22)
F42	198(5)	−592(4)	2962(3)	776(23)
F43	−939(5)	−852(6)	3747(3)	1120(29)
F44	−1711(5)	483(7)	4237(3)	1269(38)
F45	−1382(6)	2026(7)	3920(3)	1343(35)
F46	−259(5)	2311(5)	3120(3)	886(24)
F52	−994(4)	3506(4)	1002(3)	714(21)
F53	−2506(5)	3710(5)	414(3)	969(27)
F54	−2872(4)	2604(5)	−321(3)	936(29)
F55	−1730(5)	1297(5)	−476(3)	996(26)
F56	−218(5)	1070(4)	112(3)	801(22)
C61	2044(7)	2772(7)	1999(4)	380(27)
O61	1983(6)	3394(5)	2200(3)	727(27)
O1	2165(4)	550(4)	1319(3)	455(18)

Table 1. (Cont.)

Atom	x	y	z	U_{eq} or B
C71	6734(14)	1512(12)	8525(6)	1339(72)
C72	7369(10)	1351(10)	8083(6)	810(47)
O2	7836(7)	727(6)	8029(4)	1052(36)
O3	7307(8)	1937(6)	7730(5)	1123(39)
C73	7799(23)	1823(15)	7264(11)	2118(126)
C74	7208(30)	1689(27)	6858(12)	3385(205)

[a] $U_{eq} = \frac{1}{3}\sum_i \sum_j [U_{ij}(a_i^* a_j^*)(\vec{a}_i \cdot \vec{a}_j)]$

* Isotropic displacement parameter, B

Table 2. Assigned Parameters for Aquo, Carbonyl Tetrakis(Pentafluorophenyl)octachloroporphyrin Ruthenium(II).

x, y, z and $U_{eq}{}^{a} \times 10^4$

Atom	x	y	z	B	
C81	2113	608	117	10.0	*
C82	3110	277	177	10.0	*
O4	3395	244	596	10.0	*
O5	3902	140	−172	10.0	*
C83	4801	−74	1	13.5	*
C84	5482	37	−378	15.0	*
C91A	4182	1901	8228	15.0	*
C92A	3256	1464	8232	10.0	*
C93A	2614	1851	8622	10.0	*
C94A	1677	1396	8619	10.0	*
C95A	1024	1765	9002	10.0	*
C96A	98	1328	9006	15.0	*
C91B	4073	2287	8474	15.0	*
C92B	3311	1674	8335	10.0	*
C93B	2440	1827	8656	10.0	*
C94B	1666	1226	8527	10.0	*
C95B	806	1382	8845	10.0	*
C96B	44	784	8715	15.0	*
C91C	3801	2164	8479	15.0	*
C92C	3028	1549	8341	10.0	*
C93C	2156	1671	8645	10.0	*
C94C	1405	1091	8521	10.0	*
C95C	545	1247	8840	10.0	*
C96C	−240	644	8712	15.0	*
H71A	6799	1075	8765	10.0	*
H71B	6886	2030	8677	10.0	*
H71C	6100	1528	8413	10.0	*
H73A	8214	1373	7293	10.0	*
H73B	8120	2321	7183	10.0	*
H74A	7585	1586	6569	10.0	*
H74B	6889	1151	6928	10.0	*

Table 2. (Cont.)

Atom	x	y	z	B	
H74C	6796	2099	6818	10.0	*
H81A	1811	602	432	10.0	*
H81B	2131	1164	−8	10.0	*
H81C	1780	265	−113	10.0	*
H83A	4956	271	279	10.0	*
H83B	4801	−643	103	10.0	*
H84A	6077	−112	−249	10.0	*
H84B	5335	−308	−657	10.0	*
H84C	5489	605	−480	10.0	*
H91A	4572	1652	7983	10.0	*
H91B	4093	2474	8150	10.0	*
H91C	4467	1853	8549	10.0	*
H91D	4606	2185	8274	10.0	*
H91E	3859	2841	8419	10.0	*
H91F	4233	2219	8818	10.0	*
H91G	4331	2059	8277	10.0	*
H91H	3589	2719	8423	10.0	*
H91I	3963	2098	8822	10.0	*
H92A	3349	891	8309	10.0	*
H92B	2975	1512	7910	10.0	*
H92D	3528	1121	8391	10.0	*
H92E	3154	1742	7991	10.0	*
H92G	3250	998	8396	10.0	*
H92H	2877	1619	7997	10.0	*
H93A	2518	2424	8546	10.0	*
H93B	2892	1803	8945	10.0	*
H93D	2227	2381	8600	10.0	*
H93E	2600	1759	8999	10.0	*
H93G	1937	2224	8590	10.0	*
H93H	2311	1603	8989	10.0	*
H94A	1777	823	8695	10.0	*

Table 2. (Cont.)

Atom	x	y	z	B	
H94B	1403	1444	8295	10.0	*
H94D	1878	672	8582	10.0	*
H94E	1505	1293	8183	10.0	*
H94G	1616	537	8577	10.0	*
H94H	1243	1158	8178	10.0	*
H95A	927	2338	8926	10.0	*
H95B	1301	1717	9325	10.0	*
H95D	593	1936	8790	10.0	*
H95E	967	1314	9189	10.0	*
H95G	334	1801	8784	10.0	*
H95H	708	1180	9183	10.0	*
H96A	−292	1577	9251	10.0	*
H96B	−187	1376	8685	10.0	*
H96C	187	755	9084	10.0	*
H96D	−483	893	8918	10.0	*
H96E	−122	850	8372	10.0	*
H96F	252	228	8771	10.0	*
H96G	−762	759	8918	10.0	*
H96H	−410	708	8370	10.0	*
H96I	−36	87	8769	10.0	*

Population Parameters: C91A to C96A, 0.302; C91B to C96B, 0.298; C91C to C96C, 0.236. Hydrogen atoms have same population as attached carbon atom; hydrogen atoms A, B and C are on 'A' carbon atoms, D, E and F on 'B' carbon atoms and G, H and I on 'C' carbon atoms. C81, C82, C83, C84 O4 and O5 have population parameter 0.5.

Table 3. Anisotropic Displacement Parameters for Aquo, Carbonyl Tetrakis(Pentafluorophenyl)octachloroporphyrin Ruthenium(II).

Atom	U_{11}	U_{22}	U_{33}	U_{12}	U_{13}	U_{23}
Ru	172(4)	413(5)	289(4)	−13(4)	−3(3)	76(4)
Cl1	392(16)	884(24)	664(21)	−5(16)	37(15)	444(18)
Cl2	327(16)	1175(30)	744(22)	194(17)	208(15)	461(21)
Cl3	358(18)	1677(40)	944(28)	362(21)	171(18)	729(28)
Cl4	400(17)	1312(30)	373(17)	47(18)	−99(13)	225(18)
Cl5	468(19)	1627(37)	343(17)	−69(21)	11(14)	200(20)
Cl6	333(16)	1384(32)	585(21)	−289(18)	−35(14)	397(21)
Cl7	341(16)	1413(34)	659(22)	−267(19)	−130(15)	389(22)
Cl8	350(16)	1152(29)	650(21)	17(17)	−67(14)	526(20)
C21	266(53)	354(63)	308(59)	38(45)	−4(44)	123(47)
C22	519(70)	408(71)	453(75)	−24(57)	−35(59)	−16(58)
C23	464(70)	910(105)	223(62)	222(70)	90(52)	87(65)
C24	286(62)	606(86)	590(86)	28(59)	60(59)	193(70)
C25	226(56)	415(70)	613(83)	−21(51)	−39(54)	117(61)
C26	244(54)	421(66)	374(65)	27(49)	−64(47)	36(53)
C31	261(58)	562(76)	347(64)	−15(54)	17(47)	126(56)
C32	314(60)	643(85)	421(68)	−79(60)	−48(51)	73(61)
C33	414(71)	536(82)	612(81)	238(62)	51(61)	180(65)
C34	243(62)	976(112)	473(76)	62(69)	−74(54)	155(74)
C35	263(62)	645(87)	581(79)	−54(61)	−104(56)	75(67)
C36	290(62)	505(79)	660(82)	−35(58)	−21(58)	134(65)
C41	230(53)	626(79)	268(60)	−47(53)	−1(45)	91(56)
C42	323(66)	863(103)	458(75)	−84(67)	−36(55)	299(73)
C43	458(77)	947(115)	560(91)	−146(77)	−133(67)	361(85)
C44	494(87)	1562(174)	348(83)	−291(103)	55(66)	90(93)
C45	473(82)	1218(137)	583(94)	11(87)	136(70)	−257(95)
C46	355(65)	759(98)	517(78)	−95(63)	49(57)	90(70)
C51	231(54)	608(77)	371(65)	21(53)	6(47)	209(58)
C52	312(63)	629(85)	477(74)	−37(57)	62(55)	100(62)
C53	339(69)	747(102)	656(89)	148(66)	−20(63)	183(75)
C54	186(60)	1063(115)	590(88)	76(71)	−90(60)	235(82)
C55	540(79)	955(106)	380(71)	−247(82)	−187(60)	63(74)
C56	410(65)	628(80)	423(69)	−6(64)	−71(53)	100(66)

Table 3. (Cont.)

Atom	U_{11}	U_{22}	U_{33}	U_{12}	U_{13}	U_{23}
F22	679(45)	876(56)	565(44)	−213(40)	65(35)	−180(39)
F23	767(50)	1276(67)	454(45)	40(46)	170(37)	−103(43)
F24	640(46)	968(57)	849(55)	−34(41)	372(41)	453(45)
F25	495(39)	514(43)	934(54)	−152(34)	45(36)	178(38)
F26	571(41)	698(46)	474(42)	−144(34)	35(32)	−85(35)
F32	564(43)	638(47)	790(51)	8(36)	−206(38)	0(39)
F33	645(47)	747(53)	910(56)	247(40)	−110(40)	54(43)
F34	435(40)	1121(61)	809(52)	162(39)	−250(37)	254(45)
F35	466(41)	945(56)	874(55)	−133(38)	−276(38)	−16(44)
F36	493(42)	722(53)	1007(59)	−118(36)	−222(39)	97(43)
F42	705(51)	603(49)	1021(62)	54(41)	119(44)	131(44)
F43	807(58)	1426(79)	1125(70)	−334(54)	−101(49)	810(63)
F44	741(55)	2569(118)	500(50)	−408(65)	317(43)	118(61)
F45	1057(70)	1987(108)	989(70)	72(69)	472(57)	−628(71)
F46	876(57)	758(57)	1028(63)	22(46)	263(48)	−212(49)
F52	466(40)	839(54)	835(53)	186(36)	−48(37)	−165(43)
F53	533(46)	1258(69)	1115(67)	474(48)	−72(44)	168(54)
F54	385(40)	1701(81)	718(52)	63(46)	−247(37)	208(52)
F55	813(56)	1311(73)	859(60)	−68(50)	−386(47)	−240(54)
F56	776(51)	780(53)	844(56)	201(44)	−269(42)	−226(43)
C61	310(59)	389(69)	442(70)	27(53)	3(50)	66(56)
O61	807(64)	587(63)	787(66)	50(49)	51(50)	−143(51)
O1	438(43)	417(44)	511(47)	−6(35)	−44(35)	3(36)
C71	1856(192)	1558(179)	601(107)	552(146)	−273(118)	−139(112)
C72	777(107)	679(106)	974(127)	5(86)	−104(92)	35(100)
O2	1119(87)	724(72)	1314(95)	293(65)	222(72)	231(67)
O3	1238(94)	876(85)	1255(100)	194(68)	−35(78)	386(75)
C73	3124(411)	1029(170)	2221(315)	292(215)	2029(317)	446(201)
C74	4265(600)	4101(521)	1808(322)	−2050(429)	1958(371)	−1157(350)

$U_{i,j}$ values have been multiplied by 10^4

The form of the displacement factor is:

$$\exp -2\pi^2(U_{11}h^2a^{*^2} + U_{22}k^2b^{*^2} + U_{33}\ell^2c^{*^2} + 2U_{12}hka^*b^* + 2U_{13}h\ell a^*c^* + 2U_{23}k\ell b^*c^*)$$

Table 4. Complete Distances and Angles for Aquo, Carbonyl Tetrakis(Pentafluorophenyl)octachloroporphyrin Ruthenium(II).

	Distance(Å)		Distance(Å)
Ru –N1	2.063(7)	C15 –Cl6	1.711(10)
Ru –N2	2.060(7)	C15 –C16	1.340(14)
Ru –N3	2.059(7)	C16 –Cl7	1.724(11)
Ru –N4	2.052(7)	C16 –C17	1.443(13)
Ru –C61	1.828(10)	C17 –C18	1.420(13)
Ru –O1	2.172(7)	C18 –C19	1.384(12)
Cl1 –C1	1.717(10)	C18 –C51	1.507(13)
C1 –C2	1.446(13)	C19 –C20	1.448(13)
C1 –C20	1.327(13)	C20 –Cl8	1.710(10)
C2 –N1	1.373(11)	C21 –C22	1.359(14)
C2 –C3	1.411(13)	C21 –C26	1.400(13)
N1 –C19	1.385(11)	C22 –C23	1.404(16)
C3 –C4	1.385(13)	C22 –F22	1.350(13)
C3 –C21	1.510(13)	C23 –C24	1.354(16)
C4 –N2	1.368(11)	C23 –F23	1.335(13)
C4 –C5	1.444(13)	C24 –C25	1.334(16)
N2 –C7	1.384(12)	C24 –F24	1.336(13)
C5 –Cl2	1.724(10)	C25 –C26	1.377(14)
C5 –C6	1.340(14)	C25 –F25	1.341(12)
C6 –Cl3	1.705(11)	C26 –F26	1.338(11)
C6 –C7	1.437(14)	C31 –C32	1.376(15)
C7 –C8	1.398(13)	C31 –C36	1.363(15)
C8 –C9	1.396(13)	C32 –C33	1.384(16)
C8 –C31	1.489(14)	C32 –F32	1.342(12)
C9 –N3	1.393(12)	C33 –C34	1.378(16)
C9 –C10	1.452(14)	C33 –F33	1.349(13)
N3 –C12	1.374(12)	C34 –C35	1.354(16)
C10 –Cl4	1.714(10)	C34 –F34	1.336(14)
C10 –C11	1.349(14)	C35 –C36	1.345(16)
C11 –Cl5	1.710(10)	C35 –F35	1.324(13)
C11 –C12	1.456(13)	C36 –F36	1.341(13)
C12 –C13	1.398(13)	C41 –C42	1.370(15)
C13 –C14	1.400(13)	C41 –C46	1.391(15)
C13 –C41	1.493(13)	C42 –C43	1.393(18)
C14 –N4	1.379(11)	C42 –F42	1.321(14)
C14 –C15	1.455(13)	C43 –C44	1.37(2)
N4 –C17	1.365(11)	C43 –F43	1.352(16)

Table 4. (Cont.)

	Distance(Å)		Distance(Å)
C44 –C45	1.33(2)	C91C –C92C	1.528
C44 –F44	*1.347(18)*	*C92C –C93C*	*1.507*
C45 –C46	1.382(19)	C93C –C94C	1.461
C45 –F45	1.345(17)	C94C –C95C	1.524
C46 –F46	1.367(14)	C95C –C96C	1.520
C51 –C52	1.402(15)	C71 –H71A	0.953
C51 –C56	1.384(15)	C71 –H71B	0.948
C52 –C53	1.365(16)	C71 –H71C	0.957
C52 –F52	1.340(13)	C73 –H73A	0.938
C53 –C54	1.333(18)	C73 –H73B	0.947
C53 –F53	1.338(14)	C74 –H74A	0.959
C54 –C55	1.360(18)	C74 –H74B	0.993
C54 –F54	1.333(15)	C74 –H74C	0.890
C55 –C56	1.387(17)	C81 –H81A	0.950
C55 –F55	1.351(15)	C81 –H81B	0.950
C56 –F56	1.323(13)	C81 –H81C	0.950
C61 –O61	*1.134(13)*	C83 –H83A	0.950
C71 –C72	1.52(2)	C83 –H83B	0.950
C72 –O2	1.213(19)	C84 –H84A	0.950
C72 –O3	1.331(19)	C84 –H84B	0.950
O3 –C73	1.44(3)	C84 –H84C	0.950
C73 –C74	1.39(5)	C91A –H91A	0.950
C81 –C82	1.535	C91A –H91B	0.950
C82 –O4	1.191	C91A –H91C	0.950
C82 –O5	1.490	C92A –H92A	0.950
O5 –C83	1.411	C92A –H92B	0.950
C83 –C84	1.421	C93A –H93A	0.950
C91A –C92A	1.503	C93A –H93B	0.950
C92A –C93A	1.526	C94A –H94A	0.950
C93A –C94A	1.530	C94A –H94B	0.950
C94A –C95A	1.512	C95A –H95A	0.950
C95A –C96A	1.503	C95A –H95B	0.950
C91B –C92B	1.515	C96A –H96A	0.950
C92B –C93B	1.539	C96A –H96B	0.950
C93B –C94B	1.507	C96A –H96C	0.950
C94B –C95B	1.524	C91B –H91D	0.950
C95B –C96B	1.494	C91B –H91E	0.950

Table 4. (Cont.)

Distance(Å)		Angle(°)	
C91B –H91F	0.950	N1 –Ru –N2	89.3(3)
C92B –H92D	0.950	N1 –Ru –N3	178.8(3)
C92B –H92E	0.950	N1 –Ru –N4	90.4(3)
C93B –H93D	0.950	N1 –Ru –C61	91.6(4)
C93B –H93E	0.950	N1 –Ru –O1	89.2(3)
C94B –H94D	0.950	N2 –Ru –N3	90.3(3)
C94B –H94E	0.950	N2 –Ru –N4	172.2(3)
C95B –H95D	0.950	N2 –Ru –C61	96.4(4)
C95B –H95E	0.950	N2 –Ru –O1	85.9(3)
C96B –H96D	0.950	N3 –Ru –N4	89.8(3)
C96B –H96E	0.950	N3 –Ru –C61	89.6(4)
C96B –H96F	0.950	N3 –Ru –O1	89.7(3)
C91C –H91G	0.950	N4 –Ru –C61	91.4(4)
C91C –H91H	0.950	N4 –Ru –O1	86.3(3)
C91C –H91I	0.950	C61 –Ru –O1	177.6(4)
C92C –H92G	0.950	Ru –C61 –O61	178.9(9)
C92C –H92H	0.950	Ru –N1 –C2	125.7(6)
C93C –H93G	0.950	Ru –N1 –C19	125.6(6)
C93C –H93H	0.950	Ru –N2 –C4	125.8(6)
C94C –H94G	0.950	Ru –N2 –C7	125.2(6)
C94C –H94H	0.950	Ru –N3 –C9	125.0(6)
C95C –H95G	0.950	Ru –N3 –C12	125.2(6)
C95C –H95H	0.950	Ru –N4 –C14	125.6(6)
C96C –H96G	0.950	Ru –N4 –C17	125.7(6)
C96C –H96H	0.950	C2 –C1 –Cl1	128.7(7)
C96C –H96I	0.950	C20 –C1 –Cl1	122.5(7)
		C20 –C1 –C2	108.4(8)
		N1 –C2 –C1	107.9(7)
		C3 –C2 –C1	127.9(8)
		C3 –C2 –N1	123.7(8)
		C19 –N1 –C2	107.9(7)
		C4 –C3 –C2	126.2(8)
		C21 –C3 –C2	116.6(8)
		C21 –C3 –C4	117.3(8)
		N2 –C4 –C3	125.5(8)
		C5 –C4 –C3	126.5(8)
		C5 –C4 –N2	107.9(8)

Table 4. (Cont.)

	Angle(°)		Angle(°)
C7 –N2 –C4	108.1(7)	C17 –C16 –C15	108.6(9)
Cl2 –C5 –C4	129.5(7)	C17 –C16 –Cl7	130.4(8)
C6 –C5 –C4	108.2(8)	C16 –C17 –N4	108.1(8)
C6 –C5 –Cl2	122.0(8)	C18 –C17 –N4	124.8(8)
Cl3 –C6 –C5	122.6(8)	C18 –C17 –C16	127.0(8)
C7 –C6 –C5	107.7(9)	C19 –C18 –C17	126.8(8)
C7 –C6 –Cl3	129.6(8)	C51 –C18 –C17	115.7(8)
C6 –C7 –N2	108.0(8)	C51 –C18 –C19	117.4(8)
C8 –C7 –N2	125.3(8)	C18 –C19 –N1	124.6(8)
C8 –C7 –C6	126.4(9)	C20 –C19 –N1	107.8(7)
C9 –C8 –C7	125.7(9)	C20 –C19 –C18	127.7(8)
C31 –C8 –C7	117.5(8)	C19 –C20 –C1	107.9(8)
C31 –C8 –C9	116.8(8)	Cl8 –C20 –C1	122.7(7)
N3 –C9 –C8	125.7(8)	Cl8 –C20 –C19	129.2(7)
C10 –C9 –C8	127.4(9)	C22 –C21 –C3	122.9(9)
C10 –C9 –N3	106.9(8)	C26 –C21 –C3	121.1(8)
C12 –N3 –C9	108.9(7)	C26 –C21 –C22	116.0(9)
Cl4 –C10 –C9	129.5(8)	C23 –C22 –C21	122.1(10)
C11 –C10 –C9	108.7(9)	F22 –C22 –C21	118.2(9)
C11 –C10 –Cl4	121.7(8)	F22 –C22 –C23	119.7(9)
Cl5 –C11 –C10	122.2(8)	C24 –C23 –C22	119.4(10)
C12 –C11 –C10	107.5(9)	F23 –C23 –C22	119.0(10)
C12 –C11 –Cl5	130.3(7)	F23 –C23 –C24	121.6(10)
C11 –C12 –N3	108.0(8)	C25 –C24 –C23	120.1(11)
C13 –C12 –N3	125.2(8)	F24 –C24 –C23	117.9(10)
C13 –C12 –C11	126.6(9)	F24 –C24 –C25	122.0(10)
C14 –C13 –C12	125.2(8)	C26 –C25 –C24	121.0(10)
C41 –C13 –C12	117.2(8)	F25 –C25 –C24	120.1(10)
C41 –C13 –C14	117.5(8)	F25 –C25 –C26	119.0(9)
N4 –C14 –C13	125.7(8)	C25 –C26 –C21	121.4(9)
C15 –C14 –C13	126.1(8)	F26 –C26 –C21	119.6(8)
C15 –C14 –N4	108.2(8)	F26 –C26 –C25	119.0(9)
C17 –N4 –C14	108.2(7)	C32 –C31 –C8	120.9(9)
Cl6 –C15 –C14	129.2(7)	C36 –C31 –C8	122.8(9)
C16 –C15 –C14	106.8(9)	C36 –C31 –C32	116.3(10)
C16 –C15 –Cl6	123.6(8)	C33 –C32 –C31	121.3(10)
Cl7 –C16 –C15	120.9(8)	F32 –C32 –C31	120.4(9)

Table 4. (Cont.)

	Angle(°)		Angle(°)
F32 –C32 –C33	118.2(9)	C54 –C53 –C52	120.2(11)
C34 –C33 –C32	119.1(11)	F53 –C53 –C52	120.0(11)
F33 –C33 –C32	119.5(10)	F53 –C53 –C54	119.8(11)
F33 –C33 –C34	121.3(10)	C55 –C54 –C53	120.3(12)
C35 –C34 –C33	119.9(11)	F54 –C54 –C53	121.3(11)
F34 –C34 –C33	118.2(10)	F54 –C54 –C55	118.3(11)
F34 –C34 –C35	121.9(10)	C56 –C55 –C54	121.5(11)
C36 –C35 –C34	119.4(11)	F55 –C55 –C54	121.2(11)
F35 –C35 –C34	117.6(10)	F55 –C55 –C56	117.3(11)
F35 –C35 –C36	123.0(10)	C55 –C56 –C51	118.9(10)
C35 –C36 –C31	123.9(10)	F56 –C56 –C51	119.6(10)
F36 –C36 –C31	118.5(9)	F56 –C56 –C55	121.5(10)
F36 –C36 –C35	117.6(10)	O2 –C72 –C71	124.5(15)
C42 –C41 –C13	123.3(9)	O3 –C72 –C71	113.1(14)
C46 –C41 –C13	119.4(9)	O3 –C72 –O2	122.2(14)
C46 –C41 –C42	117.3(10)	C73 –O3 –C72	119.2(16)
C43 –C42 –C41	120.1(11)	C74 –C73 –O3	113.0(26)
F42 –C42 –C41	120.4(10)	O4 –C82 –C81	115.5
F42 –C42 –C43	119.5(11)	O5 –C82 –C81	134.5
C44 –C43 –C42	120.8(13)	O5 –C82 –O4	108.6
F43 –C43 –C42	118.8(12)	C83 –O5 –C82	122.2
F43 –C43 –C44	120.3(12)	C84 –C83 –O5	111.7
C45 –C44 –C43	120.0(14)	C93A –C92A –C91A	110.7
F44 –C44 –C43	121.0(13)	C94A –C93A –C92A	109.7
F44 –C44 –C45	119.0(13)	C95A –C94A –C93A	111.0
C46 –C45 –C44	119.9(13)	C96A –C95A –C94A	112.0
F45 –C45 –C44	119.8(13)	C93B –C92B –C91B	110.5
F45 –C45 –C46	120.3(12)	C94B –C93B –C92B	111.8
C45 –C46 –C41	121.8(11)	C95B –C94B –C93B	111.5
F46 –C46 –C41	119.4(10)	C96B –C95B –C94B	111.1
F46 –C46 –C45	118.8(11)	C93C –C92C –C91C	113.1
C52 –C51 –C18	121.2(9)	C94C –C93C –C92C	114.3
C56 –C51 –C18	121.1(9)	C95C –C94C –C93C	111.8
C56 –C51 –C52	117.7(9)	C96C –C95C –C94C	111.9
C53 –C52 –C51	121.4(10)	H71A –C71 –C72	109.9
F52 –C52 –C51	119.2(9)	H71B –C71 –C72	110.1
F52 –C52 –C53	119.4(10)	H71C –C71 –C72	109.6

Table 4. (Cont.)

			Angle(°)				Angle(°)
H71B	-C71	-H71A	109.4	H92A	-C92A	-C91A	109.2
H71C	-C71	-H71A	108.7	H92B	-C92A	-C91A	109.2
H71C	-C71	-H71B	109.1	H92A	-C92A	-C93A	109.2
H73A	-C73	-O3	109.9	H92B	-C92A	-C93A	109.2
H73B	-C73	-O3	109.3	H92B	-C92A	-H92A	109.5
H73A	-C73	-C74	109.4	H93A	-C93A	-C92A	109.4
H73B	-C73	-C74	104.4	H93B	-C93A	-C92A	109.4
H73B	-C73	-H73A	110.7	H93A	-C93A	-C94A	109.4
H74A	-C74	-C73	107.9	H93B	-C93A	-C94A	109.4
H74B	-C74	-C73	105.6	H93B	-C93A	-H93A	109.5
H74C	-C74	-C73	112.7	H94A	-C94A	-C93A	109.1
H74B	-C74	-H74A	105.3	H94B	-C94A	-C93A	109.1
H74C	-C74	-H74A	114.0	H94A	-C94A	-C95A	109.1
H74C	-C74	-H74B	110.8	H94B	-C94A	-C95A	109.1
H81A	-C81	-C82	109.5	H94B	-C94A	-H94A	109.5
H81B	-C81	-C82	109.5	H95A	-C95A	-C94A	108.8
H81C	-C81	-C82	109.5	H95B	-C95A	-C94A	108.8
H81B	-C81	-H81A	109.5	H95A	-C95A	-C96A	108.8
H81C	-C81	-H81A	109.5	H95B	-C95A	-C96A	108.8
H81C	-C81	-H81B	109.5	H95B	-C95A	-H95A	109.5
H83A	-C83	-O5	108.9	H96A	-C96A	-C95A	109.5
H83B	-C83	-O5	108.9	H96B	-C96A	-C95A	109.5
H83A	-C83	-C84	108.9	H96C	-C96A	-C95A	109.5
H83B	-C83	-C84	108.9	H96B	-C96A	-H96A	109.5
H83B	-C83	-H83A	109.5	H96C	-C96A	-H96A	109.5
H84A	-C84	-C83	109.5	H96C	-C96A	-H96B	109.5
H84B	-C84	-C83	109.5	H91D	-C91B	-C92B	109.5
H84C	-C84	-C83	109.5	H91E	-C91B	-C92B	109.5
H84B	-C84	-H84A	109.5	H91F	-C91B	-C92B	109.5
H84C	-C84	-H84A	109.5	H91E	-C91B	-H91D	109.5
H84C	-C84	-H84B	109.5	H91F	-C91B	-H91D	109.5
H91A	-C91A	-C92A	109.5	H91F	-C91B	-H91E	109.5
H91B	-C91A	-C92A	109.5	H92D	-C92B	-C91B	109.2
H91C	-C91A	-C92A	109.5	H92E	-C92B	-C91B	109.2
H91B	-C91A	-H91A	109.5	H92D	-C92B	-C93B	109.2
H91C	-C91A	-H91A	109.5	H92E	-C92B	-C93B	109.2
H91C	-C91A	-H91B	109.5	H92E	-C92B	-H92D	109.5

Table 4. (Cont.)

	Angle(°)		Angle(°)		
H93D	-C93B -C92B	108.9	H94H	-C94C -C93C	108.9
H93E	-C93B -C92B	108.9	H94G	-C94C -C95C	108.9
H93D	-C93B -C94B	108.9	H94H	-C94C -C95C	108.9
H93E	-C93B -C94B	108.9	H94H	-C94C -H94G	109.5
H93E	-C93B -H93D	109.5	H95G	-C95C -C94C	108.9
H94D	-C94B -C93B	108.9	H95H	-C95C -C94C	108.9
H94E	-C94B -C93B	108.9	H95G	-C95C -C96C	108.9
H94D	-C94B -C95B	108.9	H95H	-C95C -C96C	108.9
H94E	-C94B -C95B	108.9	H95H	-C95C -H95G	109.5
H94E	-C94B -H94D	109.5	H96G	-C96C -C95C	109.5
H95D	-C95B -C94B	109.1	H96H	-C96C -C95C	109.5
H95E	-C95B -C94B	109.1	H96I	-C96C -C95C	109.5
H95D	-C95B -C96B	109.1	H96H	-C96C -H96G	109.5
H95E	-C95B -C96B	109.1	H96I	-C96C -H96G	109.5
H95E	-C95B -H95D	109.5	H96I	-C96C -H96H	109.5
H96D	-C96B -C95B	109.5			
H96E	-C96B -C95B	109.5			
H96F	-C96B -C95B	109.5			
H96E	-C96B -H96D	109.5			
H96F	-C96B -H96D	109.5			
H96F	-C96B -H96E	109.5			
H91G	-C91C -C92C	109.5			
H91H	-C91C -C92C	109.5			
H91I	-C91C -C92C	109.5			
H91H	-C91C -H91G	109.5			
H91I	-C91C -H91G	109.5			
H91I	-C91C -H91H	109.5			
H92G	-C92C -C91C	108.6			
H92H	-C92C -C91C	108.6			
H92G	-C92C -C93C	108.6			
H92H	-C92C -C93C	108.6			
H93G	-C93C -C92C	108.3			
H93H	-C93C -C92C	108.3			
H93G	-C93C -C94C	108.3			
H93H	-C93C -C94C	108.3			
H93H	-C93C -H93G	109.5			
H94G	-C94C -C93C	108.9			

Table 5. Intermolecular Distances Less Than 3.5 Å for Aquo, Carbonyl Tetrakis(Pentafluorophenyl)octachloroporphyrin Ruthenium(II).

	Distance(Å)		Distance(Å)
Cl1 –F25	3.140(7)	F23 –F36	3.411(10)
C1 –F43	3.423(12)	F24 –F53	3.439(10)
N1 –F43	3.353(11)	F24 –F54	2.981(10)
C4 –O4	3.436	F24 –F44	3.359(11)
N2 –F33	3.415(10)	F24 –F35	3.036(10)
N3 –O2	3.250(13)	F24 –F25	3.314(9)
Cl4 –C91B	3.460	F24 –F26	3.378(9)
Cl4 –F25	3.152(7)	F25 –F53	2.862(10)
C18 –F43	3.471(12)	F25 –F25	3.264(9)
C19 –F43	2.998(12)	F26 –F33	2.982(9)
C20 –F43	3.057(12)	F26 –F34	3.080(9)
C23 –F54	3.191(13)	F32 –C71	3.249(19)
C24 –F53	3.400(14)	F32 –C72	3.057(17)
C24 –F54	3.039(13)	F32 –O2	3.422(12)
C24 –F25	3.087(13)	F32 –O3	3.208(13)
C25 –F53	3.140(13)	F32 –C74	3.47(4)
C25 –C25	3.417(15)	F32 –C91A	3.283
C25 –F25	3.060(12)	F33 –C91A	3.203
C33 –F26	3.032(13)	F33 –C92A	3.353
C34 –F26	3.100(13)	F33 –C61	3.369(12)
C35 –F24	3.394(13)	F33 –O61	3.176(11)
C43 –F34	3.246(15)	F34 –F43	3.170(11)
C44 –F34	3.189(17)	F34 –F44	3.088(11)
C44 –F35	3.409(17)	F34 –O61	3.035(11)
C45 –F35	3.300(16)	F35 –F44	3.400(11)
C54 –F45	3.104(16)	F35 –F45	3.169(11)
C55 –C96A	3.456	F35 –C71	3.442(19)
C55 –F45	3.157(15)	F35 –O3	3.367(13)
C56 –C96A	3.444	F36 –O3	3.323(13)
F22 –C81	3.490	F36 –C91A	2.576
F22 –C82	3.154	F36 –C91B	2.652
F22 –O5	3.004	F36 –C91C	3.022
F23 –F54	3.296(10)	F42 –F52	3.318(10)
F23 –C91A	3.083	F43 –F52	3.033(11)
F23 –C91B	2.409	F43 –C61	3.362(13)
F23 –C91C	2.711	F43 –O61	3.170(12)
F23 –F35	3.491(10)	F45 –F54	3.013(12)

Table 5. (Cont.)

	Distance(Å)
F45 –F55	3.174(12)
F45 –C96A	3.393
F46 –C95A	3.328
F46 –C96A	3.253
F46 –C95B	3.230
F46 –C96B	3.465
F46 –C95C	3.214
F52 –C74	3.47(4)
F55 –C96A	2.975
F55 –C96B	3.448
F55 –C96C	3.228
F55 –C71	3.47(2)
F55 –C81	3.245
F55 –C82	3.305
F55 –O4	3.449
F56 –C81	3.428
F56 –C96A	3.017
O61 –C92A	3.305
O61 –C92C	3.389
O1 –C81	3.210
O1 –C82	3.371
O1 –O4	2.668
O1 –C96C	3.362
O1 –O2	2.683(12)
O2 –C96C	3.306
O4 –C83	3.060
O5 –O5	3.309
O5 –C84	2.343
C84 –C84	2.453

Table 6. Observed and Calculated Structure Factors for

Aquo, Carbonyl Tetrakis(pentafluorophenyl)porphyrin Ruthenium(II)

The columns contain, in order, ℓ, $10F_{obs}$, $10F_{calc}$ and $10\sigma F_{obs}$. A minus sign preceding F_{obs} indicates that F^2_{obs} is negative.

-15	0	1	
2	893	807	26
4	347	396	32
6	424	432	30
-15	1	1	
1	433	380	21
2	879	871	19
3	427	440	21
4	383	358	22
5	547	531	20
6	504	495	20
-15	2	1	
1	41	25	75
2	-74	23	56
3	507	479	20
4	404	373	21
5	418	405	21
6	227	259	29
-15	3	1	
1	608	584	19
2	127	58	43
3	417	424	21
4	179	108	34
-15	4	1	
1	170	77	35
-14	0	1	
2	663	641	25
4	170	231	45
6	897	867	25
8	179	205	44
10	631	579	26
12	600	555	27
-14	1	1	
1	246	217	26
2	523	485	19
3	153	195	35
4	304	293	23
5	67	80	58
6	608	574	18
7	242	157	26
8	711	719	18
9	301	271	24
10	337	298	23
11	234	169	28
12	-155	38	31
-14	2	1	
1	80	89	53
2	189	204	30
3	249	263	26
4	144	54	37
5	548	521	19
6	434	396	20
7	540	507	19
8	351	383	22
9	250	252	26
10	164	44	35
11	722	695	19
-14	3	1	
1	600	610	18
2	132	108	39
3	715	697	18
4	863	866	18
5	762	743	18
6	87	109	51
7	197	146	30
8	194	122	31
9	1018	994	19
10	247	253	27
11	237	266	28
-14	4	1	
1	335	336	22
2	321	347	23
3	277	229	25
4	208	126	29
5	282	255	24
6	176	7	33
7	648	672	19
8	300	281	24
9	345	326	23
10	150	201	38
-14	5	1	
1	107	0	46
2	911	870	18
3	694	705	18
4	650	608	18
5	325	341	23
6	451	495	20
7	126	55	42
8	735	663	19
-14	6	1	
1	489	514	20
2	39	71	76
3	69	24	60
4	165	201	35
5	-43	42	73
6	459	466	21
7	366	335	22
-14	7	1	
1	222	157	29
2	550	537	19
3	422	360	21
-13	0	1	
2	1663	1611	26
4	537	544	25
6	216	157	37
8	262	310	34
10	79	8	69
12	531	529	26
14	963	972	25
-13	1	1	
1	548	503	18
2	699	657	17
3	193	118	29
4	835	757	17
5	1153	1104	18
6	799	725	17
7	268	280	24
8	-127	85	34
9	-119	100	36
10	205	173	28
11	696	607	18
12	917	852	18
13	85	35	52
14	186	27	32
15	256	170	27
-13	2	1	
1	785	759	17
2	389	339	20
3	1205	1179	18
4	406	444	19
5	215	114	27
6	292	264	23
7	330	316	21
8	78	163	52
9	391	413	20
10	493	517	19
11	228	197	27
12	79	136	54
13	-17	19	91
14	464	443	20
15	790	766	19
-13	3	1	
1	383	344	20
2	390	390	20
3	268	179	24
4	187	4	29
5	945	930	17
6	380	400	20
7	113	133	42
8	-76	42	51
9	156	66	34
10	459	385	19
11	760	760	18
12	106	133	46
13	481	515	20
14	458	438	20
-13	4	1	
1	278	281	23
2	349	326	21
3	664	655	17
4	140	131	36
5	277	260	23
6	238	243	26
7	235	220	26
8	519	445	19
9	906	911	18
10	151	70	36
11	359	393	22
12	-124	2	38
13	355	337	23
14	433	420	21
-13	5	1	
1	-155	24	28
2	120	203	40
3	321	301	22
4	-66	27	56
5	189	262	30
6	360	355	21
7	456	418	19
8	271	250	25
9	235	205	27
10	247	265	27
11	-92	66	48
12	490	529	20
13	716	750	19
-13	6	1	
1	-127	24	35
2	121	236	41
3	-129	70	34
4	315	296	22
5	-47	74	68
6	-73	67	54
7	143	45	37
8	510	516	19
9	72	66	59
10	794	773	18
11	405	409	21
-13	7	1	
1	205	155	29
2	248	257	26
3	-29	75	81
4	181	237	32
5	123	23	42
6	571	556	19
7	24	62	87
8	514	441	20
9	92	27	52
10	267	237	27
-13	8	1	
1	223	183	28
2	470	491	20
3	229	207	28
4	399	466	21
5	143	196	39
6	76	108	58
7	146	131	39
8	62	37	65
-13	9	1	
1	472	444	20
2	195	188	32
3	-156	77	31
4	84	7	55
-12	0	1	
2	222	218	40
4	-229	18	22
6	1027	1071	23
8	-112	115	50
10	-207	6	27
12	808	773	24
14	663	568	25
16	462	422	28
18	287	340	35
-12	1	1	
1	84	77	53
2	320	402	24
3	-166	21	28
4	293	374	21
5	99	171	43
6	68	127	54
7	405	378	19
8	-122	125	34
9	-115	21	36
10	257	315	24
11	127	167	38
12	270	243	23
13	85	78	50
14	800	746	18
15	419	370	20
16	654	654	18
17	294	299	24
18	255	206	27
-12	2	1	
1	117	222	41
2	-131	87	31
3	187	196	28
4	-95	51	41
5	650	686	17
6	227	234	25
7	519	528	17
8	-117	1	36
9	-147	92	29
10	-126	112	34
11	278	300	23
12	257	233	24
13	313	316	22
14	225	230	27
15	111	137	44
16	531	522	19
17	614	587	19
-12	3	1	
1	-135	50	30
2	321	309	20
3	985	1035	17
4	602	620	17
5	-91	64	43
6	563	575	17
7	184	202	29
8	452	450	18
9	513	551	18
10	-176	34	24
11	-185	27	23
12	-85	58	48
13	193	176	30
14	140	121	37
15	752	755	18
16	148	112	37
17	279	156	26
-12	4	1	
1	526	550	17
2	466	433	18
3	372	327	19
4	399	408	19
5	437	492	18
6	35	139	73
7	422	373	19
8	232	235	25
9	-59	18	59
10	196	117	29
11	372	378	20
12	293	325	23
13	563	549	18
14	-139	64	33
15	154	108	36
16	262	261	26
-12	5	1	
1	-113	138	37
2	86	27	48
3	514	516	18
4	453	476	18
5	74	88	53
6	309	239	22
7	931	879	17
8	527	496	18
9	811	785	17
10	140	163	37
11	-72	11	54
12	399	389	20
13	180	151	32
14	431	386	20
15	694	702	19
16	470	436	20
-12	6	1	
1	354	324	20
2	-189	53	22
3	-10	144	93
4	-126	47	34
5	481	503	18
6	415	396	19
7	233	208	26
8	-67	47	56
9	253	252	25
10	396	387	20
11	150	195	36
12	503	488	19
13	217	267	29
14	-52	84	68
15	148	222	39
-12	7	1	
1	147	167	35
2	51	26	64
3	232	261	26
4	432	392	19
5	-49	47	65
6	543	487	18
7	147	119	36
8	945	886	18
9	223	96	28
10	543	523	19
11	305	288	24
12	160	160	36
13	269	242	26
-12	8	1	
1	470	441	19
2	369	309	21
3	355	365	21
4	439	438	20
5	210	112	29
6	797	803	18
7	295	285	24
8	196	178	31
9	438	377	20
10	683	713	19
11	214	140	30
12	364	379	23
-12	9	1	
1	151	55	36
2	224	255	28
3	178	188	32
4	374	312	21
5	94	62	50
6	389	425	21
7	386	356	22
8	426	427	21
9	559	556	20
10	157	10	38
-12	10	1	
1	355	296	22
2	202	145	31
3	110	84	46
4	182	146	33
5	743	724	19
6	231	154	29
7	677	568	19
-11	0	1	
2	1295	1283	26
4	536	490	26
6	-183	112	32
8	455	547	28
10	508	466	24
12	762	748	23
14	788	760	24
16	390	466	28
18	201	258	42
20	638	603	27
-11	1	1	
1	-113	24	38

2	51	99	65
3	-58	139	60
4	830	744	18
5	166	260	33
6	573	572	19
7	52	178	65
8	-85	57	49
9	-176	1	25
10	561	601	17
11	601	590	17
12	182	249	29
13	335	339	20
14	-141	35	30
15	337	351	21
16	538	523	18
17	-174	49	26
18	237	293	27
19	-51	41	68
20	167	130	36

-11 2 1

1	1038	1070	18
2	353	312	21
3	247	238	26
4	-132	9	33
5	317	337	23
6	-137	71	32
7	-40	127	72
8	213	334	29
9	-86	26	50
10	713	749	16
11	733	686	17
12	-88	147	45
13	917	951	17
14	337	335	21
15	388	400	20
16	-185	34	23
17	-199	78	22
18	96	162	49
19	387	389	22

-11 3 1

1	372	355	21
2	-41	126	70
3	461	472	20
4	-98	84	43
5	595	645	19
6	68	100	58
7	611	656	19
8	99	158	48
9	21	111	81
10	385	352	19
11	722	729	17
12	166	195	31
13	193	204	29
14	412	374	19
15	-105	110	41
16	-86	120	48
17	481	502	19
18	223	197	28
19	409	378	21

-11 4 1

1	1079	1075	19
2	370	331	21
3	-142	37	32
4	-160	50	28
5	-72	12	55
6	158	204	35
7	602	567	16
8	456	428	18
9	1358	1348	18
10	457	426	18
11	524	516	18
12	857	851	17
13	563	562	18
14	28	123	79
15	155	245	35
16	-156	47	29
17	-174	34	27
18	112	131	45
19	299	276	25

-11 5 1

1	427	412	21
2	151	6	36
3	1008	1030	19
4	178	207	33
5	156	117	31
6	797	785	16
7	286	358	22
8	522	558	17
9	321	256	21
10	408	394	19
11	659	665	17
12	85	110	50
13	229	231	26
14	-150	46	30
15	216	281	28
16	-66	164	59
17	531	535	19
18	371	380	22

-11 6 1

1	632	673	16
2	64	65	55
3	151	131	32
4	615	677	17
5	49	52	63
6	75	175	52
7	330	323	21
8	728	731	17
9	252	261	24
10	801	770	17
11	322	281	22
12	296	307	23
13	-145	74	31
14	363	370	21
15	185	179	32
16	72	89	59
17	378	416	22

-11 7 1

1	169	141	30
2	463	488	18
3	-82	168	47
4	-154	33	28
5	314	301	21
6	518	505	18
7	-28	100	78
8	-95	21	44
9	117	161	41
10	552	550	18
11	240	225	26
12	542	545	19
13	218	196	28
14	-126	33	37
15	403	419	21
16	346	303	23

-11 8 1

1	213	151	27
2	98	37	45
3	609	580	17
4	-146	4	30
5	-87	23	47
6	508	465	18
7	580	500	18
8	384	366	20
9	369	325	21
10	249	285	26
11	298	255	24
12	-75	63	55
13	201	138	31
14	464	465	20
15	153	143	38

-11 9 1

1	605	609	18
2	153	96	34
3	136	233	37
4	128	91	39
5	-65	38	57
6	-156	90	29
7	412	377	20
8	-30	42	80
9	282	263	25
10	178	255	33
11	288	231	25
12	311	355	24
13	394	377	22

-11 10 1

1	440	418	20
2	110	77	44
3	193	208	30
4	-87	5	49
5	121	39	42
6	404	459	21
7	391	415	21
8	-100	78	46
9	208	221	30
10	35	102	81
11	-123	116	40

-11 11 1

1	-168	66	28
2	237	291	28
3	257	230	26
4	223	82	29
5	545	543	19
6	277	273	26
7	189	211	33
8	154	195	38

-11 12 1

1	119	86	45
2	191	155	33

-10 0 1

2	617	609	24
4	2673	2595	34
6	371	285	28
8	153	199	46
10	280	306	33
12	447	503	28
14	355	368	27
16	765	782	24
18	167	228	45
20	192	208	43

-10 1 1

1	1104	1128	18
2	1697	1637	21
3	237	87	24
4	840	796	17
5	98	5	43
6	890	825	17
7	984	975	18
8	486	469	19
9	310	319	22
10	97	148	46
11	402	445	21
12	455	418	20
13	244	240	23
14	879	901	17
15	128	142	37
16	-123	35	35
17	-137	70	32
18	-134	93	33
19	176	227	32
20	632	639	19
21	449	454	20

-10 2 1

1	322	331	21
2	143	57	33
3	1529	1480	20
4	414	393	19
5	909	871	18
6	-108	23	37
7	-68	29	53
8	705	693	18
9	252	268	25
10	305	305	23
11	614	621	19
12	627	616	19
13	103	145	42
14	-119	15	35
15	39	100	70
16	526	533	18
17	758	721	17
18	29	161	79
19	-164	60	28
20	211	243	29
21	146	185	39

-10 3 1

1	1357	1292	19
2	485	488	18
3	644	623	17
4	15	107	86
5	270	223	23
6	77	90	51
7	500	509	19
8	736	734	18
9	49	84	66
10	-135	26	33
11	133	120	39
12	66	38	54
13	547	572	17
14	-104	92	39
15	491	545	18
16	54	19	62
17	218	272	27
18	63	193	60
19	374	426	21
20	241	284	27
21	195	238	32

-10 4 1

1	833	786	18
2	83	84	49
3	675	633	18
4	1125	1071	18
5	690	715	18
6	-142	47	30
7	180	218	31
8	420	361	20
9	812	865	19
10	158	149	35
11	940	944	19
12	-11	129	90
13	-114	71	36
14	208	214	27
15	423	389	19
16	-142	125	31
17	332	397	22
18	235	277	27
19	58	97	64
20	-21	108	90

-10 5 1

1	83	121	50
2	810	810	18
3	591	600	18
4	53	18	64
5	525	526	19
6	-192	66	22
7	190	304	31
8	-75	13	54
9	95	95	49
10	-95	32	41
11	-89	72	44
12	94	103	46
13	270	299	23
14	666	624	17
15	283	274	23
16	-62	166	58
17	-168	61	27
18	-107	141	42
19	237	268	28
20	174	220	35

-10 6 1

1	205	272	29
2	-74	51	52
3	293	329	24
4	397	407	21
5	44	55	71
6	-106	62	42
7	291	298	25
8	802	805	19
9	111	79	40
10	877	857	17
11	49	35	65
12	446	443	19
13	230	273	26
14	108	205	43
15	209	230	28
16	378	420	21
17	-120	95	38
18	-140	81	34
19	-176	78	28

-10 7 1

1	173	163	33
2	519	522	20
3	454	456	20
4	187	227	32
5	269	295	26
6	491	530	17
7	-80	73	47
8	506	501	18
9	254	214	24
10	400	431	19
11	-123	19	35
12	343	355	21
13	-56	121	62
14	260	280	25
15	-108	19	41
16	-192	26	24
17	-107	55	43
18	252	221	27

-10 8 1

1	303	292	21
2	425	438	18
3	-144	11	29
4	97	96	44
5	625	572	17
6	452	482	18
7	202	225	28
8	140	162	36
9	640	652	17
10	-37	22	73
11	-145	32	31
12	255	249	25
13	152	194	35
14	-74	8	55
15	111	126	45
16	355	376	22
17	-146	117	34

-10 9 1

1	-97	11	42
2	219	140	26
3	673	663	17
4	-112	103	38
5	219	146	27
6	550	572	18
7	674	656	17
8	343	275	21
9	587	575	18
10	-131	101	34
11	-108	36	41
12	242	262	27
13	307	341	24
14	477	454	20
15	102	150	49
16	-77	3	57

-10 10 1

1	505	552	18
2	218	243	27
3	-132	68	33
4	216	205	27
5	281	327	24
6	199	232	29
7	318	303	22
8	-54	83	64
9	-155	2	30
10	-42	41	72
11	442	377	20
12	397	360	21
13	-139	4	35
14	-135	3	37

-10 11 1

1	338	334	22
2	202	219	29
3	550	529	19
4	99	43	47
5	346	317	22
6	363	393	22
7	216	252	29
8	259	242	26
9	284	265	25
10	-74	7	57
11	-105	70	46
12	217	241	31

-10 12 1

1	-113	103	41
2	117	253	44
3	-108	120	43
4	51	35	69
5	397	381	21
6	348	296	23
7	94	69	52
8	101	64	50
9	72	72	79

-10 13 1

1	53	119	70
2	172	189	35
3	197	279	32

-9 0 1

2	854	902	22
4	277	302	28
6	486	488	24
8	1656	1685	26
10	649	625	24
12	594	649	25
14	470	511	28
16	347	401	28
18	-58	94	77
20	147	226	49
22	399	350	30

-9 1 1

1	585	621	16
2	439	396	17
3	462	451	17
4	431	390	17
5	287	306	20
6	1237	1133	18
7	191	248	26
8	220	222	24
9	122	133	37
10	-66	81	52
11	139	195	35
12	57	99	61
13	131	191	38
14	-119	26	38
15	746	747	19
16	148	221	33
17	475	538	18
18	444	490	19
19	-164	79	27
20	99	137	46
21	211	252	29
22	328	350	23
23	32	109	83

-9 2 1

1	262	219	21
2	-139	133	25
3	23	10	74
4	-74	9	44
5	559	540	17
6	287	283	21
7	1408	1397	19
8	626	666	17
9	421	363	19
10	-107	77	38
11	194	153	29
12	-126	44	34
13	562	542	19
14	-85	82	49
15	-154	93	26
16	551	600	17
17	-78	122	49
18	460	488	19
19	72	112	55
20	423	433	20
21	29	185	82
22	43	157	74
23	91	77	53

-9 3 1

1	292	288	20
2	183	157	26
3	85	77	43
4	1165	1147	18
5	1395	1411	19
6	682	627	17
7	41	89	66
8	455	448	18
9	459	453	19
10	163	187	32
11	1098	1085	19
12	-164	73	26
13	-129	76	35
14	442	413	21
15	-121	184	34
16	153	185	33
17	836	845	17
18	267	300	24
19	184	214	31
20	99	183	47
21	237	270	27
22	128	158	42

-9 4 1

1	1110	1053	17
2	335	333	19
3	963	950	17
4	460	382	18
5	-72	11	48
6	772	774	17
7	655	647	17
8	477	472	19
9	514	544	19
10	-99	35	42
11	152	170	35
12	210	195	29
13	-156	57	29
14	277	269	22
15	494	541	18
16	708	725	17
17	62	79	59
18	448	503	19
19	739	749	18
20	149	93	37
21	475	494	20
22	32	34	83

-9 5 1

1	354	391	19
2	-110	27	35
3	1127	1121	18
4	450	481	18
5	538	501	18
6	742	737	17
7	277	310	23
8	146	148	35
9	994	944	18
10	626	663	19
11	60	55	62
12	411	408	21
13	-70	78	51
14	523	514	17
15	398	379	19
16	825	786	17
17	212	232	28
18	152	134	35
19	374	452	21
20	44	114	72
21	184	260	33

-9 6 1

1	64	127	55
2	500	533	18
3	186	184	29
4	34	37	73
5	470	463	19
6	327	335	22
7	418	434	20
8	497	531	19
9	-74	0	54
10	157	70	36
11	773	775	19
12	339	321	20
13	286	308	22
14	606	615	17
15	308	296	22
16	145	172	36
17	-147	62	30
18	521	517	19
19	149	187	37
20	466	492	20
21	-163	27	30

-9 7 1

1	158	186	33
2	477	461	19
3	-37	35	72
4	838	800	18
5	473	470	20
6	295	270	24
7	254	236	26
8	513	512	20
9	314	357	24
10	249	276	23
11	476	435	18
12	460	522	18
13	80	171	51
14	-88	138	46
15	114	122	42
16	337	360	22
17	243	260	26
18	625	672	19
19	66	243	61
20	122	160	44

-9 8 1

1	816	782	18
2	645	607	19
3	165	163	34
4	195	221	31
5	190	111	31
6	609	587	19
7	186	150	33
8	342	385	20
9	-82	125	47
10	-138	65	31
11	112	153	42
12	456	457	19
13	-126	0	35
14	14	142	91
15	469	509	19
16	302	308	23
17	102	157	48
18	205	251	31
19	-169	12	29

-9 9 1

1	444	456	21
2	454	380	21
3	543	571	17
4	95	115	44
5	253	328	23
6	190	218	28
7	283	256	22
8	602	649	17
9	580	550	18
10	93	153	47
11	290	280	23
12	-73	111	53
13	214	328	28
14	-115	45	39
15	-99	81	45
16	-18	147	92
17	349	358	23

-9 10 1

1	148	146	34
2	289	329	22
3	309	287	22
4	146	155	35
5	369	389	20
6	264	305	24
7	537	511	18
8	454	490	19
9	252	334	25
10	134	185	38
11	305	317	23
12	-188	21	24
13	306	317	24
14	-36	55	78
15	117	181	45
16	-68	110	61

-9 11 1

1	212	208	27
2	393	389	20
3	255	241	25
4	231	230	26
5	665	592	18
6	259	249	25
7	158	123	34
8	158	161	34
9	320	374	23
10	29	69	81
11	144	178	38
12	-99	123	46
13	-149	0	33
14	50	207	72

-9 12 1

1	458	424	19
2	185	187	31
3	174	192	32
4	253	291	26
5	113	70	44
6	315	299	23
7	276	294	25
8	-70	98	57
9	-116	113	41
10	114	33	45
11	-99	115	48
12	233	279	29

-9 13 1

1	98	51	48
2	159	226	36
3	-95	7	47
4	388	347	21
5	104	58	48
6	169	175	35
7	-101	78	47
8	353	326	23

-8 0 1

2	1524	1513	24
4	559	608	21
6	126	71	43
8	605	588	22
10	61	105	68
12	300	245	30
14	507	557	26
16	537	526	27
18	984	1008	23
20	406	358	27
22	853	911	25
24	300	391	35

-8 1 1

1	1135	1158	16
2	1035	1115	16
3	571	562	15
4	467	485	16
5	425	447	16
6	362	361	17
7	571	581	16
8	1250	1175	17
9	364	339	18
10	711	768	16
11	1347	1289	19
12	585	602	17
13	333	378	21
14	699	747	18
15	-41	165	71
16	-103	109	43
17	38	119	69
18	561	557	17
19	407	367	19
20	581	579	18
21	-66	29	56
22	89	59	51
23	-86	119	51
24	146	183	39

-8 2 1

1	998	1086	16
2	223	260	21
3	806	907	15
4	-52	102	52
5	706	719	15
6	1047	1000	16
7	582	624	16
8	302	276	19
9	241	207	22
10	1245	1260	18
11	557	589	17
12	-120	42	33
13	329	376	21
14	578	586	18
15	265	329	25
16	244	265	27
17	679	652	16
18	256	231	24
19	336	323	21
20	438	445	19
21	581	556	18
22	156	67	35
23	688	678	19
24	-166	34	30

-8 3 1

1	766	835	15
2	115	164	33
3	425	441	16
4	131	69	31
5	1564	1565	19
6	89	82	40
7	372	422	18
8	61	128	52
9	936	996	17
10	811	780	17
11	578	595	17
12	105	157	42
13	599	593	18
14	72	180	55
15	479	543	20
16	416	435	21
17	423	456	18
18	-86	116	46
19	499	527	18
20	49	126	66
21	460	510	19
22	-101	98	44
23	448	430	20
24	237	249	29

-8 4 1

1	189	163	24
2	39	153	61
3	729	755	16
4	426	453	17
5	483	522	17
6	469	438	17
7	1020	1004	17
8	597	587	17
9	1305	1351	19
10	186	114	28
11	1071	1082	18
12	392	355	20
13	156	245	34
14	188	160	31
15	597	597	19
16	264	233	22
17	-31	54	75
18	146	225	35
19	-111	15	39
20	32	116	77
21	454	464	20
22	224	208	29
23	-35	122	80

-8 5 1

1	513	511	16
2	-148	58	24
3	124	140	34
4	446	479	17
5	567	572	17
6	340	373	19
7	153	102	31
8	86	22	46
9	849	854	17
10	-109	19	38
11	-152	3	28
12	230	289	27
13	671	669	19
14	477	463	20
15	394	413	19
16	-95	138	42
17	51	182	63
18	-122	94	36
19	192	216	30
20	357	360	21
21	129	212	41
22	15	58	94
23	261	257	27

-8 6 1

1	417	412	18
2	375	353	19
3	800	791	17
4	546	526	17
5	683	669	17
6	1123	1174	18
7	518	485	18
8	749	710	18
9	217	184	27
10	776	770	18
11	-33	56	76
12	193	219	31
13	193	240	31
14	729	720	16
15	420	437	19
16	241	288	25
17	-149	16	29
18	-48	92	66
19	348	357	21
20	103	150	46
21	336	265	23
22	326	338	24

-8 7 1

1	522	455	18
2	737	755	17
3	-81	70	46
4	331	289	21
5	512	476	18
6	405	414	20
7	449	419	19
8	798	731	18
9	421	447	20
10	129	44	40
11	347	365	22
12	940	973	19
13	438	429	18
14	452	454	18
15	257	265	24
16	51	161	65
17	-148	44	30
18	519	548	19
19	85	138	52
20	276	266	25
21	120	102	44

-8 8 1

1	153	25	33
2	807	819	18
3	764	821	18
4	683	670	18
5	152	175	35
6	-55	114	62
7	104	164	45
8	287	302	24
9	-130	61	35
10	553	521	20
11	113	41	40
12	618	622	17
13	267	252	23
14	127	186	39
15	-86	115	47
16	403	420	20
17	125	100	40
18	137	196	39
19	-118	53	40
20	-144	92	34

-8 9 1

1	707	671	18
2	414	381	20
3	560	492	19
4	565	598	19
5	187	197	32
6	168	199	34
7	410	445	21
8	116	152	42
9	190	240	28
10	-111	58	38
11	749	686	17
12	658	643	17
13	476	476	19
14	222	280	27
15	142	163	37
16	72	17	57
17	558	562	19
18	244	281	27
19	192	228	33

-8 10 1

1	397	394	22
2	205	111	30
3	671	655	19
4	320	322	20
5	382	391	19
6	439	448	18
7	-31	25	75
8	122	89	39
9	563	548	18
10	488	511	18
11	442	418	19
12	67	120	58
13	113	153	43
14	-96	66	45
15	649	674	18
16	-78	79	54
17	381	359	22
18	250	310	28

-8 11 1

1	466	456	18
2	327	309	21
3	151	83	33
4	322	316	21
5	83	60	50
6	240	174	25
7	763	748	17
8	92	38	48
9	211	166	28
10	151	183	35
11	-32	106	78
12	460	391	20
13	542	536	19
14	44	65	73
15	130	157	42
16	118	21	45

-8 12 1

1	-87	20	46
2	448	448	19
3	-28	21	79
4	230	236	26
5	395	379	20
6	-14	13	91
7	163	204	33
8	266	251	25
9	399	364	21
10	569	539	19
11	410	433	21
12	169	242	35
13	-114	108	42
14	-100	98	48

-8 13 1

1	115	1	42
2	115	139	42
3	186	230	31
4	385	402	21
5	-94	115	46
6	317	310	23
7	156	180	36
8	499	542	20
9	137	74	40
10	119	92	44
11	64	40	64

-8 14 1

1	-84	69	51
2	244	316	27
3	117	5	44
4	305	211	24
5	-139	67	35
6	105	16	48
7	178	227	34

-7 0 1

2	1548	1528	23
4	1553	1548	23
6	1166	1122	21
8	989	935	21
10	389	402	24
12	871	903	23
14	1338	1319	25
16	898	948	25
18	1251	1322	27
20	235	225	35
22	-81	19	66
24	-80	93	70

-7 1 1

1	716	694	14
2	1355	1316	17
3	556	485	14
4	1792	1683	19
5	498	468	15
6	607	539	15
7	-110	53	29
8	693	664	15
9	539	468	16
10	-116	85	29
11	474	491	17
12	770	807	16
13	480	514	18
14	382	391	19
15	401	416	20
16	1040	1013	18
17	168	128	33
18	379	334	22
19	303	313	21
20	989	1031	17
21	611	606	18
22	-149	55	30
23	251	316	26
24	-109	50	43
25	-144	133	35

-7 2 1

1	590	574	14
2	892	880	15
3	907	954	15
4	502	463	15
5	491	373	15
6	495	507	15
7	1459	1413	18
8	294	329	19
9	550	568	16
10	252	301	21
11	281	320	20
12	313	319	20
13	964	1020	17
14	350	312	20
15	-48	105	65
16	305	276	23
17	1441	1411	20
18	549	572	20
19	130	202	37
20	273	268	23
21	296	350	23
22	209	284	28
23	-131	40	35
24	495	436	20
25	262	305	27

-7 3 1

1	620	607	14
2	90	3	36
3	1856	1778	20
4	581	568	15
5	555	548	15
6	392	394	16
7	545	552	16
8	1086	1074	17
9	1084	1098	17
10	191	117	25
11	716	692	16
12	226	174	24
13	98	188	43
14	793	816	18
15	1613	1621	21
16	555	556	19
17	491	434	20
18	318	287	20
19	531	561	17
20	126	93	39
21	213	314	28
22	-49	173	67
23	-102	14	44
24	-119	83	40
25	-82	49	55

-7 4 1

1	869	861	15
2	111	73	33
3	453	441	16
4	634	651	15
5	888	912	16
6	278	270	19
7	280	259	20
8	399	405	17
9	128	50	33
10	151	153	30
11	788	798	17
12	242	250	24
13	777	763	17
14	524	453	19
15	934	955	18
16	247	245	26
17	550	511	20
18	654	640	17
19	691	632	17
20	442	468	19
21	-117	38	38
22	-173	16	26
23	426	423	21
24	-105	60	45

-7 5 1

1	609	542	15
2	913	863	16
3	1336	1337	18
4	741	745	16
5	151	97	28
6	-79	45	41
7	952	963	17
8	600	563	16
9	1439	1431	19
10	350	360	20
11	-67	21	52
12	36	3	71
13	547	550	18
14	1628	1638	21
15	1397	1384	20
16	502	498	20
17	451	495	18
18	330	287	21
19	343	314	21
20	374	381	20
21	387	411	20
22	-75	122	54
23	144	164	39
24	124	93	44

-7 6 1

1	713	689	16
2	1043	1023	17
3	146	181	29
4	211	203	24
5	689	737	16
6	872	889	17
7	112	132	37
8	249	233	23
9	254	278	23
10	593	552	18
11	39	21	70
12	1059	1051	18
13	328	248	22
14	534	500	19
15	141	59	38
16	64	20	56
17	177	226	30
18	557	562	18
19	-80	66	50
20	487	474	19
21	91	242	50
22	215	225	29
23	132	157	42

-7 7 1

1	308	366	20
2	748	710	16
3	219	171	24
4	786	777	17
5	40	92	65
6	163	195	30
7	177	132	29
8	954	937	18
9	295	311	22
10	621	614	18
11	120	62	41
12	301	273	23
13	1012	1017	19
14	801	819	19
15	830	777	17
16	624	607	17
17	222	212	26
18	163	263	33
19	31	93	78
20	281	257	24
21	208	190	30
22	736	725	19

-7 8 1

1	342	369	20
2	116	191	38
3	-200	17	18
4	-20	129	81
5	847	824	18
6	1712	1676	21
7	478	496	19
8	330	253	22
9	98	63	46
10	121	77	41
11	356	355	22
12	681	667	19
13	389	376	19
14	643	579	17
15	43	85	69
16	448	501	19
17	143	118	36
18	65	96	59
19	297	307	23
20	203	285	30
21	228	155	29

-7 9 1

1	-93	87	43
2	236	236	25
3	1049	1057	18
4	1124	1049	19
5	128	97	39
6	143	204	36
7	176	182	32
8	317	324	23
9	876	847	19
10	146	155	38
11	160	150	31
12	436	465	18
13	141	87	35
14	19	98	85
15	180	150	31
16	167	136	33
17	91	18	49
18	-140	4	33
19	-58	107	64
20	-48	29	72

-7 10 1

1	694	650	18
2	460	484	20
3	128	54	40
4	190	154	31
5	725	724	19
6	194	115	31
7	969	962	19
8	196	27	27
9	101	112	43
10	133	141	36
11	555	564	18
12	445	437	19
13	636	625	18
14	237	264	26
15	110	120	44
16	301	314	23
17	-135	60	35
18	217	211	29
19	563	574	20

-7 11 1

1	243	253	27
2	499	499	18
3	621	636	16
4	318	275	20
5	438	414	18
6	320	353	21
7	290	308	22
8	621	620	17
9	559	593	18
10	-69	35	55
11	601	571	18
12	-136	37	33
13	-61	94	60
14	-97	3	45
15	219	177	29
16	-62	141	62
17	192	159	33

-7 12 1

1	329	307	21
2	130	83	37
3	99	81	45
4	128	193	38
5	186	54	29
6	841	784	17
7	576	565	18
8	205	211	28
9	-79	8	51
10	-147	74	31
11	91	88	50
12	376	372	21
13	307	328	24
14	47	50	71
15	78	101	58
16	-148	28	34

-7 13 1

1	90	122	47
2	258	197	24
3	106	85	43

4	600	560	18
5	144	192	36
6	254	280	25
7	41	16	72
8	195	169	30
9	208	96	29
10	477	487	20
11	-75	100	56
12	104	59	48
13	-174	77	28

-7 14 1

1	184	65	30
2	270	280	24
3	128	192	39
4	61	99	61
5	209	201	29
6	245	305	27
7	251	266	27
8	383	395	22
9	127	103	43
10	266	231	27

-7 15 1

1	180	117	32
2	187	250	32
3	181	191	33
4	275	218	25
5	266	198	26

-6 0 1

2	507	605	19
4	2720	2526	31
6	534	521	19
8	836	806	20
10	1836	1820	26
12	524	490	23
14	395	412	26
16	1207	1232	25
18	293	351	33
20	-26	91	96
22	488	480	26
24	-142	98	45
26	724	674	26

-6 1 1

1	1650	1536	18
2	538	537	13
3	1686	1532	18
4	214	86	19
5	1084	998	15
6	1619	1481	18
7	600	593	14
8	173	199	23
9	903	882	15
10	1074	1112	16
11	1027	960	16
12	689	714	16
13	267	273	21
14	292	242	21
15	650	635	17
16	884	875	18
17	622	635	18
18	506	494	19
19	443	484	21
20	552	582	17
21	142	197	35
22	568	577	18
23	-100	12	43
24	-149	114	31
25	-192	49	24
26	429	398	21

-6 2 1

1	628	635	13
2	1118	1077	15
3	1065	999	15
4	1705	1481	18
5	284	254	17
6	120	140	29
7	921	949	15
8	616	546	15
9	1380	1365	17
10	1080	1076	16
11	628	605	16
12	106	209	36
13	932	947	17
14	201	189	26
15	812	812	17
16	698	686	18
17	871	852	18
18	368	356	22
19	237	280	28
20	795	800	17
21	172	135	31
22	-128	107	35
23	502	520	19
24	106	195	46
25	364	368	22
26	101	26	50

-6 3 1

1	1122	1083	15
2	224	329	19
3	62	112	43
4	256	229	18
5	894	816	15
6	485	516	15
7	1657	1650	19
8	1212	1253	16
9	474	381	16
10	584	510	16
11	954	927	16
12	-186	23	18
13	892	882	17
14	421	426	18
15	291	327	22
16	-32	18	75
17	690	693	18
18	462	424	20
19	701	685	19
20	124	169	38
21	-168	33	26
22	-108	71	40
23	302	327	23
24	138	172	39
25	598	573	19
26	173	142	36

-6 4 1

1	750	700	14
2	381	418	15
3	1301	1305	16
4	483	451	15
5	1035	1045	15
6	303	259	18
7	821	829	15
8	874	883	16
9	1460	1459	18
10	631	681	16
11	515	507	17
12	1013	1005	17
13	225	294	24
14	574	547	18
15	862	841	18
16	391	347	20
17	566	525	19
18	-76	76	54
19	571	514	17
20	170	172	31
21	740	774	17
22	468	492	19
23	137	207	38
24	-111	76	42
25	169	124	36

-6 5 1

1	83	65	38
2	630	574	15
3	261	196	19
4	78	99	41
5	675	610	15
6	2024	1934	21
7	741	662	15
8	734	751	16
9	203	216	24
10	33	44	67
11	771	757	17
12	820	803	17
13	525	559	18
14	382	393	20
15	253	251	25
16	431	519	20
17	506	563	20
18	416	424	18
19	530	535	17
20	196	247	29
21	128	142	39
22	172	138	32
23	477	490	20
24	512	509	20
25	214	223	31

-6 6 1

1	373	350	17
2	1330	1291	17
3	237	221	21
4	912	907	16
5	55	10	52
6	195	147	24
7	391	437	17
8	907	850	16
9	266	212	21
10	1318	1350	18
11	394	303	19
12	33	40	73
13	102	57	43
14	764	752	18
15	347	341	22
16	599	643	19
17	73	139	51
18	154	130	33
19	12	48	91
20	596	564	18
21	145	107	36
22	549	577	19
23	-77	10	55
24	123	152	44

-6 7 1

1	530	454	16
2	111	12	35
3	527	561	16
4	139	188	30
5	166	113	27
6	992	990	17
7	497	530	17
8	-52	72	57
9	306	338	21
10	254	295	24
11	617	589	18
12	1316	1314	19
13	160	139	34
14	69	69	57
15	259	266	26
16	237	243	24
17	229	251	25
18	753	736	17
19	92	99	48
20	61	102	60
21	-70	47	56
22	253	227	26
23	-57	75	65

-6 8 1

1	97	13	40
2	465	461	17
3	1114	1094	17
4	136	28	33
5	287	329	21
6	123	83	36
7	178	40	29
8	976	965	18
9	966	924	18
10	613	581	18
11	-47	68	67
12	279	291	24
13	135	154	39
14	288	251	25
15	413	422	18
16	449	422	18
17	76	154	53
18	-15	34	90
19	41	96	71
20	432	459	20
21	495	512	20
22	326	329	23

-6 9 1

1	410	396	19
2	153	218	32
3	216	232	26
4	226	228	25
5	937	958	18
6	-93	134	43
7	613	643	18
8	350	348	21
9	207	131	29
10	215	260	28
11	510	539	20
12	397	393	22
13	300	314	21
14	222	210	26
15	243	262	25
16	-151	10	29
17	-58	25	61
18	467	427	19
19	246	284	26
20	155	215	36
21	290	303	25

-6 10 1

1	378	332	20
2	73	86	53
3	381	435	20
4	-20	45	84
5	273	285	24
6	140	118	37
7	751	751	18
8	254	179	26
9	918	970	19
10	152	39	37
11	119	101	39
12	185	231	29
13	266	282	24
14	364	399	20
15	120	162	40
16	-106	9	41
17	-142	127	32
18	75	189	56
19	303	289	24
20	171	149	35

-6 11 1

1	84	158	50
2	211	224	28
3	125	130	40
4	318	313	23
5	740	716	19
6	157	89	36
7	714	683	19
8	238	266	24
9	256	298	23
10	267	337	23
11	451	473	19
12	577	575	18
13	369	378	20
14	-97	134	44
15	-66	106	57
16	-129	48	36
17	291	304	24
18	294	284	25
19	402	369	22

-6 12 1

1	510	493	17
2	534	455	17
3	339	353	20
4	350	320	20
5	365	360	19
6	-77	44	50
7	99	46	45
8	518	506	18
9	498	533	18
10	231	226	26
11	-31	27	77
12	-108	66	41
13	379	419	21
14	-80	154	52
15	-67	116	59
16	298	298	25
17	340	359	23

-6 13 1

1	455	478	18
2	306	314	21
3	213	245	26
4	306	306	21
5	264	244	24
6	592	643	18
7	265	300	24
8	289	323	23
9	151	53	35
10	381	395	21
11	124	73	41
12	247	323	27
13	25	159	86
14	305	259	24
15	109	116	48

-6 14 1

1	177	63	30
2	309	337	22
3	392	368	20
4	514	544	18
5	-82	102	49
6	123	21	40
7	232	196	27
8	468	506	20
9	-138	75	34
10	182	226	33
11	103	176	48
12	126	216	43

-6 15 1

1	291	265	23
2	449	461	20
3	131	63	39
4	108	132	44
5	303	300	23
6	303	396	24
7	244	128	27
8	259	226	27

-5 0 1

2	157	236	30
4	2323	2319	27
6	1313	1409	20
8	2245	2154	27
10	1062	974	21
12	282	259	26
14	585	464	23
16	713	656	24
18	633	666	25
20	1034	1058	26
22	484	386	26
24	577	617	26
26	408	373	30

-5 1 1

1	2075	2044	20
2	1555	1467	17
3	2047	1929	20
4	939	840	13
5	532	525	13
6	-53	35	44
7	1141	1232	15
8	928	908	14
9	371	356	15
10	352	365	16
11	-95	28	33
12	654	653	15
13	1373	1370	18
14	1198	1164	17
15	1007	967	17
16	1026	1046	18
17	764	777	18
18	791	816	18
19	154	191	35
20	223	148	29
21	359	296	20
22	958	994	17
23	108	114	43
24	214	210	28
25	101	168	48
26	503	503	20
27	197	159	33

-5 2 1

1	1900	1870	19
2	694	768	13
3	2875	2797	26
4	392	421	14
5	1421	1323	16
6	1587	1567	17
7	193	255	20
8	786	691	14
9	313	241	17
10	771	854	15
11	35	87	61
12	1427	1438	18
13	1235	1284	17
14	339	272	19
15	18	65	80
16	232	333	25
17	203	226	28
18	423	326	20

19	1395	1373	20
20	-83	6	52
21	72	117	53
22	421	391	19
23	332	321	22
24	190	220	31
25	284	334	25
26	37	113	79

-5 3 1

1	2216	2117	21
2	966	901	14
3	697	745	13
4	1401	1522	16
5	1322	1368	16
6	854	855	14
7	229	310	19
8	-114	139	27
9	496	559	15
10	253	212	19
11	1007	958	16
12	670	632	16
13	650	662	16
14	62	120	52
15	659	670	17
16	63	221	56
17	390	342	20
18	297	318	23
19	225	215	28
20	51	91	62
21	389	444	19
22	14	70	91
23	474	446	19
24	-72	42	55
25	463	428	20
26	182	180	34

-5 4 1

1	750	671	13
2	148	232	24
3	-47	23	49
4	97	36	33
5	1010	968	15
6	499	533	14
7	455	388	15
8	1222	1180	16
9	326	379	17
10	682	685	15
11	1800	1749	20
12	190	187	25
13	734	711	16
14	-99	88	37
15	84	115	47
16	345	400	21
17	351	378	21
18	434	407	20
19	172	165	34
20	451	504	18
21	219	166	27
22	405	400	20
23	641	675	18
24	-165	3	28
25	292	286	25
26	-165	15	30

-5 5 1

1	-74	7	37
2	495	546	14
3	427	423	15
4	954	940	15
5	1142	930	16
6	664	711	15
7	373	343	16
8	439	380	16
9	1131	1201	16
10	314	393	19
11	893	882	16
12	576	536	16
13	654	711	17
14	-76	138	47
15	100	113	43
16	333	408	22
17	688	707	18
18	346	325	23
19	271	321	22
20	193	184	28
21	610	658	17
22	338	355	21
23	81	161	53
24	235	253	28
25	-88	155	51

-5 6 1

1	406	352	15
2	-70	99	41
3	582	570	15
4	450	376	15
5	1554	1532	18
6	561	635	15
7	679	717	15
8	103	97	37
9	466	421	17
10	1123	1189	17
11	1472	1413	19
12	784	736	17
13	230	198	25
14	45	179	65
15	-95	79	43
16	459	460	20
17	12	139	95
18	193	242	29
19	-128	104	33
20	322	353	21
21	408	332	20
22	563	543	18
23	280	316	25
24	614	595	19
25	138	237	41

-5 7 1

1	269	206	19
2	891	895	15
3	553	545	15
4	467	412	16
5	309	346	19
6	100	143	37
7	504	551	16
8	1041	1055	17
9	341	288	19
10	797	786	17
11	325	340	20
12	340	321	20
13	366	386	20
14	223	270	27
15	333	374	22
16	-149	66	31
17	152	164	32
18	122	214	38
19	208	265	27
20	585	600	18
21	110	145	43
22	562	590	19
23	8	89	100
24	23	5	90

-5 8 1

1	279	258	19
2	193	176	24
3	156	78	28
4	677	670	16
5	536	498	17
6	711	706	16
7	-75	61	45
8	145	144	32
9	415	430	19
10	638	652	17
11	506	492	18
12	484	459	19
13	155	166	35
14	280	288	25
15	193	202	31
16	545	548	17
17	352	353	20
18	233	281	26
19	111	133	42
20	313	356	22
21	12	88	94
22	160	209	36
23	384	357	22

-5 9 1

1	209	203	24
2	258	213	22
3	1064	1047	17
4	115	47	37
5	515	495	17
6	-35	2	69
7	488	479	18
8	590	537	18
9	1347	1345	19
10	689	609	18
11	119	85	41
12	357	423	22
13	177	117	33
14	1125	1130	20
15	277	262	22
16	372	426	20
17	-117	73	37
18	-97	35	44
19	346	362	21
20	-84	10	50
21	411	426	21
22	338	291	23

-5 10 1

1	335	346	20
2	86	198	46
3	328	380	21
4	156	82	32
5	674	736	18
6	-121	8	34
7	554	528	18
8	673	644	18
9	284	292	24
10	125	113	41
11	738	750	19
12	417	408	21
13	138	93	35
14	308	315	21
15	-125	48	35
16	-72	25	53
17	561	519	18
18	-30	35	79
19	261	205	26
20	-82	164	52
21	78	51	58

-5 11 1

1	333	255	21
2	159	13	32
3	648	631	18
4	713	630	18
5	496	527	19
6	345	319	22
7	706	642	19
8	491	478	20
9	586	576	20
10	120	163	38
11	-56	59	59
12	357	275	20
13	434	484	19
14	239	231	25
15	420	472	20
16	-103	89	42
17	-79	100	52
18	106	131	47
19	163	154	36
20	214	287	31

-5 12 1

1	546	510	19
2	384	343	21
3	322	361	23
4	277	230	25
5	445	526	17
6	422	328	18
7	394	401	19
8	186	151	29
9	198	219	28
10	586	579	17
11	468	470	19
12	540	520	18
13	160	158	34
14	-100	101	43
15	86	160	52
16	417	350	21
17	262	243	26
18	392	366	22

-5 13 1

1	111	115	39
2	246	290	23
3	-119	61	34
4	-130	27	31
5	207	271	26
6	286	293	22
7	147	41	34
8	633	652	17
9	218	116	27
10	407	358	20
11	168	181	33
12	307	284	23
13	-44	81	71
14	563	599	19
15	124	50	43
16	410	424	22

-5 14 1

1	266	242	23
2	166	156	31
3	-112	76	37
4	388	344	19
5	78	104	51
6	280	306	23
7	233	172	26
8	223	132	27
9	288	297	24
10	412	404	20
11	144	87	38
12	327	319	23
13	193	203	32

-5 15 1

1	63	31	59
2	397	398	20
3	249	142	25
4	308	354	22
5	135	121	38
6	-78	82	52
7	357	394	21
8	294	258	24
9	167	117	35
10	-60	73	64

-5 16 1

1	243	238	27
2	52	130	67
3	212	251	29
4	166	93	35
5	421	383	21

-4 0 1

2	1019	617	17
4	3098	2866	33
6	634	814	17
8	141	94	33
10	1407	1533	22
12	-145	61	30
14	526	491	22
16	105	87	52
18	910	892	24
20	184	266	44
22	239	345	34
24	353	342	30
26	589	624	26

-4 1 1

1	-97	46	28
2	815	875	12
3	1587	1474	16
4	1194	1246	14
5	194	336	18
6	512	550	12
7	186	61	20
8	167	197	22
9	1326	1302	16
10	-58	40	44
11	356	361	16
12	366	321	16
13	699	680	15
14	888	860	16
15	847	896	16
16	1069	1087	17
17	-90	37	42
18	453	490	19
19	-92	137	45
20	436	468	20
21	-38	92	76
22	156	191	33
23	443	389	19
24	327	335	22
25	216	270	28
26	292	292	24
27	158	186	37

-4 2 1

1	336	348	13
2	1695	1626	17
3	1023	908	13
4	295	263	14
5	1284	1274	15
6	718	779	13
7	2087	2099	21
8	1210	1123	15
9	238	195	18
10	869	898	14
11	828	768	15
12	430	451	16
13	1625	1673	19
14	301	333	19
15	472	550	17
16	825	840	17
17	-65	154	53
18	82	142	50
19	354	403	22
20	827	805	19
21	186	218	33
22	378	441	20
23	249	289	25
24	89	24	50
25	635	608	18
26	410	326	21
27	236	256	29

-4 3 1

1	668	613	12
2	828	833	13
3	1023	969	13
4	218	156	18
5	571	595	13
6	562	595	13
7	1324	1272	16
8	-122	175	24
9	104	74	32
10	755	752	14
11	1078	1084	16
12	909	900	16
13	541	540	16
14	217	225	23
15	651	611	16
16	253	268	23
17	1090	1108	18
18	557	538	18
19	245	232	26
20	204	237	30
21	285	237	22
22	127	213	38
23	302	309	22
24	-147	2	31
25	254	212	26
26	-129	21	37
27	336	345	24

-4 4 1

1	1754	1700	18
2	699	619	13
3	742	771	13
4	657	655	13
5	199	208	19
6	1057	973	15
7	1044	1075	15
8	171	147	23
9	587	528	14
10	37	143	58
11	92	104	38
12	-89	70	36
13	427	454	17
14	383	391	18
15	989	1031	17
16	267	290	23
17	469	462	19
18	324	360	22
19	677	665	19
20	61	126	64
21	694	703	17
22	429	388	19
23	152	161	35
24	99	204	47
25	348	361	22
26	164	114	36

-4 5 1

1	307	322	15
2	911	985	14
3	383	425	14
4	382	331	15
5	856	902	14
6	991	970	15

7	156	39	25
8	750	700	15
9	472	530	15
10	1374	1345	17
11	919	836	16
12	745	788	16
13	777	789	16
14	323	343	20
15	148	6	32
16	1399	1424	19
17	962	915	18
18	271	214	25
19	56	68	65
20	104	176	42
21	137	10	36
22	443	459	19
23	316	254	22
24	-118	69	39
25	331	337	23
26	216	228	31

-4 6 1

1	183	110	21
2	1271	1366	16
3	392	416	15
4	413	403	15
5	646	603	14
6	178	229	23
7	1039	991	16
8	643	651	15
9	797	809	15
10	909	957	16
11	140	163	30
12	344	375	19
13	-41	160	63
14	1021	976	18
15	1011	1030	18
16	613	595	18
17	-42	9	70
18	270	194	25
19	166	148	30
20	1143	1138	18
21	729	713	17
22	600	569	18
23	132	149	39
24	129	198	41
25	164	146	36

-4 7 1

1	256	296	18
2	378	404	16
3	173	197	24
4	1325	1230	17
5	617	604	15
6	367	356	17
7	1029	991	16
8	595	570	16
9	500	502	16
10	662	652	16
11	1301	1310	18
12	690	682	17
13	250	271	24
14	227	258	26
15	548	543	19
16	164	277	33
17	-51	90	66
18	801	765	16
19	250	271	24
20	402	371	19
21	138	5	37
22	406	407	20
23	-66	41	59
24	734	705	19
25	358	374	23

-4 8 1

1	490	438	15
2	1538	1520	18
3	212	165	22
4	326	317	18
5	351	237	18
6	199	191	24
7	435	450	17
8	1296	1268	18
9	442	453	18
10	362	302	19
11	339	347	20
12	145	201	34
13	435	434	19
14	260	254	25
15	695	638	19
16	-51	106	67
17	233	281	24
18	-128	27	33
19	500	445	18
20	434	474	19
21	-130	44	35
22	399	455	21
23	-87	56	51
24	59	65	67

-4 9 1

1	467	458	16
2	637	616	16
3	559	619	16
4	73	40	46
5	421	408	18
6	498	466	17
7	568	596	17
8	285	214	22
9	222	254	25
10	142	169	35
11	563	562	18
12	558	577	19
13	558	558	19
14	152	81	36
15	275	313	26
16	-180	20	23
17	270	320	23
18	500	502	18
19	265	266	24
20	-169	88	26
21	152	115	36
22	62	57	63
23	753	666	19

-4 10 1

1	213	198	24
2	112	21	36
3	363	385	19
4	160	202	30
5	272	315	22
6	35	112	70
7	381	424	20
8	129	166	37
9	513	507	19
10	199	225	29
11	26	42	82
12	76	147	55
13	63	7	62
14	188	160	28
15	500	515	18
16	127	195	38
17	-166	48	26
18	-43	101	69
19	458	425	19
20	170	97	34
21	480	474	20
22	203	208	31

-4 11 1

1	232	228	25
2	303	295	21
3	138	22	34
4	380	399	20
5	504	427	18
6	48	27	65
7	510	482	19
8	316	351	23
9	338	312	22
10	-124	52	37
11	-72	29	50
12	64	63	56
13	224	235	26
14	237	231	25
15	232	206	26
16	-45	151	68
17	489	503	19
18	70	77	58
19	328	357	23
20	42	0	75

-4 12 1

1	391	408	20
2	279	274	24
3	528	519	19
4	-38	10	72
5	518	546	19
6	434	460	20
7	462	413	20
8	239	177	23
9	-108	90	38
10	110	128	41
11	-113	36	37
12	-110	38	39
13	-98	46	43
14	512	542	18
15	355	377	21
16	73	83	57
17	262	258	26
18	78	88	57
19	-7	67	103

-4 13 1

1	75	19	49
2	10	32	89
3	-74	27	49
4	330	313	20
5	366	408	19
6	369	291	19
7	281	353	22
8	-163	19	25
9	164	131	32
10	136	40	36
11	204	100	28
12	536	509	18
13	103	83	45
14	76	19	56
15	57	45	65
16	599	587	19
17	248	170	28

-4 14 1

1	240	210	24
2	258	175	23
3	91	182	46
4	177	173	30
5	394	409	19
6	506	437	18
7	95	93	45
8	176	45	30
9	190	162	29
10	183	181	31
11	195	207	30
12	-98	3	45
13	-92	58	48
14	604	584	19
15	185	31	33

-4 15 1

1	124	128	39
2	78	81	52
3	205	236	28
4	341	361	21
5	142	14	36
6	224	226	27
7	236	233	26
8	-106	6	42
9	-44	55	70
10	198	159	30
11	122	10	43
12	277	295	26

-4 16 1

1	393	343	21
2	294	289	24
3	260	194	25
4	213	239	29
5	178	198	33
6	-132	35	36
7	135	103	40

-3 0 1

2	1258	1316	17
4	253	306	20
6	2861	2643	31
8	2720	2786	30
10	964	1012	19
12	963	918	20
14	706	748	21
16	215	268	33
18	1127	1189	25
20	691	670	26
22	421	447	26
24	549	528	25
26	301	356	33
28	915	827	26

-3 1 1

1	2191	2054	20
2	1811	1798	17
3	1128	1085	13
4	155	149	21
5	781	876	12
6	154	11	22
7	2156	2246	21
8	2619	2485	24
9	1619	1636	17
10	131	130	26
11	626	560	14
12	976	994	15
13	533	582	15
14	653	614	15
15	253	272	21
16	798	781	16
17	332	340	20
18	245	227	24
19	664	693	18
20	704	691	18
21	301	355	24
22	269	253	23
23	-25	72	81
24	304	223	22
25	337	319	22
26	404	425	21
27	108	44	47
28	339	288	24

-3 2 1

1	78	125	34
2	529	602	11
3	555	685	11
4	165	83	20
5	1683	1453	17
6	1974	1787	19
7	1933	1953	19
8	1124	1076	14
9	930	874	14
10	400	409	14
11	189	193	21
12	366	375	16
13	699	721	15
14	234	282	21
15	-88	65	38
16	410	496	18
17	464	479	18
18	599	561	18
19	760	783	18
20	860	831	19
21	357	330	23
22	135	64	36
23	960	953	17
24	327	291	22
25	264	202	25
26	178	132	33
27	584	560	19

-3 3 1

1	1530	1399	16
2	765	637	12
3	169	180	20
4	1251	1018	14
5	122	8	26
6	2291	2274	22
7	2751	2750	25
8	1000	999	14
9	582	613	13
10	-45	62	50
11	251	228	18
12	935	976	15
13	826	817	15
14	620	637	16
15	-87	66	39
16	-55	119	54
17	672	641	17
18	194	255	28
19	325	322	22
20	180	125	32
21	684	668	19
22	309	359	21
23	188	111	30
24	92	4	48
25	705	722	18
26	134	135	40
27	520	483	20

-3 4 1

1	503	501	12
2	251	414	16
3	927	1030	13
4	1654	1642	17
5	1943	1997	19
6	1095	996	14
7	853	828	14
8	734	698	14
9	824	833	14
10	1178	1218	16
11	1411	1414	17
12	627	596	15
13	531	523	16
14	423	378	17
15	83	159	44
16	315	411	20
17	679	633	17
18	134	165	37
19	422	438	20
20	431	402	21
21	493	477	17
22	302	281	22
23	379	432	20
24	301	277	23
25	108	6	45
26	-152	20	32
27	276	259	26

-3 5 1

1	71	122	37
2	1012	1039	14
3	1097	1006	14
4	485	447	13
5	294	272	16
6	599	706	13
7	451	393	14
8	143	165	26
9	389	452	16
10	623	587	15
11	124	207	31
12	346	365	18
13	515	517	16
14	-49	146	56
15	-106	27	35
16	146	172	33
17	-131	91	32
18	331	341	22
19	258	252	26
20	963	901	19
21	903	897	17
22	307	332	22
23	-165	14	27
24	251	255	26
25	-84	173	51
26	706	667	19

-3 6 1

1	507	551	13
2	354	374	15
3	335	278	15
4	476	568	14
5	432	481	14
6	730	730	14
7	449	371	15
8	901	935	15
9	-129	134	25
10	708	717	15
11	219	270	22
12	-68	146	45
13	81	113	44
14	459	441	18
15	233	215	24
16	612	635	18
17	255	261	25
18	359	332	22
19	522	565	20
20	526	456	17
21	59	42	60
22	366	306	20
23	275	349	24
24	302	269	24
25	292	340	25
26	-139	1	36

-3 7 1

1	649	578	14
2	308	328	16
3	329	240	16
4	-53	99	47
5	532	455	15
6	550	575	15
7	512	449	15

8	726	774	15
9	380	397	17
10	270	381	20
11	-70	51	46
12	628	626	17
13	454	435	18
14	1057	1028	18
15	105	87	42
16	-59	73	59
17	529	446	19
18	114	137	44
19	109	2	41
20	674	717	17
21	132	154	38
22	247	295	25
23	113	149	44
24	245	180	27
25	174	200	35

-3 8 1

1	191	196	22
2	667	630	15
3	110	0	32
4	53	117	51
5	1053	1024	16
6	638	634	15
7	500	462	16
8	494	452	16
9	204	134	24
10	470	456	17
11	401	388	18
12	436	445	18
13	197	285	28
14	-73	26	52
15	515	541	19
16	275	334	25
17	191	202	32
18	771	791	17
19	419	394	19
20	169	167	32
21	246	223	25
22	453	375	20
23	156	51	36
24	479	549	20

-3 9 1

1	512	454	16
2	124	30	31
3	354	346	17
4	120	67	32
5	187	190	24
6	333	299	18
7	156	60	29
8	1050	1035	17
9	211	203	25
10	426	473	19
11	414	415	19
12	728	655	18
13	486	489	19
14	166	132	33
15	466	430	20
16	371	416	19
17	457	441	18
18	265	257	23
19	605	582	18
20	58	71	62
21	291	239	24
22	185	187	32
23	453	361	20

-3 10 1

1	145	128	30
2	74	53	46
3	367	350	18
4	110	189	36
5	284	251	21
6	567	549	17
7	-73	14	48
8	267	278	23
9	335	301	21
10	493	480	19
11	732	651	18
12	122	57	41
13	136	152	39
14	-45	63	71
15	89	17	47
16	183	212	29
17	535	544	18
18	223	245	27
19	522	505	18
20	105	11	45
21	669	589	18
22	339	318	23

-3 11 1

1	470	404	18
2	551	570	17
3	-39	28	66
4	69	81	52
5	310	325	21
6	231	208	25
7	430	413	19
8	99	7	45
9	643	703	18
10	318	267	23
11	-76	26	53
12	61	40	56
13	338	356	20
14	680	657	17
15	155	128	33
16	223	314	27
17	177	203	31
18	411	408	20
19	555	447	19
20	96	98	50
21	385	334	22

-3 12 1

1	118	155	39
2	61	8	58
3	560	539	18
4	269	218	24
5	333	335	22
6	373	358	21
7	703	671	18
8	396	358	21
9	343	315	19
10	127	140	36
11	414	456	18
12	738	710	17
13	253	264	24
14	129	132	38
15	118	120	41
16	428	414	20
17	216	256	28
18	259	207	26
19	361	392	22

-3 13 1

1	157	93	35
2	257	191	26
3	169	183	29
4	188	234	27
5	98	48	42
6	579	567	17
7	218	258	25
8	286	249	21
9	-154	22	27
10	234	259	25
11	120	59	39
12	-92	108	44
13	164	206	33
14	407	414	20
15	185	165	31
16	292	282	24
17	332	347	23
18	418	358	21

-3 14 1

1	124	151	37
2	247	286	24
3	207	154	26
4	547	544	17
5	160	1	32
6	502	460	18
7	-95	163	42
8	163	158	32
9	184	198	29
10	145	91	35
11	430	370	19
12	332	363	22
13	126	30	41
14	157	118	36
15	258	161	27

-3 15 1

1	-70	110	52
2	250	208	24
3	67	30	56
4	161	24	32
5	343	352	21
6	492	498	19
7	90	91	48
8	105	39	44
9	240	335	26
10	191	159	31
11	-67	67	58
12	180	179	33

-3 16 1

1	15	39	90
2	160	121	34
3	453	481	19
4	172	223	33
5	306	227	23
6	149	98	37
7	43	86	72
8	-91	98	48
9	50	26	69

-2 0 1

2	840	1161	13
4	924	929	15
6	2414	2276	26
8	1628	1598	21
10	-108	115	36
12	116	139	41
14	1198	1186	22
16	661	672	22
18	833	792	24
20	491	512	27
22	521	420	28
24	103	20	60
26	178	209	45
28	218	261	42

-2 1 1

1	822	430	10
2	613	432	9
3	807	992	10
4	1603	1446	15
5	762	731	11
6	1189	1083	13
7	2415	2383	22
8	943	875	13
9	1799	1844	18
10	1063	1068	14
11	401	317	14
12	959	961	15
13	980	932	15
14	549	557	15
15	51	50	54
16	1050	1075	17
17	519	524	17
18	148	166	32
19	390	444	20
20	479	430	19
21	-126	12	36
22	476	507	21
23	238	227	25
24	357	352	21
25	501	506	19
26	104	103	46
27	237	254	28
28	346	277	24

-2 2 1

1	717	797	10
2	1497	1430	15
3	1167	1022	13
4	1559	1708	15
5	2564	2376	23
6	50	95	45
7	1590	1620	16
8	738	663	12
9	795	767	13
10	212	164	19
11	397	402	15
12	276	288	18
13	1346	1324	17
14	1277	1271	17
15	836	777	16
16	-120	17	30
17	726	763	17
18	-103	11	38
19	808	816	18
20	323	284	23
21	69	25	59
22	-81	118	53
23	-50	164	64
24	-31	31	78
25	-51	11	65
26	459	471	20
27	36	85	79
28	171	186	36

-2 3 1

1	362	396	12
2	375	584	12
3	1637	1522	16
4	1261	1277	14
5	1226	1137	14
6	101	148	30
7	-138	99	20
8	393	327	13
9	509	475	13
10	734	669	14
11	1703	1655	19
12	1188	1147	16
13	139	124	28
14	546	504	16
15	1153	1138	17
16	110	150	37
17	840	828	17
18	598	584	18
19	108	181	43
20	567	557	19
21	231	261	28
22	-128	8	33
23	381	382	20
24	-77	38	52
25	-136	3	34
26	69	94	60
27	234	229	28
28	-133	135	38

-2 4 1

1	1437	1247	15
2	591	602	11
3	1179	991	14
4	223	114	17
5	2627	2637	24
6	565	476	12
7	36	63	54
8	894	856	14
9	631	548	13
10	194	92	21
11	1270	1248	16
12	505	412	15
13	724	697	15
14	244	225	21
15	883	904	16
16	505	488	17
17	100	121	42
18	-70	79	52
19	212	258	28
20	109	182	45
21	-131	0	36
22	549	544	17
23	32	61	77
24	45	69	69
25	651	572	18
26	235	172	28
27	396	382	22

-2 5 1

1	129	0	24
2	783	652	12
3	900	788	13
4	199	298	19
5	1668	1655	18
6	1136	1117	15
7	1145	1034	15
8	334	370	15
9	1040	992	15
10	350	268	16
11	1133	1144	16
12	1191	1198	17
13	45	135	57
14	823	842	16
15	919	914	17
16	670	701	17
17	57	55	59
18	229	221	26
19	-80	108	51
20	114	239	44
21	91	97	46
22	570	566	17
23	730	678	17
24	208	121	29
25	128	132	41
26	297	257	25
27	149	155	39

-2 6 1

1	809	732	13
2	1333	1342	15
3	1108	1163	14
4	558	488	13
5	838	934	14
6	438	416	14
7	871	933	14
8	737	727	14
9	210	231	21
10	416	435	16
11	149	182	28
12	786	832	16
13	537	552	16
14	683	725	16
15	-100	1	38
16	-57	79	57
17	209	177	27
18	-73	105	53
19	-107	103	42
20	304	351	21
21	-90	83	45
22	-148	53	30
23	-44	53	69
24	406	386	20
25	278	253	25
26	580	537	19

-2 7 1

1	203	200	19
2	828	779	14
3	1029	1070	15
4	916	972	14
5	606	513	14
6	666	671	14
7	834	772	15
8	1168	1185	16
9	425	450	16
10	414	399	17
11	192	268	24
12	544	515	16
13	-116	26	32
14	637	616	17
15	188	212	28
16	419	426	20
17	613	657	19
18	237	216	27
19	-147	60	28
20	366	418	20
21	194	262	29
22	437	408	19
23	161	47	34
24	876	823	18
25	336	304	23

-2 8 1

1	478	444	15
2	1586	1642	18
3	834	828	15
4	157	3	25
5	215	101	21
6	1320	1304	17
7	479	408	16
8	872	921	16
9	772	740	16
10	439	445	17
11	575	567	17
12	338	350	20
13	240	251	24
14	417	459	19
15	97	17	46
16	186	244	31
17	53	46	66
18	443	450	18
19	-125	32	34
20	428	444	19
21	296	305	23
22	314	313	22
23	500	514	19
24	278	234	25
25	254	217	28

-2 9 1

1	466	424	15
2	339	345	17

3	360	416	17
4	977	911	16
5	1533	1568	19
6	507	505	16
7	260	126	20
8	25	4	71
9	418	451	18
10	284	296	21
11	299	336	21
12	-58	121	57
13	379	390	20
14	195	252	30
15	234	256	27
16	75	184	56
17	207	188	26
18	-141	104	30
19	-145	27	30
20	262	226	24
21	444	485	19
22	140	31	38
23	587	524	19
24	177	150	35

-2 10 1

1	957	945	16
2	267	149	20
3	404	477	17
4	361	335	18
5	569	539	16
6	324	336	19
7	964	976	17
8	148	5	32
9	1065	1167	18
10	56	48	59
11	594	594	18
12	184	146	31
13	518	453	19
14	177	231	33
15	289	310	21
16	-140	31	30
17	164	162	32
18	156	186	33
19	263	281	24
20	189	196	30
21	410	322	21
22	181	155	33
23	190	224	33

-2 11 1

1	386	351	18
2	338	338	19
3	687	661	17
4	-68	38	50
5	344	398	20
6	256	334	23
7	337	348	20
8	224	188	26
9	750	763	18
10	136	21	37
11	379	457	21
12	176	64	33
13	-28	69	75
14	152	242	33
15	462	408	18
16	-17	143	87
17	-105	24	41
18	491	471	19
19	269	248	25
20	100	120	48
21	370	330	22

-2 12 1

1	158	66	32
2	569	586	18
3	176	72	30
4	455	431	19
5	282	299	23
6	296	308	23
7	486	496	19
8	511	539	19
9	460	488	20
10	164	195	29
11	184	246	28
12	403	409	19
13	535	527	17
14	22	4	82
15	-144	46	30
16	-136	47	32
17	140	141	37
18	268	284	25
19	326	334	23
20	114	164	46

-2 13 1

1	222	149	27
2	250	238	26
3	108	59	44
4	671	657	19
5	225	126	28
6	323	389	20
7	195	182	27
8	152	34	32
9	272	310	22
10	874	878	17
11	211	26	26
12	134	6	36
13	121	98	39
14	115	112	41
15	225	207	27
16	277	258	25
17	-144	13	33
18	84	38	55

-2 14 1

1	86	36	46
2	374	356	19
3	109	87	40
4	162	23	31
5	-85	39	45
6	351	367	20
7	195	157	28
8	311	351	21
9	169	58	31
10	150	14	34
11	144	211	35
12	543	558	18
13	131	124	39
14	194	210	30
15	-5	161	102
16	49	21	71

-2 15 1

1	160	121	32
2	258	289	23
3	241	239	25
4	366	313	20
5	194	158	29
6	-57	23	60
7	314	320	22
8	251	243	25
9	345	281	21
10	278	347	24
11	406	405	20
12	125	111	41
13	74	125	57

-2 16 1

1	490	434	19
2	143	44	36
3	176	187	32
4	210	185	28
5	247	296	26
6	258	241	25
7	370	356	21
8	-84	21	51
9	197	178	31

-2 17 1

1	109	15	45
2	153	23	36

-1 0 1

2	1820	1874	19
4	3047	2601	31
6	2037	1786	23
8	1940	1988	23
10	748	629	18
12	411	494	21
14	917	884	21
16	-68	98	61
18	114	114	51
20	423	468	28
22	696	670	27
24	-154	84	40
26	49	68	87
28	773	662	26

-1 1 1

1	1227	1059	11
2	1020	1264	10
3	345	152	10
4	1123	753	12
5	799	698	11
6	586	640	11
7	148	172	22
8	196	295	19
9	829	876	13
10	787	729	13
11	999	965	14
12	1783	1810	19
13	418	373	15
14	794	732	15
15	771	738	15
16	545	492	16
17	378	343	18
18	892	877	17
19	212	229	27
20	348	333	22
21	-94	146	46
22	-14	13	94
23	-126	33	34
24	384	345	20
25	57	124	63
26	315	243	23
27	182	107	33
28	299	282	25

-1 2 1

1	417	745	9
2	1439	1574	14
3	424	346	10
4	157	21	20
5	901	620	11
6	1082	960	13
7	527	438	12
8	-58	80	41
9	2986	2977	27
10	581	511	13
11	-24	114	64
12	791	709	14
13	361	308	16
14	-51	55	52
15	1357	1354	18
16	816	825	16
17	115	129	36
18	271	267	22
19	-90	41	44
20	383	405	21
21	904	910	19
22	346	309	23
23	44	148	68
24	287	338	23
25	407	416	20
26	284	252	24
27	642	549	19
28	111	104	48

-1 3 1

1	1863	1882	17
2	696	731	11
3	1502	1195	15
4	1478	1488	15
5	116	174	26
6	1064	1031	13
7	1060	998	13
8	2123	2108	21
9	728	610	13
10	526	492	13
11	1504	1517	17
12	379	392	15
13	1267	1142	17
14	842	852	15
15	91	87	40
16	190	197	25
17	1079	1094	17
18	296	257	22
19	1057	1045	18
20	309	310	23
21	236	201	28
22	-52	104	61
23	166	261	32
24	79	58	53
25	397	361	20
26	131	60	40
27	293	252	25
28	-144	122	35

-1 4 1

1	1222	1268	13
2	194	91	17
3	3459	3390	24
4	498	447	12
5	2656	2674	24
6	880	758	13
7	58	78	42
8	1838	1889	19
9	796	737	13
10	173	184	22
11	1255	1208	16
12	528	549	15
13	16	28	75
14	523	520	16
15	1093	1108	17
16	376	370	18
17	973	914	17
18	291	293	22
19	125	162	39
20	105	93	46
21	406	432	22
22	-99	21	41
23	124	208	39
24	565	575	18
25	257	293	25
26	219	225	29
27	107	143	48

-1 5 1

1	850	916	12
2	1067	1059	13
3	380	383	13
4	2124	2167	20
5	1266	1253	15
6	971	921	14
7	305	325	15
8	1056	1109	15
9	738	707	14
10	113	20	30
11	778	802	15
12	367	418	17
13	610	591	15
14	543	568	16
15	738	698	16
16	246	299	23
17	623	597	17
18	987	969	18
19	624	592	19
20	503	539	20
21	337	341	20
22	504	496	18
23	-63	132	58
24	341	360	22
25	615	585	18
26	117	150	44
27	246	293	28

-1 6 1

1	1103	1017	14
2	1303	1321	15
3	404	441	13
4	2320	2408	22
5	203	11	19
6	579	586	13
7	340	382	15
8	1442	1490	17
9	144	82	26
10	814	766	15
11	852	845	15
12	828	800	16
13	949	1000	16
14	589	576	16
15	326	373	20
16	1272	1236	19
17	629	593	18
18	422	409	20
19	-124	139	37
20	212	232	30
21	-66	51	55
22	-154	29	29
23	-163	4	27
24	190	172	31
25	-117	30	40
26	63	127	64

-1 7 1

1	609	579	13
2	348	339	15
3	384	401	14
4	360	397	15
5	1072	1110	15
6	1952	1986	20
7	281	268	17
8	945	897	15
9	423	377	16
10	830	780	15
11	663	594	16
12	32	33	66
13	-83	27	41
14	969	957	17
15	89	51	46
16	-25	95	79
17	204	177	29
18	650	645	19
19	-122	62	38
20	-162	27	26
21	478	522	18
22	322	338	22
23	225	263	27
24	415	396	20
25	110	106	46
26	217	258	30

-1 8 1

1	244	331	18
2	400	340	15
3	527	560	14
4	501	445	15
5	630	616	15
6	52	59	51
7	235	258	20
8	456	462	16
9	642	613	16
10	144	16	29
11	1032	980	17
12	290	357	21
13	211	224	26
14	-130	22	31
15	316	334	22
16	816	790	18
17	310	324	23
18	-64	28	60
19	323	389	21
20	426	435	19
21	173	160	32
22	515	475	19
23	287	317	24
24	-90	75	49
25	-164	37	30

-1 9 1

1	377	316	16
2	118	113	31
3	76	6	41
4	275	272	19
5	1307	1365	17
6	253	149	20
7	1243	1315	17
8	226	179	22
9	693	694	16
10	442	493	18
11	509	615	17
12	-55	20	57
13	267	240	23
14	325	405	22
15	319	339	23
16	-95	103	46
17	-103	78	38
18	148	195	33
19	109	202	42
20	-124	37	35
21	-119	62	37
22	-153	17	30
23	397	393	21
24	207	193	31

-1 10 1

1	501	458	16
2	390	397	17
3	600	636	16
4	214	81	23
5	561	516	16
6	76	131	46
7	335	399	19
8	-98	65	37
9	905	966	17
10	209	143	26
11	626	586	18
12	192	166	29
13	-56	97	61
14	-152	98	29

15	407	390	21
16	161	285	31
17	-129	83	33
18	265	330	24
19	373	355	20
20	125	92	40
21	521	528	19
22	157	87	36
23	276	244	26

-1 11 1

1	669	648	16
2	308	312	20
3	426	454	18
4	710	775	17
5	335	322	20
6	223	305	25
7	736	733	17
8	225	314	26
9	155	212	33
10	-118	16	35
11	187	221	30
12	139	252	37
13	255	256	26
14	-111	87	36
15	70	97	53
16	327	364	21
17	270	202	24
18	-22	48	84
19	588	580	18
20	52	49	67
21	-169	7	28
22	122	143	44

-1 12 1

1	138	113	35
2	425	386	19
3	571	504	18
4	113	160	40
5	347	382	21
6	278	283	23
7	134	143	37
8	367	339	21
9	512	529	19
10	274	315	25
11	119	159	37
12	45	85	64
13	143	77	34
14	382	406	19
15	244	196	25
16	190	183	29
17	317	299	22
18	-174	69	26
19	-44	94	71
20	236	205	28

-1 13 1

1	347	280	21
2	363	382	21
3	336	385	22
4	137	83	37
5	507	561	19
6	545	530	19
7	244	153	23
8	466	465	17
9	285	338	22
10	31	22	74
11	224	231	25
12	659	654	17
13	-77	119	49
14	48	0	66
15	53	86	64
16	105	197	45
17	-51	39	67
18	518	391	20

-1 14 1

1	152	152	31
2	208	231	26
3	203	194	26
4	209	188	26
5	15	68	86
6	-133	18	31
7	108	138	41
8	332	383	21
9	233	142	25
10	536	607	18
11	148	48	34
12	91	2	48
13	264	239	24
14	320	332	22
15	283	287	24
16	429	377	21

-1 15 1

1	483	506	18
2	253	217	24
3	110	35	41
4	-116	9	36
5	299	237	22
6	219	121	26
7	420	308	19
8	338	244	21
9	172	151	32
10	354	379	21
11	-83	44	50
12	205	243	29
13	425	366	21
14	299	213	36

-1 16 1

1	136	109	37
2	236	213	26
3	565	577	18
4	140	117	37
5	262	220	25
6	71	157	57
7	-52	109	65
8	189	154	31
9	226	256	28
10	109	66	46

-1 17 1

1	452	454	20
2	224	211	28
3	75	107	57
4	116	89	44

0 0 1

2	849	1029	11
4	-90	216	36
6	3547	3683	36
8	458	465	17
10	383	412	19
12	910	924	19
14	473	447	21
16	517	450	23
18	730	731	23
20	926	894	25
22	316	187	34
24	736	733	24
26	-99	141	60
28	130	147	57

0 1 1

1	1197	1554	-
2	2656	2719	23
3	215	231	13
4	149	340	19
5	334	85	12
6	582	518	11
7	673	622	11
8	193	272	19
9	858	856	13
10	1824	1724	19
11	400	410	14
12	287	278	17
13	720	688	14
14	623	577	15
15	1030	1040	16
16	1200	1153	17
17	573	592	17
18	174	137	29
19	230	39	25
20	549	534	19
21	674	598	19
22	1018	966	19
23	94	0	46
24	330	229	21
25	-150	39	30
26	179	183	32
27	396	369	21
28	560	515	20

0 2 1

0	1779	1968	16
1	4128	4271	35
2	2500	2477	22
3	682	326	9
4	540	585	10
5	2721	2573	19
6	50	4	45
7	585	434	12
8	1661	1625	17
9	454	460	13
10	830	773	13
11	1425	1393	17
12	1256	1232	16
13	1557	1420	18
14	292	290	18
15	260	276	20
16	925	924	16
17	619	564	17
18	407	407	19
19	1612	1579	21
20	361	290	21
21	437	383	21
22	418	370	22
23	277	279	23
24	638	625	17
25	533	481	18
26	111	145	45
27	340	335	23
28	159	59	38

0 3 1

1	876	908	10
2	1382	1119	14
3	4866	4883	42
4	1034	1042	12
5	768	714	11
6	656	645	11
7	1807	1736	18
8	-108	31	26
9	2207	2136	21
10	1434	1348	16
11	627	614	14
12	907	867	15
13	586	517	15
14	498	464	16
15	516	539	16
16	260	277	21
17	579	603	17
18	503	448	18
19	300	314	22
20	273	286	25
21	808	765	19
22	72	104	53
23	157	137	33
24	-91	84	46
25	216	153	28
26	80	75	55
27	486	496	20
28	-135	7	37

0 4 1

0	3937	3959	34
1	164	248	19
2	2025	2015	19
3	725	701	11
4	420	449	12
5	1845	1799	18
6	1808	1766	18
7	857	850	13
8	1089	1014	14
9	1319	1264	16
10	-65	98	40
11	707	699	14
12	97	136	35
13	1432	1399	18
14	303	354	19
15	332	315	18
16	504	521	17
17	935	933	17
18	1021	985	18
19	456	413	19
20	199	181	30
21	307	305	24
22	-112	84	37
23	793	758	17
24	225	157	27
25	791	726	18
26	169	141	34
27	123	132	44

0 5 1

1	1238	1370	14
2	1470	1513	15
3	207	209	17
4	1349	1417	15
5	319	357	14
6	151	219	22
7	1067	1091	14
8	522	592	13
9	80	47	36
10	326	271	16
11	909	846	15
12	327	203	17
13	922	896	16
14	280	264	20
15	-70	35	46
16	581	548	17
17	627	586	17
18	217	195	27
19	315	321	23
20	-133	52	35
21	545	542	17
22	534	487	18
23	289	305	23
24	87	64	50
25	87	69	51
26	174	140	34
27	510	524	20

0 6 1

0	265	172	15
1	145	8	22
2	123	134	25
3	1974	1997	20
4	740	794	13
5	902	803	14
6	2164	2172	21
7	780	802	14
8	807	783	14
9	835	910	14
10	1174	1169	16
11	408	431	16
12	765	750	15
13	344	285	18
14	294	346	20
15	135	154	33
16	1111	1122	18
17	379	388	20
18	844	829	18
19	-74	61	54
20	371	396	22
21	446	473	18
22	253	276	24
23	11	101	94
24	396	443	20
25	274	261	25
26	413	428	21

0 7 1

1	432	523	14
2	1247	1167	15
3	726	741	13
4	1285	1202	16
5	202	16	20
6	965	937	15
7	179	62	22
8	1371	1483	17
9	420	477	16
10	706	680	15
11	261	255	20
12	191	239	24
13	733	759	16
14	584	638	17
15	605	531	17
16	900	850	18
17	-52	89	63
18	-175	62	25
19	-145	46	32
20	307	306	21
21	151	165	34
22	671	689	17
23	156	84	35
24	-127	45	37
25	247	256	27
26	374	298	23

0 8 1

0	948	920	14
1	709	689	14
2	937	977	15
3	466	423	14
4	709	762	14
5	1198	1241	16
6	392	383	16
7	660	761	15
8	128	71	30
9	530	610	16
10	782	797	16
11	543	589	16
12	-99	87	36
13	213	116	25
14	483	516	18
15	313	360	22
16	356	386	21
17	132	129	39
18	183	259	33
19	460	488	18
20	724	752	17
21	175	26	31
22	113	158	43
23	338	324	22
24	349	376	22
25	231	263	29

0 9 1

1	682	684	15
2	70	23	43
3	682	748	15
4	170	128	25
5	944	886	16
6	428	441	16
7	372	430	17
8	1017	981	17
9	893	982	16
10	548	504	17
11	445	411	18
12	335	361	20
13	746	755	17
14	507	461	19
15	535	478	19
16	260	259	26
17	547	577	17
18	119	120	39
19	77	11	52
20	126	196	39
21	374	340	21
22	435	464	20
23	155	199	36
24	95	124	52

0 10 1

0	415	439	16
1	618	589	16
2	324	317	18
3	265	300	20
4	640	720	16
5	800	838	16
6	270	276	21
7	1187	1196	18
8	111	24	38
9	72	71	50
10	208	216	26
11	894	927	18
12	31	30	75
13	272	258	24
14	528	575	19
15	258	318	26
16	-105	139	38
17	264	279	23
18	-110	28	38
19	425	432	19
20	131	106	38
21	194	163	30
22	-90	39	49
23	288	308	25

0 11 1

1	470	431	17
2	147	104	30
3	611	525	17
4	472	441	18
5	583	538	17
6	-48	54	60
7	329	433	21
8	-18	31	84
9	753	690	18
10	242	287	25
11	660	609	18
12	188	131	30
13	513	476	20
14	536	561	17
15	122	121	38
16	69	88	54
17	-66	135	54

18	-38	31	72
19	233	218	26
20	392	383	21
21	643	629	19
22	277	250	26

0 12 1

0	124	184	36
1	454	494	18
2	370	387	20
3	508	564	18
4	354	362	20
5	-48	82	64
6	646	630	18
7	270	151	24
8	322	308	22
9	623	561	19
10	227	188	28
11	216	270	25
12	778	810	16
13	248	162	24
14	428	366	18
15	135	70	36
16	160	165	32
17	103	35	44
18	337	286	22
19	390	395	21
20	251	312	27

0 13 1

1	282	208	23
2	584	534	18
3	372	410	21
4	350	327	22
5	173	135	32
6	175	148	32
7	194	51	26
8	644	702	16
9	224	174	25
10	346	345	20
11	297	323	22
12	105	58	42
13	131	51	37
14	419	483	19
15	257	291	24
16	267	226	24
17	244	305	26
18	116	82	44

0 14 1

0	323	435	20
1	-161	43	25
2	-28	18	74
3	-12	51	88
4	126	110	36
5	74	47	51
6	393	353	19
7	481	512	18
8	140	27	35
9	203	148	27
10	247	265	25
11	156	112	33
12	552	518	18
13	252	263	25
14	159	104	34
15	171	232	33
16	218	209	29

0 15 1

1	166	76	31
2	419	443	19
3	344	260	20
4	397	469	19
5	67	51	55
6	101	166	44
7	155	151	33
8	217	199	27
9	380	443	20
10	403	351	20
11	-77	17	53
12	95	30	49
13	137	155	40
14	-32	44	81

0 16 1

0	345	321	21
1	476	439	19
2	217	167	27
3	118	35	41
4	-132	27	33
5	-86	12	48
6	-70	75	55
7	281	210	24
8	-26	67	83
9	226	319	28
10	196	186	31

0 17 1

1	280	280	25
2	232	64	27
3	305	358	24
4	201	155	30

1 0 1

0	267	203	9
2	2489	2370	25
4	198	420	21
6	545	650	15
8	540	681	17
10	3374	3287	36
12	168	168	32
14	717	685	21
16	1638	1596	25
18	1363	1273	25
20	842	761	25
22	938	859	26
24	421	336	27
26	409	368	29
28	419	355	30

1 1 1

0	1666	1310	13
1	115	256	18
2	679	603	9
3	994	731	11
4	868	799	10
5	445	230	11
6	2455	2466	22
7	1164	1077	13
8	571	601	12
9	954	913	13
10	518	491	13
11	831	825	14
12	1122	1061	15
13	211	114	21
14	594	594	15
15	-77	13	41
16	144	90	30
17	709	712	16
18	151	226	32
19	368	361	20
20	485	441	19
21	272	281	25
22	268	164	26
23	175	190	31
24	776	749	17
25	756	713	18
26	398	367	21
27	-102	79	45
28	437	369	21

1 2 1

0	823	708	8
1	408	182	9
2	1210	1123	12
3	1609	1558	15
4	1686	1848	16
5	807	626	11
6	198	254	17
7	137	160	23
8	477	427	12
9	1784	1821	18
10	766	772	13
11	1315	1322	16
12	372	333	15
13	655	669	15
14	1227	1214	17
15	1323	1340	18
16	802	781	16
17	-26	94	73
18	154	170	32
19	766	760	18
20	254	249	25
21	483	478	20
22	636	599	20
23	153	212	34
24	309	310	22
25	288	220	24
26	605	539	18
27	415	415	21
28	333	319	24

1 3 1

0	289	13	9
1	870	933	11
2	360	485	12
3	1267	1261	13
4	132	2	23
5	816	839	11
6	194	322	18
7	1579	1459	16
8	1954	1834	19
9	-166	23	16
10	630	661	13
11	1298	1356	16
12	742	721	14
13	1947	1911	21
14	575	611	15
15	277	186	20
16	763	768	16
17	663	655	17
18	-134	1	30
19	503	492	19
20	-104	91	42
21	359	358	22
22	592	602	17
23	330	342	21
24	-116	70	38
25	597	568	18
26	178	113	33
27	421	389	21
28	238	155	29

1 4 1

0	1160	1252	11
1	938	1165	12
2	2052	1986	19
3	4072	3967	35
4	1525	1428	16
5	733	758	12
6	188	19	18
7	2685	2789	25
8	904	957	13
9	529	484	13
10	649	665	14
11	237	217	19
12	828	923	15
13	425	430	16
14	126	120	32
15	1272	1326	18
16	327	277	19
17	968	967	17
18	465	442	19
19	291	265	23
20	-61	100	60
21	290	329	25
22	293	241	22
23	825	810	17
24	344	308	21
25	532	458	19
26	-46	174	71
27	776	777	19

1 5 1

0	283	203	10
1	1460	1504	15
2	823	839	12
3	768	705	12
4	1193	1265	14
5	1797	1793	18
6	110	168	28
7	588	606	13
8	186	207	20
9	65	46	41
10	255	188	18
11	614	656	14
12	1612	1648	19
13	324	386	18
14	436	509	17
15	43	109	61
16	678	698	17
17	1024	1039	18
18	698	691	18
19	806	803	18
20	-169	122	27
21	140	163	35
22	691	634	17
23	732	737	17
24	198	162	29
25	63	199	61
26	90	93	52
27	168	60	36

1 6 1

0	461	463	9
1	602	599	12
2	854	850	13
3	201	124	18
4	2188	2177	21
5	330	153	15
6	562	527	13
7	869	878	14
8	848	886	14
9	495	534	14
10	543	535	15
11	496	473	15
12	1131	1131	16
13	70	79	46
14	926	982	17
15	415	316	18
16	855	877	17
17	351	298	21
18	160	106	34
19	346	345	22
20	384	398	22
21	472	467	18
22	815	770	17
23	238	285	26
24	75	169	55
25	130	3	41
26	754	711	19

1 7 1

0	958	987	11
1	189	220	20
2	147	177	23
3	921	963	14
4	2228	2378	22
5	1071	1131	15
6	2210	2254	22
7	759	778	14
8	733	721	15
9	153	107	26
10	878	907	15
11	75	20	43
12	139	169	30
13	1029	1033	17
14	632	615	17
15	157	110	31
16	879	860	18
17	352	380	21
18	410	429	21
19	-110	139	42
20	704	698	17
21	774	728	17
22	333	265	21
23	151	111	35
24	583	594	19
25	263	228	26
26	609	596	20

1 8 1

0	213	211	14
1	1150	1108	15
2	432	366	15
3	707	792	14
4	614	636	14
5	331	340	17
6	309	326	17
7	730	689	15
8	935	970	16
9	237	301	21
10	419	405	17
11	383	405	18
12	429	513	17
13	-129	1	29
14	653	681	17
15	235	195	25
16	506	490	19
17	582	629	19
18	-25	115	85
19	348	309	20
20	799	829	17
21	501	452	18
22	286	260	23
23	228	244	28
24	235	198	28
25	642	602	19

1 9 1

0	536	515	11
1	1500	1485	18
2	221	122	20
3	1043	1047	16
4	676	595	15
5	1642	1654	19
6	1655	1653	19
7	411	462	17
8	384	403	18
9	370	355	18
10	94	88	41
11	-127	93	30
12	188	237	27
13	128	159	36
14	683	683	18
15	-131	33	33
16	52	138	65
17	118	156	38
18	284	321	22
19	611	652	17
20	317	323	22
21	166	196	33
22	178	147	32
23	509	494	20
24	493	432	20

1 10 1

0	717	760	11
1	119	15	32
2	149	69	28
3	896	906	16
4	163	95	27
5	-2	26	90
6	336	335	19
7	386	449	18
8	-78	97	45
9	660	688	17
10	593	623	17
11	453	411	19
12	-86	20	46
13	779	810	18
14	56	94	62
15	-94	43	45
16	83	95	47
17	317	327	21
18	168	116	31
19	517	563	18
20	244	234	25
21	458	458	20
22	188	84	32
23	219	267	30

1 11 1

0	260	266	15
1	844	887	17
2	243	249	22
3	399	428	18
4	636	677	17
5	826	786	17
6	134	48	34
7	242	244	24
8	464	525	19
9	161	108	32
10	180	34	31
11	952	1025	18
12	444	338	20
13	586	547	18
14	-93	67	41
15	109	111	40
16	446	480	18
17	565	548	17
18	256	229	24
19	456	460	19
20	592	593	18
21	164	98	35

1 12 1

0	403	429	14
1	-112	73	36
2	512	495	18
3	591	607	18
4	138	37	35
5	138	188	35
6	287	298	23
7	141	11	36
8	545	574	19
9	444	448	20
10	329	403	23
11	153	199	32

12	122	21	37
13	365	377	19
14	424	436	19
15	209	111	27
16	140	79	35
17	-88	64	46
18	114	99	42
19	120	89	42
20	305	377	24

1 13 1

0	745	789	13
1	179	126	31
2	440	399	20
3	159	38	34
4	231	237	27
5	223	234	28
6	242	255	23
7	132	24	34
8	49	26	62
9	164	7	31
10	567	577	17
11	302	328	22
12	718	713	17
13	281	261	23
14	405	374	19
15	-136	51	32
16	326	295	22
17	-47	97	68
18	499	482	19

1 14 1

0	151	107	23
1	299	262	21
2	567	595	17
3	108	119	40
4	388	420	19
5	78	55	50
6	163	176	31
7	254	256	23
8	516	498	18
9	214	100	27
10	346	334	21
11	102	0	44
12	-56	97	61
13	253	185	25
14	472	492	19
15	66	134	60
16	290	311	25

1 15 1

0	433	423	13
1	197	91	27
2	-74	70	50
3	69	67	54
4	370	325	20
5	148	131	34
6	488	449	18
7	-91	48	44
8	134	25	37
9	133	204	38
10	229	220	27
11	507	541	19
12	452	460	20
13	301	324	24

1 16 1

0	150	71	25
1	240	310	25
2	169	78	32
3	428	449	19
4	225	141	27
5	102	21	45
6	145	100	36
7	139	224	38
8	85	115	52
9	494	478	20
10	210	140	30

1 17 1

0	282	217	17
1	179	190	32
2	52	5	67
3	-45	28	71
4	153	82	35

2 0 1

0	340	114	10
2	719	644	12
4	802	738	14
6	1181	1048	17
8	1970	1778	24
10	3055	3079	34
12	1455	1368	22
14	97	134	49
16	247	219	30
18	843	887	24
20	991	905	25
22	625	656	27
24	904	908	24
26	185	134	44
28	549	461	28

2 1 1

0	240	407	9
1	683	400	9
2	1197	1321	12
3	1509	1489	14
4	812	877	11
5	186	134	18
6	365	249	12
7	1158	984	14
8	1307	1278	15
9	1207	1286	15
10	418	368	14
11	435	434	14
12	694	676	14
13	209	198	21
14	937	864	16
15	716	705	16
16	477	486	17
17	139	157	32
18	177	4	29
19	616	579	18
20	775	752	18
21	148	29	37
22	738	688	19
23	325	264	21
24	637	541	18
25	586	537	18
26	518	467	19
27	426	364	21
28	464	494	21

2 2 1

0	955	948	9
1	211	73	14
2	1084	614	12
3	1906	2030	18
4	109	206	27
5	197	109	17
6	1379	1372	15
7	785	866	12
8	985	833	13
9	1305	1348	15
10	929	885	14
11	1735	1612	19
12	658	589	14
13	479	408	15
14	247	245	20
15	360	325	18
16	950	951	17
17	127	67	35
18	816	764	17
19	649	596	18
20	109	31	44
21	-152	49	30
22	494	464	17
23	578	546	17
24	194	75	29
25	635	609	18
26	32	24	80
27	105	71	48
28	184	41	34

2 3 1

0	178	219	13
1	1135	1224	12
2	2251	2131	15
3	605	369	11
4	999	1129	12
5	1536	1701	16
6	1977	2090	19
7	1559	1649	16
8	-65	61	37
9	1306	1282	15
10	1219	1251	15
11	122	80	28
12	1108	1093	16
13	956	964	15
14	413	380	17
15	201	268	24
16	1174	1125	18
17	308	337	21
18	302	277	22
19	887	859	18
20	65	3	60
21	472	496	20
22	-148	88	29
23	467	466	18
24	455	419	19
25	484	461	19
26	109	103	46
27	615	571	19

2 4 1

0	281	348	10
1	2257	2131	21
2	1666	1726	17
3	192	230	18
4	337	162	13
5	612	645	12
6	315	467	14
7	2343	2347	22
8	291	270	15
9	153	228	23
10	1286	1208	16
11	1405	1375	17
12	170	73	24
13	1027	1056	16
14	669	702	16
15	189	212	25
16	148	148	31
17	1657	1659	20
18	285	252	23
19	549	546	19
20	156	222	36
21	496	530	20
22	73	174	53
23	691	607	17
24	482	452	19
25	121	118	42
26	-18	129	92
27	-116	2	42

2 5 1

0	465	518	9
1	398	373	12
2	505	569	12
3	559	484	12
4	751	684	12
5	1786	1556	18
6	-40	95	50
7	540	426	13
8	782	642	14
9	502	482	14
10	240	255	19
11	410	430	15
12	335	330	17
13	1059	1092	16
14	626	611	16
15	-89	60	39
16	337	277	20
17	1043	1018	18
18	262	286	25
19	479	478	20
20	305	300	24
21	-98	111	41
22	717	739	17
23	469	479	19
24	-90	96	47
25	117	213	43
26	3	130	106
27	14	71	98

2 6 1

0	579	541	9
1	590	552	13
2	1050	1103	14
3	233	26	17
4	283	252	16
5	140	51	24
6	1047	1025	15
7	851	950	14
8	799	874	14
9	699	720	14
10	647	638	15
11	236	321	20
12	178	216	25
13	628	596	16
14	261	234	21
15	370	385	19
16	1409	1377	19
17	257	252	24
18	653	681	18
19	54	74	66
20	-67	93	53
21	270	273	23
22	738	728	17
23	111	120	43
24	-17	169	90
25	-161	33	30
26	114	165	47

2 7 1

0	91	40	24
1	364	359	14
2	800	735	14
3	251	252	17
4	807	901	14
5	406	275	15
6	353	404	16
7	117	81	30
8	1583	1529	18
9	195	67	23
10	419	409	16
11	169	212	25
12	177	204	26
13	194	158	25
14	1190	1262	18
15	169	96	30
16	743	684	18
17	189	230	30
18	184	215	32
19	134	204	35
20	718	745	17
21	264	216	24
22	142	224	36
23	209	205	29
24	-150	129	31
25	-83	9	53

2 8 1

0	797	819	11
1	511	462	14
2	280	284	17
3	742	752	14
4	653	698	14
5	126	171	29
6	891	862	15
7	337	283	17
8	142	110	29
9	470	484	16
10	570	573	16
11	113	29	35
12	835	856	17
13	114	41	38
14	-67	85	51
15	218	213	26
16	-107	0	39
17	-161	189	27
18	473	506	17
19	41	0	68
20	174	168	31
21	207	191	28
22	26	148	82
23	102	142	47
24	184	195	33
25	187	134	33

2 9 1

0	568	599	11
1	457	476	15
2	566	503	15
3	38	109	58
4	113	10	33
5	145	102	28
6	558	582	16
7	767	769	16
8	1023	1096	17
9	443	451	17
10	220	268	24
11	570	588	17
12	217	247	25
13	651	618	18
14	340	337	21
15	425	477	20
16	500	459	20
17	154	184	31
18	241	271	24
19	757	776	17
20	460	482	19
21	-109	121	40
22	-167	98	27
23	23	79	87
24	165	154	36

2 10 1

0	288	208	14
1	547	554	16
2	131	166	31
3	355	274	18
4	409	412	17
5	982	958	17
6	488	444	17
7	505	592	17
8	22	44	78
9	30	41	73
10	116	94	39
11	571	632	18
12	699	647	18
13	329	402	22
14	169	227	33
15	227	193	24
16	501	456	17
17	505	579	17
18	354	372	20
19	204	181	28
20	86	59	50
21	-53	62	65
22	-154	30	31
23	543	513	20

2 11 1

0	366	318	13
1	304	342	20
2	87	42	44
3	746	744	17
4	172	195	28
5	254	216	23
6	259	185	23
7	449	507	19
8	197	53	28
9	996	1008	18
10	145	120	36
11	-93	77	45
12	160	94	35
13	336	384	19
14	756	724	16
15	928	930	17
16	299	251	21
17	107	84	42
18	267	248	24
19	496	488	19
20	237	212	27
21	580	551	19

2 12 1

0	423	451	14
1	492	489	18
2	144	102	34
3	214	128	26
4	576	628	18
5	414	319	20
6	370	389	21
7	534	502	19
8	440	427	20
9	192	55	31
10	249	106	23
11	573	608	17
12	290	242	22
13	494	516	18
14	154	171	33
15	27	86	78
16	524	518	18
17	452	399	19
18	374	361	21
19	181	232	32
20	219	217	29

2 13 1

0	516	548	14
1	185	23	30
2	652	586	18
3	521	510	19
4	443	398	20
5	133	106	39
6	128	0	35
7	183	169	28

8	668	649	16
9	223	274	25
10	345	424	20
11	287	229	22
12	171	121	31
13	335	261	21
14	381	447	20
15	109	133	43
16	252	307	25
17	219	209	28
18	381	383	21

2 14 1

0	660	638	12
1	185	42	28
2	69	9	52
3	59	97	57
4	124	82	37
5	146	1	33
6	510	474	17
7	212	182	26
8	110	111	41
9	44	27	67
10	354	393	20
11	343	221	21
12	598	669	18
13	155	119	35
14	221	203	28
15	258	203	26
16	309	324	24

2 15 1

0	87	12	35
1	134	157	36
2	306	322	21
3	282	227	22
4	215	151	26
5	327	363	21
6	111	1	41
7	151	145	-34
8	389	362	20
9	352	310	21
10	186	191	31
11	114	118	44
12	-58	0	63
13	186	187	33

2 16 1

0	216	177	19
1	86	109	50
2	99	96	46
3	133	127	38
4	69	0	56
5	395	402	20
6	104	129	46
7	111	16	44
8	-115	34	39
9	64	90	62

2 17 1

0	82	12	40
1	161	168	35
2	189	159	31

3 0 1

0	2946	2686	26
2	432	551	15
4	197	65	23
6	3377	3168	35
8	279	233	21
10	693	720	18
12	597	609	20
14	2750	2698	33
16	352	288	26
18	910	846	24
20	1352	1303	27
22	-176	30	33
24	670	608	24
26	49	132	88
28	217	69	43

3 1 1

0	1243	1019	11
1	2138	2032	20
2	455	595	11
3	1769	1543	17
4	2557	2245	23
5	1955	1985	19
6	349	276	13
7	707	693	12
8	-91	135	29
9	-99	28	28
10	272	270	16
11	235	257	19
12	1621	1595	18
13	74	136	42
14	329	321	18
15	189	159	25
16	914	921	17
17	284	256	21
18	635	610	18
19	351	350	21
20	181	114	32
21	427	375	21
22	434	411	18
23	-120	24	36
24	126	1	40
25	126	191	40
26	364	377	22
27	-119	7	41
28	516	519	20

3 2 1

0	941	768	9
1	1174	1176	13
2	268	417	14
3	702	551	11
4	927	805	12
5	1005	943	13
6	598	621	12
7	542	582	12
8	869	924	13
9	839	917	13
10	928	897	14
11	394	344	15
12	-150	21	20
13	949	912	15
14	615	615	16
15	771	785	16
16	59	22	53
17	210	200	25
18	208	199	27
19	863	882	18
20	125	101	41
21	628	582	19
22	92	2	46
23	483	466	18
24	-104	110	42
25	209	289	29
26	327	319	23
27	65	92	63

3 3 1

0	1075	1102	10
1	1856	2024	18
2	1490	1347	10
3	328	343	13
4	2022	1938	19
5	888	806	13
6	-51	165	44
7	628	565	13
8	-53	10	44
9	1010	1002	14
10	150	64	24
11	1584	1540	18
12	125	49	29
13	202	264	23
14	117	86	34
15	461	493	17
16	208	125	25
17	1538	1524	20
18	68	5	55
19	-112	58	39
20	295	342	24
21	507	544	20
22	568	527	17
23	630	615	17
24	-53	73	64
25	-58	132	62
26	179	161	33
27	360	382	23

3 4 1

0	516	460	9
1	736	840	12
2	412	396	12
3	901	1031	13
4	-99	143	26
5	153	107	22
6	390	405	14
7	1032	996	14
8	228	96	18
9	2071	1968	21
10	157	9	24
11	512	513	15
12	715	719	15
13	925	963	16
14	1024	1006	16
15	461	448	17
16	-37	39	66
17	136	11	35
18	-63	111	56
19	261	290	25
20	154	242	36
21	246	285	24
22	107	162	43
23	208	220	28
24	-86	103	48
25	600	581	19
26	127	123	42
27	471	475	21

3 5 1

0	242	78	12
1	590	589	12
2	1290	1400	15
3	340	229	14
4	942	917	13
5	186	243	20
6	173	160	21
7	986	939	14
8	531	527	14
9	597	575	14
10	972	964	15
11	1691	1674	19
12	557	567	15
13	449	459	16
14	541	565	16
15	505	513	17
16	1002	972	18
17	759	764	18
18	280	327	24
19	105	126	46
20	357	432	23
21	8	161	94
22	745	780	17
23	601	551	18
24	-24	17	84
25	483	515	20
26	351	360	23

3 6 1

0	329	299	10
1	1369	1243	16
2	799	674	13
3	90	71	32
4	-77	24	34
5	55	138	45
6	496	478	14
7	576	487	14
8	1037	1028	15
9	433	414	15
10	202	216	22
11	103	76	36
12	-95	27	35
13	476	430	17
14	960	932	17
15	50	5	60
16	213	208	26
17	-52	118	62
18	-161	15	27
19	121	54	42
20	682	683	17
21	235	155	25
22	179	92	31
23	361	331	21
24	435	418	20
25	184	119	33
26	514	481	20

3 7 1

0	856	841	11
1	1042	1018	15
2	137	93	25
3	500	543	14
4	1293	1351	16
5	364	386	16
6	573	537	15
7	702	771	15
8	98	89	36
9	774	790	15
10	785	790	16
11	639	564	16
12	195	162	25
13	39	134	64
14	-63	174	52
15	379	412	20
16	737	717	18
17	-86	1	47
18	590	628	19
19	238	277	24
20	337	321	21
21	601	610	18
22	668	673	18
23	364	301	21
24	777	743	18
25	363	372	23

3 8 1

0	1111	1138	12
1	601	621	14
2	1412	1352	17
3	120	75	30
4	847	820	15
5	343	306	17
6	278	156	19
7	930	939	16
8	701	686	16
9	-15	91	78
10	347	361	18
11	-49	94	57
12	441	424	18
13	787	783	17
14	851	815	18
15	58	194	60
16	-106	156	40
17	190	213	31
18	-108	152	37
19	302	304	21
20	761	749	17
21	199	204	29
22	462	471	19
23	269	247	25
24	167	65	35

3 9 1

0	788	778	11
1	417	437	16
2	151	116	27
3	214	163	22
4	479	509	16
5	1162	1082	17
6	824	807	16
7	169	213	27
8	418	466	18
9	-92	105	39
10	100	160	41
11	752	714	17
12	737	730	17
13	199	205	28
14	171	148	32
15	70	50	56
16	432	430	17
17	423	443	18
18	262	265	23
19	221	261	26
20	180	215	30
21	-70	70	55
22	-86	2	49
23	656	653	19

3 10 1

0	96	102	28
1	889	885	16
2	465	413	17
3	806	809	16
4	55	2	54
5	-82	41	42
6	183	177	27
7	776	761	17
8	111	4	39
9	487	496	18
10	384	449	20
11	167	167	32
12	253	174	25
13	390	387	21
14	131	157	40
15	678	658	16
16	282	250	22
17	-20	31	82
18	191	231	28
19	226	213	26
20	137	102	37
21	635	663	18
22	141	198	39

3 11 1

0	19	33	64
1	656	682	17
2	180	168	28
3	390	350	19
4	469	530	18
5	660	599	17
6	182	139	29
7	635	654	18
8	106	82	43
9	57	63	61
10	485	448	19
11	859	823	19
12	131	151	35
13	523	535	17
14	328	250	20
15	107	239	41
16	174	157	30
17	295	278	22
18	-157	1	27
19	294	302	23
20	-98	49	45
21	144	6	38

3 12 1

0	78	74	38
1	-140	37	29
2	322	274	21
3	790	787	18
4	250	125	25
5	471	418	19
6	40	22	71
7	72	15	55
8	355	255	22
9	749	752	16
10	154	137	31
11	-15	220	86
12	162	124	31
13	248	304	24
14	349	304	20
15	285	315	23
16	-129	35	34
17	157	173	34
18	277	283	24
19	-124	57	37

3 13 1

0	653	633	13
1	335	377	22
2	308	252	23
3	195	94	26
4	148	91	31
5	499	467	17
6	847	884	16
7	304	137	21
8	306	397	21
9	88	40	47
10	191	133	28
11	153	112	33
12	395	367	20
13	124	56	39
14	-105	79	41
15	218	270	28
16	309	286	23
17	40	65	74

3 14 1

0	243	217	17
1	394	368	19
2	381	318	19
3	226	282	25
4	133	135	35
5	-71	9	51
6	102	141	43
7	180	198	29
8	599	584	17
9	181	184	30
10	142	272	36
11	169	110	32
12	-15	1	91
13	131	27	39
14	322	318	23
15	-88	81	50

3 15 1

0	214	216	19
1	84	86	49
2	122	121	38
3	-140	16	30
4	26	10	78
5	306	295	22
6	169	180	31
7	75	21	53
8	195	211	29
9	88	16	50
10	-75	112	53
11	319	238	23
12	139	194	39

3 16 1

0	301	291	16
1	354	330	21
2	-16	47	89
3	305	288	23
4	179	237	31
5	-107	61	41
6	209	214	29
7	160	153	35
8	86	45	53
9	338	306	23

4 0 1

0	1079	919	13
2	352	375	18
4	1701	1844	21
6	3703	3591	39
8	1231	1199	19
10	589	467	19
12	1360	1325	22
14	38	95	78
16	615	560	23
18	-100	65	54
20	886	876	26
22	407	452	27
24	942	912	24
26	203	168	42

4 1 1

0	923	907	10
1	618	494	11
2	1655	1709	17
3	916	924	12
4	653	635	12
5	3209	3069	29
6	2558	2577	24
7	2005	1903	20
8	1934	1987	19
9	1212	1134	15
10	724	703	14
11	1178	1240	16
12	43	110	54
13	65	73	47
14	946	957	16
15	67	82	49
16	225	164	24
17	295	268	22
18	404	412	20
19	-52	91	64
20	539	532	19
21	452	467	21
22	-130	17	33
23	-140	106	32
24	285	231	24
25	66	72	60
26	541	503	19
27	148	68	39

4 2 1

0	1465	1427	13
1	942	987	12
2	162	206	20
3	1296	1301	14
4	1452	1397	15
5	1525	1512	16
6	317	226	14
7	774	778	13
8	567	585	13
9	512	548	14
10	316	270	16
11	600	612	14
12	-139	56	23
13	-113	92	29
14	18	10	75
15	475	480	17
16	951	959	17
17	23	132	79
18	151	170	34
19	173	210	32
20	194	207	31
21	150	154	33
22	183	190	30
23	-77	182	51
24	408	423	20
25	516	480	19
26	98	3	50
27	239	231	29

4 3 1

0	1566	1592	14
1	1265	1201	14
2	1500	1429	16
3	2037	2002	20
4	2442	2403	23
5	1100	1019	14
6	-38	2	50
7	858	882	14
8	280	271	16
9	362	370	15
10	53	150	48
11	922	925	15
12	501	494	15
13	1266	1320	17
14	994	1040	16
15	1079	1085	17
16	668	649	17
17	-80	66	47
18	-115	89	37
19	643	647	19
20	-103	105	44
21	309	350	21
22	-56	195	60
23	-177	19	25
24	-173	0	26
25	300	296	24
26	127	57	42
27	460	451	21

4 4 1

0	657	725	9
1	2058	2029	20
2	1525	1568	16
3	1856	1812	13
4	970	904	13
5	1356	1452	16
6	2087	2063	21
7	590	506	14
8	526	599	14
9	-101	7	30
10	217	165	21
11	385	409	16
12	321	361	18
13	323	332	18
14	825	866	16
15	742	732	17
16	-12	94	87
17	1001	1004	18
18	24	165	82
19	198	176	30
20	61	76	64
21	211	178	27
22	-100	129	42
23	-64	153	58
24	125	157	40
25	348	353	22
26	83	129	55

4 5 1

0	947	813	11
1	682	640	13
2	1675	1527	18
3	238	248	17
4	95	34	31
5	541	490	14
6	687	684	14
7	677	664	14
8	971	975	15
9	379	385	16
10	330	314	17
11	230	234	21
12	1239	1242	17
13	564	510	16
14	823	795	17
15	898	891	17
16	-93	20	41
17	-107	27	39
18	112	137	43
19	713	693	19
20	232	281	25
21	198	251	28
22	265	255	24
23	-105	110	41
24	64	50	61
25	271	215	26
26	217	234	30

4 6 1

0	565	629	10
1	488	531	14
2	635	578	13
3	1301	1383	16
4	1258	1353	16
5	1136	1151	15
6	302	309	17
7	607	593	14
8	509	527	15
9	440	459	16
10	1057	1078	16
11	278	279	20
12	595	582	16
13	905	929	17
14	138	177	33
15	-92	46	42
16	438	442	19
17	118	227	41
18	714	654	19
19	473	441	17
20	-30	159	75
21	277	324	23
22	503	470	18
23	204	206	29
24	439	455	20
25	262	333	27

4 7 1

0	564	531	10
1	274	50	17
2	1225	1138	16
3	517	515	14
4	809	768	15
5	580	459	15
6	1176	1093	16
7	134	57	29
8	446	410	16
9	283	302	19
10	362	324	18
11	103	136	38
12	86	117	44
13	296	347	21
14	596	554	18
15	154	142	33
16	-59	12	59
17	429	440	20
18	-122	116	33
19	274	354	22
20	404	447	19
21	137	216	36
22	123	126	40
23	78	95	55
24	359	405	22
25	-110	64	44

4 8 1

0	334	306	12
1	-46	71	52
2	275	326	18
3	460	348	15
4	1072	1118	16
5	577	545	15
6	94	5	38
7	691	618	16
8	116	82	34
9	311	309	19
10	293	291	20
11	645	641	17
12	301	236	21
13	135	126	36
14	191	147	29
15	-23	51	83
16	363	344	22
17	162	160	30
18	-178	1	23
19	93	245	46
20	-139	82	31
21	-80	1	50
22	462	477	19
23	289	298	25
24	405	423	22

4 9 1

0	158	45	19
1	1111	1160	17
2	415	339	17
3	490	537	16
4	208	238	23
5	746	791	16
6	693	643	16
7	567	627	17
8	-107	80	35
9	185	203	28
10	-93	44	41
11	-90	45	42
12	434	450	19
13	243	265	26
14	256	300	25
15	166	169	34
16	131	182	35
17	-104	74	39
18	334	302	21
19	209	175	27
20	328	378	21
21	59	158	62
22	221	189	28
23	252	287	27

4 10 1

0	160	97	21
1	-47	88	58
2	78	15	46
3	501	479	17
4	297	234	20
5	676	644	17
6	101	37	41
7	240	208	24
8	461	423	18
9	412	371	19
10	137	129	36
11	684	652	18
12	117	74	42
13	282	242	25
14	324	232	20
15	96	73	44
16	459	489	18
17	309	263	21
18	151	114	34
19	-82	33	49
20	-132	28	34
21	380	406	21
22	156	62	37

4 11 1

0	493	411	13
1	452	403	18
2	229	144	25
3	581	530	17
4	165	119	31
5	294	327	22
6	165	198	31
7	383	368	20
8	291	266	23
9	544	533	19
10	90	113	50
11	47	100	62
12	-58	4	56
13	144	144	34
14	287	322	22
15	98	69	44
16	341	382	21
17	-119	66	36
18	-91	131	46
19	314	292	23
20	143	155	38

4 12 1

0	158	193	24
1	-77	95	49
2	178	67	31
3	521	525	19
4	365	243	21
5	924	902	18
6	232	193	27
7	378	407	21
8	187	230	27
9	211	229	25
10	266	314	22
11	101	119	43
12	156	95	32
13	95	181	45
14	360	315	20
15	355	369	21
16	323	260	22
17	-3	146	102
18	110	93	44
19	245	266	27

4 13 1

0	205	93	18
1	143	91	32
2	364	311	19
3	312	333	20
4	186	194	27
5	-76	9	47
6	156	130	31
7	122	64	37
8	196	173	27
9	-65	74	54
10	-88	92	45
11	155	80	33
12	348	285	21
13	176	204	31
14	547	444	18
15	123	166	41
16	-90	82	48
17	110	45	46

4 14 1

0	288	246	15
1	130	158	36
2	308	308	21
3	161	47	31
4	562	545	17
5	225	77	25
6	332	331	21
7	182	37	29
8	490	453	18
9	103	19	44
10	344	298	21
11	61	51	61
12	278	188	24
13	128	175	41
14	200	197	31

4 15 1

0	237	254	18
1	137	139	36
2	346	346	21
3	130	63	37
4	195	236	29
5	-40	15	69
6	388	384	20
7	293	295	23
8	241	268	26
9	264	250	25
10	-96	30	46
11	176	62	33

4 16 1

0	114	128	31
1	-139	50	32
2	78	61	54
3	231	239	27
4	153	74	35
5	339	271	22
6	136	168	39
7	-89	60	49

5 0 1

0	3500	3501	31
2	2766	2774	30
4	2601	2474	29
6	1898	1851	24
8	276	321	23
10	326	424	22
12	731	712	20
14	106	180	48
16	1111	1163	24
18	227	58	37
20	292	302	35
22	805	828	24
24	470	423	27
26	317	292	33

5 1 1

0	479	522	9
1	517	501	12
2	2366	2234	22
3	258	263	15
4	1252	1278	15
5	1147	1165	14
6	1025	1061	14
7	892	808	14
8	487	520	14
9	521	457	14
10	398	277	15
11	478	501	15
12	963	977	15
13	359	388	17
14	628	641	16
15	542	551	17
16	359	289	19
17	904	946	18
18	776	757	18
19	362	352	22
20	118	201	44
21	100	69	44
22	600	545	17
23	-32	18	77
24	190	167	31
25	341	333	22
26	371	356	22
27	509	488	20

5 2 1

0	99	101	22
1	1335	1367	15
2	182	201	19
3	324	345	14
4	62	32	40
5	1787	1826	18
6	574	529	13
7	329	288	15
8	261	257	17
9	793	825	14
10	997	1027	15
11	2025	2062	21
12	280	356	19
13	-72	102	42
14	118	140	34
15	1220	1213	18
16	-31	75	71
17	150	48	33
18	801	796	18
19	187	184	31
20	-77	99	54
21	789	768	17
22	100	145	45
23	250	303	25
24	311	360	23
25	130	108	41
26	101	55	49

5 3 1

0	669	622	9
1	1737	1803	18
2	1185	1037	15
3	632	630	13
4	276	306	16
5	957	942	14
6	-99	143	28
7	107	93	30
8	357	252	15
9	1249	1181	16
10	967	983	15
11	913	917	16
12	524	519	16
13	454	497	17
14	84	107	43
15	303	307	20
16	-112	61	35
17	417	426	19
18	1123	1095	19
19	276	301	25
20	321	363	20
21	330	335	21
22	282	300	23
23	389	419	20
24	186	162	31
25	213	299	30
26	258	303	27

5 4 1

0	373	307	10
1	300	232	15
2	1109	1020	15
3	601	635	13
4	583	627	13
5	69	170	39
6	98	70	32
7	300	140	16
8	364	402	16
9	1516	1508	18
10	295	201	18
11	160	149	27
12	289	285	19
13	547	542	16
14	197	249	26
15	540	567	17
16	561	590	18
17	309	339	22
18	90	11	49
19	676	677	19
20	432	459	18
21	-177	50	24
22	106	186	44
23	246	229	26
24	222	212	28
25	342	345	23
26	-120	84	41

5 5 1

0	1187	1234	12
1	498	561	14
2	1147	1220	15
3	993	928	15
4	1365	1465	17
5	45	18	50
6	649	666	14
7	113	66	32
8	872	947	15
9	1094	1072	16
10	387	380	17
11	107	139	36
12	388	412	18
13	329	338	20
14	143	240	33
15	177	188	29
16	390	387	20
17	51	71	65
18	487	490	20
19	88	27	46
20	333	347	20
21	325	379	21
22	196	203	29
23	221	264	28
24	242	305	27
25	187	236	33

5 6 1

0	-62	62	33
1	489	452	15
2	293	416	17
3	231	242	20
4	339	302	16
5	656	633	15
6	59	12	48
7	1026	976	16
8	758	712	15
9	363	341	17
10	386	368	18
11	860	862	16
12	362	316	19
13	505	487	18
14	279	254	23
15	673	696	18
16	-126	54	34
17	212	198	28
18	501	517	17
19	250	316	23
20	564	585	17
21	180	197	30
22	-93	77	45
23	199	143	30
24	377	387	22
25	-120	202	41

5 7 1

0	-86	67	27
1	257	227	19
2	718	718	15
3	602	524	15
4	341	421	17
5	407	419	16
6	618	630	15
7	84	29	40
8	165	148	27
9	141	74	30
10	878	940	17
11	616	630	17
12	173	73	29
13	-47	29	63
14	-119	124	36
15	379	401	21
16	634	632	19
17	216	210	25
18	-89	71	44
19	-71	29	52
20	-135	59	32
21	128	176	38
22	690	694	18
23	112	36	45
24	80	178	57

5 8 1

0	1391	1340	14
1	317	305	18
2	533	556	16
3	314	375	18
4	420	505	16
5	433	447	17
6	820	856	16
7	291	328	20
8	750	768	16
9	50	17	59
10	862	862	17
11	330	363	21
12	1084	1065	18
13	160	143	33
14	-98	111	43
15	-140	66	32
16	-112	92	36
17	-62	27	55
18	-129	25	33
19	-173	17	24
20	195	251	29
21	169	127	32
22	59	13	63
23	-21	80	89

5 9 1

0	84	74	32
1	777	789	16
2	582	540	16
3	409	409	17
4	482	477	17
5	192	207	25
6	162	122	29
7	-22	76	77
8	59	24	56
9	756	765	17
10	831	809	18
11	587	548	18
12	207	104	28
13	-87	127	48
14	268	247	26
15	265	193	22
16	541	580	17
17	439	451	19
18	-40	5	69
19	-92	9	45
20	-134	67	33
21	368	349	21
22	-93	159	48

5 10 1

0	177	182	20
1	769	712	17
2	280	268	22
3	106	89	39
4	314	335	21
5	540	554	17
6	250	91	24
7	1390	1410	19
8	335	262	21
9	-53	146	62
10	-122	41	35
11	332	345	22
12	307	399	20
13	522	563	17
14	510	520	17
15	97	204	45
16	-132	45	32
17	-111	30	38
18	162	173	33
19	531	487	19
20	432	396	20
21	170	179	34

5 11 1

0	-82	6	35
1	86	33	48
2	113	131	40
3	604	565	18
4	236	118	25
5	835	846	18
6	233	135	26
7	181	34	31
8	166	206	33
9	415	404	21
10	205	200	26
11	570	545	17
12	130	174	36
13	333	343	20
14	196	201	28
15	-40	99	69
16	391	338	20
17	259	278	25
18	102	1	47
19	-139	30	34

5 12 1

0	313	264	16
1	417	466	20
2	335	339	22
3	348	284	22
4	207	132	29
5	228	67	23
6	849	851	16
7	281	237	21
8	756	771	16
9	386	279	19
10	-48	64	63
11	365	418	20
12	424	392	19
13	268	305	23
14	199	223	29
15	102	36	45
16	80	210	53
17	-108	1	42
18	467	425	20

5 13 1

0	84	78	35
1	176	195	29
2	113	10	39
3	207	237	26
4	432	429	18
5	342	385	20
6	312	346	21
7	38	110	69
8	605	614	17
9	211	163	27
10	375	417	20
11	77	194	52
12	-107	43	40
13	182	175	31
14	188	183	31
15	180	157	32
16	471	443	20

5 14 1

0	284	322	16
1	27	44	77
2	157	152	32
3	73	65	52
4	89	35	47
5	91	154	46
6	435	474	19
7	220	170	26
8	320	299	22
9	233	220	26
10	197	272	30
11	128	93	40
12	321	371	23
13	206	168	30

5 15 1

0	-124	6	26
1	-63	51	57
2	186	259	30
3	371	364	20
4	302	304	23
5	211	179	28
6	246	219	26
7	148	80	36
8	231	339	27
9	210	218	29
10	238	262	27

5 16 1

0	150	149	27
1	309	260	23
2	141	110	38
3	269	241	25
4	-128	76	36
5	243	252	27

6 0 1

0	300	293	15
2	1404	1353	21
4	512	595	19
6	869	900	19
8	699	663	19
10	1469	1552	23
12	608	552	21
14	621	637	22
16	928	947	24
18	179	198	43
20	333	371	28
22	512	578	25
24	142	207	51
26	297	258	35

6 1 1

0	2248	2117	19
1	358	300	14
2	2165	2003	21
3	1087	1136	15
4	407	454	14
5	728	830	13
6	16	46	68
7	606	603	14
8	-91	51	31
9	-80	149	37
10	621	650	15
11	32	35	62
12	865	821	16
13	107	234	35
14	232	177	22
15	370	315	19
16	802	782	17
17	492	520	19
18	504	468	19
19	553	599	19
20	38	165	70
21	39	69	71
22	-130	57	34
23	306	289	23
24	488	502	19
25	240	272	28
26	479	448	21

6 2 1

0	806	843	10
1	1046	984	14
2	978	897	14
3	919	852	14
4	796	838	14
5	246	194	17
6	1316	1150	16
7	1202	1173	16
8	292	393	17
9	553	548	15
10	1062	1058	16
11	893	906	16
12	234	212	21
13	43	52	59
14	621	683	17
15	1212	1196	18
16	225	177	25
17	349	400	21
18	177	152	32
19	51	29	68
20	77	65	51
21	537	543	18
22	121	189	40
23	186	151	31
24	103	36	47
25	-87	101	51
26	373	318	23

6 3 1

0	975	1011	11
1	645	676	14
2	326	334	15
3	269	249	17
4	1288	1317	16
5	273	308	17
6	59	4	44
7	234	335	19
8	459	366	15
9	784	739	15
10	882	855	15
11	600	629	16
12	94	131	39
13	1186	1241	18
14	990	986	17
15	652	637	17
16	141	148	35
17	778	818	18
18	199	138	30
19	400	362	18
20	303	339	21
21	212	282	27
22	326	314	22
23	557	555	18
24	129	150	41
25	494	448	20

6 4 1

0	533	497	10
1	159	162	23
2	580	470	14
3	971	1003	15
4	655	624	14
5	90	33	35
6	595	604	14
7	1348	1402	17
8	241	286	20
9	1798	1786	20
10	603	569	15
11	788	740	16
12	-116	56	31
13	168	149	29
14	456	502	18
15	920	864	18
16	132	22	37
17	291	270	23
18	371	385	22
19	346	389	19
20	116	216	40
21	433	439	19
22	86	17	50
23	484	407	19
24	246	279	27
25	-51	107	70

6 5 1

0	1297	1243	13
1	1452	1501	17
2	252	237	19
3	676	622	14
4	713	701	15
5	865	770	15
6	369	354	16
7	681	699	15
8	752	687	15
9	207	153	23
10	415	498	17
11	114	142	36
12	1217	1178	18
13	1053	1049	18
14	595	626	18
15	85	9	49
16	268	294	25
17	269	244	25
18	1156	1169	17
19	562	556	17
20	-126	28	34
21	238	274	25
22	526	524	18
23	280	158	24
24	574	563	19
25	378	367	22

6 6 1

0	413	433	12
1	1206	1173	17
2	1056	1015	16
3	316	320	18
4	1023	1068	16
5	1230	1195	17
6	405	357	16
7	594	641	16
8	758	738	16
9	382	336	18
10	728	732	17
11	366	333	19
12	125	113	37
13	-105	79	38
14	305	295	23
15	505	481	19
16	1034	1052	19
17	365	372	19
18	163	136	31
19	218	222	26
20	117	126	40
21	413	354	20
22	818	773	18
23	592	570	19
24	-111	55	43

6 7 1

0	1857	1818	17
1	926	871	16
2	377	382	17
3	203	84	23
4	1096	1099	17
5	681	581	16
6	1277	1218	18
7	555	530	16
8	462	492	17
9	223	215	24
10	187	129	28
11	370	441	20
12	453	415	19
13	428	445	20
14	190	195	30
15	296	266	24
16	110	109	40
17	122	163	38
18	707	698	17
19	365	301	20
20	628	609	18
21	486	443	19
22	243	201	26
23	289	291	25

6 8 1

0	159	138	21
1	214	191	24
2	845	783	16
3	780	757	16
4	645	670	16
5	534	549	17
6	206	197	24
7	176	97	28
8	207	224	26
9	1029	1005	18
10	877	860	18
11	193	171	29
12	259	288	25
13	-95	40	45
14	-76	133	54
15	276	267	22
16	649	687	17
17	61	51	59
18	367	382	20
19	86	83	50
20	241	170	26
21	634	577	18
22	625	624	19

6 9 1

0	241	217	17
1	1140	1197	18
2	387	323	19
3	323	316	20
4	375	364	19
5	796	841	17
6	464	409	18
7	1498	1498	20
8	146	53	34
9	103	131	43
10	313	357	22
11	184	176	31
12	55	187	64
13	228	298	24
14	-154	10	27
15	211	210	26
16	-165	28	26
17	140	175	36
18	160	54	33
19	681	626	18
20	404	395	21
21	213	167	30

6 10 1

0	56	128	46
1	319	322	21
2	114	26	39
3	963	983	18
4	153	8	33
5	455	443	19
6	169	157	31
7	259	250	24
8	257	189	25
9	220	212	28
10	408	402	21
11	257	276	22
12	65	104	54
13	-111	34	37
14	130	174	37
15	456	471	18
16	234	205	26
17	594	554	18
18	62	134	61
19	119	11	43
20	14	58	96

6 11 1

0	326	301	16
1	385	408	20
2	155	161	34
3	-111	31	38
4	149	145	35
5	325	311	22
6	682	685	18
7	137	52	33
8	47	32	62
9	86	73	46
10	248	207	23
11	374	373	19
12	-99	30	41
13	365	374	20
14	237	217	25
15	278	376	23
16	-91	91	46
17	303	303	23
18	49	31	69
19	225	266	29

6 12 1

0	105	107	29
1	110	104	39
2	664	656	16
3	182	117	28
4	639	613	16
5	91	21	44
6	276	329	22
7	573	567	17
8	405	410	19
9	231	171	25
10	452	425	18
11	249	268	24
12	216	256	27
13	125	79	39
14	122	150	40
15	274	266	24
16	310	301	23
17	124	94	43

6 13 1

0	206	198	19
1	353	360	20
2	154	111	32
3	33	125	72
4	113	18	40
5	250	231	24
6	166	194	31
7	124	121	38
8	440	395	19
9	112	18	41
10	358	292	21
11	211	197	28
12	282	243	24
13	119	177	42
14	436	441	20
15	207	153	30

6 14 1

0	98	37	33
1	111	78	41
2	282	238	23
3	156	61	33
4	236	143	25
5	48	111	65
6	129	57	38
7	43	64	69
8	287	324	23
9	189	172	30
10	269	261	25
11	71	139	58
12	175	35	34

6 15 1

0	307	358	16
1	-50	18	66
2	240	189	26
3	-145	33	31
4	219	178	28
5	276	236	24
6	273	208	25
7	-106	23	42
8	247	157	27

7 0 1

0	978	854	15
2	72	141	53
4	1407	1307	22
6	2122	2153	27
8	396	476	22
10	1950	1866	27
12	1411	1330	24
14	233	154	33
16	263	70	32
18	400	432	29
20	165	7	43
22	175	84	43
24	843	864	25

7 1 1

0	297	369	12
1	689	635	14
2	1518	1437	18
3	1050	964	15
4	733	793	14
5	548	552	14
6	432	402	15
7	760	792	15
8	1341	1398	17
9	832	769	15
10	584	566	16
11	677	639	16
12	207	58	24
13	423	481	18
14	683	729	17
15	431	408	18
16	862	896	18
17	240	274	25
18	-78	35	51
19	544	566	17
20	454	470	18
21	905	912	17
22	695	661	18
23	110	61	44
24	130	24	41
25	539	484	20

7 2 1

0	1166	1150	12
1	1860	1794	20
2	218	195	20
3	326	356	16
4	374	362	16
5	1918	1974	20
6	795	776	15
7	1110	1155	16
8	1079	1040	16
9	1248	1214	17
10	363	319	17
11	1624	1636	19
12	884	890	16
13	395	423	18
14	399	420	19
15	333	277	21
16	412	365	20
17	381	339	21
18	865	851	19
19	140	239	34
20	256	219	23
21	471	390	18
22	190	217	30
23	571	563	19
24	455	489	20
25	760	741	19

7 3 1

0	149	142	18
1	293	301	17
2	136	106	27
3	1311	1299	17
4	955	1022	15
5	920	885	15
6	635	672	15
7	1059	1011	16
8	632	653	15
9	793	756	16
10	107	56	35
11	83	54	43
12	170	95	28
13	463	443	18
14	129	61	36
15	684	663	18
16	49	20	66
17	678	709	19
18	176	44	29
19	-75	10	49
20	153	186	33
21	659	655	17
22	25	32	82
23	215	261	28
24	109	187	46
25	20	35	92

7 4 1

0	517	563	11
1	920	958	15
2	157	199	26
3	356	347	17
4	158	133	26
5	638	628	15
6	786	756	15
7	1792	1716	20
8	192	159	23
9	153	92	28
10	957	941	16
11	81	125	44
12	112	167	38
13	871	898	17
14	428	453	19
15	238	274	26
16	348	356	22
17	864	865	19
18	152	45	32
19	1208	1240	18
20	42	17	68
21	-194	6	21
22	254	270	25
23	254	291	26
24	394	427	22

7 5 1

0	254	309	14
1	-20	3	71
2	768	794	15
3	378	362	17
4	1454	1440	18
5	393	363	17
6	633	587	15
7	445	386	16
8	637	612	16
9	563	551	16
10	683	693	16
11	405	367	18
12	318	352	21
13	477	550	19
14	392	429	20
15	414	421	20
16	591	635	19
17	591	614	17
18	172	8	30
19	266	228	23
20	294	255	22
21	186	164	30
22	366	363	21
23	237	278	27
24	195	218	32

7 6 1

0	1379	1356	14
1	340	277	18
2	100	87	37
3	415	374	17
4	176	238	26
5	353	392	18
6	1441	1458	18
7	980	959	17
8	137	134	32
9	158	215	29
10	137	71	34
11	164	119	31
12	394	414	20
13	106	84	43
14	527	534	19
15	74	55	56
16	476	415	17
17	217	263	26
18	1119	1085	18
19	83	88	50
20	272	312	24
21	178	207	32
22	258	269	26
23	-162	4	30

7 7 1

0	437	410	12
1	662	690	16
2	147	85	30
3	796	824	16
4	974	987	17
5	194	48	25
6	531	524	17
7	333	374	20
8	195	252	26
9	286	270	22
10	701	682	18
11	230	183	26
12	-109	8	39
13	-105	101	42
14	338	333	23
15	252	246	23
16	875	859	17
17	249	180	24
18	159	176	33
19	249	291	25
20	563	590	18
21	150	65	36
22	276	299	25

7 8 1

0	283	276	15
1	991	950	17
2	155	41	31
3	379	393	19
4	363	330	20
5	561	562	18
6	849	863	17
7	840	841	17
8	527	539	18
9	295	299	23
10	438	493	20
11	201	236	29
12	-149	53	30
13	556	570	17
14	293	292	21
15	398	392	19
16	24	126	81
17	358	310	21
18	551	530	18
19	454	409	19
20	293	311	24
21	201	212	31

7 9 1

0	-64	78	41
1	243	279	25
2	578	575	18
3	867	888	18
4	201	150	28
5	171	33	31
6	189	111	29
7	320	332	22
8	862	842	18
9	491	455	19
10	-59	65	61
11	753	716	16
12	38	51	69
13	-114	3	37
14	220	196	26
15	607	570	17
16	350	290	21
17	235	240	26
18	-78	29	52
19	499	454	19
20	544	588	19

7 10 1

0	230	230	19
1	416	411	20
2	545	502	19
3	315	279	22
4	63	129	58
5	447	382	20
6	151	12	35
7	325	298	22
8	542	465	16
9	339	358	19
10	271	289	22
11	146	74	33
12	208	136	27
13	899	905	17
14	407	426	19
15	171	96	32
16	241	276	26
17	471	449	20
18	154	40	36
19	486	500	20

7 11 1

0	253	237	19
1	510	498	20
2	222	176	24
3	499	480	17
4	123	105	36
5	293	266	21
6	463	470	17
7	683	665	16
8	120	62	38
9	261	252	23
10	591	574	17
11	425	451	19
12	131	130	37
13	252	270	25
14	256	245	25
15	475	479	19
16	341	268	22
17	465	411	20

7 12 1

0	684	703	12
1	153	135	32
2	318	264	20
3	285	281	22
4	337	326	20
5	535	478	17
6	219	118	25
7	343	361	20
8	445	427	18
9	112	140	41
10	98	14	45
11	132	79	38
12	469	435	19
13	339	358	22
14	372	352	21
15	400	398	21

7 13 1

0	171	159	22
1	107	58	41
2	749	795	17
3	333	270	21
4	419	392	19
5	169	150	31
6	232	167	25
7	238	131	25
8	241	196	25
9	166	93	33
10	290	241	24
11	8	29	98
12	219	199	28
13	150	66	37

7 14 1

0	394	408	14
1	-44	47	68
2	314	272	22
3	-91	72	46
4	355	326	21
5	106	155	44
6	280	208	24
7	-78	0	51
8	148	213	36
9	82	37	54
10	150	93	37

7 15 1

0	155	215	26
1	282	266	25
2	360	395	22
3	207	167	30
4	114	73	44
5	111	148	45

8 0 1

0	422	479	16
2	2097	2170	27
4	1396	1342	23
6	544	469	22
8	432	400	23
10	44	19	76
12	492	371	25
14	966	948	25
16	287	345	33
18	153	89	42
20	539	495	24
22	172	290	44
24	277	247	36

8 1 1

0	1162	1178	13
1	291	301	18
2	-22	5	69
3	87	92	39
4	930	888	16
5	144	250	28
6	216	222	22
7	483	537	16
8	1189	1245	17
9	220	192	22
10	822	818	16
11	837	777	17
12	1227	1208	18
13	1086	1084	18
14	1000	972	18
15	210	93	27
16	217	256	27
17	432	441	17
18	265	308	22
19	490	494	17
20	404	476	19
21	323	332	21
22	251	209	25
23	-99	38	45
24	372	415	22

8 2 1

0	289	345	13
1	1376	1382	18
2	291	277	18
3	344	388	17
4	581	565	15
5	1015	979	16
6	573	583	15
7	920	884	16
8	356	361	18
9	250	232	21
10	1428	1436	19
11	505	462	17
12	301	254	21
13	1126	1079	18
14	691	674	18
15	553	541	18
16	208	120	28
17	682	680	16
18	381	367	19
19	615	617	17
20	250	244	24
21	427	412	19
22	458	481	19
23	-64	166	60
24	112	92	46

8 3 1

0	105	105	26
1	-67	40	45
2	-124	16	27
3	412	437	17
4	82	42	41
5	149	187	28
6	1158	1174	17
7	814	812	16
8	181	132	25
9	440	401	17
10	93	13	42
11	843	892	17
12	92	59	44
13	1065	1072	18
14	584	594	18
15	237	151	26
16	750	713	19
17	448	444	18
18	137	180	35
19	325	321	21
20	157	179	33
21	125	149	39
22	186	193	31
23	679	671	18

8 4 1

0	672	673	11
1	1030	1081	16
2	869	825	16
3	504	473	16
4	-114	74	30
5	86	10	41
6	74	59	45
7	238	213	22
8	459	474	17
9	892	870	17
10	56	54	56
11	305	318	21
12	125	15	37
13	844	852	18
14	282	319	23
15	255	236	25
16	409	425	18
17	146	255	33
18	243	181	24
19	699	698	17
20	509	531	18
21	254	271	25
22	112	92	44
23	356	367	22

8 5 1

0	394	329	12
1	716	731	16
2	435	402	17
3	803	813	16
4	673	620	16
5	717	691	16
6	737	723	16
7	947	930	17
8	759	726	17
9	371	413	19
10	717	672	17
11	1104	1107	18
12	604	630	18
13	54	41	62
14	337	329	22
15	469	459	17
16	-100	39	40
17	576	598	17
18	960	947	17
19	541	568	18
20	-149	86	30
21	-81	59	51
22	615	607	19
23	381	345	22

8 6 1

0	617	587	12
1	493	524	17
2	92	15	41
3	925	938	17
4	88	49	43
5	97	147	41
6	221	140	24
7	134	21	34
8	1401	1424	19
9	959	951	18
10	674	689	18
11	253	248	24
12	455	464	19
13	558	566	19
14	72	140	51
15	-158	4	26
16	361	391	20
17	348	316	20
18	319	270	22
19	248	301	25
20	478	512	19
21	298	259	24
22	449	477	21

8 7 1

0	1027	1027	13
1	22	9	78
2	64	106	54
3	-66	95	51
4	194	87	27
5	586	533	17
6	1310	1286	19
7	574	542	18
8	243	131	24
9	131	89	37
10	610	632	18
11	238	195	26
12	543	449	19
13	322	361	20
14	409	427	19
15	65	165	56
16	485	528	18
17	312	291	22
18	641	577	18
19	186	85	31
20	481	459	20
21	325	313	23

8 8 1

0	82	138	37
1	173	118	30
2	1012	990	18
3	781	761	18
4	1385	1385	20
5	374	292	20
6	347	335	21
7	551	520	19
8	857	886	18
9	383	382	21
10	494	459	20
11	274	277	22
12	492	498	17
13	470	443	18
14	382	425	19
15	428	432	19
16	351	382	21
17	223	248	27
18	77	18	55
19	443	400	20
20	479	477	20

8 9 1

0	597	585	13
1	882	850	18
2	320	287	23
3	105	19	45
4	164	22	34
5	766	812	18
6	759	756	19
7	141	45	38
8	-71	27	50
9	-61	16	55
10	-44	59	65
11	407	416	19
12	499	548	18
13	117	95	40
14	-87	106	46
15	296	308	23
16	-97	79	44
17	519	521	19
18	227	229	28
19	534	503	20

8 10 1

0	290	290	18
1	277	201	25
2	230	174	28
3	946	928	19
4	249	115	23
5	185	122	28
6	433	379	18
7	687	664	16
8	120	45	38
9	820	850	17
10	205	76	27
11	223	215	26

12	363	343	20
13	394	458	20
14	-166	24	26
15	299	324	23
16	174	191	33
17	312	270	24

8 11 1

0	538	529	12
1	480	461	18
2	405	385	19
3	155	94	32
4	245	135	24
5	941	952	17
6	374	277	19
7	690	715	17
8	321	277	21
9	159	112	32
10	215	96	27
11	812	801	17
12	111	64	42
13	271	287	24
14	-130	21	35
15	169	141	34
16	418	456	21

8 12 1

0	35	70	58
1	317	346	21
2	496	428	18
3	582	634	17
4	634	550	17
5	469	499	18
6	189	118	29
7	196	124	28
8	247	227	24
9	284	288	23
10	296	312	23
11	132	134	39
12	187	106	31
13	20	136	89
14	314	303	24

8 13 1

0	610	652	13
1	121	25	40
2	153	148	34
3	203	57	28
4	393	407	20
5	183	234	30
6	529	511	18
7	235	189	26
8	184	170	31
9	-83	18	50
10	342	317	22
11	199	254	31

8 14 1

0	-94	53	34
1	-121	0	37
2	569	599	18
3	120	12	41
4	70	161	57
5	-137	81	33
6	135	20	39
7	92	53	50

9 0 1

0	751	752	16
2	646	683	22
4	1423	1478	24
6	265	322	29
8	246	123	31
10	273	273	31
12	124	37	51
14	316	21	32
16	658	828	22
18	-104	82	52
20	66	118	72
22	491	493	27

9 1 1

0	-45	142	44
1	216	183	23
2	2009	1991	22
3	354	377	18
4	216	215	23
5	385	382	18
6	182	252	26
7	1011	969	17
8	1333	1408	18
9	643	641	17
10	371	382	19
11	147	162	33
12	239	109	25
13	1426	1427	20
14	1106	1133	19
15	300	234	20
16	224	34	24
17	87	24	47
18	301	326	21
19	-147	45	28
20	-58	156	58
21	-169	28	25
22	286	320	24
23	386	368	21

9 2 1

0	837	845	12
1	634	602	16
2	1075	1051	17
3	445	447	17
4	646	623	16
5	560	568	16
6	738	777	16
7	142	32	31
8	290	342	21
9	56	25	57
10	798	789	17
11	1097	1068	18
12	1219	1205	19
13	397	254	20
14	235	71	27
15	475	481	17
16	756	779	16
17	905	908	17
18	257	305	23
19	-108	15	38
20	-87	35	46
21	-118	37	37
22	-102	62	43
23	473	475	20

9 3 1

0	162	194	20
1	89	181	41
2	102	163	38
3	299	286	20
4	151	97	30
5	-72	42	46
6	470	504	17
7	671	658	17
8	346	322	20
9	611	594	17
10	379	376	20
11	348	320	21
12	508	468	19
13	984	947	18
14	434	431	20
15	595	645	16
16	582	560	17
17	202	20	27
18	420	418	19
19	338	320	21
20	194	255	29
21	244	268	26
22	186	219	32

9 4 1

0	245	145	16
1	1693	1674	20
2	316	298	20
3	-63	43	50
4	391	387	18
5	1232	1228	18
6	261	296	22
7	82	65	47
8	-79	100	45
9	804	788	17
10	961	925	18
11	1399	1373	20
12	157	51	33
13	664	677	19
14	103	71	40
15	516	496	17
16	579	573	17
17	488	534	18
18	-74	39	51
19	289	330	23
20	161	190	34
21	110	124	45
22	444	464	21

9 5 1

0	-135	50	21
1	450	433	18
2	112	39	38
3	1197	1186	18
4	519	467	18
5	313	348	21
6	284	258	22
7	470	436	18
8	486	496	18
9	779	784	18
10	213	92	27
11	580	535	18
12	147	190	36
13	85	22	45
14	931	901	16
15	847	876	16
16	514	509	17
17	179	232	30
18	242	270	25
19	365	341	21
20	552	578	19
21	511	508	20

9 6 1

0	937	910	13
1	87	15	46
2	423	429	19
3	197	22	27
4	1264	1244	19
5	508	487	18
6	464	405	19
7	139	2	35
8	383	398	20
9	324	282	22
10	1251	1225	19
11	647	646	19
12	409	437	18
13	725	719	16
14	270	217	22
15	239	236	24
16	580	560	18
17	94	4	47
18	321	337	22
19	581	587	19
20	191	209	31
21	154	201	49

9 7 1

0	379	401	14
1	183	63	30
2	1260	1242	19
3	496	469	19
4	466	453	19
5	519	494	19
6	304	309	23
7	167	148	32
8	771	837	18
9	100	39	46
10	565	604	16
11	122	63	36
12	83	88	47
13	297	287	21
14	284	256	22
15	191	216	29
16	92	100	48
17	206	211	29
18	474	541	20
19	137	135	39
20	497	492	20

9 8 1

0	572	571	14
1	542	492	19
2	224	165	27
3	408	430	20
4	600	590	19
5	477	439	20
6	356	324	22
7	387	378	21
8	453	471	17
9	324	335	20
10	33	153	72
11	540	541	17
12	-80	84	47
13	231	260	25
14	346	361	21
15	158	201	34
16	280	365	24
17	241	244	27
18	483	493	20
19	265	259	26

9 9 1

0	159	116	26
1	446	484	21
2	395	315	20
3	749	704	16
4	230	123	24
5	-39	49	68
6	133	96	35
7	642	641	17
8	384	410	19
9	642	596	17
10	-88	69	43
11	73	54	53
12	-50	64	63
13	-145	15	30
14	242	254	26
15	107	163	45
16	236	263	27
17	247	153	27

9 10 1

0	116	177	29
1	-125	47	34
2	288	199	22
3	540	509	17
4	339	297	20
5	711	741	17
6	141	54	35
7	252	259	24
8	113	80	41
9	95	142	46
10	216	212	27
11	215	263	28
12	-156	23	29
13	163	184	34
14	-92	93	48
15	218	207	29
16	-77	120	55

9 11 1

0	93	138	35
1	512	485	18
2	427	374	19
3	731	773	17
4	209	116	27
5	141	137	36
6	335	333	21
7	361	363	20
8	304	222	22
9	478	461	19
10	197	200	29
11	108	81	44
12	96	51	49
13	358	330	22
14	125	47	43

9 12 1

0	475	372	14
1	428	414	20
2	154	80	34
3	216	222	27
4	292	253	23
5	550	540	18
6	199	214	29
7	132	39	38
8	-109	115	40
9	95	42	48
10	-107	59	42
11	374	420	22

9 13 1

0	124	177	30
1	205	137	30
2	428	427	20
3	236	258	27
4	-48	21	68
5	97	131	47
6	140	132	38
7	-93	11	47
8	250	274	26

9 14 1

0	344	360	23

10 0 1

0	1345	1307	19
2	1776	1653	27
4	-111	75	47
6	884	944	24
8	1652	1656	27
10	678	714	25
12	271	260	34
14	1248	1258	23
16	200	120	38
18	182	215	41
20	363	406	29

10 1 1

0	748	720	12
1	150	110	32
2	581	532	17
3	96	148	43
4	591	608	17
5	64	156	54
6	262	245	23
7	699	737	17
8	346	315	20
9	306	286	22
10	237	271	25
11	581	570	18
12	163	90	33
13	308	274	20
14	373	298	19
15	457	465	18
16	598	611	17
17	420	397	19
18	499	488	18
19	-101	106	42
20	232	226	27
21	370	367	21

10 2 1

0	664	622	12
1	1398	1342	19
2	-67	26	51
3	913	900	17
4	-97	12	39
5	488	460	18
6	489	455	18
7	1181	1211	18
8	421	438	19
9	284	296	23
10	415	432	20
11	655	642	18
12	409	392	21
13	663	646	16
14	389	405	18
15	729	720	17
16	131	178	36
17	514	545	18
18	247	252	25
19	255	273	25
20	413	448	20
21	255	212	26

10 3 1

0	153	162	23
1	254	234	23
2	153	178	32
3	282	311	22
4	173	30	30
5	1371	1352	19
6	668	628	18
7	454	378	19
8	82	98	49
9	129	116	38
10	465	439	19
11	539	575	19
12	116	152	37
13	216	237	25
14	116	144	38
15	331	331	20
16	157	197	32
17	686	686	17
18	-134	80	32
19	269	271	24
20	128	101	40
21	406	383	21

10 4 1

0	156	195	23
1	135	118	35
2	1271	1231	19
3	88	73	47
4	166	198	31
5	250	191	24
6	-87	101	45
7	121	134	39
8	463	487	19
9	479	541	19
10	339	380	22
11	330	335	19
12	-114	90	34
13	269	236	22
14	414	406	18
15	391	421	19
16	38	124	70
17	-50	53	63
18	24	94	82
19	628	642	18
20	398	348	21

10 5 1

0	856	842	13
1	62	77	58
2	67	4	56
3	624	625	18
4	545	539	19
5	177	139	31
6	829	841	18
7	577	568	19
8	179	115	31
9	545	560	19
10	260	256	22
11	537	546	17
12	-73	59	49
13	146	204	33
14	202	228	27
15	469	449	18
16	104	149	43
17	85	139	49
18	151	215	35
19	404	395	21
20	237	190	28

10 6 1

0	434	408	14
1	342	333	22
2	404	357	20
3	134	115	38
4	80	64	52
5	231	211	27
6	159	162	34
7	157	163	35
8	377	315	18
9	522	494	17
10	-116	9	34
11	81	78	48
12	206	213	26
13	484	489	18
14	456	463	18
15	111	116	41
16	-110	33	38
17	-72	15	54
18	522	502	19
19	140	4	39

10 7 1

0	260	278	18
1	-115	100	39
2	809	789	19
3	-62	11	59
4	-67	57	57
5	842	787	19
6	636	601	16
7	205	149	26
8	600	578	17
9	479	410	17
10	397	403	19
11	-77	89	48
12	580	536	17
13	303	291	22
14	67	106	55
15	-120	35	36
16	402	352	20
17	-143	97	32
18	555	553	19

10 8 1

0	496	501	12
1	-37	40	69
2	123	128	37
3	223	261	25
4	-132	41	31
5	116	89	39
6	605	635	17
7	537	428	17
8	1128	1108	17
9	236	191	24
10	105	86	42
11	-45	93	65
12	428	349	19
13	142	193	35
14	271	354	24
15	250	257	26
16	309	335	23
17	242	250	28

10 9 1

0	104	148	32
1	108	50	42
2	-184	8	22
3	189	200	29
4	-124	25	34
5	285	277	22
6	349	307	20
7	156	15	33
8	197	165	28
9	586	600	17
10	370	336	20
11	324	276	21
12	144	110	35
13	432	428	20
14	284	298	24
15	173	59	34

10 10 1

0	227	216	19
1	376	349	20
2	259	157	24
3	548	560	18
4	-78	7	50
5	-164	69	26
6	283	233	23
7	908	882	17
8	260	209	24
9	198	117	29
10	-120	18	36
11	76	80	54
12	238	182	27
13	423	416	21
14	-67	111	60

10 11 1

0	-101	0	32
1	310	284	23
2	308	291	23
3	158	164	34
4	112	43	43
5	714	703	18
6	234	52	27
7	304	302	23
8	240	229	27
9	123	116	41
10	233	232	27
11	248	248	27

10 12 1

0	265	303	18
1	85	115	53
2	302	281	24
3	148	166	37
4	39	77	75
5	140	94	39
6	172	209	34
7	228	265	28
8	402	374	21

10 13 1

0	126	131	32
1	-71	89	59
2	63	23	64
3	52	3	86

11 0 1

0	453	434	19
2	773	823	25
4	-156	25	38
6	311	353	31
8	429	468	28
10	285	376	29
12	777	815	23
14	-146	47	39
16	673	713	24
18	634	704	25
20	154	171	50

11 1 1

0	617	573	13
1	479	498	19
2	584	558	18
3	791	761	18
4	-50	43	64
5	-54	96	61
6	534	506	19
7	-139	18	31
8	521	563	19
9	263	193	25
10	150	203	31
11	-50	16	60
12	512	502	17
13	-158	17	26
14	297	288	21
15	453	476	18
16	193	134	29
17	247	228	25
18	213	240	28
19	165	246	34

11 2 1

0	529	494	13
1	-60	134	59
2	606	617	18
3	221	240	27
4	587	631	18
5	146	269	35
6	557	579	19
7	189	132	30
8	96	102	47
9	489	475	17
10	355	378	19
11	666	725	16
12	430	428	18
13	219	269	25
14	231	231	25
15	-88	13	45
16	240	211	25
17	607	646	18
18	-163	18	28
19	125	191	41

11 3 1

0	112	108	31
1	333	363	22
2	115	117	42
3	217	176	28
4	574	521	19
5	599	617	19
6	558	592	19
7	56	20	63
8	94	90	48
9	458	451	17
10	369	411	19
11	340	370	20
12	-91	1	42
13	610	626	17
14	-131	62	32
15	495	528	18
16	462	510	19
17	233	281	26
18	114	175	43
19	306	317	24

11 4 1

0	148	181	26
1	284	295	24
2	454	458	20
3	762	774	18
4	265	252	25
5	522	485	19
6	156	210	35
7	35	59	69
8	265	316	22
9	565	580	17
10	97	31	43
11	983	1001	17
12	67	167	54
13	87	93	47
14	38	83	70
15	389	397	20
16	154	128	34
17	-169	105	26
18	-170	12	27

11 5 1

0	256	249	18
1	481	491	20
2	318	308	23
3	-49	26	67
4	-51	62	66
5	526	488	17
6	203	252	26
7	-119	63	34
8	114	199	39
9	393	404	19
10	306	323	21
11	308	333	21
12	-68	90	52
13	358	400	20
14	215	241	27
15	362	386	21
16	73	76	55
17	-132	24	34
18	316	331	23

11 6 1

0	713	678	12
1	359	381	19
2	523	499	17
3	428	428	18
4	558	550	17
5	135	94	35
6	556	566	17
7	63	8	56
8	649	668	17
9	83	117	48
10	499	475	18
11	99	58	43
12	412	410	19
13	73	118	53
14	335	361	21
15	30	150	79
16	278	273	24
17	142	167	38

11 7 1

0	866	886	12
1	587	568	17
2	736	740	17
3	-7	25	94
4	103	168	43
5	351	325	20
6	1043	1045	17
7	217	245	26
8	-90	14	44
9	84	111	48
10	-59	93	57
11	151	8	33
12	846	859	17
13	89	68	49
14	227	273	27
15	241	253	26
16	254	236	26

11 8 1

0	615	586	12
1	205	143	27
2	577	571	17
3	242	210	24
4	647	684	17
5	486	419	18
6	147	71	34
7	37	103	72
8	108	54	42
9	112	118	41
10	226	173	26
11	176	164	31
12	142	110	36
13	174	185	32
14	86	134	52
15	-57	60	63

11 9 1

0	283	259	16
1	562	545	18
2	433	427	19
3	717	711	17
4	138	13	36
5	428	365	19
6	386	386	20
7	518	505	18
8	200	140	29
9	324	272	22
10	403	482	20
11	278	279	24
12	265	280	25
13	121	174	43

11 10 1

0	21	8	69
1	-65	86	57
2	87	135	50
3	326	337	22
4	405	416	20
5	337	282	22
6	491	489	19
7	142	15	37
8	377	347	21
9	441	476	20
10	410	412	21
11	-61	38	61

11 11 1

0	-136	138	25
1	354	371	22
2	95	87	50
3	211	203	29
4	305	291	24
5	185	55	32
6	319	312	23
7	627	571	19
8	166	128	35

11 12 1

0	-107	49	33
1	-105	33	45
2	55	131	68

12 0 1

0	407	458	21
2	-71	140	73
4	300	281	29
6	1767	1846	26
8	868	801	23
10	159	70	43
12	439	472	26
14	193	202	40
16	92	164	65

12 1 1

0	136	226	29
1	-122	99	38
2	-174	88	26
3	-147	140	27
4	385	469	18
5	54	111	59
6	262	2	22
7	372	291	19
8	753	774	16
9	407	415	18
10	821	858	17
11	-56	163	58
12	132	166	36
13	-125	73	34
14	85	161	49
15	-104	62	41
16	359	377	21
17	-166	71	28

12 2 1

0	628	626	14
1	226	312	24
2	190	262	27
3	-168	42	24
4	819	792	16
5	561	578	17
6	248	191	23
7	1087	1094	17
8	254	125	23
9	243	180	24
10	208	137	26

11	135	160	35
12	-68	74	53
13	232	243	25
14	243	321	25
15	-168	36	26
16	182	277	31
17	-149	101	31

12 3 1

0	368	392	14
1	341	344	20
2	228	234	25
3	503	558	17
4	235	162	24
5	401	398	19
6	827	796	17
7	385	397	19
8	398	402	19
9	964	989	17
10	-134	93	31
11	421	433	19
12	32	134	74
13	81	110	50
14	114	19	42
15	580	608	18
16	268	309	25
17	-92	179	48

12 4 1

0	171	196	22
1	347	407	20
2	402	396	19
3	1145	1153	17
4	282	286	22
5	-23	121	80
6	104	127	42
7	-41	103	68
8	-136	7	31
9	123	211	38
10	190	242	28
11	248	312	24
12	167	152	31
13	596	635	18
14	222	126	27
15	346	379	22
16	57	141	65

12 5 1

0	638	636	12
1	-74	53	50
2	431	409	18
3	316	317	21
4	448	462	18
5	501	507	18
6	-148	43	29
7	289	306	22
8	193	260	28
9	-139	2	30
10	143	54	35
11	241	300	25
12	-132	74	33
13	78	140	53
14	265	289	25
15	358	375	22

12 6 1

0	258	259	17
1	124	2	38
2	878	903	17
3	119	128	39
4	-119	36	36
5	383	407	20
6	313	308	22
7	-76	50	50
8	-135	93	32
9	-72	120	52
10	-75	76	51
11	129	112	38
12	520	552	19
13	-78	84	51
14	332	383	22

12 7 1

0	318	329	15
1	256	173	24
2	686	621	17
3	136	46	36
4	705	675	17
5	93	49	47
6	395	402	20
7	181	215	30
8	113	170	42
9	-56	95	61
10	305	278	23
11	159	81	34
12	425	449	20
13	108	155	45

12 8 1

0	417	451	14
1	199	144	29
2	398	442	20
3	371	355	20
4	273	240	24
5	166	39	33
6	411	397	20
7	206	149	29
8	215	258	28
9	112	196	43
10	-56	34	63
11	-67	1	58
12	131	108	40

12 9 1

0	-148	18	22
1	-71	63	55
2	89	86	50
3	662	634	18
4	232	135	27
5	313	327	23
6	191	3	31
7	234	145	27
8	403	407	21
9	104	87	47
10	139	111	52

12 10 1

0	-133	55	26
1	171	267	34
2	251	227	26
3	86	186	52
4	207	128	30
5	640	665	19
6	213	163	30

13 0 1

0	200	97	28
2	68	108	72
4	612	690	24
6	563	543	24
8	741	732	24
10	765	720	24
12	239	194	36
14	542	574	26

13 1 1

0	994	1003	13
1	446	479	18
2	114	135	41
3	502	537	18
4	82	128	50
5	-22	53	82
6	803	840	17
7	33	50	74
8	708	673	17
9	222	193	26
10	191	108	29
11	112	205	42
12	590	555	18
13	552	512	18
14	452	461	20
15	242	265	27

13 2 1

0	874	854	13
1	465	396	18
2	337	313	21
3	16	72	87
4	90	123	47
5	-137	44	31
6	293	243	22
7	281	80	23
8	531	472	18
9	534	513	18
10	264	256	24
11	382	359	20
12	145	70	36
13	304	240	23
14	189	158	31
15	380	371	21

13 3 1

0	335	295	15
1	843	804	17
2	235	214	25
3	226	155	26
4	459	418	19
5	304	351	22
6	129	35	38
7	1034	1036	18
8	226	212	26
9	247	272	25
10	117	105	41
11	399	429	20
12	180	161	31
13	667	632	18
14	398	366	21

13 4 1

0	331	312	15
1	621	603	17
2	195	19	29
3	743	667	17
4	-86	81	47
5	252	239	24
6	525	487	18
7	91	89	48
8	293	306	23
9	784	778	18
10	262	223	24
11	267	243	24
12	116	171	42
13	286	304	24

13 5 1

0	454	449	13
1	395	392	20
2	190	43	29
3	127	103	39
4	196	98	29
5	109	123	43
6	441	396	19
7	411	417	20
8	190	142	30
9	170	176	32
10	162	22	34
11	623	644	18
12	302	344	24

13 6 1

0	455	449	14
1	261	142	24
2	805	751	18
3	278	197	24
4	437	438	19
5	201	110	29
6	10	37	95
7	-91	116	47
8	499	458	19
9	453	429	20
10	519	503	19
11	176	95	33

13 7 1

0	796	798	13
1	180	75	32
2	250	216	26
3	56	37	64
4	-133	28	34
5	138	74	38
6	680	676	18
7	89	105	51
8	305	265	24
9	229	184	28
10	316	286	23

13 8 1

0	280	247	18
1	102	57	47
2	386	367	21
3	520	507	19
4	567	550	19
5	203	56	30
6	460	441	20
7	117	59	44

13 9 1

0	152	211	27
1	499	481	20
2	137	141	40
3	266	225	26

14 0 1

0	650	609	18
2	292	287	32
4	588	410	25
6	539	495	26
8	552	523	26
10	400	249	29
12	395	354	30

14 1 1

0	259	254	18
1	254	237	25
2	474	487	19
3	423	366	20
4	1173	1142	19
5	311	284	23
6	227	129	27
7	450	420	19
8	511	492	19
9	347	306	22
10	797	811	18
11	-64	125	60

14 2 1

0	444	446	14
1	614	565	18
2	171	104	32
3	605	560	18
4	400	309	20
5	184	123	31
6	623	594	18
7	478	415	19
8	149	155	36
9	220	196	28
10	384	365	21
11	152	114	36

14 3 1

0	244	241	18
1	456	389	19
2	361	345	21
3	860	825	18
4	407	418	20
5	222	250	28
6	147	107	36
7	588	530	19
8	-37	9	75
9	561	535	19
10	169	141	34

14 4 1

0	374	437	15
1	906	855	18
2	175	129	32
3	36	4	76
4	319	242	23
5	703	700	18
6	241	151	27
7	527	515	19
8	316	232	23
9	204	142	30
10	363	321	22

14 5 1

0	308	273	17
1	183	158	32
2	246	166	27
3	666	679	18
4	367	316	22
5	139	3	39
6	377	355	21
7	86	125	53
8	521	455	19

14 6 1

0	829	817	13
1	219	61	29
2	541	497	19
3	214	73	29
4	500	485	20
5	386	410	22
6	579	576	19

14 7 1

0	290	251	18
1	384	290	22
2	1036	1036	19
3	261	102	27

15 0 1

0	242	231	27
2	489	539	28
4	606	592	27
6	470	515	28

15 1 1

0	621	613	14
1	262	277	26
2	323	228	23
3	629	568	19
4	650	597	19
5	355	368	22
6	464	422	20

15 2 1

0	379	422	15
1	323	287	23
2	579	572	19
3	590	581	19
4	175	104	34
5	203	8	31

15 3 1

0	390	351	15
1	635	648	19
2	173	69	35
3	122	102	44
4	183	147	33

15 4 1

0	280	270	18
1	327	331	24

Appendix 5

Transient Spectra of $RuTFPPCl_8(CO)$ at 415 nm

DATA FILE: RUO2.001 1995-2-23 9:19:52
TIME RANGE: 50 µs INPUT V RANGE: 0.320V INPUT OFFSET: 0 %
EXPERIMENT: TRANSIENT ABSORBTION
FAST (200 MHz) QUASI-DIFFERENTIAL AMP
MODE: SINGLE-ENDED

SHOTS PRE CYCLE: 10 CYCLES: 5 PMT VOLTIGE: 702 V
EXCITATION WAVELENGTH: 355 nm OBSERVATION WAVELENGTH: 415 nm
SAMPLE: RuCl8(CO)
SOLVENT: CH2Cl2
TEMPERATURE: rt
COMMENT: under dioxygen
COMMENT:

---> FIXED PARAMETER; ! ---> FIXED SIGN

$$y(t) = C0 + C1*e^{-k1*t} + C2*e^{-k2*t}$$

C0 = -5.029E-3
C1 = -1.936E-1 !k1 = 1.053E7 s^{-1}
C2 = -6.791E-5 !k2 = 1.560E5 s^{-1}

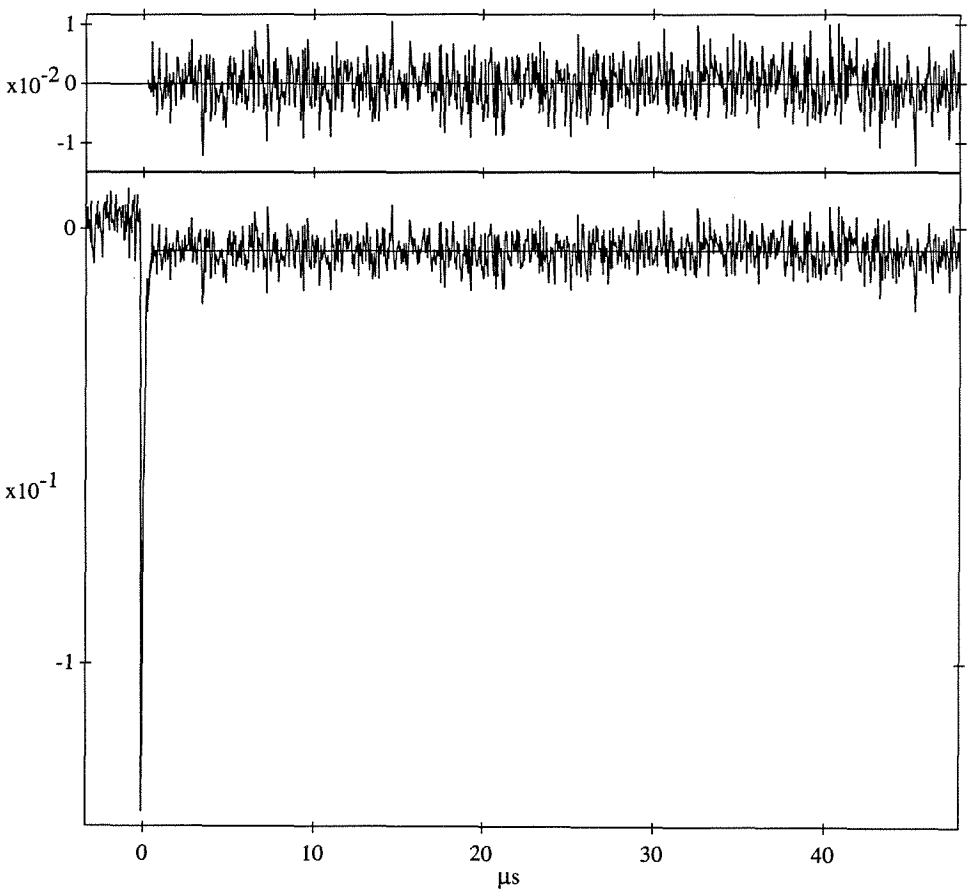

DATA FILE: RUET.002 1995-2-23 9:24:35
TIME RANGE: 50 µs INPUT V RANGE: 0.320V INPUT OFFSET: 0 %
EXPERIMENT: TRANSIENT ABSORBTION
FAST (200 MHz) QUASI-DIFFERENTIAL AMP
MODE: SINGLE-ENDED

SHOTS PRE CYCLE: 10 CYCLES: 5 PMT VOLTIGE: 702 V
EXCITATION WAVELENGTH: 355 nm OBSERVATION WAVELENGTH: 415 nm
SAMPLE: RuCl8(CO)
SOLVENT: CH2Cl2
TEMPERATURE: rt
COMMENT: under ethylene
COMMENT:

---> FIXED PARAMETER; ! ---> FIXED SIGN

$$y(t) = C0 + C1*e^{-k1*t} + C2*e^{-k2*t}$$

C0 = -1.311E-2
C1 = -9.201E-2 !k1 = 2.996E6 s^{-1}
C2 = -5.118E-3 !k2 = 4.197E5 s^{-1}

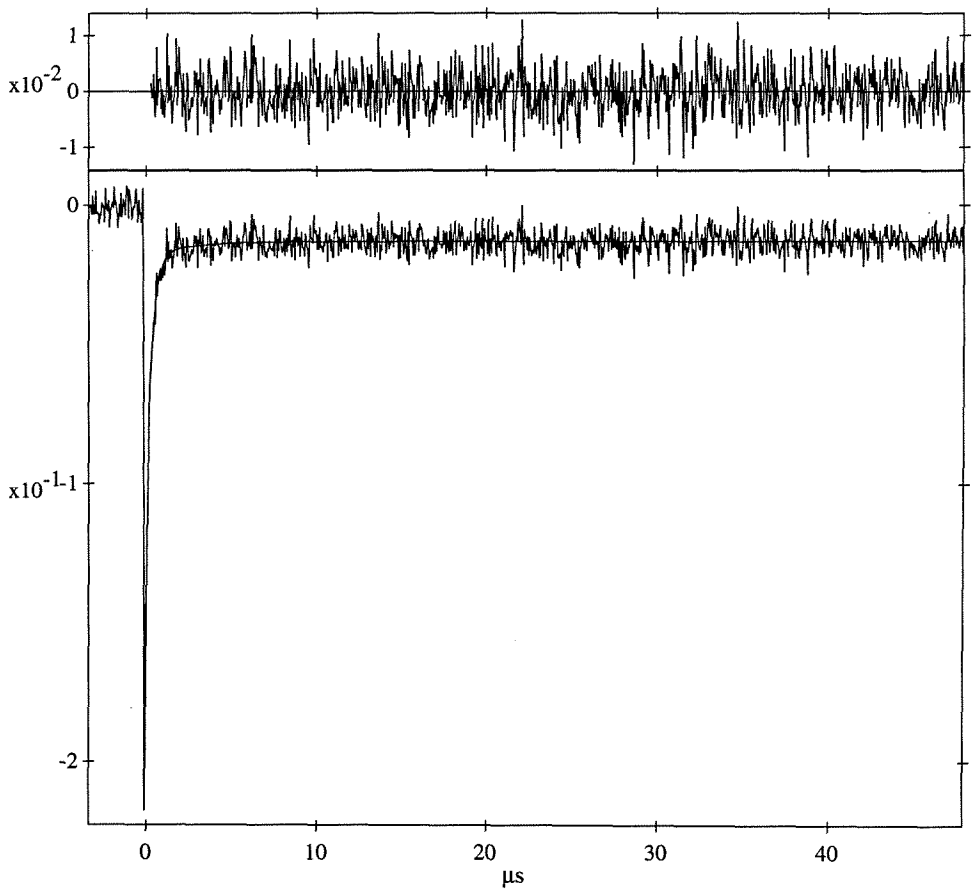

DATA FILE: RUAR.005 1995-2-23 9:14:31
TIME RANGE: 50 µs INPUT V RANGE: 0.320V INPUT OFFSET: 0 %
EXPERIMENT: TRANSIENT ABSORBTION
FAST (200 MHz) QUASI-DIFFERENTIAL AMP
MODE: SINGLE-ENDED

SHOTS PRE CYCLE: 10 CYCLES: 5 PMT VOLTIGE: 702 V
EXCITATION WAVELENGTH: 355 nm OBSERVATION WAVELENGTH: 415 nm
SAMPLE: RuCl8(CO)
SOLVENT: CH2Cl2
TEMPERATURE: rt
COMMENT: under argon
COMMENT:

---> FIXED PARAMETER; ! ---> FIXED SIGN

$$y(t) = C0 + C1*e^{-k1*t} + C2*e^{-k2*t}$$

C0 = -5.758E-3
C1 = -1.183E-1 !k1 = 5.008E6 s^{-1}
C2 = -1.920E-2 !k2 = 7.660E5 s^{-1}

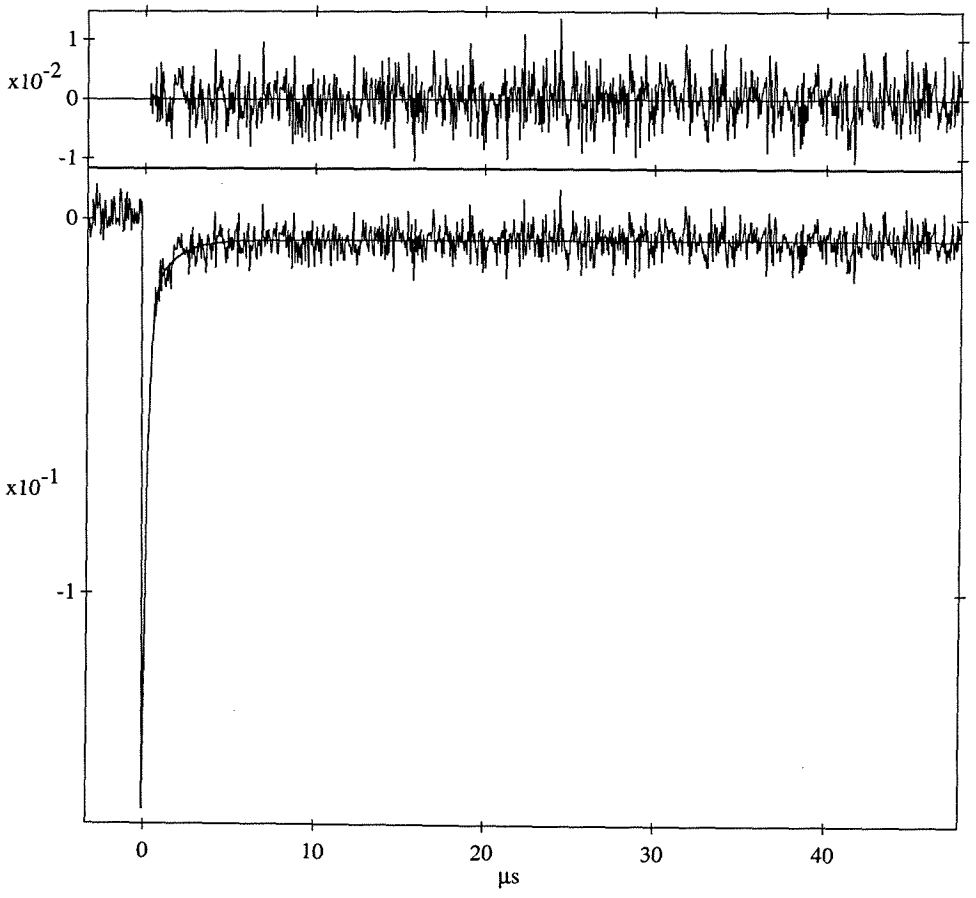

DATA FILE: RUO2.000 1995-2-23 9:18:40
TIME RANGE: 5.0 µs INPUT V RANGE: 0.320V INPUT OFFSET: 0 %
EXPERIMENT: TRANSIENT ABSORBTION
FAST (200 MHz) QUASI-DIFFERENTIAL AMP
MODE: SINGLE-ENDED

SHOTS PRE CYCLE: 10 CYCLES: 5 PMT VOLTIGE: 702 V
EXCITATION WAVELENGTH: 355 nm OBSERVATION WAVELENGTH: 415 nm
SAMPLE: RuCl8(CO)
SOLVENT: CH2Cl2
TEMPERATURE: rt
COMMENT: under dioxygen
COMMENT:

---> FIXED PARAMETER; ! ---> FIXED SIGN

$y(t) = C0 + C1*e^{-k1*t} + C2*e^{-k2*t}$

C0 = -8.692E-3
C1 = -6.069E-2 !k1 = 1.252E7 s^{-1}
C2 = -1.127E-1 !k2 = 7.463E6 s^{-1}

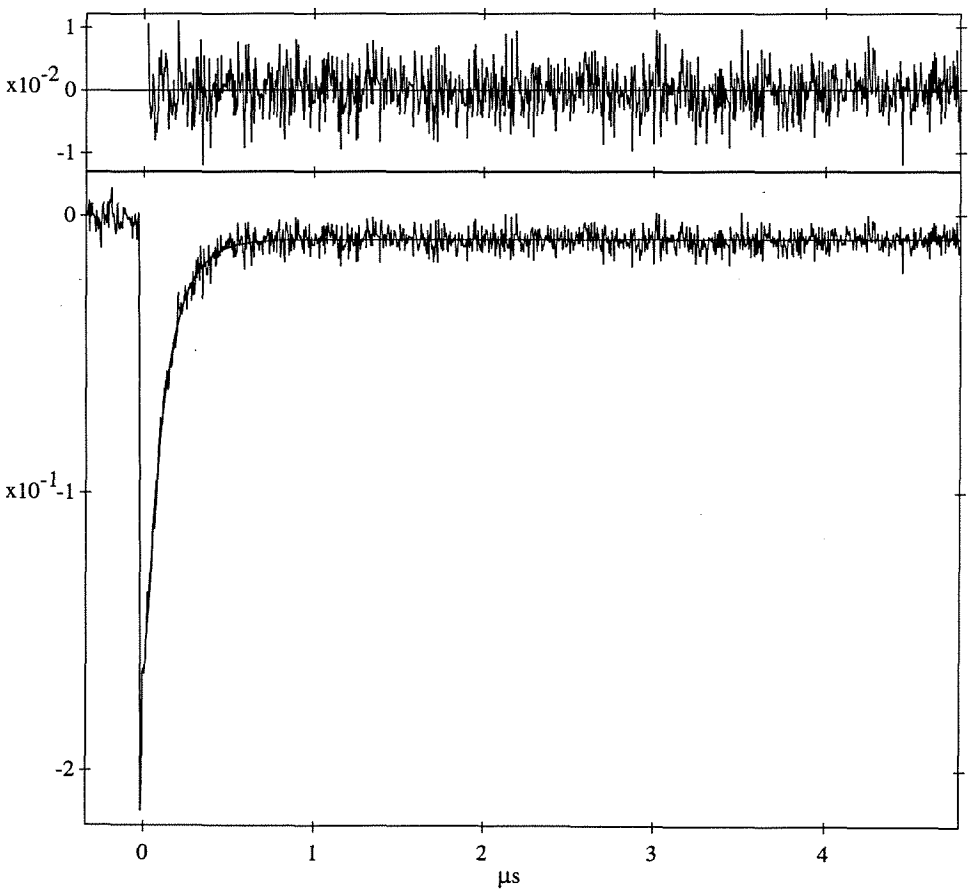

DATA FILE: RUET.001 1995-2-23 9:23:24
TIME RANGE: 5.0 µs INPUT V RANGE: 0.320V INPUT OFFSET: 0 %
EXPERIMENT: TRANSIENT ABSORBTION
FAST (200 MHz) QUASI-DIFFERENTIAL AMP
MODE: SINGLE-ENDED

SHOTS PRE CYCLE: 10 CYCLES: 5 PMT VOLTIGE: 702 V
EXCITATION WAVELENGTH: 355 nm OBSERVATION WAVELENGTH: 415 nm
SAMPLE: RuCl8(CO)
SOLVENT: CH2Cl2
TEMPERATURE: rt
COMMENT: under ethylene
COMMENT:

---> FIXED PARAMETER; ! ---> FIXED SIGN

$y(t) = C0 + C1*e^{-k1*t} + C2*e^{-k2*t}$

C0 = -1.544E-2
C1 = -1.144E-1 !k1 = 8.860E6 s^{-1}
C2 = -8.417E-2 !k2 = 2.281E6 s^{-1}

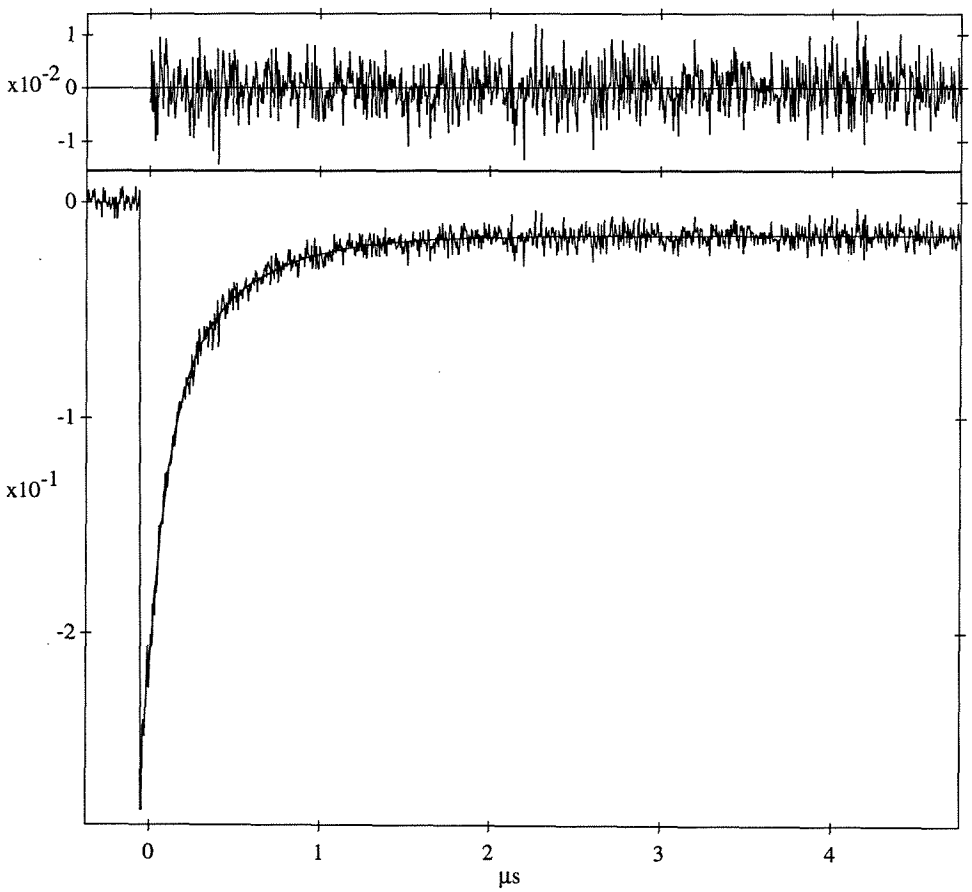

DATA FILE: RUAR.004 1995-2-23 9:13:21
TIME RANGE: 5.0 µs INPUT V RANGE: 0.320V INPUT OFFSET: 0 %
EXPERIMENT: TRANSIENT ABSORBTION
FAST (200 MHz) QUASI-DIFFERENTIAL AMP
MODE: SINGLE-ENDED

SHOTS PRE CYCLE: 10 CYCLES: 5 PMT VOLTIGE: 702 V
EXCITATION WAVELENGTH: 355 nm OBSERVATION WAVELENGTH: 415 nm
SAMPLE: RuCl8(CO)
SOLVENT: CH2Cl2
TEMPERATURE: rt
COMMENT: under argon
COMMENT:

---> FIXED PARAMETER; ! ---> FIXED SIGN

$$y(t) = C0 + C1*e^{-k1*t} + C2*e^{-k2*t}$$

C0 = -9.262E-3
C1 = -6.495E-2 !k1 = 7.124E6 s^{-1}
C2 = -8.926E-2 !k2 = 2.166E6 s^{-1}